

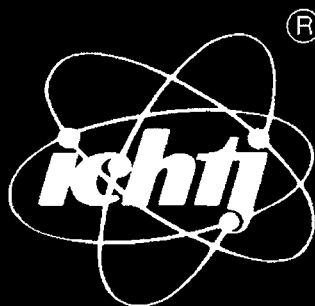
ISSN 1425-204X



PL0101523

# ANNUAL REPORT

## 2000

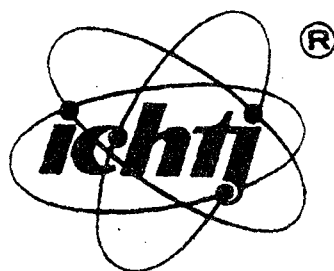


INSTITUTE  
OF NUCLEAR CHEMISTRY  
AND TECHNOLOGY

32 / 37

# ANNUAL REPORT

## 2000



INSTITUTE  
OF NUCLEAR CHEMISTRY  
AND TECHNOLOGY

## **EDITORS**

*Wiktor Smutek, Ph.D.*  
*Ewa Godlewska-Para, M.Sc.*

## **PRINTING**

*Sylwester Wojtas*

**PLEASE BE AWARE THAT  
ALL OF THE MISSING PAGES IN THIS DOCUMENT  
WERE ORIGINALLY BLANK**

# CONTENTS

<b>GENERAL INFORMATION</b>	<b>9</b>
<b>MANAGEMENT OF THE INSTITUTE</b>	<b>11</b>
<b>MANAGING STAFF OF THE INSTITUTE</b>	<b>11</b>
<b>HEADS OF THE INCT DEPARTMENTS</b>	<b>11</b>
<b>SCIENTIFIC COUNCIL (1999-2003)</b>	<b>11</b>
<b>SCIENTIFIC STAFF</b>	<b>14</b>
<b>PROFESSORS</b>	<b>14</b>
<b>ASSOCIATE PROFESSORS</b>	<b>14</b>
<b>SENIOR SCIENTISTS (Ph.D., D.Sc.)</b>	<b>14</b>
<b>SENIOR SCIENTISTS (Ph.D.)</b>	<b>15</b>
<b>RADIATION CHEMISTRY AND PHYSICS, RADIATION TECHNOLOGIES</b>	<b>17</b>
RADIATION-INDUCED CHANGES IN AMINOGLUTETHIMIDE H. Ambroz, E. Kornacka, G. Przybytniak	19
IDENTIFICATION OF RADICALS IN ELECTRON BEAM IRRADIATED IFOSFAMIDE H. Ambroz, E. Kornacka, G. Przybytniak	20
*OH RADICAL INDUCED OXIDATION OF $\alpha$ -METHYLALANINE TIME-RESOLVED AND SPIN-TRAPPING ESR STUDY P. Wiśniowski, G.L. Hug, R.W. Fessenden	21
GENERATION OF AROMATIC THIOETHER RADICAL CATIONS CONTAINING PHENYL, VINYL, ALLYL, AND METHYL SUBSTITUENTS IN ORGANIC SOLVENTS A. Korzeniowska-Sobczuk, P. Wiśniowski, K. Bobrowski, S. Naumov, L. Richter, O. Brede	23
OXIDATION PROCESSES OF N,S,-DIACETYL-L-CYSTEINE ETHYLESTER: INFLUENCE OF S-ACETYLATION P. Wiśniowski, G. Strzelczak, K. Bobrowski, N. Varmenot, S. Remita, Z. Abedinzadeh	25
SPECTRAL, KINETICS, AND THEORETICAL STUDIES OF RADICAL CATIONS DERIVED FROM THIOANISOLE AND ITS CARBOXYLIC DERIVATIVE A. Korzeniowska-Sobczuk, K. Bobrowski, G.L. Hug, I. Carmichael	26
INTERACTION OF TETRAMERIC SILVER WITH AMMONIA IN AgCs-rho ZEOLITE J. Sadło, M. Danilczuk, J. Michalik	29
A NANOSECOND PULSE RADIOLYSIS SYSTEM DEDICATED TO THE NEW LAE 10 ACCELERATOR IN THE INCT J. Mirkowski, P. Wiśniowski, K. Bobrowski	31
POST-IMPLANTATION DEFECTS. INSTABILITY UNDER 1 MeV ELECTRON IRRADIATION IN GaAs S. Warchoła, H. Rzewuski, J. Krynicki, R. Grötzschel	33
RADIATION CHEMISTRY OF POLYMERS AS RECOGNIZED BY DIFFUSE REFLECTANCE SPECTROPHOTOMETRY (DRS) Z.P. Zagórski, A. Rafalski	35
ROLE OF SPURS IN IRRADIATED POLYMER BLENDS Z.P. Zagórski	37
EPR SPECTROSCOPY OF $\gamma$ -IRRADIATED POLYCRYSTALLINE ASPARAGINE AND ASPARAGINE-CONTAINING PEPTIDES G. Strzelczak, K. Bobrowski, Ch. Houée-Levin, J. Bergés	39
MULTIFREQUENCY EPR STUDY OF RADICALS PRODUCED BY RADIATION IN SHELLS AND CORALLITE G. Strzelczak, W. Stachowicz, J. Michalik, G. Vanhaelewyn, F. Callens, E. Goovaerts	41
QUALIFICATION OF THE CONCENTRATION RATIO OF RADIATION INDUCED HYDROCARBONS IN RELATION TO FATTY ACID COMPOSITION WITH THE USE OF A GAS CHROMATOGRAPH (GC) K. Lehner, W. Stachowicz	43

DETECTION OF IRRADIATION OF FROZEN FISH MEAT BY SINGLE CELL GEL ELECTROPHORESIS K. Malec-Czechowska, Z. Szot, W. Stachowicz, M. Kruszewski	44
GELATINISATION AND AMYLOSE-LIPID COMPLEX TRANSITION OCCURRING IN NATIVE AND GAMMA IRRADIATED STARCHES STUDIED BY DIFFERENTIAL SCANNING CALORIMETRY K. Cieřła, A.-Ch. Eliasson, W. Głuszewski	46
THERMOLUMINESCENCE OF SOILS FROM KUJAWY-POMERANIAN REGION A.M. Dancewicz, K. Malec-Czechowska	47
RADIOLYTIC DEGRADATION OF HERBICIDE 2,4-DICHLOROPHENOXYACETIC ACID (2,4-D) P. Drzewicz, M. Trojanowicz, P. Panta, W. Głuszewski, M. Gryz, G. Natęcz-Jawecki, J. Sawicki, C. Duarte, M.H.O. Sampa, H. Oikawa, M. Szewczyńska, A. Al-Kaid, A.A. Al-Mowed	49
RADIATION MODIFICATION OF LDPE (BRALEN TYPE) I. Legocka, Z. Zimek, K. Mirkowski, M. Zielonka	51
RADIATION STERILIZATION OF ALLOGRAFTS I. Kałuska, Z. Zimek	54
EB DOSE CALIBRATION FOR THE LINEAR ELECTRON ACCELERATOR IN THE INCT EXPERIMENTAL PLANT FOR FOOD IRRADIATION H.B. Owczarczyk, W. Migdał, W. Stachowicz, G. Strzelczak	56
CHEMICAL DOSIMETRY. LMTD STAND FOR PRECISE $\gamma$ -IRRADIATION OF DOSIMETERS AND OTHER SMALL OBJECTS Z. Stuglik	57
<b>RADIOCHEMISTRY, STABLE ISOTOPES, NUCLEAR ANALYTICAL METHODS, GENERAL CHEMISTRY</b>	<b>59</b>
INFLUENCE OF RELATIVISTIC EFFECTS ON HYDROLYSIS OF $Ra^{2+}$ B. Włodzimirska, A. Bilewicz	61
DETERMINATION OF TRACE AMOUNTS OF CADMIUM IN GEOLOGICAL AND ENVIRONMENTAL MATERIALS BY NAA WITH PRECONCENTRATION ON AMPHOTERIC ION EXCHANGE RESIN Z. Samczyński, R. Dybczyński, B. Danko	62
PROBLEMS OF THE ATTRIBUTION OF WORKS OF ART: EXAMPLES OF 18th CENTURY CENTRAL EUROPEAN DECORATIVE GLASS J. Kunicki-Goldfinger, J. Kierzek, A.J. Kasprzak, B. Małozewska-Bućko	63
DYNAMIC ADSORPTION OF RADIOEUROPIUM FROM SIMULATED LIQUID RADIOACTIVE WASTES ON $\alpha$ -CRYSTALLINE POLYANTIMONIC ACID J. Satyanarayana, A. Bilewicz, J. Narbutt	64
DIFFUSE REFLECTION SPECTROSCOPY: STUDIES OF OXIDE LAYERS FORMED ON THE STAINLESS STEELS IN HIGH TEMPERATURE WATER L. Fuks, C. Degueldre	65
AN ATTEMPT TO FRACTIONATE URANIUM ISOTOPES IN THE ACETATE-AMALGAM SEPARATION SYSTEM W. Dembiński, M. Poniński, R. Fiedler	67
AQUEOUS SOLUBILITIES OF RARE EARTH TRIHALIDES (Cl, Br, I) AT 298 K T. Mioduski	67
STUDIES ON DETERMINATION OF SOME TRANSITION METALS IN BIOLOGICAL MATERIALS BY ION CHROMATOGRAPHY K. Kulisa, H. Polkowska-Motrenko, R. Dybczyński	68
SIMPLE PC SOFTWARE FOR ROUTINE ANALYSIS OF GAMMA-RAY SPECTRA Z. Szopa, R. Dybczyński	70
DIRECT PRETREATMENT OF ANALYTICAL SAMPLES IN A GRAPHITE FURNACE TUBE IN ATOMIC ABSORPTION SPECTROMETRY L. Pszonicki, W. Skwara, J. Dudek	71
DETERMINATION OF TRACE CONCENTRATION OF PLATINUM IN ENVIRONMENTAL SAMPLES BY GRAPHITE FURNACE ATOMIC ABSORPTION SPECTROMETRY AFTER PRECONCENTRATION ON A SORBENT J. Chwastowska, W. Skwara, E. Sterlińska, J. Dudek, L. Pszonicki	72
RADIONUCLIDE CONCENTRATION MEASUREMENTS IN SOLUTION AND SOIL J. Kierzek, J. Parus, B. Małozewska-Bućko	73

SURFACE MODIFICATION OF PARTICLE TRACK-ETCHED MEMBRANES D. Wawszczak, W. Malicki, M. Buczkowski	75
RADIATION RESISTANCE OF PARTICLE TRACK-ETCHED MEMBRANES M. Buczkowski, B. Sartowska, D. Wawszczak, W. Starosta	76
SYNCHROTRON SAXS STUDY OF PERMEATING MEMBRANE DEPENDING ON ITS DEPTH H. Grigoriew, S. Bernstorff, A. Wolińska-Grabczyk, A.G. Chmielewski	78
SYNTHESIS OF $\text{LiCoO}_2$ AND $\text{LiMg}_{0.05}\text{Co}_{0.95}\text{O}_2$ THIN FILMS ON POROUS $\text{Ni/NiO}$ CATHODES FOR MCFC BY COMPLEX SOL-GEL PROCESS (CSGP) W. Łada, A. Deptuła, B. Sartowska, T. Olczak, A.G. Chmielewski, M. Carewska, S. Scaccia, E. Simonetti, L. Giorgi, A. Moreno	79
$\text{LiCoO}_2$ NANOCOMPOSITE DOPED $\text{SiO}_2$ , $\text{TiO}_2$ , $\text{Al}_2\text{O}_3$ FOR RECHARGEABLE LITHIUM BATTERIES A. Deptuła, F. Croce, W. Łada, D. Deptuła, T. Olczak, D.L. Chua	81
THE CRYSTAL STRUCTURE OF TETRA-n-BUTYLAMMONIUM TETRAIODODINATE(III) K. Rudawska, H. Ptasiiewicz-Bąk, S. Siekierski	83
ASYMMETRIC HYDROGEN BONDS IN CENTROSYMMETRIC ENVIRONMENT: NEUTRON STUDY OF THE VERY SHORT HYDROGEN BOND IN POTASSIUM HYDROGEN DICHLOROMALEATE I. Olovsson, H. Ptasiiewicz-Bąk, T. Gustafsson, I. Majerz	84
ANTIFERROMAGNETIC ORDER IN $\text{RIrSi}$ ( $\text{R}=\text{Tb-Er}$ ) COMPOUNDS A. Szytuła, M. Hofmann, J. Leciejewicz, B. Penc, A. Zygmunt	85
NEUTRON SCATTERING SPECTROSCOPY AND AB INITIO STUDY OF L-THREONINE A. Pawlukojć, J. Leciejewicz, J. Tomkinson, S.F. Parker	85
CRYSTAL CHEMISTRY OF COORDINATION COMPOUNDS WITH HETEROCYCLIC CARBOXYLATE LIGANDS. PART XXXII: THE CRYSTAL AND MOLECULAR STRUCTURE OF A CALCIUM(II) COMPLEX WITH PYRIDINE-2,6-DICARBOXYLATE AND WATER LIGANDS W. Starosta, H. Ptasiiewicz-Bąk, J. Leciejewicz	87
CRYSTAL CHEMISTRY OF COORDINATION COMPOUNDS WITH HETEROCYCLIC CARBOXYLATE LIGANDS. PART XXXIII: THE CRYSTAL AND MOLECULAR STRUCTURES OF TWO POLYMORPHIC FORMS OF A CALCIUM(II) COMPLEX WITH PYRIDINE-2,6-DICARBOXYLATE, WATER AND NITRATE LIGANDS W. Starosta, H. Ptasiiewicz-Bąk, J. Leciejewicz	88
CRYSTAL CHEMISTRY OF COORDINATION COMPOUNDS WITH HETEROCYCLIC CARBOXYLATE LIGANDS. PART XXXIV: THE CRYSTAL AND MOLECULAR STRUCTURES OF LEAD(II) COMPLEXES WITH FURAN-2-CARBOXYLATE AND FURAN-3-CARBOXYLATE LIGANDS B. Paluchowska, J.K. Maurin, J. Leciejewicz	90
<b>RADIOBIOLOGY</b>	<b>93</b>
EXPRESSION OF TP53 EFFECTOR PROTEINS AND STRESS KINASES IN L5178Y SUBLINES I. Grądzka, I. Szumiel, D. Kowalczyk, P. Janik	95
CAFFEINE-INHIBITABLE CONTROL OF THE RADIATION-INDUCED G2 ARREST IN L5178Y-S CELLS DEFICIENT IN NON-HOMOLOGOUS END-JOINING I. Szumiel, I. Grądzka, M. Kapiszewska	96
EXAMINATION OF MICRONUCLEI FREQUENCY AS AN IONIZING RADIATION SENSITIVITY MARKER IN A PANEL OF LYMPHOID CELL LINES A. Jaworska, P. De Angelis, I. Szumiel, J. Reitan	97
EXAMINATION OF THE ROLE OF DOUBLE STRAND BREAK REPAIR IN THE ADAPTIVE RESPONSE OF HUMAN LYMPHOCYTES: NEUTRAL COMET ASSAY M. Wojewódzka, I. Grądzka, I. Buraczewska	98
EXAMINATION OF THE ROLE OF DOUBLE STRAND BREAK REPAIR IN THE ADAPTIVE RESPONSE OF HUMAN LYMPHOCYTES: PULSE FIELD ELECTROPHORESIS I. Grądzka, M. Wojewódzka, I. Buraczewska	99
CYTOTOXIC EFFECTS OF CIS-PLATINUM AND PALLADIUM(II) CHLORIDES COMPLEXED WITH A NOVEL STABLE LIGAND STUDIED IN MOUSE LYMPHOMA CELL LINES DIFFERING IN DNA REPAIR SYSTEMS M. Kruszewski, E. Boużyk, T. Oidak, K. Samochocka, L. Fuks, W. Lewandowski, W. Priebe	101
DNA DAMAGE INFLICTED IN MOUSE LYMPHOMA CELL LINES BY CIS-PLATINUM AND PALLADIUM(II) CHLORIDES COMPLEXED WITH A NOVEL STABLE LIGAND (wp1-1) M. Kruszewski, E. Boużyk, K. Samochocka, L. Fuks, W. Lewandowski, W. Priebe	102
DIFFERENTIAL ANTI-PROLIFERATIVE PROPERTIES OF NOVEL HYDROXYDICARBOXYLATOPLATINUM(II) COMPLEXES WITH HIGH OR LOW REACTIVITY WITH THIOLS I. Buraczewska, E. Boużyk, J. Kuduk-Jaworska, K. Waszkiewicz, I. Szumiel	103

G2 PHASE ARREST CAUSED BY HYDROXYDICARBOXYLATOPLATINUM(II) COMPLEXES WITH LOW REACTIVITY WITH THIOLS I. Buraczewska, J. Kuduk-Jaworska, K. Waszkiewicz, A. Gasińska, I. Szumiel	104
CYTOPLASMIC ACTIVITY OF TYROSINE PROTEIN KINASE, c-Abl, IN L5178Y MURINE LYMPHOMA CELL SUBLINES - A LINK TO DIFFERENTIAL APOPTOSIS PRONENESS? B. Sochanowicz, I. Szumiel	104
VALIDATION OF THE MICRONUCLEUS-CENTROMERE ASSAY FOR BIOLOGICAL DOSIMETRY A. Wójcik, M. Kowalska, E. Boużyk, I. Buraczewska, G. Kobiątko	105
INCREASE IN LABILE IRON POOL IN MOUSE LYMPHOMA CELL LINES TREATED WITH HYDROGEN PEROXIDE M. Kruszewski, T. Bartłomiejczyk, P. Lipiński	106
<b>NUCLEAR TECHNOLOGIES AND METHODS</b>	<b>109</b>
<b>PROCESS ENGINEERING</b>	<b>111</b>
INDUSTRIAL DEMONSTRATION PLANT FOR ELECTRON BEAM FLUE GASES TREATMENT A.G. Chmielewski, E. Iller, B. Tymiński, Z. Zimek, J. Licki	111
ELECTRON BEAM TREATMENT OF POLYAROMATIC HYDROCARBONS, EMITTED FROM COAL COMBUSTION A.G. Chmielewski, A. Ostapczuk, J. Licki	112
REDUCTION OF ENERGY CONSUMPTION FOR NO <sub>x</sub> REMOVAL IN ELECTRON BEAM FLUE GAS TREATMENT BY USING AN ALCOHOL AS SCAVENGER A.G. Chmielewski, Y. Sun, Z. Zimek, S. Bułka, J. Licki	113
AEROSOL FORMATION AND ITS PRECIPITATION IN ELECTRON BEAM FLUE GAS TREATMENT E. Iller, A.G. Chmielewski, B. Tymiński, G. Zakrzewska-Trznadel, J. Licki, Cz. Ryguta, J. Bartosiak	114
ELECTRON BEAM STIMULATION OF THE REACTIVITY OF CELLULOSE PULPS E. Iller, A. Kukielka, A.G. Chmielewski, J. Michalik, Z. Zimek, H. Stupińska, W. Mikołajczyk, H. Struszczyk	114
MEMBRANE PROCESSES FOR RADIOACTIVE LIQUID WASTE TREATMENT A.G. Chmielewski, M. Harasimowicz, G. Zakrzewska-Trznadel, B. Tymiński, W. Tomczak, A. Cholerzyński	115
APPLICATION OF CERAMIC MEMBRANES FOR RADIOACTIVE WASTE PURIFICATION G. Zakrzewska-Trznadel, M. Harasimowicz, B. Tymiński, A.G. Chmielewski	117
HYDROCHEMICAL AND ISOTOPE BACKGROUND FOR GROUNDWATER IN THE REGION OF SZCZERCÓW LIGNITE DEPOSIT W. Sołtyk, J. Walendziak, A. Owczarczyk	117
DETERMINATION OF SULFUR ISOTOPE RATIOS IN COAL FROM POLISH COALFIELDS A.G. Chmielewski, R. Wierchnicki, M. Derda	118
SULFUR ISOTOPE EFFECTS IN CHEMICAL REACTIONS A.G. Chmielewski, R. Wierchnicki, A. Mikołajczuk	119
<b>MATERIAL ENGINEERING, STRUCTURAL STUDIES, DIAGNOSTICS</b>	<b>121</b>
PROVENANCE STUDIES OF ALABASTER AND MARBLE SCULPTURES FROM POLAND BY INAA E. Pańczyk, M. Ligęza, L. Waliś	121
INVESTIGATIONS OF TRACK ETCHED MEMBRANE SURFACES USING SEM WITH DIFFERENT WORKING CONDITIONS B. Sartowska, O. Orelovitch	123
NEW WOOD PRESERVATIVES BASED ON COOPER COMPLEXES OF ETHANOLAMINE AND POLYAMINOTRIAZOLE A. Łukasiewicz, L. Rowińska, L. Waliś	124
SILICA GEL MODIFIED WITH MANGANESE II AS A SELECTIVE SORBENT FOR GOLD AND SILVER A. Łukasiewicz, L. Rowińska, L. Waliś	125
STRUCTURE AND COMPOSITION OF Pd-Ti SURFACE ALLOY FORMED BY PULSED PLASMA BEAMS Z. Werner, J. Piekoszewski, A. Barcz, R. Grötzschel, F. Prokert, J. Stanisławski, W. Szymczyk	126
INTERFACE IN Ti-Al <sub>2</sub> O <sub>3</sub> SYSTEM MANUFACTURED WITH THE USE OF HIGH INTENSITY PULSED PLASMA BEAMS J. Piekoszewski, J. Stanisławski, R. Grötzschel, W. Matz, J. Jagielski	127



DOPING OF TITANIUM WITH SILICON USING INTENSE PULSED PLASMA BEAMS E. Richter, J. Piekoszewski, F. Prokert, J. Stanisławski, L. Waliś	128
<b>NUCLEONIC CONTROL SYSTEMS AND ACCELERATORS</b>	<b>130</b>
XRF ANALYSIS OF LIGNITE ASH USING PARTIAL LEAST SQUARE CALIBRATION MODEL E. Kowalska, P. Urbański	130
FEASIBILITY OF PLS CALIBRATION MODELS FOR INSTRUMENTS MEASURING ASH IN COAL USING GAMMA RAY SCATTERING METHODS E. Kowalska, P. Urbański	131
PORTABLE RADON-IN-AIR CONCENTRATION MONITOR RMR-1 J. Bartak, J.P. Pieńkos	132
USE OF MULTIVARIATE PROCESSING IN GAUGES FOR RADON AND RADON DAUGHTERS CONCENTRATION IN AIR B. Machaj, P. Urbański	133
GAUGE FOR MEASUREMENT OF DOSERATE AND ACTIVITY OF Ru-106 BETA SOURCE FOR IRRADIATION OF EYE CANCER B. Machaj, E. Świstowski, C. Do-Hoang	135
PERFORMANCES OF LAE 10 ACCELERATOR WITH A THREE ELECTRODE ELECTRON GUN WITH MESH GRID Z. Dźwigalski, Z. Zimek	137
<b>THE INCT PUBLICATIONS IN 2000</b>	<b>139</b>
<b>THE INCT REPORTS IN 2000</b>	<b>158</b>
<b>NUKLEONIKA</b>	<b>159</b>
<b>THE INCT PATENTS AND PATENT APPLICATIONS IN 2000</b>	<b>162</b>
PATENTS	162
PATENT APPLICATIONS	162
<b>CONFERENCES ORGANIZED AND CO-ORGANIZED BY THE INCT IN 2000</b>	<b>163</b>
<b>Ph.D./D.Sc. THESES</b>	<b>170</b>
Ph.D. THESES	170
D.Sc. THESES	170
<b>EDUCATION</b>	<b>171</b>
Ph.D. PROGRAMME IN CHEMISTRY	171
TRAINING OF STUDENTS	171
<b>RESEARCH PROJECTS AND CONTRACTS</b>	<b>173</b>
RESEARCH PROJECTS GRANTED BY THE POLISH STATE COMMITTEE FOR SCIENTIFIC RESEARCH IN 2000 AND IN CONTINUATION	173
IMPLEMENTATION PROJECTS GRANTED BY THE POLISH STATE COMMITTEE FOR SCIENTIFIC RESEARCH IN 2000 AND IN CONTINUATION	173
IAEA RESEARCH CONTRACTS IN 2000	174
IAEA TECHNICAL CONTRACTS IN 2000	174
EUROPEAN COMMISSION RESEARCH PROJECTS IN 2000	174
OTHER FOREIGN CONTRACTS IN 2000	174
<b>LIST OF VISITORS TO THE INCT IN 2000</b>	<b>175</b>

<b>THE INCT SEMINARS IN 2000</b>	<b>178</b>
<b>SEMINARS DELIVERED OUT OF THE INCT IN 2000</b>	<b>179</b>
<b>AWARDS IN 2000</b>	<b>182</b>
<b>INSTRUMENTAL LABORATORIES AND TECHNOLOGICAL PILOT PLANTS</b>	<b>183</b>
<b>INDEX OF THE AUTHORS</b>	<b>194</b>

## GENERAL INFORMATION

The Institute of Nuclear Chemistry and Technology (INCT) is one of the successors of the Institute of Nuclear Research (INR) which was established in 1955. The latter Institute, once the biggest Institute in Poland, has exerted a great influence on the scientific and intellectual life in this country.

The INCT came into being as one of the independent units established after the dissolution of the INR in 1983.

The fundamental research on radiobiology, radio- and coordination chemistry and radiation chemistry is continued.

The Institute offers academic and research programmes for Ph.D. and D.Sc. thesis in chemistry.

Institute is one of the most advanced science and technology centres working on development of technologies and methods in the field of:

- radiation chemistry and technology,
- application of nuclear methods in material and process engineering,
- design and manufacturing of instruments based on nuclear techniques,
- trace analysis and radioanalytical techniques,
- environmental research.

At this moment, with its nine electron accelerators in operation and with the staff experienced in the field of electron beam applications, the Institute is one of the most advanced centres of science and technology in this domain. The following activity should here be mentioned:

- pilot plant for radiation sterilization of medical devices and transplantations,
- pilot plant for radiation modification of polymers,
- experimental pilot plant for food irradiation,
- pilot plant for removal of SO<sub>2</sub> and NO<sub>x</sub> from flue gases.

Based on the technology elaborated in this Institute, an industrial plant for electron beam flue gas treatment has been completed at the EPS "Pomorzany" (Dolna Odra PS Group). With its 1200 MW electron accelerators, the plant is the biggest radiation processing facility ever built in the world. On the turn of the XX century, a new challenge emerges before radiation chemistry, researchers and engineers in the field of nuclear process engineering.

This event together with the above mentioned plants in operation places the Institute among the most developed world accelerator centers.

In 2000 the Institute organized:

- The First Coordination Consortium Meeting for Project "Electron Beam Processing of Flue Gases, Emitted in Metallurgical Processes, for Volatile Organic Compounds Removal",
- An International Mini-Symposium on "Radiation-Induced Radical Processes in Systems of Biological Relevance"

and co-organized

- A Bilateral Workshop on "Radiation-Induced Paramagnetic Defects in Solids", Ghent, Belgium;
- A Seminar on "Polish Science and Technology for Nuclear Energy of To-morrow", Maðralin, Poland.

The Institute also sponsored the 30th Annual Meeting of the European Society for Radiation Biology "European Radiation Research 2000".

Common research projects were performed in the frame of grants from the European Union:

- Accreditation for high dose measurement (INCO Copernicus);
- Electron beam for processing of flue gases, emitted in metallurgical processes for volatile organic compounds removal.

At the 3rd International Exhibition of Invention "Innowacje'2000" (Gdańsk, Poland) the Institute has been awarded with the Cup of President of the Polish State Committee for Scientific Research for the separation of water isotopomers by a porous hydrophobic membrane and the bronze medal for the method of making hollow spherical ceramic and metallic materials, reduced by hydrogen. The congratulations were sent to the Institute by the Prime Minister.

Two scientific workers of the Institute received D.Sc. degree, two other Institute's researchers were granted with Ph.D. degree.

Two students from Ecole des Mines de Nantes (France) and thirteen fellowship holders from the IAEA were trained at the Institute.

The Institute is the editor of NUKLEONIKA - a world wide recognized journal for nuclear research.

## MANAGEMENT OF THE INSTITUTE

### MANAGING STAFF OF THE INSTITUTE

Director

Assoc.Prof. **Lech Waliś**, Ph.D.

Deputy Director for Research and Development

Prof. **Andrzej G. Chmielewski**, Ph.D., D.Sc.

Deputy Director for Administration

**Edmund Freliszka**, M.Sc.

Accountant General

**Barbara Kaźmirska**

### HEADS OF THE INCT DEPARTMENTS

- Department of Nuclear Methods of Material Engineering  
Assoc.Prof. **Lech Waliś**, Ph.D.
- Department of Structural Research  
**Wojciech Starosta**, M.Sc.
- Department of Radioisotope Instruments and Methods  
Prof. **Piotr Urbański**, Ph.D., D.Sc.
- Department of Radiochemistry  
Prof. **Jerzy Narbutt**, Ph.D., D.Sc.
- Department of Nuclear Methods of Process Engineering  
Prof. **Andrzej G. Chmielewski**, Ph.D., D.Sc.
- Department of Radiation Chemistry and Technology  
**Zbigniew Zimek**, Ph.D.
- Department of Analytical Chemistry  
Prof. **Rajmund Dybczyński**, Ph.D., D.Sc.
- Department of Radiobiology and Health Protection  
Prof. **Irena Szumiel**, Ph.D., D.Sc.
- Experimental Plant for Food Irradiation  
**Wojciech Migdał**, Ph.D., D.Sc.
- Laboratory for Detection of Irradiated Foods  
**Wacław Stachowicz**, Ph.D.
- Laboratory for Measurements of Technological Doses  
**Zofia Stuglik**, Ph.D.

### SCIENTIFIC COUNCIL (1999-2003)

1. Assoc.Prof. **Aleksander Bilewicz**, Ph.D., D.Sc.  
Institute of Nuclear Chemistry and Technology  
•radiochemistry, inorganic chemistry
2. Prof. **Krzysztof Bobrowski**, Ph.D., D.Sc.  
Institute of Nuclear Chemistry and Technology  
•radiation chemistry, photochemistry, biophysics
3. Prof. **Andrzej G. Chmielewski**, Ph.D., D.Sc.  
Institute of Nuclear Chemistry and Technology  
•chemical and process engineering, nuclear chemical engineering, isotope chemistry
4. Prof. **Jadwiga Chwastowska**, Ph.D., D.Sc.  
Institute of Nuclear Chemistry and Technology  
•analytical chemistry

5. **Jakub Dudek**, M.Sc.  
Institute of Nuclear Chemistry and Technology  
• analytical chemistry
6. Prof. **Rajmund Dybczyński**, Ph.D., D.Sc.  
Institute of Nuclear Chemistry and Technology  
• analytical chemistry
7. Prof. **Zbigniew Florjańczyk**, Ph.D., D.Sc.  
Warsaw University of Technology  
• chemical technology
8. **Zyta Głębowicz**  
Institute of Nuclear Chemistry and Technology  
• staff representative
9. Assoc.Prof. **Edward Iller**, Ph.D., D.Sc.  
Institute of Nuclear Chemistry and Technology  
• chemical and process engineering, physical chemistry
10. Prof. **Janusz Jurczak**, Ph.D., D.Sc.  
Polish Academy of Sciences, Institute of Organic Chemistry; Warsaw University  
• organic chemistry, stereochemistry
11. **Iwona Kałuska**, M.Sc.  
Institute of Nuclear Chemistry and Technology  
• radiation chemistry
12. **Barbara Kaźmirska**  
Institute of Nuclear Chemistry and Technology  
• staff representative
13. **Marcin Kruszewski**, Ph.D.  
Institute of Nuclear Chemistry and Technology  
• radiobiology
14. **Gabriel Kuc**, M.Sc.  
Institute of Nuclear Chemistry and Technology  
• radiation chemistry
15. Prof. **Janusz Lipkowski**, Ph.D., D.Sc.  
Polish Academy of Sciences, Institute of Physical Chemistry  
• physico-chemical methods of analysis
16. Prof. **Andrzej Łukasiewicz**, Ph.D., D.Sc.  
Institute of Nuclear Chemistry and Technology  
• material science
17. **Kazimiera Malec-Czechowska**, M.Sc.  
Institute of Nuclear Chemistry and Technology  
• radiation chemistry
18. Prof. **Bronisław Marciniak**, Ph.D., D.Sc.  
Adam Mickiewicz University in Poznań  
• physical chemistry
19. Prof. **Józef Mayer**, Ph.D., D.Sc.  
Łódź Technical University  
• physical and radiation chemistry
20. Prof. **Jacek Michalik**, Ph.D., D.Sc.  
(Co-chairman)  
Institute of Nuclear Chemistry and Technology  
• radiation chemistry, surface chemistry, radical chemistry
21. Prof. **Jerzy Narbutt**, Ph.D., D.Sc.  
Institute of Nuclear Chemistry and Technology  
• radiochemistry
22. **Ewa Pańczyk**, M.Sc.  
Institute of Nuclear Chemistry and Technology  
• nuclear physics
23. **Jan Paweł Pieńkos**, Eng.  
Institute of Nuclear Chemistry and Technology  
• electronics
24. Prof. **Leon Pszonicki**, Ph.D., D.Sc.  
(Chairman)  
Institute of Nuclear Chemistry and Technology  
• analytical chemistry
25. **Zbigniew Samczyński**, Ph.D.  
Institute of Nuclear Chemistry and Technology  
• analytical chemistry
26. Prof. **Sławomir Siekierski**, Ph.D.  
Institute of Nuclear Chemistry and Technology  
• physical chemistry, inorganic chemistry
27. Prof. **Irena Szumiel**, Ph.D., D.Sc.  
(Co-chairman)  
Institute of Nuclear Chemistry and Technology  
• cellular radiobiology
28. Prof. **Jan Tacikowski**, Ph.D.  
(Co-chairman)  
Institute of Precision Mechanics  
• physical metallurgy and heat treatment of metals
29. Prof. **Marek Trojanowicz**, Ph.D., D.Sc.  
Institute of Nuclear Chemistry and Technology  
• analytical chemistry
30. Prof. **Piotr Urbański**, Ph.D., D.Sc.  
Institute of Nuclear Chemistry and Technology  
• radiometric methods, industrial measurement equipment, metrology
31. Assoc.Prof. **Lech Waliś**, Ph.D.  
Institute of Nuclear Chemistry and Technology  
• material science, material engineering
32. **Paweł Wiśniowski**, M.Sc.  
Institute of Nuclear Chemistry and Technology  
• radiation chemistry, photochemistry, biophysics
33. Prof. **Stanisław Wroński**, Ph.D., D.Sc.  
Warsaw University of Technology  
• chemical engineering

34. Prof. **Zbigniew Zagórski**, Ph.D., D.Sc.

Institute of Nuclear Chemistry and Technology

- physical chemistry, radiation chemistry, electrochemistry

36. **Zbigniew Zimek**, Ph.D.

Institute of Nuclear Chemistry and Technology

- electronics, accelerator techniques, radiation processing

35. **Wiesław Zieliński**, M.Sc.

Institute of Nuclear Chemistry and Technology

- staff representative

#### HONORARY MEMBERS OF THE INCT SCIENTIFIC COUNCIL (1999-2003)

1. Prof. **Maria Kopeć**, Ph.D., D.Sc.

Institute of Haematology and Blood Transfusion

- haematology, radiobiology

2. Prof. **Antoni Danciewicz**, Ph.D., D.Sc.

Institute of Nuclear Chemistry and Technology

- biochemistry, radiobiology

## SCIENTIFIC STAFF

### PROFESSORS

- |   |   |
|---|---|
| 1. <b>Ambroż Hanna B.</b><br>physical and radiation chemistry, biological chemistry, photochemistry                   | 11. <b>Piekoszewski Jerzy</b><br>solid state physics  |
| 2. <b>Bobrowski Krzysztof</b><br>radiation chemistry, photochemistry, biophysics                                      | 12. <b>Pszonicki Leon</b><br>analytical chemistry   |
| 3. <b>Chmielewski Andrzej G.</b><br>chemical and process engineering, nuclear chemical engineering, isotope chemistry | 13. <b>Radoszewski Tomasz</b><br>radiometry   |
| 4. <b>Chwastowska Jadwiga</b><br>analytical chemistry   | 14. <b>Rzewuski Henryk</b><br>solid state physics   |
| 5. <b>Dancewicz Antoni</b><br>biochemistry, radiobiology  | 15. <b>Siekierski Sławomir</b><br>physical chemistry, inorganic chemistry                     |
| 6. <b>Dybczyński Rajmund</b><br>analytical chemistry  | 16. <b>Szot Zbigniew</b><br>radiobiology  |
| 7. <b>Leciejewicz Janusz</b><br>crystallography, solid state physics, material science                                | 17. <b>Szumiel Irena</b><br>cellular radiobiology   |
| 8. <b>Łukasiewicz Andrzej</b><br>material science   | 18. <b>Trojanowicz Marek</b><br>analytical chemistry  |
| 9. <b>Michalik Jacek</b><br>radiation chemistry, surface chemistry, radical chemistry                                 | 19. <b>Urbański Piotr</b><br>radiometric methods, industrial measurement equipment, metrology |
| 10. <b>Narbutt Jerzy</b><br>radiochemistry  | 20. <b>Zagórski Zbigniew</b><br>physical chemistry, radiation chemistry, electrochemistry     |

### ASSOCIATE PROFESSORS

- |   |  |
|---|--|
| 1. <b>Bilewicz Aleksander</b><br>radiochemistry, inorganic chemistry                              | 6. <b>Parus Józef</b><br>analytical chemistry                  |
| 2. <b>Grigoriew Helena</b><br>solid state physics, diffraction research of non-crystalline matter | 7. <b>Waliś Lech</b><br>material science, material engineering |
| 3. <b>Iller Edward</b><br>chemical and process engineering, physical chemistry                    | 8. <b>Wójcik Andrzej</b><br>cytogenetics                       |
| 4. <b>Legocka Izabella</b><br>polymer technology  | 9. <b>Żółtowski Tadeusz</b><br>nuclear physics                 |
| 5. <b>Tomasz Mioduski</b><br>lanthanide and actinide chemistry                                    |  |

### SENIOR SCIENTISTS (Ph.D., D.Sc.)

1. **Migdał Wojciech**  
chemistry



## SENIOR SCIENTISTS (Ph.D.)

1. **Bartłomiejczyk Teresa**  
biology
2. **Borkowski Marian**  
chemistry
3. **Boużyk Elżbieta**  
biology
4. **Bryl-Sandelewska Teresa**  
radiation chemistry
5. **Buczkowski Marek**  
physics
6. **Cieśla Krystyna**  
chemistry
7. **Danko Bożena**  
analytical chemistry
8. **Dembiński Wojciech**  
chemistry
9. **Deptuła Andrzej**  
chemistry
10. **Dobrowolski Andrzej**  
chemistry
11. **Do-Hoang Cuong**  
nuclear physics
12. **Dźwigalski Zygmunt**  
high voltage electronics, electron injectors, gas lasers
13. **Fuks Leon**  
chemistry
14. **Gniazdowska Ewa**  
chemistry
15. **Grądzka Iwona**  
biology
16. **Grodkowski Jan**  
radiation chemistry
17. **Harasimowicz Marian**  
technical nuclear physics, theory of elementary particles
18. **Jaworska Alicja**  
biology
19. **Kierzek Joachim**  
physics
20. **Kleczkowska Hanna**  
biology
21. **Krejzler Jadwiga**  
chemistry
22. **Kruszewski Marcin**  
radiobiology
23. **Krynicky Janusz**  
solid state physics
24. **Kunicki-Goldfinger Jerzy**  
conservator/restorer of art
25. **Machaj Bronisław**  
electricity
26. **Mirkowski Jacek**  
nuclear and medical electronics
27. **Nowicki Andrzej**  
organic chemistry and technology, high-temperature technology
28. **Owczarczyk Andrzej**  
chemistry
29. **Owczarczyk Hanna B.**  
biology
30. **Palige Jacek**  
metallurgy
31. **Panta Przemysław**  
nuclear chemistry
32. **Pawlukojć Andrzej**  
physics
33. **Pogoński Dariusz**  
radiation chemistry, pulse radiolysis
34. **Polkowska-Motrenko Halina**  
analytical chemistry
35. **Przybytniak Grażyna**  
radiation chemistry
36. **Ptasiewicz-Bąk Halina**  
physics
37. **Rafalski Andrzej**  
radiation chemistry
38. **Sadło Jarosław**  
chemistry
39. **Skwara Witold**  
analytical chemistry
40. **Samczyński Zbigniew**  
analytical chemistry
41. **Sochanowicz Barbara**  
biology
42. **Stachowicz Wacław**  
radiation chemistry, EPR spectroscopy
43. **Strzelczak Grażyna**  
radiation chemistry
44. **Stuglik Zofia**  
radiation chemistry
45. **Szpilowski Stanisław**  
chemistry
46. **Tymiński Bogdan**  
chemistry

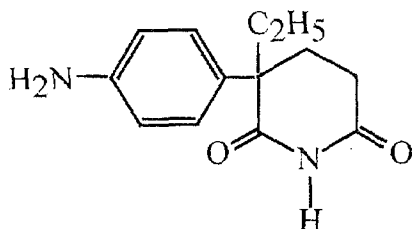
- 
- |   |  |
|---|--|
| 47. <b>Walicka Małgorzata</b><br>biology  | 51. <b>Wojewódzka Maria</b><br>radiobiology  |
| 48. <b>Warchoń Stanisław</b><br>solid state physics                                     | 52. <b>Wrońska Teresa</b><br>chemistry   |
| 49. <b>Wąsowicz Tomasz</b><br>radiation chemistry, surface chemistry, radical chemistry | 53. <b>Zakrzewska-Trznadel Grażyna</b><br>process and chemical engineering             |
| 50. <b>Wierzchnicki Ryszard</b><br>chemical engineering                                 | 54. <b>Zimek Zbigniew</b><br>electronics, accelerator techniques, radiation processing |

**RADIATION CHEMISTRY**  
**AND PHYSICS**  
**RADIATION TECHNOLOGIES**

## RADIATION-INDUCED CHANGES IN AMINOGLUTETHIMIDE

Hanna AmbroŹ, Ewa Kornacka, Grażyna Przybytniak

In this paper we present EPR investigations of paramagnetic species in aminoglutethimide (AA), which has a wide application in anticancer therapy and is administered to patients to block adrenal androgen secretion, e.g. in male breast cancer [1,2]. AA (3-ethyl-3-(p-aminophenyl)-2,6-dioxopiperidine, see Scheme) was obtained from the Institute of Pharmacy, Warszawa, Poland. The samples were irradiated to a dose of 25 kGy under aerated conditions.



AA

Scheme.

EPR spectra were measured with a Bruker X-band ESR-300 spectrometer at room temperature or at 77 K using a microwave power of 2 mW. After irradiation AA was stored at ambient temperature. Double integration of the experimental spectra and the signals recorded for standard DPPH-benzene solu-

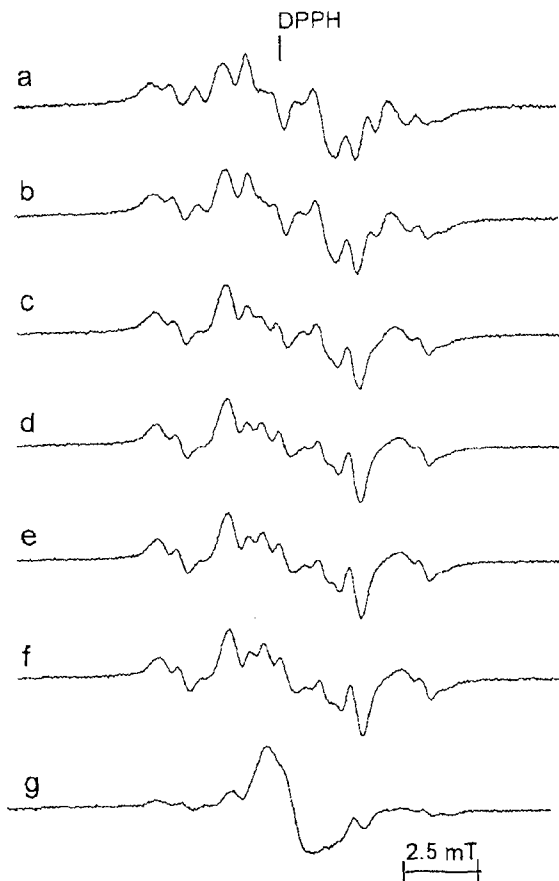


Fig.1. Spectra of AA radicals and radical pairs: (a) on irradiation, (b) after 1 h, (c) after 3 h, (d) after 1 day, (e) after 3 days, (f) after 6 days, and (g) after 5 months.

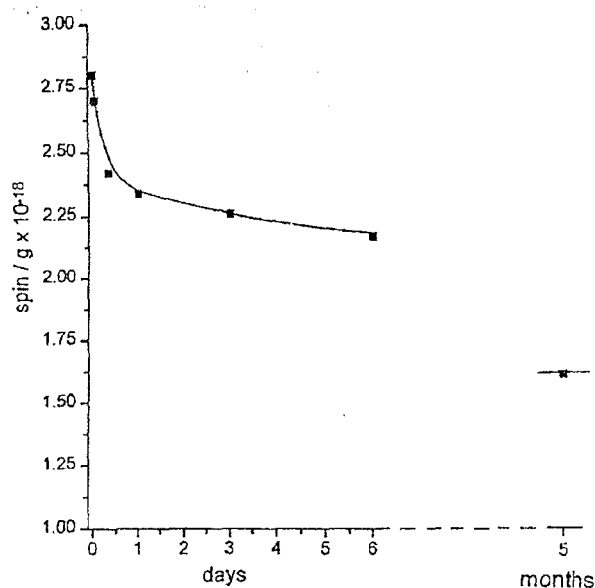


Fig.2. Decay of paramagnetic intermediates of AA vs. time.

tion enabled us to estimate the concentrations of spins in the irradiated materials. EPR signals were measured after irradiation and subsequently after days and months of storage. The results of studies carried out at room temperature are depicted in Figs.1 and 2. Two radical pairs were detected with the following ZFS parameters: (1st radical pair):  $d_{\perp} = 4.8$

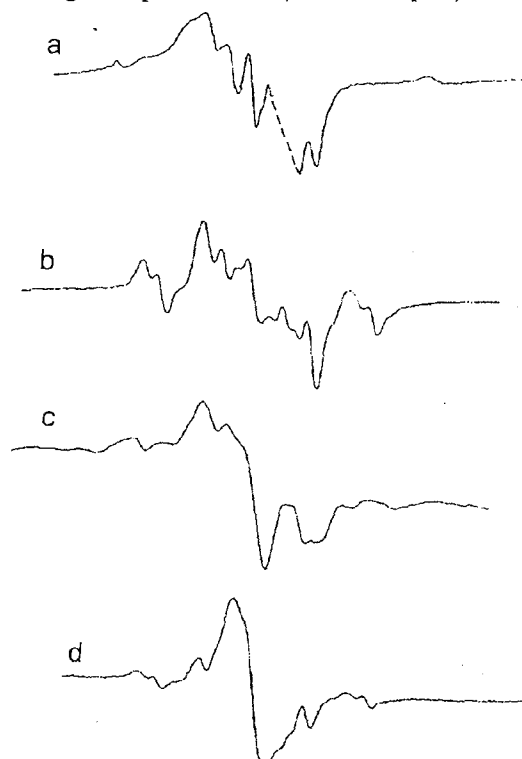


Fig.3. EPR spectra of AA: (a) irradiated, kept and recorded at 77 K, the dashed line indicates the zone distorted by a signal of quartz tube; (b) irradiated and measured at room temperature soon after irradiation; (c) irradiated at room temperature, measured at 77 K soon after irradiation; (d) irradiated and recorded at room temperature after 4 weeks room temperature storage.

mT and  $d_{\parallel}=9.8$  mT,  $r_{\perp}=0.83$  nm and  $r_{\parallel}=0.83$  nm, and (2nd radical pair):  $d_{\perp}=3.2$  mT and  $d_{\parallel}=8.5$  mT,  $r_{\perp}=0.95$  nm and  $r_{\parallel}=0.87$  nm. The unpaired spin concentration just after radiolysis is ca.  $2.8 \times 10^{18}$  per gram. The spectrum recorded after 5 months of storage still exhibits weak features of radical pairs and, furthermore, anisotropic, slightly resolved central absorption of g factor = 2.0050.

The primary radicals of the samples irradiated and examined at 77 K (Fig.3a) exhibit a broad anisotropic signal and a highly resolved spectrum which belongs to radicals of clearly different line widths (central part of the spectrum is not depicted as it was distorted by the intense signal of the quartz EPR tube). No fine interaction can be observed on (a) the contrary to spectrum (b) of the sample irradiated and examined at room temperature. Comparison of spectra (a) and (b) suggests that the primary radicals combine or rearrange at higher temperature (higher mobility of the species) leaving more stable secondary radicals in pairs. Spectrum (c) recorded at 77 K, following irradiation at room temperature, seems to indicate that the higher mobility of the paramagnetic species in spectrum (b) forces the unpaired spins to localisations, which lead to non-zero energy splitting at zero magnetic field. The stable set of free radicals (spectrum (d)), recorded at room temperature after

4 weeks of storage) reveals that the radical pairs are still visible but remain as a little admixture to the now dominating transients exhibiting doublet and singlet lines, which are evident in spectrum (b). The character and stability of radicals and their pairs following ionising radiation vary, depending on their structure and the propensities of the solid matrix towards radical trapping and stabilisation. The population of paramagnetic species and their stability in time are very important for an estimation of possible chemical changes in the pharmaceutical products and for the determination of recommended time before irradiated drugs are administered to the patient. Although it is impossible to predict radiation-induced physico-chemical changes, the sensitivity towards irradiation measured by EPR spectroscopy gives fast and reliable results [3]. As paramagnetic species may remain in a crystalline matrix even for a few years it seems appropriate to determine a drug's post-treatment quarantine before products are delivered to patients.

#### References

- [1]. Ahmed S.: *Theochem.-J. Mol. Structure*, **422**, 271-284 (1998).
- [2]. Stierer M.: *Onkologie*, **21**, 160-166 (1998).
- [3]. Gopal N.G.S., Patel K.M., Sharma G., Bhalla H.L., Wills P.A., Hilmy N.: *Radiat. Phys. Chem.*, **32**, 619-622 (1988).



PL0101464

## IDENTIFICATION OF RADICALS IN ELECTRON BEAM IRRADIATED IFOSFAMIDE

Hanna Ambroż, Ewa Kornacka, Grażyna Przybytniak

Ionising radiation can be applied as a convenient method of drug decontamination, particularly recommended for unstable substances, e.g. thermolabile or unsuitable for chemical sterilisation. As ionising radiation generates paramagnetic products, especially stable in solid state materials, it is important to control radical concentrations and their stability. This study was undertaken to determine the kinetics of the decays and structures of generated radical intermediates in 3-(2-chloroethyl)-2-[2-chloroethyl] amino]tetrahydro-2H-1,2,3-oxazaphosphine-2-oxide (ifosfamide, IA). In addition, we consider, possible mechanisms of formation of the radicals and their fate during storage, all on the basis of developments and transformations of their EPR spectra.

IA play an increasing role in combination of chemotherapy with other antitumour agents. This heterocyclic compound consists of a six-membered ring including three saturated carbon, oxygen, nitrogen and phosphorus atoms, substituted with two chloroalkyl groups, thus presenting a system making the stabilisation of paramagnetic centres of the various possible sites. We separated two signals from the composite EPR spectrum recorded after irradiation (Fig.1). One of them (radical A, Scheme) belongs to the radical formed upon the loss of chlorine atom due to breakage of weak C-Cl bonds. We cannot unambiguously confirm which chlorine

atom is detached as the difference in their EPR signals is probably insignificant. Both resulting intermediates might exhibit hfs originating from  $\alpha$

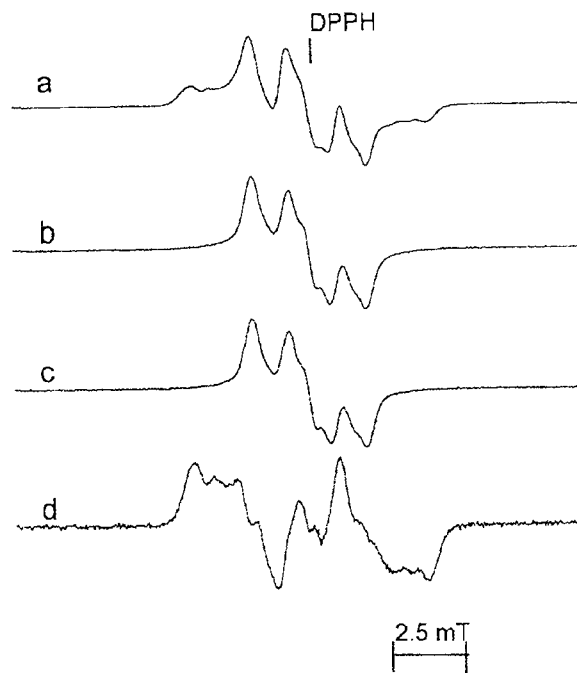
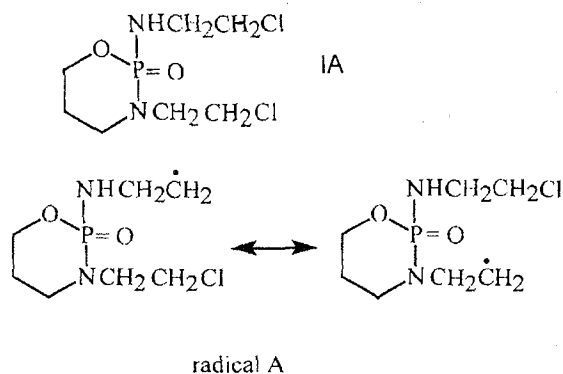


Fig.1. EPR spectra of IA radicals; (a) experimental spectrum upon irradiation, (b) experimental spectrum after 1 day, (c) spectrum of radical A and (d) spectrum of radical B, see text.



Scheme.

and  $\beta$  protons, respectively  $a(2H)=1.8$  mT and  $a(2H)=0.55$  mT. The Cl substituent remaining in the IA molecule probably stabilises the paramagnetic centre in the crystalline matrix. The spectrum of the other component (radical B) reveals a broad anisotropic signal reflecting a strong hyperfine interaction,  $a(1P)=5.3$  mT, characteristic of a phosphorus atom, together with a narrow splitting of 0.7 mT due to unidentified protons. If the major, or even a significant spin-density, was localised on the 5-valent phosphorus atom, then one should expect very high hyperfine coupling constants [1,2] as  $A_{iso}$  for the  $^{31}P$  nuclei equals to 363.2 mT. Since radical B does not reveal such strong interactions and, moreover, the influence of other atoms is distinct, we believe that the paramagnetic centre is not situated at the phosphorus atom. The much lower stability of radical B (its characteristic spectrum decays after 1 day, Fig.2) indicates, that, for example, a fast hydrogen atom transfer can be taking place.

Only 30% of the initial radicals remains after 6 days, which might result from the low melting point of IA (47°C) and, therefore, from the lower rigidity of the microcrystalline matrix as compared to that exhibited by other drugs at the storage temperature. This property of FA influences the level of radicals produced with different sources of ionising radiation. The gradual character of irradiation using a  $\gamma$ -source, at a dose rate of only 5 kGy/h means the sample is only slightly warmed due to effective heat exchange between the irradiated object and its

environment. On the other hand, if irradiation is performed with an electron beam, then the temperature increases significantly [3] due to the adiabatic character of energy absorption, which results in

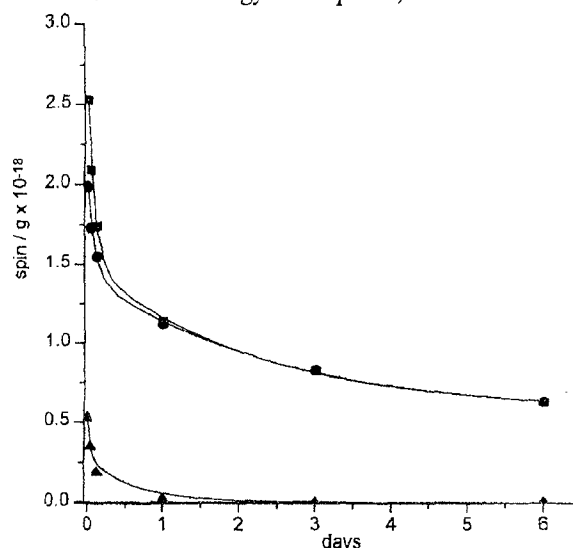


Fig.2. Concentrations of IA radicals: (■) all radicals, (●) radical A and (▲) radical B, vs. time.

a pronounced thermal effect and a subsequent reduction of spin population in radicals derived from IA. For a system of such a low melting point even variations in ambient temperature can modify considerably the radical concentration. These thermal effects are the reasons why, 5 months after electron beam irradiation, no radical species were detected, whereas in previous studies [4], using gamma-irradiation, the radicals seem to be highly populated and more stable.

## References

- [1]. Begum A., Lyons A.R., Symons M.C.R.: J. Chem. Soc. (A), 2388-2392 (1971).
- [2]. Begum A., Symons M.C.R.: J. Chem. Soc., Faraday Trans., 2, 69, 43-48 (1973).
- [3]. Zagórski, Z.P.: Thermal and electrostatic aspects of radiation processing of polymers. In: Radiation processing of polymers. Eds. A. Singh, J. Silverman. Hanser Publishers, Munich 1992, pp. 272-287.
- [4]. Ambroź H.B., Kornacka E.M., Marciniec B., Ogrodowczyk M., Przybytniak G.: Radiat. Phys. Chem., 58, 357-366 (2000).

## <sup>1</sup>OH RADICAL INDUCED OXIDATION OF $\alpha$ -METHYLALANINE TIME-RESOLVED AND SPIN-TRAPPING ESR STUDY

Paweł Wiśniowski, Gordon L. Hug<sup>1/</sup>, Richard W. Fessenden<sup>1/</sup>

<sup>1/</sup> Radiation Laboratory, University of Notre Dame, USA



PL0101465

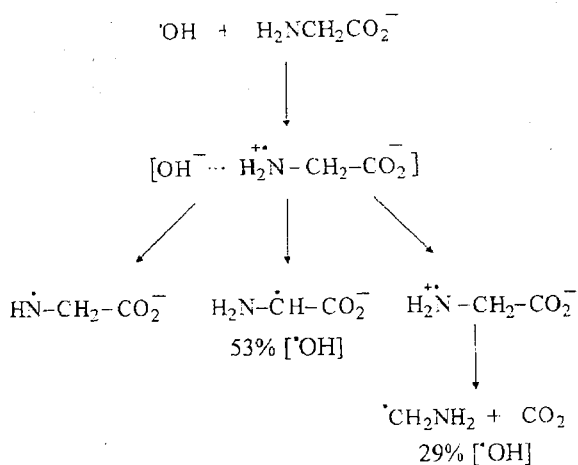
### Introduction

Precise chemical mechanisms of amino acid oxidation are of interest to understanding the fate of proteins under oxidative stress in biological systems. Recently, the oxidation mechanism of glycine anions was proposed that attempts to explain systematically all the processes from subnanosecond to steady-state time scales. Several radicals were postulated [1] as being involved in the beginning steps of glycine anions oxidation with two main primary radicals,

$H_2N^+-CH_2-CO_2^-$  and  $HN^+-CH_2-CO_2^-$  (Scheme). Initially, the aminyl radicals  $HN^+-CH_2-CO_2^-$  were only inferred from scavenging reactions with hydroquinones [1], but they were subsequently identified in steady-state radiolysis experiments with the aci-anion ( $CH_2=NO_2^-$ ) of nitromethane as a spin-trap [2].

### Aim

The aminyl radicals appeared to play a more significant role when glycine was substituted with methyl groups [3].  $\beta$ -Scission of the aminyl radicals



Scheme.

with the formation of  $\text{CO}_2^\bullet$  radicals, was thought to be a significant decay channel for these radicals, especially for  $\text{HN}^\bullet-\text{C}(\text{CH}_3)_2-\text{CO}_2^-$  from  $\alpha$ -methylalanine (2-aminoisobutyric acid). The purpose of the current work was to look closely at TRESR (Time-Resolved ESR) and also spin-trapping experiments involving  $\alpha$ -methylalanine in order to see if this aminyl radical does exist and to see if  $\beta$ -scission of any resulting aminyl radical does occur. Even though,  $\alpha$ -methylalanine has been studied previously under steady-state in situ radiolysis with ESR detection [4], no radicals left over from a decarboxylation were observed, however, carbon dioxide has been determined in steady-state  $\gamma$ -radiolysis [5]. Thus, the radical corresponding to the decarboxylated fragment of  $\alpha$ -methylalanine should be present.

#### Experimental

Radiolysis was carried out with electrons from a Van de Graaff accelerator. The chemical samples were contained in a quartz cell of 0.4 mm thickness, and the cell was irradiated edge-on. The solution to be irradiated was passed through a heat-exchange unit before entering the ESR cell in order to cool the solution, so that the formation of  $\text{N}_2\text{O}$  bubbles could be avoided. The measurements were made at a temperature of about 288 K. A bubble trap was also used in most of the experiments.

#### Time-resolved ESR experiments

The TRESR was operated in both the kinetic-profile and the BOXCAR mode. Both of these modes are based on obtaining kinetic profiles with no frequency modulation [6]. The signal-averaged data are accumulated by summing pairs of matched kinetic traces. One trace in each pair is acquired at the nominal external magnetic field. The matching trace is acquired at an external magnetic field that is shifted to a spectral position where no transition is located (ideally, at least in the kinetic-profile mode). This shifted field is produced by a current through external coils on the cavity. These on- and off-resonance traces are subtracted, and the procedure is repeated with each intermediate result being folded into the average. In the BOXCAR-scanning mode of operation of the ESR spectrometer, the external field is slowly scanned, at the

same time that the kinetic traces are being accumulated. The data consists of the amplitude difference between traces over a selected time interval. The external magnetic field is slowly scanned through a range to display a spectrum. Since the field steps are generally much smaller than in the kinetic-profile mode, the spectra have a first derivative form.

#### Spin-trapping ESR experiments

The spin-trapping experiments were done in the steady-irradiation mode. The external magnetic fields were scanned, but now there was a frequency-modulation signal employed as part of the detection unit. The spin-trap was the aci-anion of nitromethane,  $\text{CH}_2=\text{NO}_2^-$ . Radicals are trapped by radical addition to the carbon across the double bond, forming an N-centered radical on the nitrogen of the nitro group.

#### Results

##### Time-resolved ESR in $\alpha$ -methylalanine

The reducing radical  $\text{H}_2\text{N}^\bullet-\text{C}(\text{CH}_3)_2$  was found to be present immediately following the radiolytic pulse, consistent with the spin-relaxation dynamics of the radicals in the joint magnetic field of the

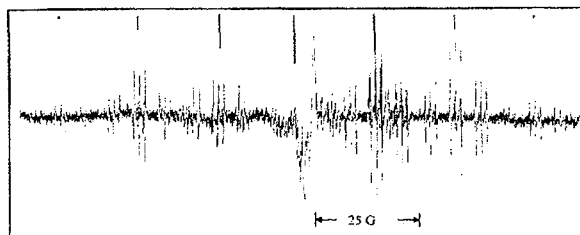


Fig.1. Time-resolved ESR spectrum (BOXCAR method) of the  $\text{H}_2\text{N}^\bullet-\text{C}(\text{CH}_3)_2$  radical.

external magnet and the microwave radiation. From TRESR ESR (Figs.1 and 2), the pattern can be seen to be made up of 7 groups of lines with a splitting between the centers of adjacent groups of 18.86 G. The pattern is indicative of 6 equivalent protons. Furthermore, the intensities of these groups are not inconsistent, if account is taken for the spin polarization, with the 1:6:15:20:15:6:1 expected for such a set of equivalent protons. Each of the 7 major groups of lines is further split into a 1:2:1 triplet by the two equivalent protons from the  $\text{NH}_2$  group. The splitting corresponds to a hyper-

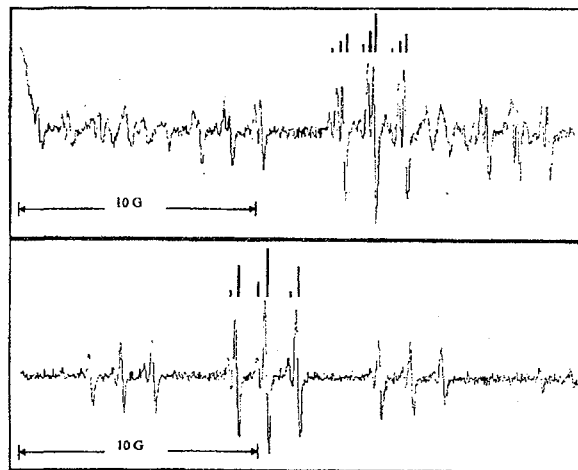


Fig.2. Second order splittings of the  $\text{H}_2\text{N}^\bullet-\text{C}(\text{CH}_3)_2$  radical.

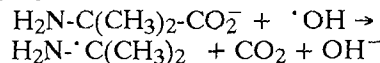
fine coupling of 6.06 G. Finally, each of these smaller groups of lines are split into an even triplet with a hyperfine coupling of 1.3 G for the contribution from the nitrogen nuclei. The g-factor associated with this spectrum is 2.0027. This spectrum is assigned to the decarboxylated radical,  $\text{H}_2\text{N}\cdot\text{C}(\text{CH}_3)_2$ . This radical has not been reported earlier, even in steady-state radiolysis.

The central major group of lines (corresponding to relative intensity 20 for 6 equivalent protons) is severely distorted by the electron signal from the irradiated quartz. However, the next two major line groupings (corresponding to relative intensities 15 and 6 for 6 equivalent protons) show typical second-order splittings. The lines making up the high field "intensity 15" group of lines should all be split into three lines of relative intensity 9:5:1. The lines, making up the high field "intensity 6" group, should, for the same reasons, each be split into two lines with a relative intensity 5:1. The existence of these second-order splitting patterns, associated with six equivalent protons, further supports the assignment of all these lines to the  $\text{H}_2\text{N}\cdot\text{C}(\text{CH}_3)_2$  radical. Relatively broad lines from another radical can be seen in the middle of the sharper lines from the  $\text{H}_2\text{N}\cdot\text{C}(\text{CH}_3)_2$  radical. There are indications that other lines of this radical are present at lower magnetic fields, and additional experiments are scheduled for more detailed scanning of these spectral regions. However, it is significant to note that these lines do not match the lines assigned to the  $\text{NH}_2\text{-C}(\text{CH}_3)(\cdot\text{CH}_2)\text{CO}_2^-$  radical seen in steady-state in situ radiolysis of  $\alpha$ -methylalanine [4]. These lines also do not correspond to the  $\cdot\text{N}=\text{C}(\text{CH}_3)_2$  seen in steady-state radiolysis [4] and later assigned [7]. Lines corresponding to neither of these radicals were seen in the time window of the scan. This is not all that surprising for the  $\cdot\text{N}=\text{C}(\text{CH}_3)_2$  radical since it is likely derived from secondary processes.

#### Spin-trapping in $\alpha$ -methylalanine

Aminyl radical  $\text{NH}\cdot\text{-C}(\text{CH}_3)_2\text{-CO}_2^-$ . As an alternative, the spin-trapping ESR method was used to trap the aminyl radical with the nitromethane aci-anion  $\text{CH}_2=\text{NO}_2^-$ , following in situ steady-state radiolysis. The spin-adduct of the  $\cdot\text{CO}_2^-$ ,  $^-\text{O}_2\text{C-CH}_2\cdot\text{NO}_2^-$  radical was detected. The  $\cdot\text{CO}_2^-$  radical was previously proposed to be formed by b-scissions of aminyl radicals.

#### Conclusions



A new carbon-centered radical  $\text{H}_2\text{N}\cdot\text{C}(\text{CH}_3)_2$  has been discovered in the radiolytic oxidation of  $\alpha$ -methylalanine. A little-used TRESR method of collecting data was employed that permitted the observation of a short-lived radical that had previously escaped detection when steady-state ESR was used. The existence of  $\cdot\text{CO}_2^-$  in the spin-trapping experiments is consistent with the aminyl radical being present and the  $\beta$ -scission process, taking place as predicted.

These experiments were performed during the scientific visit at the Radiation Laboratory, University of Notre Dame, USA, 1999-2000 sponsored by IAEA.

This part of work was presented at the 6th International Conference on Pulse Investigations in Chemistry, Biology and Physics PULS'2000, 9-15 September 2000, Łeba, Poland.

#### References

- [1]. Bonifacic M., Stefanic I., Hug G.L., Armstrong D.A., Asmus K.-D.: J. Am. Chem. Soc., **120**, 9930-9940 (1998).
- [2]. Hug G.L., Fessenden R.W.: J. Phys. Chem. B, submitted.
- [3]. Bonifacic M., Armstrong D.A., Carmichael I., Asmus K.-D.: J. Phys. Chem. B, **104**, 643-649 (2000).
- [4]. Neta P., Fessenden R.W.: J. Phys. Chem., **75**, 738-748 (1971).
- [5]. Asmus K.-D., Stefanic I., Bonifacic M., Armstrong D.A.: private communication.
- [6]. Fessenden R.W.: J. Chem. Phys., **58**, 2489-2500 (1973).
- [7]. Fessenden R.W.: Chem. Phys. Lett., **29**, 364-367 (1974).

## GENERATION OF AROMATIC THIOETHER RADICAL CATIONS CONTAINING PHENYL, VINYL, ALLYL, AND METHYL SUBSTITUENTS IN ORGANIC SOLVENTS

Anna Korzeniowska-Sobczuk, Paweł Wiśniowski, Krzysztof Bobrowski, Sergej Naumov<sup>1/</sup>,  
Lothar Richter<sup>2/</sup>, Ortwin Brede<sup>2/</sup>

<sup>1/</sup> Institute of Surface Modifications, Leipzig, Germany

<sup>2/</sup> University of Leipzig, Germany

Radical cations derived from organic sulfides, containing aromatic and unsaturated substituents, play an important role in a variety of chemical processes extending from those of industrial importance (organic synthesis) [1] to the enzymatic oxidations in biological systems [2,3]. A certain amount of information on the nature and kinetic parameters of intermediates formed from aryl-substituted sulfides is available [4-6], however, no similar studies have been performed for the sulfides with unsaturated substituents. Quantitative information on these sys-

tems would be of chemical and biochemical interest since the nature of the species is expected to be influenced by the degree of spin delocalization in the aromatic ring and the double bond. The last feature should affect the propensity of the radical cations to form dimers.

The basic spectral and kinetic behaviour of radical cations and radicals observed in pulse radiolysis of the corresponding organic sulfides with the aromatic and unsaturated substituents are provided in n-butyl chloride and cyclohexane solutions. In



PL0101466



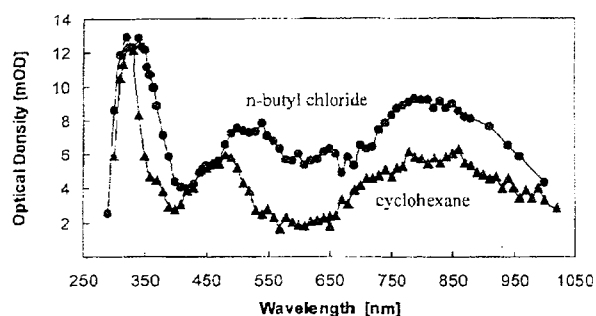


Fig. 1. Transient absorption spectra recorded after pulse irradiation of  $O_2$ -saturated (●) n-butyl chloride and (▲) cyclohexane solutions containing allyl-phenyl sulfide (5 mM) 250 ns after the pulse (50 Gy).

order to support spectral assignments, quantum mechanical calculations were performed that pro-

vided information about the spin density distribution in sulfur monomeric radical cations and the stabilization energy of sulfur dimeric radical cations and sulfur-chloride three electron bond complexes.

Quantum chemical calculations were performed using Density Functional Theory (DFT) Hybrid B3LYP with 6-31G(d) parameter set method (Gaussian 98W). Equilibrium geometries, energies of the systems, electronic structures, atomic spin densities, and Mulliken atomic charges distribution for the ground states, neutral radicals and radical cations were calculated both for gas phase and unpolar solvent. The solvent effect was taken into account using Tomasi's Polarized Continuum Model (PCM) of the Self-Consistent Reaction Field (SCRF). For simulation of the BuCl as a solvent,

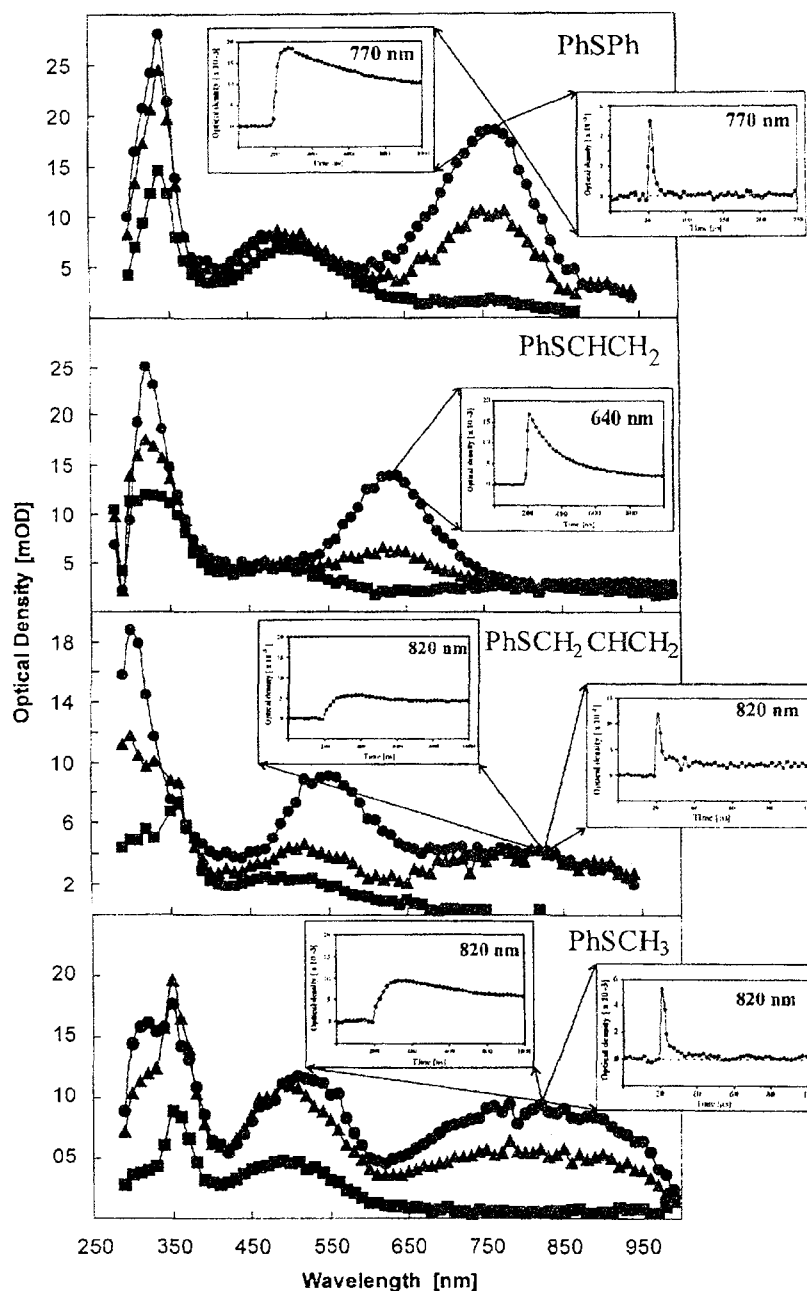


Fig. 2. Transient absorption spectra recorded after pulse irradiation of  $N_2$ -saturated n-butyl chloride solutions containing 1 mM of thioethers: (A) diphenyl sulfide (●) 270 ns, (▲) 950 ns, and (■) 58  $\mu$ s; (B) phenyl-vinyl sulfide (●) 250 ns, (▲) 430 ns, and (■) 950 ns; (C) allyl-phenyl sulfide (●) 250 ns, (▲) 970 ns, and (■) 31  $\mu$ s; (D) methyl-phenyl sulfide (●) 330 ns, (▲) 970 ns, and (■) 31  $\mu$ s after the pulse (50 Gy).

the calculation were made with dielectric constant  $\epsilon=7.58$  and 60 points/sphere implemented in Gaussian 98W program. Owing to their low ionization potential, the aromatic thioethers are good electron donors and can react with the n-butyl radical cations ( $\text{BuCl}^{+\bullet}$ ) and cyclohexane radical cations ( $\text{RH}^{+\bullet}$ ) via charge transfer forming monomeric sulfur radical cations (Fig.1). These radical cations exhibit very similar UV and VIS spectra with strong absorption bands located between 340-350 nm, and weaker absorption bands located at 490-510 nm. Location of the third absorption band (in the near IR region) is affected by the character of the second substituent at the thioether group (Fig.2). In contrast to aliphatic thioether radical cations, they do not undergo dimerization

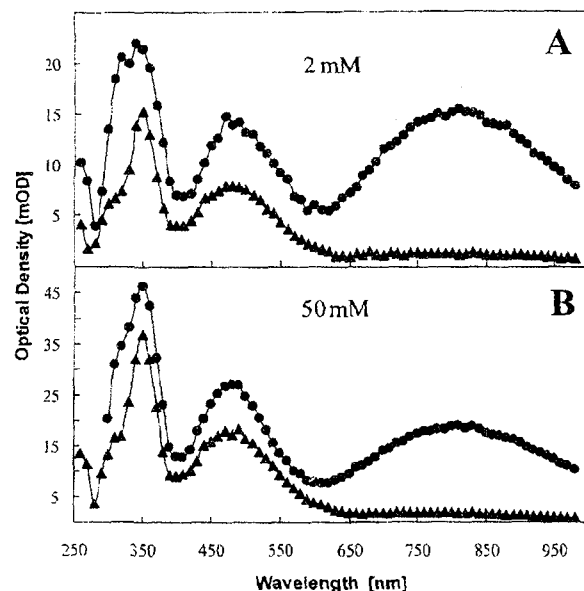


Fig.3. Transient absorption spectra recorded after pulse-irradiation of  $\text{N}_2$ -saturated n-butyl chloride solutions containing methyl-phenyl sulfide: (A) 2 mM (●) 250 ns and (▲) 31  $\mu\text{s}$ ; (B) 50 mM (●) 250 ns and (▲) 62  $\mu\text{s}$  after the pulse (50 Gy).

(via formation of a three-electron bond with the parent thioethers up to 50 mM) (Fig.3).

In n-butyl chloride solutions monomeric sulfur radical cations decay via inhomogeneous and ho-

mogeneous neutralization with  $\text{Cl}^-$  (Fig.4) forming a relatively long-lived sulfur-chlorine three-electron bond adduct ( $>\text{S}:\text{Cl}$ ) characterized by two absorption bands peaking at 340 and 500 nm (Fig.3).

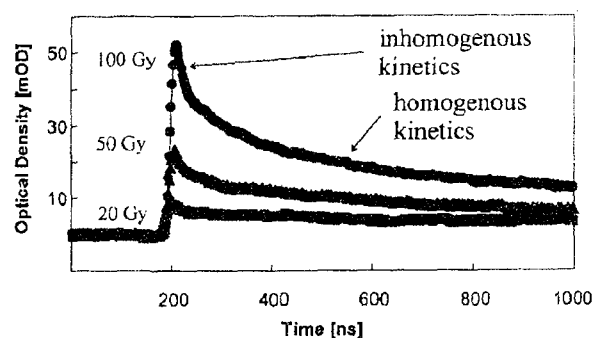


Fig.4. Optical density vs. time profiles recorded after pulse irradiation of  $\text{N}_2$ -saturated solutions containing diphenyl sulfide (50 mM) at different doses (■) 20 Gy, (▲) 50 Gy, and (●) 100 Gy.

Stabilization energies of the ( $>\text{S}:\text{Cl}$ )-adducts are three-fold higher than the stabilization energies of the corresponding dimeric sulfur radical cations ( $\text{S}:\text{S}^+$ ) as found applying quantum chemical calculations, using DFT.

The work described herein was supported by the Programme of Scientific and Scientific-Technological Collaboration between Poland and Germany.

This part of work was presented at the 6th International Conference on Pulse Investigations in Chemistry, Biology, and Physics PULS'2000, 9-15 September 2000, Łeba, Poland.

## References

- [1]. Chatgililoglu C., Bertrand M.P., Ferreri C.: In: S-centered radicals. Ed. Z.B. Alfassi. John Wiley&Sons Ltd., Chichester 1999, pp. 311-354.
- [2]. Ozaki S., de Montelano O.: J. Am. Chem. Soc., **117**, 7056-7064 (1995).
- [3]. Stubbe J.A., van der Donk W.A.: Chem. Rev., **98**, 705-762 (1998).
- [4]. Ioele M., Steenken S., Baciocchi E.: J. Phys. Chem. A, **101**, 2979-2987 (1997).
- [5]. Mohan H., Mittal J.P.: J. Phys. Chem. A, **101**, 10012-10017 (1997).
- [6]. Yokoi H., Hatta A., Ishiguro K., Sawaki Y.: J. Am. Chem. Soc., **120**, 12728-12733 (1998).

## OXIDATION PROCESSES OF N,S-DIACETYL-L-CYSTEINE ETHYLESTER: INFLUENCE OF S-ACETYLATION

Paweł Wiśniowski, Grażyna Strzelczak, Krzysztof Bobrowski, Nicolas Varmentot<sup>1/</sup>, Samy Remita<sup>1/</sup>, Zohreh Abedinzadeh<sup>1/</sup>

<sup>1/</sup>Laboratoire de Chimie Physique, Université René Descartes, Paris, France

This presentation reports the results of investigations on the radical-induced oxidation mechanism of N,S-diacetyl-L-cysteine ethylester (SNACET) and focuses particularly on the effect of the electron-withdrawing functional group (acetyl group,  $\text{CH}_3\text{C}(=\text{O})$ ) on the stability of hydroxy-sulfuranyl radical and sulfur radical cationic intermediates. In the case of the latter species the stability of the monomeric sulfur radical cation ( $\text{R}_2\text{S}^{+\bullet}$ ) should be

relatively high because of spin delocalization onto the carbonyl group [1].

The mechanism of the  $\cdot\text{OH}$ -induced oxidation of N,S-diacetyl-L-cysteine ethylester (SNACET) was investigated in aqueous solutions using pulse radiolysis and steady-state  $\gamma$ -radiolysis combined with chromatographic and ESR techniques. The underlying mechanism involves a very fast fragmentation of an initially formed hydroxysulfuranyl radical ( $k_{\text{fragm}} \geq$



$7.9 \times 10^7 \text{ s}^{-1}$ ) into acyl radicals ( $\text{H}_3\text{O}-\text{CO}^\cdot$ ) and the respective sulfenic acid ( $\text{RSOH}$ ). Subsequently, these intermediates react via a hydrogen abstraction reaction that yields acetaldehyde and the respective sulfinyl radical ( $\text{RSO}^\cdot$ ). In contrast, in very acidic solutions ( $\text{pH} < 2$ ), the  $^\cdot\text{OH}$ -induced oxidation results in formation of the monomeric sulfur radical cation ( $\text{SNACET} > \text{S}^{+\cdot}$ ) which absorbs at  $\lambda_{\text{max}} = 420 \text{ nm}$ . This intermediate is formed with the absolute bimolecular rate constant  $k = 3.9 \times 10^9 \text{ M}^{-1} \text{ s}^{-1}$ . It de-

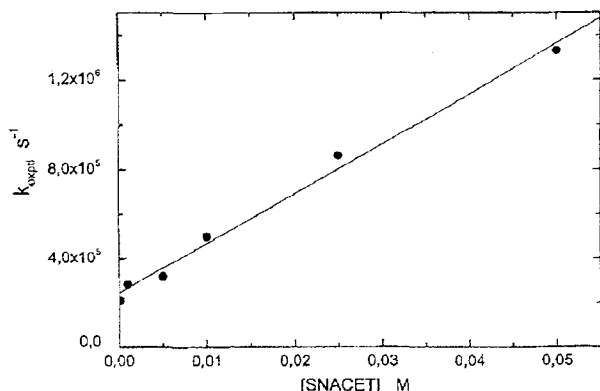


Fig. A plot of the observed first-order rate constants of the decay of  $\text{SNACET}(>\text{S}^{+\cdot})$  as a function of the SNACET concentration.

cays in a SNACET concentration-independent process ( $k_d = 2.5 \times 10^5 \text{ s}^{-1}$ ) and in a SNACET concentration-dependent process ( $k_{\text{S-S}} = 2.2 \times 10^7 \text{ M}^{-1} \text{ s}^{-1}$ ), (Fig.). The first process involves mainly fragmenta-

tion of the carbon-sulfur bond and yields the acetylthiyl radical ( $\text{CH}_2=\text{C}(\text{OH})-\text{S}^\cdot$ ). The latter intermediate was identified via its reaction with oxygen as the thiylperoxyl radical ( $\text{RSOO}^\cdot$ ), characterized by a transient absorption band with  $\lambda_{\text{max}} = 540 \text{ nm}$  [2]. The second process represents the association of the monomeric sulfur radical cation ( $\text{SNACET} > \text{S}^{+\cdot}$ ) with a second nonoxidized SNACET molecule to form the intermolecularly three-electron-bonded dimeric radical cation ( $>\text{S}^\cdot \cdot \text{S} <^+$ ). The low rate constant ( $k_{\text{S-S}}$ ) is in line with the high stability of the monomeric sulfur radical cation ( $\text{SNACET} > \text{S}^{+\cdot}$ ) because of spin delocalization in the carbonyl group. The monomeric radical cation ( $\text{SNACET} > \text{S}^{+\cdot}$ ) is alternatively produced in slightly acidic solutions using the sulfate radical anion,  $\text{SO}_4^{\cdot-}$ , as an one-electron oxidant. This work provides further evidence that the nature of the neighboring group affects the ultimate course of the sulfide oxidation [3].

The work described herein was supported by the Programme of Scientific and Scientific-Technological Collaboration between Poland and France POLONIUM 2000 No 0 15 75 RD.

## References

- [1]. Zhao R., Lind J., Merenyi G., Eriksen T.E.: *J. Phys. Chem. A*, **103**, 71-74 (1999).
- [2]. Tamba M., Simone G., Quintilani M.: *Int. J. Radiat. Biol.*, **50**, 595-600 (1986).
- [3]. Asmus K.-D.: In: *S-centered Radicals*. Ed. Z.B. Alfassi. John Wiley & Sons Ltd., Chichester 1999, pp 141-191.

## SPECTRAL, KINETICS, AND THEORETICAL STUDIES OF RADICAL CATIONS DERIVED FROM THIOANISOLE AND ITS CARBOXYLIC DERIVATIVE

Anna Korzeniowska-Sobczuk, Krzysztof Bobrowski, Gordon L. Hug<sup>1/</sup>, Ian Carmichael<sup>1/</sup>

<sup>1/</sup> Radiation Laboratory, University of Notre Dame, USA

Considerable attention has been devoted to the chemistry of sulfur-centered radicals and radical cations because of their importance as intermediates in many chemical processes including those of organic synthesis [1], environmental [2], and biological significance [3,4]. Most of the information on sulfur-centered radical cations has come from those derived from aliphatic thioethers ( $\text{R}_2\text{S}$ ). An important feature of monomeric sulfur radical cations derived from aliphatic thioethers is their propensity to form relatively stable dimeric radical cations through the reaction of monomeric radical cations with a neutral parent molecule [5].

On the other hand, sulfur-centered radical cations, derived from aromatic thioethers ( $\text{ArS}$ ), have been investigated much less extensively. It has recently been shown that the oxidation of selected aromatic thioethers using  $\text{SO}_4^{\cdot-}$  or  $\text{Ti}^{2+}$ , results in the formation of sulfur monomeric radical cations ( $\text{ArS}^{+\cdot}$ ). However, no dimeric sulfur radical cations ( $\text{ArS}^\cdot \cdot \text{SAr}$ )<sup>+</sup> were formed because of the spin delocalization onto the aromatic ring [6]. In opposition, it has been proposed that  $^\cdot\text{OH}$ -induced oxidation of thioanisole and 2-(phenylthio)ethanol

leads to monomer radical cations with a positive charge localized on the benzene ring ( $\text{Ar}^{+\cdot}\text{S}$ ), in addition to sulfur-centered dimeric radical cations ( $\text{ArS}^\cdot \cdot \text{SAr}$ )<sup>+</sup> [7,8].

In the light of the above controversy, it is of interest to re-examine the nature of intermediate species formed during the oxidation of aromatic thioethers. In this presentation we report the results of pulse- and  $\gamma$ -radiolysis studies of thioanisole ( $\text{Ph-S-CH}_3$ ) and its carboxylic derivative, phenylthioacetic acid ( $\text{Ph-S-CH}_2\text{-COOH}$ ), in aqueous solutions. Particular emphasis is placed on  $^\cdot\text{OH}$ -induced oxidation since it allows a detailed quantification of the relative contribution of the  $^\cdot\text{OH}$  addition to the benzene ring and to the thioether functionality. Furthermore, in order to support our conclusions, quantum mechanical calculations were performed using Density Functional Theory (DFT) that provided information on the relative stabilization energies of  $\text{Ph}^{+\cdot}\text{-S-CH}_3$  and  $\text{Ph-S}^{+\cdot}\text{-CH}_3$  radical cations.

### Reaction of $\text{SO}_4^{\cdot-}$ radicals with thioanisole

The  $\text{SO}_4^{\cdot-}$  radical anion is known to react with thioanisole through one-electron oxidation, form-



PL0101468

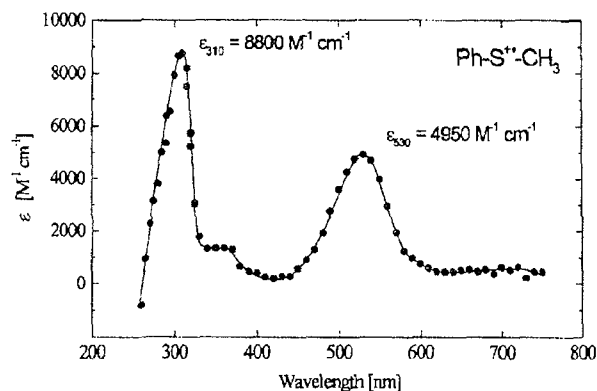
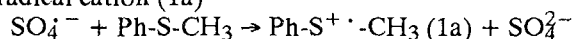


Fig. 1. Transient absorption spectrum recorded after pulse irradiation of an Ar-saturated aqueous solution containing 0.2 mM thioanisole, 2 mM Na<sub>2</sub>S<sub>2</sub>O<sub>8</sub>, and 0.1 M tert-butanol 7 μs after the pulse at pH 5.6. The ε values are based on G(radical)=G(SO<sub>4</sub><sup>•-</sup>)=2.15.

ing the corresponding monomeric sulfur-centered radical cation (1a)



Pulse radiolysis studies were carried out to generate the transient optical absorption spectrum of (1a) in order to obtain quantitative spectral data on (1a) with the same pulse radiolysis setup used to obtain transient optical absorption spectra formed during the <sup>•</sup>OH-induced oxidation of thioanisole. Our absorption spectrum in Fig. 1 can positively identify the transient as (1a) because the overall spectrum exhibits two strong characteristic absorption maxima located at λ<sub>max</sub>=310 and 530 nm with ε<sub>310</sub>=8800 M<sup>-1</sup>cm<sup>-1</sup> and ε<sub>530</sub>=4950 M<sup>-1</sup>cm<sup>-1</sup>.

#### Reaction of <sup>•</sup>OH radicals with thioanisole

The pulse radiolysis of aqueous, N<sub>2</sub>O-saturated solutions containing thioanisole at pH 6.7 yields a

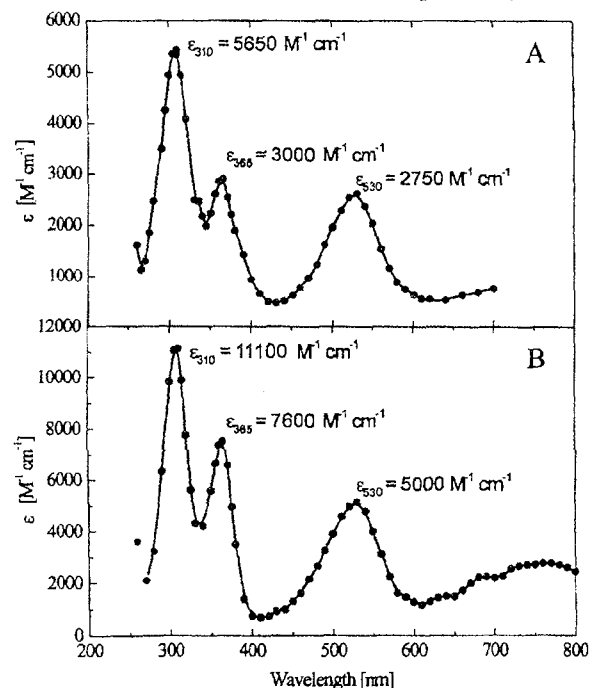


Fig. 2. Transient absorption spectra recorded after pulse irradiation of (A) N<sub>2</sub>O-saturated aqueous solution containing 1 mM thioanisole, 1.4 μs after the pulse at pH 6.7. The ε values are based on G(radical)=G(<sup>•</sup>OH)=5.6; (B) N<sub>2</sub>O-saturated aqueous solution containing 1 mM thioanisole, 1.4 μs after the pulse at pH 0. The ε values are based on G(radical)=G(<sup>•</sup>OH)=2.8.

complex spectrum transients with absorption maxima at λ<sub>max</sub>=310, 365, and 530 nm with apparent extinction coefficients of ε<sub>310</sub>=5650 M<sup>-1</sup>cm<sup>-1</sup>, ε<sub>365</sub>=3000 M<sup>-1</sup>cm<sup>-1</sup>, and ε<sub>530</sub>=2750 M<sup>-1</sup>cm<sup>-1</sup> (Fig. 2A). Since the 530-nm absorption band does not overlap with the absorption bands of the other species, the fraction of the <sup>•</sup>OH radicals that induced oxidation of the thioether functionality, leading to Ph-S<sup>•+</sup>-CH<sub>3</sub> radical cations (1a) can be calculated as ~0.55. Several corrections have to be made for the 365-nm absorption since the apparent ε<sub>565</sub> has contributions from both the <sup>•</sup>OH-adduct to the aromatic ring (2a) (hydroxycyclohexadienyl radical) (~0.45 of the available <sup>•</sup>OH radicals) and from the <sup>•</sup>H atom adduct to the aromatic ring (cyclohexadienyl radical) (~10% relative to the <sup>•</sup>OH radicals). A transient spectrum obtained after electron pulsing in N<sub>2</sub>-saturated solutions containing thioanisole at pH 0, exhibits a complex spectrum of transients with absorption maxima at λ<sub>max</sub>=310, 365, and 530 nm with apparent extinction coefficients of ε<sub>310</sub>=11100 M<sup>-1</sup>cm<sup>-1</sup>, ε<sub>565</sub>=7600 M<sup>-1</sup>cm<sup>-1</sup>, and ε<sub>530</sub>=5000 M<sup>-1</sup>cm<sup>-1</sup> (Fig. 2B). The latter value of the apparent extinction coefficient clearly indicates that the monomeric sulfur radical cations (1a) are formed with 100% of the available <sup>•</sup>OH radicals. Thus, the strong 365-nm absorption band can be assigned exclusively to the <sup>•</sup>H atom adduct to the aromatic ring and to (1a).

#### Reaction of <sup>•</sup>OH radicals with phenylthioacetic acid

The pulse irradiation of an N<sub>2</sub>O-saturated solution, pH 6.97, containing phenylthioacetic acid, leads to the spectra consisting of two distinct absorption bands with λ<sub>max</sub>=310 and 550 nm which are assigned to the monomeric sulfur radical cation (1b) and the distinct 360-nm absorption band attributed both to hydroxycyclohexadienyl (2b) and cyclohexadienyl type radicals (Fig. 3A). After decay of (1b), the spectrum is dominated by an absorption spectrum at λ<sub>max</sub>=330 nm assigned to the Ph-S-CH<sub>2</sub> radicals. At pH 1, pulsed irradiation of N<sub>2</sub>-saturated solutions of phenylthioacetic acid leads again to the formation of 310-nm and 530-nm absorption bands, indicating the formation of (1b). Following the decay of (1b), the spectrum observed is again dominated by an absorption band at λ<sub>max</sub>=330 nm assigned to the Ph-S-CH<sub>2</sub> radicals. These radicals are produced from the decarboxylation of (1b) which is, in turn, corroborated by the formation of CO<sub>2</sub>. Up to pH ~3.5, the measured G(CO<sub>2</sub>) yields accounts for ca. 100% of the available <sup>•</sup>OH radicals. Above pH 3.5, there is a progressive decrease in G(CO<sub>2</sub>) on going from pH 4.0 to 5.0 until a plateau is reached between pH 5 and 7. The G(CO<sub>2</sub>) yields measured on the plateau account for ca. 50% of the available <sup>•</sup>OH radicals (Fig. 3B).

#### Reaction mechanism

Hydroxyl radicals (<sup>•</sup>OH) react with thioanisole (Ph-S-CH<sub>3</sub>) via two competitive addition pathways: with the thioether functionality and with the aromatic ring (Scheme 1). At neutral pH, <sup>•</sup>OH addition leads to the prompt formation of monomeric sulfur radical

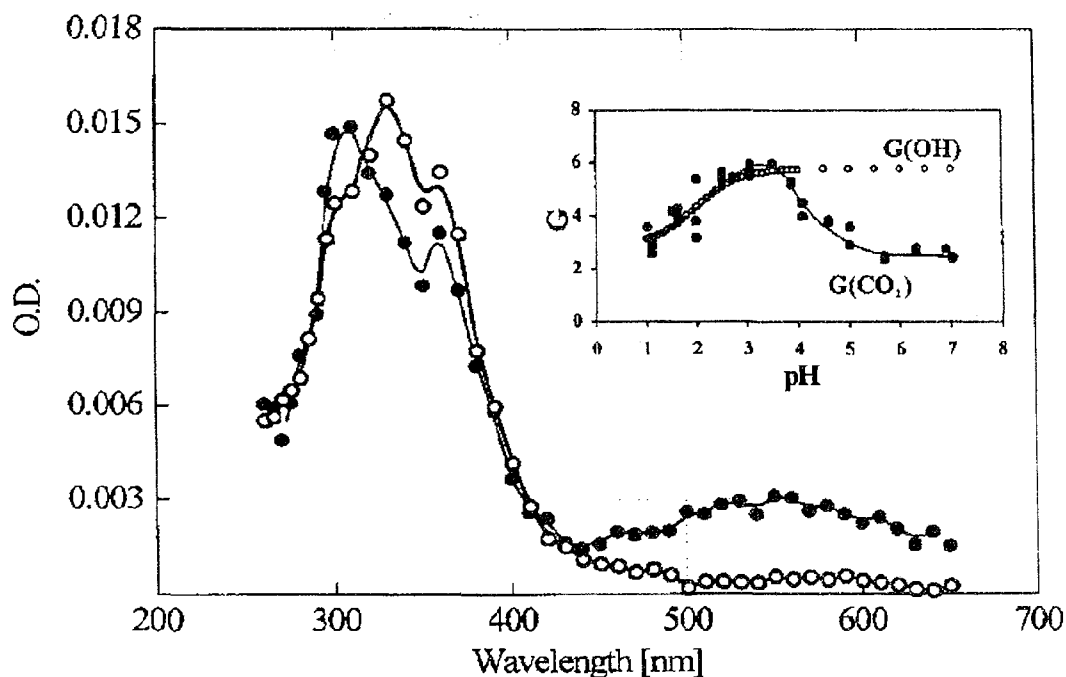
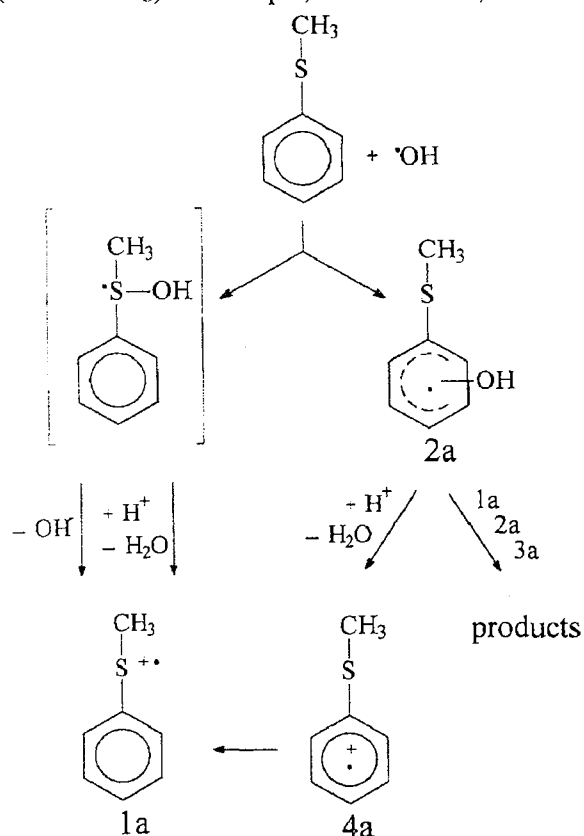


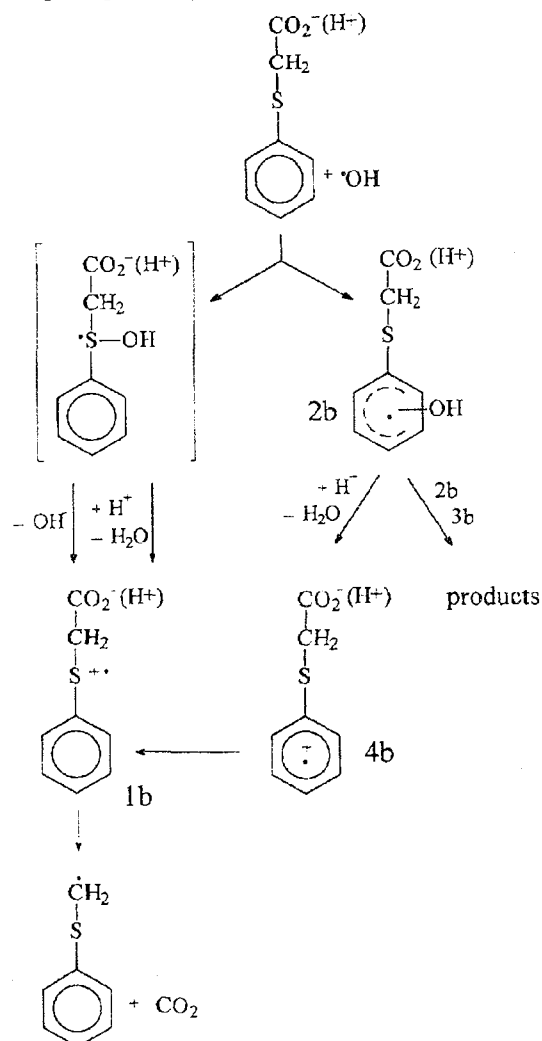
Fig.3. Transient absorption spectra recorded after pulse-irradiation of N<sub>2</sub>O-saturated aqueous solution containing 2 mM phenylthioacetic acid (●) 140 ns and (○) 1.4 μs after the pulse at pH 6.97. Inset: G(CO<sub>2</sub>) measured as a function of pH after γ-radiolysis of N<sub>2</sub>O-saturated aqueous solution containing 2 mM phenylthioacetic acid.

cations (Ph-S<sup>+</sup>-CH<sub>3</sub>, addition to the thioether group) with the radiation chemical yield that accounts for only ca. 55% of the available <sup>•</sup>OH radicals, and hydroxycyclohexadienyl radicals (Ph<sup>•</sup>-(OH)-S-CH<sub>3</sub>, addition to the aromatic ring). The latter radicals subsequently decay into products, which do not include the corresponding radical cations with delocalized positive charge on the aromatic ring (Ph<sup>+</sup>-S-CH<sub>3</sub>). At low pH, <sup>•</sup>OH addition, both to

the thioether functionality and to the aromatic ring, leads promptly only to Ph-S<sup>+</sup>-CH<sub>3</sub> radical cations



Scheme 1.



Scheme 2.

equal to  $\sim 100\%$  of the available  $\cdot\text{OH}$  radicals. These observations are rationalized in terms of the highly unstable nature of  $\text{Ph}^+\cdot\text{-S-CH}_3$  radical cations (formed via proton-catalyzed water elimination from  $\text{Ph}^+\cdot\text{-(OH)-S-CH}_3$  radicals) and their rapid conversion into  $\text{Ph-S}^+\cdot\text{-CH}_3$  radical cations.

An additional experimental support for the instability of radical cations derived from aromatic thioethers with delocalized positive charge on their aromatic rings has been obtained from the  $\cdot\text{OH}$ -induced oxidation studies of phenylthioacetic acid ( $\text{Ph-S-CH}_2\text{-COOH}$ ) (Scheme 2). At low pH,  $\text{Ph-S-CH}_2\text{-COOH}$  undergoes complete (relative to the available  $\cdot\text{OH}$  radicals) quantitative decarboxylation, in contrast to neutral pH, where the yield of decarboxylation accounts for only the half available  $\cdot\text{OH}$  radicals.

Our conclusion about the instability of the  $\text{Ph}^+\cdot\text{-S-CH}_3$  radical cation was supported by quantum mechanical calculations using Density Functional Theory (DFT) that provided information about the relative stabilization energies of  $\text{Ph}^+\cdot\text{-S-CH}_3$  and  $\text{Ph-S}^+\cdot\text{-CH}_3$  radical cations.

This work described herein was supported by the Polish State Committee for Scientific Research, grant 3 T09A 037 19.

This part of work was presented at the 6th International Conference on Pulse Investigations in Chemistry, Biology, and Physics PULS'2000, 9-15 September 2000, Łeba, Poland.

## References

- [1] Chatgililoglu C., Bertrand M.P., Ferreri C.: In: S-centered radicals. Ed. Z.B. Alfassi. John Wiley & Sons Ltd., Chichester 1999, pp. 311-354.
- [2] Tobien T., Cooper W.J., Nickelsen M.G., Pernas E., O'Shea K.E., Asmus K.-D.: *Env. Sci., Technol.*, (2000), in print.
- [3] Ozaki S., de Montelano O.: *J. Am. Chem. Soc.*, **117**, 7056-7064 (1995).
- [4] Stubbe J.A., van der Donk W.A.: *Chem. Rev.*, **98**, 705-762 (1998).
- [5] Asmus K.-D.: In: S-centered radicals. Ed. Z.B. Alfassi. John Wiley & Sons Ltd., Chichester 1999, pp. 141-191.
- [6] Ioele M., Steenken S., Baciocchi E.: *J. Phys. Chem. A*, **101**, 2979-2987 (1997).
- [7] Mohan H., Mittal J.P.: *J. Phys. Chem. A*, **101**, 10012-10017 (1997).
- [8] Gawandi V.B., Mohan H., Mittal J.P.: *Phys. Chem. Chem. Phys.*, **1**, 1919-1926 (1999).

## INTERACTION OF TETRAMERIC SILVER WITH AMMONIA IN AgCs-rho ZEOLITE

Jarosław Sadło, Marek Danilczuk, Jacek Michalik

### Introduction

Molecular sieves have unique abilities to stabilise cationic silver clusters produced radiolytically or by hydrogen reduction.

The most stable cationic silver clusters were found in an AgCs-rho zeolite, in which the tetrameric clusters,  $\text{Ag}_4^{3+}$  are stable till 400 K [1-3]. The silver tetramer, which is formed in gamma-irradiated AgCs-rho zeolites exposed to  $\text{NH}_3$ , shows an ESR spectrum with a substantial reduction of Ag hyperfine splitting in comparison with  $\text{Ag}_4^{3+}$  in dehydrated zeolites. Based on this result, we postulated earlier the formation of an  $\text{Ag}_4^{3+}(\text{NH}_3)_n$  multicore complex in rho zeolite [2].

In the present studies the analogous ESR experiments with  $^{14}\text{NH}_3$  and  $^{15}\text{NH}_3$  were carried out in order to solve the structure of ammonia ligands.

The experimental details of the preparation, irradiation and ESR measurements of AgNaCs-rho/ $\text{NH}_3$  samples are given in [4].

### Results and discussion

The X-band ESR spectrum of dehydrated AgCs-rho zeolite irradiated at 77 K and recorded after annealing of the sample to room temperature is shown in Fig.1a. It is composed of three sets of lines: anisotropic signal B, singlet S and five-line multiplet Q due to three types of paramagnetic species. The two lines denoted as  $B_\perp$  and  $B_\parallel$  represent divalent silver cations  $\text{Ag}^{2+}$ : ( $g_\perp=2.051$ ,  $g_\parallel=2.315$ ). In A zeolite, in which  $\text{Ag}^{2+}$  cations are stabilised more efficiently giving a stronger ESR spectrum,  $B_\perp$  and  $B_\parallel$  components are splitted into doublets separated about 40 G. Isotropic singlet S ( $g_{\text{iso}}=2.010$ ,  $\Delta H_{\text{pp}}=2.2$  mT) we assigned tentatively

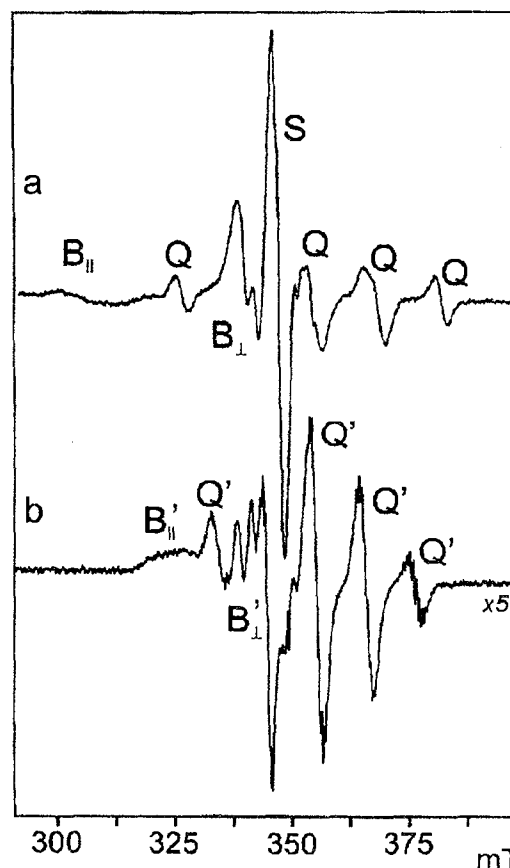


Fig.1. ESR spectra of AgCs-rho zeolite irradiated at 77 K and annealed to room temperature: a - dehydrated zeolite; b - zeolite exposed to  $^{15}\text{NH}_3$  ammonia.

to a signal derived from radiation-induced defects in zeolitic framework because such a singlet with



similar ESR parameters ( $g_{\text{iso}}=2.012$ ,  $\Delta H_{\text{pp}}=1.5$  mT) was recorded in a gamma irradiated sodium-cesium form of zeolite rho. A positive  $g$  shift suggests that this center has the nature of a trapped hole. In fact, in a silica-alumina gel a similar signal was interpreted as a positive hole trapped on the bridging oxygen atom that is bonded to the aluminum present substitutionally in the silica matrix. The isotropic pentet Q with spin Hamiltonian parameters  $A_{\text{iso}}=13.9$  mT and  $g_{\text{iso}}=1.973$  represents the tetrameric silver cluster  $\text{Ag}_4^{3+}$  located inside an octagonal prism [2]. Similar signals were observed in AgCs-rho zeolite after  $\text{H}_2$  reduction [1] as well as in  $\gamma$ -irradiated AgH-rho zeolite [2]. The third and fourth lines of pentet Q show some additional features and their intensities are lower than one would expect from the binominal intensity ratio. We earlier proposed that those irregularities resulted from overlapping of the low intensity quartet of  $\text{Ag}_3^{3+}$  cluster which is a precursor of the silver tetramer.

The X-band spectrum of AgCs-rho zeolite exposed to  $^{15}\text{NH}_3$  before irradiation reveals also the signals of  $\text{Ag}^{2+}$  and  $\text{Ag}_4^{3+}$  denoted in Fig.1b as B' and Q', respectively. The ESR parameters of both species  $\text{Ag}^{2+}$  ( $g_{\perp}=2.033$ ,  $g_{\parallel}=2.148$ ) and  $\text{Ag}_4^{3+}$  ( $g_{\text{iso}}=1.967$ ,  $A_{\text{iso}}=10.7$  mT) are distinctly different from those in dehydrated zeolite. The perpendicular component of  $\text{Ag}^{2+}$  spectrum and the outer lines of  $\text{Ag}_4^{3+}$  pentet show clearly an additional structure due to the interaction with the  $^{15}\text{N}$  nuclei.

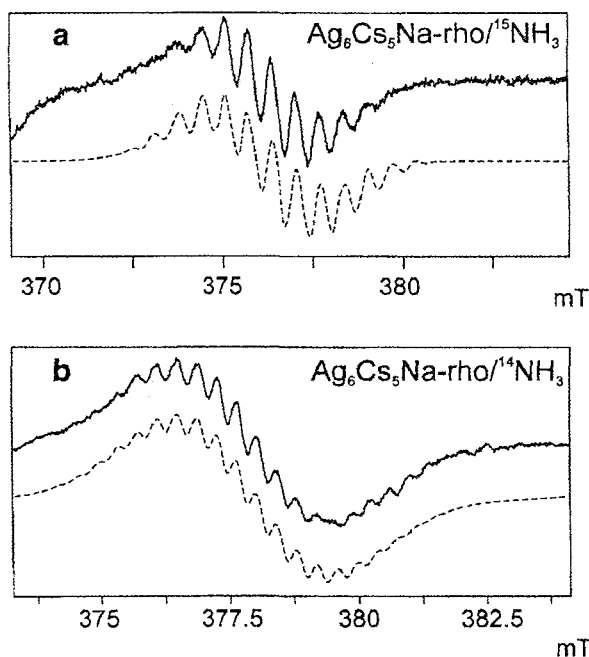


Fig.2. High field line of  $\text{Ag}_4^{3+}$  pentet showing superhyperfine splitting due to the interaction with  $\text{NH}_3$  molecules: a -  $^{15}\text{NH}_3$ , b -  $^{14}\text{NH}_3$ . The dashed lines represent simulated spectra.

The ESR pentet of  $\text{Ag}_4^{3+}$  in AgCs-rho/ $\text{NH}_3$  zeolite, in contrast with the dehydrated sample, shows almost a perfect binomial intensity ratio 1:4:6:4:1 indicating that the ESR spectrum represents only the  $\text{Ag}_4^{3+}$  cluster.

The decrease of Ag hyperfine splitting from 13.9 mT for  $\text{Ag}_4^{3+}$  in dehydrated zeolite to 10.7 mT for zeolite exposed to  $\text{NH}_3$  is due to the substantial shift of spin density from the silver nuclei to the  $\text{NH}_3$  molecules located in the nearest vicinity. The calculated spin density on 5s silver molecular orbital is  $0.623 \pm 0.05$  for  $\text{Ag}_4^{3+}(\text{NH}_3)_n$  and is by 22% lower than that for  $\text{Ag}_4^{3+}$  in dehydrated zeolite, suggesting strongly that the  $\text{NH}_3$  ligands are coordinated by the tetrameric cluster. A direct proof of the formation of multicore  $\text{Ag}_4^{3+}(\text{NH}_3)_n$  complex was obtained from the analysis of superhyperfine structure of  $\text{Ag}_4^{3+}$  pentet recorded in AgCs-rho exposed to  $^{15}\text{NH}_3$  and  $^{14}\text{NH}_3$ . Fig.2a and b show a high field line of  $\text{Ag}_4^{3+}$  pentet on which an additional structure due to the superhyperfine interaction with nitrogen is seen most clearly. Both spectra are different proving univocally that the superhyperfine structure results from the interaction with nitrogen nuclei.  $^{15}\text{N}$  and  $^{14}\text{N}$  have different spins, 1/2 and 1, respectively, thus a different number of superhyperfine lines is expected for the interaction with  $^{15}\text{N}$  and  $^{14}\text{N}$  nuclei. The best fit of the simulation of  $^{15}\text{N}$  superhyperfine pattern was obtained for the two closer nitrogens:  $A_{\text{iso}}^1(^{15}\text{N})=1.16$  mT and for the four more distant ones:  $A_{\text{iso}}^2(^{15}\text{N})=0.56$  mT (Fig.2a). For  $^{14}\text{N}$  the best simulation we obtained for the same numbers of interacting nitrogen nuclei with superhyperfine splitting  $A_{\text{iso}}^1(^{14}\text{N})=0.76$  mT and  $A_{\text{iso}}^2(^{14}\text{N})=0.36$  mT, respectively (Fig.2b). In both cases dashed lines represent simulated spectra.

Based on these results we are able to propose the structure of multicore complex as  $\text{Ag}_4^{3+}(\text{NH}_3)_2(\text{NH}_3)_4$ .  $\text{Ag}_4^{3+}$  is trapped in the octagonal prism coordinating two  $\text{NH}_3$  molecules situated in two  $\alpha$ -cages interconnected

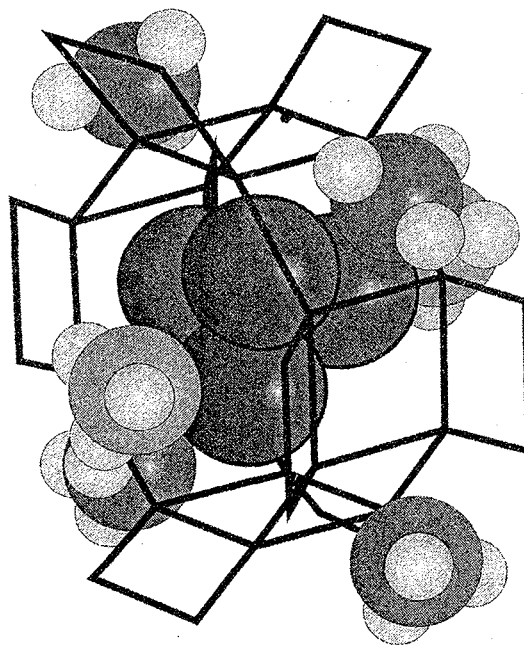


Fig.3. The schematic configuration of  $\text{Ag}_4^{3+}(\text{NH}_3)_2(\text{NH}_3)_4$  complex.  $\text{Ag}_4^{3+}$  cluster is located in octagonal prism interacting with two close ammonia (less grayish circles depicting N atoms) in the  $\alpha$ -cages connected with the prism through octagonal windows. Four more distant  $\text{NH}_3$  molecules (more grayish circles) are located in  $\alpha$ -cages connected to the prism through the square windows.

by the prism with  $\text{Ag}_4^{3+}$  inside, close to two octagonal windows of the prism. Four other  $\text{NH}_3$  molecules are located in four further  $\alpha$ -cages interacting with the tetramer through square windows. Schematically our model is presented in Fig.3.

### Conclusions

Based on the EPR results it is postulated that the  $\text{Ag}_4^{3+}$  clusters in AgCs-rho zeolite exposed to  $\text{NH}_3$  are formed directly during radiolysis at 77 K by trapping electron by the arrangements of  $4\text{Ag}^+$  in the same octagonal prism. This mechanism is unlike to the gradual silver agglomeration is dehydrated AgCs-rho, which requires migration of silver atoms and cations to produce  $\text{Ag}_4^{3+}$ . The decrease of  $\text{Ag}_4^{3+}$  hyperfine splitting from 13.9 mT in dehydrated zeolite to 10.7 mT in zeolite exposed to ammonia indicates a strong interaction with  $\text{NH}_3$  molecules.

The formation of multicore  $\text{Ag}_4^{3+}(\text{NH}_3)_n$  complex was proved univocally by the presence of superhyperfine pattern on the  $\text{Ag}_4^{3+}$  lines. The number of superhyperfine lines is different for zeolites exposed to  $^{14}\text{NH}_3$  and  $^{15}\text{NH}_3$ . The best simulation of

$^{14}\text{N}$  and  $^{15}\text{N}$  superhyperfine patterns were obtained assuming the interaction with the two close nitrogen nuclei and the four distant ones. Matching ligand configuration to the zeolite structure, we postulated that the  $\text{Ag}_4^{3+}$  cluster in the octagonal prism coordinates through octagonal windows two close  $\text{NH}_3$  molecules in the nearest  $\alpha$ -cages. Four further ammonia molecules are placed in the next-neighboring  $\alpha$ -cages interacting with the tetramer through square windows.

The  $\text{Ag}_4^{3+}(\text{NH}_3)_2(\text{NH}_3)_4$  complex is also formed when ammonia is adsorbed on dehydrated zeolite with  $\text{Ag}_4^{3+}$  clusters already produced by irradiation indicating that the silver tetramer is located in the site accessible for adsorbates.

### References

- [1]. Xu B., Kevan L.: J. Phys. Chem., **95**, 1147 (1991).
- [2]. Michalik J., Sadko J., Yu J-S., Kevan L.: Colloids Surfaces A, **115**, 239 (1996).
- [3]. Michalik J., Sadko J., Kodaira T., Shimomura S., Yamada H.: J. Radioanal. Nuclear Chem., **232**, 135 (1998).
- [4]. Sadko J., Danilczuk M., Michalik J.: Phys. Chem. Chem. Phys., **3**, 1705 (2001).

## A NANOSECOND PULSE RADIOLYSIS SYSTEM DEDICATED TO THE NEW LAE 10 ACCELERATOR IN THE INCT

Jacek Mirkowski, Paweł Wiśniowski, Krzysztof Bobrowski

Pulse radiolysis is an invaluable tool for studying the kinetics and spectra of transient chemical species. This method has found a broad range of important applications in chemistry and biochemistry, extending far beyond the scope of radiation chemistry to which it was first applied [1].

With the advent of microprocessors all aspects of the generalized experiment are susceptible to computer control. In this report we describe a computer-controlled pulse radiolysis system based on a fast digital storage oscilloscope (DSO) [2,3]. The oscilloscope produces a sufficient number of time points that multiple time scales can be generated by the computer from a single kinetic trace originating from DSO. Thus, one can in principle, with a single kinetic trace, resolve time constants from a few nanoseconds to tens, or even hundreds of microseconds. The simultaneous recording transient absorption data on multiple time scales is valuable for saving both experimental time and the amount of valuable samples.

The measurement room, with an accelerator gun, an analytical light source lamp, a dose meter and other devices, is separated from the operator room by a shielding wall and fiber optic connectors used for noise interference minimization (Fig.1). Analytical light, after passing the measurement cell, periscope and monochromator SpectraPro-275 (controlled by the host PC) is converted to electric current signal in a photomultiplier Hamamatsu R-955. The signal, after subtraction of the reference light and signal amplification (DI) (1, 10 or 100x), is measured by a LeCroy 9354AL oscilloscope. Other analog signals (reference light-I0 and dose monitor)

are measured using AD converters in ADAM modules (Advantech).

All peripherals are connected to a host computer (PC) using two types of interfaces: a GPIB-parallel bus and RS232/RS485 serial buses with an optical isolation. The fast oscilloscope LeCroy 9354AL is connected to the PC using the parallel bus GPIB. This bus is also used for connecting an HV Power Supply PS310 (not shown in Fig.1). Other peripherals are connected to the PC using a single RS485 serial communication port.

Digital signals, pre-trigger, dose strobe, reference light strobe, are sent from the host computer to target elements using digital (open collector) outputs through specialized ADAM modules. The pre-trigger pulse is sent to the accelerator using fiber optic connections. The trigger signal from the accelerator, after passing through fiber optics and converters, is sent to the LeCroy 9354AL oscilloscope. The monochromator, equipped with RS232 interface, is connected to the host PC using the ADAM 4521 addressable module that converts RS485 standard to RS232 standard. The program RD2000, which controls pulse radiolysis setup, works under Windows 9X/NT operating system. This program was created using Delphi 3.0 (Borland) Pascal type programming tools.

The Operator Desktop (Fig.2) consists of five sub-windows:

- One-Shot Data, for the actual measured kinetics (not shown);
- Final Data, for the averaged data, which are displayed after each accelerator shot at a selected wavelength;







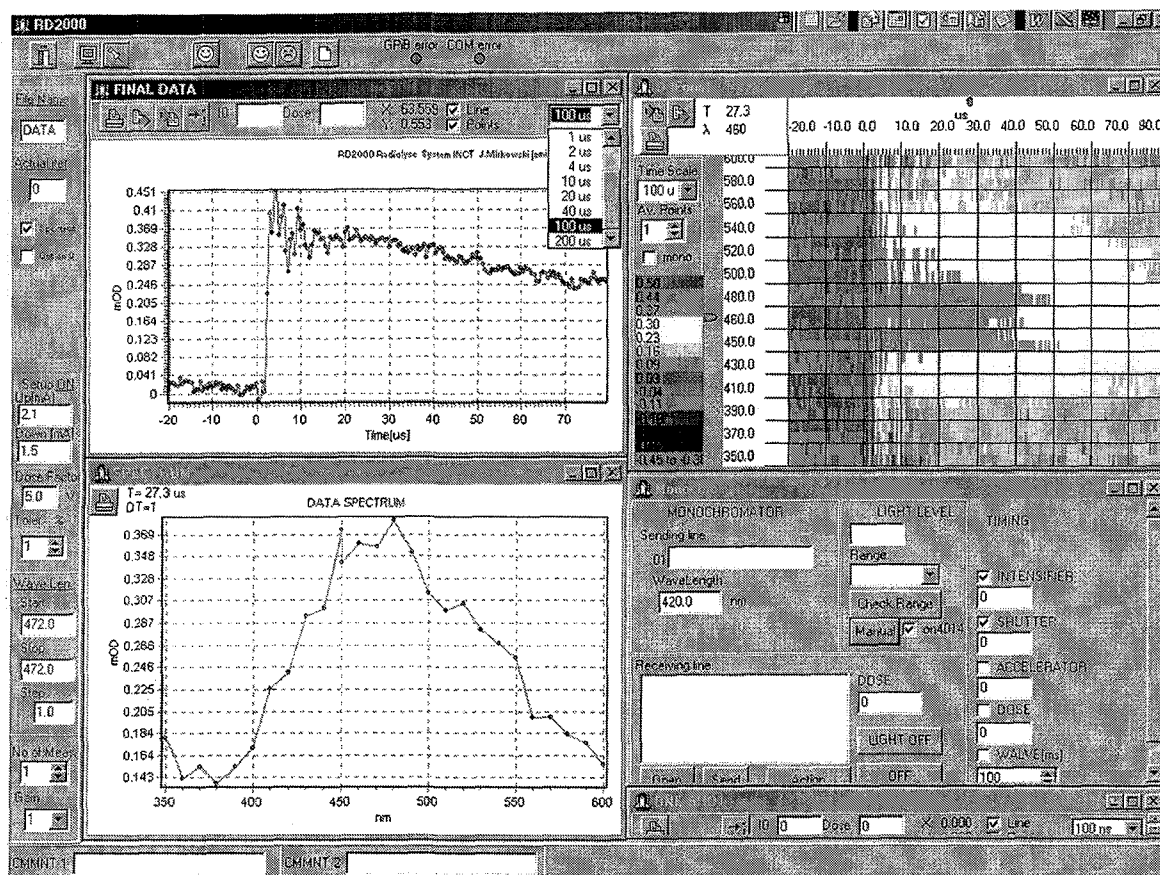


Fig.2. General view of the operator desktop after data collection.

parameters, trigger parameters and active buffer parameters. The active buffer parameters are used for positioning the front of the electron pulse accurately at the 20% time scale position point. In the current version, the buffer length and the time scale are fixed parameters.

The Final Data window shows an unwrapped box with optional values of the time scale parameter for the displayed kinetics. In the current version the system collects data on 11 time domains: starting from 100 ns and ending on 200 ms. All kinetics are stored in 200-points data buffer per each time domain.

The operator can choose independently any time scale for each window, i.e. One Shot Data, Final Data, D3Form1. Data, in the Data Spectrum Window, are displayed accordingly with the position of the horizontal marker (time positioning) on mapped data.

The current version of the pulse system (without light pulser) allows measurements of the optical density in the range of tenths of mOD.

Experimental data are collected and stored in standard formats (e.g. DBF) easily accessible by common programs (Lotus, Excel, Origin, Access etc.).

The new pulse radiolysis system, due to its modular structure and applied programming tools, is very flexible, adopted easily to all changes, and friendly for the users.

Part of this work was presented at the 6th International Conference on Pulse Investigations in Chemistry, Biology, and Physics PULS'2000, 9-15 September 2000, Łeba, Poland.

## References

- [1]. Photochemistry and Radiation Chemistry. Eds. J.F. Wishart, D.G. Nocera. Advances in Chemistry Series 254, American Chemical Society, Washington, D.C. 1998.
- [2]. Thomas M.D., Hug G.L.: Computers Chem., **22**, 491-498 (1998).
- [3]. Hug G.L., Wang Y., Schöneich Ch., Jiang P.-Y., Fessenden R.W.: Radiat. Phys. Chem., **54**, 559-566 (1999).

## POST-IMPLANTATION DEFECTS. INSTABILITY UNDER 1 MeV ELECTRON IRRADIATION IN GaAs

Stanisław Warchoń, Henryk Rzewuski, Janusz Krynicki, Rainer Grötzschel<sup>1/</sup>

<sup>1/</sup> Forschungszentrum Rossendorf e.V., Dresden, Germany

One of the main drawbacks of ion implantation into semiconductor crystals is generation of lattice damage which deteriorates their physical parameters. There-

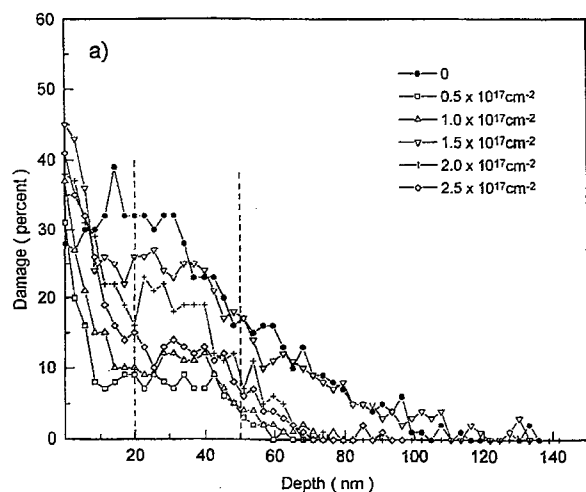
fore, it is necessary to remove post-implantation defects in order to activate the implanted impurities and to obtain the desired electrical activity of the crystal.



PL0101471

In our previous work [1] we reported the results of the influence of 300 keV electron irradiation on GaAs single crystals implanted with 150 keV As<sup>+</sup> at RT. The results revealed a distinct increase of post-implantation damage level - the effect opposite to defect annealing.

The aim of the present work [2] was to determine how the post-implantation defects in GaAs evolve at different depths below the surface and how such evolution depends upon the fluence of 1 MeV electron irradiation.



first three electron fluences and then runs oscillating to some asymptotic value of about 50% of total amorphization, much higher than the initial, as implanted level, of about 28%.

The other two curves b and c, representing damage level variations at 20 and 50 nm, show at the onset a decrease of damage followed by damped oscillations. It is worth to notice that the damage levels of curves b and c for the maximum electron fluence  $5.0 \times 10^{17} \text{ cm}^{-2}$  amount to 21 and 13%, and are lower than their initial as-implanted values - 32

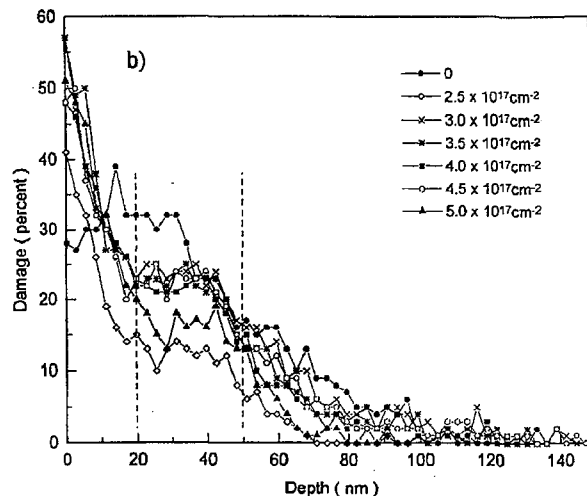


Fig.1. Depth distributions of damage as extracted from the channeling spectra obtained for different 1 MeV electron fluences.

The n-type GaAs wafers of (100) orientation were implanted with 150 keV As<sup>+</sup> ions below the amorphization threshold at RT using the implantation dose of  $2 \times 10^{13} \text{ ions cm}^{-2}$  at a constant flux of  $0.1 \mu\text{A cm}^{-2}$ . Then the implanted samples were irradiated with a scanned beam of 1 MeV electrons from a Van de Graaff accelerator in a dose range of  $(0.5-5.0) \times 10^{17} \text{ cm}^{-2}$  at 320 K. RBS and channeling spectroscopy of 1.7 MeV  $^4\text{He}^+$  ions were used to determine the depth distribution of defect concentration before and after 1 MeV irradiations using the classical relation by Chu et al. [3]. The damage distributions related to both Ga and As peaks in the RBS spectra were calculated using the "Defect" computer program [1]. The RBS measurements were performed at the Forschungszentrum Rossendorf e.V., Germany.

Fig.1a,b presents the damage depth distributions (damage profiles) as extracted from the measured  $\langle 100 \rangle$  channeling spectra. In order to show more clearly the behavior of damage profiles under 1 MeV electron irradiation Fig.2 presents the damage fluctuations in three selected depths of the damage distributions, namely for 0, 20 and 50 nm (curves a, b, and c, respectively) from the surface of a sample. The curve a represents damage level variations at the surface, but the curves b and c - show these variations at the maximum and at the slopes of the damage profiles. An "oscillatory" behavior of the damage at these selected depths under increasing electron fluence is very well seen. These variations occur in the whole range of electron fluences.

In the case of the subsurface defect concentration (curve a), the damage level increases with the

and 17%, respectively. Apart from the oscillatory behavior, this decrease indicates that defect annihilation processes take place at these depths, decreasing the defect concentration to some asymptotic values.

Using pulsed electron beam annealing of Si<sup>+</sup> and Cr<sup>+</sup> implanted GaAs, Alberts et al. [4] found a significant increase of a damage peak which occurred after several peaks decreasing from the amorphization level. The authors argue that this effect is probably related to a disrupted surface structure being a result of transient surface melting, which takes place above  $0.7 \text{ J cm}^{-2}$  energy density of the electron beam pulses, and subsequent regrowth of the implanted layer. In our case, the appearance of damage level oscillations at three various sample depths shows a repeated increase and decrease of damage. Since the crystalline GaAs can hardly be amorphized by a single dose of  $0.5 \times 10^{17} \text{ cm}^{-2}$  of 1

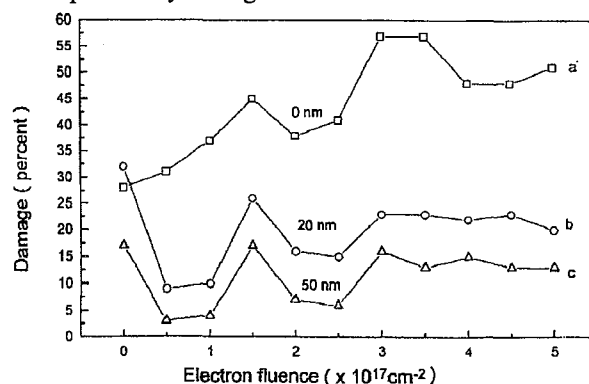


Fig.2. Damage level fluctuations at 0, 20 and 50 nm from the surface of the sample as a function of 1 MeV electron fluences.

MeV electrons at RT, we have a heavily damaged layer as can be inferred from the RBS-c measurements. The reason of great differences between Albert's [4] and our results depends very likely on the experimental conditions, i.e. amorphization and partial damage of the implanted layer, low (pulsed) and high (scanned) electron energy irradiations and different implanted ions of Si, Cr, and As, respectively. TEM investigations on weakly damaged GaAs layers by Wesch et al. [5] indicate that in these layers defect structures consisting of point defects, point defect clusters and amorphous zones exist. High resolution electron microscopy studies on individual displacement cascades by Bench et al. [6] provides a strong proof that the damage within the core of isolated cascades is amorphous. It is evident that in the implanted layer these various defect structures are not uniformly distributed along the path of ions.

Assuming a similar distribution of post-implantation defect structures in our weakly damaged samples, transformation processes of defects should proceed in a different way, leading to the observed damage level behavior at various subsurface regions of the implanted layer.

The present results support our view from the previous paper [5] on the processes responsible for the increase of defect concentration under electron irradiation. The charge state of defects is changed in the field of ionization and modifies the energy barrier for their migration. At least a part of them out-diffusing from the damaged zones and migrating through the sample will make stable associations with the intrinsic or impurity atoms in the crystal, increasing in this way defect concentration [5]. The participation of Frenkel pairs created by 1

MeV electrons in the transformation processes should be rejected because their concentration is several orders of magnitude lower than the concentration of defects introduced by implantation.

It has been shown using RBS-c spectroscopy of 1.7 MeV  $^4\text{He}^+$  ions that 1 MeV electron irradiation of GaAs implanted with 150 keV  $\text{As}^+$  ions at RT induces damped oscillations in the damage level. The increase of defect concentration appearing during oscillations confirms the results obtained in our previous paper [1]. This effect can be attributed to ionization induced alteration of a defect charge state and to the enhanced out-diffusion of simple defects from the damaged zones making then associations with other defects in a crystal. The asymptotic value of ionization induced damage oscillations indicates that some of the radiation-produced defects are stable under ionizing radiation. Further investigations are necessary to explain in more detail the oscillating behavior of a damage level taking place in the implanted GaAs under electron irradiation, especially at lower electron energy, close or below the energy threshold for atomic displacement.

The authors wish to thank Mr. J. Toruń for technical assistance.

## References

- [1]. Warchol S., Rzewuski H.: *Nukleonika*, **43**, 1, 23-29 (1998).
- [2]. Warchol S., Rzewuski H., Krynicki J., Groetzschel R.: *Nukleonika*, **45**, 4, 225-228 (2000).
- [3]. Chu W.K., Mayer J.W., Nicolet M.A.: *Backscattering Spectroscopy*. Academic Press., New York 1978.
- [4]. Alberts H.W., Gaigher H.L., Friedland E.: *Mat. Sci. & Eng.*, **B9**, 331-335 (1991).
- [5]. Wesch W., Gartner K., Jordanow A., Goetz G.: *Nucl. Instr. and Meth. in Phys. Res.*, **B22**, 447-449 (1987).
- [6]. Bench M.W., Robertson J.M.: *Nucl. Instr. and Meth. in Phys. Res.*, **B59/60**, 372-376 (1991).

## RADIATION CHEMISTRY OF POLYMERS AS RECOGNIZED BY DIFFUSE REFLECTANCE SPECTROPHOTOMETRY (DRS)

Zbigniew P. Zagórski, Andrzej Rafalski

Execution of plans of our Institute in the field of solid state radiation chemistry demands the development of new measurement techniques, especially the quantitative-optical ones. The diffuse reflectance spectrophotometry is the most recent. Research on radiation chemistry of polymers consist of chemical, physico-chemical and, last but not least, physical methods. These methods become more and more sophisticated, contributing to deeper understanding of reactions of polymers, helping to control properties and even tailoring them according to technological needs. A particular method of investigations of polymers is the spectrophotometric method in the region of UV and visible wavelengths. Species formed by the action of ionising radiation have usually molar extinction coefficients ( $\epsilon$ ) in order of hundreds and thousands of  $\text{M}^{-1}\text{cm}^{-1}$ , thus allowing observation of radiation effects sometimes even after the absorbed dose as low as 10 grays. Conventional spectrophotometry requires reasonably transparent

samples, e.g. of background not exceeding 2 units of optical density (OD). Some modern spectrophotometers are offering a tolerance of OD of background up to 5, but high dissipation of light impairs the chances of spectral investigations. Virgin polymers, as appearing from polymerisation line, exceed even that liberal threshold of OD and demand a new approach.

We have found it in the application of diffuse reflectance absorption spectrophotometry (DRS) of general application in the investigation of radiolysis of polymers. The reflection from metallic surface (Fig.1, left part of the diagram), so called specular reflection, involves a few atomic layers only and explains the colour of certain metals, e.g. of gold and copper. The reflected spectrum is also of application in the construction of optical devices, in which as high yield of reflection is desired as possible, e.g. in selected regions of infra red. In the radiation chemistry of polymers, the specular reflection is of no



PL0101472

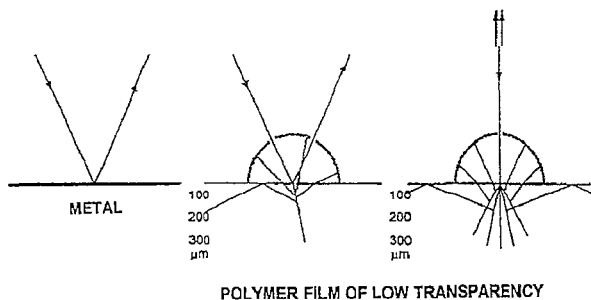


Fig. 1. Simplified picture of the origin of diffuse reflectance spectroscopy. Explanations in the text.

use; on the contrary, every effort is made to get rid of it, as it does not carry any information originating from the inside of the sample. The bulk of polymer, under the surface is probed by the beam of light which is penetrating the polymer. According to laws of optics, the analysing beam falling diagonally on the surface of transparent material even at a low degree, is partly reflected (specular reflection) and partly refracted into the material. This fraction of light is the most important, because due to internal reflections, it is able to leave the sample, but is attenuated by absorption by species formed in the sample. The escaping beam of light carries important information about the absorption at particular wavelength. Some instruments are using a vertical beam of analysing light. In that case the reflected specular beam escapes along the same route as the incident beam. The beam intruding inside the sample causes similar phenomena as in the case of diagonal beam, i.e. produces reflected stray light, containing information about new compounds in the sample. The distribution of emitted light is random; the amount of escaping light is low, and the losses are substantial, due, e.g. to the total internal. Therefore efforts are made to collect as much of the reemitted light as possible.

In all spectrophotometric measurements the question of reference sample arises. It is a fortuitous situation in radiation chemistry, when we can compare irradiated sample vs. unirradiated one, compensating all factors influencing spectrum, like roughness of the surface, presence of crystalline and amorphous phases in the polymer etc. Such a simple measurement may be performed only with spectrophotometers of specific construction. We have found that a spectrophotometer of Perkin-Elmer Lambda 9 fulfils the requirements: it is a double beam apparatus with the light integrating sphere with two windows - the first for the reference, the second for the sample. The beam of analytical light probes alternately the irradiated and unirradiated samples in the sphere, recording only the difference of absorptions. The computer program determines the wavelengths of maxima of absorption bands, allows to change scales and to record results of other measurements for comparison etc. The measurement is as simple as in conventional spectrophotometry and consists of placing unirradiated and irradiated samples (in the shape of a film, or a powder in the suprasil cell) at respective windows (Fig. 2). Pressure applied by the lid is very useful,

because it forces the film to be planar, which is impossible in the case of Varian-Cary 4 or 5 instruments.

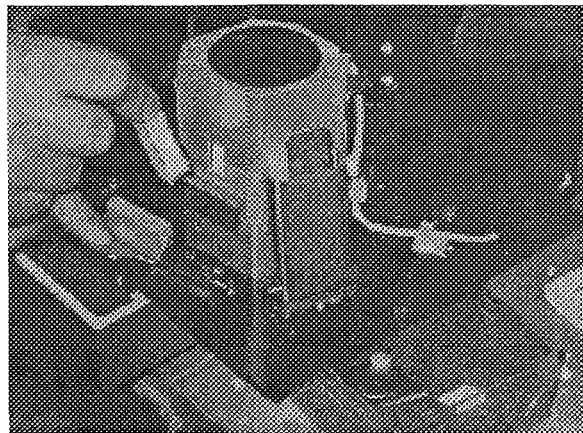


Fig. 2. Insertion of the irradiated sample into a Lambda 9 spectrophotometer with DRS light integrating equipment.

Although the instrumental part of the DRS method requires the modern state of art of optoelectronics and computer assisted acquisition and data processing, the theory of diffuse reflection spectroscopy dates back almost to the first quarter of the XX Century. Frequently quoted, an early paper by Kubelka and Munk [1] does not explain bases of the method and the theory behind it; only the second one published after the WWII by the mentioned leading author [2] reveals complicated mathematics behind it. More information can be found in later comments [3] and [4]. These papers have presented the theoretical treatment of the phenomenon, leading to equations connecting the new approach with traditional equations of extinction, known as the Lambert-Beer law. New equations involve  $\epsilon$ , the molar extinction coefficient. However, a simple determination of  $\epsilon$  from the diffuse reflection measurement is not possible, because the Kubelka-Munk function  $F(R)$  involves the coefficient  $S$  describing a scattering coefficient of the matrix. Therefore, the calculation of  $\epsilon$  is difficult especially in the case of polymers, and in some cases seems to be impossible to solve at the time being. Nevertheless, the comparative value of changes of spectrum after irradiation, effect of reactions with gases, etc is of a great value.

The shape of the sample of polymer is in principle unrestricted, however, there may not be any differences in the surface of unirradiated and irradiated samples. That condition is fulfilled in the case of powders, like widely investigated by our team - virgin polypropylene, or composites of polyethylene with solids like alanine or sodium chloride. Films of smooth surface, which yield much of specular reflection, can cause difficulties in keeping exact identity of the surface of reference and irradiated sample. Therefore we have introduced during the year 1999 a technique of roughening of the surface of such polymers. After such treatment, the relation of light reemitted from the inside of the sample to the amount reflected is increased, improving the precision of the measurement.

A comparison of spectrophotometric results with EPR spectra shows an additional advantage of the DRS method, because spectrophotometry detects any species showing electronic spectra, whereas EPR spectroscopy is limited to paramagnetic species, not necessarily present in irradiated material, long time after the irradiation. Another advantage is signalled, namely the positive role of investigation of rather shallow surface layer of polymer. The information needed often at higher LET radiation effects in polymer systems is easily supplied by DRS. Low range of high LET radiations is of advantage, because most of the energy is deposited close to the surface, i.e. in the layer "seen" preferably by the DRS. Low intensity of high LET radiations demands a several days lasting exposure to reach the dose sufficient to observe spectral effects. The method works efficiently at similar depths as the range of ionising particles in the material.

Our new approach to the radiation chemistry of solid state has helped already to quantify the solid state dosimetry as labels, previously only semiquantitative [5] in the estimate, but we hope that a wider application of DRS to the radiation chemistry of polymers will result in a much more important field.

## References

- [1]. Kubelka P., Munk F.: Ein Beitrag zur Optik der Farbanstriche. *Z. Tech. Phys.*, **12**, 593 (1931).
- [2]. Kubelka P.: New contributions to the optics of intensely light-scattering materials. Part I. *J. Opt. Soc. Amer.*, **38**, 448 (1948).
- [3]. Kortüm G.: *Reflexionsspektroskopie*. Springer, Berlin, Göttingen etc. 1966.
- [4]. Perkampus H.-H.: *UV-VIS spectroscopy and its applications*. Springer, Berlin, Heidelberg etc. 1992.
- [5]. Zagórski Z.P., Rafalski A.: Diffuse reflectance spectroscopic quantification of absorbed dose indicated by labels. *Radiat. Phys. Chem.*, **57**, 725 (2000).

## ROLE OF SPURS IN IRRADIATED POLYMER BLENDS



PL0101473

Zbigniew P. Zagórski

Radiation processing of polymers, applied for the purpose of modification of properties, is connected with radiolytic changes in molecules of components and additives. Ionising energy deposition is distributed to absorbing moieties according to their contribution to the electron pool in the material. The participation of primary ionisation acts in additives of low concentration is negligible, but these compounds take part in secondary reactions. Radiation induced modification of properties, (e.g. commercially important crosslinking of neat polyethylene) is correlated with chemical changes. These are detected by product analysis and specific techniques for the determination of transients, e.g. by electron paramagnetic resonance (EPR). Important product analysis methods, i.e. UV-Vis absorption spectrophotometry can be applied in polymer chemistry only as diffuse reflection spectrophotometry (DRS) [1].

In the last decades, radiation processing of polymers has been developed on a large scale and commercially implemented due to the availability of large gamma and electron beam sources of low linear energy transfer (LET) ionising radiation. Many basic questions are not answered yet and also the number of possible combinations of polymers and blends remains far to be exhausted. Radiation chemistry of polymers shows that in spite of identical starting point of reactions, i.e. the single ionisation spurs (80% of deposited energy, independently of the kind of polymer), a diversity of subsequent chemical reactions occurs, specific for particular types of polymers. These reactions are influenced by additives present for the purpose of conventional processing and by uncontrolled reagents like oxygen in surrounding atmosphere, extremely reactive with free radicals formed by the interaction of ionising radiation in the polymer. Although the primary products induced by radiation

are formed randomly in particular moieties of the material, in the proportion resulting from their electron participation in the mixture or blend, the transfer of energy in the initial stage or transfer of intermediates occurs in subsequent stages of the development of reactions. In the result, variety of final products is formed, identified in the course of product analysis. The latter involves stable products as well as intermediates of different stability.

The remaining 20% of energy deposited in the polymer appears in multi-ionisation spurs with products different from those which are produced in the dominating single-ionisation spurs. The participation of multi-ionisation spurs rises sharply with increasing linear energy transfer (LET) values of the applied radiation. Ten MeV protons already double the participation of large spurs in comparison with low LET radiation ( $\gamma$ -rays, X-radiation and fast electrons used in radiation processing). Multi-ionisation spurs dominate over single-ionisation spurs in the case of heavy ions beams, which cause the destruction of polymers along their tracks, producing negligible yields of free radicals characteristic for low LET radiations. That phenomenon is common for all irradiated media, liquid and solid [2] and has to be taken into account also in the field of radiation chemistry of polymers. This paper shows that products of single-ionisation spurs can be different to those of multi-ionisation spurs. They are different in the most popular case, i.e. of water radiolysis, where single-ionisation spurs are the source of free radicals, i.e. hydrated electrons, hydrogen atoms and hydroxyl radicals. Multi-ionisation spurs yield hydrogen peroxide and molecular hydrogen of completely different, low reactivity. A more complicated situation is in the case of solids, as seen on a simple model of alanine. Here the main product of single-ionisation spurs is ammonia, but also ammonia is the product of



multi-ionisation spurs, where it is one of the debris of one molecule of alanine or a cluster of molecules of alanine, which obtained too much energy to survive. A single molecule of alanine ionised in a single ionisation spur survives easily, as an anion radical  $\text{CH}_3\text{C}^+\text{HCOO}^-$ . However, among the products of radiolysis is  $\text{CO}_2$ , which is a constituent of debris of a molecule or cluster, which has obtained a substantial excess of energy. There is no other way, on which  $\text{CO}_2$  could be formed. Even the loss of an electron in single ionisation on  $\text{CO}_2^-$  zwitterion does not result in decarboxylation and the dominating reaction in the single ionisation spur is deamination of alanine. Therefore the radiation yield of carbon dioxide is a measure of the yield of multi-ionisation spurs.

Looking for products which may indicate the role of multi-ionisation spurs, one has to find the effect of concentrated deposits of energy in a casual place in the polymeric chain. What is likely in the case of polymers? The basic radiation induced reaction, originating in all types of ionisation spurs is dehydrogenation (abstraction of hydrogen), therefore the radiation yield of  $\text{H}_2$  has been taken as the most general indicator of energy transfer in Figs.3 and 4 in paper [3]. The dehydrogenation causes subsequent reactions, mainly the formation of unsaturated moieties in the polymer, but with very different secondary consequences, from cross-linking to degradation. Both reactions are running parallel, but in polyethylene the final crosslinking is dominating, being the base of production of heat-shrinkable polymers, whereas in polypropylene radiation leads to the degradation. The latter phenomenon spoils the application of polypropylene, undergoing radiation processing, if proper additives are not applied. Ethylene-polypropylene copolymers have a comparatively good radiation resistance, because negative effects of polypropylene degradation are counterbalanced by cross-linking of polyethylene. Unfortunately, the dominating effect of formation of  $\text{H}_2$  in irradiated polymers, cannot be taken as indicator of single- or multi-ionisation spurs, because it dominates in every size of spurs. One has to look in more complicated details of radiation chemistry of polymers. Such features have been observed in the case of aliphatic-aromatic blends of polymers, reported by Żuchowska, Zagórski, Przybytniak, Rafalski [4].

Aromatic compounds are more resistant towards ionising radiation because of mechanisms directing the dissipation of energy straightforward into heat. That property of aromatics, also of polymers [3] with aromatic moieties, is partially protecting aliphatic blocks present in the material from radiolysis. Therefore, butadiene-styrene elastomer is more resistant toward the ionising radiation than polybutadiene rubber, as expressed e.g. by radiation yield of hydrogen. In our previous papers, effects of radiation on PE-linear SBS [4] have been described. Processes in PE-SBS blends with 25, 50 and 75% of SBS were not the simple sum of processes observed in neat PE and neat SBS polymer, which indicates

interactions between two components of the blend. Our next paper [5] deals with the absorption of ionising energy in thermoplastic elastomer-PP blends in a full range of proportions, which helps to assume the mechanisms of energy transfer. Fig.1a-c in that paper show the EPR spectra of PP-SBS blends in the function of time elapsed after 60 kGy irradiation at room temperature and the storage time at the same temperature. All spectra are shown without deconvolution and separation of particular signals. Fig.2 in [5] shows the decay of radicals in the same system, but expressed as concentration of spins, which is important for the hypothetical explanation of mechanism of phenomena in terms of spurs. The spectroscopic investigations (diffuse reflectance spectrophotometry, DRS) were performed on samples of the same composition. The method allows to record optical absorption spectra in polymer blends of poor transparency. Fig.3 in [5] shows the spectra of products absorbing in UV, in irradiated blends of polypropylene containing no SBS, 10, 25 and 75% of SBS and the SBS alone. The products exhibit main absorption band at 312 nm and are more stable than free radical products (except peroxides) observed by the EPR method. Although a precise identification of these semi-stable products is not possible at the time being, the most probable explanation of the UV absorption is that it is due to unsaturated moieties (UM) in the polypropylene chain. However, there is a striking difference between the dependence of the concentration of unsaturated species on the composition of aliphatic-aromatic composition. In our case, the fact of dramatic reduction of formation of UM already by a 10% addition of SBS is a remainder of the classic concave curve of radiolysis vs. composition of an aliphatic-aromatic mixture in radiation chemistry, including polymers [3]. The radiolysis of aromatic component is not only less extensive in comparison with the aliphatic participant, but also a protection effect is exhibited by the aromatic participant. The phenomenon is explained by energy transfer of single-ionisation spurs to the energy dissipating constituent. Therefore, the 10% participant in energy absorption, by a 10% concentration of SBS turns in ca. 30% the effect due to the energy transfer of single ionisation spurs in polypropylene (90% participation in primary energy absorption) to the SBS moieties.

The same PP-SBS systems show an opposite picture in the EPR investigation: the yield of spins in irradiated samples, shows no diminishment of radical concentration in the blend containing 10% of SBS but even a slight increase, immediately after irradiation, 3 h after irradiation and 3 days after! This strange difference can be explained only by in-deep discussion of early stages of radiolysis in polymers, in terms of single- and multi-ionization spurs. As it is known, in general, radiation chemistry, almost from the beginning of that discipline, the products of both kinds of spurs are more or less different, depending on the chemistry of irradiated

system. In the case of low linear transfer of energy (LET) radiations, i.e.  $\gamma$  and high energy electrons, ca. 80% of energy is deposited in single-ionisation spurs, responsible for free radicals, and the rest is located in multi-ionization spurs, which produce mainly the debris of a region of the molecule and in the case of polymers cause the non-repairable scission of the chain. Therefore, two loose ends of a chain are formed, being the sites of radicals, able to react with oxygen to peroxides, with hydrogens on neighbouring chains etc. The location of multi-ionisation spurs is completely random and is not a subject to any energy transfer, or influence, as it is in the case of single ionisation spurs, mentioned above in connection with EPR measurements. The main support for the assumption that the latter are connected with multi-ionisation spurs, is the radiation yield of spins, in other words of free radical sites on the chains, in our case mainly at their new ends, formed during scission. The yield of these effects is, in the case of EPR measurements, close to 0.53 per 100 eV of absorbed energy (or 0.055  $\mu$ moles per J in the SI system). The precision of the measurement of yields of spin, by comparison with the concentration of spins in DPPH (a standard practice in the EPR methodics), measured in the same conditions, is  $\pm 25\%$ , but even taking the upper limit of the confidence, the yield is adequate to the 20% energy-yield of multi-ionisation spurs.

Presented results of free radical species measurements and of optical absorption spectra of products

formed during radiolysis allow to ascribe first group of the mentioned results to the effects of multi-ionisation spurs and the second to the single ionisation spurs and energy transfer phenomena. The first observation of different effects from single- and multi-ionisation spurs in polymers ever, is the foundation of further research on generalisation of the role of spur size in polymers in future years. The investigations are continued.

Part of the report was used in the invited lecture "Modification, degradation and stabilization of polymers in view of the classification of radiation spurs" on the MoDeSt 2000 Conference, Palermo, Italy, 3-8 September 2000.

## References

- [1] Zagórski Z.P., Rafalski A.: Radiation chemistry of polymers as recognized by diffuse reflectance spectrophotometry (DRS). In: INCT Annual Report 2000.
- [2] Zagórski Z.P.: Solid state radiation chemistry - features important in basic research and applications. *Radiat. Phys. Chem.*, **56**, 559-565 (1999).
- [3] Zagórski Z.P.: Wybrane zagadnienia chemii radiacyjnej polimerów (Selected features of the radiation chemistry of polymers). *Polimery*, **42**, 141-147 (1997).
- [4] Przybytniak G.K., Zagórski Z.P., Żuchowska D.: Free radicals in electron beam irradiated blends of polyethylene and butadiene-styrene block copolymer. *Radiat. Phys. Chem.*, **55**, 655-658 (1999).
- [5] Żuchowska D., Zagórski Z.P., Przybytniak G.K., Rafalski A.: Influence of butadiene/styrene copolymers on the stabilisation of polypropylene in electron beam irradiations. *Int. J. Polym. Mater.*, in print.

## EPR SPECTROSCOPY OF $\gamma$ -IRRADIATED POLYCRYSTALLINE ASPARAGINE AND ASPARAGINE-CONTAINING PEPTIDES

Grażyna Strzelczak, Krzysztof Bobrowski, Chantal Houée-Levin<sup>1/</sup>, Jacqueline Bergés<sup>2/</sup>

<sup>1/</sup> Université Paris-Sud, Orsay, France

<sup>2/</sup> Université Pierre et Marie Curie, Paris, France

### Introduction

The most commonly observed hydrolytic reactions (spontaneous, nonenzymatic) that occur in peptides and proteins involve asparagine residues. Many factors, both endogeneous (e.g. primary, secondary, tertiary, and quaternary structures) and exogeneous (e.g. pH, buffer concentration) can influence the rate of hydrolytic reactions. It is well established that asparaginyl residues are prone to spontaneous deamidation, at rates that vary widely as a function of their amino acid sequences. It was shown that in various pentapeptides containing asparaginyl residues in the central position that the half-lives of the spontaneous deamidation varied from 6 days to 9 years. This observation led to the hypothesis that the amino acid sequences around asparaginyl residues in various enzymes might have been selected for through evolutionary pressures to serve as biological clocks to govern the rates of turnover of enzymes in vivo. This concept is consistent with the fact that the in vivo rates of enzyme turnover increase with the content of asparaginyl residues. The age-related accumulation of abnor-

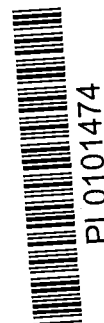
mal forms of enzymes have been attributed to the deamidation of asparaginyl residues. The most convincing evidence that deamidation contributes to the age-related pool of altered enzymes comes from the studies showing that the accumulation of labile isoenzymic forms of triose phosphate isomerase in bovine eye lens and cultured dermal fibroblasts of individuals with premature aging diseases, i.e. progeria, Werner's syndrome is due to the sequential deamidation of two asparagine residues (Asn<sup>71</sup> and Asn<sup>15</sup>).

### Aim

Oxidation constitute additional major degradation pathway of peptides and proteins. In contrast to the extensive information available about the hydrolytic asparagine (Asn) degradation pathways, there is, at present, considerably less mechanistic understanding of the underlying oxidation mechanisms, both in the aqueous medium and in the solid state.

The following problems are addressed:

- identification of radical transients formed on  $\gamma$ -radiolysis of polycrystalline asparagine and methionyl-asparagine dipeptide;





- analysis of the final product: carbon dioxide;
- stability of the free radical cations coming from electron ejection by ionizing radiation;
- ease of decarboxylation vs. deamidation processes as a consequence of energy deposition;
- loss of hydrogen atom as a consequence of irradiated sample warming-up.

### Experimental

The samples of polycrystalline asparagine (Asn), methionyl-asparagine (Met-Asn) and valyl-asparagine (Val-Asn) were evacuated and irradiated in liquid nitrogen with a dose of 4 kGy in a  $^{60}\text{Co}$ - $\gamma$ -source. The radicals produced by radiation were studied over the temperature range of 77-293 K by applying an electron spin resonance (ESR) technique using a Bruker ESP-300 spectrometer with a variable temperature unit. The ESR spectra were analyzed by computer simulation program (provided by Dr. D. Dulling from NIH, USA). Carbon dioxide analysis was performed by means of a gas chromatographic head-space technique using a Shimadzu GC-14C gas chromatograph equipped with a thermal conductivity detector and a Porapak Q column.

### Quantum chemical calculations

Preliminary ab initio calculations have been applied for bond dissociation energies of some selected radicals under study. All isolated species were optimized using large basis sets (6-31G\*0 at the MP2 level using the program Gaussian 98. Our previous works demonstrated the necessity of using such large basis sets. Solvent effects were studied using the SCRF option of Gaussian. In this case DFT was used (B3LYP) with the same basis set.

### Results

#### EPR

In asparagine-containing peptides anion carbonyl radicals formed by the addition of electron to the carbonyl group of peptide bond (singlet  $g=2.003$  and  $\Delta H=8$  G) were detected at 77-95 K. In asparagine and the amide anion a radical is observed (doublet with  $a=24$  G). At 180-250 K hydrogen abstraction radicals from the methylene group in the side chain of asparagine were detected in asparagine as well as in Met-Asn and Val-Asn (with the hyperfine splitting of  $a_{\text{H}}=16$  G and  $a_{2\text{H}}=3.5$  G). Additionally, in Val-Asn at 200 K deamidation radical is observed (triplet with  $g=2.003$  and  $a_{2\text{H}}=19.5$  G) from valine residue and  $\alpha$ -(alkylthio)alkyl radical (triplet with  $g=2.0045$  and  $a_{2\text{H}}=20$  G) in Met-Asn. On further warming to above 250 K, in asparagine and asparagine-containing peptides the decarboxylation from the Asn-residue are presumably observed with ( $a_{\text{H}}=16$  G and  $a_{2\text{H}}=19.5$  G). In asparagine, additionally (triplet of doublets) is observed with hyperfine splittings ( $a_{2\text{H}}=36$  G and  $a_{\text{H}}=10$  G), which can be assigned to the deamidation radicals. (Figs.1 and 2).

At room temperature, H-abstraction radicals from the  $\alpha$ -carbon of asparagine and Asn-residue in Met-Asn (Fig.3) and Val-Asn dipeptides are formed (triplet with  $a_{2\text{H}}=17$  G).

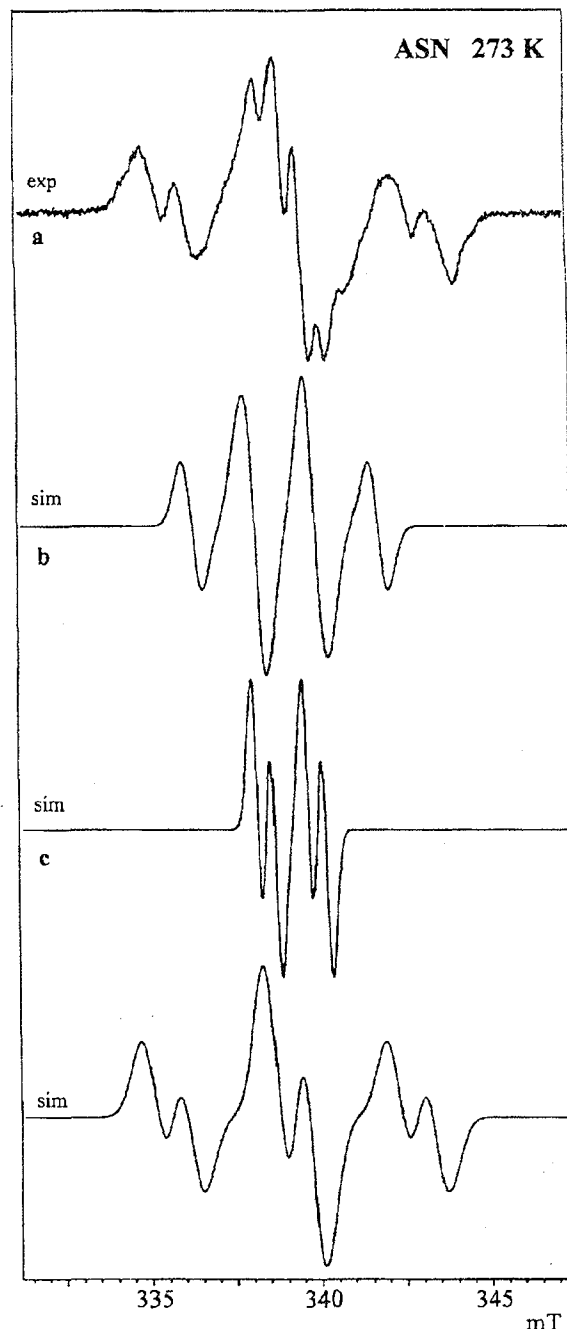


Fig.1. EPR spectra of asparagine: a - decarboxylation radicals, b - H-abstraction radicals from the methylene group in the side chain of asparagine, c - deamidation radicals.

### Quantum chemical calculations

Asparagine radicals: the radical cation is unstable: during the optimization process, the  $\text{C}_{\alpha}\text{H}-\text{COOH}$  bond is lengthened up to bond dissociation. The cation undergoes "spontaneous decarboxylation". However, the bond dissociation energy of the latter is higher than that of  $\text{C}_{\beta}\text{CONH}_2$ , indicating that deamidation is less energy-consuming than decarboxylation. Free radicals resulting from hydrogen atom abstraction were fully optimized. Hydrogen atom abstraction from the  $\text{C}_{\alpha}$  requires less energy and gives a more stable radical. The energy difference is ca.  $22 \text{ kcal} \cdot \text{mol}^{-1}$ .

Asparagine-containing peptides radicals: in the radical cation, no bond is lengthened upon ion-

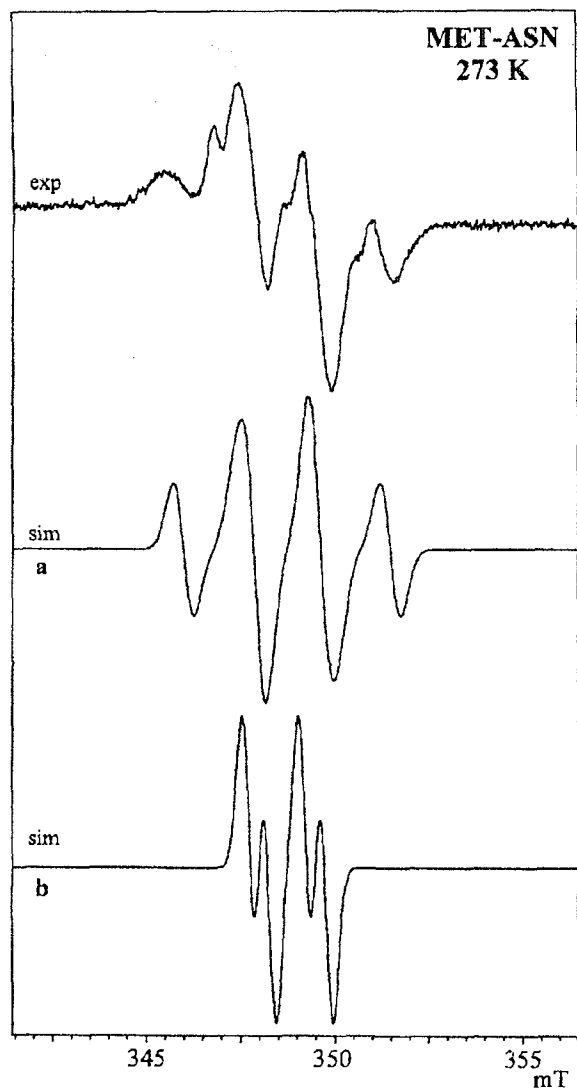


Fig.2. EPR spectra of Met-Asn peptide: a - decarboxylation radicals, b - H-abstraction radicals from the methylene group in the side chain of asparagine.

ization, hence the ionization potential was calculated as 8.7 eV. Deamidation requires less energy than decarboxylation. However, the BDE for deamidation is higher for Asn-containing peptides, as compared with BDE in free Asn. On the other hand, the BDE for decarboxylation is similar, both in peptides and Asn. These calculations rationalize

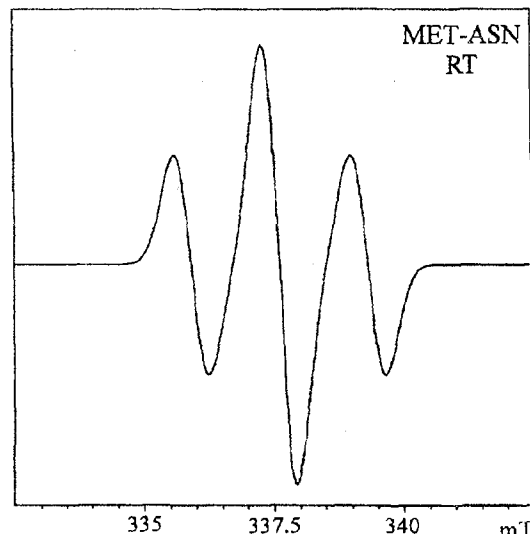


Fig.3. EPR spectrum of Met-Asn and Asn, H-abstraction radicals from  $\alpha$ -carbon of Asn residue.

higher  $\text{CO}_2$  yields measured in Asn-containing peptides, as compared with Asn. Similarly to Asn, hydrogen abstraction from the  $\text{C}_\alpha$  requires less energy, as compared to  $\text{C}_\beta$ , and gives a more stable radical. The energy difference is ca.  $14 \text{ kcal} \cdot \text{mol}^{-1}$ .

#### Conclusions

Anion carbonyl radicals are formed by the addition of an electron to the carbonyl group of the peptide bond in asparagine-containing peptides at low temperature, that further undergo deamidation process. In asparagine the amide anion is observed, and deamidation does not occur.

At 180-250 K hydrogen abstraction radicals from the methylene group in the side chain of asparagine were detected in asparagine as well as in Met-Asn and Val-Asn.

At a temperature above 250 K decarboxylation radicals are observed in asparagine and asparagine-containing peptides. However, decarboxylation yields are higher in peptides.

Additionally, in asparagine EPR spectrum was detected which can be assigned to the deamidation radicals.

H-abstraction radicals from the  $\alpha$ -carbon in asparagine and in Asn-residue in Val-Asn and Met-Asn dipeptides were detected at room temperature.

## MULTIFREQUENCY EPR STUDY OF RADICALS PRODUCED BY RADIATION IN SHELLS AND CORALLITE

Grażyna Strzelczak, Wacław Stachowicz, Jacek Michalik, Gauthier Vanhaelewyn<sup>1/</sup>, Freddy Callens<sup>1/</sup>, Etienne Goovaerts<sup>2/</sup>

<sup>1/</sup> Ghent University, Ghent, Belgium

<sup>2/</sup> University of Antwerp, Belgium

### Introduction

Shells of molluscs and corals of sea water are composed mainly of calcium carbonate and partly of organic matrix. Calcium carbonate appears in two main crystal forms: as calcite and as aragonite. Many organisms (molluscs and corals) build their skeletons of aragonite.

Under the action of ionising radiation a lot of paramagnetic species are produced in shells, which are usually very stable and can be studied by an EPR technique at room temperature.

Radicals or defects produced by radiation in the mineral part of shells are utilised for many applications: e.g. - dating of archeological remnants,



PL0101475

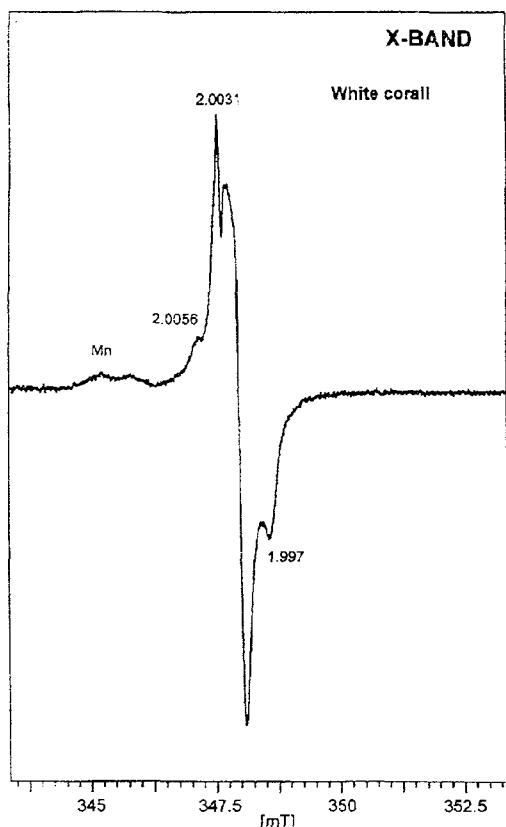


Fig.1. Experimental EPR spectrum recorded with powdered corallite of white coral; X-band measurement.

retrospective dosimetry using tooth enamel, for detection of bone containing food, in medical studies.

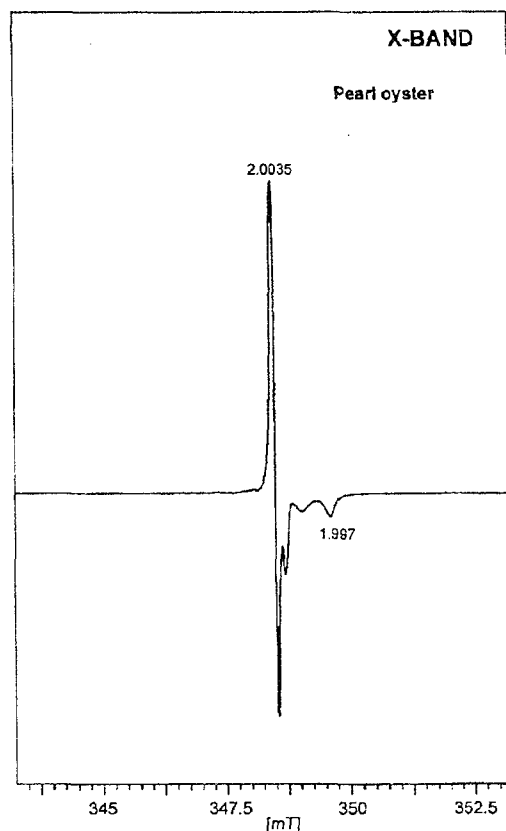


Fig.3. Experimental EPR spectrum recorded with powdered pearl oyster shell (*Meleagrina vulgaris*); X-band measurement.

### Experimental

The samples of shells and corals were irradiated with a  $^{60}\text{Co}$  gamma-source at a dose of 7 kGy and

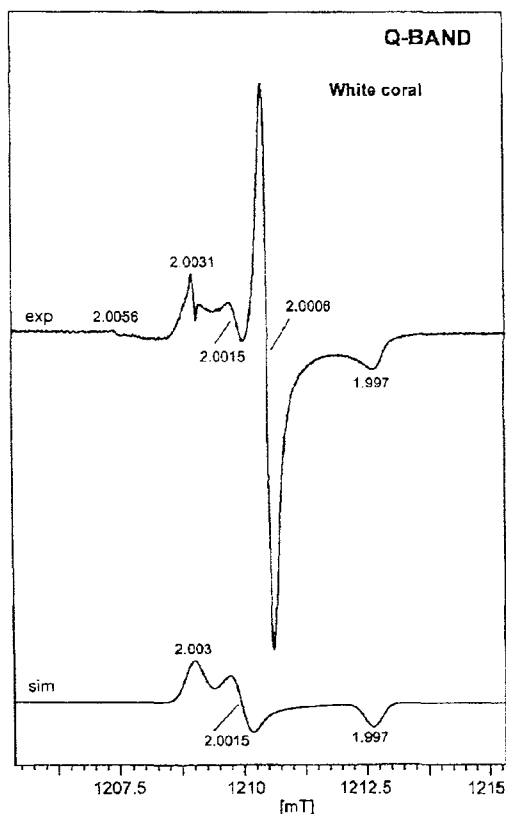


Fig.2. Experimental EPR spectrum recorded in white coral; Q-band measurement. Lower spectrum - simulation of the orthorhombic  $\text{CO}_3^{2-}$ .

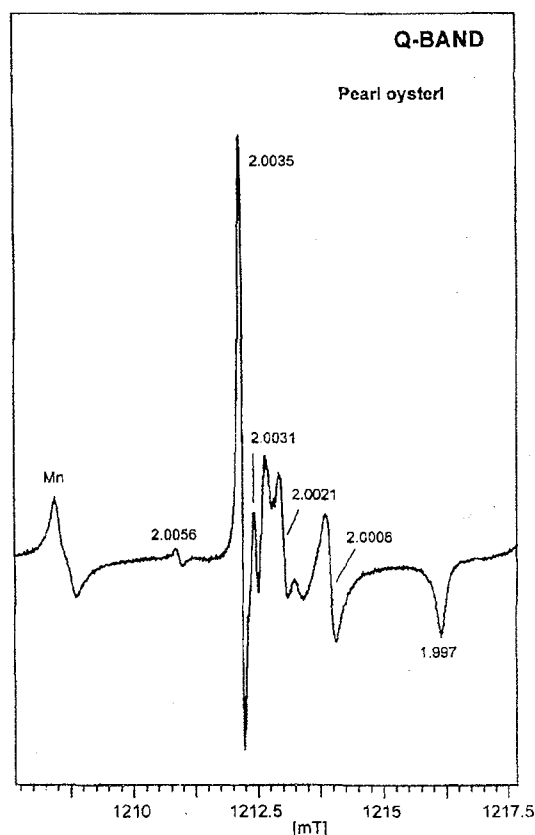


Fig.4. Experimental EPR spectrum recorded in pearl oyster shell; Q-band measurement.

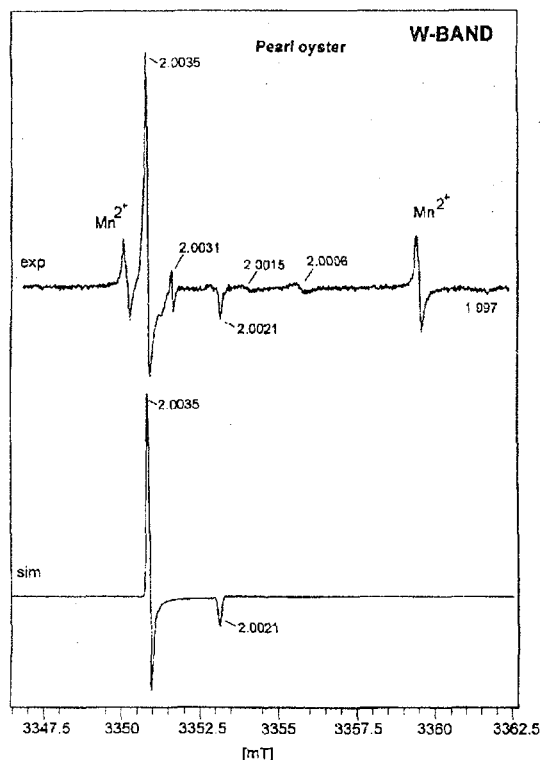


Fig.5. Experimental EPR spectrum recorded in pearl oyster shell; W-band measurement. Lower spectrum - simulation of the axial  $\text{SO}_3^-$  radical anion.

with an X-ray tube at a dose of about 20 kGy. The paramagnetic species produced by radiation in them were subsequently studied by X, Q and W-bands EPR spectroscopy. The EPR X-band measurement have been done in this Institute by using a Bruker ESP 300 spectrometer. Q-band measurements were performed in the Ghent University by using a Bruker Elexys E-500. W-band measurements were carried out in the University of Antwerp with the use of a Bruker Elexys E-600 spectrometer.

#### Results

The most stable, long living paramagnetic centre identified in all the investigated shells and corals is the anion radical  $\text{CO}_2^-$  which appears as:

- $\text{CO}_2^-$  isotropic with  $g=2.0006$  and  $\Delta H=0.3$  mT and
- $\text{CO}_2^-$  orthorhombic with  $g_x=2.0030$ ,  $g_y=1.9970$ ,  $g_z=2.0015$  and  $\Delta H=0.25$  mT.

In the spectrum of white coral sample recorded at the X-band, the lines assigned to both  $\text{CO}_2^-$  ion radicals are overlapped (Fig.1). The records of the same sample taken at the Q-band show the spectra better resolved with individual lines characterised by the g-values corresponding to both types of ion radicals (Fig.2).

Additional two signals were distinguished in the spectra: one with  $g=2.0031$  could be probably derived from  $\text{SO}_3^-$  isotropic and the second with  $g=2.0056$  attributed to  $\text{SO}_2^-$  isotropic radical ion.

A computer simulation was used to prove the identity of the components of experimental spectra.

In the EPR spectrum of pearl oyster shell recorded at X-band, the lines are overlapped (Fig.3), but in the Q and W-band spectra we have observed the manganese  $\text{Mn}^{2+}$  paramagnetic ion which is very well seen (Figs.4 and 5). Besides, a strong signal presumably attributed to isotropic  $\text{SO}_2^-$  ( $g=2.0056$ ) radical, and another one to  $\text{SO}_3^-$  axial with  $g_{\perp}=2.0035$  and  $g_{\parallel}=2.0021$  were observed.

#### Conclusion

The EPR spectra of natural shells and corals exposed to ionising radiation when recorded in X-band are complex and not easy to be interpreted because the individual EPR lines are rather narrow and superimposed. The spectra recorded in Q and W-bands were found to be resolved satisfactorily and the assignments of single paramagnetic species in complex spectra were possible to be done.

This work has been done in the frame of Scientific and Technological Cooperation Belgium-Poland, BIL 97/174B 1698.

The extended version of this article is accepted for publication in "Radiation Research".

## QUALIFICATION OF THE CONCENTRATION RATIO OF RADIATION INDUCED HYDROCARBONS IN RELATION TO FATTY ACID COMPOSITION WITH THE USE OF A GAS CHROMATOGRAPH (GC)

Katarzyna Lehner, Wacław Stachowicz

Ionising radiation induces in foodstuffs, which contain fat, some complex chemical changes leading, among others, as compared with unirradiated food, to an increased release of hydrocarbons. Generally, the cleavage of certain chemical bonds in triglycerides results in the formation of two groups of hydrocarbons: (1)  $\text{C}_{n-1}$  (hydrocarbons which have one C atom less than the original fatty acid) and (2)  $\text{C}_{n-2:1}$  (hydrocarbons with two C atoms less than the original fatty acid and additional double bond in position 1). The detection and quantitation of these hydrocarbons is the basis for the identification of

irradiated food. Natural fat consist of fatty acids containing even numbers of C atoms in a molecule, the most often 16 or 18 (that is for animal fat). The saturated fatty acids are palmitic acid (16:0) and stearic acid (18:0) as well as the unsaturated ones, i.e. oleic acid (18:1) and linoleic acid (18:2). The treatment of foods with ionizing radiation induced usually formation of the following hydrocarbons: pentadecane (15:0), tetradecene (14:1), heptadecane (17:0), hexadecene (16:1), heptadecene (17:1), hexadecadiene (16:2), heptadecadiene (17:2), hexadecatriene (17:3). These products appear in small



PL0101476

quantities ( $\mu\text{g/g}$  fat), depending on the dose of irradiation and the numbers of fatty acids present in triglyceride.

Previously some preliminary experiment have been done with chicken meat. At present, the more advanced experiments were conducted with 2 types of red meat, beef and pork as well as with chicken carcasses. After portioning, the meat was irradiated with three doses of gamma rays: 1.5, 3.0 and 5.0 kGy. The preparation of samples for GC measurement were done by the procedure which is based on the European Standard No 1784 [1]. Some modifications have been done in order to obtain higher yields of hydrocarbons. This makes, according to our expedience, the GC analysis more reliable and reproducible.

The GC measurements of hydrocarbons have been done with a capillary column installed with a Perkin Elmer Mode 8700 apparatus equipped with a flame-ionisation detector (FID). At the beginning, the instrument was tested with the use of hydrocarbon standards to prove the reproducibility of quantitation i.e. determination of the proportions between GC peaks assigned to individual hydrocarbons.

The GC examination involved a comparison of the number and the quantity (normalised GC peak heights) of produced hydrocarbons with the number and the content of original acids in food, in obedience to the procedure given in the European Standard EN 1784. In the case of chicken carcasses the full coincidence of our results with the data given in the Standard was achieved. On the other hand, in the case of beef and pork the results strayed a bit from the standard. This might be caused by the different fatty acid composition in the local (Polish) food, arising probably from different feeding. This important suggestion should be confirmed by studying the fatty acid composition in meats, which were the subject of present experiments. A more detailed information on this study will be found elsewhere [2].

## References

- [1]. European Standard: Foodstuffs - Detection of irradiated food containing fat - Gas chromatographic analysis of hydrocarbons. (BS EN 1784). BSI, 1997.
- [2]. Lehner K., Stachowicz W.: Wykrywanie i oznaczanie radiacyjnie indukowanych węglowodorów za pomocą chromatografii gazowej jako metoda identyfikacji napromieniowania żywności. Raporty IChTJ. Seria B nr 7/2000. IChTJ, Warszawa 2000.

## DETECTION OF IRRADIATION OF FROZEN FISH MEAT BY SINGLE CELL GEL ELECTROPHORESIS

Kazimiera Malec-Czechowska, Zbigniew Szot, Waław Stachowicz, Marcin Kruszewski

Single cell gel electrophoresis (comet assay) is a method of detection of DNA damage at the cellular level. The method is widely used nowadays in basic and applied science and has many applications, for example, in biomonitoring, medicine and toxicology. Since several years the comet assay is also tested as a tool for the detection of irradiated food [1]. The identification of irradiated beef, pork and chicken meat with the use of comet assay is also carried out in the Laboratory for Detection of Irradiated Foods, INCT. The results of these experiments were presented in earlier publications [2,3]. Recently, we performed a study on the identification of fish meat, i.e. carp, trout and salmon.

The fresh fishes were purchased in a retail trade. From each fish three parallel samples were prepared and immediately frozen at  $-21^{\circ}\text{C}$ . Two samples taken from each fish were irradiated with gamma rays from a  $^{60}\text{Co}$  source with a dose of 1.5 or 3.0 kGy. All samples were stored until examination in the frozen state (about one month). The procedure for identification of irradiation of food by the comet assay consists of the following steps [1,4]:

- preparation of cell suspension from a food sample;
- transfer of agarose cell suspension onto a slide precoated with a thin agarose layer;
- lysis of the cells in order to disrupt cell membranes with the use of a lysis buffer;
- gel electrophoresis of fragmented DNA; during electrophoresis DNA fragments will stretch or migrate out of the cell nucleus;

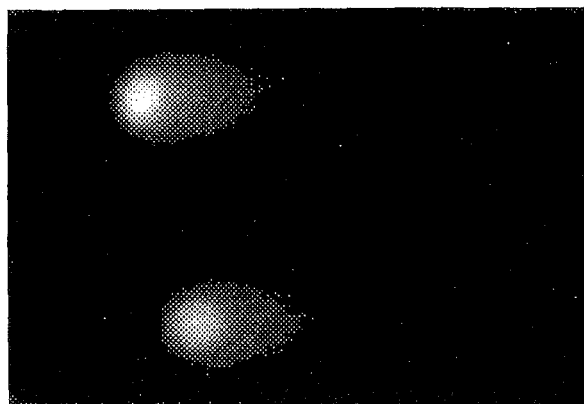
- staining the cells on slides for microscopic evaluation of the pattern of DNA migration.

Application of the comet assay to a new type of foodstuff requires an individual evaluation of each step of the procedure. Special attention should be paid to the optimisation of lysis conditions, i.e. concentration of the lysis buffer, treatment time, and to electrophoresis conditions. Based on the results obtained in this Laboratory, we propose to adapt the following procedure for the evaluation of irradiation of fish meat by comet assay: Place 1.5 g of fish muscles (thin slices) in a small beaker containing 5 ml of cold PBS. Place the beaker in an ice-cold water bath and homogenise the content with a magnetic stirrer for 5 min. Filter the suspension through a  $250\ \mu\text{m}$  sieve cloth and leave to sediment for 5 min in the ice-cold water bath. Mix  $300\ \mu\text{l}$  of the cell suspension with 1 ml of warm ( $45^{\circ}\text{C}$ ) 0.8% agarose in PBS and put  $100\ \mu\text{l}$  of this suspension on a microscope slide precoated with a water solution of 0.5% agarose. Immediately place a cover slip on it. Place the slide on ice for 5 min until a stable gel is formed. Remove the cover slip and place the slides in a lysis solution (2.5% SDS in electrophoresis buffer) for 8 min. After lysis immerse the slides in electrophoresis buffer ( $0.5 \times \text{TBE}$ ) for 5 min. After conditioning, place the slides in the horizontal electrophoresis chamber and fill the tank with fresh electrophoresis buffer. Conduct electrophoresis at room temperature, at a potential of 2 V/cm for 2 min. Remove the slides from the electrophoresis chamber and immerse in water for 5

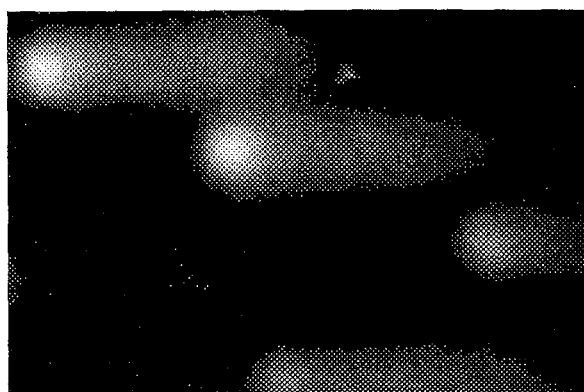


PL0101477

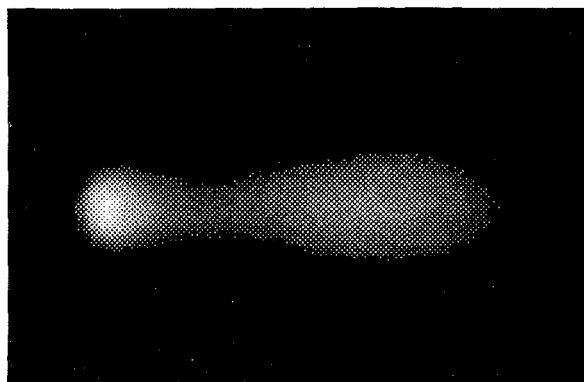
## DAPI staining



Dose 0 kGy



Dose 1.5 kGy



Dose 3.0 kGy

## Silver staining

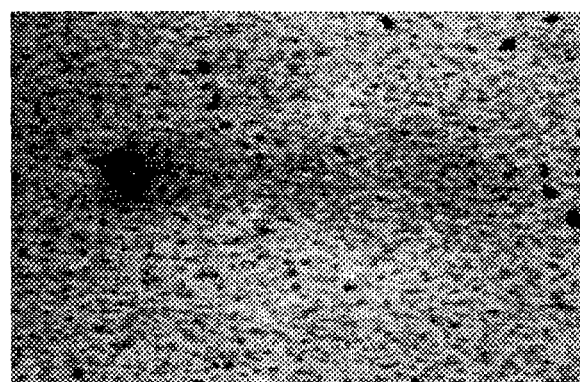
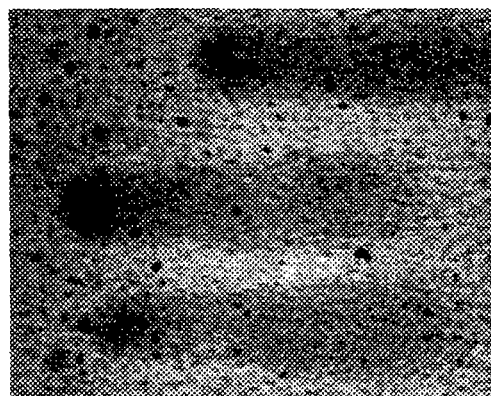
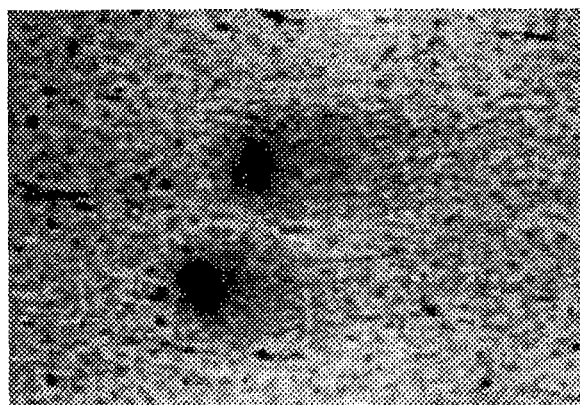


Fig. Comet assay microscopic images of cells isolated from carp muscles non-irradiated and exposed to gamma radiation with doses 1.5 and 3.0 kGy.

min. Subsequently the slides are stained with a fluorescent dye (DAPI) according to Kruszewski et al. [2] or with silver according to Delincée [4]. The microscope images of cells taken from carp samples are presented in Fig. The images of cells taken from the trout and salmon samples are similar (data not shown). It is clearly seen from the images that the amount of DNA in the comet tail (the DNA migrated from the nucleus due to the irradiation) of irradiated and non-irradiated fish is considerably different. Comets with a short tail or without tail at all easily identify the non-irradiated samples. On the other hand, comets from the irradiated samples

have a distinct head and a long well visible tail of different width. The comets obtained after applying the dose of 3 kGy are slightly different than those observed in the samples irradiated with 1.5 kGy; the end of tail was wider than the head. The results of present examination confirm the applicability of the comet assay for identification of irradiation of fish. This is a new approach in the application of comet assay to the identification of irradiated food. However, our study was performed on model samples kept at proper storage conditions and further investigations are necessary to confirm our results on samples available on the market. We cannot ex-

clude that in case of samples of unknown storage conditions, e.g. imported frozen products or products stored in ice, the comet assay may be applied as screening method only. The positive identification of samples (i.e. irradiation) needs to be proved by other methods less sensitive to inappropriate storage conditions, e.g. EPR spectroscopy of bone excised from fish. This limitation of the comet assay method arises from the fact that fragmentation of DNA is not specific for radiation treatment only. It can be also caused by some physical, chemical or

biological factors like repeated freezing and thawing, storage under unsuitable conditions (enzymes action) etc.

## References

- [1]. Cerda H., Delincée H., Haine H., Rupp H.: *Mutat. Res.*, 375, 167-181 (1997).
- [2]. Kruszewski M., Malec-Czechowska K., Dancewicz A.M., Iwanefiko T., Wojewódzka M.: *Nukleonika*, 43, 2, 147-160 (1998).
- [3]. Malec-Czechowska K., Stachowicz W., Dancewicz A.M., Szot Z.: *Nukleonika*, 44, 4, 549-560 (1999).
- [4]. Delincée H.: *Comet Newsletter*, July (1995).

## GELATINISATION AND AMYLOSE-LIPID COMPLEX TRANSITION OCCURRING IN NATIVE AND GAMMA IRRADIATED STARCHES STUDIED BY DIFFERENTIAL SCANNING CALORIMETRY

Krystyna Cieśla, Ann-Charlotte Eliasson<sup>1/</sup>, Wojciech Głuszewski

<sup>1/</sup> Center of Chemistry and Chemical Engineering, University of Lund, Sweden

The course of gelatinisation and amylose-lipid complex transition, occurring during heating of starch and flour suspensions depends on the structure of starch granules. It was found previously that gamma irradiation influences these processes [1,2]. Significant differences between the maximum viscosities were detected during heating of water suspensions of non-irradiated and irradiated wheat and rye flour. Smaller values of enthalpy were always determined by DSC for both processes taking place in the samples irradiated with doses of 20 and 30 kGy, in comparison to those occurring in the non-irradiated reference samples under the same conditions. Differences between the peak and onset temperatures were also found. The result shows changes in lipids surrounding and confirm the conclusions concerning the decrease in starch granules ordering [3,4] caused by irradiation.

At present, DSC studies were continued for pure samples of wheat starch (product of Sigma) waxy-maize and waxy-potato starches (Lyckeby Starkelsen, Kristianstad) as well as several starch samples extracted from potato, applying various conditions. The samples were irradiated with <sup>60</sup>Co radiation in a gamma cell Issledovatel in the INCT applying doses of 5, 10, 20, 30 kGy with a dose rate of ca. 3 kGy/h. DSC measurements were carried out in the temperature range 10-150°C with heating and cooling rates 10, 5 and 2.5°C/min for the suspensions (closed hermetically in Al pans) with low concentration of starch (20-25%) and with high concentration (45-50%). A Seiko DSC 6200 calorimeter installed in the University of Lund was used. With the purpose of examination of the reversible amylose-lipid complex transition, characterised by a weak thermal effect, DSC studies were carried out during heating-cooling-heating cycles (up to 3 heating processes).

In the case of 20-25% starch suspensions a single endothermal effect of gelatinisation is observed, while in the case of the suspensions with concentration of 45-50% two processes occur in the temperature range 55-90°C (Fig.). In the case of wheat

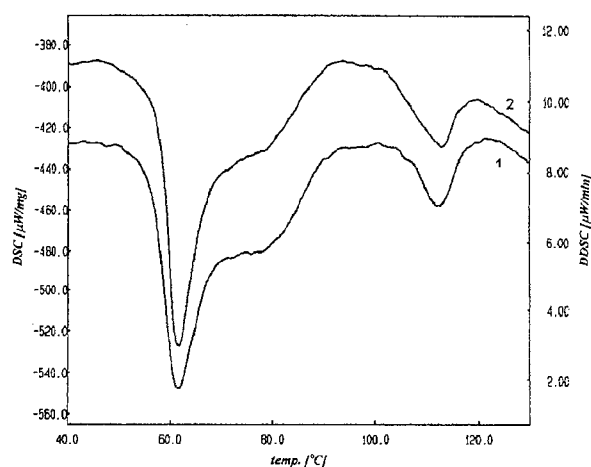


Fig. Examples of the normalised DSC curves recorded during the first heating at a rate of 10°C/min of ca. 50% suspensions of wheat starch (curve 1 - the initial starch, curve 2 - the sample irradiated with a dose of 30 kGy).

starch (Fig.) the reversible amylose-lipid complex transition takes place at higher temperature.

Only gelatinisation was observed during the first heating of potato and waxy-maize starch. It was stated that gelatinisation of the irradiated waxy-maize starch, and waxy-potato starch (both containing essentially pure amylopectin) occur always at lower temperature than gelatinisation taking place in the appropriate reference samples under the same experimental conditions. For example, the peak temperature values equal to 68.5, 67.5 and 66.7°C were determined in the case of 20% suspensions of the initial waxy-potato starch and the samples irradiated with doses of 10 and 20 kGy, respectively, heated at a rate of 10°C/min. The radiation influence on gelatinisation temperature differs in the case of the other potato starch samples, in dependence on the conditions of sample preparation and the resulting crystalline properties of granules.

Influence of irradiation on the structural properties differs for particular starches. It might be concluded, for example, that irradiation of the



PL0101478

potato starch lead at first to destruction of the crystalline regions with lower ordering (melted at lower temperature) while in the case of the wheat starch the crystalline regions with higher ordering are destroyed in the first step.

Table. The values of peak temperature ( $^{\circ}\text{C}$ ) determined on the basis of several reproducible measurements for thermal effect of the amylose-lipid complex transition, occurring in the 50% suspensions of the initial wheat starch sample and the samples irradiated with various doses. The suspensions were heated at a rate of  $10^{\circ}\text{C}/\text{min}$ .

Dose [kGy]	Heating cycles			Cooling cycles		
	I	II	III	I	II	III
0	112.1	116.0	116.2	99.4	99.9	100.2
5	112.5	115.7	115.6	99.5	99.5	99.7
10	112.6	114.9	114.6	98.8	98.3	97.8
20	112.3	113.9	113.7	97.4	96.5	96.1
30	112.2	113.4	112.6	96.3	95.3	94.9

The amylose-lipid complex transition was investigated during first heating and subsequent heating and cooling of wheat starch (Fig., Table), beside to the gelatinisation process observed only on first heating. During the first heating, the transition was observed for all the samples in the similar temperature range. During the subsequent heating and cooling, the transition occur in the samples irradiated with doses of 10, 20, 30 kGy at a temperature lower than in the initial sample (examples are given in Table). Moreover, in the irradiated sample the transition occurs during the subsequent cooling at a temperature lower than in the preceding one, in opposite to the initial sample. Small differences

were noticed between the initial sample and the sample irradiated with a dose of 5 kGy. The results were confirmed for the non-irradiated and irradiated samples of wheat starch gelatinised in a dryer at  $105^{\circ}\text{C}$ , and afterwards examined by DSC. Therefore, it might be deduced that the amylose-lipid complex symmetry is diminished by the way of subsequent thermal treatment of the irradiated samples, while improved in the case of the initial one.

It was stated that the retrogradation occurs easier in the gels with a low concentration (20%) obtained from the irradiated starch samples, than in the similar gels obtained from the initial samples. A smaller retrogradation was observed, however, in the concentrated (50%) gels prepared from the irradiated samples, than in such gels prepared from the reference samples.

## References

- [1] Cieřla K., Svensson E., Eliasson A.-Ch.: Preliminary differential scanning calorimetry studies of radiation-induced transformations in starch and flour. *J. Thermal. Anal. Calorim.*, **56**, 1197-1202 (1999).
- [2] Cieřla K., Eliasson A.-Ch.: Influence of gamma radiation on potato starch gelatinization studied by differential scanning calorimetry. *Radiat. Phys. Chem.*, submitted.
- [3] Cieřla K., Gwardys E., Źółtowski T.: Changes of relative crystallinity of potato starch under gamma irradiation. *Starch/Stärke*, **43**, 251 (1991).
- [4] Cieřla K., Źółtowski T., Diduszko R.: Detection of physico-chemical changes occurring in flour under gamma irradiation by small-angle X-ray scattering. *Food Structure*, **12**, 175 (1993).

## THERMOLUMINESCENCE OF SOILS FROM KUJAWY-POMERANIAN REGION

Antoni M. Danciewicz, Kazimiera Malec-Czechowska

Measurement of thermoluminescence (TL) of silicate minerals, which are inherent or contaminating components of foodstuffs is presently a standardised method for detection of their irradiation [1]. Intensity of TL in minerals increases upon irradiation of food to a level many times higher than in non-irradiated sample.

To gain some information on the level of TL in soils and their silicate minerals, which appear in

foodstuffs, we have measured TL intensity of various cultivated soils from the Kujawy-Pomeranian region. Other properties of these soils are being investigated by Prof. Halina Dąbkowska-Naskręć, Soil Science Department, Academy of Agriculture in Bydgoszcz, who supplied us with the soil samples. TL intensity has been measured in triplicates using ca. 1 mg of soil as such and silicate minerals isolated according to the method described as standard

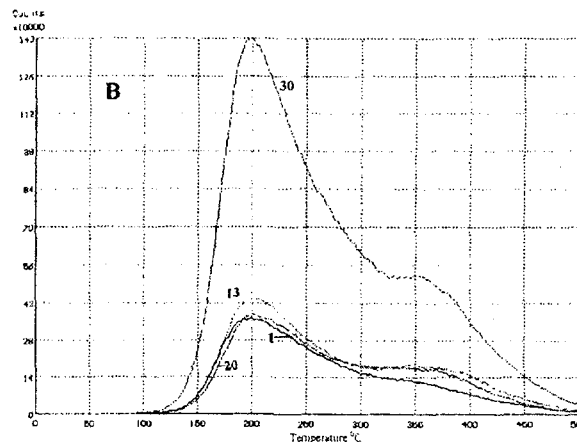
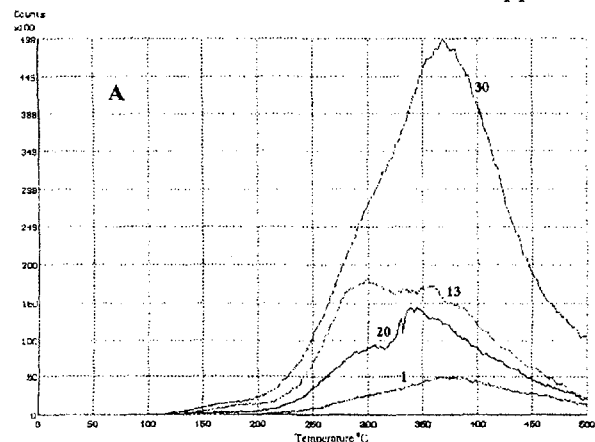


Fig.1. Thermoluminescence (glow curves) of selected soil samples from Kujawy-Pomeranian region (Table): A - non-irradiated, B - irradiated with 1 kGy.



PL0101479



procedure for TL measurement. TL measurements were also carried out on soil samples and silicate

This results probably from the difference in the composition of silicate minerals, (the content of po-

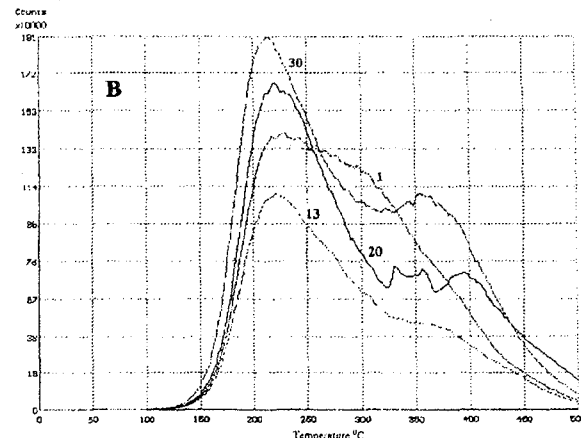
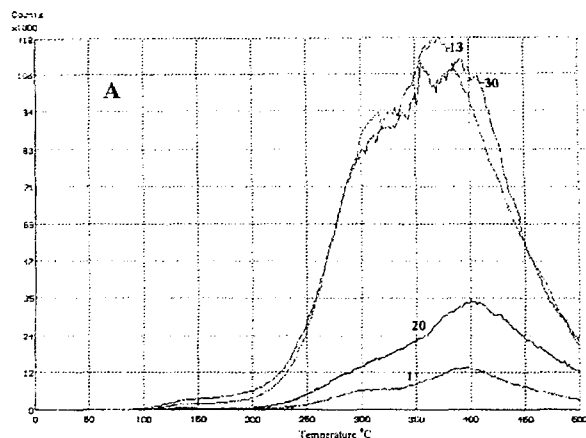


Fig.2. Thermoluminescence (glow curves) of silicate minerals isolated from selected samples of soils (Table): A - non-irradiated, B - irradiated with 1 kGy.

minerals, which were subjected to gamma radiation with a dose of 1 kGy.

The results obtained with 18 different samples of soils show conclusively that the shape of TL glow curve coincide with that of a mixture of feldspar and quartz [2,3], the minerals, generally present in different proportions in soils. The maximum of TL

tassium feldspar), and from the difference of absorbed dose due to natural radioactivity of soils. On the one hand, the loss of luminescence because of the action of temperature and light (bleaching) on soil, takes place. The latter effect has clearly been proved in samples of soils collected from the surface layer, which often is turned over. TL intensity

Table. Thermoluminescence of soils collected from different localities in the Kujawy-Pomeranian region. The temperatures of maximal thermoluminescence ( $T_{max}$ ) and its intensities (area under glow curve for the temperature interval from  $T_{max} - 20^{\circ}\text{C}$  to  $T_{max} + 20^{\circ}\text{C}$ ) are given for soils as such and for silicate minerals isolated from them.

Locality	Sample		Silicate minerals [%]	Soils		Silicate minerals	
	Number	Code		$T_{max} [^{\circ}\text{C}]$	TL intensity $\cdot 10^3 \pm \text{SD}$	$T_{max} [^{\circ}\text{C}]$	TL intensity $\cdot 10^3 \pm \text{SD}$
Szadkowice	1	Ap	74.2	380	$138 \pm 68$	393	$262 \pm 114$
	2	A2	70.5	381	$78 \pm 13$	381	$861 \pm 171$
Cieřlin	6	Ap	75.2	367	$243 \pm 231$	386	$1076 \pm 614$
	7	A2	73.8	378	$98 \pm 46$	375	$1052 \pm 431$
Gnojno	13	Ap	76.3	335	$310 \pm 50$	349	$2254 \pm 164$
	14	Aa	71.5	323	$403 \pm 170$	362	$2202 \pm 957$
Dobre	19	Ap	64.3	385	$183 \pm 147$	379	$640 \pm 192$
	20	A2	70.4	328	$280 \pm 80$	377	$973 \pm 325$
Liszkowo	24	Ap	76.9	375	$180 \pm 66$	399	$659 \pm 50$
	25	Eet	79.1	369	$506 \pm 18$	320	$2046 \pm 1213$
Zduny	29	Ap	85.2	379	$158 \pm 113$	415	$263 \pm 72$
	30	Eet	85.4	366	$923 \pm 283$	384	$1950 \pm 435$
Batkowo	34	Ap	74.2	380	$124 \pm 36$	379	$976 \pm 368$
	35	B1br	63.9	363	$493 \pm 104$	360	$8138 \pm 1908$
Peckowo	39	Ap	76.8	331	$307 \pm 80$	374	$1609 \pm 25$
	40	B1br	61.8	337	$2445 \pm 936$	343	$15605 \pm 7583$
Starogr3d	0-15	-	74.2	379	$77 \pm 25$	418	$271 \pm 8$
	15-30	-	73.0	398	$101 \pm 20$	421	$337 \pm 65$

intensity appears at an interval of temperature between 300 and 400°C. Upon irradiation, the TL intensity increases and the shape of glow curve changes. There is a shift of TL maximum observed down to around 200°C. The descent part of glow curve is slightly influenced by the presence of a maximum found in non-irradiated sample, which is seen as a small peak or shoulder on TL curve around 350°C (Fig.1). A similar shape of glow curves has been obtained for silicate minerals isolated from non-irradiated and the soil samples irradiated with 1 kGy of gamma rays (Fig.2). The intensities of TL of all 18 samples of soils as examined through the study differ significantly (Table).

of samples has been found lower than that of samples taken from the same locality but from the deeper layer which is usually not moved during cultivation.

The extended version of this communication with more detailed discussion is being prepared for publication elsewhere.

#### References

- [1]. EN 1788. Foodstuffs - Detection of irradiated food from which silicate minerals can be isolated - Method by thermoluminescence. European Committee for Standardization. Brussels 1996.
- [2]. Singhvi A.K., Mejdahl V.: Nucl. Tracks, **10**, 137-161 (1985).
- [3]. Sojka Ch., Delincée H.: Lebensm. Wiss. u-Technol., **33**, 431-439 (2000).

## RADIOLYTIC DEGRADATION OF HERBICIDE 2,4-DICHLOROPHENOXYACETIC ACID (2,4-D)

Przemysław Drzewicz, Marek Trojanowicz, Przemysław Panta, Wojciech Głuszewski, Michał Gryz<sup>1/</sup>,  
Grzegorz Nałęcz-Jawecki<sup>1/</sup>, Józef Sawicki<sup>1/</sup>, Celina Duarte<sup>2/</sup>, Maria H.O. Sampa<sup>2/</sup>, Hiroshi Oikawa<sup>2/</sup>,  
Małgorzata Szewczyńska<sup>3/</sup>, Abeer Al-Kaid<sup>4/</sup>, Abed A. Al-Mowed<sup>4/</sup>

<sup>1/</sup> Department of Environmental Health Sciences, Medical University of Warsaw, Poland

<sup>2/</sup> Institute of Energetic and Nuclear Research IPEN, São Paulo, Brazil

<sup>3/</sup> Central Institute of Labor Protection, Warszawa, Poland

<sup>4/</sup> Syrian Atomic Energy Commission, Damascus, Syria

2,4-dichlorophenoxyacetic acid (2,4-D) is a common herbicide widely used in agriculture, on pastures and lawns, in parks and for the protection of rail roads [1-3]. In living organisms as well as in the natural environment as a result of metabolic processes of 2,4-D, various toxic and cancerogenic chloroorganic compounds are formed, mostly 2,4-dichlorophenol [2,3]. In Poland and in several other countries also one of severe environmental problems is the storage of unused and unwanted expired pesticides including large amounts of 2,4-D [4,5]. They are stored in concrete tombs and their leakage to soil and underground waters has been already reported because of ageing and gradual destruction of all protective materials used. A search for appropriate technology of their destruction is an important environmental issue.

Environmental remediation using radiation chemistry is one of the promising advanced oxidation processes, but there is lack of the ability to predict

factors on the effectiveness of radiolytic degradation of 2,4-D and toxicity changes of irradiated solutions.

Experimental conditions and instrumentation used was practically the same as employed earlier for a batch study of radiolytic degradation of 2,4-dichlorophenol [13]. Aerated aqueous solutions of 2,4-D (250 ml) were irradiated in cylindrical glass cells (55 mm in diameter, 160 mm in height) in a Russian  $\gamma$ -irradiation source Issledovatel with <sup>60</sup>Co with a dose rate of 2.72 kGy/h and a mean energy of 1.25 MeV. Electron beam irradiations were carried out in glass Petri dishes of diameter 14.5 cm with the thickness of a solution layer 3.7 mm using a 1.5 MeV accelerator Dynamitron from Radiation Dynamics.

Analytical measurements of yield of 2,4-D decomposition and the detection of products formed were carried out using reversed-phase HPLC. In optimized conditions, as eluent was used a mixture of

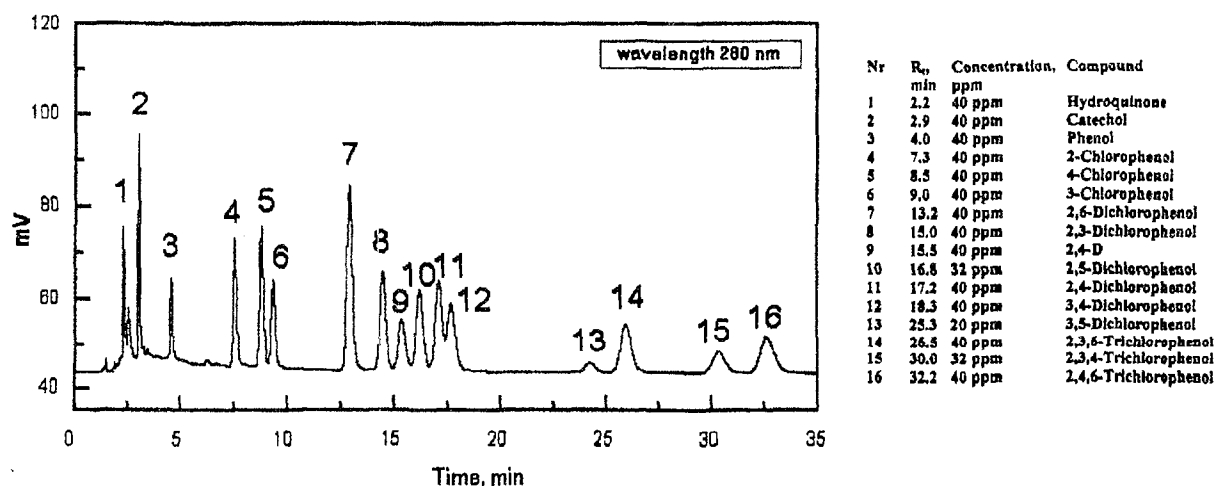
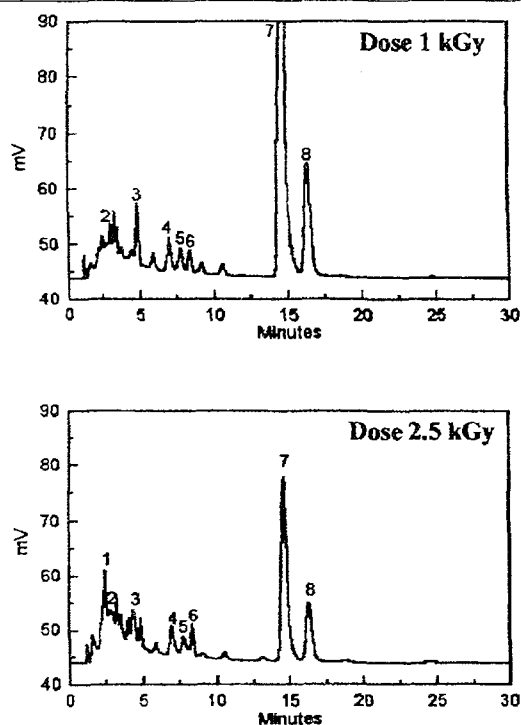


Fig.1. Reversed-phase chromatogram of a mixture of 2,4-D, selected phenols and dihydroxybenzenes in optimized conditions with UV detection at 280 nm. Injection volume 20  $\mu$ l, flow-rate 1.5 ml/min. Concentration of injected solutes and identification of analytes shown in the Fig.

and control the radiation chemical processes in complex environmental systems [6,7]. The current status of environmental application of ionizing radiation has been recently reviewed for natural and drinking water purification [8] and for treatment of wastewater [9]. Recently, there were already some attempts to employ this technology for the decomposition of pesticides, including triazine herbicides [10-12] and also carbamate insecticide and chlorinated organic pesticides [11].

The aim of this environmentally oriented work was to study the effect of various experimental

water, acetonitrile and methanol (60:35:5 vol. %), containing 2 g/l citric acid and applying UV detection at 280 nm. As it is shown in an example chromatogram (Fig.1), the optimized conditions allow to resolve 2,4-D, di- and monochlorophenols, unsubstituted phenol and dihydroxybenzenes. A 20-fold solid-phase preconcentration was carried out using a commercial Merck sorbent LiChrolutEN (500 mg bed). Total Organic Carbon determinations were carried out with a Shimadzu TOC-5000 analyzer. Measurements of toxicity, based on bacterial chemiluminescence, were carried out with a Microtox



Number	Compound
1	Hydroquinone
2	Catechol
3	Phenol
4	2-Chlorophenol
5	4-Chlorophenol
6	3-Chlorophenol
7	2,4-D
8	2,4-Dichlorophenol

Fig. 2. Reversed-phase chromatograms recorded in optimized conditions for 50 mg/l 2,4-D aerated solutions of pH 7.0 irradiated with 1 and 2.5 kGy doses.

M500 Toxicity Analyzer from Azur Environment (Beckshire, UK).

At a 50 mg/l level of 2,4-D, complete radiolytic decomposition of the substrate in aerated neutral solutions requires at least a 5 kGy dose, but a complete release of inorganic chloride occurs at an about 7.5 kGy dose. This is due to the transient formation of other different chloroorganic compounds such as mono- and dichlorophenols (see chromatograms in Fig. 2 for two different doses). Using ion-chromatography with conductivity detection for the determination of other than chloride ionic products as main products at doses up to 20 kGy, formates and acetates were found (Fig. 3). A complete mineralization of aqueous 2,4-D solutions requires, however, much larger doses. Experiments performed with electron beam irradiation and infrared TOC determination have shown that in a 20 mg/l 2,4-D solution at 200 kGy only 50% mineralization occurs. In 100 mg/l 2,4-D solutions irradiation with a 20 kGy dose results in a 10% decrease of TOC, only.

The yield of 2,4-D degradation can be substantially reduced in the presence of other competing scavengers of hydroxyl radicals. A strong indirect scavenging effect was found for nitrate present in irradiated 2,4-D solutions. In the presence of 50

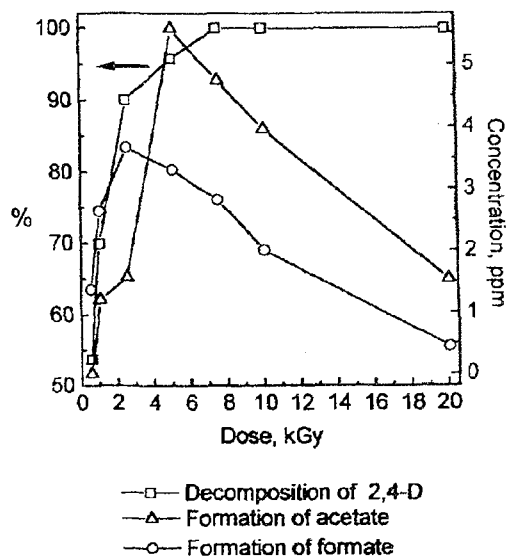
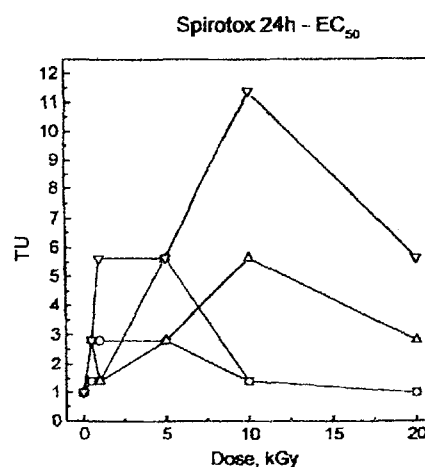
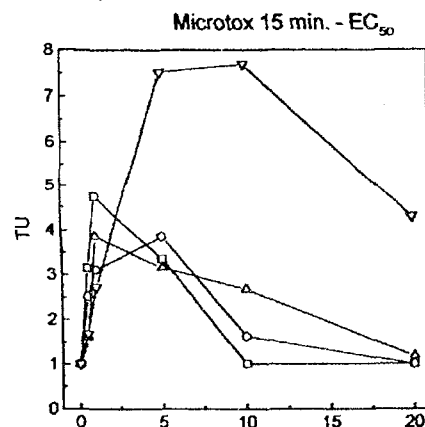


Fig. 3. Effect of radiation dose on yield of 2,4-D decomposition and concentration of acetate and formate formed during irradiation of 50 mg/l 2,4-D aerated solutions at pH 7.0.

mg/l nitrate, decomposition of 50 mg/l 2,4-D requires a 10 kGy dose, which is a twice larger dose



- 50 ppm 2,4-D
- 50 ppm 2,4-D, 10 ppm NO<sub>3</sub><sup>-</sup>
- △— 50 ppm 2,4-D, 20 ppm NO<sub>3</sub><sup>-</sup>
- ▽— 50 ppm 2,4-D, 50 ppm NO<sub>3</sub><sup>-</sup>

Fig. 4. Effect of radiation dose on changes of toxicity of irradiated 50 mg/l 2,4-D solution with various nitrate concentration measured with Microtox and Spirotox toxicity tests.

than in the absence of nitrate. A similar increase of needed dose was found in the presence of 400 mg/l bicarbonate in neutral irradiated solutions of 2,4-D. No scavenging effect was found, however, in the presence of humic substances up to 50 mg/l, and on the contrary, in the presence of humic acid a more efficient release of inorganic chloride was found (100% at 5 kGy in irradiation of 50 mg/l 2,4-D solution).

The examined substrate 2,4-D exhibits phytotoxicity, hence, their solutions prior to the irradiation do not give positive response with the used Microtox and Spirotox tests. The products formed during radiolysis of 2,4-D, however, are much more toxic (e.g. 2,4-dichlorophenol and other phenolic compounds) [14], therefore these tests can be applied in this case for environmental purpose. As it can be seen in Fig.4, a complete reduction of toxicity of irradiated 50 mg/l solution of 2,4-D is observed at a 10 kGy dose for both tests. This reduction of toxicity is significantly affected by the presence of nitrate in irradiated solutions (Fig.4), and to some smaller extent also by the presence of bicarbonate.

In the present state of these studies, the following conclusions about the radiolytic degradation of 2,4-D can be made. For the examined range of 2,4-D concentrations, at doses up to 1 kGy, in the irradiation of aerated solutions of 2,4-D, the main process is the release of glycolate and formation of highly toxic 2,4-dichlorophenol. At doses from 1 to 5 kGy a release of inorganic chloride occurs with

the formation of monochlorophenols and hydroxybenzenes. At doses higher than 5 kGy a destruction of the benzene ring takes place with the formation of simple carboxylic acids. The yield of these processes may be affected by the presence of scavengers of hydroxyl radicals.

## References

- [1]. Starak A.: Chemiczne substancje toksyczne w środowisku i ich wpływ na zdrowie i życie człowieka. Wydawnictwo PAN, Warszawa 1990.
- [2]. Różański L.: Przemiany pestycydów w organizmach żywych i środowisku. Agra-Enviro Lab, Poznań 1998.
- [3]. 2,4-dichlorophenoxyacetic acid (2,4-D) - Environmental Aspects, Environmental Health Criteria 84. World Health Organization, Geneva 1989.
- [4]. Barcelo D., Hennion M.C.: Trace Determination of Pesticide and Their Degradation Products in Water. Elsevier, Amsterdam 1997.
- [5]. Zaleska A., Hupka J.: Waste Manag. Res., **17**, 220-226 (1999).
- [6]. Trifunac A.: Radiat. Phys. Chem., **57**, 53 (2000).
- [7]. Final Report of "Research Needs and Opportunities in Radiation Chemistry Workshop". Chesterton, USA, 1998; <http://www.er.doe.gov/production/bes/chm/RadRprt.doc>.
- [8]. Pikaev A.K.: High Energy Chem., **34**, 1-12 (2000).
- [9]. Pikaev A.K.: High Energy Chem., **34**, 55-73 (2000).
- [10]. Karpel vel Leitner N., Berger P., Gehringer P.: Radiat. Phys. Chem., **55**, 317-322 (1999).
- [11]. Dessouki A.M., Aly H.F., Sokker H.H.: Czech. J. Phys., **49**, 521-533 (1999), Suppl. S1.
- [12]. Angelini G., Bucci R., Carnevaletti F., Colosimo M.: Radiat. Phys. Chem., **59**, 303-307 (2000).
- [13]. Drzewicz P., Panta P., Głuszeński W., Trojanowicz M.: J. Radioanal. Nucl. Chem., **242**, 601-609 (1999).
- [14]. Kaiser K.L.E., Palabrica V.S.: Water Poll. J. Canada, **26**, 362-431 (1991).

## RADIATION MODIFICATION OF LDPE (BRALEN TYPE)

Izabella Legocka, Zbigniew Zimek, Krzysztof Mirkowski, Maria Zielonka<sup>1/</sup>

<sup>1/</sup> Industrial Chemistry Research Institute, Warszawa, Poland

A study have been started at this Institute on the development of new PE composites better suited to application properties of heat shrinkable products. The effect of electron beam irradiation on blends of the LDPE Bralen type with an ionomer resin based on ethylene/methacrylic acid (Surlyn) has been investigated.

Irradiated polymers are non melting, exhibiting perfect elasticity above their crystalline melting point. Three dimensional network of bonds is formed between polymer chains during crosslinking process initiated by ionizing radiation. It creates a shape memory effect. Crosslinking of polyethylene products may improve their properties like flexibility, impact and chemical resistance and modify their tensile and thermal properties. The polyethylene chains can be also degraded which is being observed at higher dose level. On the other hand, the irradiation creates the hydrocarbon radicals, which, with suitable additive presence, react more quickly leading to higher efficiency of crosslinking process and lowering the irradiation dose.

New types of polyethylene based materials are offered on the market. The mixtures based on semi-crystalline polyethylene give composite materials

with different supermolecular structures and visco-elastic properties. The selection should be performed to determine a material with best physical properties. The radiation dose and degree of crosslinking should be optimized as well. Economic and customer demands are creating a broad field for research and development in the polymer radiation processing technology. Lower dose required in radiation induced crosslinking process and better performances of the final products are typical scopes of the research leading to better economic parameters and better response on customer demands regarding product quality.

Multiphase polymers are of great importance in the development of new synthetic materials. However, the development of new useful blends is severely limited by a strong immiscibility of many polymer pairs of interest. The miscibility of homopolymer/copolymer blends has been successfully achieved by the presence of specific intermolecular interactions [1-3]. This interactions include hydrogen bonding in bulk or solution and charge transfer complexes [4]. Numerous studies have been based on anion-cation and ion-dipole interactions as miscibility enhancers [5,6]. The addition of selected



PL0101481

compounds, which may promote better miscibility, increases the crosslinking homogeneity of irradiated polymer blends as it was described in the literature [7-9].

The physical properties of the samples were measured to establish the effectiveness of irradiation process and sample composition influence on final product parameters. The following analytical methods have been applied:

1. The gel fraction measurements were done by extracting soluble components in boiling xylene for totally 8 h at temperature 125°C using a Soxhlet apparatus and after drying the residue at 135°C for 15 min.
2. The effect of radiation on the mechanical properties of the sample were measured on an Instron tensile testing machine. The results of the tests included: elongation at break and tensile strength of the samples.
3. The melting behavior of the samples were studied on a Perkin-Elmer DSC-7 differential scanning calorimeter. A sample, approximately 7 mg in weight, was heated at 10°C/min in nitrogen. Two main characterization values have been derived from the recorded DSC curves: the peak temperature and heat of fusion.
4. Rheological characteristics of the samples were investigated by a Dynamic Spectrometer RDS-II machine, at temperature 150°C. The following parameters were measured: viscosity  $\eta^*$ , complex dynamic shear modulus  $G^*$  ( $G'$  - shear storage modulus; real part of  $G^*$  and  $G''$  - shear loss modulus; imaginary part of  $G^*$ ) vs. vibration frequency ( $10^{-1}$ - $10^3$  rad/s) to evaluate the tendency of structural changes and formulate conclusions leading to optimization of the dose and LDPE blend composition.

LDPE Bralen type RB-0323 (MFI - 0.35 g/10 min; density - 918 kg/m<sup>3</sup>) from one producer was included to performed investigations. A commercially available additive ionomeric resin Surlyn was applied as well. The raw material and the added component were in the form of pellets suitable for a conventional extrusion equipment. The ionomeric resin, Surlyn type, is a metal salt of an ethylene/organic acid copolymer.

Samples were obtained by mixing and after extruding raw materials at 130°C using a Brabender type machine. Samples were prepared in the following proportions:

Sample No	Sample composition
0	100% Bralen
1	95% Bralen + 5% Surlyn
2	90% Bralen + 10% Surlyn
3	85% Bralen + 15% Surlyn

The samples were irradiated at room temperature (20 ± 3°C). Electron beam with an energy of 10 MeV was applied during irradiation of samples in the LAE 13/9 accelerator. Total doses of 70, 90, 120, 150 kGy were collected in a multi pass system. One pass of absorbed dose level was not higher than 25 kGy. The dose rate during irradiation process was controlled by the calorimetric method.

Table 1. Gel fraction content [%].

Sample No	LDPE sample composition	Dose [kGy]			
		70	90	120	150
0	Bralen	52.1	59.1	66.0	70.6
1	Bralen + 5% Surlyn	59.2	63.1	67.0	70.6
2	Bralen + 10% Surlyn	59.8	62.9	65.3	69.0
3	Bralen + 15% Surlyn	60.2	66.2	68.0	68.8

The relation between the gel fraction content and the absorbed dose in the samples is given in Table 1. It can be stated that for the samples prepared on the basis of Bralen and at a low dose level the gel fraction is significantly higher than that for the investigated raw material. Significant improvement was obtained for polymer blends with respect to the polymer based matrix. The best results have been found for the mixture (85% PE + 15% Surlyn).

Table 2. Mechanical properties.

Sample No	Performances	Dose [kGy]				
		0	70	90	120	150
0	Tensile strength [MPa]	17.0	17.2	17.8	17.0	16.8
	Elongation at break [%]	519	500	492	450	455
1	Tensile strength [MPa]	16.4	17.4	18.2	18.0	17.4
	Elongation at break [%]	502	500	482	490	496
2	Tensile strength [MPa]	15.8	18.8	21.8	20.1	19.0
	Elongation at break [%]	450	430	415	470	468
3	Tensile strength [MPa]	14.6	15.8	22.4	20.1	18.2
	Elongation at break [%]	480	465	452	446	488

The results of measurements related to tensile strength and elongation at break of the irradiated samples are shown in Table 2. These results were obtained for the dose up to 150 kGy. The higher gel fraction level corresponds with the higher tensile strength in the performed mechanical tests. The samples irradiated with a dose of 120 and especially of 150 kGy are characterized by a lower tensile strength value which indicate the influence of degradation process on the mechanical properties of those samples [10]. The analysis of elongation at break results of the measurements leads to similar conclusions.

Table 3. Melting behavior of raw materials.

Sample No	Peak temperature [°C]		Heat of fusion [J/g]	
	Dose [kGy]		Dose [kGy]	
	0	90	0	90
0	116.78	115.85	115.70	88.57
1	-	115.70	-	84.2
2	-	115.94	-	78.99
3	-	115.75	-	91.4

The results of performed measurements of the melting behavior of the samples with different composition and irradiated with a dose of 90 kGy are shown in Table 3. The comparison of those results indicates a significant change of fusion heat

after irradiation, specially for sample 2 and 3 (10 and 15% of Surllyn content). The wider and splitted melting peak is observed which is related to structural reconfirmation processes in those samples [11].

No influence has been found of the sample composition with the ionomeric resin Surllyn type on the viscosity  $\text{Eta}^*$  and moduli  $G'$  and  $G''$  in non irradiated samples. The uniform interaction with ionizing radiation can be expected due to this fact. The influence of the dose on moduli  $G'$  ( $G'$  and  $G''$ ) was investigated using sample No 2 (90% Bralen + 10% Surllyn). The applied dose range

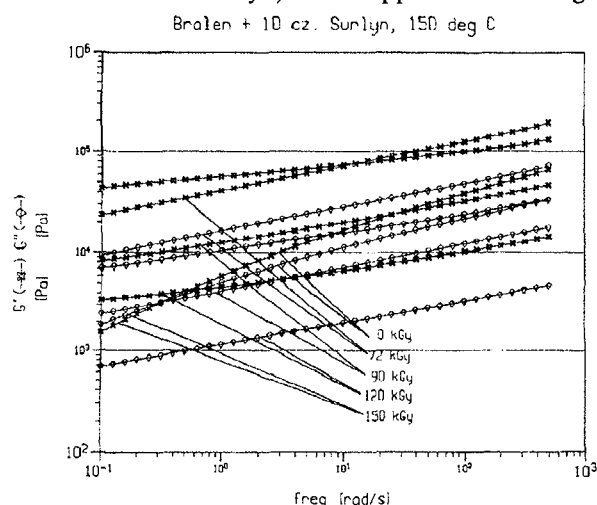


Fig.1. The moduli  $G'$  and  $G''$  vs. vibration frequency rate: irradiated sample No 2 for different dose level.

0-150 kGy, Fig.1, shows the modulus components  $G'$  and  $G''$  behaviour vs. vibration frequency. Fig.2 is related to viscosity coefficient  $\text{Eta}^*$ . It may be noticed that value of  $G'$ ,  $G''$  and  $G''/G'$  of non irradiated samples are the lowest (excluding the value obtained for the dose 120 kGy where a saturation effect is observed). The shape of curves of the irradiated samples is slightly different as compared with the non irradiated ones. This indicates homogeneity of the polymer blends as compared with the initial polymer and the lack of significant distortion of the material structure. It should be noticed that

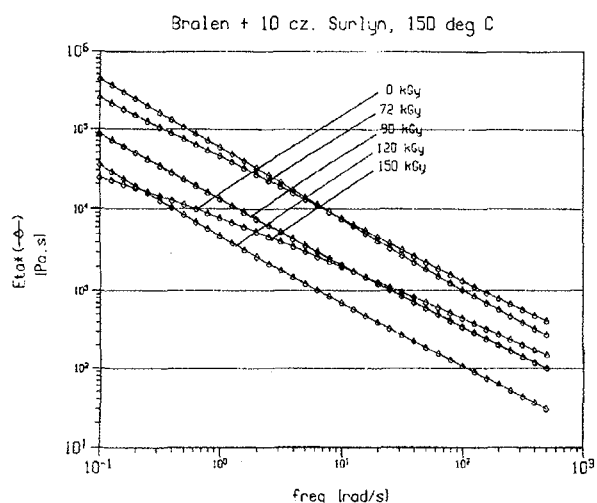


Fig.2. The viscosity  $\text{Eta}^*$  vs. vibration frequency rate: irradiated sample No 2 for different dose level.

the shape of the curves  $G'(\omega)$  and  $G''(\omega)$  for the sample irradiated with the dose 72 kGy and the non irradiated one are similar, but the value of  $G'$  and  $G''$  coefficients are higher after irradiation. This is correlated with the crosslinking process proved by the gel fraction content. The sample become stiffer, but the effect of degradation has not been observed as yet (increasing value of  $G''$  coefficient). The gel fraction and mechanical properties are not satisfactory for the dose 72 kGy. When the dose 90 kGy is applied the values of  $G'$  and  $G''$  coefficients are lower, but the  $G''/G'$  is higher than for the dose 72 kGy. However, the gel fraction content and mechanical properties are better. In spite of the more intense degradation process, the final properties were significantly improved. Degradation process is manifested by lower viscosity which also leads to lower homogeneity of the material, which can be observed for the sample irradiated with the dose 120 kGy (lower value of  $G'$  and  $G''$  coefficients and higher  $G''/G'$ ). It should be noticed that the gel fraction has practically the same level and mechanical properties are deteriorated. A higher value of  $G'$ ,  $G''$  and  $G''/G'$  for the dose 150 kGy and a similar gel fraction coefficient are observed. The mechanical properties are becoming worse as well as the elongation at break, which is related to material degradation. The same time of recombination process of macroradicals may create more branched polymer forms, which makes more difficult material deformation. Taking into account the above consideration, the dose 90 kGy has been selected as an optimum due to a certain level of gel fraction and mechanical properties of the material.

The influence of the added modifier and the irradiation process on LDPE properties can be illustrated by the value of  $G'$  and  $G''$  coefficients. Those coefficients for samples 1 and 3 are lower than for sample 2 (dose 72 kGy). This can indicate that for such a low dose, the added material has not been used sufficiently well (sample 3). At the same time this makes the sample softer. On the other hand, when the modifier content is too low (sample 1) its influence on the material properties is limited as well. When the dose is higher (90 kGy), the value of  $G'$  and  $G''$  coefficients for the samples 1 and 2 are similar but  $G''/G'$  value for sample 2 is significantly higher for higher vibration frequencies, which may suggest a higher viscosity caused by the differentiated structure. When the added modifier content is higher (sample 3), the value of  $G'$  and  $G''$  coefficients grow effectively suggesting more stiff structure caused by the crosslinking process. The value of  $G''$  for higher vibration frequency level may indicate polymer degradation but without adequate influence on mechanical properties at ambient temperature. When the dose is 120 kGy, the samples with different modifier content are showing similar results. The observed higher value of  $G'$  coefficient may indicate a non homogenous structure caused by crosslinking and degradation processes. It is also reflected in mechanical properties measured at ambient temperature.

The application of ionomeric resin as a LDPE modifier allows to obtain homogenous blends. The gel fraction in all samples increases with increasing dose level. The gel fraction of irradiated LDPE blends are higher than for pure LDPE. The dose 90 kGy has been found to be sufficient to obtain a suitable gel fraction content. This has been supported by measurements of mechanical and rheological properties. The obtained results prove the assumption that the different polymer composition require a different dose to obtain suitable crosslinking efficiency.

The results of the tensile tests of irradiated samples show changes of tensile strength and elongation induced by crosslinking density of the sample. The effect of oxidative degradation, leading to main chain scission, can be observed as well. The results of melting behavior show that the peaks of melting endotherms of unirradiated samples are slightly higher than the irradiated ones. The peaks of irradiated samples move to the low temperature side and became shorter and broader and the heat of fusion also decreases. The experimental data coming from rheological property measurements performed at higher temperature are well correlated with mechanical properties measured at ambient temperature and provide more complex information regarding structural changes incorporated by the crosslinking process initiated by ionizing radiation.

Generally, the obtained characteristics of PE blends are significantly different from those which

are relating to pure LDPE. Particularly, the dose which is required for the effective crosslinking process was significantly reduced. The final conclusion, regarding the optimum content of added modifier (10-15% of ionomeric resin content) may require more precise optimisation.

## References

- [1]. Paul D.R., Newman S.: Polymer blends. Academic Press, New York 1978.
- [2]. Utracki L.A.: Polymer alloys and blends. Thermodynamics and Rheology. Hanser, Munich 1990.
- [3]. Dubin P. et al.: Macromolecular Complexes in Chemistry and Biology. Springer Verlag, Berlin 1994.
- [4]. Rutkowska M., Eisenberg A.: Macromolecules, 17, 821 (1984).
- [5]. Plante M., Bazuin C.G., Jerome R.: Macromolecules, 28, 1567 (1997).
- [6]. Al-Salah H.A.: J. Appl. Polymer Sci., 1, 17 (2000).
- [7]. Wiesner L.: Effects of radiation on polyethylene and other polyolefins in the presence of oxygen. Radiat. Phys. Chem., 37, 1, 77-81 (1991).
- [8]. Waldron R.H., McRae H.F., Madison J.D.: The effect of various monomers on crosslinking efficiency. Radiat. Phys. Chem., 25, 4-6, 843-848 (1985).
- [9]. Mateev M., Karageorgiev S.: The effect of electron beam irradiation and content of EVA upon the gel-forming process in LDPE-EVA films. Radiat. Phys. Chem., 51, 2, 205-206 (1998).
- [10]. Datta S.K., Chaki T.K., Tikku V.K., Pradhan N.K., Bhownik A.K.: Heat shrinkage of electron beam modified EVA. Radiat. Phys. Chem., 50, 4, 399-405 (1997).
- [11]. Gal O., Kostecki D., Babic D., Stannett V.T.: DSC melting behavior of irradiated low density polyethylene containing antioxidants. Radiat. Phys. Chem., 28, 3, 259-267 (1986).

## RADIATION STERILIZATION OF ALLOGRAFTS

Iwona Kałuska, Zbigniew Zimek

### Introduction

Allografts such as bones, tendons, cartilage, dura mater, heart valves and skin, prepared and distributed by tissue banks, are widely used for reconstructive surgery. The main aim of tissue banks is to provide safe and effective allografts for transplantation. The risk of infectious disease transmission with tissue allografts is the main concern in tissue banking practice. Microorganisms can be introduced into grafts during tissue procurement, processing, preservation and storage. Even if all these procedures are carried out under aseptic conditions, the possibility of bacterial, fungal or viral disease transmission of donor origin cannot be excluded. Therefore, tissue allografts should be sterilized [1]. One of the sterilization methods is the radiation sterilization. The main advantages distinguishing radiation sterilization of allografts with electron beam are:

- there is a possibility to provide the process at room temperature or at dry ice temperature,
- sterilization is carried out in the whole volume,
- it does not involve neither toxic chemicals nor radio-active materials,
- sterilized material can be used immediately after exposure.

### Radiation sterilization

Radiation sterilization is a physical process, involving the exposure of a product to high energy

radiation. The product packaged in sealed units is exposed, in a specially designed equipment, to gamma rays from the cobalt-60 or cesium-137 radionuclides, or to a beam from an electron generator. At the Institute of Nuclear Chemistry and Technology (INCT) two high energy electron beam accelerators are used for this purpose. Mainly medical devices of single use are sterilized in our facility but also four Polish tissue banks are availing of our services.

### Choice of radiation dose

One of the most important thing when radiation sterilization is applied is the determination of sterilization dose.

There is far more easier to establish conditions of irradiation for medical devices than for tissue allografts. The reason for this is that medical devices are manufactured in well known, stable conditions. This means that the bioburden (population of viable microorganisms on a product) can be easily determined.

There are several standards dealing with radiation sterilization. According to EN 556 [2], which describes the requirements for medical devices to be labelled sterile, the product is sterile only when the sterility assurance level (SAL) achieves  $10^{-6}$ . EN 552 [3] provides two approaches for establishing the sterilizing dose to achieve compliance with EN 556 and hence provide a SAL of  $10^{-6}$ :



PL0101482

- selection of sterilizing dose capable of achieving compliance with EN 556 by identifying the number of the innate microbial population present on, or in the medical devices and its resistance to radiation, or
- the product is treated with a minimum dose of 25 kGy.

Also in the second case the manufacturer must substantiate the effectiveness of 25 kGy as an irradiation dose. This is something new, because in the past the dose 25 kGy was established following inactivation studies on bioburden and generally accepted as adequate for the purpose of sterilization and no further investigations were needed. To demonstrate that 25 kGy is appropriate for the products, the manufacturer has to have an access to microbiological laboratory. Till now, the Polish Authority responsible for medical devices distribution allows only a traditional approach, it means that the product has to be treated with a minimum dose of 25 kGy, despite, it is obvious that such an approach may increase costs for the manufacturer [4]. Dose setting methods 1 and 2 listed in Annex B of ISO 11137 [5] can be used to determine the sterilization dose based on data generated to provide a knowledge of the product bioburden numbers and resistance. They can also be used to substantiate that 25 kGy will achieve the required sterility assurance level. Both of these dose setting methods have a requirement to audit the continued validity of the sterilizing dose every 3 months. For products manufactured in a large number (more than 1000 product units), the principal envisaged method of substantiation was performing a dose setting exercise employing either Method 1 or 2 of ISO 11137, provided that the outcome of the exercise was the establishment of a sterilization dose that is less than 25 kGy. Methods 1 and 2 have severe limitations in determining product-specific doses for product units with low bioburden. At levels below approximately three microorganisms per products unit, the method becomes less discriminating because it is not always able to detect resistant microorganisms that occur at low probability. Such organisms may, however, affect sterility when product units are exposed to the selected sterilizing dose. The lowest value for average bioburden given in the procedural table of Method 1 is 0.06. For product manufactured in small quantities, either as a single batch or as batches produced infrequently, substantiation using Method 1 or 2 is not practicable due to the relatively high number of product units needed to perform a dose setting exercise. So, a new document was published in 1996 as ISO/TR 13409 [6], which is an adaptation of Method 1. However, the European Standardization Body, CEN, has recommended on technical grounds that ISO/TR 13409 should not be adopted in the European standard system. The reason for that is that, while it universally provides safe outcomes within the limits placed on sample size and bioburden levels, it frequently gives outcomes that are incorrect; the latter do not allow substantiation of 25 kGy in circumstances where

this dose would give an SAL of  $10^{-6}$ . This failure to discriminate properly is attributed to a design fault of the method.

An alternative approach to choosing verification doses for substantiation of 25 kGy was proposed by J. Kowalski and A. Tallentire. This approach is valid for sample size from 10 to 100 product units, corresponding to SALs of  $10^{-1}$  to  $10^{-2}$ . The procedural elements are:

- perform a bioburden determination;
- with a knowledge of the number of product units to be used for the verification dose experiment, conduct a simple calculation to obtain the maximal verification dose characteristic of the resultant bioburden estimate;
- perform a verification dose experiment, and accept or reject substantiation of a 25 kGy sterilization dose based upon the outcome of the verification dose experiment.

The approach aims to:

1. link directly the outcome of the verification dose experiment with the attainment of an SAL of  $10^{-6}$  at 25 kGy;
2. provide the maximal verification dose that is consistent with this linkage and provide a level of conservativeness at least equivalent to that built into the standard distribution of resistances (SDR).

The SDR is a hypothetical distribution, albeit based on measurements of the radiation resistances of selected microbial isolates, comprising a series of increasing  $D_{10}$  values and associated probabilities of occurrence [7].

All the mentioned above standards concern medical devices. Can they be applied for tissue allografts? The selection of a sterilization dose is a compromise between a dose that is high enough to inactivate as many microorganisms as possible and low enough to preserve important biological properties of tissue allografts. With respect to human tissue allografts it is very difficult, or simply impossible to determine the bioburden each time, since initial contamination may vary greatly from tissue to tissue and from one donor to another. These standards do not take this into account because they concern health care product where biological aspects are not important.

Dose of minimum 25 kGy is routinely applied in many tissue banks in the world, however, the Central Tissue Bank in Warsaw has recommended a dose of 35 kGy, so other multi-tissue banks in Poland also have implemented a dose of 35 kGy. However, the validation of sterilization dose of 35 kGy for tissue allografts has not been performed. Mainly because of the troubles with an appropriate dosimetric system which will work in frozen state. Most of the bone allografts are irradiated in frozen state. Only lyophilized bone allografts are irradiated at room temperature.

There are other problems associated with irradiation of tissue allografts which should be investigated to improve the quality of the process. For example, the definition of batch and determination



of batch size or amount of samples which can be available for verification dose experiments.

## References

- [1]. Dziedzic-Gocławska A.: The application of ionizing radiation to sterilize connective tissue allografts. In: Radiation Tissue Banking. Ed. G.O. Phillips (In-Cooperation with IAEA). Singapore, London, New York 2000, 35 p.
- [2]. EN 556: Sterilization of medical devices - Requirement for terminally sterilized devices to be labelled sterile. CEN, European Committee for Standardization, Brussels 1995. Polish standard PN-EN 556:1999 is a translation of EN 556.
- [3]. EN 552: Sterilization of medical devices - Validation and routine control of sterilization by irradiation. CEN, European Committee for Standardization, Brussels 1994. Polish standard PN-EN 552:1999 is a translation of EN 552.
- [4]. Kałuska I., Zimek Z.: The impact of European standards concerning radiation sterilization on the quality assurance of medical products in Poland. IAEA-TECDOC-1070, Vienna 1999, pp. 327-330.
- [5]. ISO 11137: Sterilization of health care products - Requirements for validation and routine control - Radiation sterilization. International Organization for Standardization, Geneva 1995.
- [6]. ISO Technical Report 13409: Sterilization of health care products - Radiation sterilization - Substantiation of 25 kGy as a sterilization dose for small or infrequent production batches. International Organization for Standardization, Geneva 1996.
- [7]. Kowalski J.B., Aoshuang Y., Tallentire A.: Radiat. Phys. Chem., 58, 77-86 (2000).

## EB DOSE CALIBRATION FOR THE LINEAR ELECTRON ACCELERATOR IN THE INCT EXPERIMENTAL PLANT FOR FOOD IRRADIATION

Hanna B. Owczarczyk, Wojciech Migdał, Wacław Stachowicz, Grażyna Strzelczak

In the INCT Experimental Plant for Food Irradiation the absorbed dose of electron beam (EB) irradiation generated from a 10 MeV, 8 kW linear electron accelerator Elektronika is routinely controlled with water calorimeters individually pre-calibrated before use. The rate of temperature decrease and thermistor sensitivity (read out of the voltage) are determined. Styrofoam embedded calorimeters are calibrated with the use of a ferrous sulphate (Fricke) dosimeter based on the spectrophotometric measurements of its oxidation product - ferric ions. Precision limits of  $\pm 1\%$  is attained. Solutions of the Fricke dosimeter, prepared exactly according to a generally accepted procedure, are exposed to gamma rays from a  $^{60}\text{Co}$  the INCT irradiator (actual dose rate 2.7 kGy/h) and to the beam of 10 MeV electrons. In the latter case thin wall 10 mm deep flasks are used. The absorbed dose in the INCT irradiator has been evaluated basing on the NIST (US National Institute of Standards and Technology) alanine dosimeters traceable to a  $^{60}\text{Co}$  gamma ray calibration in the NIST. The overall uncertainty of dose evaluation was  $\pm 3.5\%$  at a 95% confidence level (NIST Report of Special Measurement, NIST DB 926:104-107). However, by applying the Fricke dosimeter it is possible to measure accurately the dose between 40 and 400 Gy only and for technical reason the read out of the dose within this range is not very accurate under the beam of electrons. On the other hand, for food irradiation much higher doses are usually applied (from 1000 to 8000 Gys) and thus, for dose calibration the extrapolation of the results obtained with the Fricke dosimeter are always needed.

Taking advantage of the methodology of calibration used by the NIST experts during the special dosimetric measurements mentioned above, the control measurements of dose in the linear electron accelerator have been done. Instead of l-alanine standard pellets as in the NIST measurements, the powdered l-alanine (crystalline product from Aldrich-Chemie, 99% of purity CHR) was used, while the sample holder for the positioning of test samples inside the

irradiation chamber had exactly the same construction as that delivered by the NIST specialists.

The procedure of calibration was as follows:

30 samples of l-alanine weighing from 101 to 119 mg each were sealed in small polyethylene bags (EB irradiation); the same number of samples was closed in small polyethylene ampoules with caps (gamma irradiation). The samples were exposed: (a) to the action of 10 MeV electron beam on an accelerator conveyor, the applying doses being 2.3, 3.4, 6.2, 12.8 and 25.3 kGy as estimated with a water calorimeter calibrated with the Fricke dosimeter (three measurements for each dose) and (b) to the action of gamma rays from the INCT irradiator by applying the doses of 3.0, 5.0, 15.0 and 30.0 kGy (three measurements for each dose) as established (exposition time) on the basis of the NIST calibration data with the correction for  $^{60}\text{Co}$  decay in time. Standard error of the dose measurement done with the linear accelerator did not exceed 7%, while that with the gamma irradiator - 3%.

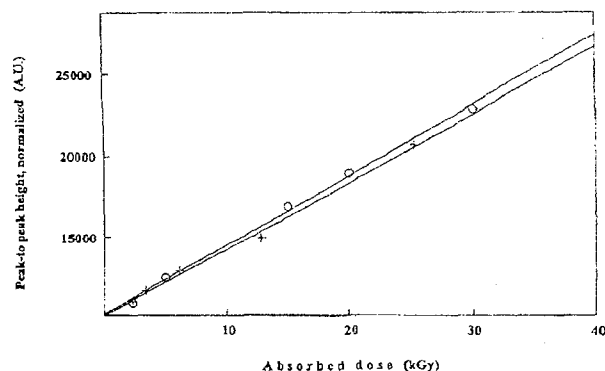


Fig. A comparison of dose calibration curve obtained on the basis of the NIST special measurement with gamma rays from a 18 kCi  $^{60}\text{Co}$  irradiator (opened circle points - o) with dose calibration curve obtained on the basis of water calorimeter and Fricke dosimeter measurements done with the beam of 10 MeV electrons from the linear accelerator (cross marked points - +). In abscissas the normalized peak heights of the central line in the EPR spectrum of irradiated l-alanine are given in arbitrary units (peak-to-peak heights as measured by a spectrometer computer and normalized to the weight of sample and  $\text{Mn}^{2+}$  standard 5th peak height).



PL0101483

The samples were transferred from irradiation containers (bags and ampoules) to the EPR measuring tubes, 3 mm in diameter, made of Spectrosil glass. Each of tubes was weighed before and after the L-alanine sample was poured inside, to receive true weights of each sample. The EPR measurements were done at X-band with a Bruker ESB 300 EPR spectrometer. The basic settings were as follows: microwave power - 1 mW, modulation frequency - 100 kHz and modulation amplitude - 3.5 mT. The internal EPR standard ( $\text{Mn}^{2+}$ ) was used to correct a small difference in the cavity response when samples of different weights are measured.

The results of calibration are shown in Fig. There is only a slight difference between the slopes

of two curves constructed for gamma ray and EB irradiations. The dose points (average of three peak to peak signal heights), corresponding to gamma irradiation, are usually located higher as compared with those which correspond to EB irradiation. In consequence, there is a difference between the slopes of two curves (straight lines within the investigated range of doses) which characterise the dose vs. EPR signal intensity relationship for gamma and EB irradiation. Thus, the numbers which correspond to gamma irradiation are by 5% higher. Taking the NIST calibration data as the reference point, we adapted in the INCT Experimental Plant for Food Irradiation the 5% correction factor which is routinely used by the EB dose measurements.

## CHEMICAL DOSIMETRY. LMTD STAND FOR PRECISE $\gamma$ -IRRADIATION OF DOSIMETERS AND OTHER SMALL OBJECTS

Zofia Stuglik

Every dosimetry system traceable to national or international standards has to include an element which allows for precise dose reconstruction. In the case of the Laboratory for Measurements of Technological Doses (LMTD), the INCT, it is a  $^{60}\text{Co}$  gamma source Issledovatel (Fig.1) whose construction is similar to the well-known Gammacell 220, Nordion, Canada.

In the Issledovatel there are actually 36 gamma sources with a total activity of  $\sim 130$  TBk (3.5 kCi) and a place for additional 18 sources. The sources

are placed at fixed positions around the cylindrical working area with dimensions:  $l=20$  cm,  $\varnothing=14$  cm. A biological shielding enable to work in the vicinity to the source all the time without over-crossing the permissible doses. The irradiated samples are put into a stand (it fulfils an approximate electronic equilibrium condition) and lifted into the working area automatically.

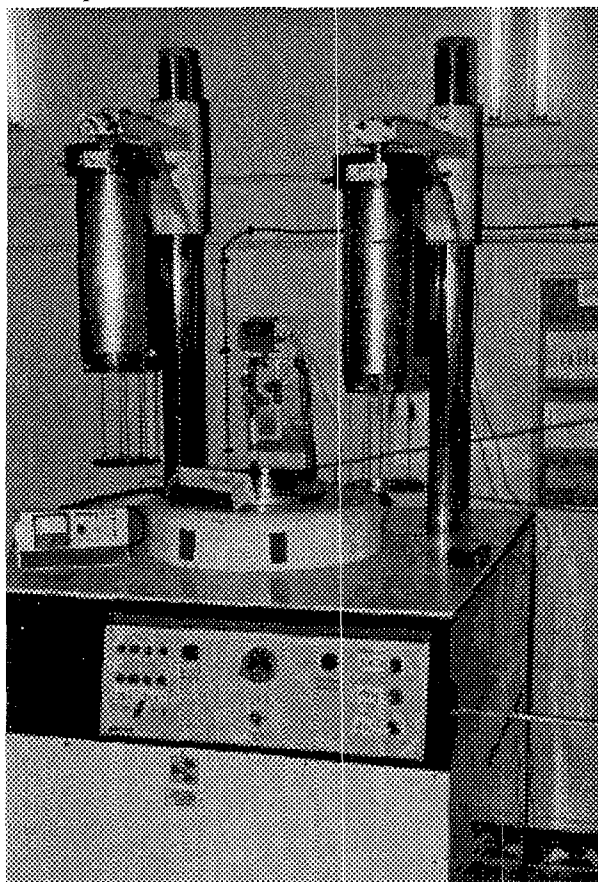


Fig.1. An overview of a  $^{60}\text{Co}$  gamma source Issledovatel.

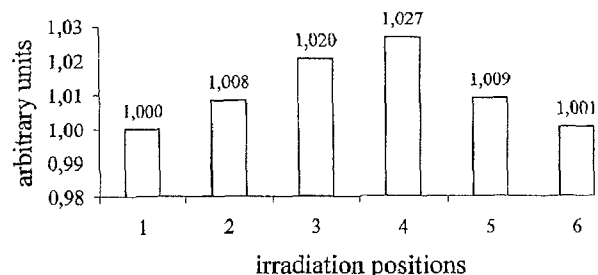


Fig.2. Small but distinct differences between the dose rates at 1-6 irradiation positions in the LMTD stand positioned at the central part of Issledovatel (relative values).

During the irradiation, the stand is positioned in the central part of the working area with the best homogeneous dose. Six liquid dosimeters (2 ml each) or 24 foil dosimeters can be irradiated simultaneously. Our measurements by means of Fricke and dichromate dosimeters showed small but distinct differences between the dose rates at different irradiation positions. They are presented in Fig.2.

Table. Dose rates at 1-4 irradiation positions determined by the LMTD Fricke dosimeter and the NPL low dose dichromate dosimeter (transfer standard).

Date	Position	Dt [Gy/min]		LPDT/NPL
		LPDT Fricke	NPL LD dichromate	
01.12.1999	1	48.83	48.73	1.002
01.12.1999	2	49.24	49.24	1.000
01.12.1999	3	49.82	49.47	1.007
01.12.1999	4	50.13	49.49	1.013



PL0101484

During realization of the EU Inco-Copernicus project IC-15-CT-96-0824 we have the possibility to compare our results with the dose measurements done at Centre for Ionizing Radiation Metrology, National Physical Laboratory (Teddington, United Kingdom). Low dose dichromate dosimeters were used as transfer standard dosimeters. The results

presented in Table confirmed a high precision of the LMTD dose measurements.

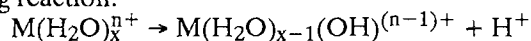
The LMTD offers for today  $\gamma$ -irradiation of dosimeters or other small objects in the dose range 10 Gy - 100 kGy with temperature control and with a combined uncertainty  $\pm 2.8\%$  at a 95% confidence level.

**RADIOCHEMISTRY**  
**STABLE ISOTOPES**  
**NUCLEAR ANALYTICAL METHODS**  
**GENERAL CHEMISTRY**

INFLUENCE OF RELATIVISTIC EFFECTS ON HYDROLYSIS OF  $\text{Ra}^{2+}$ 

Barbara Włodzimirska, Aleksander Bilewicz

The metal cations hydrolysis is shown in the following reaction:



Generally, hydrolysis is related to the interaction between the oxygen in water molecule and the metal cation [1]. Therefore, the tendency to hydrolyze increases with increasing oxidation state of the cation and decreasing ionic radius. This is understandable because with decreasing M-O distance, the polarizing effect of smaller cation on the O-H bond in the aqua ligand increases, which, in turn results in easier loss of the proton from the hydrated cation. Because of that, hydrolysis should decrease down each Group of the Periodic Table with increasing radius of the outermost shell in the ion.

Unexpectedly, for 1+ cations of Group 11, 2+ cations of Group 12, and 3+ cations of Group 13 the heaviest members in each group ( $\text{Au}^+$ ,  $\text{Hg}^{2+}$  and  $\text{Tl}^{3+}$ , respectively) hydrolyse much more easily than their lighter congeners. Table 1 presents the first hydrolysis constants

$$K_1 = \frac{[\text{M}(\text{OH})(\text{OH}_2)_{x-1}^{(n-1)+}][\text{H}^+]}{[\text{M}(\text{OH}_2)_x^{n+}]}$$

and radii of the maximum charge density of the outermost orbital ( $r_{\text{max}}$ ) in the Group 11, 12 and 13 metal cations.

The  $\text{Cu}^+$  and  $\text{Au}^+$  aqua ions are known to be unstable in aqueous solution, especially under alkaline

Table 1.  $\text{pK}_1$  [2,3] and  $r_{\text{max}}$  [4] for Groups 11, 12 and 13 cations.

Group 11			Group 12			Group 13		
cation	$r_{\text{max}}$ [pm]	$\text{pK}_1$	cation	$r_{\text{max}}$ [pm]	$\text{pK}_1$	cation	$r_{\text{max}}$ [pm]	$\text{pK}_1$
$\text{Cu}^+$	32.3	-	$\text{Zn}^{2+}$	30.5	8.96	$\text{Ga}^{3+}$	28.6	3.6
$\text{Ag}^+$	54.5	12	$\text{Cd}^{2+}$	52.1	10.08	$\text{In}^{3+}$	49.4	4.0
$\text{Au}^+$	64.0	3.8	$\text{Hg}^{2+}$	61.5	3.40	$\text{Tl}^{3+}$	58.9	0.6

line conditions. However, gold (I) solutions in mixtures of acetonitrile and dilute mineral acids have been used to determine the first hydrolysis constant of  $\text{Au}^+$  [3]. The aim of the present work was to study the hydrolysis for cations of 7th period in comparison with lighter homologs.

Table 2.  $\text{pK}_1$  and  $r_{\text{max}}$  [4] for Groups 2 cations.

Cation	$r_{\text{max}}$ [pm]	$\text{pK}_1$	$\text{pK}_1$ (literature) [2]
$\text{Ca}^{2+}$	55.66	13.22	13.36
$\text{Sr}^{2+}$	70.14	13.83	13.775
$\text{Ba}^{2+}$	88.08	14.05	13.996
$\text{Ra}^{2+}$	96.98	14.07	

Until now, the first hydrolysis constant for  $\text{Fr}^+$ ,  $\text{Ra}^{2+}$  and  $\text{Ac}^{3+}$  have not been determined. These cations exist only in submicroamount and a simple potentiometric method cannot be applied. The ion exchange method based on the various partition of the  $\text{Ra}^{2+}$  and  $\text{RaOH}^+$  cations was used. This method permits to work with extremely diluted  $\text{Ra}^{2+}$  radioactive solutions. From the plotted relationship

between the values of  $\log K_d$  and  $\log[\text{OH}^-]$ , the first hydrolysis constants have been determined for  $\text{Ra}^{2+}$  and also for comparison for  $\text{Ca}^{2+}$ ,  $\text{Sr}^{2+}$  and  $\text{Ba}^{2+}$ . The results are presented in Table 2, and compared with values obtained from other work

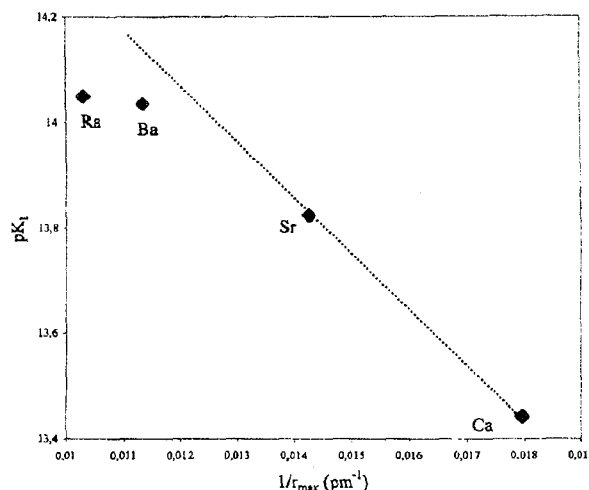


Fig. Dependence of the first hydrolysis constants on the radius of the outermost shell.

[2]. Table 2 shows that the hydrolysis of  $\text{Ra}^{2+}$  is close to the hydrolysis of  $\text{Ba}^{2+}$ , despite that the hydrolysis should decrease down each group of the Periodic Table. As shown in Fig., the  $\text{pK}_1$  value for  $\text{Ra}^{2+}$  do not fit well to the straight line created by

$\text{Ca}^{2+}$ ,  $\text{Sr}^{2+}$  and  $\text{Ba}^{2+}$  cations. The reason of higher than expected  $\text{Ra}^{2+}$  hydrolysis is the influence of relativistic effects on bonding orbitals. Due to relativistic stabilization of  $7s$  and  $7p_{1/2}$  orbitals, the first hydrolysis constant of  $\text{Ra}^{2+}$  is similar to that of  $\text{Ba}^{2+}$ , in spite of the difference in their outermost orbital radii equal to 8 pm. The influence of relativistic effect on  $\text{Ra}^{2+}$  hydrolysis is smaller than for the heaviest member of Group 11, 12 and 13 because  $\text{Ra}^{2+}$  forms octahydrate cations. Participations of  $s$  and  $p_{1/2}$  relativistic stabilized orbitals in M- $\text{H}_2\text{O}$  bonding in  $\text{Ra}(\text{H}_2\text{O})_8^{2+}$  is lower than in two coordinate  $\text{Au}(\text{H}_2\text{O})_2^+$  and six coordinate  $\text{Hg}(\text{H}_2\text{O})_6^{2+}$  and  $\text{Tl}(\text{H}_2\text{O})_6^{3+}$ .

## References

- [1]. Baes C.F. Jr., Messmer R.E.: The Hydrolysis of Cations. Krieger Publishing Company, Malabar Fl. 1986.
- [2]. Smith R.M., Martell A.E.: Critical Stability Constants. Vol.4. Plenum Press, New York 1976, pp.1-12.
- [3]. Kissner R., Welti G., Geier G.: J. Chem. Soc., Dalton Trans., 1773-1777 (1997).
- [4]. Desclaux J.P.: Atom Data Nucl. Data, 12, 311 (1973).

# DETERMINATION OF TRACE AMOUNTS OF CADMIUM IN GEOLOGICAL AND ENVIRONMENTAL MATERIALS BY NAA WITH PRECONCENTRATION ON AMPHOTERIC ION EXCHANGE RESIN

Zbigniew Samczyński, Rajmund Dychczyński, Bożena Danko

Cadmium is an element of toxic properties, concentration of which in the environment systematically increases. The main sources of Cd pollution are: the metallurgical industry, production of batteries, anti-corrosive coating of metals, pigments, burning of coal etc. [1,2]. Accurate and sensitive determination of this metal is then very important, especially while evaluating the extent of human exposure. Only a few instrumental analytical techniques can assure reliable determination of cadmium at trace and ultratrace concentrations [2,3], namely AAS, ICP-AES, MS and ICP-MS. Neutron Activation Analysis (NAA) is also quoted among them. Despite of their high sensitivity, most of them suffer, to a smaller or greater extent, from various interferences [2-4]. In the case of NAA, direct counting of cadmium photopeaks in instrumental version of the method is strongly disturbed by huge radioactivity of the matrix. These difficulties can be practically completely overcome performing radiochemical separation of the analyte. However, while analyzing geological and environmental materials, even after a few days of cooling, activity of the sample is often still too high to accomplish any chemical operations in a normal isotope laboratory. In this situation the only solution is the isolation of cadmium from accompanying elements before neutron irradiation. In this work an attempt was made to modify the analytical method for the determination of trace amounts of Cd in biological materials by RNAA devised by us previously [5-7], and to adopt it for samples of geological and environmental origin. Separation of cadmium is based on ion exchange with the use of an amphoteric ion exchanger Retardion 11A8.

Retardion 11A8 contains strongly basic quaternary ammonium anion exchange groups and an equivalent amount of weakly acidic carboxylic cation exchange groups [8]. Depending on the composition of the external solution being in contact with the resin, simultaneous sorption of both cations and anions is possible. Ion exchange behaviour of cadmium in hydrochloric acid and ammonia solutions ( $0.01\text{--}12\text{ mol}\cdot\text{l}^{-1}$ ) was investigated. Results revealed that in both systems distinct concentration ranges can be distinguished where Cd exhibits high affinity towards Retardion 11A8 [5,7]. Hence, establishing appropriate composition and sequence of eluents, exploiting both anion and cation exchange function of the resin, this metal can be selectively retained on the column, whereas many accompanying elements are eluted. The separation scheme based on the stepwise elution, underlying very accurate method for the determination of low and ultra low concentrations of cadmium in biological materials, was devised [5-7].

In the present work, basing on the earlier investigations, the main effort was made to apply Retar-

dion 11A8 for the determination of trace amounts of Cd in geological and environmental materials by neutron activation analysis. Two ion exchange separation procedures have been elaborated. The first is performed before, the second after neutron activation. Zinc exhibits a similar ion exchange behaviour on Retardion 11A8 like cadmium and, moreover, both the elements can be separated from one another [5,7]. Hence, determination of both metals in a single analytical cycle is feasible.

A sample is digested with  $\text{HNO}_3 + \text{HF}$  (2+1) using a microwave technique and finally introduced onto the Retardion 11A8 column in  $2\text{ mol}\cdot\text{l}^{-1}$  hydrochloric acid solution. During elution with  $2\text{ mol}\cdot\text{l}^{-1}$  HCl and  $1\text{ mol}\cdot\text{l}^{-1}$   $\text{NH}_3 + 0.1\text{ mol}\cdot\text{l}^{-1}$   $\text{NH}_4\text{Cl}$  cadmium and zinc are retained on the bed, which enables their separation from many accompanying elements present in analyzed materials. The analytes are then washed out by means of  $0.01\text{ mol}\cdot\text{l}^{-1}$  HCl and the effluent is concentrated and evaporated to dryness in a quartz ampoule. Ampoules with the isolated, in the above manner, traces of Cd and Zn are irradiated, together with standards, in a nuclear reactor. The aim of the ion exchange procedure realized after neutron activation is to remove some residual trace elements with  $2\text{ mol}\cdot\text{l}^{-1}$  HCl and  $1\text{ mol}\cdot\text{l}^{-1}$   $\text{NH}_3 + 0.1\text{ mol}\cdot\text{l}^{-1}$   $\text{NH}_4\text{Cl}$  and to separate zinc using of  $0.05\text{ mol}\cdot\text{l}^{-1}$   $\text{NH}_3 + 2.0\text{ mol}\cdot\text{l}^{-1}$   $\text{NH}_4\text{Cl}$ . Finally, cadmium is stripped from the column with the aid of  $8\text{ mol}\cdot\text{l}^{-1}$   $\text{NH}_3 + 1.0\text{ mol}\cdot\text{l}^{-1}$   $\text{NH}_4\text{Cl}$ .

The accuracy of the elaborated method was tested by determining cadmium and zinc content in two available reference materials: Lake Sediment (SL-1) [9] of environmental and Zinnwaldite ZW-C [10] of geological origin. The results of quantitative determinations show good agreement with the certified values. Gamma ray spectra of zinc and cadmium fractions are practically free from other activities apart from those, which are normally observed in the background. Analytical results were corrected for the blank resulting from used reagents, glassware and contact with atmosphere when isolation of analytes before neutron activation is accomplished. Considerable minimization and good reproducibility of the blank was finally achieved.

## References

- [1]. Stöppler M.: In: *Metals and Their Compounds in the Environment*. Ed. E. Merian. Wiley, New York 1991.
- [2]. Łobiński R., Marczenko Z.: *Spectrochemical Trace Analysis for Metals and Metalloids*. In: *Wilson & Wilson's Comprehensive Analytical Chemistry*. Vol. XXX. Ed. S.G. Weber. Elsevier, Amsterdam 1997.
- [3]. Alfassi B.Z.: *Determination of Trace Elements*. VCH, Weinheim 1994.
- [4]. Szczepaniak W.: *Metody instrumentalne w analizie chemicznej*. PWN, Warszawa 1996.



PL0101486

- [5]. Samczyński Z., Dybczyński R.: *Chem. Anal. (Warsaw)*, **41**, 873-890 (1996).  
[6]. Samczyński Z., Dybczyński R.: *J. Chromatogr. A*, **789**, 157-167 (1997).  
[7]. Samczyński Z.: *Rozdzielcze i analityczne zastosowanie jonitów amfoterycznych*. Ph.D. thesis. IChTJ, Warszawa 1999.  
[8]. Hatch M.J., Dillon J.A., Smith H.B.: *Ind. Eng. Chem.*, **49**, 812 (1957).

- [9]. Dybczyński R., Suschny O.: Final Report on the Intercomparison Run SL-1 for the Determination of Trace Elements in a Lake Sediment. IAEA Report, IAEA/RL/64, 1979.  
[10]. Govindaraju K., Rubeska I., Paukert T.: *Geostandards Newsletter*, **18**, 1 (1994).



PL0101487

## PROBLEMS OF THE ATTRIBUTION OF WORKS OF ART: EXAMPLES OF 18TH CENTURY CENTRAL EUROPEAN DECORATIVE GLASS

Jerzy Kunicki-Goldfinger, Joachim Kierzek, Aleksandra J. Kasprzak<sup>1/</sup>, Bożena Małozewska-Bućko

<sup>1/</sup>National Museum, Warszawa, Poland

Aim of the study is the assistance to the historians in supplying them with a new tool for technological and provenance study of monuments and objects of art. The procedures that have been worked out during the research can be applied to study the different kinds of historical and artistic objects, although the presented project has been only concerned with a historic glass.

Since the beginning of 2000, the first part of the project entitled "Problems of the Attribution of Works of Art: Examples of 18th Century Central European Decorative Glass" has been conducted. It has been thought as a continuation of the previous one that has been already reported [1-5]. That new project is to be accomplished by the end of the 2001 [6]. The examination has been executed thanks to the co-operation of the Institute of Nuclear Chemistry and Technology and the National Museum (Warszawa) as well as thanks to the Boards of many other museums which made the vessels available for examination: National Museums (Kraków, Poznań and Wrocław), Royal Castle in Warsaw, District Museum in Tarnów, Museum in Nieborów, Museum-Palace in Wilanów and Historical Museum in Warsaw.

The main objective of the presented study is to characterise the glass formulation made by central European factories in the 18th century, on the basis of chemical composition. This knowledge is of high importance for further technological and provenance studies of historic glass.

The project covers over 1000 vessels originating from the numerous Polish, German, Bohemian, Silesian and Russian glasshouses. In establishing the experimental procedures, the following limitations were taken into account: only non-destructive and non-sampling methods can be used to glass objects; measurements have to be carried out in a museum's display interior; very limited comparative chemical analyses data of 18th century tableware made in Central Europe, is available for cross reference. Energy dispersive X-ray fluorescence analysis (EDXRF) is used together with a short-wave ultraviolet radiation (UV-C) to examine the glass vessels. Examination of glass surfaces under a magnification is also conducted. The results of stylistic analysis and the results of physicochemical analysis, together with information from written documentary sources are discussed. Part of the examined objects has unques-

tioned attributes that have been taken as the basis for the grouping of the remaining glasses. Multivariate analyses of the analytical results (cluster, principal component and discriminating analysis) are to be applied.

The EDXRF analysis was used as a main analytical tool. The examined objects were placed directly on an excitation source shield. The analysed area of the glass surface was about 2 cm<sup>2</sup>. Two measurement set-ups were used. In the first one, X-ray spectra were measured using an 80 mm<sup>2</sup> Si(Li) detector with a 180 eV resolution for MnK $\alpha$  and a <sup>109</sup>Cd annular source (~740 MBq) to excite the elements in the glass. In the second set-up, the X-ray spectra were excited with an <sup>241</sup>Am annular source (~370 MBq) and measured using a 16 mm<sup>2</sup> HPGe low-energy detector with a 195 eV resolution at 5.9 keV. The live time of the measurements was 600 s in both cases.

The accumulated spectra were analysed using the AXIL-QXAS software, supplied by the International Atomic Energy Agency in Vienna. Over 2000 spectra have been evaluated and the corrections for the differences in matrix absorption and for the measurement geometry have been taken into account.

The research was supported by the Polish State Committee for Scientific Research, under grant No 1 H01E 028 18, as well as partly by Berthold EG&G ORTEC (Vienna) and NDT Systems (Warszawa).

### References

- [1]. Kunicki-Goldfinger J.J., Kierzek J., Kasprzak A.J., Małozewska-Bućko B.: *Raporty IChTJ. Seria B nr 2/99*. IChTJ, Warszawa 1999.  
[2]. Kunicki-Goldfinger J.J., Kierzek J., Kasprzak A.J., Małozewska-Bućko B.: In: *INCT Annual Report 1998*. INCT, Warszawa 1999, pp. 130-132.  
[3]. Kunicki-Goldfinger J.J., Kierzek J., Kasprzak A.J., Małozewska-Bućko B.: *Proceedings of the 6th International Conference on Non-Destructive Testing and Microanalysis for the Diagnostics and Conservation of the Cultural and Environmental Heritage*, Rome, Italy, 17-20 May 1999, AIPND, ICR, Rome 1999, vol. II, pp. 1539-1552.  
[4]. Kunicki-Goldfinger J.J., Kierzek J., Kasprzak A.J.: *Archäometrie und Denkmalpflege - Kurzberichte 2000*. Mensch & Buch Verlag, Berlin 2000, pp. 107-109.  
[5]. Kunicki-Goldfinger J.J., Kierzek J., Kasprzak A.J., Małozewska-Bućko B.: *X-Ray Spectrom.*, **29**, 4, 310-316 (2000).  
[6]. Kunicki-Goldfinger J.J.: *Glass & Ceramics Conservation. Newsletter of the ICOM Committee for Conservation, Working Group "Glass, Ceramics and Related Materials"*, **7**, 13-14 (2000).

# DYNAMIC ADSORPTION OF RADIOEUROPIUM FROM SIMULATED LIQUID RADIOACTIVE WASTES ON $\alpha$ -CRYSTALLINE POLYANTIMONIC ACID

Jujjavarapu Satyanarayana<sup>1/</sup>, Aleksander Bilewicz, Jerzy Narbutt

<sup>1/</sup>Ghandi Institute of Technology and Management, Visakhapatnam, India

The purpose of the work was to continue and conclude studies on the removal and immobilisation of hazardous long-lived radionuclides:  $^{137}\text{Cs}$ ,  $^{90}\text{Sr}$  and actinides(III) from liquid radioactive wastes containing various salts and complexing agents, with the use of inorganic ion exchangers. The problem of inorganic ion exchangers as selective adsorbents and potential primary barriers for radionuclides has recently been reviewed [1].  $\alpha$ -Crystalline polyantimonic acid (CAA) has been selected as a promising ion exchanger for the removal of long-lived radionuclides:  $^{90}\text{Sr}$  and actinides(III) from liquid radioactive wastes [2]. CAA is an ion exchanger highly effective toward metal cations which have radii in the range from about 95 to 120 pm, i.e.  $\text{Na}^+$ ,  $\text{Ca}^{2+}$  and  $\text{Sr}^{2+}$  [3]. Recently, CAA was studied in detail as the adsorbent for radiostrontium in the column process [4]. In the present work also the sorption of  $\text{Eu}^{3+}$  ions on CAA was investigated under dynamic conditions.

Adsorption properties of CAA towards micro-amounts of europium were investigated in the reverse-run column process [4], using standard CAA grains of size 0.1-0.3 mm, with the bed of  $\phi=4$  mm and  $h=35$  mm, at room temperature,  $21 \pm 3^\circ\text{C}$ . The

rates, from  $0.57$  to  $2 \text{ m} \cdot \text{h}^{-1}$ , i.e. from 16.3 to 57 bed volumes (BV) per hour. The effluent samples each of  $100 \text{ cm}^3$  were collected and their radioactivity was measured. The early breakthrough obtained (at ca. 200-300 BV) was probably due to the slow kinetics of  $\text{Eu}^{3+}$  adsorption on CAA and to a rather high pH (9-10) of the solution, at which dissociated EDTA strongly complexed the metal ions [2]. Additional measurements on adsorption kinetics for  $^{85}\text{Sr}$  and  $^{152}\text{Eu}$ , performed by the batch method [2], have confirmed the great effect of pH on  $\text{Eu}^{3+}$  adsorption: almost no  $\text{Eu}^{3+}$  uptake from the alkaline solution within the 24 h equilibration time, and over 98% adsorption from the acidified (the equilibrium pH of 2-2.5) solution (at the CAA-to-solution mass ratio of 1:200). On the contrary, in both cases  $\text{Sr}^{2+}$  was completely adsorbed on CAA. Therefore, in further experiments the simulated waste solution was adjusted to pH 3 and passed through the PAA column at low flow rates. Fig. shows the breakthrough curves obtained at the flow rates of 2 and  $0.57 \text{ m} \cdot \text{h}^{-1}$ .

In the first case, the decontamination factor (the ratio of the specific activity of the influent to that of effluent) of 10 was attained already at 230 BV, whereas in the second - at about 1100 BV of effluent. The former value may sometimes be accepted for waste purification, but in general, still better efficiency is required. This can be attained either by a further decrease in the flow rate, and/or with increasing bed length. Otherwise, a long lasting batch process can be recommended to treat large volumes of liquid radioactive waste.

The work has been carried out during the visit of J. Satyanarayana to the INCT, financed by the Polish State Committee for Scientific Research and DST in the frame of Indo-Polish Scientific Collaborative Research Programme (Project No INT/POL/010.00).

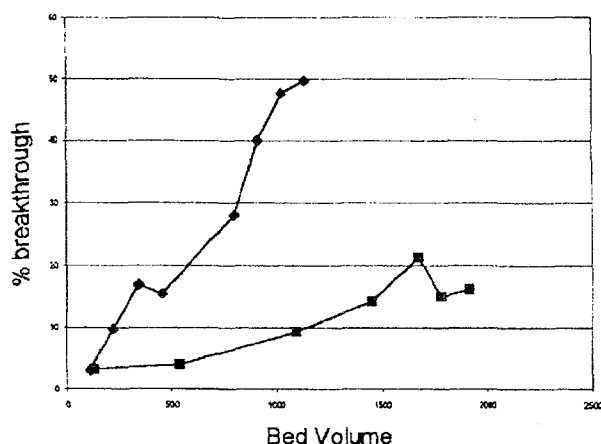


Fig. The breakthrough curves of  $\text{Eu}^{3+}$  traces on the CAA column (4/35 mm) from the simulated radioactive waste solution at pH 3, obtained at flow rates of: 2 ( $\blacklozenge$ ) and  $0.57 \text{ m} \cdot \text{h}^{-1}$  ( $\blacksquare$ ).

solution labelled with  $^{152,154}\text{Eu}^{3+}$  ions contained: EDTA (45 ppm), oxalic acid (50 ppm), citric acid (50 ppm),  $\text{CaCl}_2$  ( $0.1 \text{ g} \cdot \text{dm}^{-3}$ ),  $\text{Na}_2\text{SO}_4$  ( $1 \text{ g} \cdot \text{dm}^{-3}$ ) and  $\text{KOH}$  ( $1 \text{ g} \cdot \text{dm}^{-3}$ ), to model the composition of most common liquid radioactive waste treated in the Department of Radioactive Waste Management of the Institute of Atomic Energy at Świerk [2,5]. The column process was studied at different flow

## References

- [1]. Narbutt J.: Inorganic ion exchangers as selective adsorbents and potential primary barriers for radionuclides. In: *The Environmental Challenges of Nuclear Disarmament*. Eds. T.E. Baca, T. Florkowski. Kluwer Academic Publishers, 2000, pp. 237-243.
- [2]. Satyanarayana J., Bilewicz A., Narbutt J.: *Nukleonika*, **43**, 531-538 (1998).
- [3]. Bilewicz A.: *Radiochim. Acta*, **69**, 137-140 (1995).
- [4]. Bilewicz A., Krejzler J., Narbutt J.:  $\alpha$ -Crystalline polyantimonic acid - an adsorbent for radiostrontium and actinides(III) from liquid waste, and a potential primary barrier in Nuclear Waste Repositories. 5th International Conference on Nuclear and Radiochemistry, Pontresina, Switzerland, 3-8 September 2000, Extended Abstracts, pp. 251-253.
- [5]. Tomczak W. (Institute of Atomic Energy, Świerk): personal information.





# **DIFFUSE REFLECTION SPECTROSCOPY: STUDIES OF OXIDE LAYERS FORMED ON THE STAINLESS STEELS IN HIGH TEMPERATURE WATER**

Leon Fuks, Claude Degueldre<sup>1/</sup>

<sup>1/</sup>Paul Scherrer Institute, Villigen, Switzerland

The unique technique of Diffuse Reflection Spectroscopy (DRS) may be advantageous, even when the traditional spectroscopic techniques fail. So, it has been successfully used in many analytical fields, e.g. in the study of rough pitted surfaces [1], in the analysis of rust on weathering steels [2] or in the observation of iron oxide reflectivity [3]. All DRS applications are based on the fact that a large majority of substances in their natural state (e.g. powders, rough surface solids, various particle suspensions or dyes) exhibit so-called diffuse reflections, i.e. the incident light is scattered in all directions, as opposed to specular (mirror-like) reflection where the angle of incidence equals the angle of reflection.

Although the DR spectra are complex and strongly depend on the conditions under which they are obtained, this problem is completely outweighed by the great advantage of its non-invasive quality, which is essential in many applications [4]. In a series of papers we have shown that correctly realized in a long series of successive measurements DRS can directly provide a great number of important data concerning the kinetics of the oxide layer build-up [5-7]. So, finally we undertook an attempt to examine the possibility of extension of the DRS measurements with the aim of the analysis of chemical com-

position of the relatively thick oxide layers formed on the stainless steel under the BWR conditions. In the case of the catalysts, e.g. of metallic nanolayers formed on the surface of the silica or aluminum oxides, UV-Vis DRS has been already successfully applied and contributed numerous important details concerning their chemical composition [8-13].

It has been already observed that independently of the differences in the properties of circulating nuclear reactor cooling water, composition of the oxide layer formed on the surface of metal parts remains more or less the same [14]. As a rule, corrosion oxide films consist of two main layers:

1. an amorphous, or poorly textured, inner oxide next to the metal; it is probably quite thin in low oxygen water;

2. a duplex corrosion film (called also an outer oxide) consisting of:

- an inner sub-layer formed by small crystallites, which have some porosity and are not highly protective,
- a discontinuous, outer sub-layer, consisting of large crystals; they are quite protective where they exist.

Thickness, composition and structure of an outer oxide strongly depend on the type of the material

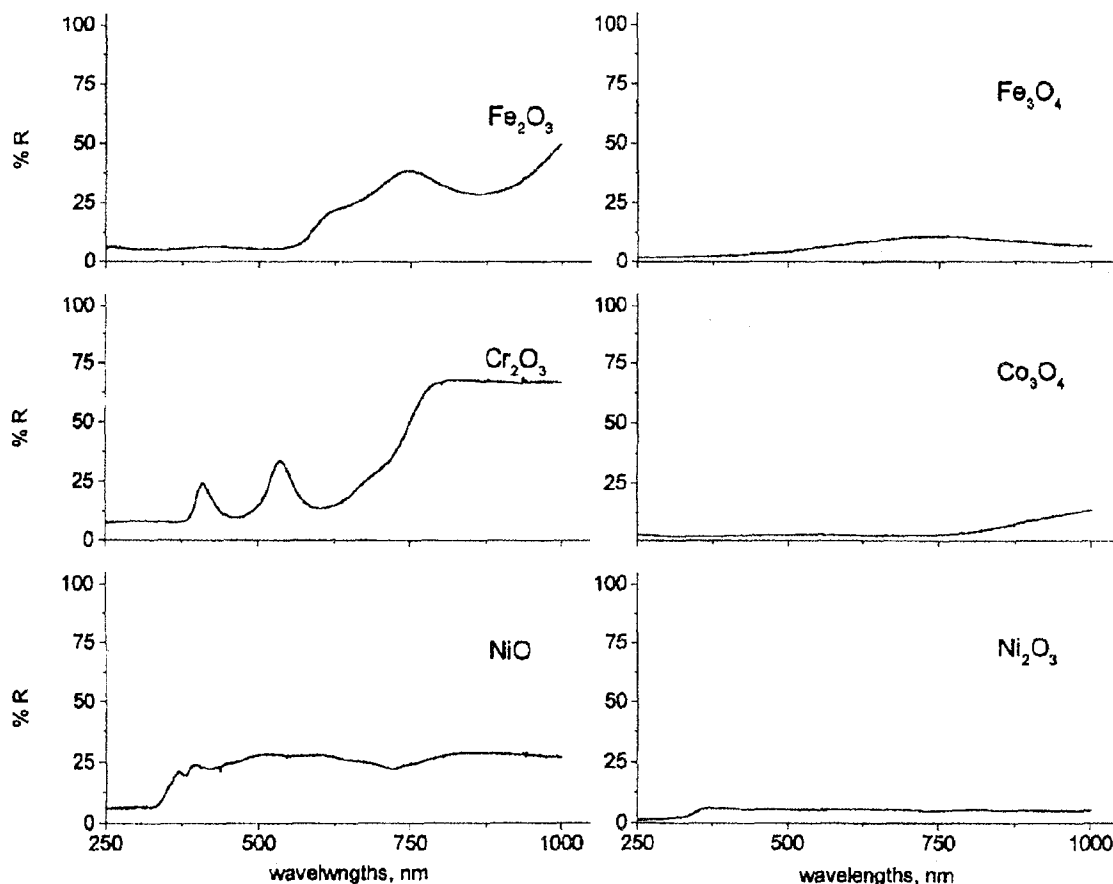


Fig.1. DRS spectra of the artificial oxide samples.

used. It differentiates the release of the corrosion products into the circulating coolant. Because of their different solubility in water, both sub-layers, formed mainly by precipitation of the dissolved compounds, exhibit various properties [14]. In de-oxygenated, hot, pressurized water the outer oxide consists mainly of octahedral magnetite  $\text{Fe}_3\text{O}_4$  which contains nickel spinel-type oxides ( $\text{Ni}_x\text{Fe}_{3-x}\text{O}_4$ ). The size of the grains ranges from ca. 100 to 1500 nm. In oxygenated high temperature water, in turn, outer layer contains additionally the Fe(III) oxides and oxyhydroxides, e.g. large particles of  $\gamma\text{-Fe}_2\text{O}_3$ , small particles of  $\alpha\text{-Fe}_2\text{O}_3$  or  $\text{FeOOH}$ . Certain amount of NiO or  $\text{Cr}_2\text{O}_3$  particles can be also incorporated.

The inner oxide consists mainly of chromium rich spinel oxides ( $\text{Ni}_x\text{Cr}_y\text{Fe}_{3-x-y}\text{O}_4$ ) with non-stoichiometric composition. Different values are reported for x and y with  $\text{Fe}_2\text{CrO}_4$ ,  $\text{FeCr}_2\text{O}_4$  and  $\text{NiCr}_2\text{O}_4$  as limiting cases [14].

The DRS spectra, recorded in the UV-Vis-Near IR spectral region, of the selected oxides which can be expected to exist in the corrosion film are presented in Fig.1. Each spectrum represents one oxide (powder sample) registered with  $\text{BaSO}_4$  as the non-absorbing reference medium. As one can see, the spectra are adequate to the chromatic properties of the investigated species. For the intensively green powder of  $\text{Cr}_2\text{O}_3$ , two distinct spectro-

$\text{Fe}_2\text{O}_3$  these peaks shift towards longer wavelength values (about 630 and 745 nm, respectively) and significantly broaden. Finally, in the spectrum of NiO (green-black) both broad peaks are very difficult to assign, but we estimate that their maxima lie at about 550-600 (green) and 800 nm, respectively. Percentage of the reflectivity of the oxide remains on the same level for all the above mentioned peaks. Other investigated samples are black in color and their spectra do not show any maxima. Percentage of the reflectivity is much lower than for the colored samples and is close to zero, characteristic for the perfectly absorbing media.

Fig.2, in turn, presents a comparison of spectra obtained for NiO and  $\text{Cr}_2\text{O}_3$  with that recorded for the real oxide film formed on the surface of the electropolished AISI 316 stainless steel (68% of Fe, 17% of Cr, 12% of Ni, 2.5% of Mo, max. 0.08% of C). Two distinct peaks in the spectral regions of 674 and 452 nm, accompanied by the small one in the region of 385 nm, can be attributed to those observed for the  $\text{Cr}_2\text{O}_3$  powder sample. Observed shifts of the peak maxima towards the low wavelengths seem to be related to the formation of the nickel-chromium-iron oxides solid solution. The artificial samples, in turn, were prepared only by mechanical mixing of the appropriate compounds.

Thanks are due to the Polish State Committee for Scientific Research for financial assistance in the scientific co-operation between the Institute of Nuclear Chemistry and Technology and Paul Scherrer Institute, as well as to the Swiss Federal Nuclear Safety Inspectorate for partial financial support.

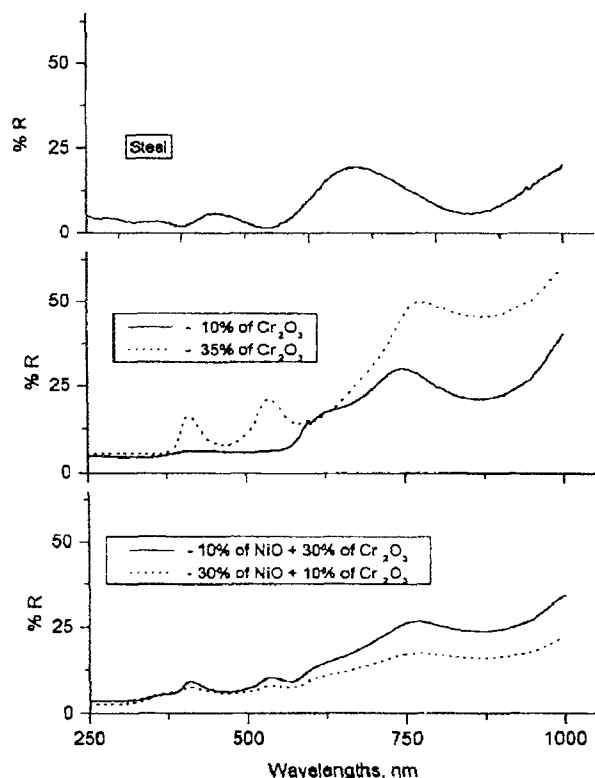


Fig.2. DRS spectrum of an oxide formed on the surface of the stainless steel during hydrothermal treatment compared with  $\text{Cr}_2\text{O}_3$  and NiO.

scopic peaks can be observed at wavelengths of 407 and 535 nm, respectively. For the reddish-gray

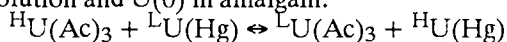
## References

- [1] Lunder O., Nisancioglu K., Hunderi O.: In-situ measurement of the pitted area by diffuse light scattering. Proceedings of the International Congress on Metallic Corrosion, National Research Council of Canada, Toronto 1984, Vol.1, 481 p.
- [2] Raman A., Kuban B.: Natl. Assoc. of Corrosion Engineers, 44, 483 (1988).
- [3] Schubnell M., Tschudi H.R., Kuhn P., Ries H.: Reflectivity as a Probe for Chemical Reactions. *Proced. Acad. Sci. Chem. Soc.*, 105, 671 (1993).
- [4] McGuire G.E., Swanson M.L., Parikh N.R., Simko S., Weiss P.S., Ferris J.H., Nemanich R.J., Chopra D.R., Chourasia A.R.: *Anal. Chem.*, 67, 199R (1995).
- [5] Degueldre C., O'Prey S., Francioni W.: *Corrosion Sci.*, 38, 1763 (1996).
- [6] Degueldre C., Fuks L., Schenker E.: *Meas. Sci. Technol.*, 9, 809 (1998).
- [7] Degueldre C., Fuks L., Schenker E.: *Appl. Surface Sci.*, 134, 254 (1998).
- [8] Scheffer B., Heijeinga J.J., Moulijn J.A.: *J. Phys. Chem.*, 91, 4752 (1987).
- [9] Okamoto Y., Nagata K., Adachi T., Imanaka T., Inamura K., Takyu T.: *J. Phys. Chem.*, 95, 3102 (1991).
- [10] Weckhuysen B.M., Schoonheydt R., Jehng J.-M., Wachs E., Cho S.J., Ryoo R., Kijstra S., Poels E.: *J. Chem. Soc. Faraday Trans.*, 91, 3245 (1995).
- [11] Sazonov V.A., Prokudina N.A., Ismagilov Z.R., Bolyfyreva N.N., Arendarskii D.A., Ushakov V.A., Rogov V.A., Gavrilov V.Yu.: *Russ. J. Appl. Chem.*, 70, 87 (1996).
- [12] Tolstoi E.V., Tolstoi V.P.: *Russ. J. Gen. Chem.*, 69, 856 (1999).
- [13] Tolstoi V.P.: *Russ. J. Appl. Chem.*, 72, 1326 (1999).
- [14] Stellwag J.: *Corrosion Sci.*, 40, 337 (1998).

AN ATTEMPT TO FRACTIONATE URANIUM ISOTOPES  
IN THE ACETATE / AMALGAM SEPARATION SYSTEMWojciech Dembiński, Marek Poniński, Rudolf Fiedler<sup>1/</sup><sup>1/</sup> International Atomic Energy Agency, Safeguards Analytical Laboratory, Seibersdorf, Austria

The isotope effects which occur in the two uranium red-ox systems U(III)-U(IV) and U(IV)-U(VI) are well known and even used for uranium enrichment on the pre-industrial scale. However, no data were published on the isotope effect in the third red-ox uranium system: U(0)-U(III).

Continuing our studies on the relation between the isotope effect and the isotope mass we tried to fractionate uranium isotopes by means of the exchange reaction between acetate complexes of U(III) in solution and U(0) in amalgam:



where: H and L are the heavier and lighter isotopes.

The chemical procedure was similar to that successfully applied in our studies on the fractionation of samarium and ytterbium isotopes [1,2]. To attain a 4-stage separation, a simple cascade procedure with two branches, solution (S) and amalgam (A), was applied. The isotope ratios in the final S and A fractions were determined by means of a mass spectrometer with a multicollector system (Finnigan MAT 262). In order to eliminate the mass fractionation effect, the method of total evaporation of the sample was applied [3].

The values of the separation gain was found to be  $-0.034 \pm 0.02$  for  $^{234/238}\text{U}$  and  $+0.00045 \pm 0.00015$ . The precision of the measurements was estimated by standard deviation of the mean,  $\text{SD}/\sqrt{8}$ .

The results revealed a different behavior of  $^{234}\text{U}$  and  $^{235}\text{U}$  with respect to  $^{238}\text{U}$  in the investigated acetate/amalgam system. From the values of the separation gains it follows that  $^{234}\text{U}$  is concentrated in the solution phase, whereas  $^{235}\text{U}$  is concentrated in the amalgam phase. The difference may be related to the even and odd mass number of the isotopes, however, because of the rather high experimental error the conclusion should be confirmed by additional studies.

## References

- [1]. Dembiński W., Poniński M., Fiedler R.: Sep. Sci. Technol., 33(11), 1693 (1998).
- [2]. Dembiński W., Poniński M., Fiedler R.: J. Radioanal. Nucl. Chem., (2001), in print.
- [3]. Fiedler R., Donohue D., Grabmueller G., Kurosawa A.: Int. J. Mass Spectrom. Ion Processes, 132, 207-205 (1994).

## AQUEOUS SOLUBILITIES OF RARE EARTH TRIHALIDES (Cl, Br, I) AT 298 K

Tomasz Mioduski

Recently, the aqueous solubilities of rare earth(III) trifluorides reported in the literature have been compiled and critically evaluated [1]. The present work is a summary of critically evaluated source literature data on the solubilities of scandium, yttrium, lanthanum and lanthanide trichlorides, tribromides and triiodides in water at 298 K (Table). The lanthanides, as actinide homologues, are of interest for radiochemistry. The data on solubility of their salts may be helpful, e.g. to analytical chemistry and technology of rare earths, and to the treatment of radioactive wastes which contain large amounts of lanthanide and yttrium fission products (the maxima on both humps of the fission yield curve).

The high solubility of  $\text{ScCl}_3$  is indicative, as in the case of the fluoride system studied [1], of the coordination number 6 for scandium in the monomeric non-hydrolysed  $[\text{Sc}(\text{OH}_2)_6]^{3+}$  aqua ion in acidic solutions.

In the  $\text{LnCl}_3\text{-H}_2\text{O}$  system Y is shifted to Tm-Yb, i.e. in the opposite direction, compared to the quasi-Tb behaviour in the  $\text{LnF}_3\text{-H}_2\text{O}$  system, as far as the solubilities listed in Table are concerned. This phenomenon must result from a "softer" environment of the two chloride ions and six water molecules vs. "hard" eight fluoride ions in the fluoride crystal lattice. In other words, the nephelauxetic effect is larger, and the participation of the

4f-electrons of the  $\text{Ln}^{3+}$  ions in bonding is more pronounced, in the trichloride hexahydrate crystal lattice  $\{[\text{Ln}(\text{OH}_2)_6(\text{Cl})_2]\text{Cl}\}$  than in the  $\text{Ln}_{\text{aq}}^{3+}$  species, i.e. octaaqualanthanides(III), and to a larger extent than in the crystal lattice of the  $\text{LnF}_3 \cdot 0.5\text{H}_2\text{O}$  salts at the same CN 8. Therefore, the Ln(III) series is shifted with regard to Y(III) which does not possess the f-electrons, in the opposite directions for these two binary aqueous halide systems.

The solubilities of  $\text{LnCl}_3$  in water at 298 K vs. Z, given in Table, demonstrate a minimum extended over a broad Sm-Dy range with the lowest value of  $3.588 \text{ mol} \cdot \text{kg}^{-1}$  at Eu. With increasing temperature, and the concentrations involved, this broad minimum tends to narrow, and to dislocate towards the heavier lanthanides. Similarly, while at 273 and 298 K, the solubility is more or less constant in the La-Nd range or even it slightly increases, at 333 K the solubility turning point is transferred from Nd to Ce. This may indicate that the equilibrium solid phase (i.e. the least soluble) for  $\text{PrCl}_3$  and  $\text{CeCl}_3$  at 333 K is not the heptahydrate any more but the hexahydrate.

The solubility plots of lanthanide bromides have been assumed to be parallel to those of the chlorides since the energies of their crystal lattices are exactly parallel [7]. Thus, the solubility of lantha-

Table. Solubilities (in mol · kg<sup>-1</sup> water) of rare earth trihalides in water at 298 K - recommended values.

RE	Trichlorides <sup>a</sup>	Tribromides <sup>b</sup>	Triiodides <sup>c</sup>	Equilibrium solid phase (X = Cl, Br)
Sc	6.22	7.1	6.17	RE(X) <sub>3</sub> · 6H <sub>2</sub> O, [RE(OH <sub>2</sub> ) <sub>9</sub> ]I <sub>3</sub>
Y	3.948	4.50	4.19	as above
La	3.895	4.52	4.39	RE(X) <sub>3</sub> · 6H <sub>2</sub> O, [RE(OH <sub>2</sub> ) <sub>9</sub> ]I <sub>3</sub>
Ce	3.84	4.45	4.12	as above
Pr	3.89	4.50	3.97	as above
Nd	3.93	4.43	3.95	RE(X) <sub>3</sub> · 6H <sub>2</sub> O, [RE(OH <sub>2</sub> ) <sub>9</sub> ]I <sub>3</sub>
Sm	3.641	4.22	3.73	as above
Eu	3.588	4.10	3.67	as above
Gd	3.590	4.10	3.81	as above
Tb	3.60	4.13	3.92	as above
Dy	3.631	4.15	3.99	as above
Ho	3.695	4.21	4.06	as above
Er	3.783	4.30	4.19	as above
Tm	3.877	4.42	4.25	as above
Yb	4.003	4.57	4.19	RE(X) <sub>3</sub> · 6H <sub>2</sub> O, [RE(OH <sub>2</sub> ) <sub>8</sub> ]I <sub>3</sub>
Lu	4.12	4.70	4.15	as above

<sup>a</sup> Precision of the recommended chloride solubilities is about 0.2%, and the accuracy is around 0.4%, except for Ce, Pr, Nd, Tb, Lu and Sc, where presumably it is somewhat worse. The respective value for Nd may be minutely high. Literature sources: [2] for Y and Ln except for Ce, Te; [3] for Sc.

<sup>b</sup> Precision is about ±3% and the accuracy is estimated to be about ±10%. Literature sources: [4].

<sup>c</sup> The precision and accuracy as for bromides. Literature sources: [5]. For the composition of the equilibrium solid phase see [6].

nide bromides in water at 298 K is slightly falling from La to Pr, then steeper, up to the minimum value at Eu-Gd, to rise sharply on going from Dy to Lu. At higher temperatures, and consequently at higher concentrations, the minimum solubility is probably shifted to Tb-Dy as for the chlorides.

The minimum solubilities of lanthanide(III) iodides, bromides and chlorides in the Sm-Tb range of the Ln series can be explained as in the case of ethylsulphates [8]. These minima for the triiodides denote that for the octaaqualanthanides(III), [Ln(OH<sub>2</sub>)<sub>8</sub>]<sup>3+</sup><sub>aq</sub>, up to Tm (and not to Er [2]), the Gibbs free energies of hydration decrease (i.e. they are becoming more exothermic) with Z more rapidly than the respective lattice free energies for the enneahydrates do. The reason of such behaviour is that the Ln-OH<sub>2</sub> distances are smaller for CN 8 than for CN 9, and the enthalpy, entropy and free enthalpy changes with Z are steeper for the lower coordination number. For the smallest ions of the Ln(III) series, viz. Yb<sup>3+</sup> and Lu<sup>3+</sup>, where CN=8 in the phases of both [Ln(OH<sub>2</sub>)<sub>8</sub>]I<sub>3</sub> and [Ln(OH<sub>2</sub>)<sub>8</sub>]<sup>3+</sup><sub>aq</sub> is held, the solubility trend is reversed.

## References

- [1]. Mioduski T.: Peculiarities of the aqueous rare earth fluoride systems. *Comments Inorg. Chem.*, **22** (6), (2000).
- [2]. Powell J.E.: Aqueous solubilities of rare earth chlorides. U.S. Atomic Energy Commission, 1959, Report IS-15; Saeger

V.W., Spedding F.H.: Some physical properties of rare-earth chlorides in aqueous solution. U.S. Atomic Energy Commission, 1960, Report IS-338; Spedding F.H., De Kock C.W., Pepple G.W., Habenschuss A.: Heats of dilution of some aqueous rare earth electrolyte solutions at 25°C. 3. Rare earth chlorides. *J. Chem. Eng. Data*, **22**, 58-70 (1977).

- [3]. Samodelov A.P.: Rastvorimost' khlorda skandiya v solyanoi kislothe pri 25°C. *Zh. Neorg. Khim.*, **10**, 1735-1737 (1965).
- [4]. Zwietasch K.J., Kirmse E.M., Krech I.: Solubility and compound formation in the lanthanum chloride-lanthanum bromide-water system. *Z. Chem.*, **24**, 144-145 (1984); Zholaliev Z.M., Sulaimankulov K., Isakova S.: Sistemy bromid ceriya-acetilkarbamid-voda i sulfat ceriya-acetilkarbamid-voda pri 25°C. *Zh. Neorg. Khim.*, **25**, 835-837 (1980); Sulaimankulov K., Abykeev K.: Spravochnik po rastvorimosti karbamidnykh solevykh sistem. Mektep, 1981.
- [5]. Rukk N.S., Savinkina E.V., Kravchenko V.V., Alikberova Z.Yu.: The formation of polyiodoiodate ions in systems containing lanthanum and yttrium iodides. *Rus. J. Coord. Chem.*, **23**, 208-210 (1997); Danilenko T.V., Emel'yanov V.I., Venskovich N.U., Ezhov A.I.: Preparation and properties of holmium iodide crystal hydrates. *Zh. Neorg. Khim.*, **43**, 139-142 (1998); Emel'yanov V.I., Molodkin A.K., Sukhov N.I., Dolganov V.P.: Sistemy Ln<sub>2</sub>O<sub>3</sub>-HI-H<sub>2</sub>O, LnI<sub>3</sub>-HI-H<sub>2</sub>O (Ln = Er, Tm, Yb) pri 25°C. *Zh. Neorg. Khim.*, **35**, 490-494 (1990).
- [6]. Heinio O., Leskela M., Niinisto L.: Structural and thermal properties of rare earth triiodide hydrates. *Acta Chim. Scand.*, **A34**, 207-211 (1980).
- [7]. Sun Tong-Shan, Wang Feng-Lian, Xiao Yu-Mei: A thermochemical study of rare-earth bromide hydrates. *Thermochim. Acta*, **311**, 21-27 (1998).
- [8]. Mioduski T., Siekierski S.: Hydration changes in the lanthanide series as reflected in the solubility of the ethylsulphates. *J. Inorg. Nucl. Chem.*, **38**, 1989-1992 (1976).

## STUDIES ON DETERMINATION OF SOME TRANSITION METALS IN BIOLOGICAL MATERIALS BY ION CHROMATOGRAPHY

Krzysztof Kulisa, Halina Polkowska-Motrenko, Rajmund Dybczyński

In our previous work the possibility of transition metals determination in water samples was tested using an ion chromatograph Dionex 2000i/SP with

an Ion Pac CS5 analytical column, an Ion Pac CG5 guard column and a post column Ion Membrane Reactor [1]. Two eluents were applied: 6mM PDCA

+ 50mM CH<sub>3</sub>COOH + 50mM CH<sub>3</sub>COONa and 50mM oxalic acid+95 mM LiOH. In the year 2000 investigations have been carried out (continued) on biological samples. A method for the determination of Fe, Cu, Pb, Ni, Cd, Zn, Mn and Co in certain biological materials (plant and animal tissue) has been elaborated. The reliability of the method has been checked using CRMs with a certified content of elements in question and by applying for some of the elements analyzed the "definitive" and/or "very accurate" methods elaborated previously in our Laboratory (Cu, Co, Ni, Cd) [2-8]. A procedure of preparation of biological samples for ion chromatography (IC) determination has been elaborated. The procedure consists of two stages: mineralization of biological matrices [9,10] and preparation of sample solution for injection into the ion chromatographic column.

Table 1. Results of Cd, Co, Cu and Ni determination in certified reference materials.

CRMs	Element [mg/kg dry mass]											
	Cd			Co			Cu			Ni		
	IC method	certified value	definitive method value	IC method	certified value	definitive method value	IC method	certified value	definitive method value	IC method	certified value	definitive method value
CTA-OTL-1	nd	1.12 ±0.12	1.17 ±0.08	1.36 ±0.42	0.879 ±0.039	0.964 ±0.017	12.5 ±2.8	14.1 ±0.5	-	6.1 ±2.5	6.32 ±0.65	5.96 ±0.40
CTA-OTL-2	nd	1.52 ±0.17	-	nd	0.429 ±0.026	0.424 ±0.006	17.3 ±2.6	18.2 ±0.9	-	nd	1.98 ±0.21	2.17 ±0.18
IAEA H8	191.6 ±12.9	189 ±6	188 ±5	nd	0.118 ±0.009	-	34.08 ±1.52	32.8 ±4.8	32.3 ±0.86	nd	0.29 ±0.41	-

graph (IC) determination has been elaborated. The procedure consists of two stages: mineralization of biological matrices [9,10] and preparation of sample solution for injection into the ion chromatographic column.

The samples of biological material (ca. 350 mg each) were weighed into PTFE vessels and digested

some elements determined, e.g. Co, Pb, Ni and Cd is close to detection limits of the IC method, at least for some materials. Mn can be determined only with the use of oxalic acid + LiOH eluent. The results for Mn using the PDCA + CH<sub>3</sub>COOH + CH<sub>3</sub>COONa eluent are considerably lower than the certified values. It seems that after digestion Mn is present in the solution in various valency states and only when using the first eluent one can obtain the required Mn complex.

In the case of determination of trace elements in biological materials by the IC method the blank of the method is critical. The blank contains usually

trace quantities of some elements determined (Fe, Cu) and also other elements, which influence the detection limits. The accuracy of the IC method has been verified using "definitive" and/or "very accurate" methods based on radiochemical neutron activation analysis for the following elements: Cu, Ni, Co, Cd (Table 1). As can be seen, good agreement

Table 2. Results of Fe, Mn, Pb and Zn determination in certified reference materials.

CRMs	Element [mg/kg dry mass]							
	Fe		Mn		Pb		Zn	
	IC method	certified or information value	IC method	certified value	IC method	certified value	IC method	certified value
CTA-OTL-1	1014±82	(989)	410±2	412±14	5.5 ±1.1	4.91±0.80	48.9±2.1	49.9±2.4
CTA-OTL-2	1040±49	1083±33	81.1±3.6	79.7±2.6	nd	22.1±1.2	43.1±3.9	43.3±2.1
IAEA H8	265.5±12.5		nd	5.62±0.29	nd	0.57±0.13	186.5±12.6	192.3±3.9

in a microwave oven (Plasmatronika Service, Wrocław) with 5 ml of concentrated HNO<sub>3</sub>. After mineralization the solutions were transferred quantitatively into PTFE evaporation dishes. Concentrated HF was added into each of the samples, and the solutions were evaporated to wet residues in order to remove silica. Finally, the residues were dissolved in HNO<sub>3</sub> (1+4). All reagents used were of spectral purity. The blank solutions were prepared in the same way. The obtained solutions (samples and blanks) were analyzed by ion chromatography according to [1]. The results of determinations of transition metals for three reference materials: Oriental Tobacco Leaves CTA-OTL-1, Virginia Tobacco Leaves CTA-VTL-1 and IAEA H8 Horse Kidney are given in Tables 1 and 2 [11-13].

As can be seen from Tables 1 and 2, in general, good or satisfactory agreement between the determined and certified values was observed. Content of

has been achieved for Co in CTA-OTL-1, Ni in CTA-OTL-1, Cu in IAEA H8 and Cd in IAEA H8. It seems that modifying digestion solution can improve detection, especially in the case of Co, Ni and Pb. Also some changes should be made to maintain Mn at 2+ valency state. These investigations will be continued.

## References

- [1] Kulisa K., Polkowska-Motrenko H., Dybczyński R.: In: INCT Annual Report 1999. INCT, Warszawa 2000, p. 74.
- [2] Dybczyński R., Wasek M., Maleszewska H.: J. Radioanal. Nuclear Chem., Articles, 130, 365 (1989).
- [3] Dybczyński R., Danko B., Maleszewska H.: J. Anal. Chem. (Moscow), 49, 31 (1994).
- [4] Dybczyński R., Danko B.: J. Radioanal. Nuclear Chem., 181, 43 (1994).
- [5] Dybczyński R., Danko B.: Biol. Trace Element Research, 43/45, 615 (1994).
- [6] Polkowska-Motrenko H., Dybczyński R., Danko B., Becker D.A.: J. Radioanal. Nuclear Chem., 207, 401 (1996).

- [7]. Dybczyński R., Samczyński Z.: J. Radioanal. Nuclear Chem., 150, 143 (1991).  
 [8]. Samczyński Z., Dybczyński R.: Chem. Anal. (Warsaw), 41, 873 (1996).  
 [9]. Polkowska-Motrenko H., Danko B., Dybczyński R., Koster-Ammerlaan A., Bode P.: Anal. Chim. Acta, 408, 89 (2000).  
 [10]. Danko B., Polkowska-Motrenko H., Dybczyński R.: J. Radioanal. Nuclear Chem., 246, 279 (2000).  
 [11]. Dybczyński R., Polkowska-Motrenko H., Samczyński Z., Szopa Z.: Raporty IChTJ. Seria A nr 1/96. IChTJ, Warszawa 1996.  
 [12]. Dybczyński R., Polkowska-Motrenko H., Samczyński Z., Szopa Z.: Raporty IChTJ. Seria A nr 3/97. IChTJ, Warszawa 1997.  
 [13]. Intercomparison of Cadmium and Other Elements in IAEA Horse Kidney (H8). Progress Report No 1. IAEA, Vienna 1985.

## SIMPLE PC SOFTWARE FOR ROUTINE ANALYSIS OF GAMMA-RAY SPECTRA

Zygmunt Szopa, Rajmund Dybczyński

Both the instrumental version of neutron activation analysis (INAA) [1,2] as well as the radiochemical one (RCNAA) [1,3] have been widely applied in various branches of science and technology. They play a significant role in trace/ultratrace analysis, as a control method for other analytical methods/techniques and frequently participate in certification of certified reference materials/reference materials CRMs/RMs [3-5].

As it is well known, the high-resolution gamma-ray spectrometry is an important part of the NAA method and, therefore, the reliability of the whole method strongly depends on reliable spectra analysis itself [6,7]. Recently, the growing spread of computer based multichannel analysers (MCA) [8] in NAA laboratories, together with the rapid development of the computer technology (ComTech), make it possible to use quite a sophisticated software for spectra analysis that few years ago could only be applied at mainframes in big computer centers [9-12].

The purpose of the present work was the elaboration of a new computer software that could be used for large-scale analyses of spectra that were acquired with the aid of computer based MCA [13] and, at the same time, avoiding the malfunction/doubtful performance of some selected functions connected with automatic peak searching for commercial software implemented therein [7]. This software was called "SAWAP-PC", similarly as its parent code working at mainframe computer [9]. It also comprises majority of the functions and features of its parent computer code and can be used for both qualitative and quantitative analyses of spectra acquired by the Polish MCA Tukan (version 2.0). This "user-friendly" PC software works under MS-DOS operation system and enables fast reduction of large data files. It has been written and run using RMFOR-86 and MS-FOR-90 compilers. From the view-point of its organisation, it is a "close-type" software handling all the required data from-and-to the computer disc, where the reduced data could be printed out and visualised for various purposes (off-line) in different ways later on.

The simplified flow chart of the SAWAP-PC program presents Fig.1., where there are 2 files called SAW.INP and SPEC.TRA (default) at the input. They contain the control data that are determining the way of spectra processing and the  $\gamma$ -ray spectra accordingly. In its default run, the program does the energy calibration, automatically searches for all real peaks in the spectrum and saves the required information in SAW.OUT (default) file at

the output. Automatic peak searching is based on digital spectrum differentiation [10], while their acceptance on several height, width and shape's tests. For all the found and accepted peaks it calculates

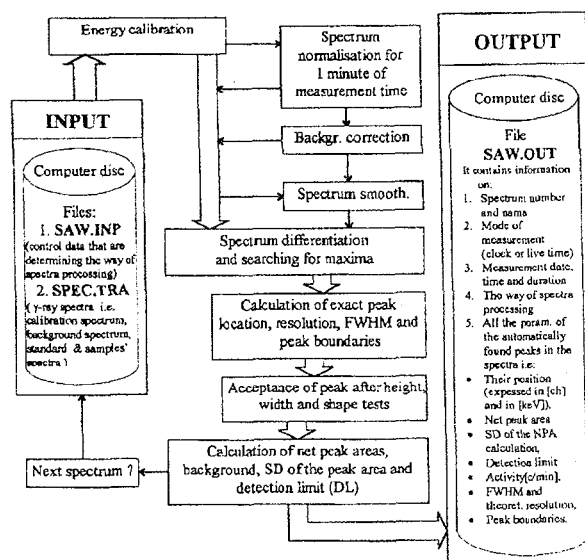


Fig.1. Simplified flow chart of SAWAP-PC spectrometrical program.

net peak area (NPA), the background "under" the peak, standard deviation (SD) of the net peak area calculation, the detection limit [10,14], the counting rate (counts/min), FWHM of the peak, the theoretical resolution and the peak boundaries. Optionally, the SAWAP may normalise the spectra for a unit of measurement time, correct each spectrum for background and smooth the spectra before processing [15]. At output SAWAP creates a file SAW.OUT containing information concerning subsequently all the processed spectra. Each contains the spectrum number and name, the measurement mode (clock/live time mode), measurement date and its duration, the way of spectra processing and then all relevant parameters for all peaks found in the spectrum. The latter could be used for further quantitative NAA.

Recently, this new software has been used for routine INAA analyses of air-borne particulates collected on cellulose filters. For the estimation of the method reliability, some CRMs have been analysed using the same procedure as that applied for filter analysis. The results obtained with the aid of SAWAP package vs. those obtained with the use of standard TUKAN [7,8] procedure for some selected radionu-



PL0101492

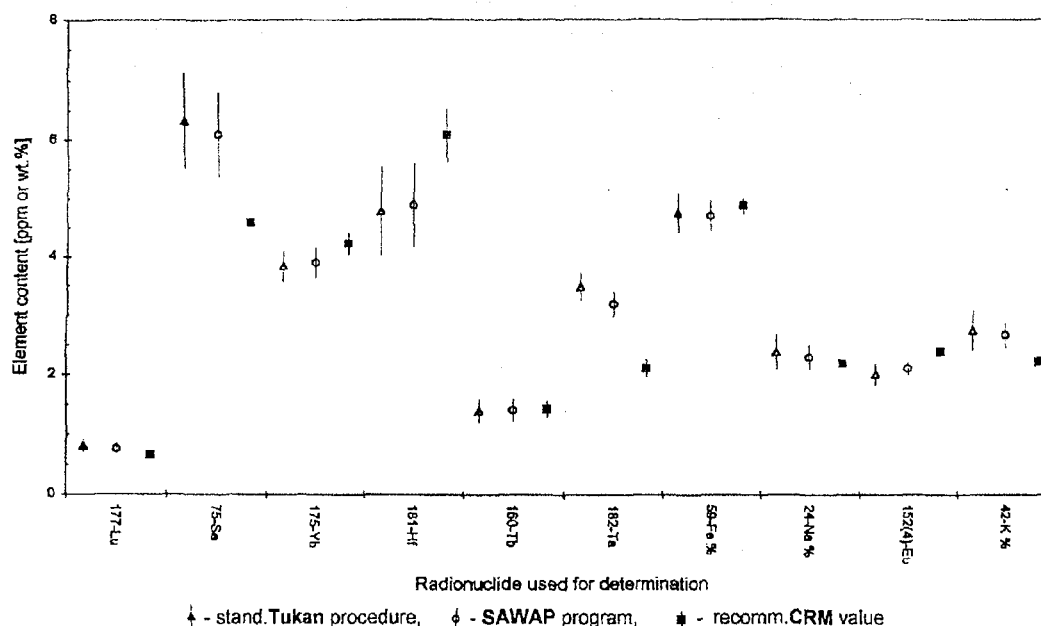


Fig.2. Comparison of some INAA results obtained for CTA-FFA-1 CRM.

lides induced in CRM CTA-FFA-1 have been shown in Fig.2. For comparison, the certified (recommended/information) values have been plotted in the same Fig. Along the x-axis the radionuclides used for quantitative determination were shown, while the element content along the y-axis. The results have been shown together with the error bars (vertical lines) displaying the standard deviation of the single determination, while the certified values together with their confidence limits. Generally, for majority of the determined elements, no significant differences between the results obtained with the aid of standard TUKAN procedure and SAWAP package have been observed although those obtained by SAWAP were generally closer to the certified values. For Se, Ta and Eu both those results could be considered as different from the certified values but they may occur due to other factors of analysis (eg. standardization) and do not depend on the spectra analysis method.

## References

- [1]. Hoste J., Op de Beeck J., Gijbels R., Adams F., Van den Winkel P., De Soete D.: *Instrumental and Radiochemical Activation Analysis*. Butterworths, London 1971.
- [2]. *Non-destructive Activation Analysis*. Ed. S. Amiel. Elsevier, New York 1981.
- [3]. Dybczyński R.: *Chem. Anal.*, 30, 749 (1985).
- [4]. Reeves R.D., Brooks R.R.: *Trace Element Analysis of Geological Materials*. Chapt.13. Wiley-Interscience Publication, N.Y.-Chichester-Brisbane-Toronto 1978.
- [5]. Dybczyński R.: *Proceedings of International Conference "Neutrons and Their Applications"*, Crete, Greece, 12-18 June 1994, SPIE, Vol. 2339, p. 448; *Chem. Anal.*, 30, 749 (1985).
- [6]. Szopa Z., Dybczyński R., Kulisa K., Sterliński S.: *Chem. Anal.*, 39, 497 (1994).
- [7]. Wasek M., Szopa Z., Dybczyński R.: *Raporty IChTJ. Seria B nr 6/97*. IChTJ, Warszawa 1997.
- [8]. Profel, "TUKAN - wielokanałowy analizator amplitudy impulsów" wersja 2.0. Warszawa 1996.
- [9]. Szopa Z., Staszelski J., Plejewska M.: *INR-1945/VIII/E/B*, Warszawa 1982.
- [10]. Op de Beeck J.: *A Programme for Complete Quantitative Neutron Activation Analysis Using Ge(Li) Detector Gamma-Ray Spectrometry*. INS, Ghent University, Ghent 1984.
- [11]. Routti J.T., Prussin S.G.: *Nucl. Instr. Meth.*, 72, 125 (1969).
- [12]. McNelles L.A., Campbell J.L.: *Nucl. Instr. Meth.*, 127, 73 (1975).
- [13]. Landsberger S., Cizek W.D., Campbell R.H.: *J. Radioanal. Chem.*, 180, 155 (1994).
- [14]. Currie L.A.: *Anal. Chem.*, 40, 586 (1968).
- [15]. Savitzky A., Golay M.J.: *Anal. Chem.*, 36, 1627 (1964).

## DIRECT PRETREATMENT OF ANALYTICAL SAMPLES IN A GRAPHITE FURNACE TUBE IN ATOMIC ABSORPTION SPECTROMETRY

Leon Pszonicki, Witold Skwara, Jakub Dudek

In the chemical analysis by graphite furnace atomic absorption spectrometry one observes sometimes negative peaks, i.e. in place where the atomisation peak of the element to be determined should be formed, the measured absorbance drops down, sometimes very deeply, to the negative values. It happens usually in the analysis of samples containing large amounts of sodium, potassium, calcium, chlorides, sulphates or organic compounds. This deformation results from the overcorrection of non-specific absorption caused by a dense cloud of

atomic or molecular vapours of the matrix components attending the atomic vapours of analyte. The size of this phenomenon depends on the type of spectrometer, on the kind of applied correction and on the gradient of temperature during the atomization process [1,2].

Usually this interfering phenomenon may be eliminated by a proper chemical pretreatment of the samples before introducing them into the graphite tube. The organic matter should be carefully mineralised and the mineral components should be

either removed or transformed in more refractory forms, e.g. in chlorides or nitrates that pyrolyse into oxide. Such pretreatment, however, is time-consuming and during the determination of trace elements at a very low concentration level it may cause the sample contamination and enhancement of the blank. Therefore, it erases an idea to carry out the preliminary chemical treatment of samples directly in the graphite tube before starting the atomization process. The aim of the presented investigation was to check this idea on the basis of samples requiring such treatment.

As analytes for this investigation, arsenic, cadmium, lead and selenium were chosen since the determination of these elements in various food products and environmental samples is often required. As inorganic matrices, samples of highly salted mineral waters, used in medicine, and as organic matrices - ethylvanillin and  $\beta$ -apo-8'-carotenal, both used in the food industry, were applied.

In normal analytical procedures the samples of all investigated mineral waters required, before their introducing into the graphite tube, double evaporation to dryness with nitric acid and dissolution of the residue in dilute nitric acid. In our investigations 10  $\mu$ l of the solution containing a mixed magnesium-palladium nitrate modifier was introduced into the tube, evaporated and dried in the usual way using the first stage of the spectrometer atomization programme. Then, the programme was stopped and the tube was cooled down to room temperature. 10  $\mu$ l samples of natural mineral waters were put directly into the tube on the dried modifier, heated slowly during 40 s up to 120°C and dried in this temperature during 10 s. This operation was repeated twice after the addition into the tube, each time, 10  $\mu$ l of nitric acid (1+1). After that, the normal atomization programme was carried out and the atomization peak registered. In all steps of this procedures, with the exception of

atomization and measurement steps, the maximum flow of argon was used to assure the removing of volatile compounds from the tube. When selenium is determined in mineral waters having a large amount of sulphates, e.g. source "Karol" from Solec Kujawski, then, the mixed palladium-magnesium-barium nitrate modifier should be used. The presence of barium removed the interferences caused by sulphates [3].

Both the investigated organic matrices require a very careful mineralization in the closed vessel, preferably using a microwave heating, before the determination of inorganic components. This troublesome treatment may be eliminated when the same procedure, as described for mineral waters, is applied. In such a case, the organic sample may be introduced directly into the tube either in the form of stable suspension in water, e.g.  $\beta$ -apo-8'-carotenal, or as solution in an organic solvent, e.g. ethylvanillin in ethanol.

All the analytical results obtained by the proposed procedure were exactly of the same quality as those obtained by the preliminary chemical treatment of the sample. They indicate that these direct procedure may be applicable to many types of analytical samples. This direct procedure enables to eliminate the time-consuming preliminary preparation of samples, to shorten the time of analysis to few minutes and to minimise the possibility of the sample accidental contamination. The last is particularly important in the determination of trace components at a very low concentration level.

#### References

- [1]. Aller A.J., Garcia-Ollala C.: J. Anal. At. Spectrom., **7**, 753 (1992).
- [2]. Garcia-Ollala C., Aller A.J.: Anal. Chim. Acta, **259**, 295 (1992).
- [3]. Welz B., Bozsai G., Sperling M., Radziuk B.: J. Anal. At. Spectrom., **7**, 505 (1992).

## DETERMINATION OF TRACE CONCENTRATION OF PLATINUM IN ENVIRONMENTAL SAMPLES BY GRAPHITE FURNACE ATOMIC ABSORPTION SPECTROMETRY AFTER PRECONCENTRATION ON A SORBENT

Jadwiga Chwastowska, Witold Skwara, Elżbieta Sterlińska, Jakub Dudek, Leon Pszonicki

Trace amounts of platinum, a major noble metal applied in the automobile catalysts, are ejected with exhausted gases and contaminate roads and their surrounding area. Most of the emitted platinum is probably in the metallic or oxide form and in this form it is considered to be biologically inert. However, platinum is able to form reactive ligand systems, the most effective of which are the chloride ligands. In this form it can be solubilised and enter soils, sediments waters and plants and, in consequence, it may enter the food chain [1]. Numerous toxicities, observed for organo-platinum compounds applied as cytotoxic drugs, indicate that platinum in this form is not inert against the living organism [2]

and the answer for the following questions is of great interest: can platinum be accumulated in the living organisms and what is its physiological effect? The answer to these questions requires the determination of ultra-trace amounts of platinum at a ng/g and sub-ng/g concentration level.

The most suitable analytical methods for the platinum determination at such a low concentration level are electrothermal atomic absorption spectrometry (ET AAS), mass spectrometry with ICP ionisation (ICP-MS) and neutron activation analysis (NAA). However, the direct determination by all these techniques is restricted owing to interferences caused by environmental sample matrices and,



usually, a preliminary platinum separation and enrichment is required. Large application of NAA, although it offers very low detection limit, is restricted by the access to a nuclear reactor. Application of ICP-MS is limited by the high matrix concentrations in the investigated samples causing spectral interferences occurring because of the limited resolution of the generally applied quadrupole mass spectrometers. Although the ET AAS shows similar shortcomings, the equipment for this technique is available in most laboratories and a method basing on it has a chance to be in common use.

The aim of the presented work was to elaborate a method of platinum determination in the road dust, soil and plant samples by an ET AAS technique after its preliminary separation on a dithizone sorbent. This type of sorbent was chosen since dithizone in a strong acidic medium forms stable complexes, beside platinum, only with palladium, gold, silver, mercury and, partially, with copper. All these elements may be present in the environmental samples at a low trace concentration level and neither of them interferes with the platinum determination by ET AAS.

The samples (5 g) were digested with hot aqua regia. The dried plant samples were burned at 400°C before digestion. The solution after digestion was filtered and transformed into the chloride form by double evaporation with hydrochloric acid. Platinum in the solution was reduced to platinum(II), using tin(II) chloride, and separated from the matrix elements by passing the solution at 0.8 ml/min through the column filled with 0.2 g of dithizone

sorbent. The diameter of the column was equal to 4 mm. The sorbent was prepared in our laboratory by immobilisation of dithizone on the microporous resin Diaion HP-2M6 (acrylic ester polymer). A maximum amount of dithizone immobilised on the resin was 25 mg/g. The sorbent prepared in this way and stored in a refrigerator is stable during six weeks. Platinum was desorbed from the column by 10 ml of a 5% thiourea solution in 0.1 N hydrochloric acid. 50 µl of the solution was used for platinum determination by ET AAS. The following measurement parameters were applied: pyrolytic graphite tube, pyrolysis temperature 1250°C; atomization temperature 2550°C; deuterium arc non-specific absorption correction; peak high absorbance at a wavelength of 265.9 nm was measured.

The parameters of the proposed analytical method for platinum determination are as follows: lower limit of determination 5 Pt ng/g; relative standard deviation calculated on the basis of seven parallel determinations SDR=0.09; recovery of the added standards varies in the range 95-100%, depending on the type of sample matrix.

In the samples of road dust, soil and grass collected on, or beside, the busy suburban road on the north side of Warszawa (Modlińska Street) the following average level of platinum concentration was found: in the road dust - 25 ng/g, in the grass - below 2 ng/g, in the soil - 35 ng/g.

#### References

- [1]. Farago M.E., Kavanag P., Blanks R., Kelly J., Kazantzis G., Thornton I., Simpson P.R., Cook J.M., Delves H.T., Hall G.E.M.: *Analyst*, **123**, 451-454 (1998).
- [2]. Balcerzak M.: *Analyst*, **122**, 67R-74R (1997).

## RADIONUCLIDE CONCENTRATION MEASUREMENTS IN SOLUTION AND SOIL

Joachim Kierzek, Józef Parus, Bożena Małozewska-Bućko

### Introduction

The International Atomic Energy Agency's Analytical Control Services organised in the first half of 2000 a proficiency test for participants of the regional project on Quality Control and Quality Assurance for Nuclear Analytical Techniques. More than 10 laboratories from the Central and Eastern Europe expressed their wish to participate in this exercise. The main objective of the test was twofold:

- to check the accuracy and precision with which the analyst can measure environmentally important radionuclides using their characteristic modes of radiation that generate alpha-, beta- and gamma-rays;
- to examine the effect of matrix on the accuracy and precision of radionuclide measurements.

We participated in the measurement of gamma emitting nuclides.

It was requested to measure the activity concentration of the following nuclides:  $^{241}\text{Am}$ ,  $^{57}\text{Co}$ ,  $^{60}\text{Co}$ ,  $^{134}\text{Cs}$ ,  $^{137}\text{Cs}$  and  $^{65}\text{Zn}$  in the delivered by the IAEA solution and soil samples. The required reference date for results was 2000.01.01.

### Standards and samples preparation for measurements

#### Activity standards

POLATOM Isotope Centre (Świerk, Poland) delivered 3 radioactive standard solutions:

1. Mix S1  $^{109}\text{Cd}$  - 22.93 kBq/g  
 $^{57}\text{Co}$  - 0.62 kBq/g  
 $^{113}\text{Sn}$  - 2.94 kBq/g  
 $^{137}\text{Cs}$  - 4.56 kBq/g  
 $^{60}\text{Co}$  - 6.03 kBq/g
2. JM/5/0  $^{241}\text{Am}$  - 8.1 kBq/g
3. JM/6/0  $^{134}\text{Cs}$  - 6.9 kBq/g

#### Preparation of standard solutions

20 ml liquid scintillation vials were used as containers. To 3 vials portions of about 0.3 g of each standard solution were weighed out. All solutions were diluted with distilled water to 3 ml and weighed.

#### Preparation of the IAEA solution

The content of the ampoule was transferred with a pipette (2.38 ml total volume of solution) to the counting vial and weighed (2.5560 g). 620 µl of water was added and weighed again.



PL0101493

*Preparation of a powdered standard*

About 250 g of a dry ground soil (grain size below 100  $\mu\text{m}$ ) was mixed with 150 g of acetone. To this mixture (pulp) 300  $\mu\text{l}$  (by weight) of each standard solution was added. The pulp was mixed for 1 h with the use of a multiaxial blender. After drying to the initial weight, the soil was mixed again during 30 min. Finally, the powder was transferred to a measurement container of 70 mm internal diameter.

*Preparation of the powdered IAEA sample*

The sample was blended during 1 hour in the multiaxial blender. Then, it was transferred to the measurement container identical to the one in which the powdered standard was prepared. The height of layer of both the standard and sample was 45 mm for the same mass of both. In this way a correction for density was avoided.

**Equipment and counting method**

The measurements were performed with the use of a gamma-ray spectrometer equipped with an ORTEC detector of GEM-90205-P type, 1.9 keV FWHM at 1.33 MeV and 92.4% relative counting efficiency and a 16 k digital signal processor of DSPEC type.

For isotopes present in standards, the activity concentration was determined based on counting efficiency for each specific radionuclide. The samples and standards in identical containers were placed directly on the detector top.

$$A_u(i) = \frac{R_u(i,E) \times f_d(i)}{\varepsilon_i \times m} \quad (1)$$

where:  $A_u(i)$  - the activity concentration of radionuclide  $i$ , in Bq/g;  $R_u(i,E)$  - the net counting rate per second in full energy peak of energy  $E$  associated with radionuclide  $i$ ;  $\varepsilon_i$  - the radionuclide specific counting efficiency for radionuclide  $i$ ;  $m$  - the mass of the sample, in g;  $f_d(i)$  - the correction factor for decay of radionuclide  $i$  between the reference data (2000.01.01) and the time of measurement and during the measurement.

The activity concentration of  $^{65}\text{Zn}$ ,  $A_{\text{Zn}}$ , for which a counting efficiency was determined from the counting efficiency curve as a function of energy, the following formula was used:

$$A_{\text{Zn}} = \frac{R_{\text{Zn}} \times f_d(\text{Zn})}{\varepsilon_{1115} \times p_{1115} \times m} \quad (2)$$

where:  $R_{\text{Zn}}$  - the net counting rate per second in the 1115 keV peak of  $^{65}\text{Zn}$ ,  $f_d(\text{Zn})$  - the correction factor for decay,  $\varepsilon_{1115}$  - the detector efficiency at 1115 keV energy,  $p_{1115}$  - the gamma-ray emission probability per disintegration for 1115 keV energy.

The results of the activity concentration measurements for all nuclides in both samples are given in Table. For comparison the IAEA values are included. These values were made known for us after receiving our results. All the results are reported with a measurement uncertainty at  $\pm 1\sigma$  level (in

Table. The IAEA and our values of activity concentration measurements.

Material	Nuclide	IAEA value Bq/g $\pm 1\sigma$ (%)	Our value Bq/g $\pm 1\sigma$ (%)
Reference Solution	$^{241}\text{Am}$	$16.45 \pm 0.82$ (5.0)	$15.77 \pm 0.41$ (2.6)
	$^{57}\text{Co}$	$14.95 \pm 0.30$ (2.0)	$16.23 \pm 0.32$ (2.0)
	$^{60}\text{Co}$	$16.60 \pm 0.33$ (2.0)	$15.66 \pm 0.26$ (1.7)
	$^{134}\text{Cs}$	$6.65 \pm 0.13$ (2.0)	$6.45 \pm 0.17$ (2.6)
	$^{137}\text{Cs}$	$21.73 \pm 0.43$ (2.0)	$20.94 \pm 0.52$ (2.5)
	$^{65}\text{Zn}$	$10.59 \pm 0.21$ (2.0)	$10.54 \pm 0.29$ (2.7)
Soil	$^{241}\text{Am}$	$92.60 \pm 7.5$ (8.1)	$88.9 \pm 4.4$ (4.9)
	$^{57}\text{Co}$	$33.13 \pm 1.02$ (3.1)	$35.2 \pm 0.8$ (2.3)
	$^{60}\text{Co}$	$93.50 \pm 2.24$ (2.4)	$86.0 \pm 1.5$ (1.7)
	$^{134}\text{Cs}$	$73.00 \pm 1.87$ (2.6)	$69.3 \pm 2.3$ (3.3)
	$^{137}\text{Cs}$	$84.20 \pm 2.2$ (2.6)	$79.5 \pm 2.1$ (2.6)
	$^{65}\text{Zn}$	$29.34 \pm 1.3$ (4.4)	$30.1 \pm 1.2$ (3.7)

Due to the lack of  $^{65}\text{Zn}$  standard, the measurements of samples and standards were additionally carried out at a distance of 14 cm from the detector. For this geometry a counting efficiency curve was prepared and the counting efficiency for  $^{65}\text{Zn}$  found.

The counting time of IAEA samples was 24 h and for standards it was 3000 s. The count rate in all measurements was not higher than 1000 cps.

For the single, well resolved peaks a total area method was used with the background from 3 channels on each side of the peak. For the closely separated or overlapped peaks the Gamma Vision-32 program of ORTEC was applied.

**Results and discussion**

The activity concentration of:  $^{241}\text{Am}$ ,  $^{57}\text{Co}$ ,  $^{60}\text{Co}$ ,  $^{134}\text{Cs}$  and  $^{137}\text{Cs}$  for each of which the standards were available was calculated from the formula:

per cent in parentheses). The uncertainties are smaller for the solution than for the soil. All the activity concentration values measured by us agree within  $\pm 2\sigma$  with the IAEA values.

The calculation of the relative uncertainty of activity concentrations is done by combining the relative uncertainties of the count rate for unknown and standard sample and activity of the standard source [1-3]:

$$\frac{S(A_u)}{A_u} = \sqrt{\left(\frac{S(R_s)}{R_s}\right)^2 + \left(\frac{S(A_s)}{A_s}\right)^2 + \left(\frac{S(R_u)}{R_u}\right)^2} \quad (3)$$

with the relative uncertainty  $S(A_s)/A_s$  of standard activity obtained from certificate and relative uncertainties of the count rate  $S(R_s)/R_s$  and  $S(R_u)/R_u$  for standard and unknown sample, respectively,

where  $S(\dots)$  is an estimator of the standard deviation of a variable given in parentheses.

The first two terms under the square root of equation (3) describe the uncertainty of detection efficiency,  $\varepsilon_i$ , for the radionuclide  $i$ . The relative uncertainty of the count rates was calculated from the fivefold measurement. In this way the uncertainties of counting statistics, the repeatability of peak areas calculation, the background stability, the reproducibility of a source position in relation to the detector, were taken into account.

The uncertainties of the sample and standard weighing, of the gamma-ray branching ratios and the decay constants are small in comparison to the uncertainties considered and they have been neglected. For example, the relative uncertainty of weighing is not more than 0.1%.

The relative uncertainty of the specific activity for  $^{65}\text{Zn}$  was calculated from the formula:

$$\frac{S(A_{\text{Zn}})}{A_{\text{Zn}}} = \sqrt{\left(\frac{S(R_{\text{Zn}})}{R_{\text{Zn}}}\right)^2 + \left(\frac{S(\varepsilon_{\text{Zn}})}{\varepsilon_{\text{Zn}}}\right)^2} \quad (4)$$

where:  $S(R_{\text{Zn}})/R_{\text{Zn}}$  - the relative uncertainty of net area count rate calculated from 3 measurements;  $S(\varepsilon_{\text{Zn}})/\varepsilon_{\text{Zn}}$  - the relative uncertainty of the Zn counting efficiency,  $\varepsilon_{\text{Zn}}$ , calculated from the counting efficiency curve.

### References

- [1]. American National Standard Calibration and Use of Germanium Spectrometers for the Measurement of Gamma-Ray Emission Rates of Radionuclides. ANSI, N42.14-1991.
- [2]. Debertin K., Helmer R.G.: Gamma- and X-Ray Spectrometry with Semiconductor Detectors. Elsevier, Amsterdam 1988.
- [3]. De Regge P., Fajgelj A.: The IAEA Guide on Quantifying Uncertainty in Nuclear Analytical Measurements. IAEA Laboratories, Seibersdorf 2000.



PL0101494

## SURFACE MODIFICATION OF PARTICLE TRACK-ETCHED MEMBRANES

Danuta Wawszczak, Wojciech Malicki, Marek Buczkowski

Particle track-etched membranes (PTMs) a product of advanced cyclotron technology can be used for precision microfiltration. An important parameter in the case of such application is the rate of microfiltration that should be enough high [1,2]. Increas-

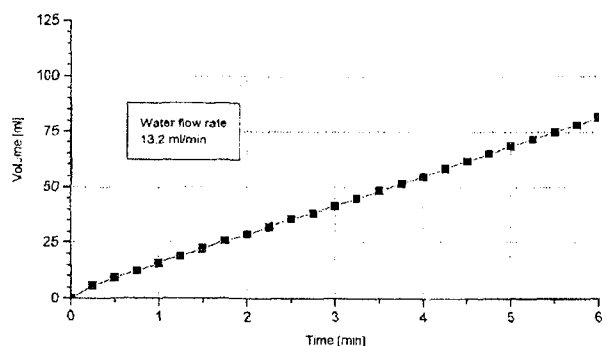


Fig.1. Volume of distilled water flow vs. time in the case of a virgin PTM with a nominal pore size  $0.45 \mu\text{m}$  made of PET film,  $10 \mu\text{m}$  thick.

ing of this rate can be introduced by surface modification of membranes. Methods of the modification depend on the treatment of membranes by proper solutions or on surface activation by using UV radiation or electron beam [3].

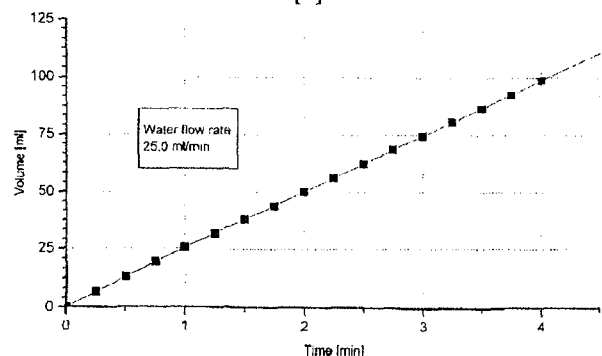


Fig.2. Volume of distilled water flow vs. time in the case of PTM moistened with isopropanol (PTM parameters as in Fig.1).

For introductory experiments, samples of PTM with nominal pores diameter  $0.45 \mu\text{m}$  made of PET

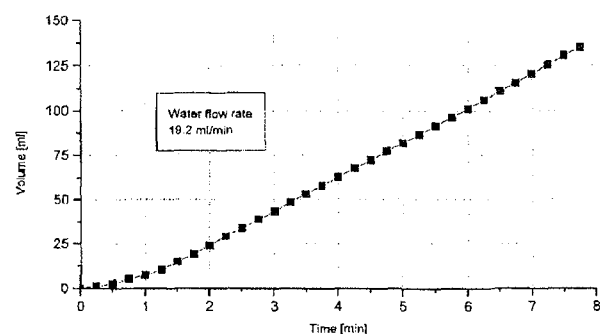


Fig.3. Volume of distilled water flow vs. time in the case of PTM moistened with PEG solution (PTM parameters as in Fig.1).

film have been taken. The samples of disc form (diameter -  $2.5 \text{ cm}$ ) were placed into a dismountable syringe holder and then distilled water was

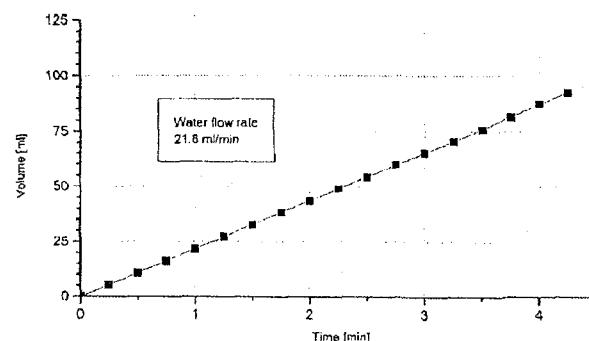


Fig.4. Volume of distilled water flow vs. time in the case of a virgin PTM moistened with PEG and then activated by a 10 MeV electron beam (PTM parameters as in Fig.1).

given under a pressure of  $0.015 \text{ MPa}$ . Amount of water coming through the membrane vs. time was determined by using a precise balance.

Samples of PTM were moistened with water solutions of poly(ethylene glycol) (PEG) 2000 type (2.5%), isopropanol, maleic acid. Some of the samples were additionally activated by using UV radiation (250 nm) or a 10 MeV electron beam at a dose of 105 kGy.

The most important results are given in Figs.1-4. In comparison with the results for a virgin membrane (Fig.1), increasing of microfiltration rate in the case of membranes moistened with isopropanol (90%), and with PEG (46%) was observed. After activation by the electron beam, increasing of microfiltration efficiency took place only for the samples treated earlier with the PEG solution (relative value 20%).

Future work in this subject should explain and develop the obtained results, which seem to be important for further application of PTMs.

## References

- [1] Buczkowski M., Starosta W., Wawszczak D., Żółtowski T.: Application of particle track membranes - Polish experiences. In: Proceedings of VI International School - Seminar Heavy Ion Physics, Dubna, Russia, 22-27 September 1997. Eds. Yu.Ts. Oganessian, R. Kalpakchieva, World Scientific, Singapore 1997, pp. 761-769.
- [2] Apel P.Yu.: Radiat. Meas., 25, 667-674 (1995).
- [3] Hagiwara M.: Polymers and Track Membranes. In: Proceedings of VI International School - Seminar on Heavy Ion Physics, Dubna, Russia, 22-27 September 1997. Eds. Yu.Ts. Oganessian, R. Kalpakchieva, World Scientific, Singapore 1997, pp. 754-760.

## RADIATION RESISTANCE OF PARTICLE TRACK-ETCHED MEMBRANES

Marek Buczkowski, Bożena Sartowska, Danuta Wawszczak, Wojciech Starosta

Particle track-etched membranes (PTMs) can be used in many fields, first of all in biomedicine and biotechnology [1]. Because of such application it is important to have data about the radiation resistance of PTMs and the possibility of their radiation sterilization. Research in this field have been undertaken in the 90's by two co-operating institutes: the Joint Institute for Nuclear Research (JINR) in Dubna and the Institute of Nuclear Chemistry and Technology (INCT) in Warszawa [2].

Widening of the possibility of PTMs application is connected, among others, with the production of new kinds of membranes. Nowadays PTMs are manufactured of PET and PC films with a nominal thickness of 20  $\mu\text{m}$  [3]. Attempts to manufacture PTM using a PEN film have been undertaken in the INCT [4]. Lack of data concerning the radiation resistance of the above polymeric films and PTMs has become a reason for doing this work.

Samples of both PTM and their base polymers have been investigated. The following PTM sample materials were prepared (see the legends of the proper Figs.): PET films of 10 and 20  $\mu\text{m}$  thick (JINR), PET and PC films 20  $\mu\text{m}$  thick (Whatman-Cyclopore, Belgium), PEN films 25  $\mu\text{m}$  thick (irradiated at a U-400 cyclotron - JINR, etched in

the INCT). The following polymeric films samples were taken: the PET film of 10 and 19  $\mu\text{m}$  thick, Estrofol ET type (Nitron-Erg, Poland); the PEN film 25  $\mu\text{m}$  thick, Kaladex type (ICI, UK); the PP film 20

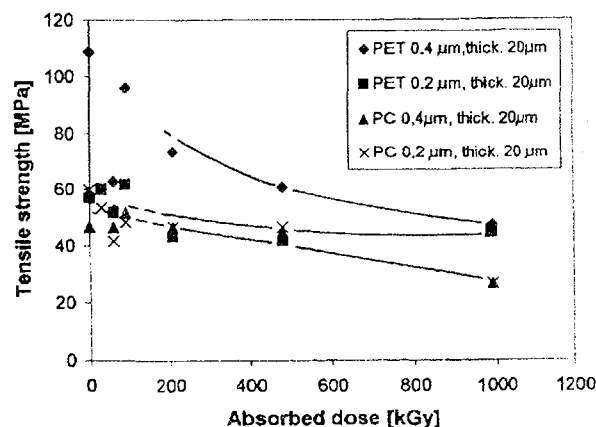


Fig.2. Tensile strength vs. absorbed dose for TEMs made of PET and PC films.

$\mu\text{m}$  thick, BG 2001 type (Petrochemia Płock, Poland).

Samples of PTM and polymeric films were irradiated using an electron beam in air of 10 MeV energy. The irradiation was made at the linear

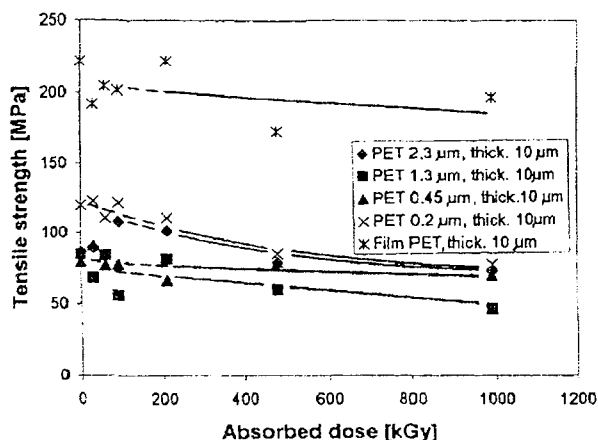


Fig.1. Tensile strength vs. absorbed dose for a PET film 10  $\mu\text{m}$  thick and TEMs made of that film.

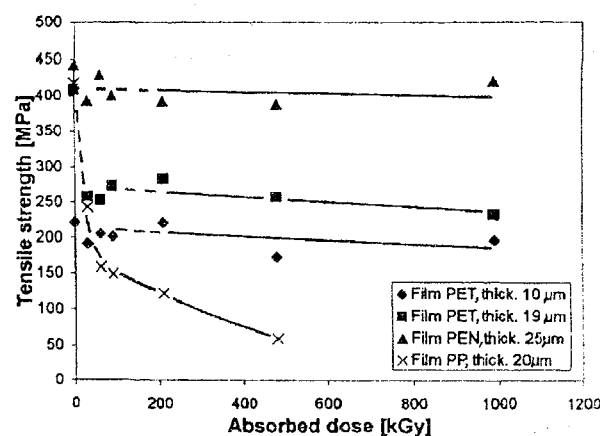


Fig.3. Tensile strength vs. absorbed dose for different polymeric films.



PL0101495

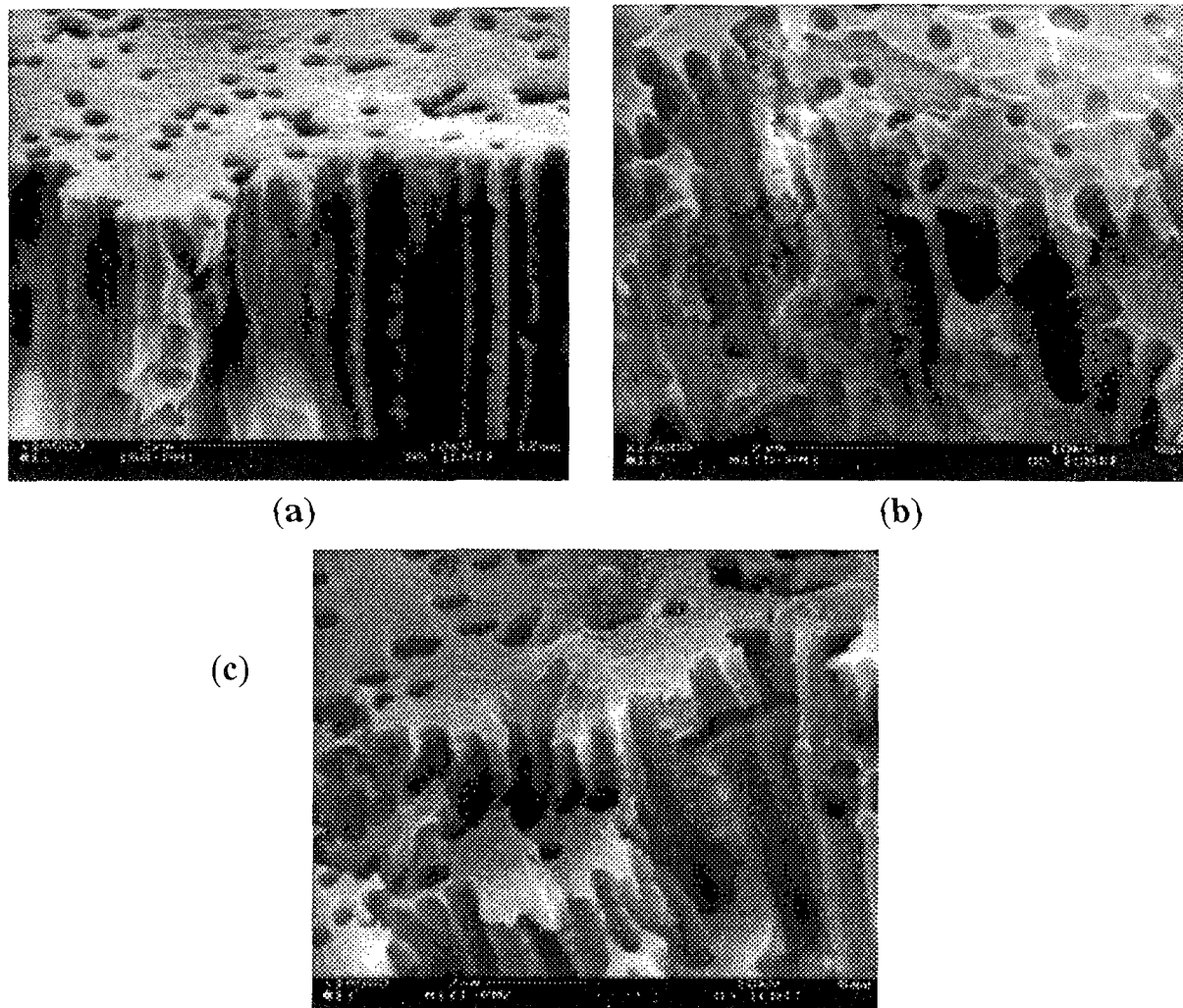


Fig.4. SEM photographs of the virgin TEM ( $0.4\ \mu\text{m}$  pores size) made of PET film  $20\ \mu\text{m}$  thick (a) and irradiated to a dose of 480 kGy (b) and 990 kGy (c).

electron accelerator LAE-13/9 type that is exploited in the Department of Radiation Technology of the INCT. The doses used were in the range from 30 to 990 kGy.

The measurements were made using a simple tensile testing machine. It gave directly the value of breaking force for standard strips of the investigated materials. Results were averaged and given in pressure units.

Results concerning tensile strength vs. absorbed dose are shown in Figs.1-3 and give a comparison of the behaviour of different PTMs and films. Fig.4 shows SEM photographs of surfaces and fractured sides of PTMs samples before and after irradiation at doses of 480 and 990 kGy, respectively.

PTMs made of the PEN film are more resistant against electron irradiation than PTMs made of the PET films of similar thickness and membrane parameters (pore diameter and pore density).

In the case of PTMs (with similar porosity) made of PET  $10\ \mu\text{m}$  thick, the tensile strength does not practically depend on the pore diameter and slightly decreases at a dose of 990 kGy (the difference is about 30%).

In the case of membranes made of polymeric materials as PET and PC (the pore density at the same level of magnitude) but with different thick-

nesses (10 and  $20\ \mu\text{m}$ ), the results concerning the tensile strength and the burst strength are similar up to the dose 990 ky.

The SEM photographs show small changes on membranes surfaces at the highest dose.

All the investigated types of PTM and films, apart from PP films, can be radiation sterilized.

For the investigation of tensile strength, the standard samples of the PTMs and polymeric films from different centres have been used. In the case of more precise measurements, it is necessary to take into account the anisotropic structure of biaxially oriented polymeric films. Moreover, it seems to be useful to carry out detailed measurements in the range up to a dose of 100 kGy because of the considerable scatter of the obtained results in the latter case.

## References

- [1]. Buczkowski M., Starosta W., Wawszczak D., Żółtowski T.: Application of particle track membranes - Polish experiences. In: Proceedings of VI International School - Seminar on Heavy Ion Physics, Dubna, Russia, 22-27 September 1997. Eds. Yu.Ts. Oganessian, R. Kalpakchieva. World Scientific, Singapore 1997, pp. 761-769.
- [2]. Zhitariuk N.I., Fiderkiewicz A., Buczkowski M., Kovalev G.N., Orelovich O.L., Żółtowski T.: Eur. Polym. J., 32, 391-395 (1996).
- [3]. Apel P.Yu.: Radiat. Meas., 25, 667-674 (1995).
- [4]. Starosta W., Wawszczak D., Sartowska B., Buczkowski M.: Radiat. Meas., 31, 149-152 (1999).

## SYNCHROTRON SAXS STUDY OF PERMEATING MEMBRANE DEPENDING ON ITS DEPTH

Helena Grigoriev, Sigrid Bernstorff<sup>1/</sup>, Aleksandra Wolińska-Grabczyk<sup>2/</sup>, Andrzej G. Chmielewski

<sup>1/</sup> Sincrotrone Trieste, Italy

<sup>2/</sup> Institute of Coal Chemistry, Polish Academy of Sciences, Gliwice, Poland

Up to now studies of permeation through a dense polymer membrane have not involved experimental measurements of any parameter step by step in the range covering the whole membrane thickness, during permeate transport. This is due to experimental difficulties. All information, which have been obtained, come from outside the membrane, from its supplying and/or expelling side, eventually some parameters referring to the whole membrane volume can be registered. Numerous theories and models of permeation exist and all of them have been verified

and 4,4-diaminodiphenylmethane and soft segments - derived from poly(oxytetramethylene) diol. The copolymer is of heterogenous lamellar structure. The model sample represented a membrane section, 5 mm thick, and was of proper thickness (0.3 mm) for X-ray measurements in transmission. To avoid evaporation, both sides of the sample (20x5 mm) were covered by a thin (1  $\mu\text{m}$ ) layer of aluminium deposited in vacuum. Just before SAXS measurements the lower part of the sample was dipped in a solvent (benzene) to reach saturation (Fig.1).

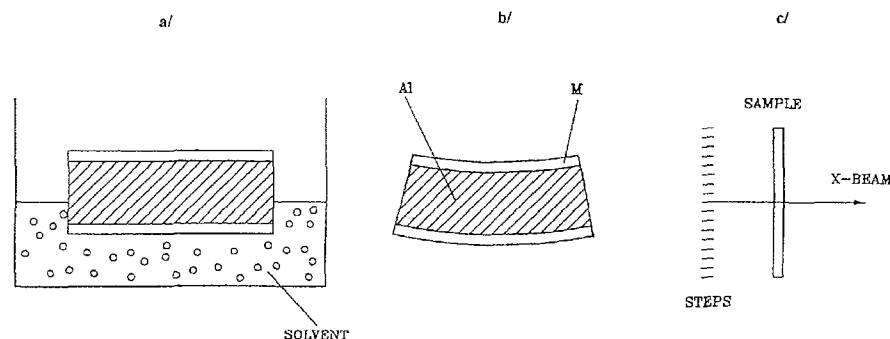


Fig.1. (a) saturation at the bottom part of the sample with benzene, (b) the sample shape after saturation, M - membrane, Al - aluminium, (c) SAXS measurement in subsequent steps.

only by a summary effect outside the membrane. On the basis of classical rules, the model with phase transition level (from liquid to vapor solvent) inside the polymer membrane is generally used.

The aim of this work was to perform a first experiment gathering measurements made step by step in the range from supplying to expelling side of the membrane during permeation. It was the SAXS synchrotron experiment, carried out on a model sample, which was prepared in the 10:1 scale, of dimensions 5x20x0.3 mm. The sample was prepared from a copolymer poly(urea-urethane) foil containing hard segments - formed from 2,4-tolylene diisocyanate

The SAXS measurements were carried out at the Austrian SAXS beamline of the synchrotron ELETTRA, Trieste, Italy. They were performed for subsequent vertical shifts of the sample table, in steps of 0.2 mm each, from the supplying to expelling side of the sample.

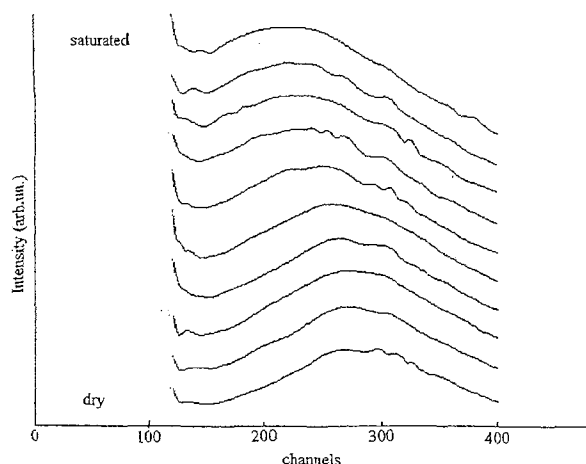


Fig.2. SAXS curves for subsequent steps of the sample height. Other curves are shown for better clarity.

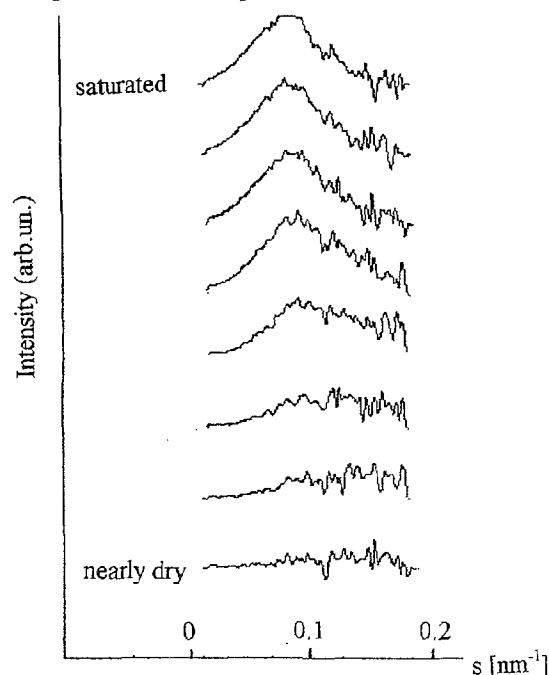


Fig.3. The results of subtraction of the SAXS curve for the dry membrane from subsequent SAXS curves of increasing degree of saturation (Lorentz corrected).

The measurement data were subjected to a preliminary treatment using the OTOKO program and displayed in Fig.2. One can see from Fig.2 that successive SAXS curves change in a monotonic sequence. The change is from the curve for dry to the curve for saturated sample. This monotonic change excluded the possibility of existence of the phase-transition level inside the membrane.

To find the way in which solvent influences the lamellar structure of the sample, we analyzed the inter-lamellar distance,  $L$ , as a sum of two components: a more dense layer and a less dense (amorphous) layer. The theory assumes that the second derivative of the correlation function represents distribution of distances between interfaces. We elaborated a computer program which enabled us to calculate this function from experimental SAXS data. It occurred that during a sorption, the solvent enters the soft domains only and hard domains remain impermeable.

As one can see from Fig.2, the slope of the SAXS peaks on the side of greater  $s$  is the same for all

curves. A shift of their maximum for subsequent steps of depth is caused only by the shift of the slope on the side of smaller  $s$ . This one-side change inclined us to subtract the SAXS curve for the dry membrane from each subsequent curve. It occurs that there is visible formation of a peak that emerges from experimental noises at steps nearly of the expelling side and becomes greater, more close and shifted to smaller  $s$  nearly the supplying side of the sample (Fig.3). The generation of the second peak indicates the formation of a new kind of aggregates (probably also lamellar) as a result of an interaction between the polymer and the solvent. The new phase is very susceptible to the solvent amount. So, the whole change in SAXS curves is caused by the new phase, while the previous one, observed for dry polymer, remains unchanged. Further study are forecasted.

#### References

- [1]. Grigoriew H., Bernstorff S., Wolińska-Grabczyk A., Domańska J., Chmielewski A.G.: *J. Membr. Sci.*, in print.

### SYNTHESIS OF $\text{LiCoO}_2$ AND $\text{LiMg}_{0.05}\text{Co}_{0.95}\text{O}_2$ THIN FILMS ON POROUS $\text{Ni/NiO}$ CATHODES FOR MCFC BY COMPLEX SOL-GEL PROCESS (CSGP)

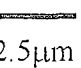
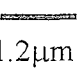
Wiesława Łada, Andrzej Deptuła, Bożena Sartowska, Tadeusz Olczak, Andrzej G. Chmielewski,  
Maria Carewska<sup>1/</sup>, Silvera Scaccia<sup>1/</sup>, Elisabetta Simonetti<sup>1/</sup>, Leonardo Giorgi<sup>1/</sup>, Angelo Moreno<sup>1/</sup>

<sup>1/</sup> ENEA, C.R.E. Casaccia, Italy

Fuel cells are commonly recognized as the most promising power generation systems. However, the energy from fuel cells is actually several times more expensive than the energy from conventional power

generation systems. The main perspective for a substantial cost reduction is the elaboration of cheaper components of fuel cells and the improvement of their quality.

Table 1. SEM micrographs of  $\text{Ni/NiO}$  cathodes covered with  $\text{LiMg}_{0.05}\text{Co}_{0.95}\text{O}_2$  fired for 4 h at 650°C.

Type of sol $\Rightarrow$	Parent sol (PS) Viscosity( $\eta$ )= 35.4 cSt Concentration of $\Sigma$ Me 46.8 g/l	1 volume of PS 1 volume of Ethanol $\eta$ =14 cSt	1 volume PS 3 $\text{H}_2\text{O}$ 4 volume Ethanol $\eta$ = 2.6 cSt
Surface  2.5µm			
Cross Section  1.2µm	 $t=1.78\mu\text{m}$	 $t=1.14\mu\text{m}$	 $t=0.78\mu\text{m}$



PL0101499



One of the most important fuel cells, highly efficient and environmentally clean, are the Molten Carbonate Fuel Cells (MCFC) composed generally of a Ni anode and a NiO cathode operating at 600-700°C in the presence of a corrosive liquid Li/K carbonate. The major disadvantage of this type of cathode is its dissolution in the K/Li electrolyte, which significantly decreases the cell lifetime [1]. LiCoO<sub>2</sub> cathodes show a lower solubility, however, they are far more expensive.

h at 400°C, and calcined for 4 h at 650°C, using a low heating and cooling rate of 1°C/min. The SEM micrographs of LiMg<sub>0.05</sub>Co<sub>0.95</sub>O<sub>2</sub> films are presented in Table 1. It is evident that the best films were obtained from the mixed sol 1 volume of parent sol (PS) : 1 volume of ethanol. The film thicknesses (t) increase with sol concentration and viscosity.

The results of microporosity are shown in Table 2. Ni plates are very porous with a large total pore area

Table 2. The results of microporosity of porous Ni plates treated also in an ambient atmosphere and covered with LiCoO<sub>2</sub>.

No of samples and treatment procedures	Ni	Ni/NiO 20 h, 700°C	Ni/NiO covered with LiCoO <sub>2</sub> , 1 h, 800°C
TOTAL INTRUSION VOLUME	0.3339 ml/g	0.1606 ml/g	0.1784 ml/g
TOTAL PORE AREA	18.250 m <sup>2</sup> /g	0.067 m <sup>2</sup> /g	5.301 m <sup>2</sup> /g
MEDIAN PORE DIAMETER (VOL.)	12.4681 μm	12.9861 μm	11.9271 μm
MEDIAN PORE DIAMETER (AREA)	0.0045 μm	5.6988 μm	0.0039 μm
AVERAGE PORE DIAMETER	0.0732 μm	9.6229 μm	0.1346 μm
BULK DENSITY	2.1330 g/ml	2.9336 g/ml	2.8479 g/ml
APPARENT (SKELETAL) DENSITY	7.4092 g/ml	5.5484 g/ml	5.7897 g/ml

Note. Densities of metallic: Ni=8.90 g/cm<sup>3</sup>, NiO=6.72 g/cm<sup>3</sup>.

sive. The aim of the present work was the preparation of LiCoO<sub>2</sub> and LiMg<sub>0.05</sub>Co<sub>0.95</sub>O<sub>2</sub> thin films on Ni/NiO in order to protect the cathode body against dissolution. Variant of a sol-gel dipping technique, elaborated in this Institute [2] was selected. The Li<sup>+</sup>-Co<sup>2+</sup>-(Mg<sup>2+</sup>) starting sols were prepared by a new type [3] of the sol-gel process, namely a Complex Sol-Gel Process (CSGP). Sols have been prepared by adding 4M LiOH to 1M aq. acetate solution of Co<sup>2+</sup>-(Mg<sup>2+</sup>) with ascorbic acid (0.5M), then, by alkalizing it with aqueous ammonia to pH=8. The sols were then diluted with water and ethanol.

The coatings were prepared by an immersion of porous sintered Ni plates in the sol. Commercial Ni plates were initially oxidized by heating at various temperatures. Their microstructure and mechanical properties as a function of temperature were observed. Heat treatment should be carried out under the dead load of the ceramic plates in order to avoid their waving. The best non-folded plates were obtained by treating them for 1 h at 550°C. The covered substrates after withdrawing from the sol were maintained (also under the dead load of ceramic plates) for 1 h at RT and soaked for 72 h at 200°C, then for 1

and about 15% of closed pores. It is evident that during heating a total pore area and skeletal density decrease, but it appears that the closed pores volume remains at a similar level. The LiCoO<sub>2</sub> layer strongly protects Ni against oxidation and fully limits the decrease of a total pore volume.

The chemical stability of the LiCoO<sub>2</sub>-Ni/NiO cathode in molten carbonates was determined by an immersion test. The mixture used was composed of 62 mol% Li<sub>2</sub>CO<sub>3</sub> and 38 mol% K<sub>2</sub>CO<sub>3</sub>. The carbonate (35 g) was contained in a pure alumina crucible, over which an air/CO<sub>2</sub> 70/30 gas mixture was passed at a 50 ml/min flow rate. The LiCoO<sub>2</sub>-Ni cathode (0.2 g, 2 mm in diameter) was accommodated at the bottom of the crucible. The immersion test was performed for 350 h at 650°C. About 1 g of the melt has been periodically extracted from the crucible using an alumina pipette and transferred on a gold plate. The cooled melts were dissolved in nitric acid and analyzed for the content of Ni and Co by AAS [4]. After the immersion test, the cathode was washed in dilute acetic acid and dried for taking the scanning electron micrographs (SEM) and energy-dispersive X-ray (EDAX) analysis. The spectra of the covered

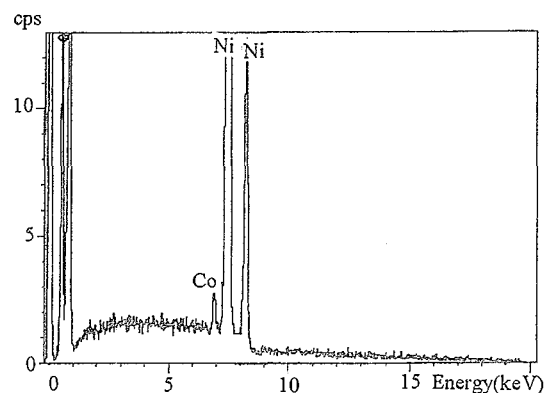
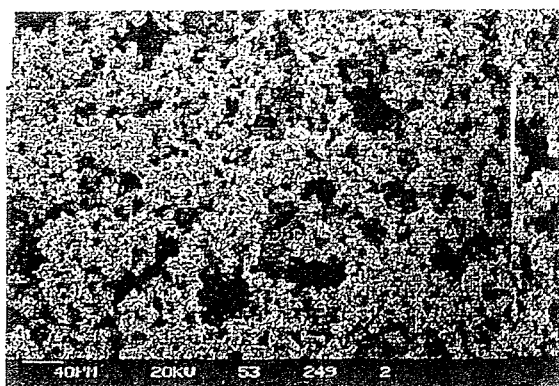


Fig.1. SEM micrograph and EDAX spectrum of Ni/NiO/LiCoO<sub>2</sub> cathode before treatment.



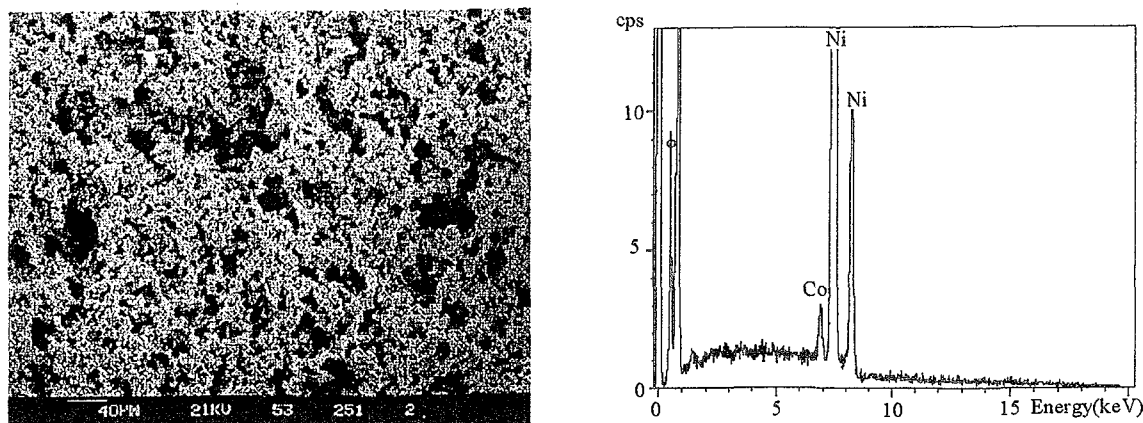


Fig.2. SEM micrograph and EDAX spectrum of Ni/NiO/LiCoO<sub>2</sub> cathode after 350 h treatment at 650°C in (Li<sub>0.62</sub>K<sub>0.38</sub>)<sub>2</sub>CO<sub>3</sub> and pCO<sub>2</sub>=0.3 atm, pO<sub>2</sub>=0.14 atm.

electrode before and after a 350 h immersion test are shown in Figs.1 and 2, respectively. The results of the analyzed melts indicate that the Ni/NiO/LiCoO<sub>2</sub> cathode is stable during the test because no traces of cobalt and nickel were detected by chemical analysis. In contrast, the separately prepared LiCoO<sub>2</sub> powder exhibited a small solubility of several ppm of Co. As can be seen, no changes in the morphological features of the electrodes, as well as in the mean size of particles, have been noticed. The EDAX analysis confirmed the presence of cobalt in the specimen before and after the test.

The authors would like to thank A. Jarzębski and A. Lachowski (Institute of Chemical Engineering, Polish Academy of Sciences) for porosity measurements.

#### References

- [1]. Fukui N.T., Okawa H., Tsunoka T.: J. Power Sources, 71, 239 (1998).
- [2]. Łada W., Olczak T., LeGeros R.Z., LeGeros J.P.: Method for preparing of calcium phosphates layers, especially hydroxyapatite. Polish Patent No 180602.
- [3]. Deptuła A., Łada W., Olczak T., Lanagan M., Dorris S.E., Goretta K.C., Poeppel R.B.: Method for preparing of high temperature superconductors. Polish Patent No 172618.
- [4]. Scaccia S.: Talanta, 49, 467 (1993).

## LiCoO<sub>2</sub> NANOCOMPOSITE DOPED SiO<sub>2</sub>, TiO<sub>2</sub>, Al<sub>2</sub>O<sub>3</sub> FOR RECHARGEABLE LITHIUM BATTERIES



Andrzej Deptuła, Fausto Croce<sup>1/</sup>, Wiesława Łada, Danuta Deptuła, Tadeusz Olczak, David L. Chua<sup>2/</sup>

<sup>1/</sup> Dipartimento di Chimica, Università "La Sapienza", Roma, Italy

<sup>2/</sup> Max Power Inc., Harleysville, USA

The exponentially growing demand for portable electronics, such as laptop computers and cellular phones, has rocketed interest for the development of cheaper and more efficient Li-ion batteries [1]. At present, commercially available cells use LiCoO<sub>2</sub> as cathodic material, but, in an effort to improve energy density, both LiNiO<sub>2</sub> and mixed LiNi<sub>y</sub>Co<sub>1-y</sub>O<sub>2</sub> layered compounds have been extensively studied

[2,3]. Despite of its high specific capacity, LiNiO<sub>2</sub> has shown some major drawbacks, which induced the scientific community to focalize on the parent "phase-stabilized" compounds LiNi<sub>y</sub>Co<sub>1-y</sub>O<sub>2</sub> having y ranging between 0.5 and 0.8. These latter mixed oxides, however, while showing an improvement in both specific energy and capacity respect to LiCoO<sub>2</sub>, still suffer from the capacity fading more evident at

Table 1. Thermal processing of gel nanocomposites.

Phase composition LiCoO <sub>2</sub> +	Foaming temp. [°C] and effect evaluation*	SIT [°C]	Final thermal treatment [°C], time [h], with intermediate grinding 0.5 h
+0.5% SiO <sub>2</sub>	130-s	454	800-18
+1% SiO <sub>2</sub>	140-m	454	800-18
+4% SiO <sub>2</sub>	150-m	454	800-18
+0.5% TiO <sub>2</sub>	120-vs	580	760-6; 760-6;760-6
+1% TiO <sub>2</sub>	120-m	590	760-6; 760-6;760-6
+4% TiO <sub>2</sub>	no	520	760-6; 760-6;760-6
+0.5% Al <sub>2</sub> O <sub>3</sub>	no	540	760-6; 760-6;760-6
+1% Al <sub>2</sub> O <sub>3</sub>	no	570	760-6; 760-6;760-6
+4% Al <sub>2</sub> O <sub>3</sub>	110 vs	560	760-6; 760-6;760-6

\*Foaming effect evaluation - increasing of volume: vs≥3 times, s=1.5-3 times, m=0.5-1.5 times, no = effect not observed.

high current density. Out of any doubts, both the capacity and energy retention upon cycling and the rate capability of the cathodic materials are topic aspects for the realization of practical Li-ion batteries.

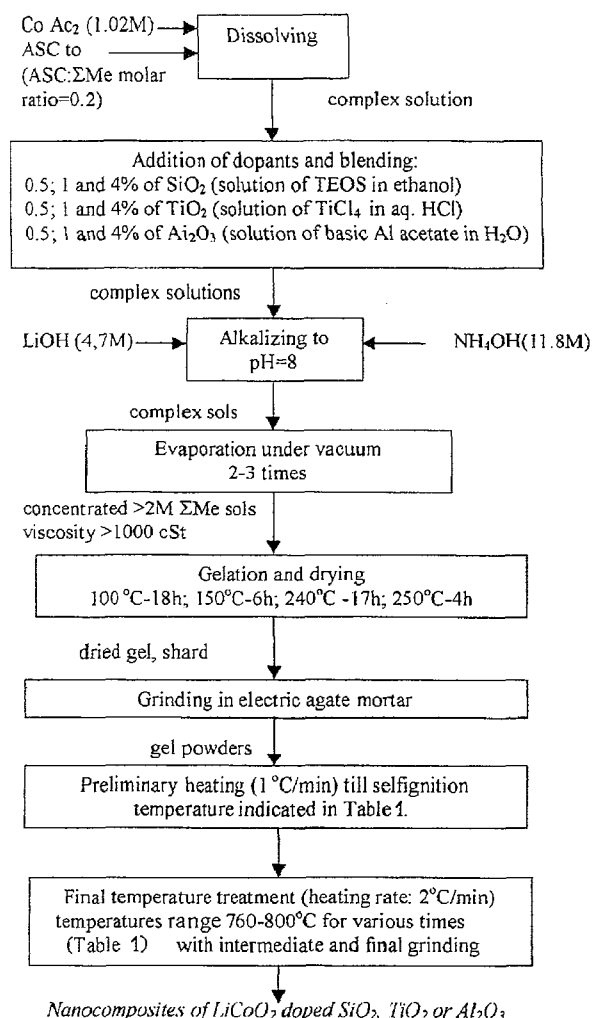


Fig.1. Experimental procedure for preparation of nanocomposites LiCoO<sub>2</sub> by Complex Sol-Gel Process.

In order to try to cope with these difficult tasks, we have adopted a "nanocomposite" strategy. Composites are a very broad class of materials generally defined as heterogeneous multiphase solids. Commonly, they are constituted by a matrix, the phase present as a major constituent and dispersoids, finely dispersed second phase particles. Physico-chemical properties of the composites start to be dominated by of the interphase regions, when the dispersoids dimensions approach a nanometer-scale (nm-scale). Often, the properties of the composites are surprisingly different

Table 2. Discharge comparison at a 70th cycle at 1 mA/cm<sup>2</sup> at 25°C.

Property	Composition				
	LiCoO <sub>2</sub> +	+0.5% SiO <sub>2</sub>	+0.5% TiO <sub>2</sub>	+0.5% Al <sub>2</sub> O <sub>3</sub>	+1% Al <sub>2</sub> O <sub>3</sub>
mAh/g	125.4	132.4	131.7	128.2	131.4
mid voltage	3.66	3.82	3.89	3.86	3.88
Wh/kg	459.0	506.2	511.9	494.7	509.8

ent from those of the separate components. Here we have prepared "composite" cathodic materials consisting of an intimate mixing, on a nm-scale, of a

main active phase and a second "inert" phase. To prepare our samples, and to achieve the best intimate

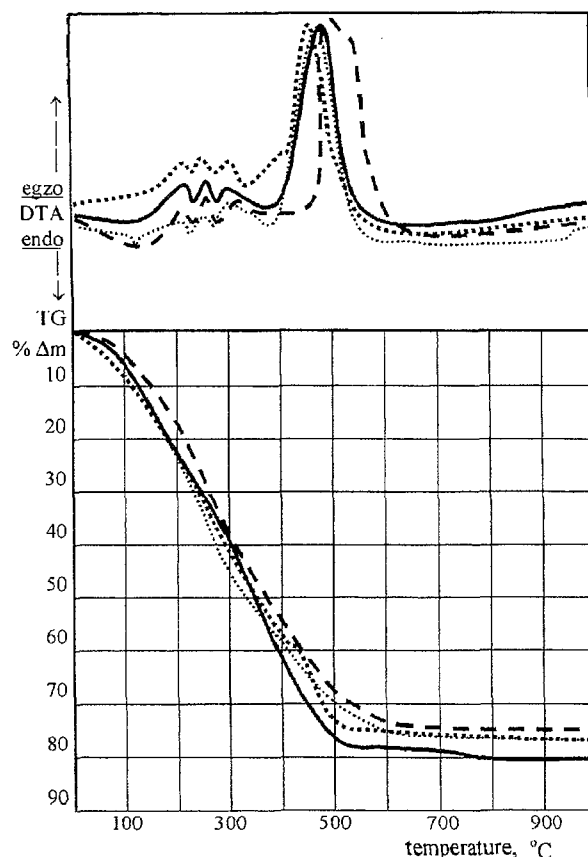


Fig.2. Thermal analysis of nanocomposite gels: ..... - LiCoO<sub>2</sub>, 25°C, 48 h; --- LiCoO<sub>2</sub> + 1.0% SiO<sub>2</sub>, 25°C, 48 h; ..... LiCoO<sub>2</sub> + 0.5% TiO<sub>2</sub>, 25°C, 48 h; — LiCoO<sub>2</sub> + 1.0% TiO<sub>2</sub>, 25°C, 48 h.

mixing between the two different phases, we have chosen to utilize a Complex Sol-Gel Process successfully applied in our former work [4] for the preparation of LiNi<sub>y</sub>Co<sub>1-y</sub>O<sub>2</sub> compounds. Essentially, the modification consists of introduction of LiOH instead LiAc<sub>2</sub>. A simplified flow chart is shown in Fig.1. Thermal analysis of gel samples shown in Fig.2 indicates that a general course of the decomposition of gels is very similar. Only for the SiO<sub>2</sub> dopant end of mass weight loss, accompanied by a very strong exothermic effect and formation of final phase take place at ~650°C, it is ~70°C higher than for the remaining materials.

Some preliminary results obtained for the composites formed by LiCoO<sub>2</sub> as the main active phase and, respectively, TiO<sub>2</sub> or Al<sub>2</sub>O<sub>3</sub> as a second foreign phase are reported below. These new 2-phase cathodic ma-

terials, despite of the relatively low concentration levels (between 0.5 and 1.0 mass %) of the dispersoids, are capable of being charged to 4.3 V vs. Li/Li<sup>+</sup>

and capable of sustaining very high discharge rates (5 mA/cm<sup>2</sup>). Furthermore, (Table 2) they all show major improvement in the cathodic rate and both in energy and capacity capability when compared with the pure, single-phase, LiCoO<sub>2</sub> parent compound.

## References

- [1]. Scrosati B.: *Nature*, 373, 557 (1995).
- [2]. Dahn J.R., Fuller E.W., O'Bravac M., von Sacken U.: *Solid State Ionics*, 109, 265 (1994).

- [3]. Croce F., Nobili F., Deptuła A., Łada W., Tossici R., D'Epifanio A., Scrosati B., Marassi R.: *Electrochem. Commun.*, 1, 605-608 (1999).
- [4]. Croce F., D'Epifanio A., Ronci F., Deptuła A., Łada W., Ciancia A., Di Bartolomeo A., Brignocchi A.: *Synthesis and Electrochemical Characterization of LiNi<sub>1-y</sub>Co<sub>y</sub>O<sub>2</sub> Powders Obtained by Complex Sol-Gel Process* MRS Spring'99 Meeting, 4-9 April 1999, San Francisco, USA. Symposium CC. "New materials for batteries and fuel cells", Proceedings, 2000, Vol. 575, p. 97.

## THE CRYSTAL STRUCTURE OF TETRA-*n*-BUTYLAMMONIUM TETRAIODOINDATE(III)

Kinga Rudawska, Halina Ptasiwicz-Bąk, Sławomir Siekierski

Structures of tetra-*n*-butylammonium salts of InCl<sub>4</sub><sup>-</sup>, InBrCl<sub>3</sub><sup>-</sup>, InBr<sub>3</sub>Cl<sup>-</sup> and InBr<sub>4</sub><sup>-</sup> were described in paper [1]. It was found that in spite of increasing size of the anion all compounds crystallize in the orthorhombic space group Pnna. The calculated In-X distance in the anion increases from the average 2.350 in InCl<sub>4</sub><sup>-</sup> to 2.479 Å in InBr<sub>4</sub><sup>-</sup>. In the InCl<sub>4</sub><sup>-</sup> anion there are two pairs of distances differing by 0.01 Å, while the four In-Br distances were found to be equal. The In-I distance in the tetrahedral InI<sub>4</sub><sup>-</sup> anion is known from measurements on In[InI<sub>4</sub>] salt (space group Pnna). In this compound there are two distances of 2.711(1) and 2.717(1) Å [2]. A similar, probably average, distance of 2.71 Å was found for the monoclinic space group C2/c [InI<sub>2</sub>(Me<sub>2</sub>SO)<sub>4</sub>][InI<sub>4</sub>] salt [3]. Comparison of the two salts of InI<sub>4</sub><sup>-</sup> suggests that a change from orthorhombic to monoclinic system may be related to increasing size of the cation. Therefore, it was interesting to know whether further increase in the size of the InX<sub>4</sub><sup>-</sup> anion when iodine is substituted for bromine would also result in decreased symmetry, and whether such a decrease would be accompanied by distortion of the [InI<sub>4</sub>] tetrahedron. To answer these questions we have studied the structure of tetra-*n*-butylammonium salt of InI<sub>4</sub><sup>-</sup> and compared it with the structure of tetra-*n*-butylammonium salts of InCl<sub>4</sub><sup>-</sup> and InBr<sub>4</sub><sup>-</sup>.

The results show that the Bu<sub>4</sub>N[InI<sub>4</sub>] (Fig.) salt crystallizes in the monoclinic space group P2<sub>1</sub>/n, in contrast with Bu<sub>4</sub>N[InCl<sub>4</sub>] and Bu<sub>4</sub>N[InBr<sub>4</sub>] [1], which crystallize in the orthorhombic Pnna space group. However, in each case there are four moieties per unit cell. Comparison with the published data [1] shows that the unit cell volume increases from 2483 Å<sup>3</sup> for InCl<sub>4</sub><sup>-</sup> to 2621 Å<sup>3</sup> for InBr<sub>4</sub><sup>-</sup> and then to 2855 Å<sup>3</sup> for the InI<sub>4</sub><sup>-</sup> salt. The almost twice as big increase in the volume difference between the I and Br than that between the Br and Cl salts results, as expected, in lower symmetry. However, it should be noted that the unit cell of the InI<sub>4</sub><sup>-</sup> salt is smaller than expected from a linear correlation between unit cell volume and anion volume.

The structures of the three Bu<sub>4</sub>N[InCl<sub>4</sub>], Bu<sub>4</sub>N[InBr<sub>4</sub>] and Bu<sub>4</sub>N[InI<sub>4</sub>] salts are similar. In

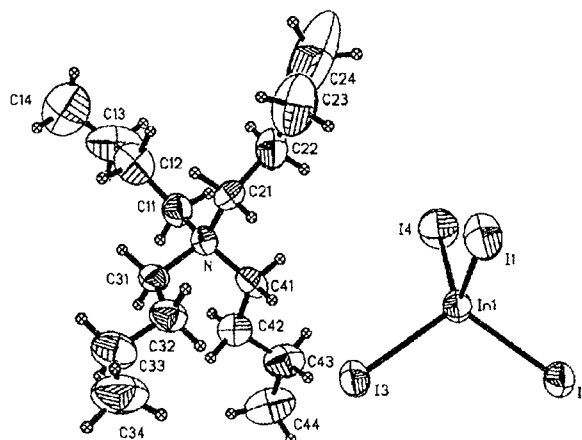


Fig. Stereoscopic picture of crystal structure of Bu<sub>4</sub>N[InI<sub>4</sub>].

each of them the InX<sub>4</sub><sup>-</sup> anion is surrounded by five nearest Bu<sub>4</sub>N<sup>+</sup> cations which occupy corners of a distorted trigonal bipyramid.

Contrary to cations, the structure of anions in the Bu<sub>4</sub>N[InX<sub>4</sub>] salts shows much larger differences. In the monoclinic iodide salt the InI<sub>4</sub><sup>-</sup> anion displays four different metal-to-ligand distances equal to 2.695(2), 2.699(2), 2.704(1) and 2.709(1) Å, while in the orthorhombic chloride and bromide salts there are either two pairs of distances, 2.345(3) and 2.355(3) Å, or only one distance equal to 2.479(2) Å, respectively.

As far as distortion of the [InX<sub>4</sub>] tetrahedron in the tetra-*n*-butylammonium salts is concerned, one could expect a correlation between the specific In-X distance and the X-N or the X-(nearest C) distance. For the title anion there is a general trend of increasing In-I distance with decreasing average I-N distance (two nearest N atoms) and decreasing average I-C distance (five nearest C atoms). However, the relationships are non-monotonic and in each of the two plots a different In-I distance deviates from the monotonic dependence.

## References

- [1]. Khan M.A., Tuck D.G.: *Acta Cryst.*, B38, 803 (1982).
- [2]. Khan M.A., Tuck D.G.: *Inorg. Chim. Acta*, 97, 73 (1985).
- [3]. Einstein F.W.B., Tuck D.G.: *Chem. Comm.*, 1182 (1970).

# ASYMMETRIC HYDROGEN BONDS IN CENTROSYMMETRIC ENVIRONMENT: NEUTRON STUDY OF THE VERY SHORT HYDROGEN BOND IN POTASSIUM HYDROGEN DICHLOROMALEATE

Ivar Olovsson<sup>1/</sup>, Halina Ptasiwicz-Bak, Torbjorn Gustafsson<sup>1/</sup>, Irena Majerz<sup>2/</sup>

<sup>1/</sup> Inorganic Chemistry, Ångström Laboratory, University of Uppsala, Sweden

<sup>2/</sup> Faculty of Chemistry, University of Wrocław, Poland

The structure of the title compound has been studied by neutron diffraction at 30 and 295 K with emphasis on the location of the protons. There are two crystallographically independent hydrogen atoms in two very short H-bonds (2.45 Å).

The structure could be refined successfully in the centrosymmetric space group P-1, with the hydrogen atoms located at the centres of symmetry. However, the form of the thermal ellipsoids of hydrogen could be interpreted as indicating either asymmetric H-bonds or of overlap of two closely spaced, partially occupied positions around the centres of symmetry. Refinements in space group P-1 were then made with the hydrogen atoms slightly shifted away from the two centres of symmetry, with partially occupied positions on either side of the centres. However, the hydrogen atoms moved back to the centres of symmetry. A fundamental problem in a least squares refinement of diffraction data is the large correlations between refined parameters of the atoms in the donor and acceptor units when these are close to related by a centre of symmetry (or by a similar symmetry operation, like a mirror plane or a twofold axis). Attempts to refine the

e.g. away from the middle of the O---O bond. One strategy to determine the actual proton position would be to impose an exact symmetry constraint on the donor and acceptor units but allow the proton to refine without this constraint. The possibility was then considered that the structure is only pseudo-centrosymmetric and that the H-bonds are in reality asymmetric. Two different series of refinements were then performed: In the first, all atoms except hydrogen were constrained in P-1, whereas hydrogen was allowed to refine without any constraints. Anisotropic refinement of all atoms resulted in clearly off-centred hydrogen positions. In the second series, all atoms were refined without constraints in P-1. This resulted in hydrogen positions quite close to those obtained in the constrained refinements. The atomic positions were within the combined standard deviations the same in both cases but as the standard deviations were about ten times larger for the heavier elements in P-1, the results from the constrained refinement were finally accepted as the most suitable description of the structure. This structure may be described as "pseudo-centrosymmetric with non-centred pro-

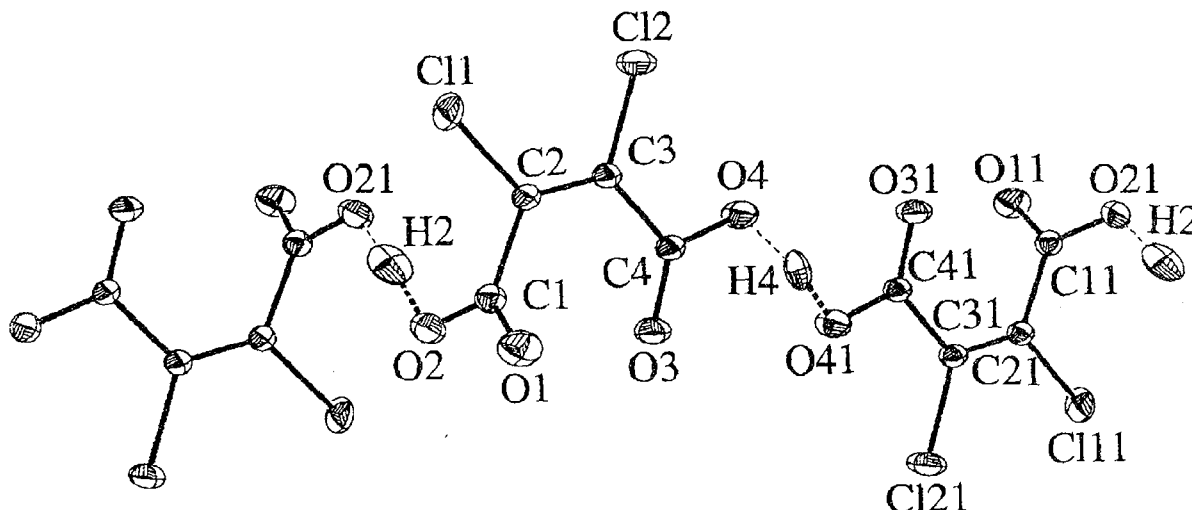


Fig.

parameters in a space group of lower symmetry will mostly diverge in this situation and the "symmetric" space group has to be chosen. The proton will then also adopt this higher symmetry. The potential energy curve for the proton motion in such a pseudo-symmetric situation has a quite broad minimum and very little energy is needed to shift the proton,

tons". Significance tests at the 0.005 level also showed that a hypothesis involving centred protons is unphysical. The shifts from the centres of symmetry are 0.15(1) Å for H2 and 0.12(1) Å for H4 at 30 K, 0.15(1) Å for both H2 and H4 at RT. At 30 K: R(F)=0.036 for 1485 reflections; at 295 K: R(F)=0.035 for 1349 reflections;  $\lambda_{\text{neutrons}}=1.207$  Å.

## ANTIFERROMAGNETIC ORDER IN RIrSi (R=Tb-Er) COMPOUNDS

Andrzej Szytuła<sup>1/</sup>, Michael Hofmann<sup>2/</sup>, Janusz Leciejewicz, Bogusław Penc<sup>1/</sup>, Adam Zygmunt<sup>3/</sup><sup>1/</sup> Institute of Physics, Jagiellonian University, Kraków, Poland<sup>2/</sup> Hahn-Meitner Institut, Berlin-Wannsee, Germany<sup>3/</sup> Trzebiatowski Institute of Low Temperatures and Structural Research, Polish Academy of Sciences, Wrocław, Poland

Crystal and magnetic structures of a series of ternary intermetallic compounds with the composition RIrSi, where R is Tb, Dy, Ho and Er were studied using X-ray, neutron diffraction and magnetometric methods. RIrSi compounds crystallize in the orthorhombic TiNiSi type structure (space group Pmna). Isostructural compounds RIrGe compounds were reported to be antiferromagnetic at low temperatures [1]. Neutron diffraction data collected at low temperatures have shown that below the Neel point at 32 K, TbIrSi shows a sine modulated magnetic order described by the wave vector  $k=[0, 0.2938(2), 0]$  with the magnetic moment of  $8.96(16)\mu_B$  at 1.5 K, localized on the  $Tb^{3+}$  ion and aligned along the c-axis. The collinear antiferromagnetic structure with the wave vector  $k=[1/2, 0, 1/2]$  and the magnetic moment of  $9.9(1)\mu_B$  parallel to the b-axis has been observed in HoIrSi at 1.5 K. In the vicinity of the Neel temperature at 4.6 K, this structure coexists with a sine modulated order described by the

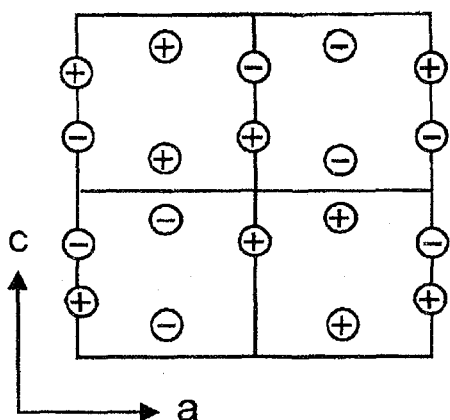


Fig.1. Schematic representation of the collinear magnetic structure of HoIrSi viewed along the tetragonal axis.

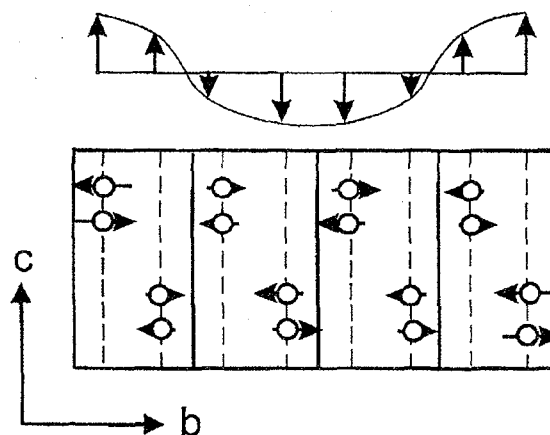


Fig.2. Schematic representation of the sine modulated magnetic ordering in HoIrSi observed near the Neel point at 4.6 K.

wave vector  $k=[0.215(2), 0, 0.458(2)]$ . The former structure is schematically displayed in Fig.1, the latter - in Fig.2. ErIrSi exhibits the sine modulated magnetic structure described by the wave vector  $k=[0, 0.184(1), 0.297(3)]$ . The magnetic moment of  $6.5(2)\mu_B$  at 1.5 K, localized on the  $Er^{3+}$  ion is aligned in the (100) plane. The Neel point of ErIrSi is at 3.8 K. Due to the large absorption cross section for thermal neutrons of the Dy and Ir nuclei, it was not possible to record neutron diffraction spectra of DyIrSi. Magnetometric measurements carried out in the temperature range from 4 K to the room temperature in magnetic field of 50 Oe indicate that the DyIrSi is also antiferromagnetic with the Neel point at 7 K.

## References

- [1]. Penc B., Hofmann M., Leciejewicz J., Ślaski M., Szytuła A.: J. Alloys Comp., 282, 18 (1999).

## NEUTRON SCATTERING SPECTROSCOPY AND AB INITIO STUDY OF L-THREONINE

Andrzej Pawlukoje<sup>1/</sup>, Janusz Leciejewicz, John Tomkinson<sup>2/</sup>, Stewart F. Parker<sup>2/</sup><sup>1/</sup> Frank Neutron Physics Laboratory, Joint Institute of Nuclear Research, Dubna, Russia;  
Institute of Nuclear Chemistry and Technology, Warszawa, Poland<sup>2/</sup> CLRC, Rutherford-Appleton Laboratory, Chilton, United Kingdom

L-threonine (2-amino-3-hydroxybutanecarboxylic acid) is one of the members of aliphatic hydroxy amino acids series. The studies of its crystal structure have shown that the molecules of L-threonine occur in the crystalline state in the zwitterion form, similarly as in L-serine (2-amino-3-hydroxy propanecarboxylic acid). In both compounds, amino and hydroxy hydrogen atoms take part in a system of hydrogen bonds, largely responsible for their biological significance. The method of IINS is

now broadly used in the studies of molecular motions (particularly of hydrogen bonds) in crystals, since the internal modes, in which hydrogen nuclei take part, produce IINS spectra with much higher intensities than other modes. This effect is due to the large cross section of hydrogen for the incoherent scattering of thermal neutrons, in addition, the substitution of hydrogen by deuterium permits the identification of the modes due to the hydrogen vibrations, since, as compared to



PL0101501

hydrogen, the incoherent cross section of deuterium is almost 40 times smaller, while the oscillator mass is twice as large. Commercial grade (Fluka Chemie AG) polycrystalline sample of L-threonine was used for IINS data collection. The deuterated sample, in which 95% of amino and hydroxy hydrogen atoms were substituted by deuterium, was recrystallized from the heavy water  $D_2O$ .

The IINS spectra were measured using TFXA, an indirect geometry inelastic spectrometer at the ISIS Pulsed Neutron Facility in Rutherford-Appleton Laboratory. Its energy resolution is about 2%. The spectra were recorded at 10 K. Time-of-flight spectra were converted to  $S(Q, \omega)$  and corrected for the background scattering using standard procedures. The  $S(Q, \omega)$  against energy transfer curves are displayed in Fig.

Gaussian 98 programme package has been adopted for optimization of the molecular structure in the zwitterion form using the data available from a neutron diffraction study at 12 K reported in [1]. The calculations were carried out at HF, MP2 and B3LYP levels with the 6-31G\*, 6-311G\*, 6-311G\*\* and 6-311++G\*\* basis sets.

The vibrational frequencies for the normal and deuterated sample of L-threonine were calculated using the optimized geometries derived from HF/6-31G\*, HF/6-311G\*, HF/6-311G\*\* and HF/6-311++G\*\* models of the zwitterion form. The frequencies were scaled by the scale factor 0.8927 as recommended for the FH methods. The harmonic force field (second derivative of energy with respect to internal coordinates) and potential energy distribution (PED) were evaluated at HF/6-311G\* level using the GAMES pro-

gram. All computations were performed using the HP-SPP computer in Dubna.

The calculated bond lengths, in which carbon, oxygen and nitrogen atoms are involved have shown fair agreement with the experimental data, however, the bond distances, in which hydrogen atoms take part, are longer than the experimental values. The bond angles computed using all four basis sets gave reasonable agreement with the experimental values - maximum deviation amounts to ca. 5 degrees. In the case of torsional angles the deviations are about 15 degrees and for some of the hydrogen bonds even 30 degrees, with the exception of those computed for hydroxyl hydrogen bonds which fit the experimental values with a reasonable accuracy. The above discrepancies are caused by the fact that the computations were carried out for the free molecule without allowing for the temperature effects - the experimental data listed in [1] refer to a molecule in the crystal kept at a temperature of 12 K.

Since the torsional angles computed using the HF/6-311G\* model show the best agreement with experimental data, only this basis set has been adopted for the interpretation of vibrational spectra.

Vibrational assignments were done for the amino group, methyl group, hydroxyl group, methine group, carbonyl group modes and skeleton deformation modes. The energies of the latter modes, apart falling in the same range, were observed to be mixed with other modes, so that they were not fully separated and could not be identified in a unique manner. A detailed analysis of the vibration modes of the amino group has shown that the bending modes produce strong peaks observed on the IINS

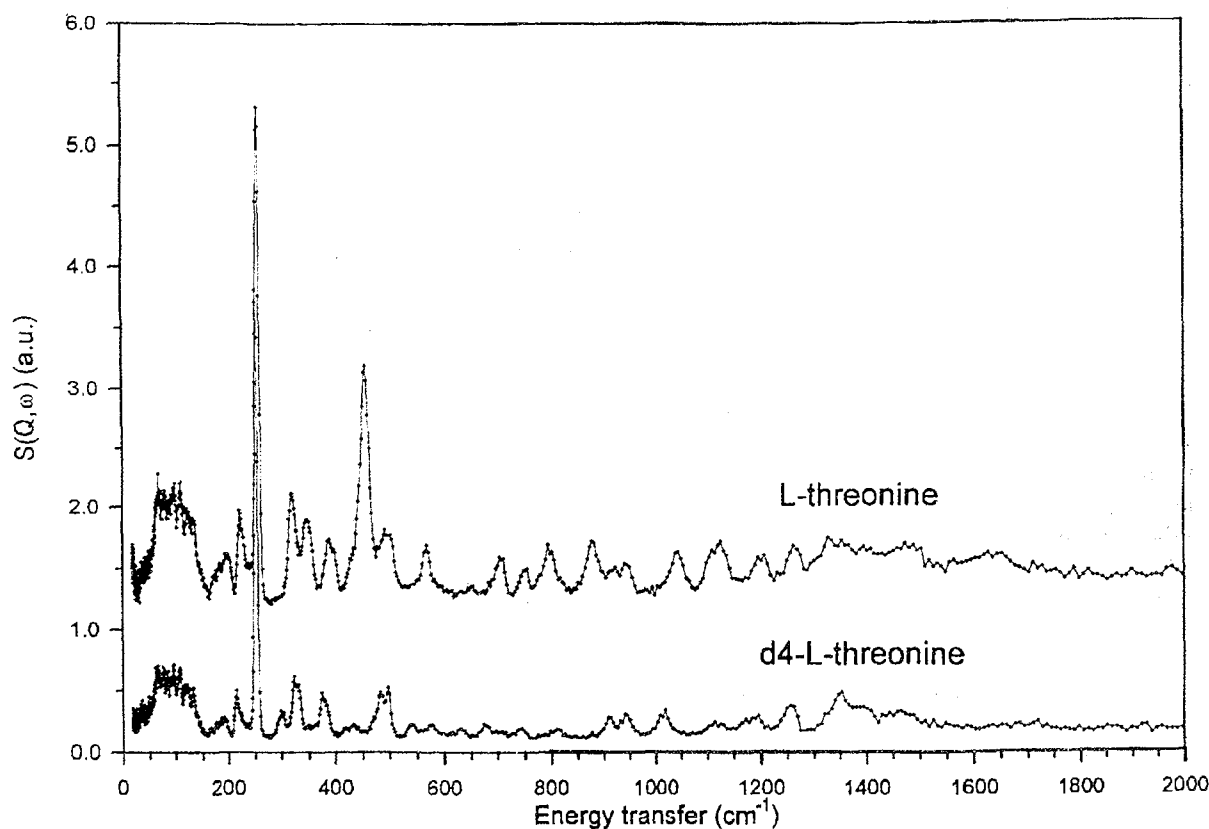


Fig. Phonon density vs. energy transfer curve for L-threonine.

spectrum of normal L-threonine at the energies of ca. 1600, 1550 and 1415  $\text{cm}^{-1}$  and at the energies of 1180, 1155 and 1010  $\text{cm}^{-1}$  on the spectrum of the deuterated sample. The ratios of respective energies is thus not far from square root two. The vibrations of the rocking type were found to be mixed with those due to other types. Therefore, a unique assignment was not possible. The intense peak observed at the energy 456  $\text{cm}^{-1}$  on the IINS spectrum of the normal sample, does not appear on the spectrum of the deuterated sample. It is assumed that the torsional mode of the  $\text{NH}_3$  group is mixed with the  $\text{CCC}_{\text{bend}}$  mode. The calculated energy of the torsional vibration of the  $\text{NH}_3$  group amounts to 239  $\text{cm}^{-1}$  and is much smaller than the observed value. This effect is caused by strong  $\text{N-H}\cdots\text{O}$  hydrogen bonds. A shift of the energy due to the torsional vibration of the amino group towards larger energies has been also detected in other aliphatic amino acids studied up to now using the IINS spectroscopy. The torsional vibration of the  $\text{ND}_3$  group is observed at the energy of 300  $\text{cm}^{-1}$ .

The most intense peak on the IINS spectrum at the energy 256  $\text{cm}^{-1}$  has been assigned to the  $\text{CH}_3_{\text{tors.}}$  mode. A second peak on the IINS spectrum observed at the energy 506  $\text{cm}^{-1}$  has been identified as the first overtone of the  $\text{CH}_3_{\text{tors.}}$  mode. The peak observed on the IINS spectrum at 320  $\text{cm}^{-1}$  was assigned to the torsional vibration of the OH group. The analysis of the neutron spectroscopy data obtained for the normal and deuterated samples of polycrystalline L-threonine combined with the ab initio calculations made it possible to identify the majority of vibrations modes due to particular molecular groups and to separate modes due to hydrogen bond vibrations in the crystals of the title compound. As in the previous studies, the IINS method proved to be an effective tool to investigate the hydrogen bond dynamics in the crystals of amino acids.

#### References

- [1]. Janczak J., Zobel D., Luger P.: Acta Cryst., **C53**, 1901 (1997).

### CRYSTAL CHEMISTRY OF COORDINATION COMPOUNDS WITH HETEROCYCLIC CARBOXYLATE LIGANDS. PART XXXII: THE CRYSTAL AND MOLECULAR STRUCTURE OF A CALCIUM(II) COMPLEX WITH PYRIDINE-2,6-DICARBOXYLATE AND WATER LIGANDS

Wojciech Starosta, Halina Ptasiwicz-Bąk, Janusz Leciejewicz

The crystals of bis[ $\mu$ -pyridine-2,6-dicarboxylato-  
-O,N-O')]bis[trisaqua-calcium(II)] di(pyridine-

-2,6-dicarboxylic acid) contain dimeric molecules  
composed of two calcium(II) ions and two ligand

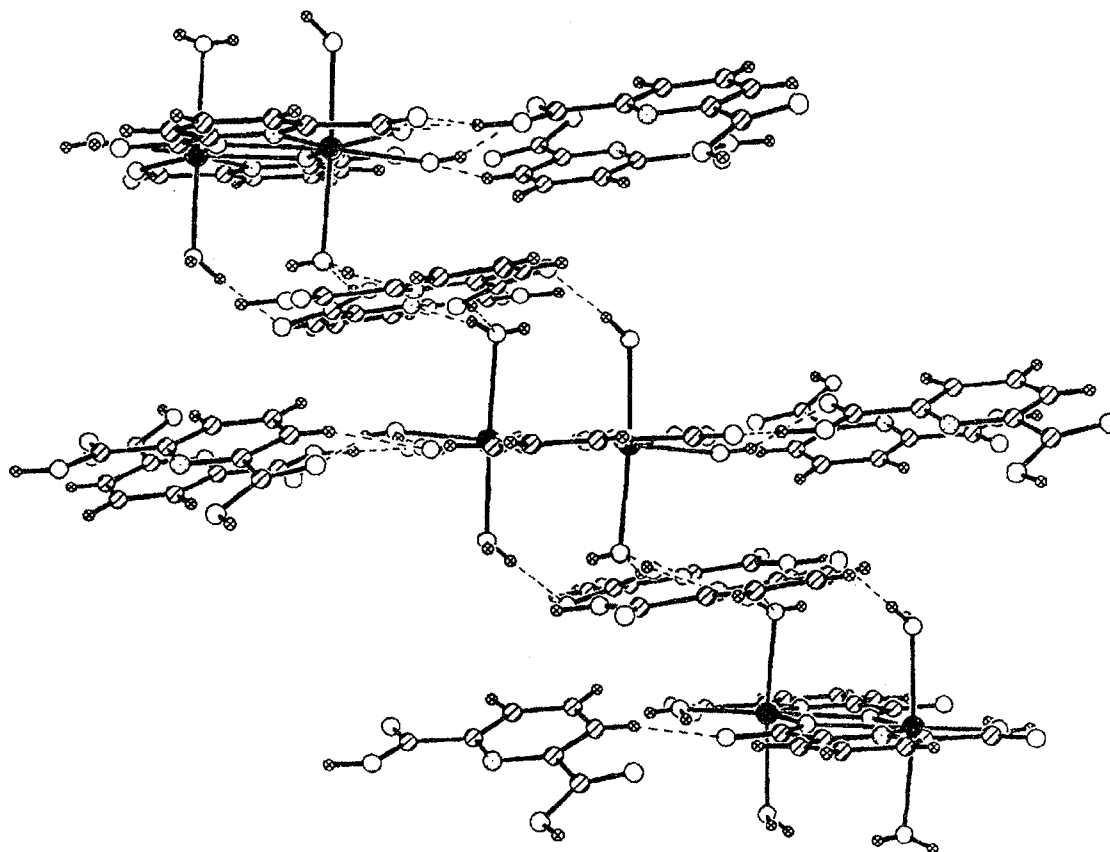


Fig. The structure of  $\text{Ca}_2(2,6\text{-PDDC})_2(\text{H}_2\text{O})_6 \cdot 2\text{H}_2(2,6\text{-PDDC})$ . Black circles represent the  $\text{Ca}(\text{II})$  ions.

molecules. Calcium ions are bridged by two bidentate oxygen atoms each donated by one carboxylic group of the ligand [Ca-O 2.438(2) Å; Ca-O 2.409(2) Å]. Apart from the two bridging oxygen atoms the coordination around each Ca(II) ion is composed of the heteroring nitrogen atom [Ca-N 2.467(2) Å], a monodentate oxygen atom of the second carboxylic group of the ligand [Ca-O 2.484(2) Å] and three oxygen atoms, each donated by a water molecule [mean Ca-O 2.388(2) Å]. The dimer is shown in Fig. The coordination polyhedron around the Ca(II) ion is a distorted pentagonal bipyramid. Its equatorial plane is composed of three carboxylate oxygen atoms, heteroring nitrogen atom and a water oxygen atom. Two other water oxygen atoms constitute the vertices of the bipyramid. Acid molecules were found in the space between the dimers. An extended network of intra- and intermolecular hydrogen bonds with lengths ranging from 2.543(3) to 2.965(3) Å is operating in the crystal. The crystals of  $\text{Ca}_2(2,6\text{-PDDC})_2(\text{H}_2\text{O})_6 \cdot 2\text{H}_2(2,6\text{-PDDC})$  are monoclinic (space group  $P2_1/c$ ):  $a=9.307(2)$ ,  $b=14.880(3)$ ,  $c=12.265(3)$  Å,  $\beta=97.24(3)^\circ$ . X-ray diffraction measurements were carried out using

the KUMA KM4 four circle diffractometer at this Institute. Data processing and structure refinement was performed using SHELXL programme package.

### References

- [1]. Part XXVI. Ptasiwicz-Bak H., Leciejewicz J.: Molecular ribbons composed of calcium(II) ions bridged by carboxylate and water oxygen atoms in the crystals of Ca(II) complex with 5-methylpyrazine-2-carboxylate ligands. *J. Coord. Chem.*, **49**, 301 (2000).
- [2]. Part XXVII. Ptasiwicz-Bak H., Leciejewicz J.: The crystal structure of monoaquabis (trans-5-methylpyrazine-2-carboxylato-N,O)copper(II) trihydrate. *Polish J. Chem.*, **74**, 877 (2000).
- [3]. Part XXVIII. Paluchowska B., Maurin J.K., Leciejewicz J.: X-ray diffraction study on manganese(II) complexes with thiophene-2-carboxylate and furan-3-carboxylate ligands. *J. Coord. Chem.*, **51**, 335 (2000).
- [4]. Part XXIX. Paluchowska B., Maurin J.K., Leciejewicz J.: The crystal and molecular structure of a furan-2-carboxylate heterobimetallic complex  $[\text{Zn}(\text{H}_2\text{O})_6]^{2+} [\text{Zn}_8\text{Na}_2(\text{C}_5\text{H}_3\text{O}_5)_{18}(\text{OH})_2]^{2-}$ . *J. Coord. Chem.*, **52**, 252 (2001).
- [5]. Part XXX. Starosta W., Ptasiwicz-Bak H., Leciejewicz J.: Polymeric molecular pattern in the crystals of calcium(II) complex with pyridine-3,4-dicarboxylate and water ligands. *J. Coord. Chem.*, **52**, 265 (2001).
- [6]. Part XXXI. Starosta W., Ptasiwicz-Bak H., Leciejewicz J.: Dimeric molecules in the crystals of calcium complex with pyridine-3,5-dicarboxylate ligands. *J. Coord. Chem.*, in press.

## CRYSTAL CHEMISTRY OF COORDINATION COMPOUNDS WITH HETEROCYCLIC CARBOXYLATE LIGANDS. PART XXXIII: THE CRYSTAL AND MOLECULAR STRUCTURES OF TWO POLYMORPHIC FORMS OF A CALCIUM(II) COMPLEX WITH PYRIDINE-2,6-DICARBOXYLATE, WATER AND NITRATE LIGANDS

Wojciech Starosta, Halina Ptasiwicz-Bak, Janusz Leciejewicz

The structures of two calcium(II) complexes with pyridine-2,6-dicarboxylate (dipicolinate or 2,6-PDDC)

ligand have been solved and described. The crystals of the complex denoted by the present authors as "cal-

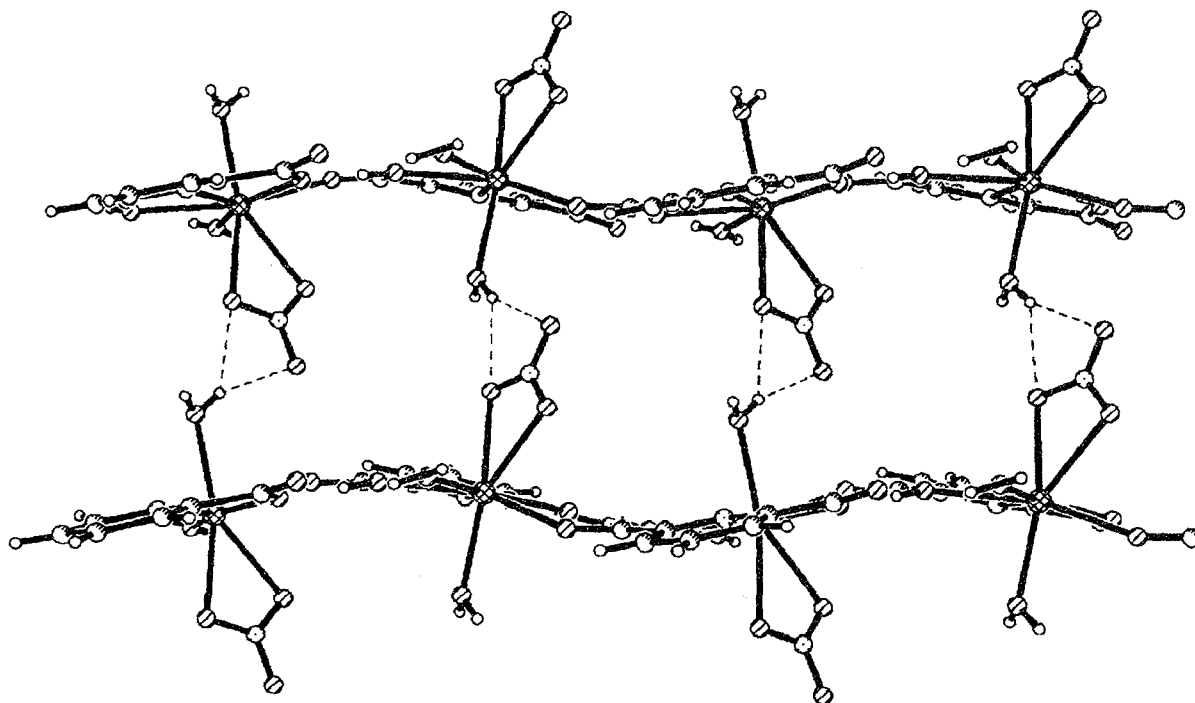


Fig.1. Molecular ribbons in the structure of the  $\alpha$ -form of  $\text{Ca}[\text{H}(2,6\text{-PDDC})](\text{H}_2\text{O})_2\text{NO}_3$ .



cium dipicolinate trihydrate" contain dimeric units composed of two calcium(II) ions and two 2,6-PDDC ligand molecules. The Ca(II) ions are bridged by two bidentate oxygen atoms donated by only one carbo-

nitrogen atom, two water oxygen atoms and two oxygen atoms of a nitrate group giving rise to a distorted pentagonal bipyramid as a coordination polyhedron. The structures of the polymorphic modifications dif-

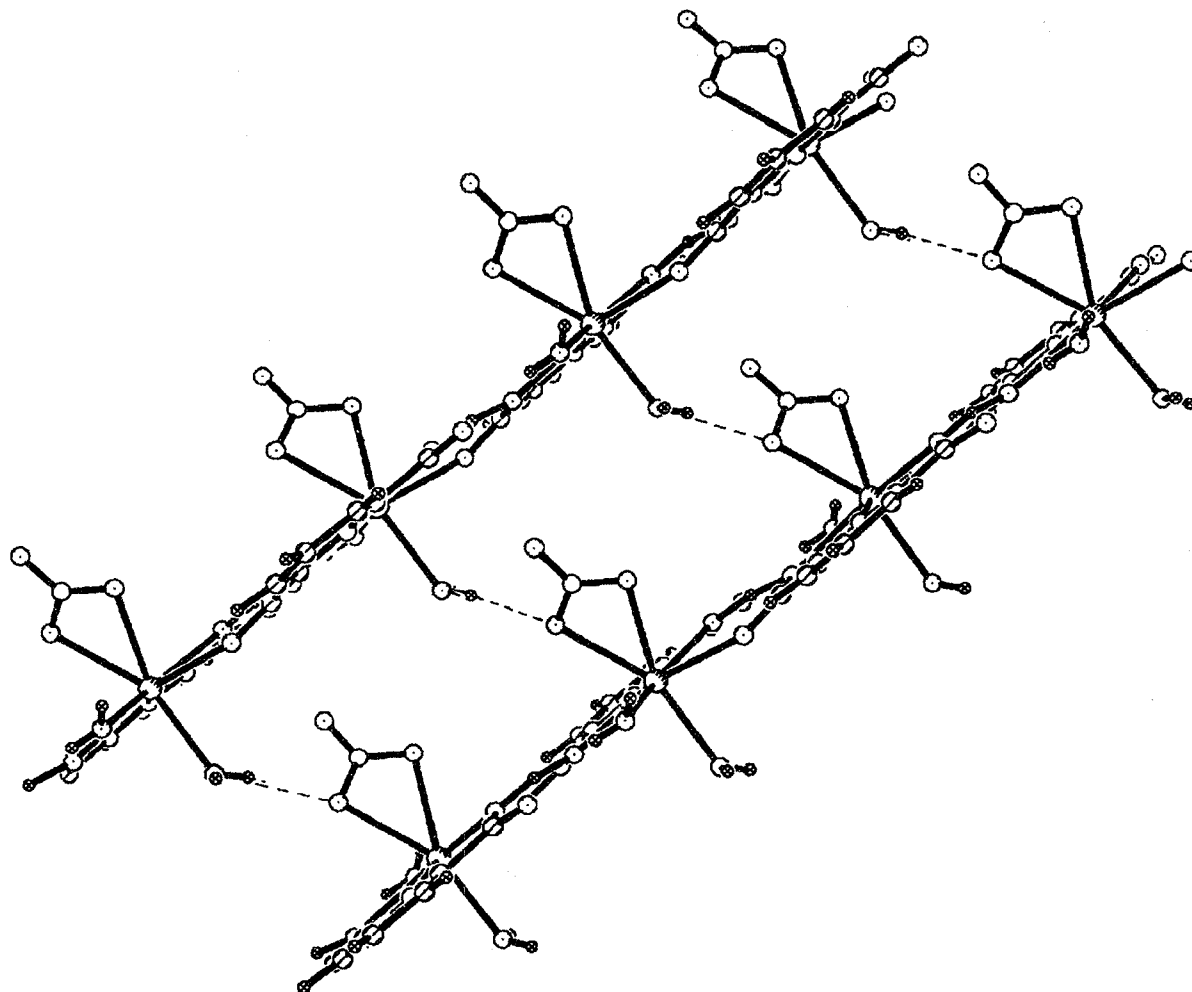


Fig.2. Molecular ribbons in the structure of the  $\beta$ -form of  $\text{Ca}[\text{H}(2,6\text{-PDDC})](\text{H}_2\text{O})_2\text{NO}_3$ .

xylate group of each 2,6-PDDC ligand. In turn, the Ca(II) ions in adjacent dimers are bridged by two water oxygen atoms giving rise to a polymeric molecular pattern [1]. Discrete dimeric molecules have been also observed in the structure of another calcium(II) complex with 2,6-PDDC and water ligands, in which free dipicolinic acid molecules have been found to be accommodated in the space between the dimers resulting in removal of the bridging via water molecules [2]. Calcium(II) complex: catena-mono( $\mu$ -pyridine-2,6-dicarboxylato-O:O:N;O') (diaqua-O) mono (nitrate-O:O) calcium(II) exists in two polymorphic forms. Each contains molecular ribbons in which adjacent Ca(II) ions are bridged by monodentate oxygen atoms donated by one carboxylate group of the pyridine-2,6-carboxylate ligand. Apart from this bridging oxygen atom, the Ca(II) ion is coordinated by two carboxylate oxygen atoms contributed by a different carboxylate group of the ligand molecule, the heteroring

fer in the way in which the nitrate ligands are oriented in respect to the equatorial planes of the adjacent coordination polyhedra: the trans mode in the  $\alpha$ -form, the cis mode in the  $\beta$ -form. In both modifications hydrogen bonds operate between the carboxylate oxygen atoms, water oxygen atoms and nitrate oxygen atoms. Figs.1 and 2 show schematically the molecular ribbons in the  $\alpha$  and  $\beta$  forms, respectively. Both are monoclinic: space group  $P2_1/n$ . The unit cell volumes are:  $V=1209 \text{ \AA}^3$  ( $\alpha$ -form) and  $1175 \text{ \AA}^3$  ( $\beta$ -form). X-ray diffraction measurements were carried out using the KUMA KM4 four circle diffractometer at this Institute. Data processing and structure refinement was performed using SHELXL programme package.

#### References

- [1]. Strahs G., Dickerson R.E.: Acta Cryst., B24, 571 (1968).
- [2]. Starosta W., Ptasiwicz-Bak H., Leciejewicz J.: J. Coord. Chem., in press.

# CRYSTAL CHEMISTRY OF COORDINATION COMPOUNDS WITH HETEROCYCLIC CARBOXYLATE LIGANDS. PART XXXIV: THE CRYSTAL AND MOLECULAR STRUCTURES OF LEAD(II) COMPLEXES WITH FURAN-2-CARBOXYLATE AND FURAN-3-CARBOXYLATE LIGANDS

Beata Paluchowska<sup>1/</sup>, Jan K. Maurin<sup>1,2/</sup>, Janusz Leciejewicz

<sup>1/</sup> Institute of Atomic Energy, Świerk, Poland

<sup>2/</sup> Drug Institute, Warszawa, Poland

The crystals of the lead(II) 2-furoate contain tetrameric structural units  $Pb_4(2-FCA)_8(H_2O)_2$  in which four Pb(II) ions are bridged by carboxylate oxygen atoms forming a circular centrosymmetric moiety. In addition, pairs of Pb(II) ions are bridged by carboxylate oxygen atoms inside this moiety. The coordination around one Pb(II) ion is ninefold: apart from the carboxylate oxygen atom it is coordinated by a water oxygen atom and three hetero-ring oxygen atoms donated by adjacent ligand molecules. The other Pb(II) ion exhibits eightfold coordination consisting of five carboxylate oxygen atoms and three hetero-ring oxygen atoms. The Pb-O bond distances range from 2.356(15) to 2.966(15) Å. Fig.1 shows one circular moiety with atom and 2-furoate ligand numbering schemes.

The molecular pattern observed in the lead(II) complex with the 3-furoate ligand is polymeric. It consists of  $Pb(3-FCA)_2(H_2O)$  structural units bridged by carboxylate oxygen atoms donated by the furan-3-carboxylate (3-FCA) ligands which act as bidentate, using both their carboxylate oxygen atoms for chelation. Three of them, however, are also engaged in bridging adjacent Pb(II) ions forming thus a three-dimensional, highly irregular molecular framework. The coordination around the Pb(II) ion is ninefold - it includes four carboxylate oxygen atoms donated by two ligand molecules, three bridging carboxylate oxygen atoms contributed by the adjacent ligands, a water oxygen atom and an oxygen atom donated by the furan ring of the adjacent ligand molecule. The Pb-O bond distances range from 2.341(11) to 3.693(12) Å. A view of

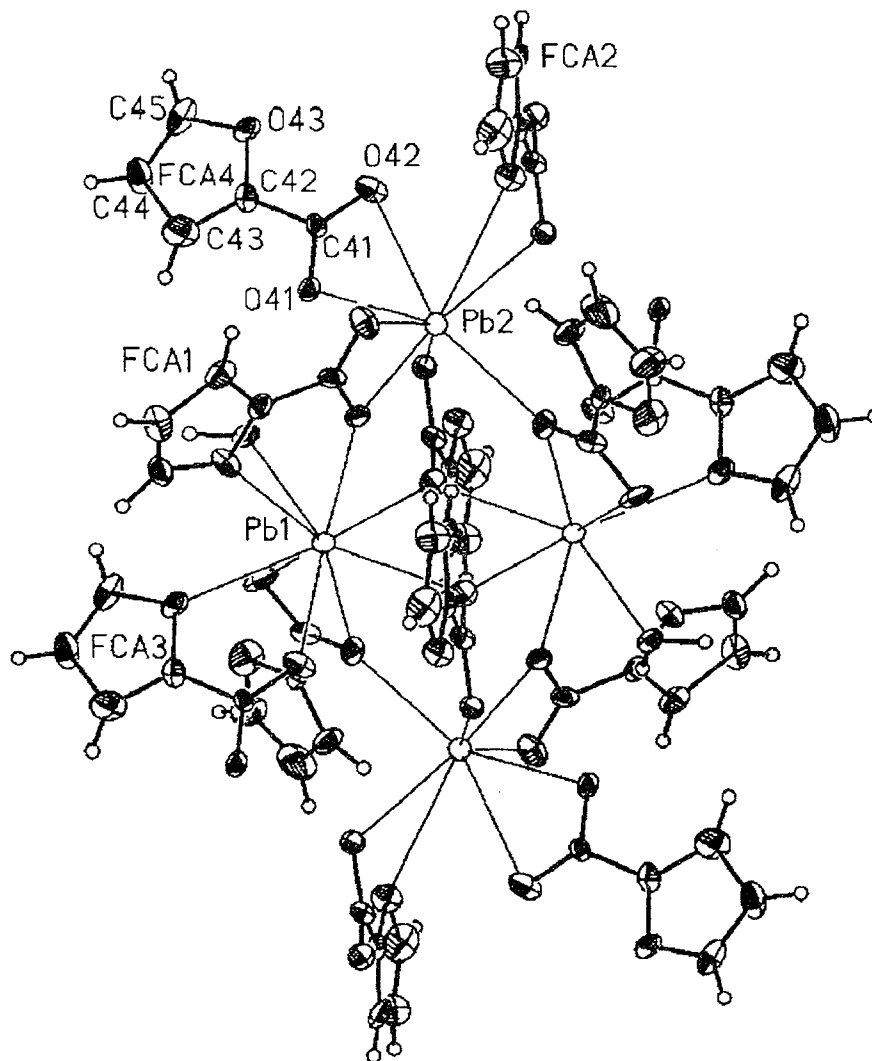


Fig.1. A circular moiety observed in the structure of lead(II) complex with 2-furoate (FCA) and water ligands.

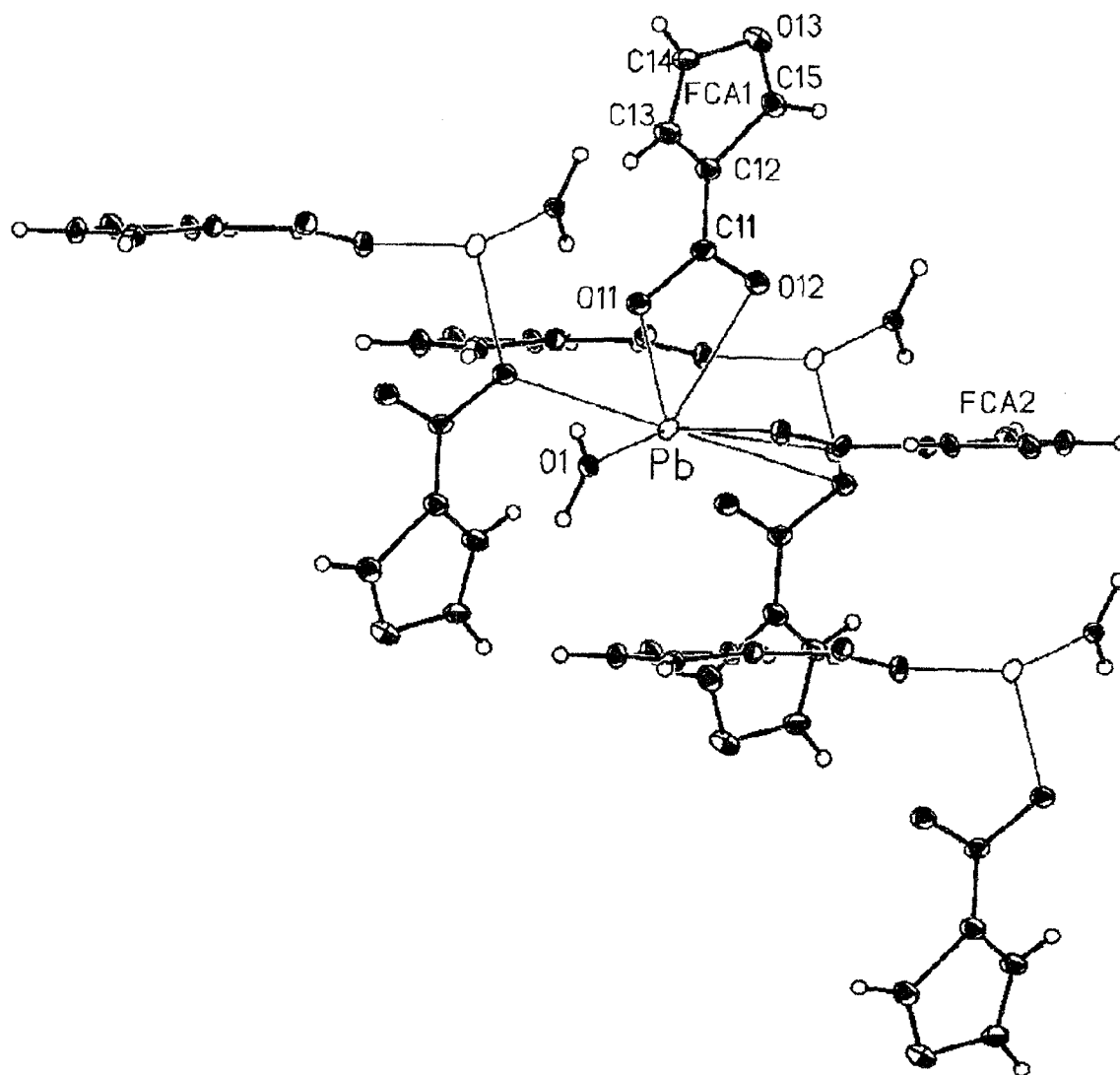


Fig.2. A fragment of the structure of lead(II) complex with 3-furoate (FCA) ligand.

a number of structural units is shown in Fig.2. The crystals of both complexes are triclinic; space group P1. X-ray diffraction measurements were carried out

using the KUMA KM4 four circle diffractometer at this Institute. Data processing and structure refinement was performed using SHELXL programme package.

# **RADIOBIOLOGY**

## EXPRESSION OF TP53 EFFECTOR PROTEINS AND STRESS KINASES IN L5178Y SUBLINES

Iwona Grądzka, Irena Szumiel, Dariusz Kowalczyk<sup>1/</sup>, Przemysław Janik<sup>1/</sup>

<sup>1/</sup>Department of Cell Biology, Oncology Center, Warszawa, Poland

Two L5178Y sublines are heterozygous for a Tp53 mutation (TGC→CGC; codon 170). Mutation at this site impairs the function of the Tp53 DNA binding domain and thus, indirectly, its transactivating capacity. The main reason for the high radiation sensitivity of LY-S cells is a deficiency in DNA double strand break (DSB) repair [1], apparently caused by impaired non-homologous end-joining (NHEJ) [2], whereas homologous recombination repair is functional [3]. In LY-R cells both repair systems are functional. The cell sublines differ in several features of response to ionising radiation that may depend on cellular signalling. In continuation of long term studies on these cells, we determined the expression of gadd45 and p21/WAF1 genes, which usually are induced by moderate radiation doses and are important in cell cycle control. Also, we checked whether Jnk and Erk protein kinases that are part of the response to various types of stress signals are present in LY cell extracts.

The cells were  $\gamma$  irradiated at 0°C with the use of a cobalt-60 gamma source (MINEOLA), at a dose

rate of 60.5 Gy/h. Protein kinases were determined with Western blotting with the use of specific antibodies. Transcription of p21/WAF1 and gadd45 was assayed by RT-PCR (reverse transcriptase-polymerase chain reaction).

Fig.1A shows that both LY sublines constitutively express gadd45 at a comparable level, and this is not affected by irradiation. LY-R cells, predictably for a Tp53 mutant, constitutively express p21/WAF1; irradiation does not enhance the expression (Fig.1B). LY-S cells express p21/WAF1 neither constitutively nor after irradiation (Fig.1B), in agreement with a recent report [4]. Fig.2 shows that the abundance of Erk1 and 2, as well as Jnk1 and 2 does not change after irradiation for up to 4 h. So, these kinases are not responsible for the differential response of LY sublines to ionising radiation. In contrast, there are recent reports on the anti-apoptotic action of p21/WAF1, apparently due to inhibition of pro-caspase-3 activation [4]. It is plausible to assume that

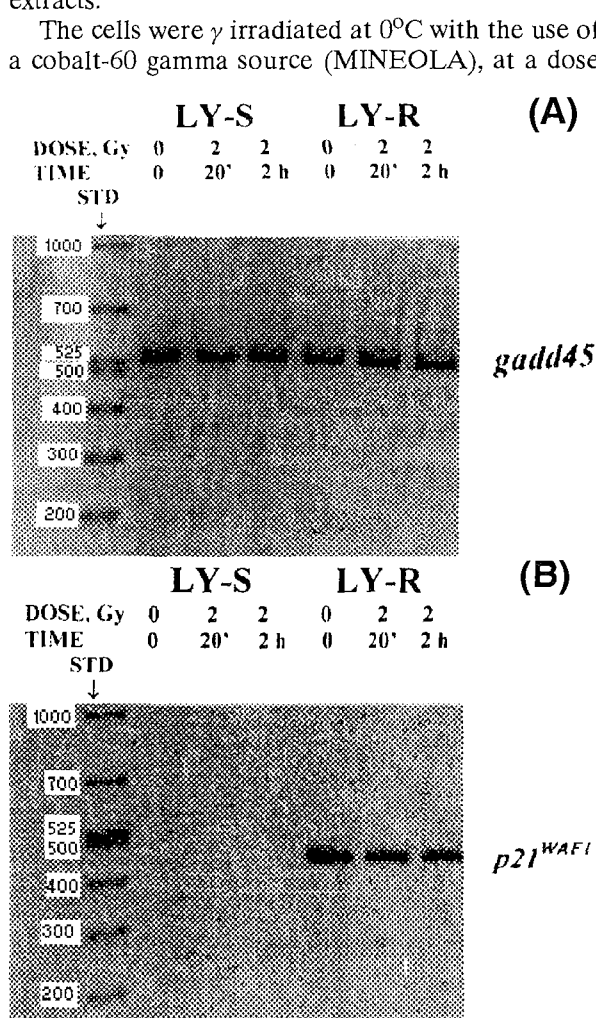


Fig.1. Expression of gadd45 (A) and p21/WAF1 (B) examined by RT-PCR in control and X-irradiated LY cells, 2 and 4 h after irradiation. STD - standard (base pairs).

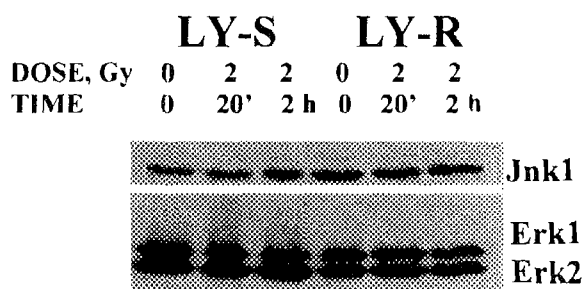


Fig.2. Western blots of Erk1, Erk2 (30  $\mu$ g protein per lane), Jnk1 and Jnk2 (20  $\mu$ g protein per lane) in control and X-irradiated LY cells, 2 and 4 h after irradiation.

this effect can take place in the X-irradiated LY-R cells, whereas LY-S cells do not express p21/WAF1 and are deprived of this protection. Although direct proof is lacking, this assumption is compatible with the previously reported [5] relative radiation-induced apoptosis proneness of LY-S cells as compared to LY-R cells.

Supported by the Polish State Committee for Scientific Research grant for the Institute of Nuclear Chemistry and Technology.

### References

- [1]. Włodek D., Hittelman W.N.: *Radiat. Res.*, **115**, 566-575 (1988).
- [2]. Kruszewski M., Wojewódzka M., Iwanefko T., Szumiel I., Okuyama A.: *Mutat. Res.*, **409**, 31-36 (1998).
- [3]. Grądzka I., Skierski J., Szumiel I.: *Cell Biochem. Funct.*, **16**, 239-252 (1998).
- [4]. Ostapenko V.V., Wang X.J., Ohnishi K., Takahashi A., Yamamoto I., Tanaka Y., Ohnishi T.: *Radiat. Res.*, **152**, 321-327 (1999).
- [5]. Szumiel I., Jaworska A., Kapiszewska M., John A., Grądzka I., Sochanowicz B.: *Radiat. Environ. Biophys.*, **39**, 33-39 (2000).

# CAFFEINE-INHIBITABLE CONTROL OF THE RADIATION-INDUCED G2 ARREST IN L5178Y-S CELLS DEFICIENT IN NON-HOMOLOGOUS END-JOINING

Irena Szumiel, Iwona Grądzka, Maria Kapiszewska<sup>1/</sup>

<sup>1/</sup> Institute of Molecular Biology, Jagiellonian University, Kraków, Poland

Duration of the radiation-induced G2 arrest in mammalian cells may be expected to be directly related to the proportion of DNA damage left unrepaired, although no general relationship of these two parameters to radiation sensitivity could be found [1]. Nevertheless, the response to X-rays of L5178Y (LY) sublines which differ in radiation sensitivity and double strand break repair competence [2] very well meets this expectation. The radiation sensitive variant, LY-S, has an exceptionally long mitotic delay (11 h/Gy), whereas the parental, more radiation resistant LY-R line, about 4 h/Gy [3].

Caffeine treatment enhanced the killing effect of X-irradiation in LY-S cells (enhancement factor equal to 1.2 from clonogenic survival), whereas it did not change survival of the X-irradiated LY-R cells [3]. In both cell lines the G2 phase fraction was considerably diminished in caffeine-treated and irradiated cells as compared to the irradiated ones.

Caffeine inhibits the kinase activity of ATM (ataxia telangiectasia mutated) [4,5] and hence, the whole signalling pathway to the cyclin B1/Cdc2 complex, thus abrogating the G2 arrest.

The treatment also increases the DNA damage (Fig.1) that is estimated with the comet assay 18 h after irradiation with 5 Gy (ca. 23% of the initial value for X and ca. 47% for X + caffeine). This indicates that either the repair has not been completed or the apoptotic DNA fragmentation has been initiated (or both). The same treatment applied to X (5 Gy)-irradiated LY-R cells (G2 arrest = 4 h/Gy) has no radiosensitizing effect and induces no apoptosis. It also does not alter the amount of DNA damage left unrepaired (ca. 28%). The results are compatible with the assumption that inhibition of the Atm-dependent G2 checkpoint pathway by caffeine brings differential effects in LY sublines because of the DNA repair defect in LY-S cells. Atm controls the activity of recombination repair, which is functional in LY-S cells. So, in these cells caffeine treatment can both inhibit DSB rejoining and abrogate the Atm-dependent G2 checkpoint control. In consequence, the LY-S cells with incompletely repaired DNA are subject to accelerated apoptosis (Fig.2). On the contrary, LY-R cells can repair DNA damage by the non-homologous end-joining, which is not affected by caffeine.

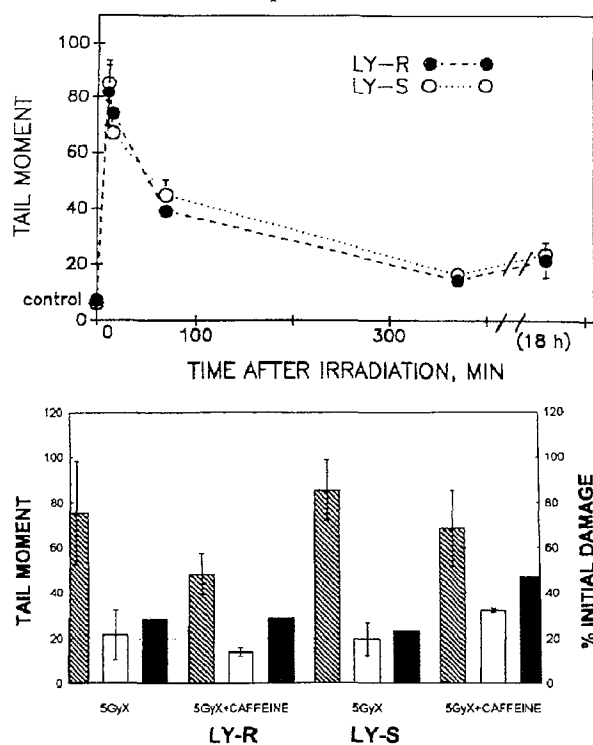


Fig.1. DNA damage repair is equal in both LY sublines X-irradiated with 5 Gy, as estimated by the alkaline comet assay (upper panel). There is more unrepaired DNA damage left in LY-S cells after 18 h incubation in 2 mM caffeine-supplemented medium than after incubation in the absence of caffeine. In LY-R cells the residual DNA damage level is not changed by caffeine (lower panel). Hatched bar - initial damage; open bar - damage after 18 h; black bar - damage after 18 h expressed as % of the initial damage. Caffeine reproducibly causes chromatin condensation resulting in a decrease in the mean tail moment. Therefore, the percentages of unrepaired damage (black bars in the lower panel) should be compared for irradiation alone and combined with caffeine, instead of the absolute tail moment values.

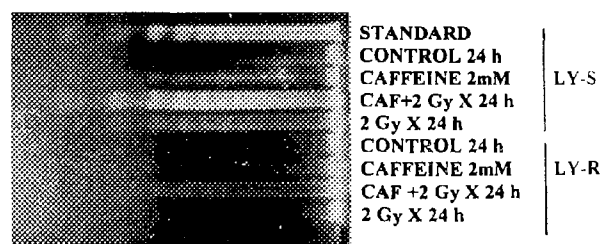


Fig.2. Apoptosis in X-irradiated and 2 mM caffeine treated LY cells. The cell cultures were X-irradiated with 2 Gy (LY-S) or 5 Gy (LY-R), harvested 24 h after irradiation; patterns of DNA electrophoresis are shown (standard - DNA from apoptotic, heat-treated LY-R cells).

Hence, abrogation of the Atm-dependent G2 checkpoint control by caffeine does not involve marked lethal consequences. Additionally, recent reports point to a possible anti-apoptotic effect of p21/WAF1; this would protect LY-R, but not LY-S cells, because of lack of expression of that protein in the latter cells.

Supported by the Polish State Committee for Scientific Research grant for the Institute of Nuclear Chemistry and Technology

## References

- [1]. Hwang A., Muschel R.J.: Radiat. Res., **150** (Suppl.), S52-S59 (1998).
- [2]. Włodek D., Hittelman W.N.: Radiat. Res., **115**, 566-575 (1988).

- [3]. Szumiel I., Wlodek D., Johnson K.J., Sundell-Bergman S.: Br. J. Cancer, **6** (Suppl.), 33-8, 33-38 (1984).  
 [4]. Blasina A., Price B.D., Turenne G.A., McGowan C.H.: Curr. Biol., **7**, 1135-1138 (1999).

- [5]. Sarkaria J.N., Busby E.C., Tibbetts R.S., Roos P., Taya Y., Karnitz L.M., Abraham R.T.: Cancer Res., **59**, 4375-4382 (1999).



PL0101526

## EXAMINATION OF MICRONUCLEI FREQUENCY AS AN IONIZING RADIATION SENSITIVITY MARKER IN A PANEL OF LYMPHOID CELL LINES

Alicja Jaworska<sup>1/</sup>, Paula De Angelis, Irena Szumiel, Jon Reitan<sup>1/</sup>

<sup>1/</sup> Department of Radiation Medicine, Norwegian Radiation Protection Authority, Oslo, Norway

A search for new markers of individual sensitivity to ionising radiation is of constant interest, mainly due to application of radiation in cancer therapy, and to occupational exposure in certain professions. The best and most reliable markers (survival, chromosomal damage) are time consuming and exacting to determine. A recent review on biomarkers [1] discusses the biological variables that affect the response to irradiation and the difficulties involved in linking the expression of specific genes with increased sensitivity to radiation. Among the most often proposed biomarkers of clinical and environmental protection use are apoptosis-related proteins and generally, propensity to apoptosis, micronucleus test and DNA damage estimated with the alkaline comet assay.

how suitable it is as an indicator for revealing radiation sensitivity of human or murine cells.

The cytokinesis-block micronucleus (CBN) assay was performed according to Fenech [2] with modifications appropriate for the differences between the cell lines concerning generation time, mitotic delay and cytochalasin B (cytB, Sigma) concentration. After irradiation, the medium was changed and  $10^5/\text{ml}$  and  $2 \times 10^5/\text{ml}$  in 10 ml T25 were taken for CBN test for mouse and human cells respectively. CytB was added 1 h after irradiation to all cultures. LY-S cells were incubated with  $1.5 \mu\text{g}/\text{ml}$  cytB for 17 h (controls) and 24 h (irradiated cells), LY-R with  $3 \mu\text{g}/\text{ml}$  for 17 h (controls) and 19 h (irradiated cells), Reh cells with  $3 \mu\text{g}/\text{ml}$  cytB for 44 h, and AT cell lines with  $3 \mu\text{g}/\text{ml}$  for 48 h (controls)

Table 1. Origin, radiation sensitivity, Trp53 status and cell cycle distribution of the lymphoid cell lines studied.

Cell line	Origin and D <sub>0</sub> [Gy]	Trp53	G1 $\pm$ SD [%]	S $\pm$ SD [%]	G2 $\pm$ SD [%]
G00736A	Human ATM +/+ (0.7)	Wild type (Wt)	74.2 $\pm$ 4.5	17.3	8.5
G00717C	Human ATM +/- (0.7)	Wt	72.2 $\pm$ 2.9	19.4	8.4
LY-R	Murine lymphoma (1.0)	p53+/-	20.1 $\pm$ 0.96	61.8 $\pm$ 3.0	18.1 $\pm$ 2.6
LY-S	Murine lymphoma (0.5)	p53+/-	20.1 $\pm$ 3.5	66.3 $\pm$ 2.2	13.5 $\pm$ 2.6
Reh	Human pre-B leukemia (0.9)	Wt	46.9	9.6	43.6

We tested five relatively radiation sensitive cell lines (Table 1) following X-irradiation with doses from 0.1 to 2 Gy. These were two lymphoid AT cell lines, one homozygous and one heterozygous for the ATM gene, the human pre-B cell line, Reh, and two murine L5178Y lymphoma cell lines, LY-R and

and 50 h (irradiated cells). For each cell line 2-3 experiments were performed.

The micronuclei frequency (MN) is presented in Table 2. No significant differences in MN were observed between the examined cell lines for doses  $\leq 1$  Gy. It was not possible to perform the assay for

Table 2. Frequency of micronuclei (MN) in lymphoid cell lines after X-ray irradiation with doses 0.1-2.0 Gy; each value represents results from 2-3 replicate experiments. Numbers represent MN/1000 binucleate cells.

Dose [Gy]	G00736A	G00717C	Reh	L5178Y-R	L5178Y-S
0	14.8 $\pm$ 3.6	13.6 $\pm$ 4.3	11.8 $\pm$ 5.1	8.0 $\pm$ 4.6	11.5 $\pm$ 3.4
0.1	30.9 $\pm$ 5.4	23.5 $\pm$ 2.8	21.5 $\pm$ 6.8	24.5 $\pm$ 8.7	17.0 $\pm$ 6.80
0.2					23.3 $\pm$ 7.00
0.3					38.7 $\pm$ 12.8
0.4					41.3 $\pm$ 16.8
0.5	36.0 $\pm$ 10.8	56.3 $\pm$ 16.6	49.0 $\pm$ 17.8	49.5 $\pm$ 7.9	42.7 $\pm$ 4.20
1.0	58.5 $\pm$ 17.1	68.0 $\pm$ 9.7	77.5 $\pm$ 20.2	85.0 $\pm$ 6.2	
2.0	101.3 $\pm$ 23.5	124.8 $\pm$ 15.7	116.7 $\pm$ 21.0	190.0 $\pm$ 50.3	

LY-S. Mean lethal dose (D<sub>0</sub>) values (Table 1) are the measure of radiation sensitivity. We examined frequency of micronuclei in an attempt to establish

1 Gy in LY-S line due to the pronounced proliferation block (mitotic delay is 11 h) and the subsequent apoptosis. In spite of the extreme radiation

sensitivity of this cell line the MN for lower doses did not substantially differ from those in the other cell lines. Neither did the MN for AT cells; in this case MN may be underestimated because of the slow proliferation rate and G2 block.

The cell lines in the study were of differential but rather high radiation sensitivity, which was found unrelated to micronucleus frequency. Altogether, it can be seen that this popular and simple predictive test is not suitable for detection of radiation sensitivity as obvious as that of AT or LY-S cells.

Supported by the Polish State Committee for Scientific Research grant for the Institute of Nuclear Chemistry and Technology.

#### References

- [1]. Brooks A.L.: *Int. J. Radiat. Biol.*, **75**, 1481-1503 (1999).
- [2]. Fenech M.: The cytokinesis-block micronucleus assay in nucleated cells. In: *Mutation and the Environment. Part B.* Wiley-Liss, New York 1990, pp. 195-206.



PL0101527

## EXAMINATION OF THE ROLE OF DOUBLE STRAND BREAK REPAIR IN THE ADAPTIVE RESPONSE OF HUMAN LYMPHOCYTES: NEUTRAL COMET ASSAY

Maria Wojewódzka, Iwona Grądzka, Iwona Buraczewska

Human lymphocytes exposed to very low doses of DNA damaging agents may become less sensitive to subsequent higher doses of the DNA damaging agent. This phenomenon is called the adaptive response [1,2]. This work refers to our previous results [3,4] that showed no differences in the post-radiation DNA repair kinetics (single-strand breaks

(SSB), DSB and alkali labile sites measured at alkaline pH) between lymphocytes adapted by low doses of hydrogen peroxide or X-rays and the control ones. Nevertheless, DNA damage observed at the chromosomal level was significantly lower in the adapted compared to non-adapted lymphocytes. Thus, it could be supposed that the decrease in the

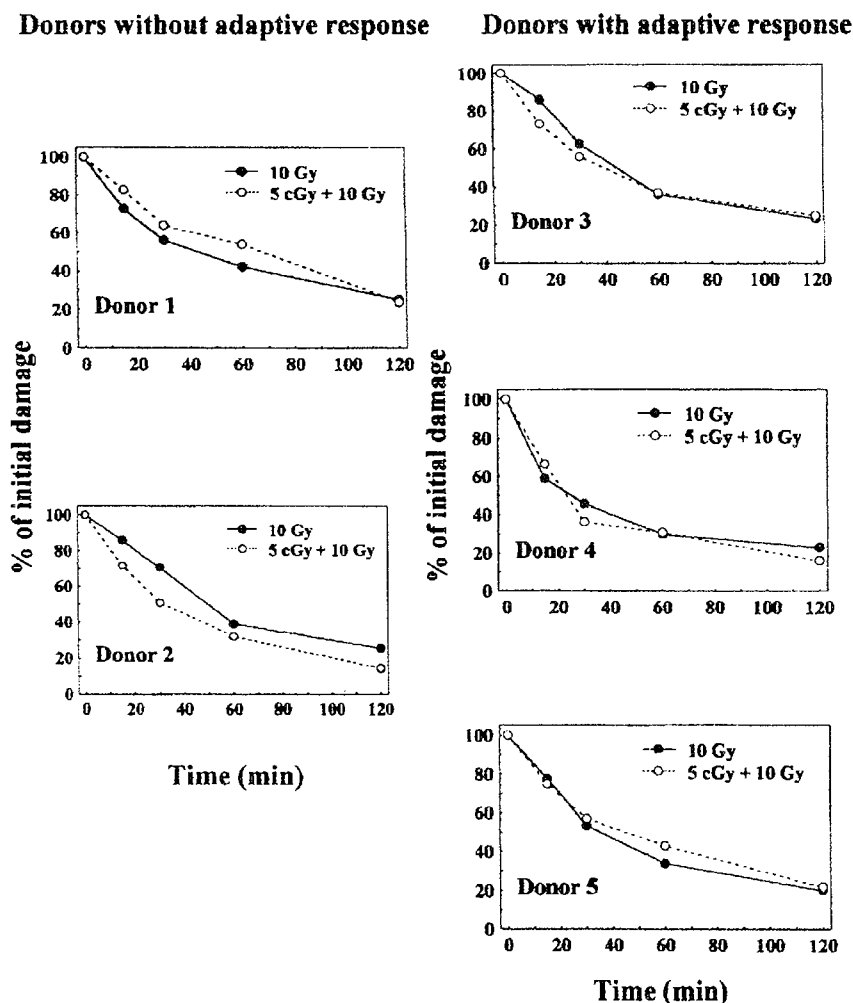


Fig. Repair of DNA DSB measured by the comet assay in the non-adapted and adapted lymphocytes irradiated with 10 Gy of X-rays. Data for donors unable or able to express radioadaptation as indicated by the results of the micronucleus assay. The results were expressed as % of the initial damage. For each time point the mean tail moment of the control value was subtracted.



chromosomal damage level in the adapted cells results from the higher DSB repair efficiency. The frequency of the DSBs induced by X-rays is about two levels of magnitude lower than the frequency of SSBs. Hence, the change in DSB repair might not be revealed by the alkaline comet assay. Therefore, we applied the neutral comet assay, which detects DSB.

Human lymphocytes isolated from whole blood and stimulated with phytohemagglutinin (PHA) were irradiated with an adaptive dose (5 cGy of X-rays) and then with a challenge dose of 2 Gy for the micronuclei assay and 10 Gy for the neutral comet assay. The frequency of micronuclei in the adapted lymphocytes was about 30% lower than that expected for an additive effect of both, adaptive and challenge doses, applied separately. Estimation of DNA damage was carried out with the use of single gel electrophoresis assay (comet assay) in neutral pH.

Fig. summarises the results of all experiments with lymphocytes from 8 donors (healthy, male, non-smokers, aged 20-28 years), including 3 who showed adaptation. The use of the neutral comet assay allowed us to suggest that the lower damage revealed in the adapted lymphocytes at the chromosomal level was unrelated to the initial level of DSBs in DNA. The differences between kinetics of DNA repair in the adapted and non-adapted lymphocytes were not significant.

Supported by the Polish State Committee for Scientific Research grant 4PO5A 022 15.

#### References

- [1]. Olivieri G., Bodycote J., Wolff S.: Science, **223**, 594-597 (1984).
- [2]. Shadley J.D., Afzal V., Wolff S.: Radiat. Res., **111**, 511-517 (1987).
- [3]. Wojewódzka M., Kruszewski M., Szumiel I.: Int. J. Radiat. Biol., **71**, 245-252 (1997).
- [4]. Wojewódzka M., Kruszewski M., Szumiel I.: Mutagenesis, **11**, 593-596 (1996).

## EXAMINATION OF THE ROLE OF DOUBLE STRAND BREAK REPAIR IN THE ADAPTIVE RESPONSE OF HUMAN LYMPHOCYTES: PULSE FIELD ELECTROPHORESIS

Iwona Grądzka, Maria Wojewódzka, Iwona Buraczewska

Human lymphocytes in culture exposed to very low doses of DNA damaging agents become less sensi-

tive to subsequent higher doses of X-rays. Such an adaptive response in human lymphocytes was first

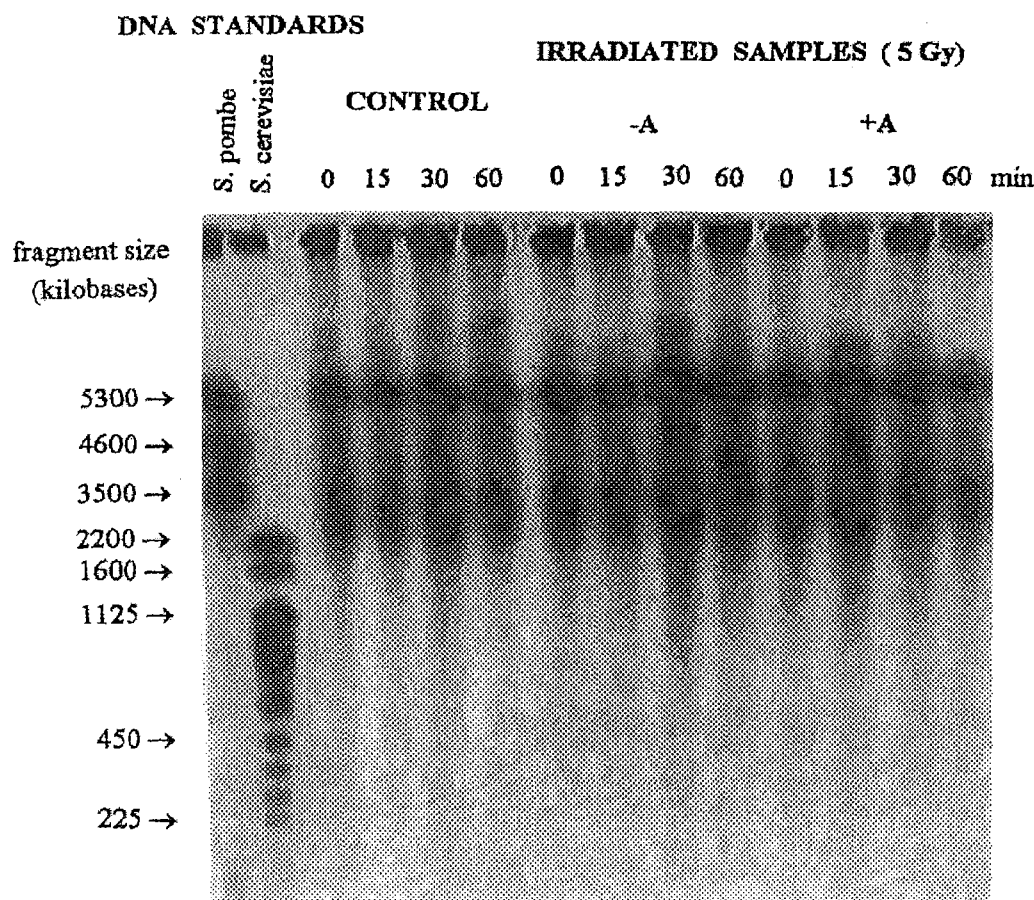


Fig.1. PFGE of DNA from human lymphocytes at sequential time points after X-irradiation (5 Gy). The cells were previously adapted (+A) or not (-A) by X-irradiation with a dose of 5 cGy. The gel was stained with ethidium bromide (1  $\mu$ g/ml).



PL0101528

identified as a decrease in chromosomal aberration frequency [1,2].

The aim of this project is to study the significance of DNA double-strand break (DSB) repair in the adaptive response of human lymphocytes exposed to X-radiation. It could be supposed that the decrease in the chromosomal damage level in the adapted cells [1,2] results from the higher DSB repair efficiency. The disposition of lymphocytes from 8 donors (healthy, male, non-smokers, aged 20-28 years) to respond adaptively was determined by comparison of the micronuclei frequency measured after irradiation with 2 Gy of X-rays in the cells adapted with 5 cGy of X-ray and the non-adapted ones. We found that in lymphocytes of the three tested donors, an adapting dose of 5 cGy of X-rays evoked a ca. 30% decrease in the frequency of micronuclei upon subsequent X-irradiation (2 Gy).

Estimation of the DSBs was carried out with the use of pulse-field gel electrophoresis (PFGE). We have examined human lymphocytes isolated from whole blood after stimulation with phytohemagglutinin (PHA). They were irradiated (or not) with 5 cGy of X-rays to induce adaptive response. The cells were embedded in low-gelling-point-agarose and lysed in a buffer containing detergents and proteinase K, pH=7.5, at 50°C, overnight. The agarose plugs containing nucleoids were placed into wells of 0.8% chromosomal grade agarose (Bio-Rad) and electrophoresed with the use of CHEF-III apparatus (Bio-Rad). The electrophoresis was performed at 1.7 V/cm and 14°C; an angle between two electric field vectors was 106°. The run was comprised of three blocks, 31 hours each, with increasing switch times: I: 50-200 s, II: 200-600 s, III: 2000-2200 s. DNA in the gel was visualised under UV-transilluminator, after staining with ethidium bromide or SYBR-Gold (Bio-Probes). The images (Fig.1) were captured with the use of a CCD camera, connected to PC. Quantification of DNA was performed using GelScan image analysis software, which measures integrated fluorescence intensities over electrophoretic path. All subsequent calculations were made using Microsoft Excel software. The level of double-strand breaks (DSB) in DNA was expressed as a sum of a percentage of a sample entering the gel, for each of individual path segments (ca. 80 segments per path), divided by an average of DNA molecular weight corresponding to this segment [3].

Fig.1 shows typical DNA electrophoresis patterns. At a dose of 5 Gy any differences in DSB levels become visible only after analysis of the fluorescence distribution. Fig.2 is the summary of all the data for the examined repair intervals, showing separately lymphocytes from donors able (a+) or unable (a-)

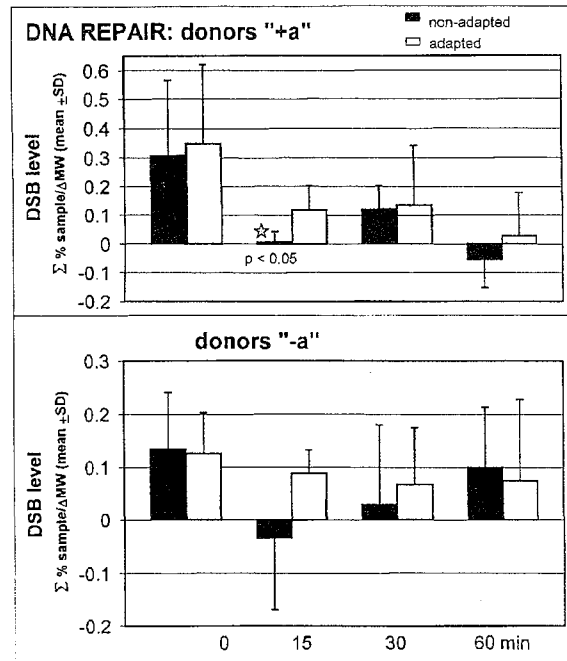


Fig.2. Comparison of DSB levels at sequential time points after irradiation with the challenge dose (5 Gy) between non-adapted (not pre-irradiated) and adapted (pre-irradiated, 5 cGy) samples, for the lymphocytes showing (+a) or not (-a) adaptive response.

for radioadaptation. Generally, rejoining kinetics for individual donors has been highly varied, but without significant difference between a+ and a- donors. Interestingly, at one repair interval (15 min) DSB are more numerous in adapted than in the non-adapted lymphocytes. Since the level of DSB is calculated from the mobility of DNA fragments and the latter parameter also depends on chromatin conformation, the outcome of adaptation may well be a chromatin conformation change.

In summary, the use of both PFGE and neutral comet (see the accompanying report) assay allowed us to suggest that the lower damage revealed in the adapted lymphocytes at the chromosomal level was unrelated to the initial level of DSBs. The differences between kinetics of DNA repair in the adapted and non-adapted lymphocytes were not statistically significant. However, the PFGE pattern differed between the DNA from adapted and non-adapted cells.

Supported by the Polish State Committee for Scientific Research grant 4PO5A 022 15.

## References

- [1] Olivieri G., Bodycote J., Wolff S.: *Science*, **223**, 594-597 (1984).
- [2] Shadley J.D., Afzal V., Wolff S.: *Radiat. Res.*, **111**, 511-517 (1987).
- [3] Cedervall B., Wong R., Albright N., Dynlacht J., Lambin P., Dewey W.C.: *Radiat. Res.*, **143**, 8-16 (1995).

# CYTOTOXIC EFFECTS OF CIS-PLATINUM AND PALLADIUM(II) CHLORIDES COMPLEXED WITH A NOVEL STABLE LIGAND STUDIED IN MOUSE LYMPHOMA CELL LINES DIFFERING IN DNA REPAIR SYSTEMS

Marcin Kruszewski, Elżbieta Boużyk, Tomasz Ołdak<sup>1/</sup>, Krystyna Samochocka<sup>2/</sup>, Leon Fuks, Włodzimierz Lewandowski<sup>3/</sup>, Waldemar Priebe<sup>4/</sup>

<sup>1/</sup> Maria Skłodowska-Curie Memorial Cancer Center and Institute of Oncology, Warszawa, Poland

<sup>2/</sup> Department of Chemistry, Warsaw University, Poland

<sup>3/</sup> Drug Institute, Warszawa, Poland

<sup>4/</sup> M.D. Anderson Cancer Center of the University of Texas, Houston, USA

Among platinum complexes, cisplatin has an established position in cancer chemotherapy [1]. This gives an incentive to seek other Pt complexes with smaller side effects and a strong anti-tumour action. Therefore, we undertook a search for new platinum compounds that would be of a relatively low cytotoxicity and good water solubility.

Cytotoxicity and antitumour activity of Pt-complexes are often sensitive to structural features such as the number of leaving groups and the nature of stable ligand. Minor variations in the structure of amine ligands can have profound effects on the antitumour activity and especially on the toxicity of these complexes. Here, we compared a platinum complex with a novel stable ligand (wp1-1) with an identical palladium complex. We measured cytotoxicity of both complexes in two mouse lymphoma L5178Y cell lines (LY) differing in the ability to NER (nucleotide excision repair) [2] and susceptibility to DNA cross-linking agents. LY-R cells are NER-deficient, whereas LY-S cells - NER-proficient.

LY cells were maintained in suspension cultures in Fischer's medium supplemented with an 8% bovine serum. Asynchronous cultures in the exponential phase of growth were used in all experiments. An appropriate aliquot of stock solution of the tested compounds (PtCl<sub>2</sub>, PdCl<sub>2</sub>, and ligand alone) was added to the final concentrations of 0.001-1.0 mg/ml for 1 h at 37°C. After incubation, the calf serum was added, the cells were centrifuged at

room temperature and re-suspended in Fischer's medium for 48 h growth tests, in order to estimate cytotoxicity. As a reference complex, cisplatin was used.

Toxicity of the ligand alone was small and similar for both LY cell lines (not shown). Toxicity of the Pt complex was similar for both cell lines (50% inhibitory concentration, IC<sub>50</sub> was 8 μM for LY-R cells and 12 μM for LY-S cells respectively) (Figs. 1 and 2). Survival curve for this compound showed the same biphasic nature that was observed in the case of cisplatin (cis-Pt). The threshold value was similar (20 μM). Interestingly, the Pd compound

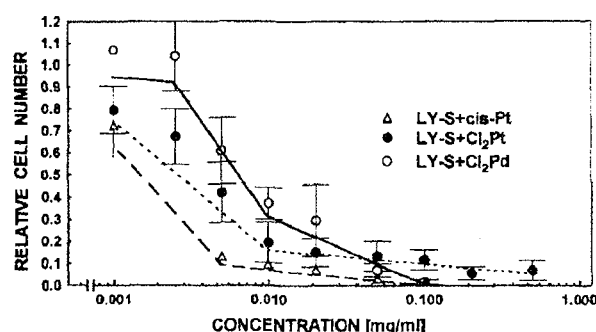


Fig. 2. Relative cell numbers in LY-S cell cultures treated with the tested drugs for 1 h and then incubated for 48 h.

was more toxic for LY-R cells than for LY-S cells (Figs. 1 and 2). Toxicity of the Pd compound for LY-R cells was similar to that of the platinum compound. Survival curve had the biphasic nature with a threshold value at 30 μM. The IC<sub>50</sub> value was 9 μM and IC<sub>10</sub> was 60 μM. Surprisingly, in LY-S cells no toxicity of the compound was found up to 6 μM concentration. The calculated IC<sub>50</sub> and IC<sub>10</sub> values were 23 and 200 μM, respectively. So, toxicity of the palladium compound in LY-S cells was lower than that of its platinum counterpart, in spite of identical ligands.

Supported by the Polish State Committee for Scientific Research grant 4PO5F 03 715.

## References

- [1] Einhorn L.H., Williams S.D.: *New Engl. J. Med.*, **300**, 289-298 (1979).
- [2] Szumiel I., Włodek D., Johanson K.J.: *Photochem. Photobiol.*, **48**, 201-204 (1988).

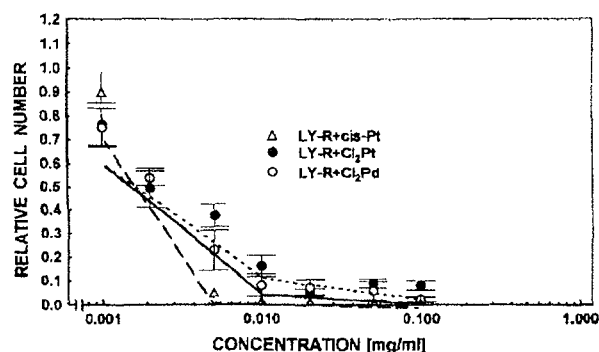


Fig. 1. Relative cell numbers in LY-R cell cultures treated with the tested drugs for 1 h and then incubated for 48 h. Relative cell number is the ratio of cell number per μl of the treated cell suspension to that in the control (untreated) one.

# DNA DAMAGE INFLICTED IN MOUSE LYMPHOMA CELL LINES BY CIS-PLATINUM AND PALLADIUM(II) CHLORIDES COMPLEXED WITH A NOVEL STABLE LIGAND (wp1-1)

Marcin Kruszewski, Elżbieta Boużyk, Krystyna Samochocka<sup>1/</sup>, Leon Fuks, Włodzimierz Lewandowski<sup>2/</sup>, Waldemar Priebe<sup>3/</sup>

<sup>1/</sup> Department of Chemistry, Warsaw University, Poland

<sup>2/</sup> Drug Institute, Warszawa, Poland

<sup>3/</sup> M.D. Anderson Cancer Center of the University of Texas, Houston, USA

We compared a platinum complex with a novel stable ligand (wp1-1) with an identical palladium complex with respect to their ability to inflict DNA damage in two mouse lymphoma L5178Y cell lines (LY) differing in the ability to NER (nucleotide excision repair) [1] and susceptibility to DNA cross-linking agents.

Asynchronous LY cell cultures in the exponential phase of growth were maintained in suspension in Fischer's medium supplemented with an 8% bovine serum. An appropriate aliquot of stock solution of the tested compounds ( $\text{PtCl}_2$ ,  $\text{PdCl}_2$ ) was added to the final concentrations of 0.001-1.0 mg/ml for 1 h at 37°C. After incubation, the calf serum was added, the cells were centrifuged at room temperature and used for the comet assay.

The comet assay (single cell gel electrophoresis) was performed according to [2] with small modifications. In brief, the cell suspension was mixed (1:1) with a 2% low melting point agarose and pipetted onto microscope slides. After agarose solidification, the slides were irradiated on ice with 2 Gy of 200 kV X-rays in an Andrex X-ray machine. After irradiation, the slides were immersed in a cold lysing solution, pH 10, for 1 hour. After lysis, the slides were placed on a horizontal gel electrophoresis unit filled with a fresh electrophoretic buffer, pH 13, allowed to stay in this buffer for 40 min for DNA unwinding and then electrophoresed (30 min, 1 V/cm). After electrophoresis, the slides were stained with DAPI and 50 randomly selected comets and analysed using image analysis software Comet v.3.0 (Kinetic Imaging Ltd., Liverpool, UK). Tail moment was measured. The tested chemicals were expected to generate DNA cross-links. Therefore, the decrease in tail moment, as compared to the irradiated, non-treated cells, was taken as a measure of DNA damage.

In growth tests we found that the Pt complex was equally toxic to both cell lines, whereas the Pd complex was much more toxic to the NER deficient LY-R cells. As shown in Fig., treatment with the Pt complex retarded DNA migration (as seen in the comet assay) similarly in both cell lines and in a dose-dependent manner. The Pd complex retarded DNA migration to a higher extent in the NER-competent cell line (LY-S), although this ability did not correspond with the compound's cytotoxicity. Since the treatment time allowed for DNA repair to continue until the measurement of DNA damage, and the damage was similar in both

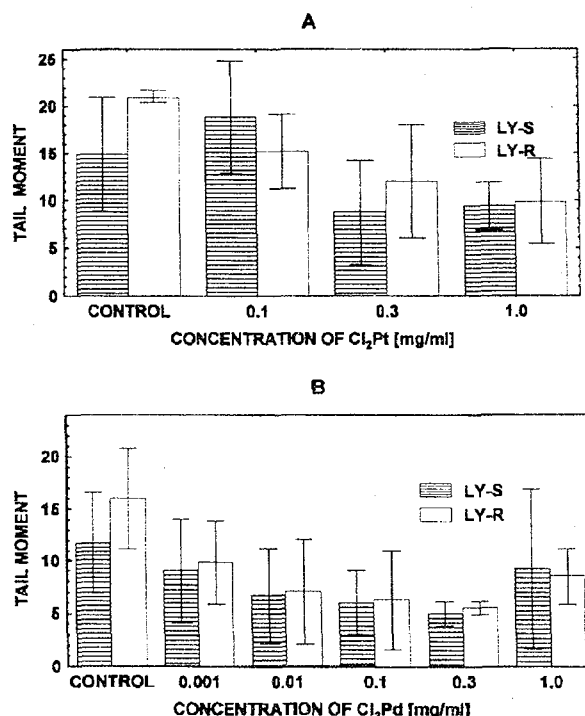


Fig. DNA damage measured with the comet assay in LY cells treated with Pt (A) or Pd complex (B). Reduction of the X-ray-induced (3 Gy) DNA migration (control) is the measure of the cross-linking ability of the complexes. See text for other explanations.

cell lines, it seems that the Pt complex does not inflict damage that is repaired by the NER system.

As mentioned above, the ability of the Pd complex to induce DNA cross-links was not reflected in its cytotoxicity. Reduction of the X-ray-induced (3 Gy) DNA migration to 30% of the initial value in LY-S cells resulted in no growth inhibition. Similarly, reduction of DNA migration by half in LY-R cells had only minor effect on cell survival (25% growth inhibition). It has been postulated that some palladium compounds induce double helix conformational changes different from those induced by cisplatin [3]. Our results support this hypothesis.

Supported by the Polish State Committee for Scientific Research grant 4PO5F 03 715.

## References

- [1]. Szumiel I., Wlodek D., Johanson K.J.: Photochem. Photobiol., 48, 201-204 (1988).
- [2]. Singh N.P., McCoy M.T., Tice R.R., Schneider E.L.: Exp. Cell Res., 175, 184-191 (1988).
- [3]. Matesanz J.: Int Biochem., 76, 29-37 (1999).

## DIFFERENTIAL ANTI-PROLIFERATIVE PROPERTIES OF NOVEL HYDROXYDICARBOXYLATOPLATINUM(II) COMPLEXES WITH HIGH OR LOW REACTIVITY WITH THIOLS

Iwona Buraczewska, Elżbieta Boużyk, Janina Kuduk-Jaworska<sup>1/</sup>, Katarzyna Waszkiewicz<sup>1/</sup>, Irena Szumiel

<sup>1/</sup> Department of Chemistry, University of Wrocław, Poland

We have examined the anti-proliferative effect of 13 recently synthesised platinum dicarboxylate complexes, very similar in their chemical, structural and kinetic properties to carboplatin. We used the L5178Y model: two murine lymphoma sublines, which differ in nucleotide excision repair (NER) ability and hence, in sensitivity to those platinum complexes that react with DNA. The anti-proliferative effect of the examined compounds mainly depends on the kind of amine ligand. Complexes with primary amine (ethylenediamine) are more effective than complexes containing tertiary amine (1-alkylimidazole). The ethylenediaminemalatoplatinum(II) complexes show a differential in vitro anti-proliferative activity in the L5178Y model; hence, it may be expected that they inflict DNA lesions that are repaired by the NER system.

Further, we evaluated the correlation between the cytotoxic properties of the examined complexes and their reactivity with GSH. The latter was measured as the concentration of unreacted GSH after 16 h incubation with the respective platinum complex. The numerical data presented in the following graphs were taken from the previous

publication [1]. The measure of cytotoxicity was inhibitory dose (ID<sub>50</sub>) that is concentration of the complex, which decreased the relative cell number in the treated cell culture to 0.5 after 48 h treatment at 37°C.

Examination of the distribution of ID<sub>50</sub> values and of the similarities between LY sublines indicates that two groups of Pt complexes can be discerned:

- 1) Pt complexes to which the LY-R cells are about twice more sensitive than the LY-S cells; here belong cisplatin and all the ethylenediaminemalatoplatinum(II) enantiomers;
- 2) 1-alkylimidazole Pt complexes, to which the LY sublines are equally sensitive.

As shown in Fig.1, the cytotoxic properties of the complexes belonging to group 1 are directly related to their reactivity with GSH; in other words, high cytotoxicity corresponds to high reactivity with GSH (LY-R cells:  $r=0.963423$ ,  $p=0.036577$ ; LY-S cells:  $r=0.995380$ ,  $p=0.004620$ ). It can be concluded, that the DNA is the cellular target of these, highly reactive with GSH, Pt complexes. In contrast, toxicity of the complexes belonging to the 2nd group is inversely related to the reactivity with GSH (Fig.2;  $r=0.8853$ ,  $p=0.000128$ ). Here belong the complexes that block cell cycle progression, bis(1-ethylimidazole) L-malatoplatinum(II) and bis(1-propylimidazole) L-malatoplatinum(II); they are the least toxic

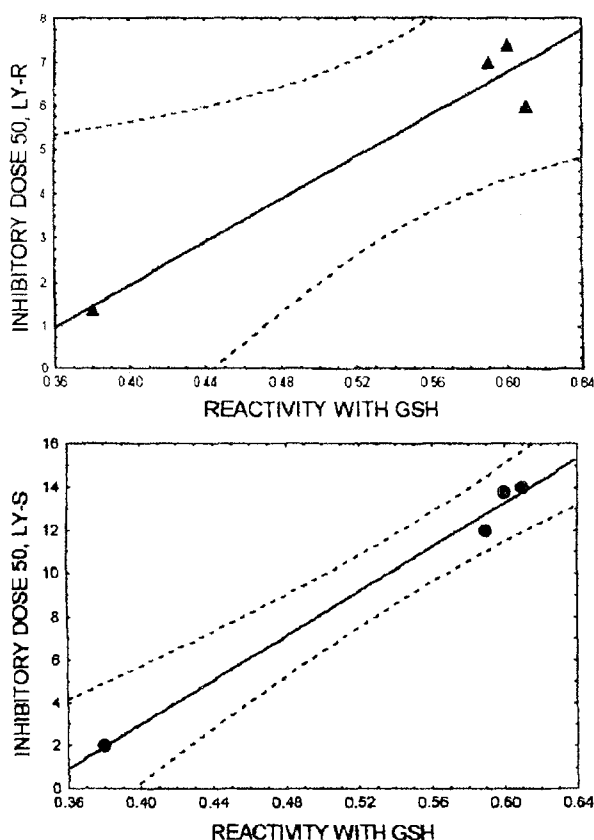


Fig.1. Correlation of the anti-proliferative activity of the group 1 platinum complexes with their reactivity with GSH. Confidence interval 95% indicated. Upper panel - data for LY-R cells; lower panel - data for LY-S cells.

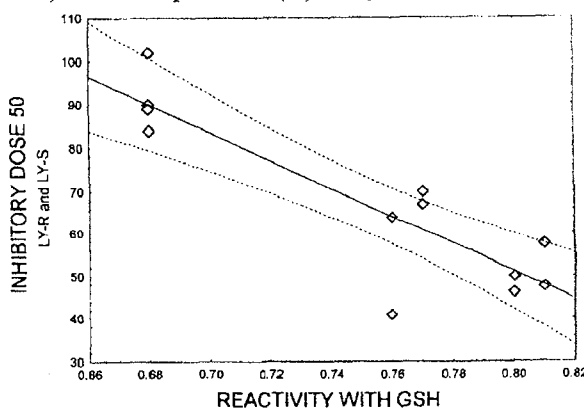


Fig.2. Correlation of the anti-proliferative activity of the group 2 platinum complexes with their reactivity with GSH. Confidence interval 95% indicated. The data for LY-R and LY-S cells are combined, because of similarity in the response to these complexes.

and of intermediate reactivity with GSH. In their case, the target seems to be different from DNA [2].

Supported by the Polish State Committee for Scientific Research grant 4PO5F 032 19.

### References

- [1]. Kuduk-Jaworska J., Waszkiewicz K.: *Trans. Met. Chem.*, **25**, 443-449 (2000).
- [2]. Buraczewska I., Kuduk-Jaworska J., Waszkiewicz K., Gasińska A., Szumiel I.: *Chem.-Biol. Interact.*, in press.

## G2 PHASE ARREST CAUSED BY HYDROXYDICARBOXYLATOPLATINUM(II) COMPLEXES WITH LOW REACTIVITY WITH THIOLS

Iwona Buraczewska, Janina Kuduk-Jaworska<sup>1/</sup>, Katarzyna Waszkiewicz<sup>1/</sup>, Anna Gasińska<sup>2/</sup>, Irena Szumiel

<sup>1/</sup> Department of Chemistry, University of Wrocław, Poland

<sup>2/</sup> Laboratory of Radiation Biology, Oncology Center, Kraków, Poland

We have examined the anti-proliferative effect of 13 recently synthesised platinum dicarboxylate complexes. We used the L5178Y model: two murine midazole) L-malatoplatinum(II), show a considerable ability to arrest cells in G2 phase (Tables 1 and 2). The property of G2 arrest induction is shared by many

Table 1. Cytometric determination of the distribution in the cell cycle of LY-R cells treated with Pt complexes for 24 h with the drug concentrations indicated (mean results from duplicate determinations  $\pm$  range).

Pt complex	Labelling index [%]	G1 phase cells [%]	S phase cells [%]	G2 phase cells [%]	LI/S	% dead cells
None (control)	59.2 $\pm$ 0.1	28.0 $\pm$ 0.1	61.7 $\pm$ 0.8	10.3 $\pm$ 0.9	0.96	3
Bis(1-ethylimidazole) L-malatoplatinum(II) 100 $\mu$ g/ml	12.7 $\pm$ 0.9	1.6 $\pm$ 0.5	26.6 $\pm$ 4.6	71.8 $\pm$ 5.1	0.48	8
Bis(1-propylimidazole) L-malatoplatinum(II) 100 $\mu$ g/ml	6.0 $\pm$ 0.2	0.65 $\pm$ 0.05	16.4 $\pm$ 1.0	82.7 $\pm$ 1.1	0.36	8

lymphoma sublines, LY-R and LY-S, which differ in nucleotide excision repair (NER) ability [1] and hence, in sensitivity to those platinum complexes

other platinum complexes; however, those examined in this report exhibit this activity at a very low toxicity level. We expect that the properties of these two pl-

Table 2. Cytometric determination of the distribution in the cell cycle of LY-S cells treated with Pt complexes for 24 h with the drug concentrations indicated (mean results from duplicate determinations  $\pm$  range).

Pt complex	Labelling index [%]	G1 phase cells [%]	S phase cells [%]	G2 phase cells [%]	LI/S	% dead cells
None (control)	58.8 $\pm$ 5.3	28.0 $\pm$ 1.1	61.6 $\pm$ 2.2	10.3 $\pm$ 1.3	0.95	2
Bis(1-ethylimidazole) L-malatoplatinum(II) 100 $\mu$ g/ml	18.3 $\pm$ 2.4	5.4 $\pm$ 0.0	29.9 $\pm$ 0.7	64.7 $\pm$ 0.7	0.61	6
Bis(1-propylimidazole) L-malatoplatinum(II) 100 $\mu$ g/ml	6.5 $\pm$ 0.0	0.7 $\pm$ 0.3	14.6 $\pm$ 2.0	84.6 $\pm$ 1.8	0.44	12

that react with DNA. We found that the 1-alkylimidazole complexes are of low toxicity and moderate to low reactivity with glutathione (GSH); in contrast to the ethylenediaminemalatoplatinum(II) complexes, their cytotoxicity is inversely correlated with reactivity with GSH [2]. Also, these 1-alkylimidazole Pt complexes, to which the LY sublines are equally sensitive, apparently do not inflict DNA damage that is repaired by the NER system. Alternatively, their target is different from DNA.

Two of the 1-alkylimidazole complexes, bis(1-ethylimidazole) L-malatoplatinum(II) and bis(1-propyli-

tinum complexes may be exploited in combined platinum complex treatment and irradiation.

Supported by the Polish State Committee for Scientific Research grant 4PO5F 032 19.

### References

- [1]. Szumiel I., Włodek D., Johanson K.J.: Photochem. Photobiol., 48, 201-204 (1988).
- [2]. Buraczewska I., Kuduk-Jaworska J., Waszkiewicz K., Gasińska A., Szumiel I.: Chem.-Biol. Interact., in press.



PL0101530

## CYTOPLASMIC ACTIVITY OF TYROSINE PROTEIN KINASE, c-Abl, IN L5178Y MURINE LYMPHOMA CELL SUBLINES - A LINK TO DIFFERENTIAL APOPTOSIS PRONENESS?

Barbara Sochanowicz, Irena Szumiel

Tyrosine protein kinase, c-Abl, is a homologue of the Abelson leukemia virus oncogene. Its biological function depends on the intracellular localisation. Nuclear c-Abl interacts with the DNA damage sensor complex and is activated by Atm in the damaged cell [1,2]. It, then, participates in cell cycle control and DNA repair regulation. It also acts as a

pro-apoptotic factor through p73. The function of the cytoplasmic c-Abl is less clear. In its activated state, as in malignant cells, it phosphorylates Ras and following Ras activation, it affects the signalling through Erk and Sapk pathways. Activated c-Abl exerts an anti-apoptotic effect independently of the Erk pathway, probably through phosphati-

dylinositol 3-kinase (PI-3K) and Bad, a pro-apoptotic protein which becomes inactive upon phosphorylation [3].

We examined the activity of c-Abl kinase in its immunoprecipitates from the total cell and nuclear extracts prepared according to [4] and [5], res-

nuclear and total cell extracts from LY-R and LY-S cells indicated a difference in the cytoplasmic activity: in LY-S subline, it was about 50% of that in the LY-R subline (Fig.).

This observation may be pertinent to the previously reported differential post-irradiation apop-

### ABL KINASE ACTIVITY

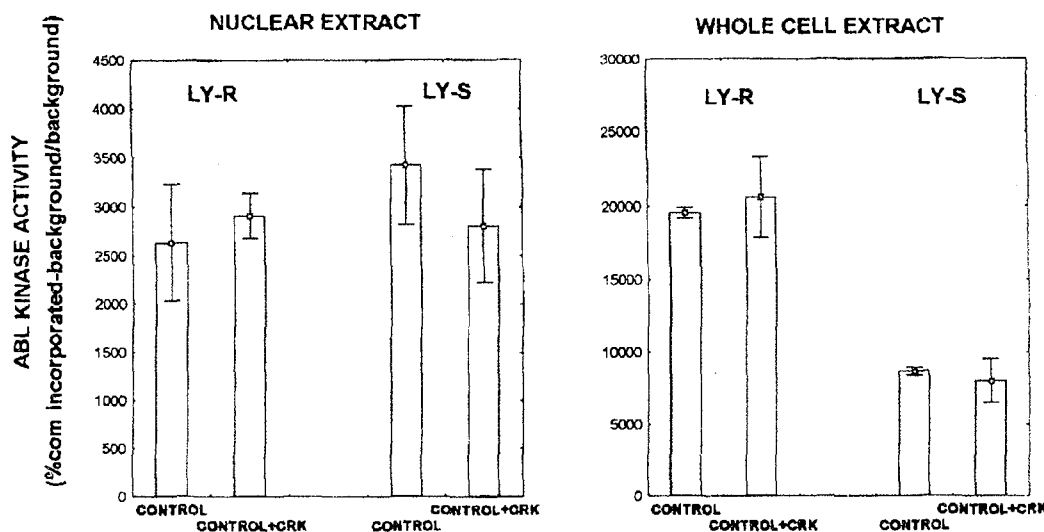


Fig. ABL kinase activity in the nuclear and whole cell extracts from LY-R and LY-S cells.

pectively. Activity determination [5] was carried out with or without GST-Crk as substrate (courtesy of Dr. D.W. Kufe). In the whole cell extract, most of the measured phosphorylation was due to autophosphorylation and phosphorylation of the co-precipitating proteins.

Irradiation (1 or 5 Gy of  $\gamma$  rays) did not appreciably alter the kinase activity in the nuclear extracts in LY-R and LY-S cells, when measured 1 or 3 h after irradiation. The activity levels were comparable in both LY sublines, with or without the crk substrate. Expression of the kinase protein, as determined by western blotting 1, 2 and 4 h after irradiation with 1 Gy, was similar in both cell lines and not altered as compared to the controls. Moreover, the co-precipitating proteins were in the molecular weight range below 66 kDa; so, there was no indication of the interaction of c-Abl with the large molecules of DNA-PK or Atm, which co-precipitate with the kinase in nuclear extracts from other cells.

On the contrary, there were co-precipitating proteins in the molecular weight range above 66 kDa in the total cell extracts, obviously of the cytoplasmic origin. Comparison of the kinase activity in the

tosis [6]. Activated c-Abl is a source of strong survival signals which counteract the pro-apoptotic signals [3]. Since apoptosis in LY sublines is p53, bcl-2 and bax-independent [6], the possibility that it is controlled through Bad and PI3-K and connected with the differential cytoplasmic activity of c-Abl, seems plausible and worth further examination.

Supported by a grant from Stiftung für Deutsch-Polnische Zusammenarbeit and by the Polish State Committee for Scientific Research (KBN), a statutory grant for the INCT.

### References

- [1] Shafman T., Khanna K.K., Kedar P., Spring K., Kozlov S., Yen T., Hobson K., Gatei M., Zhang N., Watters D., Egerton M., Shiloh Y., Kharbanda S., Kufe D., Lavin M.F.: *Nature*, **387**, 520-523 (1997).
- [2] Kharbanda S., Pandey P., Jin S., Inoue S., Bharti A., Yuan Z.M., Weichselbaum R., Weaver D., Kufe D.: *Nature*, **386**, 732-735 (1997).
- [3] Neshat M.S., Raitano A.B., Wang H.G., Reed J.C., Sawyers C.L.: *Mol. Cell Biol.*, **20**, 1179-1186 (2000).
- [4] Finnie N.J., Gottlieb T.M., Blunt T., Jeggo P.A., Jackson S.: *Proc. Natl. Acad. Sci. USA*, **92**, 320-324 (1995).
- [5] Kharbanda S., Ren R., Pandey P., Shafman T.D., Feller S.M., Weichselbaum R., Kufe D.: *Nature*, **376**, 785-788 (1995).
- [6] Szumiel I., Jaworska A., Kapiszewska M., John A., Grządka I., Sochanowicz B.: *Radiat. Environ. Biophys.*, **33**, 39-40 (2000).

## VALIDATION OF THE MICRONUCLEUS-CENTROMERE ASSAY FOR BIOLOGICAL DOSIMETRY

Andrzej Wójcik, Maria Kowalska<sup>1/</sup>, Elżbieta Boużyk, Iwona Buraczewska, Grażyna Kobiółko

<sup>1/</sup> Central Laboratory of Radiation Protection, Warszawa, Poland

Biological dosimetry is a method by which the level of radiation exposure is estimated on the basis of

radiation-induced changes in the human body. The most frequently applied method relies on measur-



PL0101531

ing the frequency of dicentric chromosomes in lymphocytes of the peripheral blood [1]. Disadvantages of the dicentric assay are a relatively high skill needed for scoring and a rather long time required for a precise analysis. An alternative method is the micronucleus (Mn) test [2], which is less time-consuming. However, its disadvantage is a weak sensitivity in the low dose region of ionising radiation.

Norppa et al. [3] were the first to suggest, that the sensitivity of the Mn assay could be enhanced by discriminating between spontaneous and clastogen-induced micronuclei. The discrimination was based on the observation that spontaneous micronuclei contain predominantly whole chromosomes, whereas clastogen-induced micronuclei contain acentric fragments. Vral et al. [4] used fluorescence in situ hybridization (FISH) with a pancentromeric DNA probe to investigate if an increased sensitivity for detection of low radiation doses could be achieved by selectively scoring those micronuclei which did not contain centromeres. Indeed, their results indicated that sensitivity of the Mn assay could be increased by analysing the frequency of centromere-negative micronuclei. The aim of the present study was to investigate whether and to what extent an enhanced sensitivity in assessing the

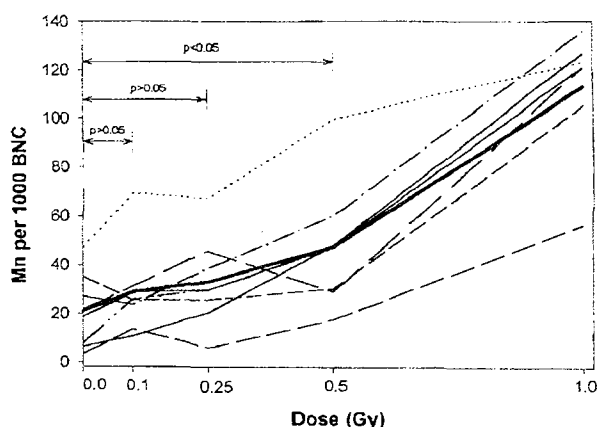


Fig. 1. Frequency of micronuclei (Mn) per 1000 binucleated cells (BNC) in human lymphocytes irradiated in vitro with increasing doses of X-rays. Separate curves for 6 donors are shown and the thick line is for mean results.

dose of ionising radiation could be achieved in our Laboratory by combining the micronucleus assay with centromere detection by FISH.

Lymphocytes of 8 donors were irradiated in vitro with different doses of ionising radiation. We esti-

mated the frequency of micronuclei in lymphocytes of all donors; the percentage of micronuclei containing centromeres (MnC+) was analysed in lymphocytes of 6 donors. The dose response curve for micronuclei in binucleated cells is shown in Fig. 1. Due to the high inter-individual variability, a statistically significant increase in the micronucleus frequency is seen only after a dose of 0.5 Gy. In accordance with the assumption that ionising radiation-induced micronuclei contain predominantly acentric fragments, the relative frequency of micronuclei containing centromeres decreased with radiation dose (Fig. 2). Due to a relatively low degree of inter-individual variability, a statistically significant difference in the frequency of MnC+ was

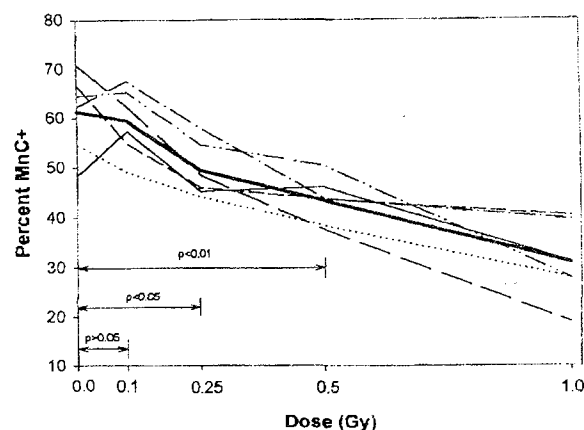


Fig. 2. Percentage of centromere-containing micronuclei (MnC+) scored in the same preparations as in Fig. 1.

observed between 0 and 0.25 Gy. It is thus evident, that the micronucleus-centromere assay is a more sensitive method to detect the exposure to ionising radiation than the conventional Mn assay. So, in the case of an accidental radiation exposure in the low dose range, the MnC+ assay is more suitable to assess the absorbed dose than the conventional Mn assay.

Supported by the Polish State Committee for Scientific Research grant 4PO5A 110 14.

## References

- [1]. Bender M.A., Awa A.A., Brooks A.L., Evans H.J., Groer P.G., Littlefield L.G.: *Mutat. Res.*, **196**, 103-159 (1988).
- [2]. Müller W.-U., Streffer C.: *Adv. Mutagen. Res.*, **5**, 1-134 (1994).
- [3]. Norppa H., Renzi L., Lindholm C.: *Mutagenesis*, **8**, 519-525 (1993).
- [4]. Vral A., Thierens H., Ridder de L.: *Int. J. Radiat. Biol.*, **71**, 61-68 (1997).

## INCREASE IN LABILE IRON POOL IN MOUSE LYMPHOMA CELL LINES TREATED WITH HYDROGEN PEROXIDE

Marcin Kruszewski, Teresa Bartłomiejczyk, Paweł Lipiński<sup>1/</sup>

<sup>1/</sup> Institute of Genetics and Animal Breeding, Polish Academy of Sciences, Jastrzębiec, Poland

Maintenance of intracellular iron metabolism demands coordination of iron uptake, utilisation and storage. The principal effectors of this regulation are transferrin receptor (TfR), a protein involved in

iron uptake, and ferritin (Ft) an iron-sequestering protein. The expression of TfR and Ft is regulated at both transcription and post-transcription levels [1,2]. The key elements in post-transcriptional regu-



lation of the expression of TfR and Ft are iron regulatory proteins (IRP1 and IRP2), that bind to the stem-loop structure (iron-responsive elements, IRE) of mRNAs coding TfR or Ft. The binding of IRP to 5'-IRE of Ft mRNA represses protein translation. On the contrary, the binding of IRP to 3'-IRE stabilises TfR mRNA and elevates its translation [2,3]. The ability of IRP1 to bind the IRE depends on the availability of weakly bound iron ions, the so called labile iron pool (LIP) [2,4]. In our previous work [5] we characterised the steady state level of LIP and the IRE binding capacity of IRP1 protein in two mouse lymphoma cell lines L5178Y-R (LY-R) and L5178Y-S (LY-S), differing in sensitivity to hydrogen peroxide (HP) [6].

In this work we studied the LIP level and the changes in IRE/IRP binding in LY cells treated with hydrogen peroxide. Interestingly, in HP treated cells we observed an increase in LIP level

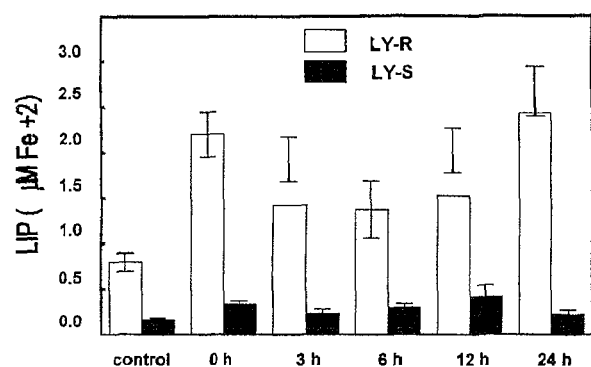


Fig.1. LIP levels in LY cells treated with HP. The cellular chelatable iron content in living LY cells was assessed as described elsewhere [5] by the method developed by Epsztejn et al. [7].

(Fig.1). This increase was more pronounced in LY-R cells than in LY-S cells. LY-R cells were already known to have a higher steady-state LIP level [5]. The increase in LIP level was correlated with an increase in the IRE binding capacity of the IRP1 protein. Similarly, this increase was more marked in LY-R cells than in LY-S cells (Fig.2). The increase in the IRE binding capacity of IRP1, indicating a total loss of the 4Fe-4S cluster, was associated with a decrease in the aconitase activity of IRP1 (Fig.2).

Our experiments revealed an intriguing phenomenon. The exposure of LY cells to exogenous oxidative stress (HP) caused an increase in the level of LIP and a corresponding increase in IRE/IRP binding that might further elevate the intracellular level of labile iron ions. The weakly bound iron ions are potentially hazardous for the cell, as they can enter the Fenton reaction - the source of highly toxic hydroxyl radicals [8]. Hence, the exposure of mammalian cells to the oxidative stress may sensi-

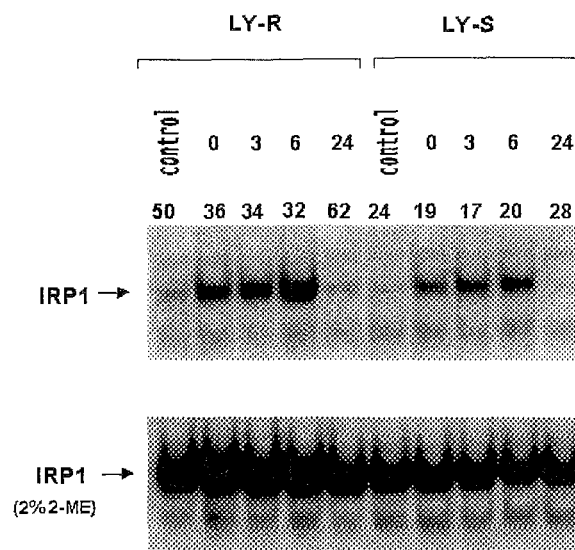


Fig.2. IRE binding activity of IRP1 protein in LY cells treated with HP. The cell extracts were prepared as previously described [5]. Two micrograms of protein were analysed in the presence or absence of 2% 2-mercaptoethanol.

tise these cells to the subsequent exposure to the oxidising agents. However, whether newly released iron ions enhance the cell's sensitivity to oxidative stress remains to be determined.

What is the source of the LIP is not known yet. Possibly, it is supplied by the oxidised iron proteins that are known to lose their iron content in response to oxidative stress [9]. Our experiments support this hypothesis, as the increase in LIP is correlated with the increase of IRE/IRP binding that requires the removal of the 4Fe-4S cluster from the IRP1 protein.

The authors are grateful to Dr. L.C. Kühn for providing the IRE containing plasmid and to Drs. P. Ponka and J. Cabantchik for the SIH and anti-calcein antibody, respectively.

Supported by the Polish State Committee for Scientific Research grant for the Institute of Nuclear Chemistry and Technology

## References

- [1] Klausner R.D., Rouault T.A., Harford J.B.: *Cell*, **72**, 19-28 (1993).
- [2] Kühn L.C.: *Nutr. Rev.*, **56**, s11-s19 (1998).
- [3] Eisenstein R.S., Blemings K.P.: *J. Nutr.*, **128**, 2295-2298 (1998).
- [4] Hentze M.W., Kühn L.C.: *Proc. Natl. Acad. Sci. USA*, **93**, 8175-8182 (1996).
- [5] Lipiński P., Drapier J.C., Oliveira L., Retmańska H., Sochanowicz B., Kruszewski M.: *Blood*, **95**, 2960-2966 (2000).
- [6] Bouzyk E., Buraczewska I., Rosiek O., Sochanowicz B., Szumiel I.: *Radiat. Environ. Biophys.*, **30**, 105-116 (1991).
- [7] Epsztejn S., Kakhlon O., Glickstein H., Breuer W., Cabantchik I.: *Anal. Biochem.*, **248**, 31-40 (1997).
- [8] Rothman R.J., Serroni A., Farber J.L.: *Mol. Pharmacol.*, **42**, 703-710 (1992).
- [9] Bouton C., Hirling H., Drapier J.C.: *J. Biol. Chem.*, **272**, 19969-19975 (1997).

**NUCLEAR TECHNOLOGIES**  
**AND**  
**METHODS**

## PROCESS ENGINEERING



PL0101502

# INDUSTRIAL DEMONSTRATION PLANT FOR ELECTRON BEAM FLUE GASES TREATMENT

Andrzej G. Chmielewski, Edward Iller, Bogdan Tymiński, Zbigniew Zimek, Janusz Licki<sup>1/</sup>

<sup>1/</sup> Institute of Atomic Energy, Świerk, Poland

The experience gathered during laboratory and pilot plant tests was the basis for the preparation of a full scale industrial plant design.

The electron dry scrubbing process has been employed at the Pomorzany Electric Power Station (Szczecin, Poland) for the simultaneous removal of SO<sub>2</sub> and NO<sub>x</sub> from flue gases emitted from Benson boilers.

After a detailed analysis it was decided to design and construct the electron beam installation treating a maximum flow of 270 000 Nm<sup>3</sup>/h of flue gas.

The Pomorzany electron beam flue gas treatment installation has been designed for the station rated output reached after a retrofit of the plant.

High concentration of NO<sub>x</sub> and relatively low content of SO<sub>2</sub> in flue gas emitted from Benson boilers establish specific conditions for flue gas treatment. The parameters of electron beam process are so chosen as to guarantee an efficient removal of NO<sub>x</sub> up to 80% and up to 70% of SO<sub>2</sub> in continuous operation of the installation. For an intermittent opera-

device. The manufacturer guaranteed high removal efficiency (particulate concentration at the outlet should be less than 20 mg/Nm<sup>3</sup>) and corrosion resistivity of the equipment. The product will then be granulated for final distribution.

The ammonia consumption is estimated to be 180-200 kg/h and the by-product yield to be ca. 800 kg/h. Ammonia water is used, as the medium for the preparation of gaseous ammonia.

At present, the Pomorzany installation passed technical tests and will be put into operation in the first quarter of the year 2001 (Figs.2 and 3) [1].

An electron beam industrial installation of capacity similar to the EPS Pomorzany has been designed and installed by the Ebara Corporation at Seito Electric Power (Sichuan Electric Power Administration) in China, primarily for the removal of SO<sub>2</sub>. Design conditions of this installation are the following:

- volumetric flow of flue gases approx. - 300 000 Nm<sup>3</sup>/h,

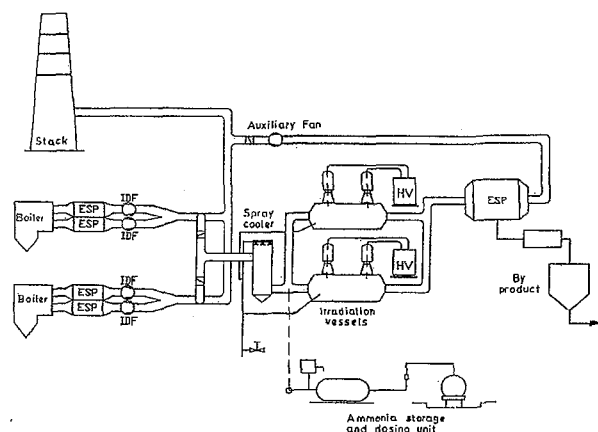


Fig.1. Process flow diagram of electron beam installation at the EPS Pomorzany.

tion up to 80% removal of NO<sub>x</sub> and 90% reduction of SO<sub>2</sub> are expected. The conceptual system arrangement of this situation is shown in Fig.1.

The flue gas will be humidified up to 10% (by volume) in a spray cooler. Ammonia is then injected before two parallel irradiation vessels equipped with two 300 kW, 800 keV accelerators installed in series (Kawęczyn pilot plant's solution). Longitudinal gas irradiation has been applied. The formed aerosol is collected in dry electrostatic precipitator with a flat heated bottom furnished with a scraping

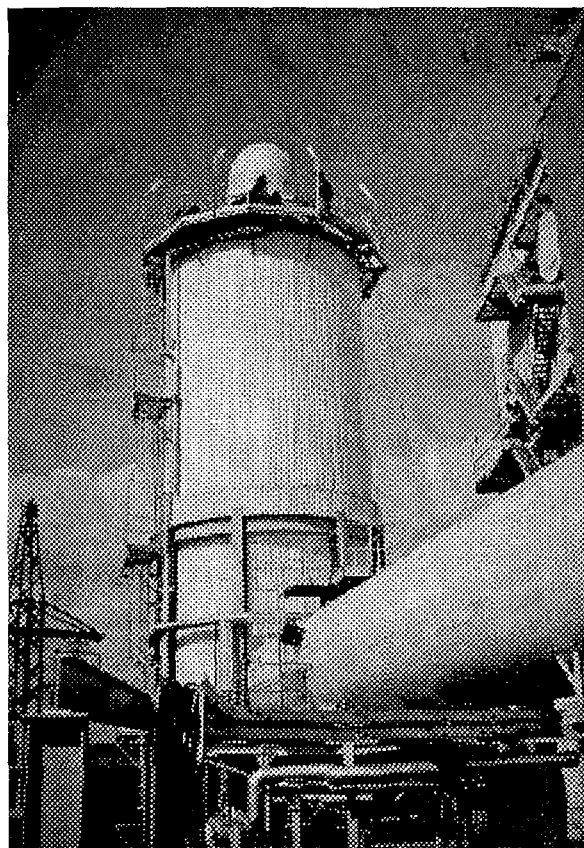


Fig.2. View of spray cooler.

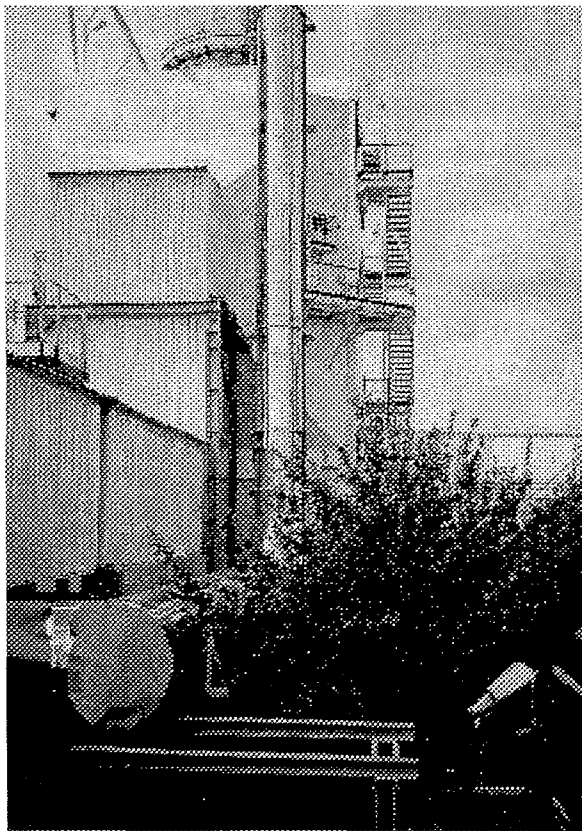


Fig.3. View of electrostatic precipitator.

- SO<sub>2</sub> content in flue gas - 1800 ppm,
- efficiency removal of SO<sub>2</sub> - 80%,
- by-product output rate - 2470 kg/h.

The Chinese electron beam installation was put into operation in May 1998 [2].

To evaluate the technology, which is applying an electron beam to react with outlet gas components, it should be recognized that the removal of both SO<sub>2</sub> and NO<sub>x</sub> is accomplished.

In Fig.4 a comparison of the investment costs for different methods of removal of SO<sub>2</sub> and NO<sub>x</sub> from flue gases is illustrated.

As follows from the cited data, the investment cost of the electron beam technology is at the level of 150-200 \$/kWe of the installed electric power generation capacity.

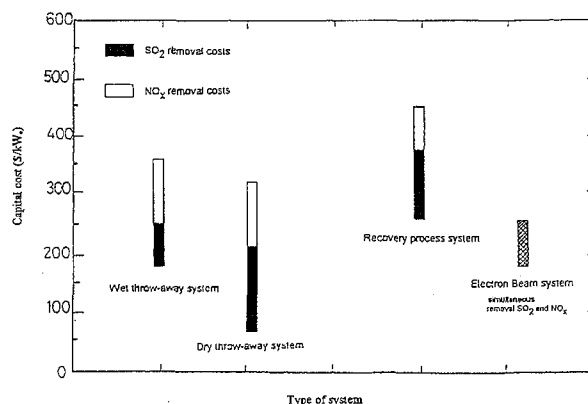


Fig.4. Comparison of the capital cost in \$/kWe vs. the type of gas purification system (based on 300 MWe unit and 2.6% sulfur content in coal).

The costs of simultaneous removal of SO<sub>2</sub> and NO<sub>x</sub> are particularly attractive for the electron beam technology when the revenues from by-product sales are taken into account.

It should be pointed out that the Electric Power Research Institute (USA) has estimated that from among 70 technologies reviewed for the simultaneous SO<sub>2</sub> and NO<sub>x</sub> removal from flue gases, the application of electron beam is one of the four most promising second-generation methods recommended for this purpose.

#### References

- [1]. Chmielewski A.G., Iller E., Tymiński B., Zimek Z., Licki J.: Przemysłowe zastosowania technologii wykorzystującej wiązkę elektronów do oczyszczania gazów spalinowych. Chem. i Inż. Ekol., 705-712 (2000).
- [2]. Hirano S., Aoki A., Izutsu M., Yuki Y.: Simultaneous SO<sub>2</sub>, SO<sub>3</sub> and NO<sub>x</sub> removal by commercial application of the EBA Process. EPRI-DOE-EPA Combined Utility Air Pollution Control Symposium: The MEGA Symposium, vol. 1-14, Atlanta, USA 1999.

## ELECTRON BEAM TREATMENT OF POLYAROMATIC HYDROCARBONS, EMITTED FROM COAL COMBUSTION

Andrzej G. Chmielewski, Anna Ostapczuk, Janusz Licki<sup>1/</sup>

<sup>1/</sup> Institute of Atomic Energy, Świerk, Poland

Combustion of fossil fuel is one of the largest source of emission of volatile organic compounds (VOCs). Emitted VOCs belong to aliphatic hydrocarbons, aldehydes, chlorinated hydrocarbons, aromatic hydrocarbons and the most dangerous polyaromatic hydrocarbons (PAHs) groups. These compounds are emitted from combustion processes with various concentrations, ranging from few ppm up to hundreds ppm, the volume of emission depending on both process conditions and the kind of used fuels [1]. The most popular method used in industry to control VOCs in flue gases is adsorption, but in the case of combustion gases, the presence of other pollutants such as SO<sub>2</sub>, NO<sub>x</sub> and dust causes this process ineffective.

Otherwise secondary pollution - the used adsorbent is generated. In the present state of art, it seems that electron beam treatment is a unique, promising method to remove SO<sub>2</sub>, NO<sub>x</sub> and VOCs from flue gases simultaneously.

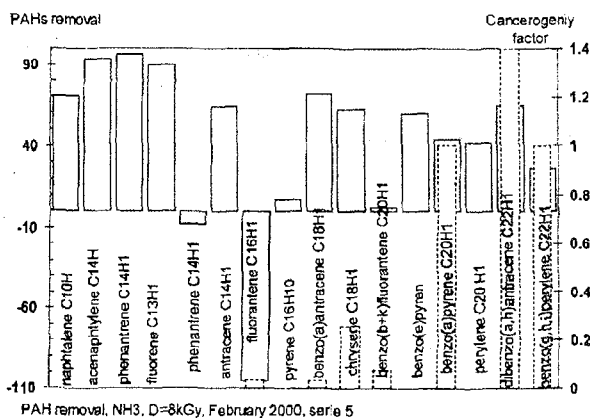
Decomposition of many VOCs by electron beam treatment has been investigated [2,3]. Numerous laboratory experiments, especially for chlorinated aliphatic hydrocarbons, have been carried out [4]. Investigated compounds have been irradiated by electron beam with doses ranging from 2 to 15 kGy, the products of radiolysis being detected by gas chromatography/flame ionisation (GC/FID) and gas chromatography/mass spectrometry (GC/MS)



PL0101503

techniques. Mechanism of organic compounds decomposition is based on the oxidation process, OH radicals are proposed [2] as the most effective oxidising species. Direct electron impact processes and negative ion dissociative attachments may contribute to the process as well [5].

The pilot plant tests to study the influence of electron beam on the chosen polyaromatic hydrocarbons during simultaneous SO<sub>2</sub> and NO<sub>x</sub> removal has been carried out at the EPS Kawczyn, equipped with 2 electron accelerators 50 kW/700 keV each. Concentration of 5 polyaromatic hydrocarbons was measured before and behind of the irradiation chamber. After filtration, the sample gas have passed through adsorbents (activated coal and XAD - 2 resin). PAHs trapped on the adsorbant material were extracted by solvents and analysed by the GC/MS technique. The experimental work has been carried out in 2 series: both with an irradiation dose of 7 kGy, in the second series 2 ammonia was injected into combustion gases. The purpose of the experiment with ammonia additive was to investigate the influence of electron beam on the PAHs during SO<sub>2</sub> and NO<sub>x</sub> removal: in this process NH<sub>3</sub> is a reagent. The removal efficiencies obtained in the pilot plant tests are presented in Fig. In the case of ammonia presence, higher removal efficiencies for all PAHs are observed. Probably when ammonia is added, sulphur and nitrogen acids are neutralised and the reaction with OH radical is promoted, or some products of VOCs with NH<sub>3</sub> are created. There is a necessity in the future work to carry out



PAH removal, NH<sub>3</sub>, D=8kGy, February 2000, serie 5

Fig.

laboratory experiments on irradiation of single compounds with and without NH<sub>3</sub> additive to recognise which kind of effect NH<sub>3</sub> causes. In pilot plant tests it is possible only to check the global influence of electron beam on the organic compounds stream. Simultaneously, high removal efficiencies of SO<sub>2</sub> (89%) and NO<sub>x</sub> (72%) were obtained.

#### References

- [1]. Hirota K., Woletz K., Paur H.-R., Mitzing H.: Radiat. Phys. Chem., 46, 1093-1097 (1995).
- [2]. Ostapczuk A., Chmielewski A.G., Honkonen V., Ruuskanen J., Tarhanen J., Svarfvar B.: Radiat. Phys. Chem., 56, 369-371 (1999).
- [3]. Paur H.-R., Jordan S.: Radiat. Phys. Chem., 31, 9-13 (1988).
- [4]. Paur H.-R.: IAEA-TECDOC-1023, IAEA, Vienna 1998.
- [5]. Kohno H., Berezin A., Chang J.-S., Yamamoto T., Shibuya A., Honda Sh.: IEE Transaction on Industry Applications, 34, (5) 953-966 (1998).

## REDUCTION OF ENERGY CONSUMPTION FOR NO<sub>x</sub> REMOVAL IN ELECTRON BEAM FLUE GAS TREATMENT BY USING AN ALCOHOL AS SCAVENGER

Andrzej G. Chmielewski, Yongxia Sun, Zbigniew Zimek, Sylwester Bułka, Janusz Licki<sup>1/</sup>

<sup>1/</sup> Institute of Atomic Energy, Świerk, Poland

Studies on the NO<sub>x</sub> removal from industrial waste-off gases have been carried out for many years. The key problem of NO<sub>x</sub> reduction is the high-energy consumption. Recently some new technologies have been used with the aim of reducing cost for NO<sub>x</sub> removal [1].

It is well known from environmental chemistry that deNO<sub>x</sub> efficiency could be increased by some organic compounds, free radicals (such as OH, HO<sub>2</sub>) chain reactions in electron beam process. Based on this, laboratory tests have been performed using the ILU-6 accelerator (Institute of Nuclear Chemistry and Technology). The laboratory setup was described earlier [2].

A simulated flue gas was prepared by the addition of NO<sub>x</sub> from a gas cylinder into the flue gas from natural - gas burner. An alcohol was selected as a scavenger. Water vapor, alcohol vapor and ammonia from the gas cylinder were added to the simulated flue gas, respectively. The simulated flue gas was passing through a reaction vessel at a flow rate of 20 m<sup>3</sup>/h and was irradiated up to 11 kGy. The SO<sub>2</sub>, NO<sub>x</sub> con-

centrations were analyzed by a SO<sub>2</sub>, NO<sub>x</sub> gas analyzer (SO<sub>2</sub>, model 40, NO<sub>x</sub>/NO, model 10AR, Thermo Environmental Instruments, USA), respectively. CO, CO<sub>2</sub>, O<sub>2</sub>, C<sub>x</sub>H<sub>y</sub> were analyzed by a portable flue gas analyzer (Lancom series II, Land Combustion Company, UK). It was found that the NO<sub>x</sub> removal efficiency was increased by 20% in the presence of alcohol at its flow rate of 30 l/h. More than 70% NO<sub>x</sub> was oxidized/reduced at 6 kGy for the initial NO concentration of 500 ppm. The humidity and ammonia addition have increased the deNO<sub>x</sub> efficiency by less than 10%. A possible mechanism was proposed.

#### References

- [1]. Gasparik R., Yamabe C., Takazaki D.: Both NO<sub>x</sub> and VOC treatment by a positive streamer corona using a series gap. Proceedings of the first Polish-Japanese hakone group symposium on non-thermal plasma processing of water and air, Sopot, Poland, 29-31 May 2000, pp. 51-54.
- [2]. Chmielewski A.G., Iller E., Zimek Z., Licki J.: Laboratory and industrial installation for electron beam flue gas treatment. Proceedings of International Symposium on Application of Isotopes and Radiation in Conservation of the Environment, Karlsruhe, Germany, March 1992. IAEA-SM-325/124.



PL0101504

## AEROSOL FORMATION AND ITS PRECIPITATION IN ELECTRON BEAM FLUE GAS TREATMENT

Edward Iller, Andrzej G. Chmielewski, Bogdan Tyminiński, Grażyna Zakrzewska-Trznadel, Janusz Licki<sup>1/</sup>,  
Czesław Rygula<sup>2/</sup>, Jerzy Bartosik<sup>2/</sup>

<sup>1/</sup> Institute of Atomic Energy, Świerk, Poland

<sup>2/</sup> Electrostatic Precipitators Factory ELWO, Pszczyna, Poland

Concentration of ammonia aerosols formed in the process of electron beam flue gas treatment (EBFGT) depends on the SO<sub>2</sub> and NO<sub>x</sub> contents, humidity of flue gas, electron beam dose and ammonia stoichiometric ratio. These parameters effect the by-product composition as well.

Recently, the electron beam pilot plant operated at the EPS Kawęczyn (20 000 Nm<sup>3</sup>/h, 2x500 kW, 700 keV accelerators) was equipped with an electrostatic precipitator (ESP) of special construction, designed and manufactured by ELWO (Pszczyna, Poland). Double compartments ESP removes of ammonia salts of aerosols from the stream of flue gases equal to 10 000 Nm<sup>3</sup>/h. A broad study of this

ESP operation in various conditions of electron beam process has been performed. Optical (laser dust-meter) and gravimetric methods for measurements of aerosol concentrations were applied. The Andersen Mark III impactor was used for the aerosol particle size distribution, while ion-chromatography for the analysis of its chemical composition. The results of operation of new type of electrostatic precipitator confirmed high efficiency removal of aerosol particles of ammonium salts. In previously reported tests for the collection of aerosol salts, a bag filter and a gravel bed filter have been applied and a comparison is given as well.

## ELECTRON BEAM STIMULATION OF THE REACTIVITY OF CELLULOSE PULPS

Edward Iller, Aleksandra Kukielka, Andrzej G. Chmielewski, Jacek Michalik, Zbigniew Zimek,  
Halina Stupińska<sup>1/</sup>, Władysław Mikołajczyk<sup>2/</sup>, Henryk Struszczyk<sup>2/</sup>

<sup>1/</sup> Pulp and Paper Research Institute, Łódź, Poland

<sup>2/</sup> Chemical Fibres Institute, Łódź, Poland

Cellulose fibres are important raw materials for the production of textile and sanitary goods. The viscose technology has not been changed through the last century, resulting in serious environmental hazards. New alternative technologies for the manufacturing of cellulose fibers are currently under research and development [1].

Institute of Chemical Fibers in Łódź has been carrying out research since 1988 to develop technology for the production of cellulose carbamate as a raw material for the production of fibers and films in order to eliminate ecological problems associated with the viscose method [2,3]. Recently, in the cooperation with the Institute of Nuclear Chemistry and Technology in Warszawa, the effect of electron beam irradiation on various type of cellulose pulps has been studied in order to improve the reactivity of raw material for the production of cellulose carbamate.

Three different types of textile pulp: Alicell, Borregaard, Ketchikan and Kraft softwood pulp were irradiated with a 10 MeV electron beam from the LAE 13/9 linear accelerator. Kraft softwood sheets selected for studying the effects of radiation dose were irradiated in the dry and wet form with a doses of 5, 10, 15, 20, 25 and 50 kGy. Textile pulps were irradiated only in the dry form with a dose of 25 kGy. After electron beam treatment, the samples of cellulose pulps have been examined by using structural and physico-chemical methods. Electron paramagnetic resonance spectroscopy (ESR) and gel permeation chromatography (GPS) were ap-

plied for the determination of structural changes in irradiated cellulose pulps. By means of physico-chemical methods such parameters as average viscosity, degree of polymerization and  $\alpha$ -cellulose contents were evaluated. The content of  $\alpha$ -cellulose was determined by gravimetric methods as per cent of pulp insoluble in a 17.5% NaOH solution.

The results of primary investigations show that electron beam irradiation with a dose of 10 kGy leads to a decrease of the degree of polymerization of textile as well as the softwood pulps by about 50%. For the Ketchikan pulp and Kraft softwood pulp the degree of polymerization decay to 467 and 544, respectively. At the same time, the content of  $\alpha$ -cellulose decreases in a meaningless way. The results are very promising, clearly indicating that the production of cellulose carbamate using as raw material the cellulose modified radiolytically should be much more effective [4,5]. It was proved, by analyzing the ESR spectra that similar radicals are formed in different types of textile and softwood pulps. However, the number of radicals stabilized in the Kraft softwood pulp at room temperature is three times higher than in Alicell, Borregaard and Ketchikan textile pulps. It is speculated that the differences in radical stability are associated with the cellulose chain flexibility which controlled by cellulose structure.

### References

- [1]. Stepanik T., Ewing D., Whitehouse R.: Electron - processing - application in the viscose industry, IAEA Advisory Group Meeting, Budapest, Hungary, 9-13 March 1998.
- [2]. Struszczyk H.: Chem. Fibres Intern., 46, 265 (1996).



PL0101505



PL0101506

- [3]. Starostka P., Mikołajczyk W., Struszczyk H.: *Fibres & Textile in Eastern Europe*, 62 (1996).
- [4]. Iller E., Kukielka A., Chmielewski A.G., Zimek Z., Michalik J., Perlińska J., Stupińska H., Mikołajczyk W., Starostka P., Strobini G.: Radiacyjna symulacja różnych rodzajów mas celulozowych przeznaczonych do wytwarzania pochodnych. *Przegl. Papiern.*, (672), 468 (2000).

- [5]. Kukielka A., Iller E., Chmielewski A.G., Zimek Z., Michalik J., Perlińska J., Stupińska H., Mikołajczyk W.: Radiation stimulation of the reactivity of different types of cellulose pulps. *Molec. Cryst. and Liquid Cryst.*, 353, 381 (2000).



PL0101507

## MEMBRANE PROCESSES FOR RADIOACTIVE LIQUID WASTE TREATMENT

Andrzej G. Chmielewski, Marian Harasimowicz, Grażyna Zakrzewska-Trznadel, Bogdan Tymiński, Włodzimierz Tomczak<sup>1/</sup>, Andrzej Cholerzyński<sup>1/</sup>

<sup>1/</sup> Institute of Atomic Energy, Świerk, Poland

### Introduction

About 10% of world's energy is produced in nuclear power plants. The share of market of electricity production will be higher in the future, there is no other alternative seen for fossil fuel. According to the agreement reached in 1998 in Kyoto, reduction of CO<sub>2</sub> emission is demanded. Also Poland has to reduce its CO<sub>2</sub> emission by 6%, therefore a national programme of power sector diversification should consider introduction of nuclear fuel in the future.

The main problem connected with further nuclear energy development is the safe treatment and disposal of radioactive waste.

In Poland, which has no nuclear power stations, radioactive wastes are generated by research reactors, medical and industrial applications. The amount of low and medium liquid wastes is close to 1000 m<sup>3</sup> annually.

Membrane processes are the technologies which are very suitable for nuclear applications. As a matter of fact, this technology as many other separation technologies, was developed in the framework of nuclear technology establishment. The effusion process adopting ceramic membranes was developed for <sup>235</sup>UF<sub>6</sub>/<sup>238</sup>UF<sub>6</sub> separation. Theory of the process (superposition of Knudsen and Pouiselle flows) and cascade calculations are till now the basic theories of gas separation.

This Institute has started its research in the field in 1985. Two Ph.D. theses were defended (M. Harasimowicz 1995, G. Zakrzewska-Trznadel 1997). Patents in USA and Poland have been received by the Institute.

The big units for UF/RO seeded enhanced process, MD plant with spiral wound module, MD stable isotopes separation cascade and full scale UF/RO unit (Governmental Strategic Programme SPR-4) have been constructed.

The INCT laboratory is equipped with a multi-channel gamma analyzer, a stable isotope mass spectrometer and a liquid scintillation detector. Membrane structure is investigated using a Culter porosimeter, an X-ray diffractometer and synchrotrone radiation (Trieste).

### Membrane radiation resistivity and cellulose membrane structure

To establish a reliable process, resistivity of membranes to gamma and electron radiation has been

studied [1] and satisfied durability of materials demonstrated.

The knowledge on membrane structure, which is important for understanding of their transport and mechanical properties, is still not adequate. X-ray and synchrotron radiation studies were performed to investigate light and heavy water transport through cellulose membranes [2,3].

### Ultrafiltration and seeded ultrafiltration

The seeded ultrafiltration includes all the processes of binding macromolecular ligands with ions and molecules present in the effluents at a very small concentration. The method makes it possible to retain part of effluent components that otherwise moved to the permeate. The removal of radioactive component using the seeded ultrafiltration method requires selection of a suitable ligand or adsorber that could bind radioactive ions.

Many different complexants and adsorbers were examined in the INCT laboratory. Polyethyleneimine (PEI), microcrystalline chitosan (MCH), and a suspension of cupric hexacyanoferrate (CuFC) were used as ligands attaching ions of Cr, Co and Cs. Best conditions under which the ions Cr<sup>3+</sup> and Co<sup>2+</sup> can be bound to PEI macromolecules were found at pH=4 to 6. The most effective absorption of ions Cs<sup>+</sup> by CuFC proceeds at pH=9.5 to 10.5.

The experiments were made on a laboratory-scale unit and on a pilot plant (UF module AMICON H26P30-43, capillary type, cut-off = 3.10<sup>4</sup> MW, membrane surface area of 2.5 m<sup>2</sup>), using simulated sewage and original LLLW. Three ligands: PEI, MCH and CuFC were simultaneously added to the samples of simulated or original waste; the concentration of each ligand was about 0.01 g/L. The sample was mixed (4 h) and after seasoning (16 h) filtered through a membrane at pH=7 and T=20°C. The volume reduction coefficient was VRC=20. Under these conditions the decontamination factors were 52 to 68 for the laboratory unit and 37 to 62 for the pilot plant [4].

### Hyperfiltration and nanofiltration

The SUF method can be applied only for wastes containing some radionuclides which are attached to the macromolecules of various ligands at the same pH value. In the case of wastes containing a great variety of radioactive ions the UF process can be used only as the first stage of purification. The products of UF process have to be directed to the next stages of the decontamination process: re-

tentate to thin-film evaporators and permeate to reverse osmosis modules.

One of the disadvantages of reverse osmosis are rather high pressures that have to be applied (up to 10 MPa). Last developments in membrane technology allow to use composite membranes (modules) working in nanofiltration range with significantly lower operating pressures - from 0.3 to 1.4 MPa. Such modules were chosen for the LLLW purification process in this Institute. Employing the low-pressure reverse osmosis (LPRO) with spiral-wound membrane modules high decontamination factors were achieved. Best results were obtained using the thin-film composite membrane element NTR 739 HF made by NITTO (Japan); it was operated at a feed pressure of 1 MPa and the retention coefficient for a 0.15% NaCl solution was 97%. The decrease of the specific activity of some radionuclides was as follows:  $^{51}\text{Cr}$  - 180,  $^{60}\text{Co}$  - 515,  $^{90}\text{Sr}$  - 320,  $^{137}\text{Cs}$  - 32,  $^{144}\text{Ce}$  - 130. For the samples of LLLW, the decontamination factors varied from 52 to 77 at a volume reduction factor VRC = 40.

On the basis of the results collected in the laboratory scale experiments, the pilot unit including three stages - UF + 2RO was designed. The pilot plant consisted of an AMICON H 26P30 capillary ultrafiltration module and two NITTO NTR 739 HF S-4 spiral wound LPRO modules. The permeate flux in the system was 80-200 L/h. The values of decontamination factors (DF), which were achieved on each stage, were as follows: pretreatment unit (PT) - 3 to 5, UF unit 1.7 to 2.4, RO1: 27 to 34, RO2: 21 to 30.

#### Membrane distillation

Membrane distillation is a process in which two aqueous solutions at different temperatures,  $T_1$  and  $T_0$ , where  $T_1 > T_0$  are separated by a hydrophobic porous membrane. The driving force of the MD process is the partial vapour pressure difference caused by the temperature gradient between the two solutions. The vapour molecules are transported through the membrane pores from the high-vapour pressure side to the low-pressure side. The component with the higher partial pressure shows a higher permeation rate.

Membrane distillation is being developed for the production of high-purity water and wastewater treatment, for the concentration of various kind of solutions near saturation conditions. The process allows the removal of salt from seawater and separation of alcohol-water solutions. For many years MD has been investigated in this Institute [5-7]. The experiences with membrane distillation led the authors to consider the process as a method for the concentration of liquid low-level radioactive wastes.

Tentative tests with liquid radwastes were carried out on a laboratory unit with a permeation test-cell holding flat sheet membrane. Polytetrafluoroethylene (PTFE) and polypropylene (PP) foils were used as hydrophobic barrier. The process was arranged in the direct contact membrane distillation configuration. The permeate condensed directly in the cold stream (distilled water) and retentate

was enriched in radionuclides. Further experiments carried out with a capillary module BFMF 06-30-33 (Euro-Sep Ltd.) with polypropylene capillaries of diameter 0.33 mm and cut off of 0.6  $\mu\text{m}$  confirmed the previous results [8]. In each experiment almost pure water (distillate) and a more concentrated solution of solids and radionuclides (retentate) were obtained as the product. The polymer membranes exhibited a high chemical and radiochemical resistance. The ions of radioisotopes did not pass through the membrane. On the basis of laboratory experiments, a pilot plant equipped with a 4 m<sup>2</sup> membrane area module, was constructed. Pilot plant experiments proved the previous statement: membrane distillation is an interesting alternative for liquid radioactive waste processing.

#### Tritiated water

Tritiated water ( $^3\text{HOH}$ ,  $\text{TOH}$ ) is generated in nuclear power plants. This product should be removed from the coolant to prevent environmental release.

There are not too many separation technologies available. However, the membrane process has been proposed by Pacific Northwest Laboratory [9] on the basis of the INCT previous works aimed to develop stable isotopes ( $^{18}\text{O}$ ,  $^{17}\text{O}$ , D) enrichment. Hydrophilic [10] and hydrophobic [11] membranes were investigated and cascade optimization modelling has been performed [12]. Three Polish and two American patents have been granted to the INCT and University of Tennessee [13-17]. A study on  $\text{T}_2\text{O}$  membrane enrichment is being carried out at the INCT as well.

Part of this work was performed in the frame of Governmental Strategic Programme SPR-4 "Radioactive wastes and spent fuel".

#### References

- [1] Chmielewski A.G., Harasimowicz M.: Influence of gamma and electron irradiation transport properties of nanofiltration and hyperfiltration membranes. *Nukleonika*, **42**(4), 857-862 (1997).
- [2] Grigoriew H., Chmielewski A.G.: X-ray study of the influence of water on the cellulose membrane structure. *J. Mat. Sci. Lett.*, **16**, 1945-1947 (1997).
- [3] Grigoriew H., Chmielewski A.G.: Capabilities of X-ray methods in studies of processes of permeation through dense membranes. *J. Membrane Sci.*, **142**, 87-95 (1998).
- [4] Chmielewski A.G., Harasimowicz M.: Application of ultrafiltration and complexation for the treatment of low-level radioactive effluents. *Sep. Sci. Technol.*, **30** (7-9), 1779-1783 (1995).
- [5] Chmielewski A.G., Zakrzewska-Trznadel G., Miljević N., Van Hook W.A.: Membrane Distillation Employed for Separation of Water Isotopic Compounds. *Sep. Sci. Technol.*, **30**, 7-9, 1653-1667 (1995).
- [6] Chmielewski A.G., Zakrzewska-Trznadel G., Miljević N., Van Hook W.A.: Multistage Process of Deuterium and Heavy-Oxygen Enrichment by Membrane Distillation. *Sep. Sci. Technol.*, **32** (1-4), 527-539 (1997).
- [7] Zakrzewska-Trznadel G., Chmielewski A.G., Miljević N.: Separation of protium/deuterium and oxygen-16/oxygen-18 by membrane distillation process. *J. Membrane Sci.*, **113**, 337-342 (1996).
- [8] Chmielewski A.G., Harasimowicz M., Zakrzewska-Trznadel G.: Purification of radioactive wastes by low temperature evaporation (membrane distillation). *Sep. Sci. Technol.*, **32**(1-4), 709-720 (1997).
- [9] Nelson D.A., Duncan G.A., Jensen S., Burton: Isotopomeric water separations with supported polyphosphazene membranes. *J. Membrane Sci.*, **12**, 105-113 (1996).
- [10] Chmielewski A.G., Zakrzewska-Trznadel G., Miljević N., Van Hook W.A.: Investigation of the Separation Factor Between



- Light and Heavy Water in the Liquid/Vapour Membrane Permeation Process. *J. Membrane Sci.*, 55, 257-262 (1991).
- [11]. Chmielewski A.G., Zakrzewska-Trznadel G., Miljević N., Van Hook W.A.:  $^{16}\text{O}/^{18}\text{O}$  and H/D Separation Factors for Liquid/Vapour Permeation of Water Through an Hydrophobic Membrane. *J. Membrane Sci.*, 60, 319-329 (1991).
- [12]. Chmielewski A.G., Matuszak A., Zakrzewska-Trznadel G., Van Hook W.A., Miljević N.: Cascades for Natural Water Enrichment in Deuterium and Oxygen-18 Using Membrane Permeation. *Sep. Sci. Technol.*, 28 (1-3), 909-927 (1993).
- [13]. Chmielewski A.G., Zakrzewska-Trznadel G., Miljević N., Van Hook W.A.: Sposób wzbogacania wody w składniki wody ciężkiej. Polish Patent 161104.
- [14]. Chmielewski A.G., Zakrzewska-Trznadel, Miljević N., Van Hook W.A.: Sposób wzbogacania wody naturalnej w tlen-18. Polish Patent 161105.
- [15]. Van Hook W.A., Chmielewski A.G., Zakrzewska-Trznadel G., Miljević N.: Enrichment of Water in Components of Heavy Water. US Patent No 5,084,181.
- [16]. Van Hook W.A., Chmielewski A.G., Zakrzewska-Trznadel G., Miljević N.: Method of Enrichment of Oxygen-18 in Natural Water. US Patent No 5,057,225.
- [17]. Chmielewski A.G., Zakrzewska-Trznadel G., Miljević N., Van Hook W.A.: Sposób wzbogacania wody naturalnej w tlen-18. Polish Patent 168 152.

## APPLICATION OF CERAMIC MEMBRANES FOR RADIOACTIVE WASTE PURIFICATION



PL0101508

Grażyna Zakrzewska-Trznadel, Marian Harasimowicz, Bogdan Tymiński, Andrzej G. Chmielewski

A study on the application of different membrane processes to nuclear technology has been conducted at the Institute of Nuclear Chemistry and Technology for many years. One application of membrane methods involves the purification and concentration of liquid low- and medium-level radioactive wastes (LLRWs and LMLRWs). Most of the wastes need proper processing to reduce the concentration of radioactive and non-active substances to the level which allows safe discharge according to the national and international regulations.

At present, the experiments with the use of MEMBRALOX<sup>®</sup> ceramic filtering elements (Fig.) are conducted. The pore size of ceramic tubes used was in the 1 kD-100 nm range. The experiments were performed with non-active and radioactive model solutions. Since the aim of the work is to remove the ions, the membranes with pores in a UF/NF range are not sufficient to achieve high decontamination factors and the process has to be enhanced by chemical complexation or adsorption. Some complexants as poly(acrylic) acid and poly(acrylic) acid salts, polyethylenimine, and cyanoferrates were tested. The experiments showed a significant increase of separation factors and decontamination factors while the macromolecular compounds were added.

Advantages of ceramic membranes employed in the nuclear industry are found in their extremely high chemical and physical stability (full pH range), resistance to oxidation and solvents, and resistance to

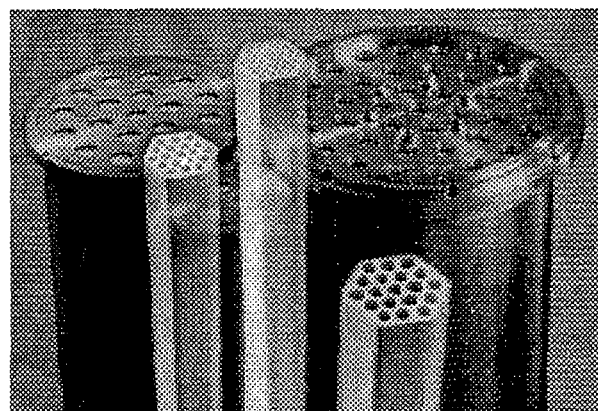


Fig. Ceramic membrane elements.

ionising radiation. Ceramic materials are advantageous when the solutions composed of organic compounds or high radioactive wastes containing alpha emitters, are filtered. High temperature resistance allows the washing with warm liquids and sterilisation by steam.

## HYDROCHEMICAL AND ISOTOPE BACKGROUND FOR GROUNDWATER IN THE REGION OF SZCZERCÓW LIGNITE DEPOSIT

Wojciech Sołtyk, Jolanta Walendziak, Andrzej Owczarczyk

The Bełchatów lignite deposit consists of two exploitation fields: Bełchatów and Szczerców. The first is being exploited now, while the second is actually prepared for future exploitation.

It has been predicted that the exploitation of Bełchatów Field resources will be completed in 2019. That is the reason why the Szczerców Field, which is going to be exploited in the period 2007-2038, is already prepared starting from 1999. A very important stage of the preparation process is the drainage of opening out excavation and surroundings. The drainage system of Szczerców Field began to work at the end of 2000. It consists of 174 wells, pumping the groundwater permanently with a

total efficiency of about 5.5 m<sup>3</sup>/s that results in the depression of groundwater table with an average velocity of 0.5 m/d. The natural hydrogeological equilibrium is entirely disturbed due to the drainage process.

The changes of water flow pattern in the ground is the reason of accelerated leaching of minerals, mixing of different water bodies, and causes hydrochemical and isotope characteristics of pumped waters being received by rivers and natural reservoirs in the region.

Aim of the present work was to investigate the isotope and hydrochemical background for the existing groundwater system before starting drain-



PL0101509

age pumping for the Szczerców Field. The water samples for investigations were taken from 112 piezometers localized in the region of the opening out excavation, salt deposit Dębina at the east edge of lignite deposit and inside the preliminary depression cone. The depth of control wells (piezometers) was in the range 23-269 m so the water

$^{34}\text{S}/^{32}\text{S}$  and  $^{18}\text{O}/^{16}\text{O}$  have been preferentially measured at hydrologic contact zones of aquifers bearing waters of different age and in geologically important regions e.g. waterbearing faults and mineralogical boundaries existing in the region under observation. Results of the hydrochemical background for the groundwaters in the opening out

Table. Results of hydrochemical and isotope measurements in opening out excavation - "Szczerców" Field.

Element (ion)		Above-deposit levels			Below-deposits levels		
Isotope	Unit	min.	max.	mean value $\pm$ stand. dev.	min.	max.	mean value $\pm$ stand. dev.
Soluble substance	mg/dm <sup>3</sup>	201	1312	269 $\pm$ 52	210	652	386 $\pm$ 113
Elect. conductivity	$\mu\text{S}/\text{cm}$	146	435	301 $\pm$ 37	203	868	440 $\pm$ 118
pH		7.40	8.63	7.68 $\pm$ 0.13	7.10	9.50	7.78 $\pm$ 0.28
Ca	mg/dm <sup>3</sup>	35.8	250.0	57.3 $\pm$ 9.9	7.6	72.2	48.0 $\pm$ 12.4
Mg	mg/dm <sup>3</sup>	2.3	16.3	7.5 $\pm$ 2.3	2.2	29.9	12.2 $\pm$ 4.3
Na	mg/dm <sup>3</sup>	3.0	35.4	9.4 $\pm$ 5.1	7.0	189.9	56.6 $\pm$ 37.7
K	mg/dm <sup>3</sup>	<2.0	8.0	2.6 $\pm$ 0.7	<2.0	14.0	5.3 $\pm$ 3.1
HCO <sub>3</sub>	mg/dm <sup>3</sup>	48.8	275.8	190.4 $\pm$ 63.1	16.4	259.3	222.5 $\pm$ 48.9
Cl	mg/dm <sup>3</sup>	7.1	83.0	18.3 $\pm$ 8.3	7.8	288.6	45.8 $\pm$ 27.7
SO <sub>4</sub>	mg/dm <sup>3</sup>	<10.0	632.0	9.8 $\pm$ 5.5	<10.0	21.0	12.6 $\pm$ 7.0
PO <sub>4</sub>	mg/dm <sup>3</sup>	0.1	2.7	0.38 $\pm$ 0.19	<0.1	4.1	0.47 $\pm$ 0.39
NH <sub>4</sub>	mg/dm <sup>3</sup>	0.27	1.99	0.83 $\pm$ 0.06	0.09	3.46	0.60 $\pm$ 0.37
Fe	mg/dm <sup>3</sup>	0.24	3.62	2.03 $\pm$ 0.98	0.33	8.60	3.20 $\pm$ 1.46
Mn	mg/dm <sup>3</sup>	<0.01	0.76	0.20 $\pm$ 0.12	<0.01	0.42	0.14 $\pm$ 0.12
Ba	$\mu\text{g}/\text{dm}^3$			12.6	0.2	120.9	12.3 $\pm$ 5.6
Br	$\mu\text{g}/\text{dm}^3$			31.0	9.1	130.8	52.7 $\pm$ 29.5
Cr	$\mu\text{g}/\text{dm}^3$			3.4	0.23	4.54	1.91 $\pm$ 1.24
J	$\mu\text{g}/\text{dm}^3$			2.2	0.6	6.1	2.1 $\pm$ 1.7
Zn	$\mu\text{g}/\text{dm}^3$			38.2	10.4	970.7	30.3 $\pm$ 13.7
Cd	$\mu\text{g}/\text{dm}^3$			0.14	0.06	0.94	0.34 $\pm$ 0.28
Cu	$\mu\text{g}/\text{dm}^3$			5.1	1.6	58.9	14.6 $\pm$ 10.6
Ni	$\mu\text{g}/\text{dm}^3$			15.5	0.2	10.7	2.2 $\pm$ 1.3
Pb	$\mu\text{g}/\text{dm}^3$			5.5	0.7	28.1	7.4 $\pm$ 5.8
Hg	$\mu\text{g}/\text{dm}^3$			0.01	<0.01	0.03	0.01 $\pm$ 0.01
Rb	$\mu\text{g}/\text{dm}^3$			2.0	0.4	16.2	2.7 $\pm$ 1.2
Ag	$\mu\text{g}/\text{dm}^3$			0.03	<0.01	11.19	0.05 $\pm$ 0.08
Sr	$\mu\text{g}/\text{dm}^3$			132.6	44.6	203.4	141.7 $\pm$ 52.0
V	$\mu\text{g}/\text{dm}^3$			0.86	0.01	2.29	0.61 $\pm$ 0.41
H-3	TU	1.6	23.1	5.5 $\pm$ 4.2	1.1	12.3	6.7 $\pm$ 4.4
Rn-222	Bq/dm <sup>3</sup>	<0.2	7.2		<0.2	3.6	
$\delta\text{S}-34$	‰ CDT	-8.00	8.42		8.42	24.21	
$\delta\text{O}-18$	‰ SMOW	-3.30	8.28		1.90	12.52	

samples taken from them were representative for all aquifers (from quaternary to mesozoic formations).

Determination of chemical water composition (macro- and microelements) as well as environmental isotopes concentration  $^3\text{H}$ ,  $^{222}\text{Rn}$  and ratios

excavation of the Szczerców Field are presented in Table.

The hydrochemical changes, which are expected after starting and further development of the drainage system, will be monitored successively in the future.



PL0101510

## DETERMINATION OF SULFUR ISOTOPE RATIOS IN COAL FROM POLISH COALFIELDS

Andrzej G. Chmielewski, Ryszard Wierzchnicki, Małgorzata Derda

In Poland hard coal occurs in three main basins, all of Upper Carboniferous age: the Upper Silesia, the Lower Silesia and the region of Lublin. There are over 120 recognized deposits, of which about 70 have been developed. Mining concentrated on the Upper

Silesian Basin, located in the south of Poland around Katowice and straddles the border with the Czech Republic. This is the most important coalfield, comprising 103 recognized deposits and covering an area of 4500 km<sup>2</sup>.

The work started with the preparation of coal samples and extraction of the particular forms of sulfur [1]. By this method, each form of sulfur has been extracted and transformed into a stable compound, which can be subsequently converted to a gas phase ( $\text{SO}_2$ ) for mass spectrometric analysis. All samples, in the form of  $\text{Ag}_2\text{S}$  and  $\text{BaSO}_4$  were incinerated to obtain  $\text{SO}_2$  using the method described by Hałas and Szaran [2,3]. Sulfur isotope ratio is obtained using the mass spectrometer DELTA plus FINNIGAN.

Table. Sulfur isotope ratios in the Polish coals.

Coal-mine	S [%]	$\delta^{34}\text{S}$ [‰]		
		Pyrite sulfur	Organic sulfur	Sulphate sulfur
Bogdanka	1.23	1.29	-2.50	-1.95
Kazimierz Juliusz	0.79	6.37	6.18	7.27
Chwałowice	0.81	1.97	3.85	1.19
Jankowice	0.64	0.33	15.88	-
Śląsk	0.74	10.50	4.40	13.71
Sośnica	2.06	-6.62	4.66	-1.88
Bełchatów*	0.30	-	9.37	-

\* Lignite.

Sulfate sulfur determinations were not performed routinely due to the low sulfate content in the studied coals (Table). Nevertheless, an acid extraction procedure was performed to remove any carbonate and other acid-soluble components from the matrix. The received results suggest that the sulfur

in coal originates from the sulfur originally bound by plants and depleted in the isotope  $^{34}\text{S}$ . The sulfur was probably produced in the process of sulphate bacterial reduction. While in the literature data for American, Australian etc. coals are presented, this study seems to be the first one performed for the coals of Polish origin. This isotope ratio can be a tracer for environmental samples (aerosol, rain, superficial water) to track the products of the combustion of a particular coal. Further work will be devoted to the application of

this method to investigate anthropogenic sulfur transport from a given coal combustion source.

#### References

- [1]. Westgate L.M., Anderson T.F.: Anal. Chem., 54, 2136 (1982).
- [2]. Hałas S., Wolacewicz W.D.: Anal. Chem., 53, 686 (1981).
- [3]. Hałas S., Szaran J.: Anal. Chem., 71, 3254 (1999).

## SULPHUR ISOTOPE EFFECTS IN CHEMICAL REACTIONS

Andrzej G. Chmielewski, Ryszard Wierzchnicki, Agnieszka Mikołajczuk

Sulphur is an important element of organic matter. Due to its high chemical reactivity, it takes part in biological and geological processes, in which isotope effects occur. It has been proved recently that to calculate the isotope effects one has to take into account not only the mass ratio but also other physical parameters of nuclides e.g. even or odd numbers of neutrons in nuclei, shape and distribution of charge, turn of nuclear spin etc. Therefore, new theoretical assumptions have been proposed on the basis of data, obtained in a study of separation processes of heavy elements, particularly uranium. It is well-known nowadays that the effects disconnected with vibration energy influence the separation of isotopes of lighter elements like iron and magnesium [1]. For sulphur isotopes question concerning these effects is still open.

Two methods are used to determine the equilibrium constants for isotope exchange reactions: theoretical calculations and experiments. Using the well-known methods of statistical mechanics, partition function ratios for many isotopic sulphur compounds have been calculated. These partition function ratios are used to determine equilibrium constant for many possible exchange reactions involving the isotopes of sulphur [2]. The results indicated that considerable fractionation of the

sulphur isotopes can be expected in laboratory and naturally occurring processes.

Recently, the isotope fractionation factors were determined for:

- $\text{H}_2\text{S}$  (gas) and sulphur species in  $\text{H}_2\text{O}$  and aqueous solution of 0.05 mol/l  $\text{Na}_2\text{S}$ . The reaction was conducted in a closed system for about 20 h at constant temperature ( $20^\circ\text{C}$ ). The products were converted into  $\text{Ag}_2\text{S}$  and further to  $\text{SO}_2$  in a

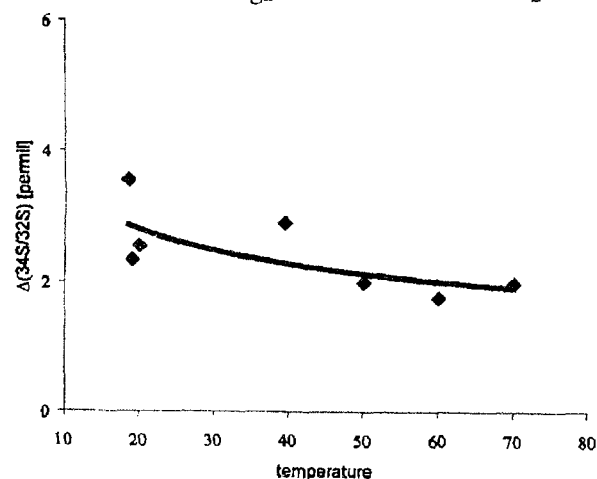


Fig. System  $\text{SO}_2\text{-H}_2\text{O}$  at  $18\text{-}70^\circ\text{C}$ ,  $\Delta^{34}\text{S}$  [‰] =  $(\alpha - 1) \times 10^3$ ,  $^{34}\text{S}$  is enriched in the solution,  $\alpha$ -isotope separation factor.

PL0101511

vacuum line [3]. The experimental results showed that the isotope fractionation factors depend on the degree of dissociation of  $\text{H}_2\text{S}$  in solution. Isotope fractionation effects can be explained by considering the vibrational behaviour of the molecules. While  $\text{H}_2\text{S}$  molecules in the gas phase vibrate almost independently, in solution there are interactions of the  $\text{H}_2\text{S}$  dipoles with the molecules and ions of the solvent, leading to different  $\text{H}_2\text{S}$  solubilities. Isotopically different  $\text{H}_2\text{S}$  molecules have various vibration energies because of the mass difference. The heavy isotope  $^{34}\text{S}$  is enriched in water solution compared with the gas phase. Changing the solvent, generally changes the vibrational behaviour of the isotopic  $\text{H}_2\text{S}$  molecules and therefore also their solubilities and finally the isotopic fractionation between solution and gas phase. In  $\text{Na}_2\text{S}$  solution, the heavy isotope  $^{34}\text{S}$  is enriched in the gas phase compared with the solution because the degree of dissociation increases [4,5].

- $^{34}\text{SO}_{2(\text{gas})} + ^{32}\text{SO}_{2(\text{aq})} = ^{32}\text{SO}_{2(\text{gas})} + ^{34}\text{SO}_{2(\text{aq})}$   
The reaction was conducted in the closed system for about 20 h, the temperature was changed from 18 to 70°C. The products were converted to  $\text{BaSO}_4$  and further to  $\text{SO}_2$  in a vacuum line. The kinetic isotope effects can be explained by the mass difference between isotopic molecules. The reaction velocity is higher for isotopically lighter molecules because it needs a smaller activation energy. The heavy isotope  $^{34}\text{S}$  is enriched in solution compared with the gas phase. While the temperature of reaction increases the solubility of the isotopic  $\text{SO}_2$  molecules decreases. The experimental results are presented graphically in Fig.

## References

- [1]. Dembiński W.: *Wiad. Chem.*, **9/10** (1999).
- [2]. Tudge A.P., Thode H.G.: *Can. J. Research*, **B28**, 567 (1950).
- [3]. Hałas S., Szaran J.: *Anal. Chem.*, **71**, 3245 (1999).
- [4]. Gessler R., Gehlen K.: *Fresenius Z. Anal. Chem.*, **324**, 130 (1989).
- [5]. Toth K., Jancso G.: *Sep. Sci. Technol.*, **26(9)**, 1267 (1991).

# MATERIAL ENGINEERING, STRUCTURAL STUDIES, DIAGNOSTICS

## PROVENANCE STUDIES OF ALABASTER AND MARBLE SCULPTURES FROM POLAND BY INAA

Ewa Pańczyk, Maria Ligęza<sup>1/</sup>, Lech Waliś

<sup>1/</sup> Academy of Fine Arts, Kraków, Poland



PL0101512

### General

Alabaster - a crypto-crystalline form of gypsum - is a sculptor's material, which is easy to process and has been used for making art objects from the Antiquity until modern times. It is characterised by a variety of colours and shapes; it is easy to be gold-coated or polychromed; however, its main disadvantage is fast destruction under the influence of atmospheric agents. Alabaster can be found in many places in Europe. In Poland such places have been identified in south-eastern regions of the country: Kraków, the Lower Silesia and the Opole Silesia (Fig.1). Also Lvov (Ukraine) should be men-

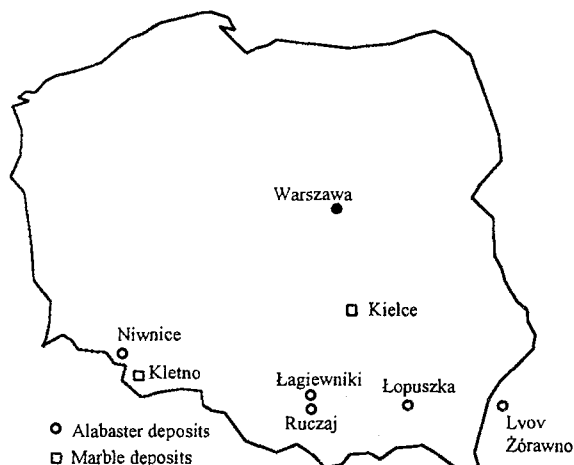


Fig.1. Location of studied alabaster and marble deposits.

tioned here. Alabaster is a pure material containing a very low concentration of trace elements and that is why in order to identify its origin in particular art objects the instrumental neutron activation analysis (INAA) has been used. Apart from the concentration of trace elements, the Ca content has been specified in particular samples taken from the art objects under analysis and from respective deposits. The fact that is very advantageous for the analysis is that the elements being the main components of  $\text{CaSO}_4 \cdot 2\text{H}_2\text{O}$  alabaster have low ( $n, \gamma$ ) reaction cross sections and the probability of the occurrence of the reaction is very low. The situation is similar in the case of marbles ( $\text{CaCO}_3$ ).

### Characteristics of art objects

The so-far examination concerned the following art objects:

- "Madonna with the Child" coming from the end of 14th century from Lvov (Fig.2) and alabaster



Fig.2. "Madonna with the Child", the end of 14th century, alabaster.

deposits closest to the place where for many centuries the sculpture was stored (Fig.1). One

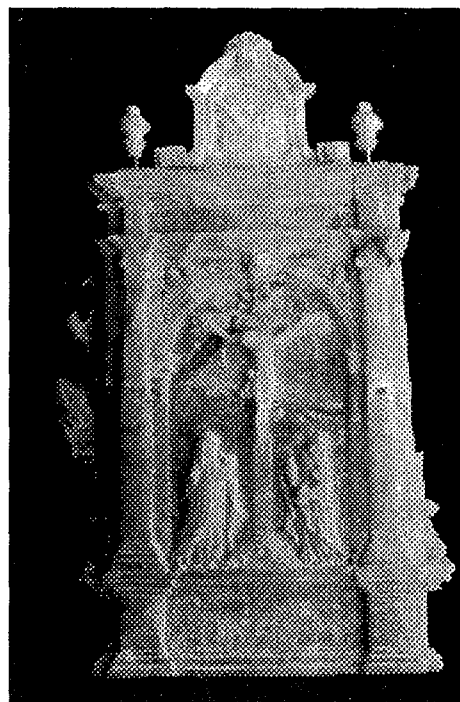


Fig.3. The "Altar with the Crucifixion of Christ", 17th century, alabaster.

of many hypotheses put forward by art historians assumed the possibility of using a native (local) alabaster for making that statuette.

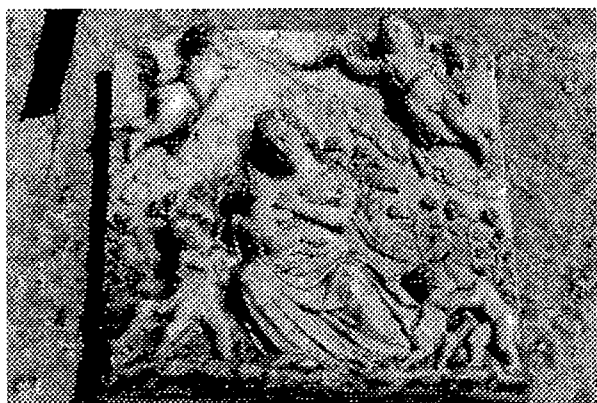


Fig.4. The relief called "Caritas", the beginning of 17th century, alabaster.

- The "Altar with the Crucifixion of Christ" dated to the 17th century of unknown origin (Fig.3), located in the convent of the Order of St. Clare



Fig.5. The relief from "Sarcophagus with cupids making armour", 2nd century A.D., marble.

- in Kraków, as well as the deposit from the Lower Silesia (the so-called "New Land" deposit).
- The relief called "Caritas" (Fig.4) dated to the beginning of 17th century of unknown origin from the National Museum in Gdańsk.
- The marble relief dated to the 2nd century A.D. (Fig.5) from Czartoryski Museum in Kraków and for two different deposits of that stone (the Kielce and Kletno marble): the so-called "White Maryann", or "Biała Marianna".

#### Analytical procedure

Samples from the deposits and sculptures under analysis have been ground in an agate mortar and afterwards samples weighing about 50 mg were taken for analysis from the prepared material. After weighing all samples were sealed in quartz ampoules and then packed together with models of 36 indexed elements. Each packet contained also Sc and Au used as monitors of the thermal neutron flux. Irradiation of the samples was carried out in a MARIA reactor at Świerk near Warszawa, at a neutron flux of  $8 \times 10^{13}$  n/cm<sup>2</sup>s. The samples were irradiated for 24 h and cooled for 12 h. The radioactivity of the samples was measured by means of a HP-Ge detector (made by ORTEC) coupled with a CANBERRA-System S100 spectrometer, controlled by an IBM computer. The analysis of gamma-ray spectra of the samples was performed with the aid of the micro-SAMPO program.

#### Analysis of results

Analysis of the results obtained should answer to the following questions:

- 1) are the distributions of trace elements in the materials analyzed characteristic of a given material?

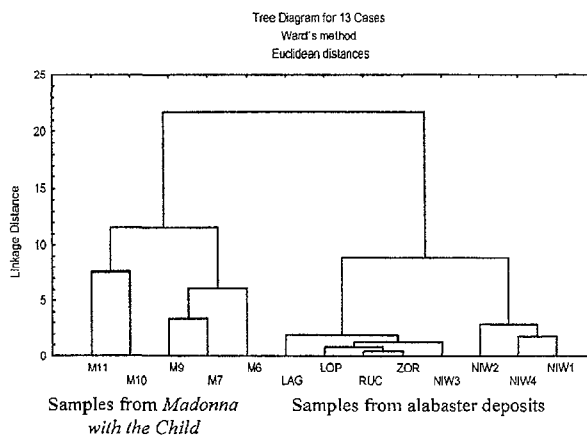


Fig.6. Cluster analysis of samples from the sculpture "Madonna with the Child" and alabaster deposits.

- 2) is it possible to establish groups of objects that exhibit the highest similarity?

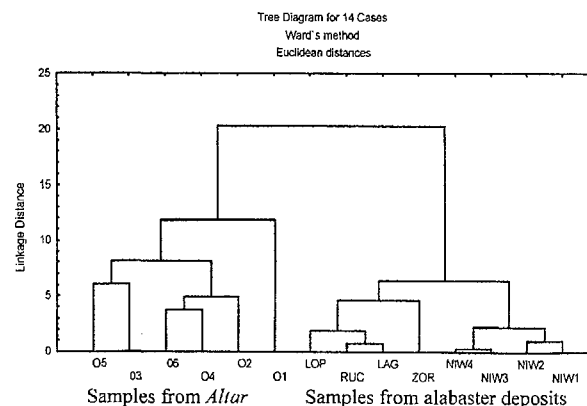


Fig.7. Cluster analysis of samples from the "Altar with the Crucifixion of Christ" and alabaster deposits.

For this purpose we employed a multivariate analysis of clusters using the STATISTICA program (StatSoft). Results are shown in Figs. 6-9.

#### Conclusions

There are major differences in the trace elements distribution both in the sculptures under analysis and in the alabaster and marble deposits. Materials taken from the sculptures under analysis do not come from the deposits analysed so far. This limits the number of hypotheses regarding the origin of alabaster and marble used in the analysed art

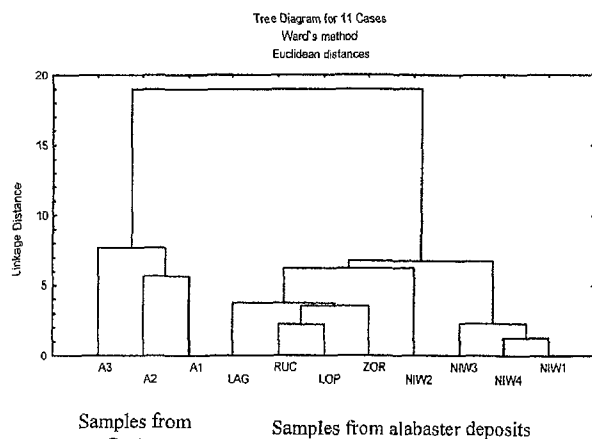


Fig. 8. Cluster analysis of samples from the relief "Caritas" and alabaster deposits.

objects. However, the last additions to the original material used in the Madonna with the Child (end of 14th century) have been specified as coming from one of the analysed alabaster deposits.

The analysis of a larger amount of alabaster deposits originating from old European mines will

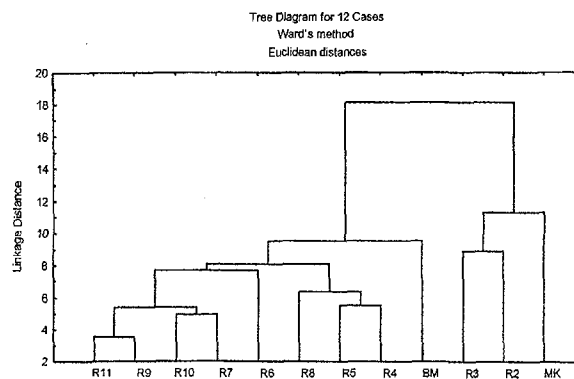


Fig. 9. Cluster analysis of samples from the "Sarcophagus with cupids marking armour" and alabaster deposits. Samples R2, R3, R4, R5, R6, R7, R8, R9, R10, R11 taken from "Sarcophagus with cupids marking armour"; MK - Kielce deposit; BM - "Biała Marianna"; Kletno deposit.

enrich the database regarding the trace elements distribution. Thus, the probability concerning the identification of the origin of that stone in various art objects will grow.



PL0101513

## INVESTIGATIONS OF TRACK ETCHED MEMBRANE SURFACES USING SEM WITH DIFFERENT WORKING CONDITIONS

Bożena Sartowska, Oleg Orelovitch<sup>1/</sup>

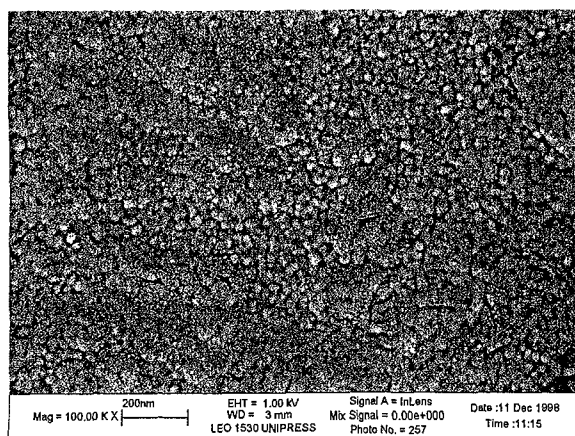
<sup>1/</sup> Flerov Laboratory of Nuclear Reaction, Joint Institute for Nuclear Research, Dubna, Russia

The process of Particle Track Membranes production is known and described in the literature [1,2]. Production and creation of new types of membranes need to analyse surface morphology and determine shape and size of pores [3]. Investigations of membrane surfaces using Scanning Electron Microscopy (SEM) need to make good conditions for presentation of small objects. New types of SEM can be used to obtain more information about details of the surface. Our last membrane investigation (1999-2000) gave us SEM picture with information, which has puzzled us and required some explanations. Cracks on the membrane surfaces can

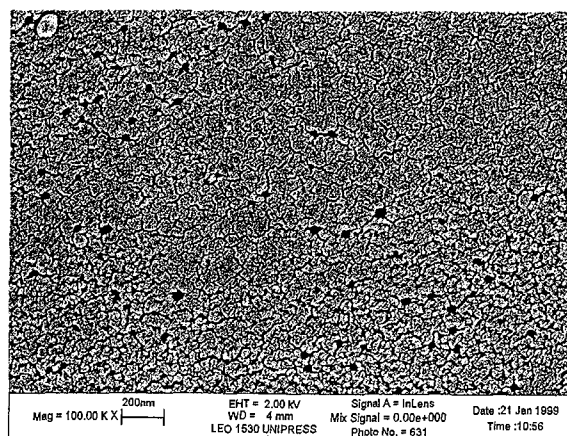
be seen. So, problem to solve appeared: are these cracks due to the effect of conditions of membrane production or method of sample preparation? (The existence of the cracks controls surface properties of the membrane).

A membrane produced from PET (polyethylene terephthalate) of thickness 15  $\mu\text{m}$  and a pore diameter of 0.45  $\mu\text{m}$  was investigated.

Our standard procedure of sample preparation was as follows: fixing the sample using a conductive glue and covered with a thin (10-20 nm) layer of Au. Two methods of covering metal were used: ion sputtering and vacuum evaporating. Process of ion



a)



b)

Fig. 1. The results of the different gold covering methods: a) with ion sputtering b) evaporated in high vacuum. Visible areas: 0.004  $\mu\text{m}^2$ .



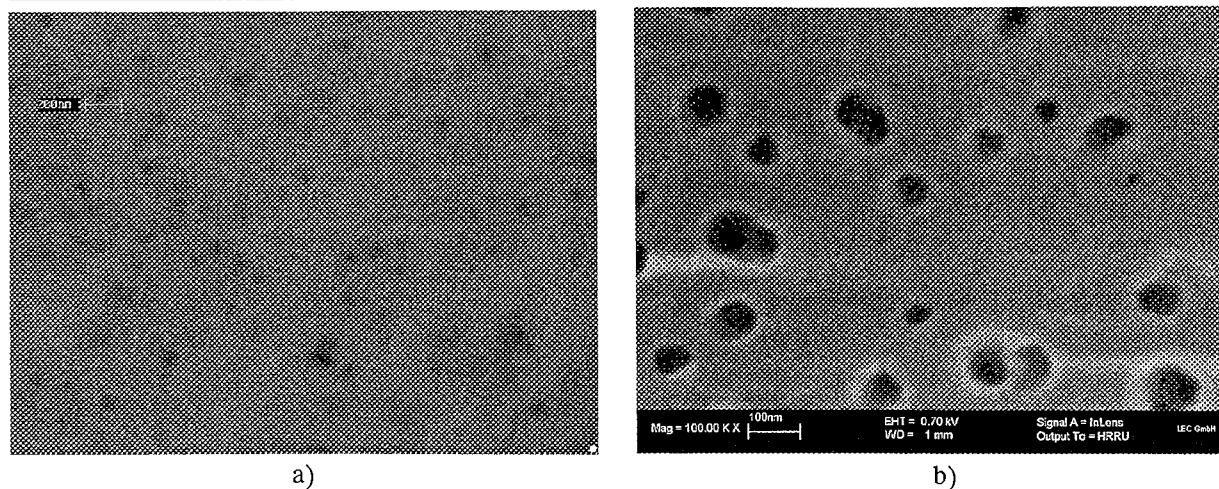


Fig.2. The view of polymer track membrane surface: a) in low-pressure mode, b) with low accelerating voltage.

sputtering was escorting with the formation of big grains of gold, which closed the small pores. The layer of this quality could not present well the details of specimen surface [4]. In the case when a vacuum evaporator was used, gold grains were smaller, details of surface can be observed, but cracks could be seen here (Fig.1).

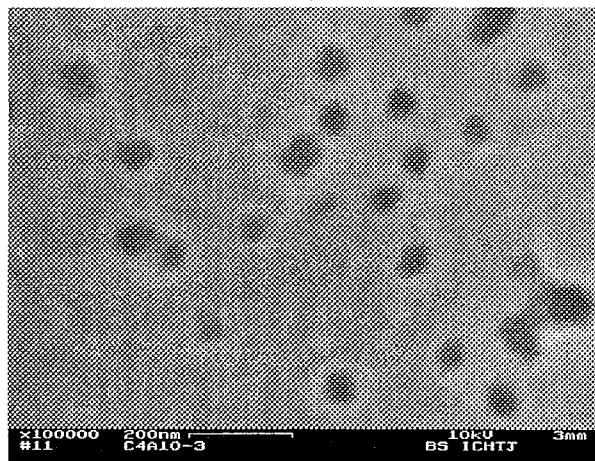


Fig.3. The surface of membrane covered with gold using the special facility (DSM 942).

To observe the non-changed membrane surface, SEMs that not required conductive covering were used. Results obtained with variable pressure mode (LEO 435VP) and with low accelerating voltage -

less than 1 kV (LEO 1530 GEMINI) show us that the cracks are not observed (Fig.2).

To minimise the influence of preparation conditions on the membrane, a special facility inside the bell of vacuum evaporator was constructed. The distance between the Au source and sample level was three times bigger than normally. Fig.3 shows us that the cracks are not viewed.

Final remarks: We have not observed cracks on the real, not changed surfaces of the investigated membranes. We could not see the cracks when the surface of the sample was not damaged during sample preparation. So, we can suggest that the previous cracks observed on the surface of the polymer track membranes were the result of the sample preparation process.

Thanks to Drs. A. Presz, M. Szudrowicz and J. Ackermann for help in SEM observations.

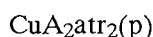
## References

- [1]. Spohr R.: Ion Tracks and Microtechnology. Principles and Applications. Vieweg, Braunschweig 1990, 272 p.
- [2]. Kuznetsov V.I., Didyk A.Yu., Apel P.Yu.: Rad. Meas., **19**, 1-4, 919-924 (1991).
- [3]. Orelowitch O., Sartowska B.: Methods of Scanning Electron Microscopy in Particle Track Membrane Investigations. X Conference on Electron Microscopy of Solids, Warszawa-Se-rock, Poland, 20-23 September 1999, pp. 397-400.
- [4]. Goldstein J.I.: Electron Microscopy and X-Ray Microanalysis, Text for Biologist, Material Scientists and Geologists. Plenum Press, New York 1992, 820 p.

## NEW WOOD PRESERVATIVES BASED ON COOPER COMPLEXES OF ETHANOLAMINE AND POLYAMINOTRIAZOLE

Andrzej Łukasiewicz, Luzja Rowińska, Lech Waliś

Studies are carried out in the Institute on new wood preservatives based on water solution of a cooper complex of polyaminotriazole (MAX) of general formula:



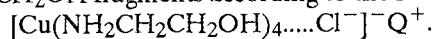
where A is the acetate anion, atr is 3-amino-1,2,4-triazole and (p) means a complex polycondensed with formaldehyde [1,2]. Good wood protection properties towards moulds were obtained by combining MAX with the cooper complex obtained by

treating  $\text{Cu}(\text{CH}_3\text{COO})_2$  or  $\text{Cu}(\text{OH})_2 \cdot \text{CuCO}_3$  with 4 moles of ethanolamine (EA) per 1 mol of Cu ( $\text{Cu}_4\text{EA}$ ). MAX +  $\text{Cu}_4\text{EA}$  (further on named as CC), showed a strong synergism of fungicidal activity after adding a quaternary alkyl ammonium salt (Q), particularly alkyl benzyl dimethyl ammonium chloride (Preventol R. Bayer product). Investigations were carried out to explain the nature of the CC-Q preparation: is it a mixture of components or it is a common complex formed by the ingredients. Ex-



tremely strong fixation of CC-Q in wood suggested the formation of a common complex. It has been found that Cu<sub>4</sub>EA binds effectively to silica gel with the formation of SiO<sub>2</sub> + Cu<sub>4</sub>EA material. This material was used for investigation of CC-Q MAX + Cu<sub>4</sub>EA

sist in the solvation of the anion (Cl<sup>-</sup> in Prevental R) by CH<sub>2</sub>OH fragments according to the formula:



Effectiveness of the CC-Q preparation in protection of wood is illustrated by the data of Table.

Table. Protection of pine wood with CC-Q towards mould *Coniophora puteana*\*.

Concentration of Cu in the preparation, % of Cu(CH <sub>3</sub> COO) <sub>2</sub>	Loss of weight [%]		
	before leaching	after leaching	control
0.2	9.5	14.4	44.8
0.4	6.7	5.3	55.1
0.7	4.7	3.9	52.8
1.0	0.7	1.1	41.9
2.0	0.0	0.0	50.3

\*This mould destroys wood causing loss of the weight.

and its water solution freshly prepared was shaken with SiO<sub>2</sub>. Cu<sub>4</sub>EA disappeared quickly but MAX remained in the solution in a considerable amount. When the mixture of MAX + Cu<sub>4</sub>EA was shaken with SiO<sub>2</sub>, after 4 h both components disappeared completely from the solution. So, a common complex MAX + Cu<sub>4</sub>EA is formed within 4 h. It has been found further that SiO<sub>2</sub>-Cu<sub>4</sub>EA binds above 3 moles of Q per 1 mol of Cu when shaken with an aqueous solution of Q. These results indicate that MAX, Cu<sub>4</sub>EA and Q form a common complex in the CC-Q preparation. The complex Cu<sub>4</sub>EA can be an interesting material for obtaining various fungicidal preparations. Mechanism of the complex formation may con-

This investigation was carried out in the Institute of Wood Protection, Warsaw Agricultural University. The CC-Q preparation is introduced to the market as wood preservative of new generation, effective and safe for the environment. Now, the method is being patented.

The work was supported by the Polish State Committee for Scientific Research - grant No 7T08E00315.

#### References

- [1]. Krajewski K.J., Łukasiewicz A., Ważny J.: 29th Annual Meeting for Wood Preservation Maastricht, the Netherlands, June 1998.
- [2]. Łukasiewicz A., Waliś L.: Mat. Lett., 30, 249 (1997).

## SILICA GEL MODIFIED WITH MANGANESE II AS A SELECTIVE SORBENT FOR GOLD AND SILVER

Andrzej Łukasiewicz, Luzja Rowińska, Lech Waliś

Silica gel (SiO<sub>2</sub>) modified with ethanolamine (EA) was described previously as an effective sorbent (SiO<sub>2</sub>-EA) for heavy metals [1,2]. SiO<sub>2</sub>-EA was not very effective for binding gold from dilute aqueous solutions. It has been found that SiO<sub>2</sub>-EA treated with MnCl<sub>2</sub> in water gives a material SiO<sub>2</sub>-EA(Mn) containing up to 5% of MnCl<sub>2</sub>. This material appeared to be a very effective sorbent for Au and Ag salts or complexes in water solution. Binding of Au or Ag consist in the reduction of the cation to the free metal by Mn<sup>2+</sup> on the sorbent surface. Due to this mechanism gold or silver can be bound selectively by the sorbent from water in the presence of other metals.

Recovery of the adsorbed metal is easily obtained by treating the sorbent with aqua regia (Au) or HNO<sub>3</sub>(Ag). Silica gel can be used again for the preparation of the sorbent SiO<sub>2</sub>-EA(Mn). Another silica-manganese sorbent was obtained from water glass (WG). WG was acidified, treated with CaCl<sub>2</sub> and then with MnCl<sub>2</sub>. The sorbent WG-Mn obtained in this way contained up to 4% of Mn.

The SiO<sub>2</sub>-EA(Mn) and WG-Mn sorbents showed a similar activity in binding Au and Ag from water. Effectiveness of binding Au from dilute water solution by the new silica-manganese sorbents is illus-

trated in Table. To 6.2 mg of AuCl<sub>3</sub> in 250 cm<sup>3</sup> of H<sub>2</sub>O, gold labelled with <sup>198</sup>Au (2.7E<sup>-5</sup>) was added and the solution was stirred for 20 min with 0.5 g of the sorbent. After complete sedimentation of the sorbent, the activity of the solution was measured. As follows from the Table, practically complete binding of Au by the sorbent from a very dilute solution (25 mg AuCl<sub>3</sub>/1 l) took place.

Table. Binding of AuCl<sub>3</sub> by the sorbents.

Sorbent	% of Au the sorbent	
	Time of sedimentation	
	1 h	24 h
SiO <sub>2</sub> -EA(Mn)	88	95
	92	94
	96*	95*
WG-Mn	-	94
	-	99*
	-	96*

\* mean value of 5 measurements.

The new silica-manganese sorbents can be used for the recovery of Au and Ag from wastes of various origin. The materials SiO<sub>2</sub>-EA(Mn, Au or Ag) and WG-Mn(Au or Ag) can also be of interest as new surface layer materials. Further investigation on properties and structure of these materials are in progress. Obtaining of the sorbents is being patented.

## References

[1]. Łukasiewicz A., Rowińska L., Waliś L.: Patent application P336188 (1999).

[2]. Łukasiewicz A., Rowińska L., Waliś L.: In: Annual Report 1999. INCT, Warszawa 2000, p. 121.

## STRUCTURE AND COMPOSITION OF Pd-Ti SURFACE ALLOY FORMED BY PULSED PLASMA BEAMS

Zbigniew Werner<sup>1/</sup>, Jerzy Piekoszewski, Adam Barcz<sup>2/</sup>, Rainer Grötzschel<sup>3/</sup>, Fridrich Prokert<sup>3/</sup>, Jacek Stanisławski<sup>1/</sup>, Władysław Szymczyk<sup>1/</sup>

<sup>1/</sup> The Andrzej Sołtan Institute for Nuclear Studies, Świerk, Poland

<sup>2/</sup> Institute of Physics, Polish Academy of Sciences, Warszawa, Poland

<sup>3/</sup> Forschungszentrum Rossendorf e.V., Dresden, Germany

High emissions of SO<sub>2</sub> and NO<sub>x</sub> from fossil fuel combustion in electric power plants create a major environmental problem over all Europe. One of the most perspective methods of these pollutants removal is an electron-beam dry scrubber process (EBDS), in which the flue gas is treated by high-power, high-energy electron beam [1]. The electron beam enters the process vessel through a 50 μm thick Ti window. The important corrosion processes occur on the flue gas side of the window, where a complex environment of ions, radicals and molecules exists during the operation of electron accelerator [2,3].

The corrosion resistance of titanium in sulfuric acid can be improved by alloying with palladium. The beneficial influence of palladium can be achieved e.g. through ion implantation (II), ion beam mixing (IBM), ion beam assisted deposition (IBAD), plasma source ion assisted deposition (PSIAD) and deposition with the use of high intensity pulsed plasma beams (HIPPB) in Deposition by Pulse Erosion (DPE) mode.

The main results obtained thus far using IBM, IBAD, PSIAD and DPE process can be summarized as follows.

Palladium coatings of up to about 400 nm thickness, deposited upon titanium by IBM, IBAD, and PSIAD produced significant improvements in the corrosion resistance of Ti foil in 0.1 M H<sub>2</sub>SO<sub>4</sub> and 0.1 M HNO<sub>3</sub> at 80°C. However, the adhesion of the coatings was weakened after 1000 h immersion, and the detachment of coating took place. The detachment occurred close to the original coating/titanium foil interface. Thus, no significant amount of Pd was detected at sites where it had detached. In contrast to the previous cases, in DPE processed samples a significant concentration of Pd (up to 70% of the original value) remains even if the thin near surface layer is also detached. At such sites, the corrosion resistance remains high due to the presence of sub-surface Ti-Pd alloy layer.

Since the inner layers of Pd-Ti alloy formed by the DPE process extends deeper than those in II, IBM, IBAD or PSIAD processed material, one can expect that the process may have advantages over conventional ion-beam-based methods. The aim of the present work was to gain insight into the structural and compositional properties of the near surface layers formed by the DPE process. The

samples used in the present work were taken from the same batches as those tested in our previous study [2,3]. They were characterized using X-ray diffraction (XRD) at a grazing angle geometry and a secondary ion mass spectroscopy (SIMS). XRD analysis showed that out of all possible stable phases in the Pd-Ti system only 3 can be identified. They are: hcp α-Ti, TiPd and TiPd<sub>3</sub>. Thus, Pd is present in our samples as a solute in Ti with grain size in the 250-300 nm range and two distinctive crystallographic phases with a grain size of 20-30 nm. The main results of SIMS analysis are as follows:

- Pd profiles exhibit a diffusive character, and their range increases monotonically from 1 to about 2 μm with the number of pulses (not taking into account a surface layer with the thickness below resolution limit of the method).
- If some experimental points close to the surface are ignored, most of the profiles can be fitted surprisingly well with gaussian distributions over almost 3 orders of magnitude. One should note that the gaussian profile is an analytical solution of the diffusion equation for a limited yield surface source, other conditions being constant.
- There is no evidence for an abrupt cut-off at the end of the profile, which must have been occurred if the melt depth was thinner than the diffusion range. This means that the melt depth was thinner than the diffusion range. This means the melt depth is at least as large as the length of undistorted diffusion profile. Basing on the computer simulation of heat evolution we estimated the diffusion time  $\tau$  as equal to about 10 μs.

Combining this result with the data on the Pd profile we estimated the diffusion constant of Pd in the liquid Ti as  $D=2.8 \times 10^{-5} \text{ cm}^2/\text{s}$ . An attempt was made to simulate the obtained Pd profiles with an appropriate theoretical model. The model assumes that (in agreement with experimental results) Pd is supplied to the surface after each pulse in portions, which diffuse into the substrate during the molten phase of the next pulse, leaving no metallic Pd at the surface. We also assume that the surface layer is molten during the pulse to a depth exceeding the diffusion range, that there is a constant period of liquid phase duration after each pulse and that the diffusion constant has a fixed value for the whole diffusion process. Thus, the



PL010101514

model assumes a multiple diffusion with limited yield source at the surface, replenished after each pulse. The problem was solved numerically by the mentioned above ETLIT program adapted for solving impurity diffusion equation instead of heat diffusion. The results of calculations are shown in Fig., in which the logarithm of concentration (in arbitrary units) is plotted vs.  $x^2$  (the "gaussian coordinates") and compared with experimental points normalized to the same total impurity content introduced by the diffusion. As we see, the theoretical fit fails since it is always a concave line in contrast with the experimental results, which follow the straight line. This result is a little surprising although obviously a number of experimental conditions are not taken into account in the simple model:

- diffusion time is not constant throughout depth - surface layers remain molten for a longer time than the deeper ones;
- diffusion constant may vary with temperature, which is also not constant over the diffusion range;
- Soret diffusion and segregation effects are ignored.

Further study is needed to clarify the mass transport in the liquid state induced by the DPE process.

In conclusion: The obtained results demonstrate that the well-defined Pd-Ti alloy layers with Pd concentration reaching 40% and depth up to  $2\ \mu\text{m}$  can be successfully produced in Ti by the DPE method. Since these layers extend deeper than those in II, IBM, IBAD or PSIAD processed material, one can expect that the DPE process may appear to be advantageous in comparison with conventional ion-beam-based methods of improving

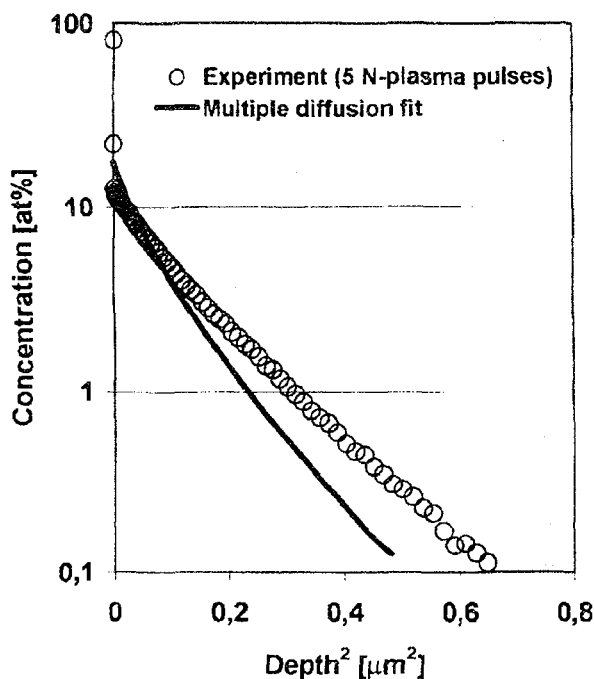


Fig. Pd profile after 5 N-plasma pulses plotted in gaussian coordinates and fitted with the theoretical results of multiple diffusion simulation normalized to the experimental content of Pd in Ti.

the corrosion properties of Ti windows used in EBDS systems.

#### References

- [1] Chmielewski A.G., Tymński B., Licki J., Iller E., Zimek Z., Dobrowolski A.: *Radiat. Phys. Chem.*, **42**, 663 (1993).
- [2] Piekoszewski J., Werner Z., Wieser E., Langner J., Grötzschel R., Reuter H., Jagielski J.: *Nukleonika*, **44**, 239 (1999).
- [3] Barson S.D., Skeldon P., Thompson G.E., Piekoszewski J., Chmielewski A.G., Werner Z., Grötzschel R., Wieser E.: *Corrosion Sci.*, **42**, 1213 (2000).

## INTERFACE IN Ti-Al<sub>2</sub>O<sub>3</sub> SYSTEM MANUFACTURED WITH THE USE OF HIGH INTENSITY PULSED PLASMA BEAMS

Jerzy Piekoszewski, Jacek Stanisławski<sup>1/</sup>, Rainer Grötzschel<sup>2/</sup>, Wolfgang Matz<sup>2/</sup>, Jacek Jagielski<sup>1/</sup>

<sup>1/</sup> The Andrzej Sołtan Institute for Nuclear Studies, Świerk, Poland

<sup>2/</sup> Forschungszentrum Rossendorf e.V., Dresden, Germany

In our previous work [1] it was shown that the high intensity pulse plasma beam (HIPPB) treatment can successfully be used in the preparation of alumina surface prior to manufacturing good alumina-cooper joints. In the present work we focused our attention on investigation of the structure and kinetics of the interface layer in the Ti-Al<sub>2</sub>O<sub>3</sub> system. Over 20 samples were prepared by irradiation of the alumina substrates with 2, 5 and 10 pulses of HIPPIB in deposition by erosion (DPE) mode, with titanium electrodes as the deposit source and nitrogen as the working gas. In addition also few samples with 20 pulses were prepared. To identify the phase structure of the processed samples, X-ray diffraction (XRD) measurements were performed on the step scan diffractometer in grazing angle geometry ( $\omega=1^\circ$ ) using CuK $\alpha$  radiation. The XRD patterns revealed evidence for the presence of

Al<sub>5</sub>O<sub>6</sub>N and AlN phases especially clearly observed for 20 pulses. The phases such as Ti<sub>3</sub>AlN and Al<sub>2</sub>TiO<sub>5</sub> can be identified with a less probability. These results are surprising for us since the TiO<sub>2</sub> (rutile) is usually considered as a phase that facilitates brazing when an active filler (containing titanium) is used. However, this rutile phase has not been identified in our samples. This results give us a hint that more detailed consideration should be undertaken toward the wettability of the phases observed in our samples. In order to get insight into the evolution of the titanium in-depth profile with the number of pulses, the Rutherford Back Scattering (RBS) measurements were performed on the processed samples. The RUMP program was used to fit the simulated spectra to the experimental data. The experimental spectrum for a given type of the sample i.e. for 2, 5 or 20 pulses was taken as an



PL0101515

average spectrum from 4 samples. The results of these fittings can be summarized as follows:

- 1) The bulk concentration of Ti atoms in the alumina substrate, i.e. beneath the surface, increases with the number of pulses as 0.17 : 0.83 : 1 for 2, 5 and 10 pulses respectively. This regularity is quite obvious in view of the fact that each pulse brings a new portion of Ti which is then mixed into the substrate by the liquid diffusion mechanism.
- 2) The aerial density of the metallic Ti film deposited on the surface (not mixed into the bulk) decreases with a number of pulses as 1 : 0.44 : 0.18 for 2, 5 and 10 pulses respectively. This is an unexpected result, since according to our understanding of the DPE process up to now, is that exclusively the last pulse in the series deposits a thin metallic film on the surface which is not mixed into the bulk. Therefore, we could have expected that the thickness of this film should not depend on the number of pulses and nominally should remain constant.

At present, we do not have yet a full understanding of the results reported in p.2. The tentative qualitative explanation of them can be as follows.

The lifetime of the molten phase (LMP) is shorter for the initial state of the substrate than that after the substantial number of pulses. Therefore, if LMP is short, the metallic atoms (and or low

energy ions) ablated from the electrodes reach the surface of the substrate when it is already solidified, being first molten by the nitrogen plasma pulse. On the contrary, if LMP is long enough, a fraction of the metallic atoms (and or low energy ions) reach the substrate when it is still molten and therefore they diffuse rapidly into the bulk. Hence, the amount of atoms forming the surface film is smaller than in the previous case. The possible reason for the difference in LMP in the virgin (or only slightly modified top layer after small number of pulses) can be twofold. First, it is possible that the new phases formed on the surface (see p.1) have lowered the melting temperature as compare to that of initial material of the substrate. Second, the heat conductivity between the top layer and bulk of the substrate decreases with the number of pulses. This would also lead to the rise of the LMP. The verification of this hypothesis requires numerical calculations of heat evolution in the substrate, basing on the thermo-physical properties of the virgin and DPE modified top layer of the system as well as on the energy spectra of the ablated metallic species. Further studies of these issues are in progress.

#### References

- [1]. Włosiński W., Krajewski A., Piekoszewski J., Stanisławski J., Waliś L.: Intense pulsed plasma beams in ceramic/metal brazing. *Nukleonika*, **45**(2), 145 (2000).

## DOPING OF TITANIUM WITH SILICON USING INTENSE PULSED PLASMA BEAMS

Edgar Richter<sup>1/</sup>, Jerzy Piekoszewski, Fridrich Prokert<sup>1/</sup>, Jacek Stanisławski<sup>2/</sup>, Lech Waliś

<sup>1/</sup> Forschungszentrum Rossendorf e.V., Dresden, Germany

<sup>2/</sup> The Andrzej Sołtan Institute for Nuclear Studies, Świerk, Poland

Strong adhesion in the coating-substrate system is a crucial issue in many technical applications. Recently [1], it has been found that silicon ion implantation into titanium enhances its adherence to the ceramic coatings thus improving the quality of the denture prosthesis based on a titanium skeleton. In the present work we attempted to manufacture a silicon surface alloy on titanium using high intensity pulsed plasma beams in two modes: PID and DPE. In PID, short intense plasma pulses ( $1 \mu\text{s}$ ,  $5 \text{ J/cm}^2$ ) serve as a source of heat to melt the near surface layer of the substrate together with the Si film pre-deposited on it. In DPE, apart from the plasma pulses also vapor of the electrode material is deposited and alloyed on the substrate. Two series of experiments have been performed. In the first one, denoted S1 titanium substrates were coated with silicon films of about 120 nm thick and then irradiated with 5 and 10 plasma pulses in PID mode with nitrogen or argon as the working (plasma) gas. In the second series S2, the DPE processing was exclusively adopted (i.e. without any external pre-deposition of silicon). Conical-shaped tips of electrodes coated with the help of the flame plasma spraying technique with about 0.1 mm thick layer of

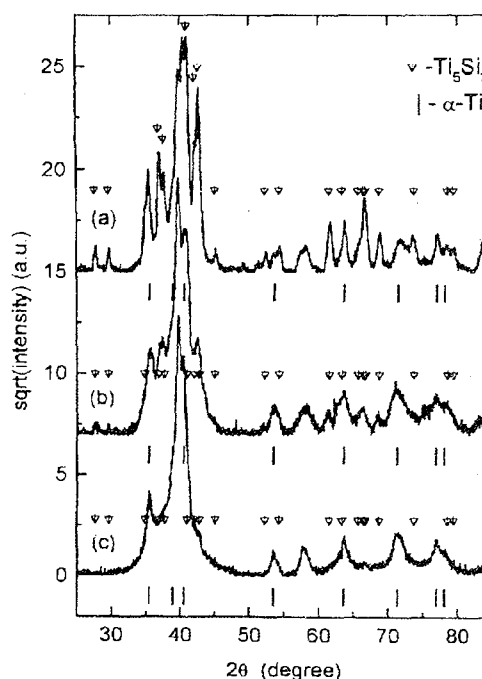


Fig. XRD patterns taken at grazing incident angle  $1^\circ$  for samples processed with 5 pulses in PID-mode (a), 10 pulses in PID-mode (b) and 5 pulses in DPE mode (c).



PL0101516

Si were the source of silicon. The samples were characterized by the following methods: Auger electron spectroscopy (AES) and X-ray diffraction (XRD) with to 1, 3 and 5° angles of grazing incidence. Fig. shows the XRD pattern taken at 1° for samples processed with 5(a) and 10(b) pulses in PID mode and for the sample processed with 5 pulses in DPE mode (c). Principal features emerging from the AES and XRD analysis are as follows:

- Mixing of Si into Ti occurs in both S1 and S2 modes of plasma processing.
- The mixing is more effective for argon than for nitrogen working gas in both the PID and the DPE modes.

- Maximum atomic concentration of silicon and the profile depth reach 40% and about 350 nm, respectively.

- The  $\text{Ti}_5\text{Si}_3$  silicide with the highest melting point (2130°C) is of all possible stable phases in the Si-Ti system formed in both S1 and S2 series.

In conclusion, it is expected that  $\text{Ti}_5\text{Si}_3$  formed in this way could be a good candidate as a diffusion barrier for oxygen in ceramic titanium joints in practical applications.

#### References

- [1]. Könönen M., Kivilathi J.: J. Biomed. Mat. Res., 28, 1027 (1994).

# NUCLEONIC CONTROL SYSTEMS AND ACCELERATORS

## XRF ANALYSIS OF LIGNITE ASH USING PARTIAL LEAST SQUARE CALIBRATION MODEL

Ewa Kowalska, Piotr Urbański

### Introduction

XRF is a very suitable method for the industrial analysis of calcium and iron in raw materials [1-3]. The same approach is proposed for the determination of these elements in the samples of lignite ash. However, one of the main problems connected with the application of XRF technique for the analysis of Fe and Ca is a strong matrix effect [1]. Moreover, when an Ar proportional counter is used for the detection of X-rays excited in the sample, the K Fe escape peak in argon and K Ca peak are overlapped. Both the factors, if not considered, can influence the accuracy of analysis, but it is possible to diminish their impact using multivariate calibration methods [4]. In the considered case, the calibration model was computed using partial least square regression (PLS) [4-6].

### Samples

The lignite ash consists of three main components:  $\text{SiO}_2$  (30-60%),  $\text{CaO}$  (20-45%) and  $\text{Fe}_2\text{O}_3$  (4-7%). To perform calibration, a set of 29 artificial reference samples was prepared. The powdered  $\text{CaCO}_3$ ,  $\text{SiO}_2$ ,  $\text{Fe}_2\text{O}_3$  and  $\text{H}_3\text{BO}_3$  were mixed together to obtain the required ranges of concentrations of  $\text{CaCO}_3$  and  $\text{Fe}_2\text{O}_3$ .

### Radiometry

X-ray fluorescence was excited with Pu-238 and Cd-109 sources and the secondary radiation was detected using Ar and Ne proportional counters. The output signal from the detector was fed to a multichannel analyser. The whole spectra registered by the multichannel analyser were used for computation of the calibration model.

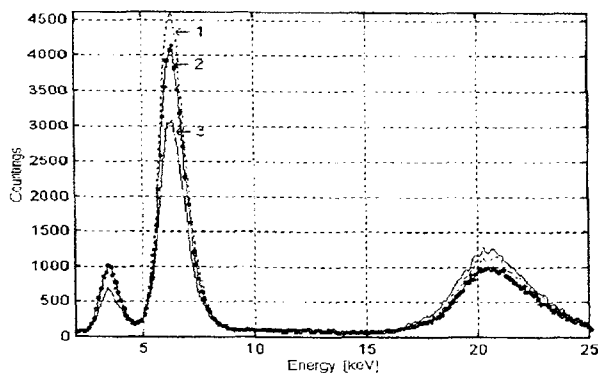


Fig.1. XRF spectra registered with the Ar proportional counter, excited with a Cd-109 source in powdered samples of different composition: 1 - 25%  $\text{CaCO}_3$ , 40%  $\text{SiO}_2$ , 6%  $\text{Fe}_2\text{O}_3$ ; 2 - 35%  $\text{CaCO}_3$ , 40%  $\text{SiO}_2$ , 6%  $\text{Fe}_2\text{O}_3$ ; 3 - 20%  $\text{CaCO}_3$ , 55%  $\text{SiO}_2$ , 4%  $\text{Fe}_2\text{O}_3$ .

### Calibration model

Spectra of the entire set of the calibration samples, registered with the various sources and detectors were used for computation of the PLS calibration models. The number of the PLS components to be included into the model was optimised using, as the figure of merit, a value of the root mean square error of crossvalidation (RMSECV). Computations were performed using PLS\_Toolbox v. 2.0 for MATLAB [7].

### Results and discussion

It was found that although for the Ne proportional counter there is no interference between the iron escape and calcium K peaks, the registered

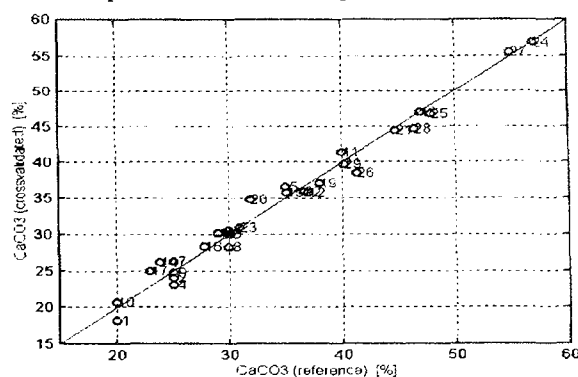


Fig.2. Relation between the  $\text{CaCO}_3$  content computed from crossvalidation and the reference values.

peak of the scattered radiation is so small that the information contained in this peak (e.g. about sample density) is lost. Also results of the iron determination were worse than in the case of the Ar counter. Both the sources, Pu-238 and Cd-109, appeared to be equally applicable. It was found that

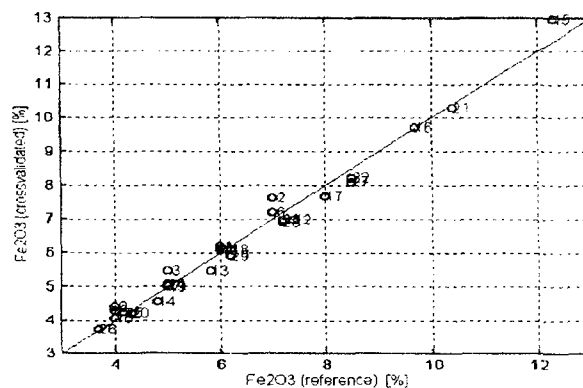


Fig.3. Relation between the  $\text{Fe}_2\text{O}_3$  content computed from the crossvalidation and reference values.

the optimal configuration is to use the Cd-109 source together with the Ar proportional counter. The spectra of the three samples of various concentration of the  $\text{SiO}_2$ ,  $\text{CaCO}_3$  and  $\text{Fe}_2\text{O}_3$ , registered in the chosen configuration, are shown in Fig.1. The minimal value of the RMSECV for the determination of calcium (1.35%  $\text{CaCO}_3$ ) was obtained for the model containing three PLS components. In the case of iron, the minimal value of RMSECV was 0.26%  $\text{Fe}_2\text{O}_3$ , and was obtained for the spectra normalised to the constant peak of the scattered radiation. The relation between the  $\text{CaCO}_3$  content computed from crossvalidation versus its reference value is shown in Fig.2. A similar relation for  $\text{Fe}_2\text{O}_3$  is presented in Fig.3.

### Conclusion

It is possible to determine iron and calcium content in powdered samples of the lignite ash using the XRF method with the PLS calibration model.

## FEASIBILITY OF PLS CALIBRATION MODELS FOR INSTRUMENTS MEASURING ASH IN COAL USING GAMMA RAY SCATTERING METHODS

Ewa Kowalska, Piotr Urbański

### Introduction

Radioisotope devices measuring the ash content and calorific value of coals have been successfully applied in the mining and energy producing industry. Among the variety of radiometric methods suitable for this purpose, the methods based on the back and forward scattering of  $\gamma$ -rays from an Am-241 source with a scintillation detector are very often applied in instruments installed in the Polish industry [1]. Due to the spectrometric feature of the scintillation detectors, the output signal from a sensor containing such a detector can be registered in the form of an energy spectrum. The aim of this work was to investigate whether the application of multivariate calibration methods (e.g. PLS [2-8]), where a full spectrum is used as the independent variable, can result in improvement of the instrument performance. Moreover, an attempt was made to compute one calibration model for the coals of variable chemical composition and originating from different mines. Such a question is very important in the case when the radiometric instruments measuring ash are installed in power stations where the coal is delivered from different mines. Calibration models were computed using PLS\_Toolbox v. 2.0 for MATLAB [9] and some home made software.

### Calibration samples

Calibration models were computed using results of measurements performed on the same set of the samples with instruments operating on the principles of back and forward scattering of the Am-241  $\gamma$ -rays. In the case of the forward scattering instrument, the result for sample No 11 was missing. The samples originated from four different mines and their composition varied considerably [7]. Fig.1 shows the relation between  $\text{Fe}_2\text{O}_3$  and ash content over the entire set of the measured samples. It can

RMSECV for the  $\text{CaCO}_3$  content within the range 25-45% is about 1.35% (abs) and for  $\text{Fe}_2\text{O}_3$  ranging from 4 to 7% is about 0.26% (abs). The analysis can be performed using a simple instrument with the radioisotope Cd-109 source and the Ar proportional counter.

### References

- [1]. Dziunikowski B.: Energy Dispersive X-Ray Fluorescence Analysis. PWN, Warszawa 1989, 431 p.
- [2]. Wasilewska-Radwańska M.: Scientific Bulletins of the Stanisław Staszic University of Mining and Metallurgy, 633 (33), (1977).
- [3]. Spiewak et al.: Poland International Cement Review, December 1994.
- [4]. Martens H., Naes T.: Multivariate Calibration. Wiley & Sons, Chichester 1991, 420 p.
- [5]. Urbański P.: Appl. Radiat. and Isot., 45, 659-669 (1994).
- [6]. Urbański P., Kowalska E.: X-Ray Spectrom., 24, 70-75 (1995).
- [7]. Wise B.M., Gallagher N.B.: PLS\_Toolbox 2.0 for use with MATLAB. Eigenvector Research Inc., 1998, 320 p.

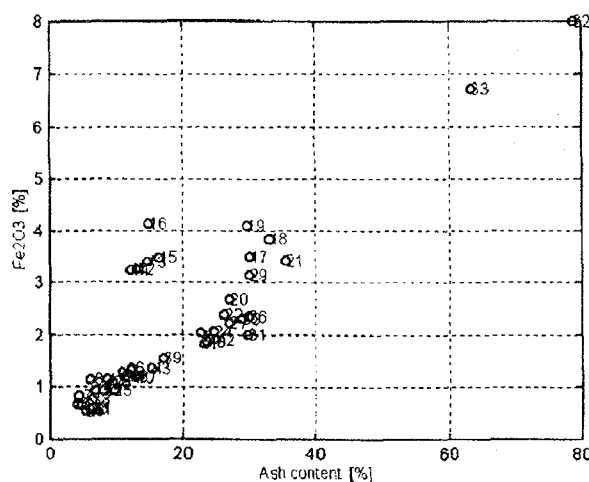


Fig.1. Concentration of  $\text{Fe}_2\text{O}_3$  versus ash content in the reference set of samples used for calibration.

be observed an unusually high iron content for a sub set of the samples No 12-16 (Fig.1).

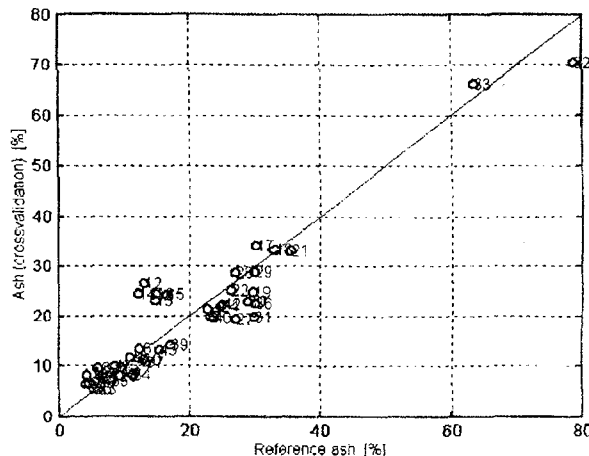


Fig.2. Results of calibration using a non-linear PLS model.



PL0101518

### Results and discussion

Four different models were investigated: linear PLS with mean centered data, linear PLS with

bration may improve performance of the instruments measuring ash in coal using back and forward scattering technique, but it is not possible fully

Table. Root mean square error of crossvalidation for different calibration models. Number of the PLS components included to the models are shown in brackets.

Radiometric method	Calibration set	PLS (mean centred)	PLS (standardised)	Non-linear PLS	MLR
$\gamma$ -rays backscattering	full spectrum, 43 samples	4.180 (4)	4.069 (3)	4.751 (1)	6.144
	full spectrum, 33 samples	2.225 (4) 3.470 (1)	4.008 (3)	2.413 (2) 2.516 (1)	3.634
$\gamma$ -rays forward scattering	full spectrum, 42 samples	4.694 (3)	3.604 (4)	4.950 (2)	6.167
	full spectrum, 32 samples	3.842 (1)	3.864 (1)	2.263 (3) 3.439 (1)	3.768

scaled data, non-linear PLS and multilinear regression (MLR) where the independent variable was determined as the area under the entire spectrum. The models were computed for the full set of samples (43 or 42 in the case of the forward scattering), as well as for the set of 33 or 32 samples obtained after removing a subset of 10 samples of very high iron content originated from one mine (No 12-16 and five others). It can be seen from the Table that the best calibration results were obtained for the non-linear PLS model for the sets containing 33 or 32 samples. The root mean square error of crossvalidation for the PLS models is considerably smaller than that for the MLR model. Differences between models computed for the back and forward scattering methods are negligible. It can be also concluded that the multivariate cali-

compensate the influence of the unusually high iron content in the measured sample (Fig.2).

### References

- [1]. Sikora T., Czerw B.: *Nukleonika*, **44**, 4, 669-674 (1999).
- [2]. Martens H., Naes T.: *Multivariate Calibration*. Wiley & Sons, Chichester 1991, 420 p.
- [3]. Urbański P.: *Appl. Radiat. and Isot.*, **45**, 659-669 (1994).
- [4]. Urbański P., Kowalska E.: *X-Ray Spectrom.*, **24**, 70-75 (1995).
- [5]. Urbański P., Kowalska E., Antoniuk W.: *Nukleonika*, **40**, 1, 61-66 (1995).
- [6]. Urbański P., Kowalska E.: *Nukleonika*, **42**, 3, 719-726 (1997).
- [7]. Kowalska E., Urbański P.: *Raporty IChTJ. Seria B nr 10/2000. IChTJ, Warszawa 2000*, 24 p.
- [8]. Urbański P., Kowalska E.: *Wielowymiarowe metody kalibracji przyrządów pomiarowych. Materiały IV Szkoły-Konferencji "Metrologia Wspomagana Komputerowo"*, Rynia k/Warszawy, 7-10 czerwiec 1999, T.3, s. 251-258.
- [9]. Wise B.M., Gallagher N.B.: *PLS\_Toolbox v. 2.0 for use with MATLAB*. Eigenvector Research Inc., 1998, 320 p.

## PORTABLE RADON-IN-AIR CONCENTRATION MONITOR RMR-1

Jakub Bartak, Jan P. Pieńkos

In the decade of 1980 a set for measurement of radon concentration in air was developed in this Institute. The set consists of a measuring head as a attachable unit GF-10 to mining radiometer RGR-13.

Increasing interest in radon measurements encouraged the development and application of a modern monitor employing a Lucas cell as radon detector, controlled by a microprocessor system. The block diagram of the monitor is shown in Fig.1. The Lucas cell is connected with a photomultiplier tube (PM) by an appropriate mechanism. The UKPP unit controls setting of PM diaphragm and is checking if the position measuring cell is correct.

The Lucas cell has a form of a cylinder, 170 cm<sup>3</sup> in volume, covered inside with a ZnS(Ag) scintillator for registration of alpha radiation. In the upper part of the cell there are two stubs allowing to flow the radon-laden-air through the cell. Generated light pulses resulting from alpha radiation produce current pulses at the output of PM tube. The pulses, after amplification in WI and discrimination by a pulse discriminator DYS, are counted in programmed time interval and processed. The operation of the monitor is controlled by a microcomputer unit that can be programmed with a keyboard placed at the front of panel (Fig.2). The

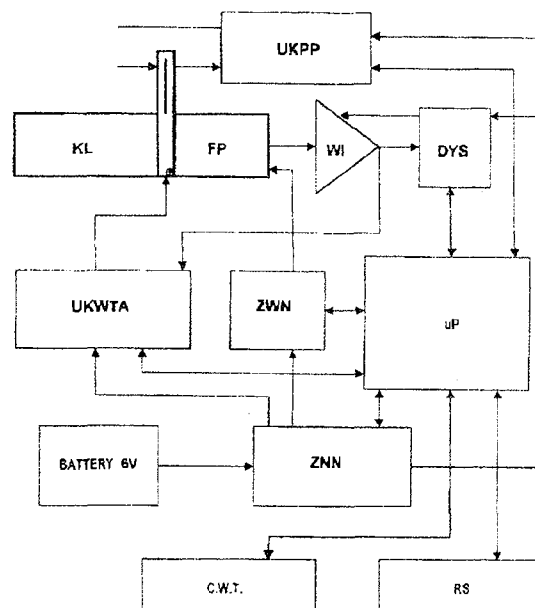


Fig.1. Block diagram of radon concentration monitor: FP - photomultiplier tube (PM); KL - Lucas cell; WI - pulse amplifier; DYS - pulse discriminator; UKPP - pulse location circuit (diaphragm position control circuit); UKWTA - gain control circuit of analog channel; ZNN - low voltage power supply; ZWN - high voltage power supply; uP - microcomputer; C.W.T. - pressure, temperature, humidity sensors; RS - serial port RS232.



PL0101519



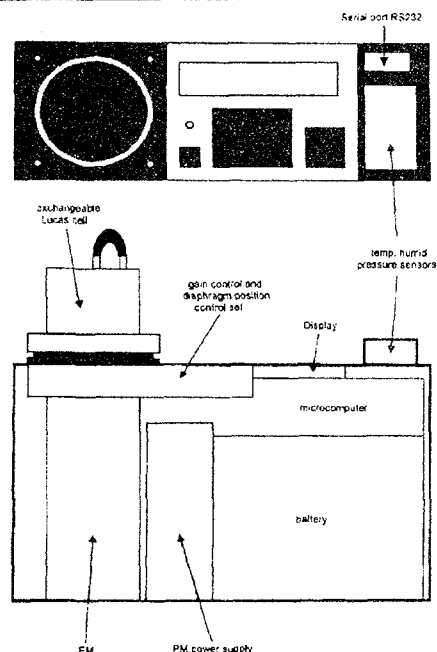


Fig.2. Components displacement of radon concentration monitor.

appropriate mode of operation, run of the measuring cycle, and results of the measurement are shown at a LED display. The measured results are also stored in the internal memory of the gauge and can be reviewed any time. A serial port RS232 enables transmission of the measured results to the external PC or to a serial printer to make a hard-copy.

Thanks to the automatic gain control circuit of the analog measuring channel, stable operation of the monitor and its accuracy is ensured, despite of the variation of ambient temperature and other agents. A built Ni-Cd battery feeds high voltage and low voltage power supplies and ensures continuous measurements of radon concentration within 300 h until recharging of the battery is necessary. The expected lower limit of detection is not worse than  $11 \text{ Bq/m}^3$ . The monitor can operate in a single reading or in a continuous mode of operation. Apart of the radon concentration, the ambient temperature, relative humidity and atmospheric pressure are also measured.

## USE OF MULTIVARIATE PROCESSING IN GAUGES FOR RADON AND RADON DAUGHTERS CONCENTRATION IN AIR

Bronisław Machaj, Piotr Urbański

### Introduction

An important factor limiting the accuracy of measurement of radon, or radon daughters concentration is a random error due to statistic fluctuations of ionizing radiation, limiting also a minimum detectable concentration of radon and its progeny. An attractive method of decreasing random error seems to be multivariate signal processing of the raw signal registered with the measuring head of a gauge.

Multivariate regression can generally be expressed as [1-3]:

$$\mathbf{Y} = \mathbf{X}\mathbf{B} + \mathbf{E} \quad (1)$$

where:  $\mathbf{Y}$  is the matrix with  $n$  rows and  $p$  columns representing  $p$  dependent variables (radon concentration),  $\mathbf{X}$  is the matrix of independent variables with  $n$  rows and  $m$  columns representing  $n$  measured signals (raw count rate spectra) in  $m$  "channels",  $\mathbf{E}$  is the matrix with  $n$  rows and  $m$  columns representing the residual error. Principal Component Analysis (PCA) is a method representing matrix  $\mathbf{X}$  of independent variables in the form:

$$\mathbf{X} = \mathbf{t}_1\mathbf{p}_1' + \mathbf{t}_2\mathbf{p}_2' + \dots + \mathbf{t}_a\mathbf{p}_a' \quad (2)$$

where:  $\mathbf{t}$  are the vectors (scores) with  $n$  rows (and 1 column) whose elements are the coordinates of the respective points on the principal component line,  $\mathbf{p}'$  are the transposed vectors (loadings) with  $m$  columns (and 1 row),  $a$  is the number of factors (number of principal components) used. The  $\mathbf{X}$  matrix of raw data is replaced by the sum of limited number  $\mathbf{t}_i\mathbf{p}_i'$  of products (usually a few) containing useful information on dependent variables and rejected higher principal components containing mainly random noise.

### Random error of PCA processed signal

Principal Component Analysis was applied to the set of 41 measurements of radon daughters concentration in air [4,5]. The measured (raw) count and PCA processed spectra are shown in Fig. It was found that PCA processed spectra with two principal components with a satisfactory accuracy carry information of the concentration of radon daughters. The spectra with 2 principal components are shown in the Fig. As can be seen from the two count rate spectra in Fig., a great part of random fluctuations responsible for random error that are superimposed on the spectra carrying information on the concentration, is removed. To investigate more in detail how great is the reduction of the random error some simulations were carried out. Employing relations describing the series decay of radon into short lived radon daughters [6] and simulating the process of deposition of the radon daughters on an air filter, the matrix of equivalent count rate spectra  $\mathbf{X}_s$  without random fluctuations were computed. The simulated spectra  $\mathbf{X}_s$  were then randomized according to Poisson distribution. Achieved in such a manner randomized spectra  $\mathbf{X}_{sr}$  were used for computation of radon daughters concentration according to standard equations (without PCA processing) and employing regression coefficients  $b$  determined earlier. This procedure was repeated 10 times, then root mean square error (RMSE) was computed for both cases. The results of computations are given in Table 1. The group 1-25 measurements corresponds to lower concentrations, whereas the 1-49 group corresponds to the full range of concentrations measured. It can be



PL0101520

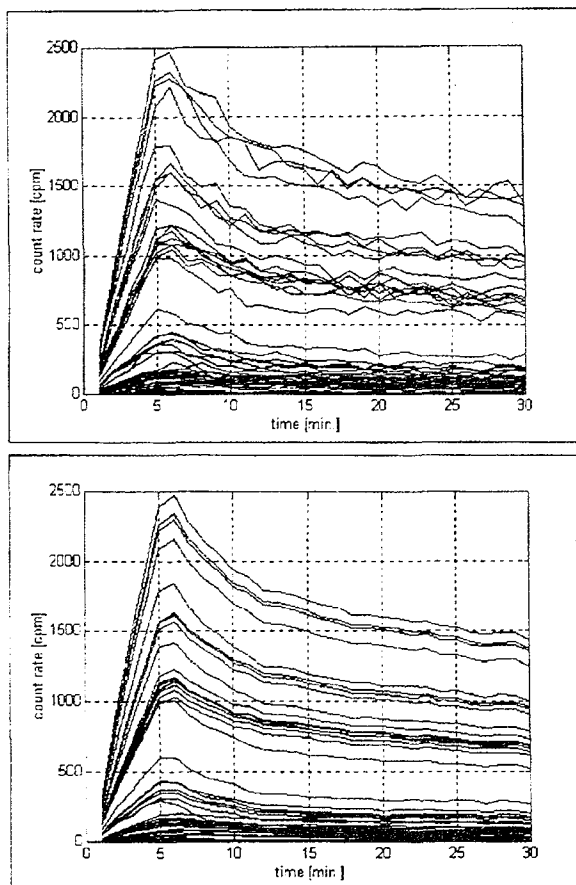


Fig. Raw (up) and PCA processed spectra (down) of the monitor of radon daughters concentration in air.

seen from the Table that thanks to PCA processing, 2-3 times reduction of random error can be

Table 1. Average RMSE of radon daughters concentration from raw and PCA processed count rate spectra with simulated random fluctuations.

Measurement number	RMSE(A) [Bq/m <sup>3</sup> ]	RMSE(B) [Bq/m <sup>3</sup> ]	RMSE(C) [Bq/m <sup>3</sup> ]	RMSE(E) [μJ/m <sup>3</sup> ]
1-25 simulated raw	157	123	99.7	0.233
1-25 PCA processed	87.0	14.9	28.1	0.058
1-49 simulated raw	434	338	269	0.647
1-49 PCA processed	207	34.4	70.7	0.132

1-25 measurement number: A=0-873 Bq/m<sup>3</sup>, B=0-797 Bq/m<sup>3</sup>, C=0-1046 Bq/m<sup>3</sup>, E=0.11-3.75 μJ/m<sup>3</sup>.

1-49 measurement number: A=0-11730 Bq/m<sup>3</sup>, B=0-9180 Bq/m<sup>3</sup>, C=0-10460 Bq/m<sup>3</sup>, E=0.11-53.7 μJ/m<sup>3</sup>.

A - <sup>218</sup>Po, B - <sup>214</sup>Pb, C - <sup>214</sup>Bi, E - alpha potential energy.

achieved. The PCA processing acts here as a kind of random noise filter [7].

Similar simulations and computations were also carried out for a gauge of radon concentration in air employing the Lucas cell as alpha radiation detector from radon and its progeny [8]. The results of computations of RMSE are shown in Table 2.

The RMSE(1-180) corresponds to the situation when the count rate was measured within 180 min after radon being introduced into the Lucas cell. In the case of RMSE(161-180), after introduction of radon into the Lucas cell it was left until a quasi radiation equilibrium inside the Lucas cell was reached and then the pulse counting started. It can be seen again from the Table that RMSE(1-180) is

Table 2. Average RMSE of radon concentration from raw and PCA processed count rate spectra with simulated random fluctuations.

Measurement number	RMSE(1-180) min [Bq/m <sup>3</sup> ]	RMSE(161-180) min [Bq/m <sup>3</sup> ]
1-10 simulated raw	87.9	125
1-10 PCA processed	38.5	115
1-21 simulated raw	213	278
1-21 PCA processed	82.4	311

1-10 measurement number: radon concentration = 405-8790 Bq/m<sup>3</sup>.

11-21 measurement number: radon concentration = 9590-45350 Bq/m<sup>3</sup>.

approximately 3 times lower (at low radon concentration) when PCA processing is used.

### Conclusions

Multivariate regression based on Principal Component Analysis applied to the raw count rates from the alpha radiation detector of radon daughters monitor improves accuracy of the gauge about 3 times. In the case of Lucas cell as radon detector, the improvement of the gauge is similar.

The multivariate signal processing is based on a set of count rates spectra measured in a fixed time period. This fact imposes limits to the application of such processing to cases where calibration of radon or radon daughters can be performed with such spectra. In case of continuous measurement of radon concentration such processing cannot be used.

The price that has to be paid for the reduction of random error employing multivariate signal processing is that the signal from the measuring head has to be measured each minute and slightly more sophisticated processing must be applied to the

signal from the measuring head. As the majority of present gauges are equipped with microprocessor systems, this is no serious problem.

### References

- [1]. Geladi P., Kowalski B.R.: Anal. Chim. Acta, 185, 1-17 (1986).
- [2]. Martens H., Naes T.: Multivariate Calibration. Wiley & Sons, Chichester 1991.
- [3]. Rencher A.C.: Multivariate statistical inference and application. John Wiley & Sons, New York 1998.
- [4]. Gierdalski J., Bartak J., Urbański P.: Nukleonika, 38, 27 (1993).
- [5]. Machaj B.: Nukleonika, 44, 479-490 (1999).
- [6]. Ewans R.D.: The Atomic Nucleus. McGraw-Hill Book Company, 1970, p. 972.
- [7]. Wold S., Anti H., Lindgren F., Ohman J.: Chemometrics and Intelligent Laboratory Systems, 44, 175-185 (1998).
- [8]. Machaj B., Urbański P.: Nukleonika, 44, 579-594 (1999).

## GAUGE FOR MEASUREMENT OF DOSERATE AND ACTIVITY OF Ru-106 BETA SOURCE FOR IRRADIATION OF EYE CANCER

Bronisław Machaj, Edward Świstowski, Cuong Do-Hoang

### Principle of operation

Medical clinics dealing with the cancer of eye, to cure the illness, nowadays, frequently employ irradiation of the tumor with beta radiation [1,2]. Irradiation beta sources have a concave shape, curvature radius 10 to 15 mm, and diameters 11 to 25 mm matching the shape of eye ball. Depending on the tumor position and the eye ball size a proper beta source is attached to the treated eye for a period ensuring that the cancer is irradiated with an exactly required dose. A physician, to be able to determine the irradiation period ensuring required dose, has to know the distribution of doserate of beta radiation emitted from the source within the eye ball. The eye ball tissue can be simulated by water with a satisfactory accuracy. Thus, the dose-rate produced by beta radiation has to be measured by the gauge in water environment. A gauge enabling such measurements is presented here.

The principle of operation of the gauge is illustrated in Figs.1 and 2. The source under investigation is fixed inside a container filled with water. A

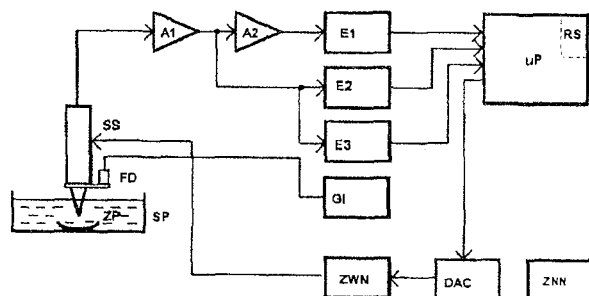


Fig.1. Functional diagram of a gauge for measurement of radiation doserate and activity of a Ru-106 beta source: SP - movable container filled with water; ZP - investigated radiation source; SS - scintillation probe; FD - light emitting diode; A1, A2 - pulse amplifiers; E1, E2, E3 - pulse discriminators; GI - pulse generator; ZWN - high voltage power supply; DAC - digital-analog converter; ZNN - low voltage power supply; uP - microprocessor.

scintillation probe employing a plastic scintillator  $\phi 2 \times 2$  mm coupled to a photomultiplier tube (PM) by a conical lightguide is used as beta radiation detector. The container with the source is moveable in horizontal and vertical direction. Additionally, the container can be rotated around the vertical axis permitting for measurement of the doserate at any point above the source area. A replaceable bronze collimator  $\phi 2 \times 23$  mm that can be put on the scintillator permits to check inequality of radioactive material on the surface of the source. The scintillation probe during measurement remains fixed. A fine micrometer screw is used to move the container with the source in horizontal and vertical direction with an accuracy of 0.01 mm. The range of horizontal and vertical movements are 25 and 50 mm, respectively, although the movement in vertical direction equal to 25 mm seems to be adequate

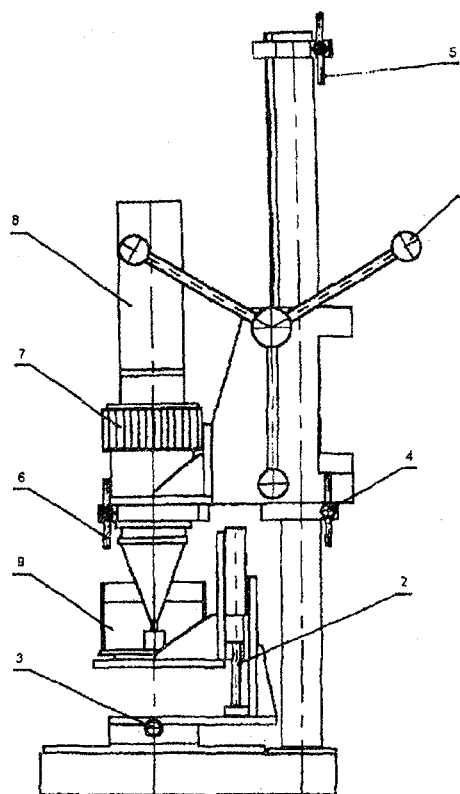


Fig.2. Measuring head of the doserate and activity gauge for Ru-106 sources: 1 - handle for moving scintillation probe in vertical direction, 2 - vertical movement screw, 3 - horizontal movement screw, 4 - lower limiter of scintillation probe, 5 - upper limiter of scintillation probe, 6 - scintillation probe lock, 7 - fine vertical adjustment of scintillation probe, 8 - scintillation probe, 9 - moveable container.

for a Ru-106 source. The vertical range of 50 mm can eventually be employed for other more penetrating radiation. A total accuracy of setting the radiation source in respect to the scintillator is not worse than 0.1 mm. Output pulses from the PM corresponding to detected beta particles after amplification and pulse discrimination E1 are fed to a microprocessor system where they are counted and processed. Prior to discrimination, the pulses from the scintillation probe are formed to a semi-Gaussian shape with the width equal to  $1 \mu\text{s}$  at a 10% level of the pulse amplitude, and a base line restorer keeps the base line level equal to zero. An automatic gain control circuit is employed to control the gain of the scintillation probe. The light emitting diode, fed from a current pulse generator, coupled to the lightguide between the scintillator and a PM photocathode produces reference light pulses. Amplitude of the light pulses is sensed by two pulse discriminators E2, E3 when the high voltage of PM tube is varied by the microprocessor (through digital-analog converter plus high voltage power).

Apart from the measurement of the doserate, the radiation activity of the source can also be mea-

sured with the gauge. To measure activity of the investigated source, the scintillation probe is raised 250 mm high in vertical direction above the source (from lower fixed position to upper fixed position of the probe, Fig.2). At such a source-detector distance, the ratio of the distance to source diameter is not lower than 10 and the source can be considered as a point source with an acceptable approximation.

The measuring results obtained in programmed counting time 20..120 s, are displayed and stored in the memory together with their parameters and comments (date and time of measurement, coordinates of scintillator with respect to the source and its type, kind of measurement) and are transmitted by RS232 serial port to a PC computer. When processing the signal from scintillation probe (pulse count rate) dead time correction is made. The gauge is equipped with an internal pulse counter allowing calibration of the gauge. Some auxiliary program functions (manual setting of PM high voltage, reference light emitting diode on/off) together with internal pulse counter enable checking proper operation of the gauge.

#### Performance

As it was already mentioned, the gauge is equipped with an automatic gain control circuit of the PM tube that is automatically activated when mains is switched on. Such a solution eliminates a long term PM tube gain variation and a long term temperature variation. The error due to the inaccu-

racy of setting the high voltage of PM tube that can be set in 2 V steps (0.2%) results in an error of count rate 0.4%. Expected maximum count rate when the scintillator housing touches the source surface is about 150 000 c/s (4 MBq source gives the count rate 42000 c/s). At such a high count rate the random error due to statistical fluctuations is well below <0.5% depending on the source-detector distance and counting time. Minimum count rate when the scintillation probe is in the upper limit position for the measurement of source activity is about 30 c/s (at 4 MBq), which at a counting time of  $t=120$  s gives random error 1.6%. Measured instability of the count rate during 7 h of operation of the gauge was <1.2% peak-to-peak.

Differential spectra of Ru-106 radiation measured in the water environment are shown in Fig.3. It can be seen that not only the count number is changed but also the shape of the spectrum varies when the source-detector distance varies due to changed geometry of measurement. Measurements of count rates with and without the plastic scintillator in the scintillation probe, in the water environment, indicate that the induced scintillations inside the lightguide connecting the scintillator with the PM photocathode is 0.4% of the count rate measured with the scintillator. Comparison of the count rate and electric charge (current) carried by analog pulses entering the pulse discriminator, proportional to light intensity induced in the scintillator, show that there is a constant ratio between the count rate and current when count rate varied from 100 (at the surface) to 5% (a few mm from the surface), and are independent of the point of measurement with respect to the source. This result suggests that variation of the shape of differential spectra shown in Fig.3 has little influence on the measuring result. Relative variation of count rate in

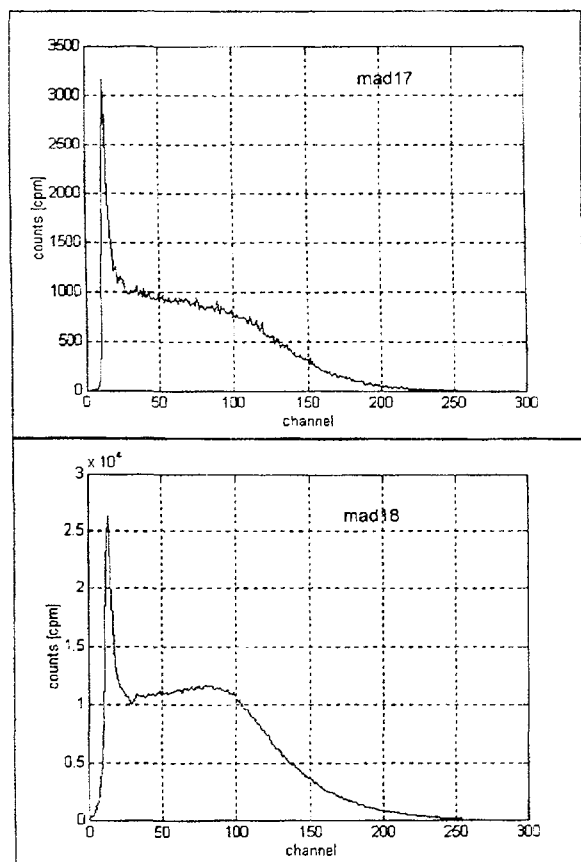


Fig.3. Differential spectra of Ru-106 measured in water environment when scintillator touches the surface in the center of the source (down) and when the distance is increased by 8 mm (up).

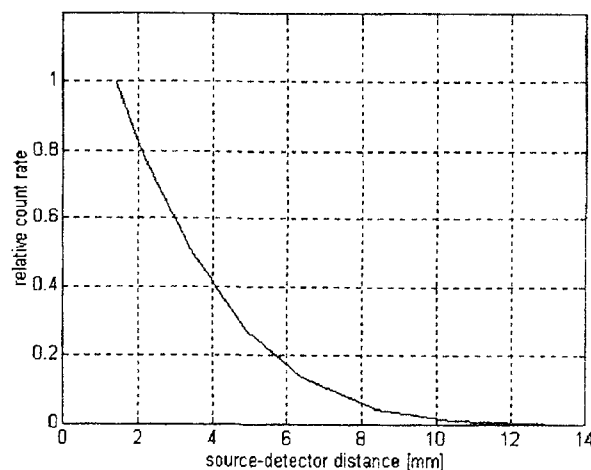


Fig.4. Relative count rate of Ru-106  $\phi 15$  mm in water environment. The source-detector distance is given from the center of the scintillator to the surface of the source in the center of the source.

water environment from the distance source-detector is shown in Fig.4.

This work was supported by the Polish State Committee of Scientific Research under the task project 8T11RE 04099 agreement No 2413/C.T11-8/99.

## References

[1]. Fluhs D., Heintz M., Wieczorek C.: *Med. Phys.*, 23, 427-435 (1996).

[2]. De Almeida C., DeWerd L., Jarvinen H., Soares C.G.: Guidelines for the calibration of low energy photon sources and beta-ray brachytherapy sources. Report International Atomic Energy Agency, 2000, IAEA DMRP-200002.

## PERFORMANCES OF LAE 10 ACCELERATOR WITH A THREE ELECTRODE ELECTRON GUN WITH MESH GRID

Zygmunt Dźwigalski, Zbigniew Zimek

## Introduction

The electron accelerator LAE 10 has been constructed in the Department of Radiation Chemistry and Technology of this Institute [1-3]. This facility is dedicated to pulse radiolysis and related experiments in the field of radiation chemistry. The following accelerator parameters are the most interesting from the point of view of experiments:

- the amplitude of the electron beam pulse;
- the duration of the accelerator electron beam pulse;
- the relation between the pedestal charge  $Q_p$  and the total charge  $Q_t$  of the accelerator pulse ratio.

The dose rate is defined by accelerator parameters. It is proportional to the duration and accelerator pulse current amplitude. The absorbed dose is proportional to the current density of the accelerator pulse. Therefore, time shape and space shape of the pulse should be measured. The smaller value  $Q_p/Q_t$  parameter may cause a smaller error in radiolysis experiment results. The pulses whose pedestal charge is less than or equal to 0.1 of total charge can be accepted, but it might be better if pedestal charge  $Q_p$  was considerably smaller. The aim of this work is to present the results of pulses shape measurements. The results was obtained for different parameters of the three electrodes electron gun. The control electrode (grid) of the gun consist of the main part with rotational symmetric and an additional element - the "flat" mesh grid. The results has been compared with the results obtained for the control electrode of the gun without mesh grid.

## Experimental arrangement

The measuring circuit - with a TDS 620 Tektronix digital oscilloscope (400 MHz band) and a specially designed Faradays cup were used [4]. The measurements of the pulse shapes between cathode and anode of the gun was realized at the same time (for selected accidents) with the assistance of the second channel of the TDS 620 oscilloscope. A high voltage pulse divider of own construction (by ratio of transformation 1:1000) was applied. The divider was made with ceramic non-inductive disk resistors M001, HVR International LTD firm. The measurements of the pulse shapes between the cathode and grid of the gun were performed using a Tektronix probe P5100 and the TDS 620 oscilloscope. We could realize these measurements only when the anode modulator was switch off because the cathode and grid were on high potential (tens kilovolts) in relation to the ground, if the modulator is in operation.

## Results and discussion

Fig.1 shows the relation between the accelerator electron beam current amplitude and the gun acce-

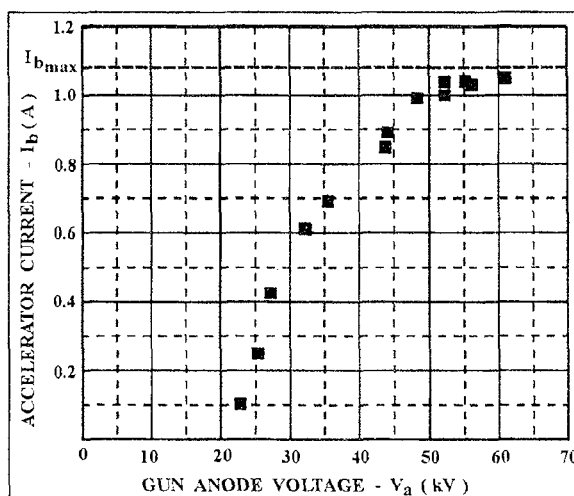


Fig.1. The relation between accelerator electron beam current amplitude and gun anode voltage.

lating voltage (gun anode voltage) amplitude  $V_a$ . The current amplitude increases with voltage amplitude and the curve is saturated when the voltage

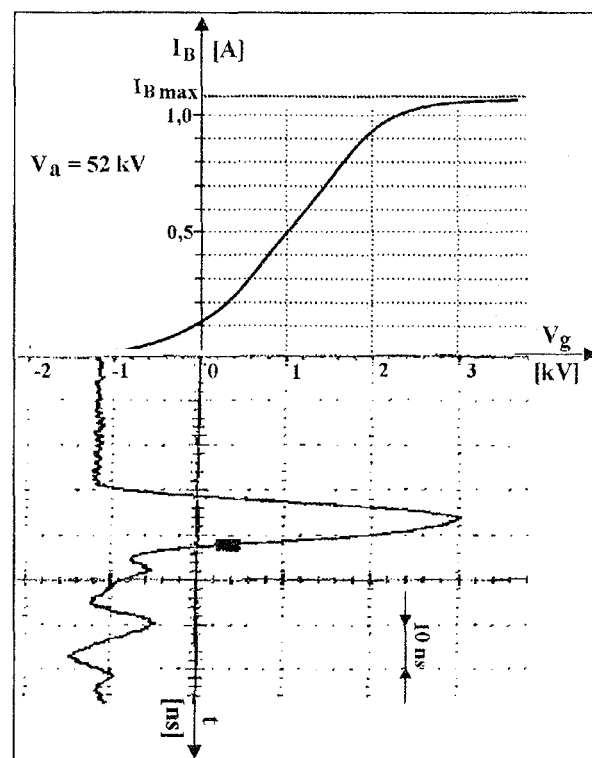


Fig.2. Characteristic features of the triode system of the accelerator electron gun.



PL0101522

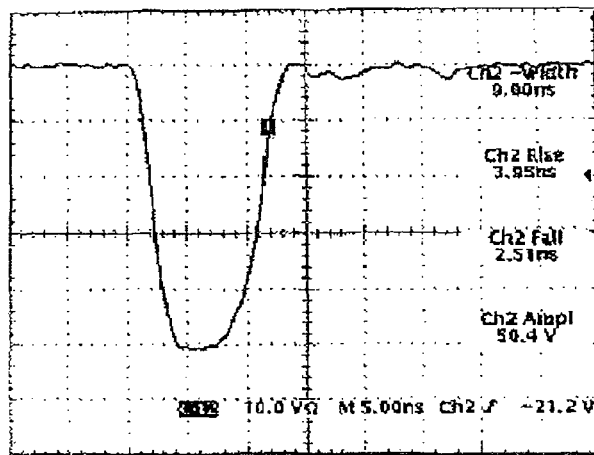


Fig.3. The shape of electron beam pulse for  $U_g = -1.25$  kV.

is about 52 kV. Accelerating structure (section) with a nominal electron output energy of 10 MeV can work with different efficiency. The efficiency depends on electron energy at the structure input. Electron energy at the input of the accelerating structure depends on the gun accelerating voltage  $V_a$ , of course. Fig.2 illustrates characteristic features of the triode system of the accelerator electron gun. The pulse, between the cathode and grid, is rather a triangle than rectangle. The pulse has inadvisable oscillations because of the not very per-

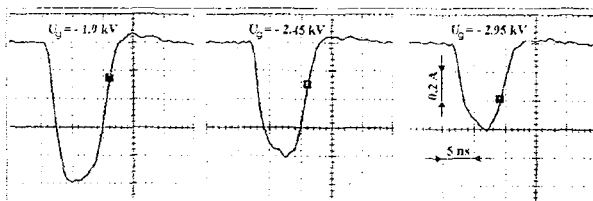


Fig.4. The shape of electron beam pulse for three different grid bias levels.

fectly gun matching to the nanosecond grid modulator. The pulse shape is little distorted by the probe 5100. The probe transmits only a 250 MHz frequency band [-3dB Bandwidth (System)]. The accelerator pulses can be obtained with different pedestal, amplitude and duration, depending on the grid bias level. Figs.3 and 4 show selected oscillograms of the pulses with different values of amplitude and duration. Fig.5 shows the relation between the pedestal charge to the total charge of the ac-

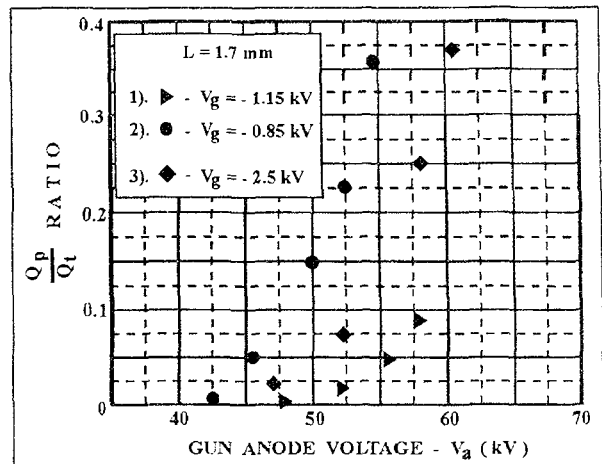


Fig.5. The relation between the pedestal charge to the total charge of the accelerator current pulse ratio and gun accelerating voltage amplitude.

celerator current pulse ratio and gun accelerating voltage amplitude. The ratio of the charges increases with the voltage amplitude and reaches a 0.05 value for 56 kV (first curve for  $V_g = -1.15$  kV) and 46 kV (second curve for  $V_g = -0.85$  kV). Such a relation for the gun without mesh grid is shown as well (third curve for  $V_g = -2.5$  kV). In conclusion, we can state that the accelerator pulses with the current amplitude congenial to the maximal possible value and with a very small pedestal charge (for example  $Q_p \leq 0.01 Q_t$ ) can be obtained only for the gun with mesh grid.

#### Final remarks

The electron accelerator type LAE 10 provides electron pulses suitable for pulse radiolysis experiments. The nanosecond grid modulator of the accelerator gun generates 10 ns, 4 kV pulses but we can change duration of the accelerator pulses in the range from 6 to 9 ns by changing the grid bias voltage level.

#### References

- [1]. Dźwigalski Z., Zimek Z.: Elektronika, 4, 19-21 (1994) (in Polish).
- [2]. Dźwigalski Z., Zimek Z.: Electron Technol., 30, 4, 331-334 (1997).
- [3]. Dąbek J., Dźwigalski Z.: Electron gun design for linear accelerator. First Congress Polish Vacuum Society, Kraków, Poland, 25-27 May 1998, pp. 120-125 (in Polish).
- [4]. Dźwigalski Z., Zimek Z.: In: INCT Annual Report 1999. INCT, Warszawa 2000, p. 138.

## THE INCT PUBLICATIONS IN 2000

1. **Ambroź H.B., Kemp T.J., Kornacka E.M., Przybytniak G.K.**  
Iron ions in damages to DNA following gamma-irradiation.  
5th Symposium Free Radicals in Biology and Medicine. Abstracts. Łódź, Poland, 7-10.06.2000, p. 96.
2. **Ambroź H.B., Kornacka E.M., Marciniec B., Ogrodowczyk M., Przybytniak G.K.**  
EPR study of free radicals in some drugs  $\gamma$ -irradiated in the solid state.  
Radiation Physics and Chemistry, **58**, 4, 357-366 (2000).
3. **Ambroź H.B., Kornacka E.M., Przybytniak G.**  
Interaction between DNA and metal ions after  $\gamma$ -irradiation in model system.  
30th Annual Meeting of the European Society for Radiation Biology "European Radiation Research 2000". Abstracts. Warszawa, Poland, 27-31.08.2000, p. 54.
4. **Aoki S., Cebula K., Chmielewski A.G., Güven O., Paur H.R.**  
Radiation processing of flue gases: Guidelines for feasibility studies (IAEA-TECDOC-1189).  
International Atomic Energy Agency, Vienna 2000, 35 pp.
5. **Bałanda M., Hofmann M., Penc B., Szytuła A., Leciejewicz J.**  
Antyferromagnetyzm związków  $RT_2X_2$  - nowe dane (Antiferromagnetism of  $RT_2X_2$  - new data).  
Ogólnopolskie Seminarium Rozpraszania Neutronów. Book of Abstracts. Kraków, Poland, 25-26.09.2000, p. [1].
6. **Baran J., Pawlukoć A., Majerz I., Malarski Z., Sobczyk L., Grech E.**  
Vibrational spectra of the adduct of 1,8-bis(dimethylamino)naphthalene with dichloromaleic acid (DMAN · DCM).  
Spectrochimica Acta, Part A, **56**, 1801-1812 (2000).
7. **Barson S.D., Skeldon P., Thompson G.E., Kolitsch A., Richter E., Wieser X., Piekoszewski J., Chmielewski A.G., Werner Z.**  
Investigation of ion assisted palladium treatments for improved corrosion resistance of titanium foil in the electron beam dry scrubber process.  
Surface and Coatings Technology, **127**, 179-192 (2000).
8. **Barson S.D., Skeldon P., Thompson G.E., Piekoszewski J., Chmielewski A.G., Werner Z., Grötzschel R., Wieser E.**  
Corrosion protection of titanium by pulsed plasma deposition of palladium.  
Corrosion Science, **42**, 1213-1234 (2000).
9. **Bartłomiejczyk T., Iwaneńko T., Kruszewski M.**  
X-ray and  $H_2O_2$ -induced DNA damage in L5178Y cell lines at the single cell level.  
30th Annual Meeting of the European Society for Radiation Biology "European Radiation Research 2000". Abstracts. Warszawa, Poland, 27-31.08.2000, p. 29.
10. **Bartłomiejczyk T., Lipiński P., Drapier J.-C., Oliveira L., Sochanowicz B., Kruszewski M.**  
Wrażliwość komórek L5178Y na  $H_2O_2$  zależy od poziomu "dostępnych" jonów żelaza (Sensitivity of L5178Y cells to  $H_2O_2$  depends on the level of labile iron pool).  
XXXVI Zjazd Polskiego Towarzystwa Biochemicznego. Streszczenia. Poznań, Poland, 13.09.2000, p. 274.
11. **Bartoś B., Bilewicz A.**  
Manganese(IV) dioxide doped by +3 transition metal cations - a new selective sorbent for radium nuclides.  
5th International Conference on Nuclear Radiochemistry. Extended Abstracts. Vol.2. Pontresina, Switzerland, 3-8.09.2000, pp. 424-425.

12. **Bartoś B., Bilewicz A.**  
Synthesis and ion exchange properties of manganese(IV) dioxide doped by +3 transition metal cations.  
Proceedings of the XVth International Symposium on Physico-chemical Methods of the Mixtures Separation "Ars Separatoria 2000". Borówno n. Bydgoszcz, Poland, 14-17.06.2000, pp. 166-167.
13. **Bażela W., Leciejewicz J., Hofmann M., Penc B., Szytuła A.**  
Frustrated magnetic behaviour of  $\text{TbRh}_{1.2}\text{Ru}_{0.8}\text{Si}_2$ .  
Journal of Alloys and Compounds, **308**, 56-59 (2000).
14. **Bażela W., Leciejewicz J., Hofmann M., Penc B., Szytuła A.**  
Influence of the atomic substitution on the magnetic order in  $\text{TbRh}_{2-x}\text{Ru}_x\text{Si}_2$  system.  
XLII Konwersatorium Krystalograficzne. Streszczenia. Wrocław, Poland, 29-30.06.2000, p.160.
15. **Bilewicz A.**  
The ionic radii of  $\text{Rf}^{4+}$ ,  $\text{Db}^{5+}$  and  $\text{Sg}^{6+}$ .  
Radiochimica Acta, **88**, 12, 833-835 (2000).
16. **Bilewicz A., Krejzler J., Narbutt J.**  
 $\alpha$ -Crystalline polyantimonic acid - an adsorbent for radiostrontium and actinides(III) from liquid waste, and a potential primary barrier in nuclear waste repositories.  
5th International Conference on Nuclear Radiochemistry. Extended Abstracts. Vol. 2. Pontresina, Switzerland, 3-8.09.2000, pp. 251-253.
17. **Bilewicz A., Włodzimirska B.**  
Determination of ionic radius of  $\text{No}^{3+}$  (Preliminary results).  
5th International Conference on Nuclear Radiochemistry. Extended Abstracts. Vol. 2. Pontresina, Switzerland, 3-8.09.2000, pp. 77-78.
18. **Błasiak J., Kowalik J., Małecka-Panas E., Drzewoski J., Wojewódzka M.**  
DNA damage and repair in human lymphocytes exposed to three anticancer platinum drugs.  
Teratogenesis, Carcinogenesis, and Mutagenesis, **20**, 119-131 (2000).
19. **Błasiak J., Trzeciak A., Małecka-Panas E., Drzewoski J., Wojewódzka M.**  
In vitro genotoxicity of ethanol and acetaldehyde in human lymphocytes and the gastrointestinal tract mucosa cells.  
Toxicology in Vitro, **14**, 287-295 (2000).
20. **Bobrowski K.**  
Oxidation processes in methionine-containing oligopeptides.  
6th International Meeting on Pulse Investigations in Chemistry, Biology and Physics PULS'2000. Book of Abstracts. Łeba, Poland, 9-15.09.2000, p. L21.
21. **Borkowski M., Choppin G.R., Moore R.C.**  
Thermodynamic modeling of metal-ligand interactions in high ionic strength NaCl solutions: the  $\text{Co}^{2+}$ -oxalate system.  
Radiochimica Acta, **88**, 9-11, 599-602 (2000).
22. **Borkowski M., Choppin G.R., Moore R.C., Free S.J.**  
Thermodynamic modeling of metal-ligand interactions in high ionic strength NaCl solutions: The  $\text{Co}^{2+}$ -citrate and  $\text{Ni}^{2+}$ -citrate systems.  
Inorganica Chimica Acta, **298**, 141-145 (2000).
23. **Boużyk E., Fuks L., Samochocka K., Lewandowski W., Fokt I., Przewłoka T., Priebe W., Kruszewski M.**  
Cytotoxicity and induction of the DNA crosslinking of platinum and palladium complexes in mouse lymphoma cell lines.  
30th Annual Meeting of European Environmental Mutagen Society. Challenges of Mutation Research for the XXIst Century. Abstracts. Budapest, Hungary, 22-26.08.2000, p. 96.
24. **Boużyk E., Grądzka I., Iwaneńko T., Kruszewski M., Sochanowicz B., Szumiel I.**  
The response of L5178Y lymphoma sublines to oxidative stress: Antioxidant defense, iron content and nuclear translocation of the P65 subunit of  $\text{NF-}\kappa\text{B}$ .  
5th Symposium Free Radicals in Biology and Medicine. Abstracts. Łódź, Poland, 7-10.06.2000, pp. 22-23.



25. **Boużyk E., Grądzka I., Iwaneńko T., Kruszewski M., Sochanowicz B., Szumiel I.**  
The response of L5178Y lymphoma sublines to oxidative stress: Antioxidant defense, iron content and nuclear translocation of the P65 subunit of NF- $\kappa$ B.  
*Acta Biochimica Polonica*, **47**, 4, 881-888 (2000).
26. **Boużyk E., Wójcik A., Kowalska M., Buraczewska I., Kobiątko G., Szumiel I.**  
Validation of the micronucleus-centromere assay for biological dosimetry.  
30th Annual Meeting of the European Society for Radiation Biology "European Radiation Research 2000". Abstracts. Warszawa, Poland, 27-31.08.2000, p. 39.
27. **Buraczewska I., Boużyk E., Kućuk-Jaworska J., Waszkiewicz K., Gasińska A., Szumiel I.**  
Differential anti-proliferative properties of novel hydroxydicarboxylatoplatinum(II) complexes with high or low reactivity with thiols.  
*Chemico-Biological Interactions*, **129**, 297-315 (2000).
28. **Chmielewski A.G.**  
Ekologiczne aspekty spalania paliw kopalnych (Ecological aspects of fossil fuel combustion).  
*Postępy Techniki Jądrowej*, **43**, 4, 36-43 (2000).
29. **Chmielewski A.G.**  
Fossil fuel combustion - crucial problem of civilization.  
Fifth International Symposium and Exhibition on Environmental Contamination in Central and Eastern Europe. Abstracts. Prague, Czech Republic, 12-14.09.2000, p. 280.
30. **Chmielewski A.G.**  
Radiation induced sulfur dioxide removal.  
*Nukleonika*, **45**, 1, 31-38 (2000).
31. **Chmielewski A.G.**  
Zintegrowany system do jednoczesnego usuwania wielu zanieczyszczeń z gazów spalinowych (Integrated system for simultaneous removal of multi contaminants from flue gases).  
Przystosowanie kominów przemysłowych i kanałów spalin w elektrowniach do odprowadzania odsiarczonych gazów spalinowych. Hadek Protective System b.v. Materiały Seminaryjne. Paszówka k/Krakowa, Poland, 30.03. - 1.04.2000, pp.[1]- [16].
32. **Chmielewski A.G., Iller E., Tymiński B.**  
Technologia oczyszczania gazów odlotowych wykorzystująca energię wiązki elektronów - możliwości rolniczego wykorzystania produktu ubocznego (Electron beam technology for flue gases treatment - the possibility of agriculture application of by-product).  
*Zeszyty Naukowe Akademii Rolniczej w Szczecinie*, **204 Agricultura**, **81**, 175-180 (2000).
33. **Chmielewski A.G., Iller E., Tymiński B., Zimek Z., Licki J.**  
Electron beam technology for multicomponent air pollution control.  
Proceedings the First Polish-Japanese Hakone Group Symposium on Non-Thermal Plasma Processing of Water and Air. Sopot, Poland, 29-31.05.2000, pp. 11-13.
34. **Chmielewski A.G., Iller E., Tymiński B., Zimek Z., Licki J.**  
Industrial plant for electron-beam flue gas treatment.  
2000 International Chemical Congress of Pacific Basin Societies. Pacificchem 2000. Book of Abstracts. Honolulu, Hawaii, 14-19.12.2000, p. ENVR 216.
35. **Chmielewski A.G., Iller E., Tymiński B., Zimek Z., Licki J.**  
Industrial plant for electron beam flue gas treatment.  
International Symposium on Radiation Technology in Emerging Industrial Applications (IAEA-SM-365). Book of Extended Synopses. Beijing, China, 6-10.11.2000, pp. 85-86.
36. **Chmielewski A.G., Iller E., Tymiński B., Zimek Z., Licki J.**  
Integrated system for air pollution control.  
Fifth International Symposium and Exhibition on Environmental Contamination in Central and Eastern Europe. Abstracts. Prague, Czech Republic, 12-14.09.2000, p. 212.

37. **Chmielewski A.G., Iller E., Tymiński B., Zimek Z., Licki J.**  
Jednoczesne usuwanie wielu zanieczyszczeń z gazów spalinowych przy użyciu wiązki elektronów (Simultaneous removal of multi component pollutants from flue gases with electron beam irradiation).  
Seminarium Naukowe "Możliwości rolniczego wykorzystania produktu powstającego w wyniku oczyszczania spalin z SO<sub>2</sub> i NO<sub>x</sub> metodą radiacyjną". Szczecin, Poland, 19.06.2000, pp. 3-8.
38. **Chmielewski A.G., Iller E., Tymiński B., Zimek Z., Licki J.**  
Przemysłowe zastosowania technologii wykorzystującej wiązkę elektronów do oczyszczania gazów spalinowych (Industrial applications of electron-beam technology for flue gases purification).  
Chemia i Inżynieria Ekologiczna, 7, 7, 705-712 (2000).
39. **Chmielewski A.G., Iller E., Tymiński B., Zimek Z., Licki J., Ostapczuk A.**  
Electron beam technology for multicomponent air pollution control - a review of Polish activities.  
Transactions of the Institute of Fluid-Flow Machinery, 107, 17-31 (2000).
40. **Chmielewski A.G., Iller E., Tymiński B., Zimek Z., Ostapczuk A., Licki J.**  
Integrated system for SO<sub>2</sub>, NO<sub>x</sub> and VOC removal.  
Proceedings of the 3rd International Scientific Conference. Invited lectures. "Air Protection in Theory & Applications". 2nd volume. Szczyrk, Poland, 29.05.-1.06.2000.  
Works & Studies of the Institute of Environmental Engineering of the Polish Academy of Sciences, 52, pp. 7-18 (2000).
41. **Chmielewski A.G., Tymiński B., Dobrowolski A., Iller E., Zimek Z., Licki J.**  
Empirical models for NO<sub>x</sub> and SO<sub>2</sub> removal in a double stage flue gas irradiation process.  
Radiation Physics and Chemistry, 57, 527-530 (2000).
42. **Chmielewski A.G., Wierzchnicki R., Derda M.**  
Determination of sulphur isotopes ratios in coal combustion process.  
V Isotope Workshop. Book of Abstracts. Kraków, Poland, 1-6.07.2000, pp. 21-22.
43. **Chmielewski A.G., Wierzchnicki R., Derda M.**  
Determination of sulphur isotopes ratios in coal combustion process.  
Fifth International Symposium and Exhibition on Environmental Contamination in Central and Eastern Europe. Abstracts. Prague, Czech Republic, 12-14.09.2000, p. 212.
44. **Chmielewski A.G., Wierzchnicki R., Mikołajczuk A.**  
Isotope effects of sulphur in chemical reaction.  
V Isotope Workshop. Book of Abstracts. Kraków, Poland, 1-6.07.2000, pp. 23-24.
45. **Chmielewski A.G., Zimek Z.**  
Nuclear technology for cleaning coal emissions.  
In: The Environmental Challenges of Nuclear Disarmament. Ed. by T.E. Baca and T. Florkowski. Kluwer Academic Publishers, Amsterdam 2000, pp. 139-148.
46. **Chmielewski A.G., Zimek Z., Iller E., Tymiński B., Licki J.**  
Industrial applications of electron-beam plasma to air pollution control.  
Journal of Technical Physics, 41, 1, 551-572 (2000).
47. **Chwastowska J., Sterlińska E.**  
Evaluation of three-stage BCR sequential extraction procedure of heavy metals in compost.  
Chemia Analityczna, 45, 395-401 (2000).
48. **Cieśla K.**  
Application of WAXS diffraction in studies of crystallinity changes in heavy ion irradiated polyester films.  
X-ray Investigations of Polymer Structures II. Szczyrk, Poland, 2-5.12.1999. In: Proceedings of SPIE. Ed. by A. Włochowicz. 4240, 2000, pp. 27-31.
49. **Cieśla K.**  
Gamma irradiation influence on starch structure studied by differential scanning calorimetry and X-ray scattering.  
IX International Starch Convention (IX ISC). Abstracts. Kraków, Poland, 13-16.06.2000, p. 77.

50. **Cieřła K., Eliasson A.-C.**  
DSC studies of gamma irradiation influence on gelatinisation and amylose-lipid complex transition occurring in potato and wheat starches.  
8th Conference on Calorimetry and Thermal Analysis and International Symposium on Thermodynamics and Structure of Liquids. Abstracts. Zakopane, Poland, 3-8.09.2000, pp. 128e-128f.
51. **Cieřła K., Roos Y., Głuszewski W.**  
Denaturation processes in gamma irradiated proteins studied by differential scanning calorimetry. Radiation Physics and Chemistry, 58, 3, 233-243 (2000).
52. **Croce F., D'Epifanio A., Deptuła A., Łada W., Ciania A., Di Bartolomeo A., Brignocchi A.**  
Synthesis and electrochemical characterization of  $\text{LiNi}_{1-y}\text{Co}_y\text{O}_2$  powders obtained by complex sol-gel process.  
Symposium held April 5-8, 1999, San Francisco, California, USA. Materials Research Society Symposium Proceedings, 375, 97-102 (2000).
53. **Dancewicz A.M.**  
Wykrywanie napromieniowania żywności (Detection of food irradiation).  
Postępy Techniki Jądrowej, 43, 2, 10-21 (2000).
54. **Danilczuk M., Yu J.-S., Brown D., Kevan L., Michalik J.**  
Conduction electron spin resonance (CESR) of metallic particles in mesoporous materials.  
Bilateral Workshop on Radiation-Induced Paramagnetic Defects in Solids. Book of Abstracts. Ghent, Belgium, 29-30.05.2000, p. [1].
55. **Danilczuk M., Yu J.-S., Brown D., Kevan L., Michalik J.**  
Conduction electron spin resonance (CESR) of metallic particles in mesoporous materials.  
Sixth International Meeting on Pulse Investigations in Chemistry, Biology and Physics PULS'2000. Book of Abstracts. Łeba, Poland, 9-15.09.2000, p. P9.
56. **Danilczuk M., Yu J.-S., Brown D., Kevan L., Michalik J.**  
Conduction electron spin resonance (CESR) of metallic particles in mesoporous materials.  
Eighth Meeting of the Benelux EPR Society. Book of Abstracts. Ghent, Belgium, 29.05.2000, p. [1].
57. **Danko B., Polkowska-Motrenko H., Dybczyński R.**  
The determination of Co in plant materials by radiochemical neutron activation analysis.  
Journal of Radioanalytical and Nuclear Chemistry, 246, 2, 279-283 (2000).
58. **Danko B., Polkowska-Motrenko H., Dybczyński R.**  
Neutronowa analiza aktywacyjna jako metoda umożliwiająca eliminację potencjalnych błędów systematycznych w analizie śladowej materiałów biologicznych. Oznaczanie kobaltu (How neutron activation analysis can help to overcome the potential sources of systematic errors in trace analysis of biological materials. Determination of cobalt).  
VI Polska Konferencja Chemii Analitycznej. Chemia Analityczna u Progu Trzeciego Tysiąclecia. Materiały konferencyjne II. Gliwice, Poland, 9-14.07.2000, p. 53.
59. **Drzewicz P., Nałęcz-Jawecki G., Głuszewski W., Panta P., Trojanowicz M.**  
Application of ionizing radiation for removing 2,4-dichlorophenol from water and wastewater.  
Fifth International Symposium and Exhibition on Environmental Contamination in Central and Eastern Europe. Abstracts. Prague, Czech Republic, 12-14.09.2000, p. 114.
60. **Drzewicz P., Panta P., Głuszewski W., Trojanowicz M., Nałęcz-Jawecki G., Gryz M.**  
Radiolytic degradation of 2,4-D herbicide for environmental purposes.  
Nuclear Future Reflecting to Construct. Book of Abstracts. Rio de Janeiro, Brazil, 15-20.10.2000, p. 417.
61. **Drzewicz P., Panta P., Głuszewski W., Trojanowicz M., Nałęcz-Jawecki G., Gryz M.**  
Radiolytic degradation of 2,4-D herbicide for environmental purposes.  
International Symposium on Radiation Technology in Emerging Industrial Applications (IAEA-SM-365). Book of Extended Synopses. Beijing, China, 6-10.11.2000, p. 197.
62. **Dybczyński R.**  
Neutronowa analiza aktywacyjna i jej wkład do nieorganicznej analizy śladowej (Neutron activation analysis and its contribution to inorganic trace analysis).

- VI Polska Konferencja Chemii Analitycznej. Chemia Analityczna u Progu Trzeciego Tysiąclecia. Materiały konferencyjne. Gliwice, Poland, 9-14.07.2000, pp. 35-66.
63. **Dybczyński R.**  
Some problems with the preparation and use of suitable reference materials for quality assurance in inorganic trace analysis.  
1st International IUPAC Symposium Trace Elements in Food. Abstract Book. Warszawa, Poland, 9-11.10.2000, pp. 35-36 (L-18).
64. **Dybczyński R., Danko B., Polkowska-Motrenko H.**  
NAA study on homogeneity of reference materials and their suitability for microanalytical techniques. Journal of Radioanalytical and Nuclear Chemistry, **245**, 1, 97-104 (2000).
65. **Dybczyński R., Danko B., Polkowska-Motrenko H.**  
Some difficult problems still existing in the preparation and certification of CRMs.  
Eight International Symposium on Biological and Environmental Reference Materials. Reference Materials for the 21st Century. Book of Abstracts. Bethesda Maryland, USA, p. Abstracts - 74.
66. **Dźwigalski Z., Zimek Z.**  
Wpływ parametrów wyrzutni elektronowej na własności nanosekundowego liniowego akceleratora elektronów LAE 10 (The influence of the electron gun parameters on the properties of the nano-second linear LAE 10 accelerator).  
VII Konferencja Naukowa "Technologia Elektronowa" ELTE 2000. Streszczenia referatów i komunikatów. Polanica Zdrój, Poland, 18-22.09.2000, p. TP41.
67. **Fuks L., Degueldre C.**  
Optical properties of  $\gamma$ -irradiated synthetic sapphire and yttria-stabilized zirconia spectroscopic windows. Journal of Nuclear Materials, **280**, 360-364 (2000).
68. **Fuks L., Majdan M.**  
Features of solvent extraction of lanthanides and actinides.  
Mineral Processing and Extractive of Metal Review, **21**, 25-48 (2000).
69. **Gackowski D., Kruszewski M., Banaszkiewicz Z., Jawien A., Oliski R.**  
DNA damage, antioxidant vitamins concentration and iron metabolism in colon cancer patients.  
5th Symposium Free Radicals in Biology and Medicine. Abstracts. Łódź, Poland, 7-10.06.2000, p. 121.
70. **Gniazdowska E., Narbutt J.**  
Hydration of dioxalkanes in aqueous solutions.  
Journal of Molecular Liquids, **84**, 273-278 (2000).
71. **Grądzka I.**  
Apoptoza: decyzja należy do mitochondrium (Apoptosis: decision rests with the mitochondrion).  
Postępy Biochemii, **46**, 1, 2-16 (2000).
72. **Grądzka I., Wojewódzka M., Buraczewska I., Szumiel I.**  
Odpowiedź adaptacyjna a naprawa podwójnoniciowych pęknięć DNA w limfocytach ludzkich (Adaptive response and repair of double strand DNA breaks in human lymphocytes).  
XXXVI Zjazd Polskiego Towarzystwa Biochemicznego. Streszczenia. Poznań, Poland, 13.09.2000, p. 41.
73. **Grigoriew H., Wolińska-Grabczyk A., Chmielewski A.G., Amenitsch H., Bernstorff S.**  
SAXS study of the influence of ethanol on the microstructure of polyurethane-based membrane. Journal of Membrane Science, **170**, 275-279 (2000).
74. **Holderna-Natkaniec K., Natkaniec I., Pawlukojć A., Khavryuchenko V.D.**  
Neutron spectroscopy and QC modelling of methyl dynamics in 1- and 2-methyl-naphthalene crystals. Physica B, **276-278**, 292-293 (2000).
75. **Hug G.L., Bobrowski K., Kozubek H., Marciniak B.**  
pH effects on the photooxidation of methionine derivatives by the 4-carboxybenzophenone triplet state.  
Nukleonika, **45**, 1, 63-71 (2000).

76. **Hug G.L., Bobrowski K., Kozubek H., Marciniak B.**  
Photo-oxidation of methionine-containing peptides by the 4-carboxybenzophenone triplet state in aqueous solution. Competition between intramolecular two-centered three-electron bonded (S:S)<sup>+</sup> and (S:N)<sup>+</sup> formation.  
Photochemistry and Photobiology, **72**, 1, 1-9 (2000).
77. **Hug G.L., Wiśniowski P.B.**  
·OH radical induced oxidation of α-methylalanine. Time-resolved and spin-trapping ESR study.  
6th International Meeting on Pulse Investigations in Chemistry, Biology and Physics PULS'2000. Book of Abstracts. Łeba, Poland, 9-15.09.2000, p. P39.
78. **Iller E., Kukielka A., Chmielewski A.G., Zimek Z., Michalik J., Perlińska J., Stupińska H., Mikołajczyk W., Starostka P., Strobin G.**  
Radiacyjna stymulacja różnych rodzajów mas celulozowych przeznaczonych do wytwarzania pochodnych (Radiation stimulation different types of cellulose pulps for production derivatives).  
Przegląd Papierniczy, **56**, 8, 468-471 (2000).
79. **Jeziórska R., Sadło J., Bojarski J., Zimek Z.**  
Procesy radiacyjne w polipropylenie modyfikowanym maleinianem rycynylo-2-oksazoliny (Radiation effects in ricinyl-2-oxazoline maleate-modified polypropylene).  
Polimery, **45**, 6, 416-422 (2000).
80. **Kaczmarek S., Majchrowski A., Kisielewski J., Kwaśny M., Wrońska T.**  
Defekty radiacyjne w monokryształach i szklach Li<sub>2</sub>B<sub>4</sub>O<sub>7</sub> (Radiation defects in single crystals and glasses of Li<sub>2</sub>B<sub>4</sub>O<sub>7</sub>).  
Biuletyn WAT, **XLIX**, 2, 87-96 (2000).
81. **Kałużka I., Zimek Z.**  
Sterylizacja radiacyjna przeszczepów i implantów (Radiation sterilization of allografts and implants).  
X Jubileuszowa Konferencja Naukowa "Biomateriały w medycynie i weterynarii". Streszczenia. Ryto, Poland, 15-18.10.2000, p. 18.
82. **Kapiszewska M., Grądzka I., John A., Szumiel I.**  
Tp-53 independent control of the radiation-induced G2 arrest is functional in L5178Y-S cells deficient in double strand break repair.  
30th Annual Meeting of the European Society for Radiation Biology "European Radiation Research 2000". Abstracts. Warszawa, Poland, 27-31.08.2000, p. 32.
83. **Kierzek J., Kunicki-Goldfinger J., Kasprzak A.J.**  
Measurements of natural radioactivity in historical glasses.  
Glass, Science and Technology (Glasstechnische Berichte), **73**, 11, 351-355 (2000).
84. **Kierzek J., Kunicki-Goldfinger J., Małozewska-Bućko B.**  
Rentgenowska analiza fluorescencyjna w badaniu dzieł sztuki. Wybrane zagadnienia (X-ray fluorescence analysis in art. Selected problems).  
Ochrona Zabytków, **LIII**, 2, 166-181 (2000).
85. **Kolenda M., Hofmann M., Leciejewicz J., Penc B., Szytuła A.**  
Neutron diffraction study of incommensurate magnetic order in TbOs<sub>2</sub>Si<sub>2</sub> and HoOs<sub>2</sub>Si<sub>2</sub>.  
Journal of Alloys and Compounds, **305**, 153-156 (2000).
86. **Korzeniowska-Sobczuk A., Hug G.L., Carmichael I., Bobrowski K.**  
Spectral, kinetics, and theoretical studies of radical cations derived from thioanisole and its carboxylic derivative.  
6th International Meeting on Pulse Investigations in Chemistry, Biology and Physics PULS'2000. Book of Abstracts. Łeba, Poland, 9-15.09.2000, p. P20.
87. **Krejzler J., Narbutt J.**  
Adsorption of radiostrontium and actinide(III) ions on a novel adsorbent apatite II.  
5th International Conference on Nuclear Radiochemistry. Extended Abstracts. 2. Pontresina, Switzerland, 3-8.09.2000, pp. 677-679.

88. **Kruszewski M., Iwaneńko T., Beaumont C., Lipiński P.**  
Oxidative damage in cells depleted in labile iron pool.  
DNA Repair Workshop. Book of Abstracts. Smolenice, Slovakia, 9-12.10.2000, p. 45.
89. **Kruszewski M., Iwaneńko T., Beaumont C., Lipiński P.**  
Oxidative DNA damage in mouse cell lines differing in labile iron pool level.  
5th Symposium Free Radicals in Biology and Medicine. Abstracts. Łódź, Poland, 7-10.06.2000, p. 172.
90. **Kruszewski M., Zastawny T.II.**  
Radiosensitivity of L5178Y cell lines correlates with the amount of initial DNA base damage but not with it's repair.  
30th Annual Meeting of the European Society for Radiation Biology "European Radiation Research 2000". Abstracts. Warszawa, Poland, 27-31.08.2000, p. 16.
91. **Kulisa K., Dybczyński R.**  
Wpływ wybranych parametrów analitycznych na zdolność rozdzielczą wysokosprawnych kolumn jonowymiennych oraz jakość wyników podczas oznaczania jonów nieorganicznych metodą chromatografii jonów (Influence of some analytical parameters on the resolution of HPIC columns and the quality of analytical results in the determination of inorganic ions by ion chromatography).  
VI Polska Konferencja Chemii Analitycznej. Chemia Analityczna u Progu Trzeciego Tysiąclecia. Materiały konferencyjne II. Gliwice, Poland, 9-14.07.2000, p. 66.
92. **Kulisa K., Polkowska-Motrenko H., Dybczyński R.**  
Wykorzystanie chromatografii jonów do kontroli procesów technologicznych w instalacjach radiacyjnego usuwania SO<sub>2</sub> i NO<sub>x</sub> z gazów odlotowych elektrowni (Application of ion chromatography to control of technological processes in installations radiation removing of SO<sub>2</sub> and NO<sub>x</sub> from flue gases of electron power station).  
Nowoczesne Metody Przygotowania Próbek i Oznaczania Śladowych Ilości Pierwiastków. Materiały IX Poznańskiego Konwersatorium Analitycznego. Poznań, Poland, 27-28.04.2000, p. 55.
93. **Kunicki-Goldfinger J., Kierzek J., Kasprzak A.**  
Some features of the 18th century glass technology used in Central Europe (Saxony, Brandenburg, Poland).  
Archäometrie und Denkmalpflege 2000. Kurzberichte 2000. Dresden, Germany, 29-31.03.2000, pp. 107-109.
94. **Kunicki-Goldfinger J., Kierzek J., Kasprzak A., Małozewska-Bućko B.**  
A study of eighteenth century glass vessels from central Europe X-ray fluorescence analysis.  
X-ray Spectrometry, 29, 310-316 (2000).
95. **Langner J., Piekoszewski J., Stanisławski J., Werner Z.**  
Present status and prospects of research in SINS on the modification of surface properties by pulsed plasma streams.  
Nukleonika, 45, 3, 193-197 (2000).
96. **Langner J., Piekoszewski J., Werner Z., Tershin V.I., Chebotarev V.V., Garkusha I., Waliś L., Sartowska B., Starosta W., Szymczyk W., Kopcewicz M., Grabias A.**  
Surface modification of constructional steels by irradiation with high intensity pulsed nitrogen plasma beams.  
Surface and Coatings Technology, 128-129, 105-111 (2000).
97. **Legocka I., Bujnowska E., Olędzki J., Mirkowski K.**  
Próby modyfikacji tlenku magnezu, tlenku cynku oraz talku niektórymi monomerami winylowymi (Preliminary study of modification of magnesium oxide, zinc oxide and talc with vinyl monomers).  
Jubileuszowy Zjazd Naukowy Polskiego Towarzystwa Chemicznego i Stowarzyszenia Inżynierów i Techników Przemysłu Chemicznego. Materiały zjazdowe. Łódź, Poland, 10-15.09.2000, pp. 145-146.
98. **Legocka I., Gałęski A., Bartczak Z., Bujnowska E., Olędzki J., Zimek Z.**  
Modification of polypropylene with oligomeric hydrocarbon resins.  
World Polymer Congress IUPAC Macro 2000. 38th Macromolecular IUPAC Symposium. Book of Abstracts. 3. Warszawa, Poland, 9-14.07.2000, p. 340.

99. **Legocka I., Zimek Z., Mirkowski K., Nowicki A.**  
Preliminary study on application PE filler modified by radiation.  
Radiation Physics and Chemistry, 57, 411-416 (2000).
100. **Legocka I., Zimek Z., Mirkowski K., Nowicki A.**  
Rheological properties of the irradiated polyethylene blends for heat shrinkable tapes.  
4th International Symposium on Ionising Radiation and Polymers. Abstract Booklet. Gouvieux-Chantilly, France, 24-28.09.2000, p. 48.
101. **Legocka I., Zimek Z., Mirkowski K., Nowicki A., Woźniak A.**  
Modification of polyethylene for heat shrinkable products application.  
4th International Symposium on Ionising Radiation and Polymers. Abstract Booklet. Gouvieux-Chantilly, France, 24-28.09.2000, p. 49.
102. **Legocka I., Zimek Z., Mirkowski K., Nowicki A., Woźniak A.**  
Polyethylene blends for heat shrinkable product application.  
International Symposium on Radiation Technology in Emerging Industrial Applications (IAEA-SM-365). Book of Extended Synopses. Beijing, China, 6-10.11.2000, p. 4.
103. **Licki J., Chmielewski A.G., Iller E.**  
Pomiary składu spalin na wylocie z instalacji ich odsiarczania lub odazotowania, w której reagentem jest amoniak (Determination of the composition of flue gas at outlet of DeSO<sub>2</sub> or DeNO<sub>x</sub> installation with ammonia injection).  
Prace i Studia Instytutu Inżynierii Środowiska PAN, 54, 110-122 (2000).
104. **Licki J., Chmielewski A.G., Iller E.**  
System monitoringu dla przemysłowej instalacji odsiarczania i odazotowania spalin przy użyciu wiązki elektronów z akceleratora (Monitoring system for industrial installation for desulphurisation and denitrification of flue gas using the electron beam from accelerator).  
Chemia i Inżynieria Ekologiczna, 7, 1-2, 153-159 (2000).
105. **Lipiński P., Bartłomiejczyk T., Drapier J.-C., Oliveira L., Sochanowicz B., Kruszewski M.**  
Different regulation of labile iron pool in L5178Y cell lines determines their susceptibility to hydrogen peroxide.  
30th Annual Meeting of European Environmental Mutagen Society. Challenges of Mutation Research for the XXIst Century. Abstracts. Budapest, Hungary, 22-26.08.2000, p. 150.
106. **Lipiński P., Drapier J.-C., Oliveira L., Retmańska H., Sochanowicz B., Kruszewski M.**  
Intracellular iron status as a hallmark of mammalian cell susceptibility to oxidative stress: a study of L5178Y mouse lymphoma cell lines differentially sensitive to H<sub>2</sub>O<sub>2</sub>.  
Blood, 95, 9, 2960-2966 (2000).
107. **Lipiński P., Drapier J.-C., Oliveira L., Retmańska H., Sochanowicz B., Kruszewski M.**  
Regulation of intracellular iron metabolism under normal and pro-oxidant conditions.  
5th Symposium Free Radicals in Biology and Medicine. Abstracts. Łódź, Poland, 7-10.06.2000, pp. 48-49.
108. **Lipiński P., Drapier J.-C., Oliveira L., Starzyński R., Kruszewski M.**  
Modulation of iron regulatory protein 1 activities by oxygen and nitrogen reactive species in a pair of mammalian cell lines displaying different intracellular REDOX environment.  
5th Symposium Free Radicals in Biology and Medicine. Abstracts. Łódź, Poland, 7-10.06.2000, p. 185.
109. **Liu W., Wang P., Komaguchi K., Shiotani M., Michalik J., Lund A.**  
Structure and dynamics of [(CH<sub>3</sub>)<sub>3</sub>N-CH<sub>2</sub>]<sup>+</sup> radical generated in γ-irradiated Al-offretite.  
Physical Chemistry Chemical Physics, 2, 2515-2519 (2000).
110. **Licki J., Chmielewski A.G., Iller E.**  
Determination of the composition of flue gas at outlet of DeSO<sub>2</sub> or DeNO<sub>x</sub> installation with ammonia injection.  
Proceedings of the 3rd International Scientific Conference "Air Protection in Theory & Applications. 1<sup>st</sup> volume. Szczyrk, Poland, 30.05.-1.06.2000, pp. 63-64.

111. **Łada W., Deptuła A., Sartowska B., Olczak T., Chmielewski A.G.**  
Preparation and characterization of  $\text{LiCoO}_2$  thin films on porous Ni/NiO cathodes for MCFC by complex sol-gel process (CSGP).  
Materials Research Society Symposium. Spring 2000 "Materials Science of Novel Oxide-Based Electronics". Abstracts. San Francisco California, USA, 24-28.04.2000, p. 340.
112. **Marciniec B., Ogrodowczyk M., Ambroź H., Przybytniak G.**  
The effect of  $\gamma$ -radiation on nitroimidazole derivatives.  
*Acta Polonica Pharmaceutica*, 57, 95-99 (2000).
113. **Michalik J., Brown D., Yu J.-S., Danilczuk M., Kim J.Y., Kevan L.**  
Conduction electron spin resonance (CESR) of metallic particles in mesoporous materials.  
33rd Annual International Meeting and 4th Meeting of European Federation of EPR Groups (EFEPR). A combined Meeting on Prospects for EPR Spectroscopy in the 21st Century. Abstracts. Norwich, United Kingdom, 10-14.09.2000, p. P42.
114. **Michalik J., Sadło J., Perlińska J.**  
Paramagnetic silver clusters in zeolites.  
Bilateral Workshop on Radiation-Induced Paramagnetic Defects in Solids. Book of Abstracts. Ghent, Belgium, 29-30.05.2000, p. [1].
115. **Michalik J., Yamada H., Perlińska J.**  
Cationic silver clusters in sodalites.  
Fifth International Meeting on Recent Advances in MR Applications to Porous Media. Abstracts. Bologna, Italy, 9-11.10.2000, p. P-33.
116. **Michalik J., Yamada H., Perlińska J.**  
Hexameric silver in sodalites.  
33rd Annual International Meeting and 4th Meeting of European Federation of EPR Groups (EFEPR). A combined Meeting on Prospects for EPR Spectroscopy in the 21st Century. Abstracts. Norwich, United Kingdom, 10-14.09.2000, p. P43.
117. **Michalik J., Yu J.-S., Sadło J.**  
ESR studies of silver clusters in the isostructural A and ZK-4 molecular sieves.  
*Bulletin of the Polish Academy of Sciences, Chemistry*, 48, 4, 293-301 (2000).
118. **Migdał W., Owczarczyk H.B., Kędzia B., Hołderna-Kędzia E., Madajczyk D.**  
Microbiological decontamination of natural honey by irradiation.  
*Radiation Physics and Chemistry*, 57, 285-288 (2000).
119. **Migdał W., Owczarczyk H.B., Świętosławski J., Świętosławski J.**  
Application of irradiation in bait production to the control of crawling insects in urban areas.  
*Radiation Physics and Chemistry*, 57, 551-553 (2000).
120. **Mirkowski J., Wiśniowski P., Bobrowski K.**  
The nanosecond pulse radiolysis system dedicated to new LAE 10 accelerator (INCT-Warsaw).  
6th International Meeting on Pulse Investigations in Chemistry, Biology and Physics PULS'2000. Book of Abstracts. Łeba, Poland, 9-15.09.2000, p. P47.
121. **Narbutt J.**  
Inorganic ion exchangers as selective adsorbents and potential primary barriers for radionuclides.  
In: *The Environmental Challenges of Nuclear Disarmament*. Ed. by T.E. Baca and T. Florkowski. Kluwer Academic Publishers, Amsterdam 2000, pp. 237-243.
122. **Nichipor H., Dashouk E., Chmielewski A.G., Zimek Z., Bułka S.**  
A theoretical study on decomposition of carbon tetrachloride, trichloroethylene and ethyl chloride in dry air under the influence of an electron beam.  
*Radiation Physics and Chemistry*, 57, 519-525 (2000).
123. **Nichipor H., Dashouk E., Chmielewski A.G., Zimek Z., Bułka S.**  
Theoretical study on decomposition of  $\text{CH}_2\text{Cl}_2$  in nitrogen and dry air under influence of electron beam.



- International Symposium on Radiation Technology in Emerging Industrial Applications (IAEA-SM-365). Book of Extended Synopses. Beijing, China, 6-10.11.2000, pp. 184-185.
124. **Nichipor H., Dashouk E., Yacko S., Chmielewski A.G., Zimek Z., Sun Y.**  
Theoretical study on decomposition of  $C_2H_2Cl_2$  and  $C_2HCl_3$  in dry and humid air under influence of electron beam.  
6th International Meeting on Pulse Investigations in Chemistry, Biology and Physics PULS'2000. Book of Abstracts. Łeba, Poland, 9-15.09.2000, p. P24.
125. **Ostapczuk A., Chmielewski A.G., Sun Y.**  
Electron beam flue gas treatment as an integrated method of  $SO_2$ ,  $NO_x$  and volatile organic compounds (VOCs) control.  
Fifth International Symposium and Exhibition on Environmental Contamination in Central and Eastern Europe. Abstracts. Prague, Czech Republic, 12-14.09.2000, p. 227.
126. **Owczarczyk H.B., Migdał W., Kędzia B.**  
The pharmacological activity of medical herbs after microbiological decontamination by irradiation.  
Radiation Physics and Chemistry, 57, 331-335 (2000).
127. **Paluchowska B., Maurin J.K., Leciejewicz J.**  
X-ray diffraction study on manganese(II) complexes with thiophene-2-carboxylate and furan-3-carboxylate ligands.  
Journal of Coordination Chemistry, 51, 335-347 (2000).
128. **Pańczyk E., Ligeza M., Kalicki A., Waliś L.**  
Nuclear methods in the examination of art objects. State in Poland.  
In: Physics in Culture I. The Solid State Physics in the Study of Cultural Heritage. Aristotle University of Thessaloniki, Thessaloniki 2000, pp. 180-185.
129. **Pańczyk E., Ligeza M., Waliś L.**  
Application of INAA to the examination of art objects: Research in Poland.  
Journal of Radioanalytical and Nuclear Chemistry, 244, 3, 543-551 (2000).
130. **Pańczyk E., Ligeza M., Waliś L.**  
Provenance studies of alabaster and marble sculptures from Poland by neutron activation analysis and electron paramagnetic resonance spectroscopy.  
32nd International Symposium Archaeometry. Program Abstracts. Mexico City, Mexico, 15-19.05.2000, p. 242.
131. **Pańczyk E., Ligeza M., Waliś L., Kalicki A.**  
Nuclear techniques in conservation of historic monuments.  
Conservator-Restorer's Bulletin, 11, 2, 138-143 (2000).
132. **Pańczyk E., Ligeza M., Waliś L., Kalicki A.**  
Techniki jądrowe w ochronie zabytków (Nuclear techniques in conservation of historic monuments).  
Biuletyn Informacyjny Konserwatorów Dzieł Sztuki, 10, 2, 5-13 (2000).
133. **Parus J., Kierzek J., Małozewska-Bućko B.**  
Determination of the carbon content in coal and ash by XRF.  
X-ray Spectrometry, 29, 2, 192-195 (2000).
134. **Pawlukojć A., Natkaniec I., Malarski Z., Leciejewicz J.**  
The dynamical pattern of the 2-aminopyrazine-3-carboxylic acid molecule by inelastic and incoherent neutron scattering, Raman spectroscopy and ab initio calculations.  
Journal of Molecular Structure, 516, 7-14 (2000).
135. **Penc B., Baran S., Hofmann M., Leciejewicz J., Szytuła A.**  
Magnetic structures of TbTX compounds.  
Physica B, 276-278, 620-621 (2000).
136. **Penc B., Baran S., Hofmann M., Leciejewicz J., Ślaski M., Szytuła A.**  
Magnetic ordering in  $RPtX$  ( $R = Gd, Tb, Dy$ ;  $X = Si, Ge$ ) compounds.  
Journal of Alloys and Compounds, 299, 79-87 (2000).

137. **Penc B., Hofmann M., Leciejewicz J., Szytuła A., Zygmunt A.**  
Magnetic properties of RPdGa (R=Gd-Er) compounds.  
Journal of Alloys and Compounds, 305, 24-31 (2000).
138. **Perlińska J., Danilczuk M., Yamada H., Michalik J.**  
Cationic silver clusters in sodalites.  
6th International Meeting on Pulse Investigations in Chemistry, Biology and Physics PULS'2000. Book of Abstracts. Łeba, Poland, 9-15.09.2000, p. P26.
139. **Perlińska J., Yamada H., Michalik J.**  
Cationic silver clusters in sodalites.  
Bilateral Workshop on Radiation-Induced Paramagnetic Defects in Solids. Book of Abstracts. Ghent, Belgium, 29-30.05.2000, p. [1].
140. **Perlińska J., Yamada H., Michalik J.**  
Cationic silver clusters in sodalites.  
Eighth Meeting of the Benelux EPR Society. Book of Abstracts. Ghent, Belgium, 29.05.2000, p. [1].
141. **Piekoszewski J., Grötzschel R., Wieser E., Stanisławski J., Werner Z., Szymczyk W., Langner J.**  
Kinetics of the pulsed erosion deposition process induced by high intensity plasma beams.  
Surface and Coatings Technology, 128-129, 394-499 (2000).
142. **Piekoszewski J., Stanisławski J., Werner Z., Richter E., Szymczyk W.**  
Pulse plasma alloyed Ti-Fe interlayer for TiN coating on tool steels.  
First International Congress on Radiation Physics, High Current Electronics, and Modification of Materials. Vol. 3. Proceedings. 5th Conference on Modification of Materials with Particle Beams and Plasma Flows. Tomsk, Russia, 24-29.09.2000, pp. 447-449.
143. **Pleschke J.M., Kleczkowska H.E., Strohm M., Althaus F.R.**  
Poly(ADP-ribose) binds to specific domains in DNA damage checkpoint proteins.  
The Journal of Biological Chemistry, 275, 52, 40974-40980 (2000).
144. **Pogocki D., Sadło J.**  
Radiation induced oxidation of thiaproline derivatives in frozen acidic aqueous solutions: theoretical and electron spin resonance study.  
Nukleonika, 45, 1, 101-108 (2000).
145. **Polkowska-Motrenko H., Danko B., Dybczyński R., Koster-Ammerlaan A., Bode P.**  
Effect of acid digestion method on cobalt determination in plant materials.  
Analytica Chimica Acta, 408, 89-95 (2000).
146. **Przybytniak G., Ambroz H.**  
The influence of DTT on DNA radicals induced by direct effect of ionising radiation.  
30th Annual Meeting of the European Society for Radiation Biology "European Radiation Research 2000". Abstracts. Warszawa, Poland, 27-31.08.2000, p. 55.
147. **Ptasiewicz-Bąk H., Leciejewicz J.**  
The crystal structure of monoaquabis(trans-5-methylpyrazine-2-carboxylato-N,O)copper(II) trihydrate.  
Polish Journal of Chemistry, 74, 877-883 (2000).
148. **Ptasiewicz-Bąk H., Leciejewicz J.**  
Molecular ribbons composed of calcium(II) ions bridged by carboxylate and water oxygen atoms in the crystals of Ca(II) complex with 5-methylpyrazine-2-carboxylate ligands.  
Journal of Coordination Chemistry, 49, 301-308 (2000).
149. **Sadło J., Amira S., Vanhaelewyn G., Callens F., Matthys P., Michalik J., Stachowicz W.**  
Paramagnetic radicals in X-ray irradiated tooth enamel heated at 400°C.  
Bilateral Workshop on Radiation-Induced Paramagnetic Defects in Solids. Book of Abstracts. Ghent, Belgium, 29-30.05.2000, p. [1].
150. **Sadło J., Danilczuk M., Callens F., Michalik J.**  
Interaction of tetrameric silver with ammonia in AgCs-rho zeolite.

- 33rd Annual International Meeting and 4th Meeting of European Federation of EPR Groups (EFEPR). A combined Meeting on Prospects for EPR Spectroscopy in the 21st Century. Abstracts. Norwich, United Kingdom, 10-14.09.2000, p. P51.
151. **Sadło J., Vanhaelewyn G., Amira S., Morent R., Matthys P., Callens F., Michalik J., Stachowicz W.**  
EPR and ENDOR study of human tooth enamel heated at 400°C.  
Bilateral Workshop on Radiation-Induced Paramagnetic Defects in Solids. Book of Abstracts. Ghent, Belgium, 29-30.05.2000, p. [1].
152. **Sadło J., Vanhaelewyn G., Amira S., Morent R., Matthys P., Callens F., Michalik J., Stachowicz W.**  
EPR and ENDOR study of human tooth enamel heated at 400°C.  
Eighth Meeting of the Benelux EPR Society. Book of Abstracts. Ghent, Belgium, 29.05.2000, p. [1].
153. **Samczyński Z., Danko B., Dybczyński R.**  
Application of Chelex 100 ion exchange resin for separation and determination of palladium, platinum and gold in geological and industrial materials by neutron activation analysis.  
*Chemia Analityczna*, **45**, 843-857 (2000).
154. **Samczyński Z., Danko B., Dybczyński R.**  
Zastosowanie jonitu CHELEX 100 do oznaczania śladowych ilości palladu, platyny i złota w materiałach geologicznych i przemysłowych metodą neutronowej analizy aktywacyjnej (Application of CHELEX 100 ion exchange resin for the determination of trace amounts of palladium, platinum and gold in geological and industrial materials by neutron activation analysis).  
VI Polska Konferencja Chemii Analitycznej. *Chemia Analityczna u Progu Trzeciego Tysiąclecia. Materiały konferencyjne II*. Gliwice, Poland, 9-14.07.2000, p. 62.
155. **Schöneich C., Pogocki D., Wiśniowski P., Hug G.L., Bobrowski K.**  
Intramolecular sulfur-oxygen bond formation in radical cations of N-acetylmethionine amide.  
*Journal of the American Chemical Society*, **122**, 10224-10225 (2000).
156. **Stachowicz W., Malec-Czechowska K.**  
Laboratorium identyfikacji napromieniowania żywności (Laboratory for detection of irradiated foods).  
*Analityka*, **4**, 26-29 (2000).
157. **Stachowicz W., Malec-Czechowska K., Danciewicz A.M., Szot Z.**  
Some methods used for detection of food irradiation.  
30th Annual Meeting of the European Society for Radiation Biology "European Radiation Research 2000". Abstracts. Warszawa, Poland, 27-31.08.2000, p. 55.
158. **Stachowicz W., Strzelczak G., Callens F.**  
Detection of irradiated food by EPR.  
Bilateral Workshop on Radiation-Induced Paramagnetic Defects in Solids. Book of Abstracts. Ghent, Belgium, 29-30.05.2000, p. [1].
159. **Starosta W., Ptasiewicz-Bąk H., Leciejewicz J.**  
The crystal and molecular structure of calcium complexes with pyridine-2,6-dicarboxylic ligand.  
XLII Konwersatorium Krystalograficzne. Streszczenia. Wrocław, Poland, 29-30.06.2000, p. 118.
160. **Strzelczak G., Bobrowski K., Kozubek H., Michalik J.**  
Electron spin resonance study of radiation induced in polycrystalline oligopeptides containing methionine.  
*Nukleonika*, **45**, 1, 93-100 (2000).
161. **Strzelczak G., Houee-Levin C., Berges J., Bobrowski K.**  
EPR spectroscopy of  $\gamma$ -irradiated polycrystalline asparagine and asparagine-containing peptides.  
6th International Meeting on Pulse Investigations in Chemistry, Biology and Physics PULS'2000. Book of Abstracts. Łeba, Poland, 9-15.09.2000, p. P32.
162. **Strzelczak G., Vanhaelewyn G., Stachowicz W., Goovaerts E., Callens F., Michalik J.**  
The advantage of Q and W band EPR in the study of radiation induced species in shells and corallite.  
Bilateral Workshop on Radiation-Induced Paramagnetic Defects in Solids. Book of Abstracts. Ghent, Belgium, 29-30.05.2000, p. [1].

163. **Strzelczak G., Vanhaelewyn G., Stachowicz W., Goovaerts E., Callens F., Michalik J.**  
Multifrequency EPR study of radicals produced by radiation in shells and corallite.  
Eighth Meeting of the Benelux EPR Society. Book of Abstracts. Ghent, Belgium, 29.05.2000, p. [1].
164. **Strzelczak G., Vanhaelewyn G., Stachowicz W., Goovaerts E., Callens F., Michalik J.**  
Multifrequency EPR study of radicals produced by radiation in shells and corallite.  
Bilateral Workshop on Radiation-Induced Paramagnetic Defects in Solids. Book of Abstracts. Ghent, Belgium, 29-30.05.2000, p. [1].
165. **Sun Y., Hakoda T., Chmielewski A.G., Hashimoto S., Zimek Z., Bułka S., Ostapczuk A., Nichipor H.**  
Decomposition of 1,1-dichloroethylene in humid air under electron beam irradiation.  
Fifth International Symposium and Exhibition on Environmental Contamination in Central and Eastern Europe. Abstracts. Prague, Czech Republic, 12-14.09.2000, p. 114.
166. **Szopa Z., Dybczyński R.**  
Porównania międzylaboratoryjne jako baza certyfikacji kandydatów na materiały odniesienia (Inter-laboratory comparison as a basis for certification of candidate reference materials).  
Analityka, 2, 4-7 (2000).
167. **Szumiel I.**  
The importance of the nuclear and cytoplasmic signalling in the cellular response to ionising radiation.  
30th Annual Meeting of the European Society for Radiation Biology "European Radiation Research 2000". Abstracts. Warszawa, Poland, 27-31.08.2000, p. 14.
168. **Szumiel I.**  
The importance of the nuclear and cytoplasmic signalling in the cellular response to ionising radiation.  
Nukleonika, 45, 4, 215-220 (2000).
169. **Szumiel I.**  
P53 and cell signalling.  
Radiotherapy & Oncology, 56, Supplement 1, p. S54 (2000).
170. **Szumiel I., Jaworska A., Kapiszewska M., John A., Grądzka I., Sochanowicz B.**  
Differential induction of apoptosis in x-irradiated L5178Y sublines bearing p53 mutation.  
Radiation Environment Biophysics, 39, 33-40 (2000).
171. **Szumiel I., Wójcik A.**  
Modne w radiobiologii - nadwrażliwość na niskie dawki promieniowania jonizującego (Trendy in radiobiology: hypersensitivity to low doses of ionising radiation).  
Postępy Techniki Jądrowej, 43, 4, 17-20 (2000).
172. **Taraszevska J., Sadło J., Michalik J., Korybut-Daszkiewicz B.**  
Stability and ESR spectra of Ni(III) tetraazamacrocyclic complexes in nitrate and chloride solutions.  
Polish Journal of Chemistry, 74, 813-822 (2000).
173. **Trojanowicz M.**  
Flow injection analysis. Instrumentation and applications.  
World Scientific, Singapore 2000, 481 p.
174. **Trojanowicz M., Drzewicz P., Panta P., Głuszewski W.**  
The effect of selected scavengers on radiolytic degradation of 2,4-dichlorophenol for environmental purposes.  
Central European Journal of Public Health, 8, 7(Suppl.), 20-21 (2000)
175. **Trzeciak A., Kowalik J., Małecka-Panas E., Drzewoski J., Wojewódzka M., Iwaneńko T., Błasiak J.**  
Genotoxicity of chromium in human gastric mucosa cells and peripheral blood lymphocytes evaluated by the single cell gel electrophoresis (comet assay).  
Medical Science Monitor, 6, 1, 24-29 (2000).
176. **Vanhaelewyn G., Lahorte P., Mondelaers W., Callens F., Michalik J., Matthys P.**  
EPR and ENDOR of irradiated sugars.  
Bilateral Workshop on Radiation-Induced Paramagnetic Defects in Solids. Book of Abstracts. Ghent, Belgium, 29-30.05.2000, p. [1].

177. **Vanhaelewyn G., Sadło J., Cailens F., Mondelaers W., Frenne De D., Matthys P.**  
A decomposition study of the EPR spectrum of irradiated sucrose.  
*Applied Radiation and Isotopes*, **52**, 1221-1227 (2000).
178. **Varmenot N., Remita S., Abedinzadeh Z., Wiśniowski P., Strzelczak G., Bobrowski K.**  
Processus d'oxydation de la N,S-diacetyl-L-cystéinate d'éthyle par le radical hydroxyle: influence du groupement acétyle.  
10<sup>èmes</sup> Journées d'Etudes de la Chimie sous Rayonnement. Programme et résumé des communications. Houffalize, Belgique, 20-25.05.2000, p. [1].
179. **Walicka M., Ding Y., Adelstein S.J., Kassis A.I.**  
Toxicity of DNA-incorporated iodine-125: Quantifying the direct and indirect effects.  
*Radiation Research*, **154**, 326-330 (2000).
180. **Warchoń S., Rzewuski H., Krynicki J., Grötzschel R.**  
Post-implantation defects instability under 1 MeV electron irradiation in GaAs.  
*Nukleonika*, **45**, 4, 225-228 (2000).
181. **Wasek M., Sterliński S., Dybczyński R., Cichowlas A.**  
Reference peak method for the analysis of doublets in gamma-ray spectrometry used in neutron activation analysis.  
*Chemia Analityczna*, **45**, 689-698 (2000).
182. **Wierzchnicki R., Mikołajczuk A., Chmielewski A.G., Miljević N.**  
Oxygen isotope ratio measurements in juices and wines for food control.  
V Isotope Workshop. Book of Abstracts. Kraków, Poland, 1-6.07.2000, pp. 257-258.
183. **Więckowski A.B., Stuglik Z., Stróżyk M., Kowalak S.**  
Generation of sulfur radicals in zeolites by means of ionization radiation.  
*Molecular Physics Reports*, **28**, 25-29 (2000).
184. **Wiśniowski P., Korzeniowska-Sobczuk A., Bobrowski K., Naumov S., Richter L., Brede O.**  
Generation of aromatic thioether radical cations containing phenyl, vinyl, allyl, and methyl substituents inorganic solvents.  
6th International Meeting on Pulse Investigations in Chemistry, Biology and Physics PULS'2000. Book of Abstracts. Łeba, Poland, 9-15.09.2000, p. P38.
185. **Włosiński W., Krajewski A., Piekoszewski J., Stanisławski J., Waliś L.**  
Intense pulsed plasma beams in ceramic/metal brazing.  
*Nukleonika*, **45**, 2, 145-146 (2000).
186. **Wojewódzka M., Grądzka I., Buraczewska I.**  
Repair of DNA DSB in human lymphocytes on single cell level.  
DNA Repair Workshop. Book of Abstracts. Smolenice, Slovakia, 9-12.10.2000, p. 40.
187. **Wojewódzka M., Grądzka I., Buraczewska I., Szumiel I.**  
Adaptive response and DSB-repair in human lymphocytes.  
30th Annual Meeting of the European Society for Radiation Biology "European Radiation Research 2000". Abstracts. Warszawa, Poland, 27-31.08.2000, p. 12.
188. **Wojewódzka M., Grądzka I., Buraczewska I., Szumiel I.**  
Adaptive response and DSB-repair in human lymphocytes.  
30th Annual Meeting of European Environmental Mutagen Society. Challenges of Mutation Research for the XXIst Century. Abstracts. Budapest, Hungary, 22-26.08.2000, p. 131.
189. **Wójcik A., Shadley J.D.**  
The current status of the adaptive response to ionizing radiation in mammalian cells.  
*Human and Ecological Risk Assessment*, **6**, 2, 281-300 (2000).
190. **Wójcik A., Shadley J.D., Szumiel I.**  
Adaptive response in lymphocytes: Is DNA repair involved?  
Eleventh International Congress of Radiation Research "Radiation Research". 2. Proceedings. Dublin, Ireland, 18-23.07.1999, [2000], pp. 434-437.

191. **Wójcik A., Szumiel I.**  
Biologiczne efekty niskich dawek promieniowania jonizującego (Biological effects of low dose ionizing radiation).  
Polska Nauka i Technika dla Energetyki Jądrowej Jutra. Seminarium Naukowe. Raport IEA-65/A Referaty. Mądralin k/Warszawy, Poland, 13-14.04.2000, pp. 117-120.
192. **Zagórski Z.P.**  
Diffuse reflection spectrophotometry (DRS) recognition of products of radiolysis in polymers.  
International Conferences on Polymer Characterization. Polychar-8 & Short Course. Program and Book of Abstracts. Denton Texas, USA, 11-14.01.2000, pp. 1-14.
193. **Zagórski Z.P.**  
Energetyka jądrowa a reszta nukleoniki (Nuclear power stations and the remaining nucleonics).  
Orbital. Wiadomości i informacje, 6, 300-301 (2000).
194. **Zagórski Z.P.**  
Modification, degradation and stabilization of polymers in view of the classification of radiation spurs.  
Proceedings of the 1st International Conference on Polymer. Modification, Degradation and Stabilization. Palermo, Italy, 3-7.09.2000, pp. 1-3.
195. **Zagórski Z.P.**  
Polimery i promieniowanie (Polymers and ionising radiation).  
Postępy Techniki Jądrowej, 43, 4, 2-13 (2000).
196. **Zagórski Z.P.**  
Radon dobry i zły (Radon - bad or beneficial).  
Sesja Naukowa "Radon w Środowisku". Streszczenia. Kraków, Poland, 14-15.06.2000, pp. 5-6.
197. **Zagórski Z.P.**  
Radon raz jeszcze (Radon once more).  
Postępy Techniki Jądrowej, 43, 3, 45-51 (2000).
198. **Zagórski Z.P.**  
Thin layer alanine dosimeter with optical spectrophotometric evaluation.  
In: Dosimetry for radiation processing. Final report of the co-ordinated research project on characterization and evaluation of high dose dosimetry techniques for quality assurance in radiation processing (IAEA-TECDOC-1156). International Atomic Energy Agency, Vienna 2000, pp. 99-106.
199. **Zagórski Z.P., Głuszewski W.**  
Single- and multi-ionization spurs in radiation chemistry of polymers.  
World Polymer Congress IUPAC Macro 2000. 38th Macromolecular IUPAC Symposium. Book of Abstracts. 3. Warszawa, Poland, 9-14.07.2000, p. 1396.
200. **Zagórski Z.P., Rafalski A.**  
Chemia radiacyjna ciała stałego tłumaczy właściwości osłonne betonu (Solid state radiation chemistry explains shielding properties of concrete).  
W: Polska Nauka i Technika dla Energetyki Jądrowej Jutra. Seminarium Naukowe. Mądralin k/Warszawy, Poland, 13-14.04.2000. Raport IAE-65/A. Otwock-Świerk, Poland, pp. 121-125.
201. **Zagórski Z.P., Rafalski A.**  
Diffuse reflectance spectroscopic (DRS) quantification of absorbed radiation dose indicated by labels.  
Radiation Physics and Chemistry, 57, 725-730 (2000).
202. **Zagórski Z.P., Rafalski A.**  
A thin, composite sodium chloride dosimeter with diffuse reflected light spectrophotometric read out.  
Journal of Radioanalytical and Nuclear Chemistry, 245, 2, 233-236 (2000).
203. **Zagórski Z.P., Rafalski A.**  
Radiation chemistry of solid thiosulfate: optical absorption spectra.  
Nukleonika, 45, 1, 109-113 (2000).
204. **Zakrzewska-Trznadel G., Chmielewski A.G., Miljević N.R., Van Hook A.**  
Membrane separation of water isotopomers.

V Isotope Workshop. Book of Abstracts. Kraków, Poland, 1-6.07.2000, pp. 267-268.

205. **Zimek Z., Bułka S., Dźwigalski Z., Roman K.**  
Short pulse electron accelerator for pulse radiolysis study.  
7th European Particle Accelerator Conference. A Europhysics Conference. Abstracts Brochure. Vienna, Austria, 26-30.06.2000, p. 46.
206. **Zimek Z., Bułka S., Dźwigalski Z., Roman K.**  
Short pulse electron accelerator for pulse radiolysis study.  
7th European Particle Accelerator Conference. A Europhysics Conference. Proceedings. Vienna, Austria, 26-30.06.2000, pp. 2379-2381.
207. **Zimek Z., Chmielewski A.G.**  
Flue gases simultaneous treatment by electron beam and streams of microwave discharge for pollutants removal.  
Fifth International Symposium and Exhibition on Environmental Contamination in Central and Eastern Europe. Abstracts. Prague, Czech Republic, 12-14.09.2000, p. 195
208. **Zimek Z., Chmielewski A.G., Bułka S.**  
Microwave discharge/electron-beam process for environmental application.  
2000 International Chemical Congress of Pacific Basin Societies. Pacificchem 2000. Book of Abstracts. Honolulu, Hawaii, 14-19.12.2000, p. ENVR 218.
209. **Zimek Z., Kałuska I.**  
Implementation of electron beam sterilization process in Poland.  
International Symposium on Radiation Technology in Emerging Industrial Applications (IAEA-SM-365). Book of Extended Synopses. Beijing, China, 6-10.11.2000, pp. 124-125.
210. **Zimek Z., Legocka I., Woźniak A.**  
Radiation processing of polymers for heat shrinkable product and medical devices application.  
6th International Meeting on Pulse Investigations in Chemistry, Biology and Physics PULS'2000. Book of Abstracts. Łeba, Poland, 9-15.09.2000, p. P7.
211. **Żuchowska D., Rajkowska M., Zagórski Z.P.**  
Struktura fizyczna mieszanin polietylenu z elastomerem termoplastycznym modyfikowanym radiacyjnie (Physical structure of blends of polymers with thermoplastic elastomers, modified by irradiation).  
IX Seminarium Tworzywa Sztuczne w Budowie Maszyn. Referaty. Kraków, Poland, 27-29.09.2000, pp. 403-406.
212. **Żuchowska D., Zagórski Z.P., Przybytniak G.K., Rafalski A.**  
Influence of butadiene/styrene copolymers on the stabilization of polypropylene in electron beam irradiation.  
International Conferences on Polymer Characterization. Polychar-8 & Short Course. Program and Book of Abstracts. Denton Texas, USA, 11-14.01.2000, p. P-28.

#### SUPPLEMENT LIST OF THE INCT PUBLICATIONS IN 1999

213. **Błasiak J., Kowalik J., Trzeciak A., Wojewódzka M.**  
Cytotoxicity and DNA damage and repair in human lymphocytes exposed to three anticancer platinum drugs.  
Neoplasma, 46, Supplement, 61-63 (1999).
214. **Błasiak J., Kowalik J., Trzeciak A., Wojewódzka M.**  
Uszkodzenia i naprawa DNA w ludzkich limfocytach ekspozowanych na przeciwnowotworowe związki platyny (DNA damage and repair in human lymphocytes exposed to anticancer platinum compounds).  
Trzecia Konferencja Naukowa poświęcona Profesorowi Antoniemu Dmochowskiemu "Aktualne kierunki badań w biochemii i biotechnologii w ochronie środowiska i życia człowieka". Abstrakty. Łódź, Poland, 14-16.12.1999, p. 4.
215. **Błasiak J., Trzeciak A., Kowalik J., Małecka-Panas E., Drzewoski J., Wojewódzka M.**  
Uszkodzenia i naprawa DNA w komórkach błony śluzowej żołądka poddanych działaniu chromu i kurkuminy (DNA damage and repair in human gastric mucosal cells exposed to chromium and curcumin).

- Trzecia Konferencja Naukowa poświęcona Profesorowi Antoniemu Dmochowskiemu "Aktualne kierunki badań w biochemii i biotechnologii w ochronie środowiska i życia człowieka". Abstrakty. Łódź, Poland, 14-16.12.1999, p. 4.
216. **Buraczewska I., Gasińska A., Grądzka I., Jarocewicz N., Sochanowicz B., Szumiel I.**  
Erbstatin-induced increase in apoptosis does not radiosensitize L5178Y cells.  
Nukleonika, **44**, 4, 561-578 (1999).
217. **Chmielewski A.G., Dobrowolski A., Iller E., Tymiński B., Zakrzewska-Trznadel G., Zimek Z., Licki J.**  
Development and application experience with technology of SO<sub>2</sub> and NO<sub>x</sub> removal from flue gas by electron beam irradiation.  
EPRI-DOE-EPA Combined Utility Air Pollution Control Symposium: The MEGA Symposium. 2: NO<sub>x</sub> and Multi-Pollutant Controls. Proceedings. Atlanta Georgia, USA, 16-20.08.1999, pp. 8-15÷8-26.
218. **Dybczyński R., Danko B., Polkowska-Motrenko H.**  
NAA study of homogeneity of reference materials and their suitability for microanalytical techniques.  
Tenth International Conference on Modern Trends in Activation Analysis. Final Program & Book of Abstracts. Bethesda Maryland, USA, 19-23.04.1999, p. 312.
219. **Kowalik J., Błasiak J., Wojewódzka M.**  
Genotoksyczność insektycydów fosforoorganicznych i ochronna rola witaminy C (Genotoxic effect of organophosphorus pesticides and protective action of vitamin C).  
Trzecia Konferencja Naukowa poświęcona Profesorowi Antoniemu Dmochowskiemu "Aktualne kierunki badań w biochemii i biotechnologii w ochronie środowiska i życia człowieka". Abstrakty. Łódź, Poland, 14-16.12.1999, p. 9.
220. **Kowalik J., Trzeciak A., Wojewódzka M., Błasiak J.**  
In vitro genotoxic effect of curcumin assessed by alkaline single cell gel/comet assay.  
Neoplasma, **46**, Supplement, 64-65 (1999).
221. **Kruszewski M., Machaj K., Ołdak T., Pojda Z.**  
Comparison of two methods of DNA isolation from the umbilical cord blood.  
American Society of Gene Therapy. 2nd Annual Meeting. Book of Abstracts. Washington D.C., USA, 9-13.06.1999, p. 68a.
222. **Kruszewski M., Wojewódzka M., Iwaneńko T., Okuyama A., Żebrowska T., Jarocewicz N., Szumiel I.**  
Differential inhibitory effect of DNA-PK inhibitor (OK-1035) on DNA repair in L5178Y mouse lymphoma cell lines.  
Neoplasma, **46**, Suppl., 32-33 (1999).
223. **Lenartowicz M., Wójcik A.**  
Preferential segregation of marker chromosomes 14 and 18 in mouse recombinant inbred strains derived from the KE and CBA/Kw strains.  
Folia Biologica, **47**, 3-4, 131-134 (1999).
224. **Przybytniak G., Ambroz H.**  
Wolne rodniki, ich identyfikacja i oznaczanie (Free radicals, their identification and determination).  
In: Metody Analityczne w Badaniach Substancji Szkodliwych i Niebezpiecznych. Praca zbiorowa pod redakcją Jerzego Gacy i in. Bydgoskie Towarzystwo Naukowe, Bydgoszcz 1999, Prace Wydziału Nauk Technicznych. Seria A. Z. Nr 26, pp. 17-26.
225. **Pszonicki L., Skwara W.**  
Behaviour of selenium and tellurium in the presence of various modifiers in electrothermal atomic absorption spectrometry.  
Journal of Analytical Atomic Spectrometry, **14**, 1925-1928 (1999)
226. **Stuglik Z.**  
Absolute and secondary dosimetry for the cyclotron ion beam radiation experiments.  
In: Techniques for High-Dose Dosimetry in Industry, Agriculture and Medicine (IAEA-TECDOC-1070). International Atomic Energy Agency, Vienna 1999, pp. 213-219.



227. **Trzeciak A., Kowalik J., Małecka-Panas E., Drzewoski J., Wojewódzka M., Błasiak J.**  
Uszkodzenia i naprawa DNA limfocytów ekspozowanych na związki chromu(VI) i malaoksonu w obecności kurkuminy (DNA damage and repair in human exposed to chromium(VI) and malaokson in present of curcumin).  
Trzecia Konferencja Naukowa poświęcona Profesorowi Antoniemu Dmochowskiemu "Aktualne kierunki badań w biochemii i biotechnologii w ochronie środowiska i życia człowieka". Abstrakty. Łódź, Poland, 14-16.12.1999, p. 19.
228. **Trzeciak A., Kowalik J., Wojewódzka M., Błasiak J.**  
Genotoxicity of chromium in human gastric mucosa cells and peripheral blood lymphocytes.  
Neoplasma, **46**, Supplement, 13-15 (1999).
229. **Trzeciak A., Wojewódzka M., Błasiak J.**  
Genotoksyczność etanolu i aldehydu octowego w limfocytach człowieka (Genotoxic effect of ethanol and acetaldehyde on human lymphocytes).  
Trzecia Konferencja Naukowa poświęcona Profesorowi Antoniemu Dmochowskiemu "Aktualne kierunki badań w biochemii i biotechnologii w ochronie środowiska i życia człowieka". Abstrakty. Łódź, Poland, 14-16.12.1999, p. 18.
230. **Wojewódzka M., Van der Schans G.P., Szumiel I.**  
DNA repair in radioadapted human lymphocytes studied by the SCGE and ELISA.  
Neoplasma, **46**, Suppl., 40 (1999).
231. **Zagórski Z.P.**  
Produkty natury - błogosławieństwa i niebezpieczeństwa (Natural products - blessings and dangers).  
W: Problemy środowiska i jego ochrony. Część 7. Red. M. Nakonieczny i P. Migula. Uniwersytet Śląski: Centrum Studiów nad Człowiekiem i Środowiskiem, Katowice 1999, pp. 115-123.
232. **Żuchowska D., Rajkowska M., Przybytniak G., Meissner W.**  
Kompozycje polietylenu z blokowym kopolimerem styren/etylen/butylen modyfikowane metodą radiacyjną (Modification of blends of polyethylene and styrene/ethylene/butylene block copolymer by radiation method).  
Materiały XIV Konferencji Naukowej "Modyfikacja Polimerów". Kudowa Zdrój, Poland, 26-30.09.1999, pp. 333-336.

## THE INCT REPORTS IN 2000

1. INCT Annual Report 1999.  
IChTJ, Warszawa 2000, 182 p.
2. Urbański P., Machaj B..  
Multivariate signal processing in measurements of radon and radon daughters in air.  
IChTJ, Warszawa 2000. Raporty IChTJ. Seria B nr 1/2000, 32 p.
3. Wojewódzka M., Grądzka I., Buraczewska I.  
Test kometowy w pH obojętnym (The neutral comet assay).  
IChTJ, Warszawa 2000. Raporty IChTJ. Seria B nr 2/2000, 18 p.
4. Radoszewski T.  
Program pomiarów pochodnych radonu w komorze radonowej (A program for radon decay products measurements in radon chamber).  
IChTJ, Warszawa 2000. Raporty IChTJ. Seria B nr 3/2000, 14 p.
5. Fuks L., Mamont-Cieśla K., Kusyk M.  
Badania polskich węgli aktywnych przeznaczonych do sorpcji i detekcji radonu (Searching of Polish activated carbons for radon sorption and detection).  
IChTJ, Warszawa 2000. Raporty IChTJ. Seria B nr 4/2000, 16 p.
6. Kowalska E., Urbański P.  
Zastosowanie wielowymiarowej kalibracji w oznaczaniu wapnia i żelaza w popiołach metodą analizy fluorescencyjnej (Application of multivariate calibration for determination of calcium and iron in ash with XRF analysis).  
IChTJ, Warszawa 2000. Raporty IChTJ. Seria B nr 5/2000, 28 p.
7. Stuglik Z.  
A high dose dosimetry system in the Institute of Nuclear Chemistry and Technology after realization of INCO-Copernicus CT96 EU 0824 Project "Accreditation for high dose measurement".  
IChTJ, Warszawa 2000. Raporty IChTJ. Seria B nr 6/2000, 14 p.
8. Lehner K., Stachowicz W.  
Wykrywanie i oznaczanie radiacyjnie indukowanych węglowodorów w próbkach mięsa za pomocą chromatografii gazowej jako metoda identyfikacji napromieniowania żywności (Detection and identification of radiation induced hydrocarbons in meats with the use of gas chromatography as one of methods for the detection of irradiated food).  
IChTJ, Warszawa 2000. Raporty IChTJ. Seria B nr 7/2000, 34 p.
9. Wojewódzka M., Grądzka I., Buraczewska I.  
Badanie roli naprawy dwuniciowych pęknięć DNA w odpowiedzi adaptacyjnej limfocytów ludzkich (Studying of the DNA DSBs repair in the adaptive response of human lymphocytes).  
IChTJ, Warszawa 2000. Raporty IChTJ. Seria B nr 8/2000, 44 p.
10. Kroh J., Bobrowski K., Chmielewski A.G., Foryś M., Kaleciński J., Rosiak J., Wolszczak M., Zimek Z.  
Stan obecny oraz perspektywy rozwoju chemii i technologii radiacyjnej w Polsce (The present status and perspectives on the development of radiation chemistry and technology in Poland).  
IChTJ, Warszawa 2000. Raporty IChTJ. Seria B nr 9/2000, 40 p.
11. Kowalska E. Urbański P.  
Wielowymiarowa kalibracja w radiometrycznych pomiarach popiołowości węgla (Multivariate calibration in the radioisotope measurements of the ash content in coal).  
IChTJ, Warszawa 2000. Raporty IChTJ. Seria B nr 10/2000, 24 p.

## NUKLEONIKA

### THE INTERNATIONAL JOURNAL OF NUCLEAR RESEARCH

#### EDITORIAL BOARD

**Andrzej G. Chmielewski** (Editor-in-Chief, Poland), **Krzysztof Andrzejewski** (Poland), **Janusz Z. Beer** (USA), **Gregory R. Choppin** (USA), **Bohdan Dziunikowski** (Poland), **Andrei Gagarinsky** (Russia), **Alexander van Hook** (USA), **Zbigniew Jaworowski** (Poland), **Larry Kevan** (USA), **Evgeni A. Krasavin** (Russia), **Stanisław Latek** (Poland), **Sueo Machi** (Japan), **Jacek Michalik** (Poland), **Tomasz Mioduski** (Poland), **James D. Navratil** (USA), **Robert H. Schuler** (USA), **Irena Szumiel** (Poland), **Piotr Urbański** (Poland)

#### CONTENTS OF No. 1/2000

1. Von Sonntag C.  
Klaus-Dieter Asmus. On the occasion of his 60th birthday.
2. Asmus K.-D.  
Odd-electron bonded sulfur- and selenium-centered radical cations as studied by radiation chemical and complementary methods.
3. Carmichael I.  
Theoretical studies on sulfur-containing radical ions.
4. Chhun S., Bergés J., Bleton V., Abedinzadeh Z.  
Intramolecular transformation of thiyl radicals to  $\alpha$ -aminoalkyl radicals: ab initio calculations on homocystein.
6. Bergés J., Fuster F., Jacquot J.-P., Silvi B., Houée-Levin C.  
Influence of protonation on the stability of disulfide radicals.
7. Chmielewski A.G.  
Radiation-induced sulfur dioxide removal.
8. Bonifacić M., Štefanić I.  
Oxidation of organic sulfides by peroxy radicals; search for an adduct intermediate.
9. Flyunt R., Makogon O., Schöneich C., Asmus K.-D.  
Radiolytically induced reductive degradation of halothane in air-saturated aqueous solutions in the presence of methionine.
10. Schöneich C.  
Reaction of sulfide radical cation complexes with hydroxide, molecular oxygen and superoxide radical anion.
11. Schuchmann M.N., Schuchmann H.-P., Knolle W., Von Sonntag J., Naumov S., Wang W.F., Von Sonntag C.  
Free-radical chemistry of thiourea in aqueous solution, induced by OH radical, H atom,  $\alpha$ -hydroxyalkyl radicals, photoexcited maleimide, and the solvated electron.
12. Hug G.L., Bobrowski K., Kozubek H., Marciniak B.  
pH effects on the photooxidation of methionine derivatives by the 4-carboxybenzophenone triplet state.
13. Wrzyszczyński A., Ścigalski F., Pączkowski J.  
Sulfur-containing initiator and coinitiators of free radical polymerization.

14. Andrzejewska E., Hug G.L., Andrzejewski M., Maciniak B.  
Photoreduction of benzophenone by trithianes as the initiation step in radical polymerization.
15. Strzelczak G., Bobrowski K., Kozubek H., Michalik J.  
Electron spin resonance study of radiation-induced radicals in polycrystalline oligopeptides containing methionine.
16. Pogocki D., Sadło J.  
Radiation-induced oxidation of thiaproline derivatives in frozen acidic aqueous solutions: theoretical and electron spin resonance study.
17. Zagórski Z.P., Rafalski A.  
Radiation chemistry of solid thiosulfate: optical absorption spectra.

#### CONTENTS OF No. 2/2000

1. Obituary: Prof. Tomasz Mioduski
2. Cebulska-Wasilewska A., Schneider K., Capała J., Coderre J.  
Biological efficiency of the Brookhaven Medical Research Reactor mixed neutron beam estimated from gene mutation in *Tradescantia stamen* hair cells assay.
3. Zieliński M., Zielińska A., Papiernik-Zielińska H., Ogrinc N., Kobal I.  
Carbon-13 isotope effect for decarboxylation of phenylpropionic acid (PPA) in concentrated phosphoric acids.
4. Sernicki J.  
Local space charge effect in conventional avalanche counters at moderate specific ionization.
5. Hryńczuk B., Weber R.  
Influence of urea and of chlorocholine chloride on accumulation of  $^{137}\text{Cs}$  in spring wheat crops.
6. Weber R., Hryńczuk B.  
Effect of leaf and soil contaminations on heavy metals content in spring wheat crops.
7. Aziz M., Andrzejewski K.  
Criticality calculations for the spent fuel storage pools for Etrr\_1 and Etrr\_2 reactors.
8. Włosiński W., Krajewski A., Piekoszewski J., Stanisławski J., Waliś L.  
Intense pulsed plasma beams in ceramic/metal brazing.

#### CONTENTS OF No. 3/2000

1. Gribkov V.A.  
Preface
2. Gribkov V.A.  
On possible formulation of problems of a Dense Plasma Focus used in materials sciences.
3. Scholz M., Miklaszewski R., Gribkov V.A., Mezzetti E.  
PF-1000 device.
4. Dubrovsky A.V., Gribkov V.A.  
Installations based on high efficiency high repetition rate miniature DPF chambers for material science.
5. Tsybenko S.P., Miklaszewski R.  
On tuning mechanisms of DPF devices.
6. Büscher S., Wrubel T., Kunze H.-J.  
Technical setup and physical properties of a gas-liner pinch
7. Freese W., Kunze H.-J.  
On the influence of a carbon solid on the properties of a helium plasma in a theta pinch discharge.

8. Sadowski M., Składnik-Sadowska E., Baranowski J., Zebrowski J., Kelly H., Lepone A., Marquez A., Milanese M., Moroso R., Pouzo J.  
Comparison of characteristics of pulsed ion beams emitted from different small PF devices.
9. Dubrovsky A.V., Silin P.V., Gribkov V.A., Volobuev I.V.  
DPF device application in the material characterization.
10. Verri G., Mezzetti F., Da Re A., Bortolotti A., Rapezzi L., Gribkov V.A.  
Fast Neutron Activation Analysis of gold by inelastic scattering,  $^{197}\text{Au}(n,n'\gamma)^{197}\text{Au}^m$ , by means of Plasma Focus device.
11. Langner J., Piekoszewski J., Stanisławski J., Werner Z.  
Present status and prospects of research in SINS on the modification of surface properties by pulsed plasma streams.
12. Sadowski M., Langner J., Stanisławski J., Matějček J., Kolman B., Chráska P.  
Surface modification of plasma-sprayed alumina deposits by high-energy ion beams.
13. Ivanov L.I., Pimenov V.N., Maslyayev S.A., Dyomina E.V., Gribkov V.A., Mezzetti F., DeChiara P., Pizzo L.  
Influence of dense deuterium plasma pulses on materials in Plasma Focus device.
14. Glazunov G.P., Volkov E.D., Lapshin V.I., Tereshin V.I., Sadowski M., Langner J., Stanisławski J.  
Some problems of plasma-material interactions in fusion devices.

#### CONTENTS OF No. 4/2000

1. Szumiel I.  
The importance of the nuclear and cytoplasmic signalling in the cellular response to ionizing radiation.
2. Zieliński M., Fry A., Zielińska A., Ogrinc N., Papiernik-Zielińska H., Kobal I.  
Carbon-13 fractionation in the oxidation of propionate of natural isotopic composition with permanganate and manganate.
3. Warchoń S., Rzewuski H., Krynicki J., Grötzschel R.  
Post-implantation defects instability under 1 MeV electron irradiation in GaAs.
4. El-Messiry A.M.  
Accidents of loss of flow for the ETTR-2 reactor: deterministic analysis.
5. Pant H.J., Saroha A.K., Nigam K.D.P.  
Measurement of liquid holdup and axial dispersion in trickle bed reactors using radiotracer technique.
6. Charewicz W.A., Zebrowski A., Walkowiak W., Borek B.  
A modified method for the determination of radioactive isotopes in building raw and construction materials with multichannel gamma spectrometry.

#### Information

#### INSTITUTE OF NUCLEAR CHEMISTRY AND TECHNOLOGY NUKLEONIKA

Dorodna 16, 03-195 Warszawa, Poland

phone: (+48-22) 811-06-56 or 811-30-21 int. 14-91; fax: (+48-22) 811-15-32;

e-mail: nukleon@orange.ichtj.waw.pl

Abstracts are available on-line at

<http://www.euronuclear.org/publications/nukleonika/index.html>

## THE INCT PATENTS AND PATENT APPLICATIONS IN 2000

### PATENTS

1. Sposób wytwarzania pustych ziaren sferycznych materiałów ceramicznych, cermetali i metali redukowanych wodorem (Method for obtaining empty spherical grains of ceramic materials, cermetals and metals reduced with hydrogen).  
A. Deptuła, A.G. Chmielewski, T. Olczak, W. Łada  
Polish Patent no. 179421
2. Sposób oczyszczania ścieków radioaktywnych (Method for purification of radioactive sewages).  
A.G. Chmielewski, G. Zakrzewska-Trznadel, M. Harasimowicz, A. Van Hook  
Polish Patent no. 179430
3. Sposób otrzymywania warstw fosforanów wapnia, w szczególności hydroksyapatytu (Method for obtaining layers from calcium phosphate, in particular hydroxyapatite).  
A. Deptuła, W. Łada, R.Z. LeGeros, T. Olczak, J.P. LeGeros  
Polish Patent no. 180602

### PATENT APPLICATIONS

1. Alaninowo-polimerowy dozymetr promieniowania jonizującego (An alanine-polymer dosimeter of ionizing radiation).  
Z. Stuglik, T. Bryl-Sandelewska, K. Mirkowski  
P. 338997
2. Sposób wytwarzania termotopliwej kompozycji klejowej z kopolimerów octanu winylu z etylenem (Method for obtaining glue composition from copolymers of vinyl acetate from ethylene).  
I. Legocka, Z. Zimek, A. Woźniak, K. Mirkowski  
P. 340068
3. Sposób usuwania lotnych zanieczyszczeń organicznych gazowych, takich jak wielopierścieniowe węglowodory aromatyczne z przemysłowych gazów odlotowych (Method for removal of volatile organic gaseous impurities such as multiring aromatic hydrocarbons from industrial flow gases).  
A.G. Chmielewski, A. Ostapczuk, K. Kubica, J. Licki  
P. 340319
4. Sposób otrzymywania paliw ciekłych z odpadów tworzyw sztucznych, zwłaszcza odpadów poliolefinowych i urządzenie do realizacji tego sposobu (Method for obtaining liquid fuels from wastes of plastics, in particular of polyolefines and the facility to realize the method).  
A.G. Chmielewski, J. Jerzy, T. Siekierski, B. Tymiński, K. Zwoliński  
P. 342248

## CONFERENCES ORGANIZED AND CO-ORGANIZED BY THE INCT IN 2000

### 1. THE FIRST COORDINATION CONSORTIUM MEETING FOR PROJECT "ELECTRON BEAM PROCESSING OF FLUE GASES, EMITTED IN METALLURGICAL PROCESSES, FOR VOLATILE ORGANIC COMPOUNDS REMOVAL", 4-5 SEPTEMBER 2000, WARSZAWA, POLAND

Organized by  
Institute of Nuclear Chemistry and Technology

#### Organizing Committee:

A. Ostapczuk, M.Sc. (Institute of Nuclear Chemistry and Technology, Warszawa, Poland); Prof. A.G. Chmielewski (Institute of Nuclear Chemistry and Technology, Warszawa, Poland); Prof. J. Piekoszewski (Institute of Nuclear Chemistry and Technology, Warszawa, Poland)

#### SCIENTIFIC PART

- Opening: general introduction into the project  
A.G. Chmielewski (Institute of Nuclear Chemistry and Technology, Warszawa, Poland)
- Consortium members and research teams presentations with emphasis on their experience in the field connected with the project  
A.G. Chmielewski (Institute of Nuclear Chemistry and Technology, Warszawa, Poland)  
V. Honkonen (Pohjois-Savo Polytechnic, Finland)  
O. Fainchtein (Institute ENERGOSTAL, Ukraine)  
H. Nichipor (Institute of Radiation Physical and Chemical Problems, Academy of Sciences of Belarus)  
N. Getoff (Ludwig-Boltzmann Institute, Austria)  
P. Skeldon (University of Manchester, Institute of Science and Technology, United Kingdom)
- General overview of the state of the basis for the project
  - Metallurgical sector in Ukraine and its impact on environment  
O. Fainchtein (Institute ENERGOSTAL, Ukraine)
  - Recent developments in electron beam flue gas treatment  
A.G. Chmielewski (Institute of Nuclear Chemistry and Technology, Warszawa, Poland)
- Project programme for the next 6 months tasks and their action plans
  - Analytical methods for experimental work  
A. Ostapczuk (Institute of Nuclear Chemistry and Technology, Warszawa, Poland)
  - Simulation programme  
V. Honkonen (Pohjois-Savo Polytechnic, Finland)
  - Analytical methods for industry tests  
O. Fainchtein (Institute ENERGOSTAL, Ukraine)
  - VOCs kinetic data  
H. Nichipor (Institute of Radiation Physical and Chemical Problems, Academy of Sciences of Belarus)
  - VOCs oxidation  
N. Getoff (Ludwig-Boltzmann Institute, Austria)
  - Solution to the material problem  
P. Skeldon (University of Manchester, Institute of Science and Technology, United Kingdom)

#### TECHNICAL VISIT TO EBFGT (COAL BOILER) PS KAWĘCZYN PILOT PLANT

#### ADMINISTRATIVE PART

## **2. INTERNATIONAL MINI-SYMPOSIUM ON "RADIATION-INDUCED RADICAL PROCESSES IN SYSTEMS OF BIOLOGICAL RELEVANCE", 18 SEPTEMBER 2000, WARSZAWA, POLAND**

**Organized by**  
**Institute of Nuclear Chemistry and Technology**

**Organizing Committee:** Prof. K. Bobrowski (Institute of Nuclear Chemistry and Technology, Warszawa, Poland)

### **OPENING ADDRESS**

A.G. Chmielewski (Institute of Nuclear Chemistry and Technology, Warszawa, Poland)

### **SCIENTIFIC SESSION I**

**Chairman:** Prof. J. Michalik (Institute of Nuclear Chemistry and Technology, Warszawa, Poland)

- One-electron oxidation and reduction processes in thioredoxin  
Ch. Houée-Levin (Université Paris-Sud, Orsay, France)
- Superoxide radical oxidation of sulfhydryls  
Z. Abedinzadeh (Université René Descartes, Paris, France)
- Radiation-induced radicals in DNA  
G. Przybytniak (Institute of Nuclear Chemistry and Technology, Warszawa, Poland)

### **SCIENTIFIC SESSION II**

**Chairman:** Z. Zimek, Ph.D. (Institute of Nuclear Chemistry and Technology, Warszawa, Poland)

- Capabilities and application of the BNL Laser-Electron Accelerator in studying electron transfer processes  
J.F. Wishart (Brookhaven National Laboratory, Upton, USA)
- One- and two-electron oxidation of dimethyl selenide  
R. Flyunt (MPI-Strahlenchemie, Muelheim, Germany; Institute of Physico-Chemistry, National Academy of Sciences of the Ukraine, Lviv, Ukraine)
- Stabilization of sulfur radical cations via intramolecular sulfur-carbonyl oxygen bond formation  
K. Bobrowski (Institute of Nuclear Chemistry and Technology, Warszawa, Poland)
- Pulse radiolysis study of formation and repair of retinoic cation radicals  
T. Sarna (Institute of Molecular Biology, Jagiellonian University, Kraków, Poland)

## **3. BILATERAL WORKSHOP ON "RADIATION-INDUCED PARAMAGNETIC DEFECTS IN SOLIDS", 29-30 MAY 2000, GHENT, BELGIUM**

**Organized by**  
**Ghent University, Institute of Nuclear Chemistry and Technology, University of Antwerp**

**Organizing Committee:** Prof. F. Callens (Ghent University, Belgium), Prof. P. Matthys (Ghent University, Belgium), Prof. E. Goovaerts (University of Antwerp, Belgium), Prof. J. Michalik (Institute of Nuclear Chemistry and Technology, Warszawa, Poland)

### **SCIENTIFIC PROGRAMME**

#### **Session 1**

**Session Chair:** Prof. F. Callens (Ghent University, Belgium)

- Paramagnetic silver clusters in zeolites  
J. Michalik (Institute of Nuclear Chemistry and Technology, Warszawa, Poland), J. Sadło (Institute of Nuclear Chemistry and Technology, Warszawa, Poland), J. Perlińska (Institute of Nuclear Chemistry and Technology, Warszawa, Poland)
- A W-band study of the D1 center in cubic boron nitride single crystals  
S.V. Nistor (National Institute for Materials Physics, Bucharest, Romania), M. Stefan (University of Antwerp, Belgium; National Institute for Materials Physics, Bucharest, Romania), D. Shoemaker (University of Antwerp, Belgium), E. Goovaerts (University of Antwerp, Belgium), G. Dinca (Dacia Synthetic Diamond Co., Bucharest, Romania)



## Session 2

**Session Chair: Prof. P. Matthys** (Ghent University, Belgium)

- The microstructure of the EL2 antisite defect in GaAs - a challenge for EPR and ENDOR  
J.R. Niklas (Technical University Bergakademie Freiberg, Germany)
- Detection of irradiated food by EPR  
W. Stachowicz (Institute of Nuclear Chemistry and Technology, Warszawa, Poland), G. Strzelczak (Institute of Nuclear Chemistry and Technology, Warszawa, Poland), F. Callens (Ghent University, Belgium)

## Session 3

**Session Chair: Prof. J. Michalik** (Institute of Nuclear Chemistry and Technology, Warszawa, Poland)

- Application of advanced EPR techniques in the study of solid state metal centers  
E. Reijerse (Catholic University of Nijmegen, the Netherlands)
- The advantage of Q and W-band EPR in the study of radiation induced species in shells and corallite  
G. Strzelczak (Institute of Nuclear Chemistry and Technology, Warszawa, Poland), G. Vanhaelewyn (Ghent University, Belgium), W. Stachowicz (Institute of Nuclear Chemistry and Technology, Warszawa, Poland), E. Goovaerts (University of Antwerp, Belgium), F. Callens (Ghent University, Belgium), J. Michalik (Institute of Nuclear Chemistry and Technology, Warszawa, Poland)

## Session 4

**Session Chair: Prof. E. Goovaerts** (University of Antwerp, Belgium)

- EPR study of paramagnetic centers generated in metastable forms of solidified water upon gamma-irradiation  
A. Pionka (Technical University of Łódź, Poland)
- EPR and ENDOR of irradiated sugars  
G. Vanhaelewyn (Ghent University, Belgium), P. Lahorte (Ghent University, Belgium), W. Mondelaers (Ghent University, Belgium), F. Callens (Ghent University, Belgium), J. Michalik (Institute of Nuclear Chemistry and Technology, Warszawa, Poland), P. Matthys (Ghent University, Belgium)
- Paramagnetic radicals in X-ray irradiated tooth enamel heated at 400°C  
J. Sadło (Institute of Nuclear Chemistry and Technology, Warszawa, Poland), S. Amira (Ghent University, Belgium), G. Vanhaelewyn (Ghent University, Belgium), F. Callens (Ghent University, Belgium), P. Matthys (Ghent University, Belgium), J. Michalik (Institute of Nuclear Chemistry and Technology, Warszawa, Poland), W. Stachowicz (Institute of Nuclear Chemistry and Technology, Warszawa, Poland)

## POSTER SESSION

- Q-band EPR and ENDOR study of  $\text{Rh}^+$  in NaCl single crystals  
H. Vrielinck (Ghent University, Belgium), F. Callens (Ghent University, Belgium), P. Matthys (Ghent University, Belgium)
- Free radicals contained in licorice-flavored sweets can be detected non-invasively after oral administration to mice using low frequency EPR  
B. Gallez (Catholic University of Louvain, Belgium), C. Baudalet (Catholic University of Louvain, Belgium), R. Debuyst (Catholic University of Louvain, Belgium)
- EPR studies of pharmaceuticals in solid phase  
M. Gibella (Catholic University of Louvain, Belgium), A. Engalytcheff (Catholic University of Louvain, Belgium), A.-S. Crucq (Catholic University of Louvain, Belgium), B. Tilquin (Catholic University of Louvain, Belgium), P. Stocker (Université d'Aix-Marseille, France), G. Lesgards (Université d'Aix-Marseille, France), J. Raffi (Université d'Aix-Marseille, France)
- Multifrequency EPR study of radicals produced by radiation in shells and corallite  
G. Strzelczak (Institute of Nuclear Chemistry and Technology, Warszawa, Poland), G. Vanhaelewyn (Ghent University, Belgium), W. Stachowicz (Institute of Nuclear Chemistry and Technology, Warszawa, Poland), E. Goovaerts (University of Antwerp, Belgium), F. Callens (Ghent University, Belgium), J. Michalik (Institute of Nuclear Chemistry and Technology, Warszawa, Poland)
- EPR and ENDOR study of human tooth enamel heated at 400°C  
J. Sadło (Institute of Nuclear Chemistry and Technology, Warszawa, Poland), G. Vanhaelewyn (Ghent University, Belgium), S. Amira (Ghent University, Belgium), R. Morent (Ghent University, Belgium), P. Matthys (Ghent University, Belgium), F. Callens (Ghent University, Belgium), J. Michalik (Institute of Nuclear Chemistry and Technology, Warszawa, Poland), W. Stachowicz (Institute of Nuclear Chemistry and Technology, Warszawa, Poland)

- Conduction electron spin resonance (CESR) of metallic particles in mesoporous materials  
M. Danilczuk (Institute of Nuclear Chemistry and Technology, Warszawa, Poland), Jong-Sung Yu (Hannam University, Taejon, Korea), D. Brown (University of Huddersfield, United Kingdom), L. Kevan (University of Houston, USA), J. Michalik (Institute of Nuclear Chemistry and Technology, Warszawa, Poland)
- Cationic silver clusters in sodalites  
J. Perlińska (Institute of Nuclear Chemistry and Technology, Warszawa, Poland), H. Yamada (National Institute for Research in Inorganic Materials, Japan), J. Michalik (Institute of Nuclear Chemistry and Technology, Warszawa, Poland)
- EPR study of Lewis-acid sites in zeolites using NO as probe molecule  
G. Catana (Catholic University of Louvain, Belgium), B.M. Weckhuysen (Catholic University of Louvain, Belgium), R.A. Schoonheydt (Catholic University of Louvain, Belgium)
- Dielectric resonator-based resonant structure for ESR measurements at high hydrostatic pressures  
A. Sienkiewicz (Institute of Physics, Polish Academy of Sciences, Warszawa, Poland; École Polytechnique Fédérale de Lausanne, Switzerland), S. Garaj (École Polytechnique Fédérale de Lausanne, Switzerland), M. Jaworski (Institute of Physics, Polish Academy of Sciences, Warszawa, Poland), C.P. Scholes (SUNNY at Albany, USA), L. Forro (École Polytechnique Fédérale de Lausanne, Switzerland)
- New opportunities offered by high-field EPR/ENDOR in the structural characterization of Mn(II) sites in zeolites  
D. Arieli (Weizmann Institute of Science, Israel), D.E.W. Vaughan (Pennsylvania State University, USA), K.G. Strohmaier (Exxon Research and Engineering Company, USA), D. Goldfarb (Weizmann Institute of Science, Israel)
- Single crystal high frequency EPR of  $\text{Fe}_4(\text{OCH}_3)_6(\text{dmp})_6$   
M. Stefan (University of Antwerp, Belgium; National Institute for Materials Physics, Bucharest, Romania), A. Bouwen (University of Antwerp, Belgium), E. Goovaerts (University of Antwerp, Belgium), D. Gatteschi (University of Florence, Italy), R. Sessoli (University of Florence, Italy), L. Sorace (University of Florence, Italy)
- Nano-scale structure of rare earth doped oxide glasses as studied by electron spin echo spectroscopy  
S.B. Orliński (Kazan State University, Kazakhstan), E.J. Reijerse (Catholic University of Nijmegen, the Netherlands)
- A Cw/pulsed heterodyne 190 GHz EPR bridge  
E.J. Reijerse (Catholic University of Nijmegen, the Netherlands), A.A.K. Klaassen (Catholic University of Nijmegen, the Netherlands), W.R. Hagen (Catholic University of Nijmegen, the Netherlands)
- Thermodynamics and kinetics of proton exchange in pH-sensitive Imidazolyl spinlabels as studied by D-band EPR  
E.J. Reijerse (Catholic University of Nijmegen, the Netherlands), V.V. Khramstov (Russian Academy of Science, Novosibirsk, Russia), I.A. Grigor'ev (Russian Academy of Science, Novosibirsk, Russia)
- Lineshape effects of distributions in zero field splitting parameters  
A.H. Priem (Catholic University of Nijmegen, the Netherlands), A.A. Klaassen (Catholic University of Nijmegen, the Netherlands), E.J. Reijerse (Catholic University of Nijmegen, the Netherlands), W.R. Hagen (Catholic University of Nijmegen, the Netherlands)

#### **4. SEMINARIUM "POLSKA NAUKA I TECHNIKA DLA ENERGETYKI JĄDROWEJ JUTRA" (SEMINAR "POLISH SCIENCE AND TECHNOLOGY FOR NUCLEAR ENERGY OF TOMORROW"), 13-14 APRIL 2000, MAĐRALIN NEAR WARSZAWA, POLAND**

##### **Organized by**

Institute of Nuclear Chemistry and Technology, Institute of Atomic Energy, National Atomic Energy Agency, Polish Nuclear Society

**Komitet Programowy:** Prof. S. Chwaszczewski - chairman (Institute of Atomic Energy, Świerk, Poland); Prof. A. Hrynkiewicz (H. Niewodniczański Institute of Nuclear Physics, Kraków, Poland); Prof. J. Marecki (Technical University of Gdańsk, Poland); Prof. Z. Celiński (Warsaw University of Technology, Poland); T. Wójcik, Ph.D. (National Atomic Energy Agency, Poland); W. Mazurek, M.Sc. (ENERGOPROJEKT-Warszawa, Poland); Prof. M. Lech (Wrocław Technical University, Poland); A. Pierzak, M.Sc. (Energy Agency Market, Poland); K. Lipko, M.Sc. (Polish Power Grid Company - International); W.

**Sikora, M.Sc.** (Ministry of Economy, Poland); **Prof. A.G. Chmielewski** (Institute of Nuclear Chemistry and Technology, Warszawa, Poland); **J. Włodarski** (National Atomic Energy Agency, Poland); **S. Szpilowski, Ph.D.** (National Atomic Energy Agency, Poland)

**Organizing Committee:** **G. Zakrzewska-Trznadel, Ph.D. - chairman** (Institute of Nuclear Chemistry and Technology, Warszawa, Poland); **A. Mikulski, Ph.D.** (Institute of Atomic Energy, Świerk, Poland); **M. Romanowski, Eng.** (Study and Design Nuclear Technique Office PROATOM, Warszawa, Poland); **W. Głuszewski, M.Sc.** (Institute of Nuclear Chemistry and Technology, Warszawa, Poland)

## LECTURES

- Analiza zapotrzebowania i prognoza struktury wytwarzania energii elektrycznej (Analysis of demand and the prognosis of the structure of electric energy production)  
S. Ciok (Energy Agency Market, Poland), A. Kerner (Energy Agency Market, Poland), J. Woroniecki (Energy Agency Market, Poland)
- Perspektywy rozwoju elektroenergetyki w Polsce (Perspectives of the development of electric power industry in Poland)  
M. Kwiatkowski (Polish Power Grid Company - International), R. Frydrychowski (Polish Power Grid Company - International)
- Energetyka jądrowa na świecie (Nuclear power industry in the world)  
T. Wójcik (National Atomic Energy Agency, Poland)
- Źródła i przetwarzanie energii w XXI wieku (Sources and energy conversion in the XXI century)  
R. Domański (Warsaw University of Technology, Poland)
- Ekonomiczne aspekty energetyki jądrowej (Economic aspects of nuclear power industry)  
Z. Celiński (Warsaw University of Technology, Poland)
- Rynek uranu i paliw reaktorowych - stan i perspektywy (Uranium and reactor fuel market - the state and perspectives)  
W. Dembiński (Institute of Nuclear Chemistry and Technology, Warszawa, Poland)
- Możliwości wykorzystania 50 lat doświadczeń w projektowaniu "Energoprojektu Warszawa" dla energetyki jądrowej w przyszłości (Fifty-year experience of ENERGOPROJEKT-Warszawa for future design work in nuclear power industry)  
M. Roguska (ENERGOPROJEKT-Warszawa, Poland), K. Grzebuła (ENERGOPROJEKT-Warszawa, Poland), A. Patrycy (ENERGOPROJEKT-Warszawa, Poland)
- Reaktory jądrowe nowej generacji (New generation of nuclear reactors)  
S. Chwaszczewski (Institute of Atomic Energy, Świerk, Poland)
- Badania plazmy i syntezy termojądrowej w IFPiLM (Plasma and thermonuclear synthesis research in the Institute of Plasma Physics and Laser Microfusion)  
A. Gałkowski (Institute of Plasma Physics and Laser Microfusion, Warszawa, Poland)
- Synteza jądrowa dla potrzeb energetyki - stan badań światowych (Nuclear synthesis for power industry needs - state-of-the-art in the world)  
Z. Składanowski (Institute of Plasma Physics and Laser Microfusion, Warszawa, Poland)
- "Modne" kierunki badań dla "niemodnej" energetyki jądrowej ("Popular" research directions for "non-popular" nuclear power industry)  
N. Gołnik (Institute of Atomic Energy, Świerk, Poland)
- Mechanizm procesu wydzielania energii z jąder-tarcz w zderzeniach hadron-jądro (The mechanism of energy emission from target nuclei in hadron-nucleus collision)  
Z. Strugalski (Institute of Atomic Energy, Świerk, Poland), E. Strugalska-Gola (Institute of Atomic Energy, Świerk, Poland)
- Nieorganiczne wymiennicze jonów jako potencjalne bariery w składowiskach odpadów promieniotwórczych (Non-organic ion exchangers as potential barriers for radioactive waste storage)  
J. Narbutt (Institute of Nuclear Chemistry and Technology, Warszawa, Poland), A. Bilewicz (Institute of Nuclear Chemistry and Technology, Warszawa, Poland), J. Krejzler (Institute of Nuclear Chemistry and Technology, Warszawa, Poland)
- Energetyka i środowisko (Electric power industry and the environment)  
A. Hryniewicz (H. Niewodniczański Institute of Nuclear Physics, Kraków, Poland)
- Ekologiczne aspekty spalania paliw kopalnych (Ecological aspects of fossil fuel burning)  
A.G. Chmielewski (Institute of Nuclear Chemistry and Technology, Warszawa, Poland)

- Analiza termodynamiczna przebiegu awarii rozszczelnieniowej w układzie z reaktorem wodnym ciśnieniowym (Thermodynamic analysis of the leakage failure in pressurised water reactor system)  
A. Fic (Silesian Technical University, Gliwice, Poland), J. Składzień (Silesian Technical University, Gliwice, Poland), J. Skorek (Silesian Technical University, Gliwice, Poland)
- System monitoringu radiologicznego w Polsce (System of radiological monitoring in Poland)  
D. Grabowski (Central Laboratory for Radiological Protection, Warszawa, Poland), W. Muszyński (Central Laboratory for Radiological Protection, Warszawa, Poland)
- Jak wzorcować aparaturę dozymetryczną? (How to calibrate dosimetric equipment?)  
K. Józefowicz (Institute of Atomic Energy, Świerk, Poland)
- Biologiczne efekty niskich dawek promieniowania jonizującego (Biological effects of low doses of radiation)  
A. Wójcik (Institute of Nuclear Chemistry and Technology, Warszawa, Poland), I. Szumiel (Institute of Nuclear Chemistry and Technology, Warszawa, Poland)
- Chemia radiacyjna ciała stałego tłumaczy właściwości osłonne betonu (Radiation chemistry explains protection procession of concrete)  
Z.P. Zagórski (Institute of Nuclear Chemistry and Technology, Warszawa, Poland), A. Rafalski (Institute of Nuclear Chemistry and Technology, Warszawa, Poland)
- Modelowanie wydzielania gazowych produktów rozszczepienia z elementów paliwowych. Postęp prac wynikający z mikro-strukturalnych obserwacji (Modelling of gaseous fission product release from fuel elements - progress based on micro-structural observations)  
M. Szuta (Institute of Atomic Energy, Świerk, Poland)
- Membranowe procesy do zateżniania odpadów promieniotwórczych (Membrane processes for concentration of radioactive wastes)  
G. Zakrzewska-Trznadel (Institute of Nuclear Chemistry and Technology, Warszawa, Poland), A.G. Chmielewski (Institute of Nuclear Chemistry and Technology, Warszawa, Poland), M. Harasimowicz (Institute of Nuclear Chemistry and Technology, Warszawa, Poland), B. Tymiński (Institute of Nuclear Chemistry and Technology, Warszawa, Poland)
- Pełna dekontaminacja elementów aluminiowych i stalowych reaktora badawczego EWA (Full decontamination of aluminium and steel components of the EWA research reactor)  
A. Bilewicz (Institute of Nuclear Chemistry and Technology, Warszawa, Poland), T. Matusiak (Institute of Atomic Energy, Świerk, Poland)
- Zastosowania betonów siarkowych do zestalania odpadów promieniotwórczych i budowy składowisk (Application of sulphur concrete for solidification of radioactive waste and construction of depository)  
A. Cholerzyński (Institute of Atomic Energy, Świerk, Poland), W. Tomczak (Institute of Atomic Energy, Świerk, Poland), J. Świtalski (Institute of Atomic Energy, Świerk, Poland)
- Koncepcja zamknięcia krajowego składowiska odpadów promieniotwórczych w Róźnie (Conception of closing of the country depository of radioactive wastes at Różan)  
W. Tomczak (Institute of Atomic Energy, Świerk, Poland), A. Cholerzyński (Institute of Atomic Energy, Świerk, Poland), J. Świtalski (Institute of Atomic Energy, Świerk, Poland)
- Zintegrowany system monitoringu radiologicznego i wspomagania decyzji po awarii elektrowni jądrowej (Integrated radiological monitoring and support system after an accident in a nuclear power plant)  
M. Borysiewicz (Institute of Atomic Energy, Świerk, Poland), S. Potemski (Institute of Atomic Energy, Świerk, Poland), R. Żelazny (Institute of Atomic Energy, Świerk, Poland)
- Elektrownie jądrowe - zajęcia dydaktyczne na wydziale mechaniczno-energetycznym Politechniki Wrocławskiej (Nuclear Power Plants - topic of activity at Mechanical-Engineering Department of Technical University in Wrocław)  
M. Lech (Wrocław Technical University, Poland)
- Fizyka i technika jądrowa na wydziale fizyki Politechniki Warszawskiej (Physics and nuclear techniques at Physics Department of Warsaw University of Technology)  
J. Pluta (Warsaw University of Technology, Poland)
- Kierunki badań radioizotopowych w zakładzie radio- i fotochemii Politechniki Poznańskiej (Radioisotope research at Radio- and Photo-Chemistry Laboratory at Poznań Technical University)  
E. Koczorowska (Poznań Technical University, Poland)
- Prezentacja zagadnień energetyki jądrowej w procesie dydaktycznym dla studentów wydziału elektrotechniki i automatyki politechniki Gdańskiej (Nuclear power presented for students of Electrical and Automation Department of Technical University of Gdańsk)  
R. Frydryk (Technical University of Gdańsk, Poland)

- Doświadczenia innych krajów w kształceniu w zakresie zjawisk związanych z promieniotwórczością (Experience of other countries in education concerning phenomenon of radioactivity)  
W. Gorączko (Poznań Technical University, Poland)
- Refleksje nad założeniami polityki energetycznej (wątpliwości postronnego obserwatora) (Remarks on energy policy (doubts of side-observer))  
S. Taczanowski (Warsaw University of Technology, Poland), W. Pohorecki (Warsaw University of Technology, Poland)

#### PANEL DISCUSSION

- Rozwój energetyki w Polsce (Electrical power industry in Poland)  
S. Ciok (Energy Agency Market, Poland)
- Informacja społeczna i nauczanie (Public information and education)  
A. Hryniewicz (H. Niewodniczański Institute of Nuclear Physics, Kraków, Poland)
- Reaktory jądrowe nowej generacji (New generation of nuclear reactors)  
S. Chwaszczewski (Institute of Atomic Energy, Świerk, Poland)
- Badania naukowe (Scientific research nuclear physics, chemistry technology and energy production)  
A.G. Chmielewski (Institute of Nuclear Chemistry and Technology, Warszawa, Poland)

## Ph.D./D.Sc. THESES

### Ph.D. THESES

1. Jarosław Sadło, M.Sc.

**Paramagnetyczne klastry srebra w sitach molekularnych (Paramagnetic silver clusters in molecular sieves)**

supervisor: Prof. Jacek Michalik, Ph.D., D.Sc.

Institute of Nuclear Chemistry and Technology, 23.03.2000

2. Ewa Gniazdowska, M.Sc.

**Hydratacja oksaalkanów w roztworach wodnych (Hydration of oxaalkanes in aqueous solutions)**

supervisor: Prof. Jerzy Narbutt, Ph.D., D.Sc.

Institute of Nuclear Chemistry and Technology, 26.10.2000

### D.Sc. THESES

1. Edward Iller, Ph.D.

**Dyspersyjny model transportu mediów w radioznacznikowych badaniach pracy wybranych instalacji przemysłowych (A dispersion model of transport media in radiotracer investigations of selected industrial installations)**

Institute of Nuclear Chemistry and Technology

2. Wojciech Migdał, Ph.D.

**Jakość mikrobiologiczna przypraw ziołowych dekontaminowanych radiacyjnie (Microbiological quality of spices decontamination by radiation)**

Academy of Economics in Poznań

## EDUCATION

### Ph.D. PROGRAMME IN CHEMISTRY

The Institute of Nuclear Chemistry and Technology holds a four year's Ph.D. degree programme to graduates of chemical, physical and biological departments of universities, to graduates of medical universities and to engineers in chemical technology and material science.

The main areas of the programme are:

- chemistry of radioactive elements and isotope effects,
- coordination chemistry,
- chemistry of separation and analytical methods,
- radiation chemistry and biochemistry,
- chemistry of fast processes,
- application of nuclear methods in chemical and environmental research and in material science,
- chemistry of radicals.

Head: Prof. Jacek Michalik, Ph.D., D.Sc.

The candidates accepted for the forementioned programme can be employed in the Institute. The candidates can apply for a doctoral scholarship.

Each participant takes part in a 45 h course of lectures of fundamental physical chemistry and a 30 h specialization course. He/she is obliged to deliver a lecture on topic of his/her dissertation at a seminar. The final requirements for the Ph.D. programme graduates, consistent with the regulation of the Ministry of National Education, are:

- submission of a formal dissertation, summarizing original research contributions suitable for publication;
- final examination and public defense of the dissertation thesis.

Applicants for the Ph.D. degree programme are accepted throughout the year. Detailed information can be obtained from Admission Secretary, Dr. Ewa Gniazdowska (phone: (+48-22) 811-27-35).

In 2000 there were held the following lecture series:

- "Radiation Types and their Radiometry" - Prof. Piotr Urbański (Institute of Nuclear Chemistry and Technology)
- "Fundamentals of Quantal Chemistry" - Prof. Grzegorz Chałasiński (Warsaw University, Department of Chemistry)
- "Supramolecular Aspects of Molecular Interactions Theory" - Prof. Lucjan Piela (Warsaw University, Department of Chemistry)
- "Group Theory in Chemistry" - Prof. Grzegorz Chałasiński (Warsaw University, Department of Chemistry)
- "Nuclear Chemistry" - Assoc. Prof. Aleksander Bilewicz, Ph.D., D.Sc. (Institute of Nuclear Chemistry and Technology)

The lectures of Prof. Chałasiński were followed by practical exercises in the Department of Chemistry, Warsaw University.

### TRAINING OF STUDENTS

Insitution	Country	Numer of participants	Period
Academy of Economics in Poznań	Poland	1	3 months
Center for Nuclear Techniques	Vietnam	1	2 months
Ecole des Mines de Nantes	France	2	3 months
		1	2 months

Electronic-Mechanical School	Poland (Warszawa)	2	01.01-30.06 1 day a week
Gent University	Belgium	1	1 week
		1	1 month
Ghandi Institute of Technology and Management	India	1	3 months
Malaysian Institute for Nuclear Technology Research	Malaysia	1	2 months
		1	4 months
Saarland University	Germany	2	1 week
Silesian Technical University, Faculty of Chemistry	Poland	1	1 week
Stanisław Staszic Academy of Mining and Metallurgy	Poland	5	2 weeks
Świętokrzyska Academy	Poland	3	3 weeks
Technical School of Chemistry	Poland (Warszawa)	4	1 month
Université Rene Descartes, Laboratoire de Chimie Physique	France	1	6 weeks
Warsaw Agricultural University, Faculty of Food Technology	Poland	35	one-day practice
Warsaw Agricultural University, Faculty of Human Nutrition and Consumer Sciences	Poland	14	one-day practice
Warsaw University	Poland	1	1 month
Warsaw University of Technology	Poland	15	one-day practice



## RESEARCH PROJECTS AND CONTRACTS

### RESEARCH PROJECTS GRANTED BY THE POLISH STATE COMMITTEE FOR SCIENTIFIC RESEARCH IN 2000 AND IN CONTINUATION

1. **New wood preservatives based on polymerized aminotriazole complexes with copper.**  
supervisor: Prof. Andrzej Łukasiewicz, Ph.D., D.Sc.
2. **Even-odd effect in separation of the isotopes of f-electron elements in the three electron exchange reactions.**  
supervisor: Wojciech Dembiński, Ph.D.
3. **Studying of the significance of DNA double-strand break repair in the adaptive response of human lymphocytes.**  
supervisor: Maria Wojewódzka, Ph.D.
4. **Analysis of centromeres in micronuclei by FISH for biological dosimetry.**  
supervisor: Assoc.Prof. Andrzej Wójcik, Ph.D., D.Sc.
5. **Electron beam processing technology for modification of various types of cellulose mass for preparation of derivatives.**  
supervisor: Assoc.Prof. Edward Iller, Ph.D., D.Sc.
6. **Influence of the structural changes in membrane-penetrant system on permeation process using synchrotron methods.**  
supervisor: Assoc.Prof. Helena Grigoriew, Ph.D., D.Sc.
7. **Radiation processing of polyolefines and their composites devoted to thermoshrinkable products.**  
supervisor: Zbigniew Zimek, Ph.D.
8. **Problems of the attribution of works of art: examples of 18th century central European decorative glass.**  
supervisor: Jerzy J. Kunicki-Goldfinger, Ph.D.
9. **Investigations in the range of functionalization technology of particle track-etched membranes and their application.**  
supervisor: Assoc.Prof. Tadeusz Żółtowski, Ph.D., D.Sc.
10. **Radiation and photochemically induced radical processes in aromatic carboxylic acids containing thioether group.**  
supervisor: Prof. Krzysztof Bobrowski, Ph.D., D.Sc.
11. **Application of ceramic membranes for liquid low- and medium-level radioactive waste processing.**  
supervisor: Grażyna Zakrzewska-Trznadel, Ph.D.
12. **Decomposition of organic compounds emitted during coal burning with the use of electron beam.**  
supervisor: Prof. Andrzej G. Chmielewski, Ph.D., D.Sc.

### IMPLEMENTATION PROJECTS GRANTED BY THE POLISH STATE COMMITTEE FOR SCIENTIFIC RESEARCH IN 2000 AND IN CONTINUATION

1. **Irradiation method for microbiological decontamination of herbal raw materials.**  
5 PO6G 004 96 C/2870
2. **Instruments for measurements of radon concentration.**  
8T10C 016 97C/3615
3. **Small dimensions universal electrofilter for inorganic hygroscopic salts capture.**  
8T10A 083 98

4. **New Polish certified reference materials of biological origin for inorganic trace analysis: tea leaves and mixture Polish herbs.**  
3T09A 001 99C/4265
5. **Development of activity and dose rate gauge of Ru-106 beta sources for irradiation of eye cancer.**  
8T 11E 04 099 C/4311
6. **The Christian art in Egypt. Studies and conservation of coptic art in the collection of the National Museum in Warsaw.**  
1HO 1E 002 99C/4402

### **IAEA RESEARCH CONTRACTS IN 2000**

1. **Decontamination of herbal raw materials and herbal drugs by irradiation.**  
10355/Regular Budget Fund  
principal investigator: Wojciech Migdał, Ph.D., D.Sc.
2. **Electron beam treatment of gaseous organic compounds emitted from fossil fuel combustion.**  
11093/RO  
principal investigator: Prof. Andrzej G. Chmielewski, Ph.D., D.Sc.

### **IAEA TECHNICAL CONTRACTS IN 2000**

1. **Industrial scale demonstration plant for electron beam purification of flue gases.**  
POL/8/014
2. **Control laboratories for radiation processing.**  
POL/8/16

### **EUROPEAN COMMISSION RESEARCH PROJECTS IN 2000**

1. **Accreditation for high dose measurement.**  
EU INCO Copernicus Project IC I5-CT96-0824  
supervisor: Zofia Stuglik, Ph.D.
2. **Electron beam for processing of flue gases, emitted in metallurgical processes for volatile organic compounds removal.**  
ICA2-CT-200010005  
supervisor: Prof. Andrzej G. Chmielewski, Ph.D., D.Sc.  
Programme coordinated by the INCT

### **OTHER FOREIGN CONTRACTS IN 2000**

1. **Elaboration of wet method for reprocessing of lithium in the form of lithium carbonate from ceramic materials  $\text{Li}_2\text{TiO}_3$ , provided by ENEA.**  
Contract with ENEA, Italy  
principal investigator: Andrzej Deptuła, Ph.D.

## LIST OF VISITORS TO THE INCT IN 2000

No	Name	Institution	Country	Period
1.	Abdul Rahman Mohd Fitri	Malaysian Institute for Nuclear Technology Research, Bangi, Kajang	Malaysia	17.10-17.12
2.	Abendizadeh Zohreh	Université René Descartes	France	08-09.09
3.	A'iasah Siti Hashim	Malaysian Institute for Nuclear Technology Research, Bangi, Kajang	Malaysia	04-17.12
4.	Al-Mowed Abed	Syrian Atomic Energy Commission	Syria	01.10-30.11
5.	Al-Kaid Abeer	Syrian Atomic Energy Commission	Syria	07.05-08.07
6.	Aten Jacob	Academic Medical Center, University of Amsterdam	Holland	12-13.10
7.	Asmus Klaus Dieter	University of Notre Dame	USA	07-09.09
8.	Bonila Fernando	University of Manchester, Institute of Science and Technology	Great Britain	07-09.09
9.	Bouton Cecile	Institute de Chimie des Substances Naturelles, Centre National de la Recherche Scientifique	France	14.01
10.	Burgess John	University of Leicester	Great Britain	15-18.05
11.	Burns Kerry	International Atomic Energy Agency	United Nations	22-26.01
12.	Cai Bin	The Guovang Power Cooperation	China	6-14.08
13.	Chen Hua	Tsinghua University, Beijing	China	6-14.08
14.	Yoon Hwan Cho	GENIX Inc., Seoul	Korea	23-24.04
15.	Dedusenko Alla	Institute ENERGOSTAL	Ukraine	03.10-02.11
16.	Delince Henry	Institute of Nutritional Physiology	Germany	18-25.04
17.	Drapkin Valery	Joint Stock Enterprise ILIP, St. Petersburg	Russia	30.01-06.02
18.	Guwen Olgun	International Atomic Energy Agency	United Nations	15-16.10
19.	Fainchtein Aleksander	Institute ENERGOSTAL	Ukraine	03-17.09
20.	Flyunt Roman	Institute of Physico-Chemistry, National Academy of Sciences of the Ukraine	Ukraine	17-21.09
21.	Frank Norman	International Business Consultants	USA	19.11-14.12
22.	Ge Xuewu	University of Science and Technology of China	China	13-19.10
23.	Ghiyas Ud-Din	Pakistan Institute of Nuclear Science and Technology, Islamabad	Pakistan	01-15.01
24.	Gooverts Etienne	University of Antwerp	Belgium	07-09.12
25.	Guven Olgun	International Atomic Energy Agency	United Nations	15-16.10
26.	Anatolij Gryzlov	State Research and Production Corporation "TORIJ", Moscow	Russia	25.01-04.02 11-23.12
27.	Hadiwinoto Kushartono	Centre for Research and Development of Isotopes and Radiation Technology, Batan	Indonesia	04-15.09 27.11-09.12
28.	Houée-Levin Chantal	Université Paris-Sud	France	08-09.09

29.	Gordon L. Hug	University of Notre Dame	USA	17-23.02 21-22.07 07-08.08
30.	Hüttermann Jürgen	Saarland University, Homburg	Germany	10-13.10
31.	Jancso Gabor	KSKI Atomic Energy Research Institute, Budapest	Hungary	01-07.07
32.	Kapoor Sudhir	Bhabha Atomic Research Centre, Bombay	India	07-09.09
33.	Kato Juran	University of California, Los Angeles	USA	18.12
34.	Kemp Terence J.	University of Warwick	Great Britain	18-23.09
35.	Kihun Joh	Samsung	Korea	08-10.08
36.	Kvitnitsky Yuriij	Slavyanskaya Power Plant, Slavyansk	Ukraine	03.10-02.11
37.	Lugao Ademar	Institute of Nuclear Energy, São Paulo	Brazil	17.07
38.	Luo Jingyu	Tsinghua University, Beijing	China	6-14.08
39.	Luxenburger Heike	Saarland University, Homburg	Germany	04-08.12
40.	Machi Sueo	Japan Atomic Industrial Forum Inc.	Japan	05-12.12
41.	Michalik Marek	University of Toronto	Canada	10.04
42.	Miljević Nada	Institute of Nuclear Sciences VINČA	Yugoslavia	14.02-13.03 08.06-08.07 21.10-21.11
43.	Mod Ali Noriah	Malaysian Institute for Nuclear Technology Research	Malaysia	04.06-02.07
44.	Morgunov Volodymyr	Institute ENERGOSTAL	Ukraine	03.10-02.11
45.	Murthy G.S.	Andhra University	India	04-17.08
46.	Nanba Tetsuya	National Institute for Resources and Environment, Tsukuba	Japan	18-25.04
47.	Nichipor Henrieta	Institute of Radiation Physical and Chemical Problems, Academy of Sciences of Belarus	Belarus	05-17.03 27.08-16.09
48.	Opos Michał	University of Toronto	Canada	10.04
49.	Aleksander Pavielev	State Research and Production Corporation TORIJ", Moscow	Russia	25.01-04.02
50.	Pimblott Simon	University of Notre Dame	USA	07-09.09
51.	Piotrovski Vladimir	Institute ENERGOSTAL	Ukraine	03-17.09
52.	Politowskij Fiodor	State Research and Production Corporation TORIJ, Moscow	Russia	25.01-04.02 11-23.12
53.	Ravoz Dalphine	Ecole des Mines, Nantes	France	06.05-06.08
54.	Satyanarayana Jujjavarapu	Ghandi Institute of Technology and Management, Visakhapatnam	India	04.08-28.10
55.	Sebastian Calvo Carlos	Instituto Peruano de Energia Nuclear	Peru	30.10-11.11
56.	Shi Wenfang	University of Science and Technology of China	China	13-19.10
57.	Singer Erik	Saarland University, Homburg	Germany	04-08.12
58.	Sinnakaruppan Kanesan	Malaysian Institute for Nuclear Technology Research, Bangi, Selangor	Malaysia	15.04-15.08
59.	Sun Jiming	Tsinghua University, Beijing	China	6-14.08
60.	Sun Weimin	China State Power Cooperation	China	06-14.08
61.	Sunaga Hiromi	Japan Atomic Energy Research Institute, Takasaki	Japan	05-07.11
62.	Tichonov Andriej	Joint Stock Enterprise ILIP, St. Petersburg	Russia	30.01-06.02
63.	Vanhaelcwyn Gauthier	Ghent University	Belgium	01-31.03
64.	Varmenot Nicolas	Université René Descartes	France	14.03-08.04 16-30.07

65.	Verhaecke Peter	International Atomic Energy Agency	United Nations	22-26.01
66.	Vigot Nicolas	Ecole des Mines, Nantes	France	06.05-05.07
67.	Vu Quoc Trong	Center for Nuclear Techniques	Vietnam	20.02-21.04
68.	Wishart James	Brookhaven National Laboratory, Upton	USA	17-19.09
69.	Wiyanto Tri Setno Dyah Larasati	National Atomic Energy Agency	Indonesia	08.05-07.08
70.	Xu Tinnyuming	Tsinghua University, Beijing	China	6-14.08
71.	Yarcheva Svetlana	Institute ENERGOSTAL	Ukraine	22.05-03.06
72.	Zhang Zhicheng	University of Science and Technology of China	China	13-19.10

## THE INCT SEMINARS IN 2000

1. Prof. Klaus-Dieter Asmus (University of Notre Dame, USA)  
Free radical and triplet induced chemistry of amino acids; electron transfer, proton transfer, abstraction reactions
2. Prof. John Burgess (University of Leicester, Great Britain)  
Solvation, reactivity and colour of iron complexes
3. Prof. Etienne Goovaerts (University of Antwerp, Belgium)  
Single crystal W-band EPR applied to the problems in solid state physics and physical chemistry
4. Assoc. Prof. Helena Grigoriew (Institute of Nuclear Chemistry and Technology, Warszawa, Poland)  
Struktura układów polimer-solvent. Nowe poglądy na podstawie wyników badań synchrotronowych (Structure of polymer-solvent systems. New views based on results from synchrotron studies)
5. Prof. Jürgen Hüttermann (Saarland University, Homburg, Germany)  
Free radicals from irradiated DNA: a survey
6. Assoc. Prof. Edward Iller (Institute of Nuclear Chemistry and Technology, Warszawa, Poland)  
Program badawczy Pracowni Technik Jądrowych w ochronie środowiska (Research programme of the Laboratory of Nuclear Techniques in the environmental protection)
7. Prof. Terence J. Kemp (University of Warwick, Great Britain)  
Crystallographic and mass spectroscopic studies of large molecules, polymers and inorganic clusters
8. Prof. Zbigniew Moroz (Institute of Nuclear Studies, Świerk, Poland)  
Sieci neuronowe i algorytmy genetyczne - niektóre zastosowania w fizyce i technice (Neuron nets and genetic algorithms - some applications in physics and techniques)
9. Prof. G.S. Murthy (Andhra University, Visakhapatnam, India)  
Nuclear waste management practice in India
10. Dr. Michał Opos (University of Toronto, Canada)  
Biologia kalretikuliny, białka osłonowego i magazynu wapnia błon endoplazmatycznego retikulum (Biology of calreticulum, a shield protein and a calcium store of endoplasmic reticulum)
11. Dr. Simon Pimblott (University of Notre Dame, USA)  
The nonhomogeneous radiation chemistry of the track-end
12. Prof. Ge Xuewu (University of Science and Technology of China)  
Radiation synthesis of nanometer composites
13. Prof. Shi Wenfang (University of Science and Technology of China)  
Application of dendritic/hyperbranched polymers in UV/EB curable coatings
14. Prof. Zbigniew Zagórski (Institute of Nuclear Chemistry and Technology, Warszawa, Poland)  
Przyszłość chemii radiacyjnej w świetle badań w USA (The future of radiation chemistry as seen in studies in the USA)
15. Prof. Zhang Zhicheng (University of Science and Technology of China)  
Radiation emulsion polymerization

## SEMINARS DELIVERED OUT OF THE INCT IN 2000

1. Andrzej G. Chmielewski  
Electron beam flue gas treatment  
Tsinghua University, Beijing, China, 07.03.2000
2. Andrzej G. Chmielewski  
Atmosphere chemistry  
Institute of Instruments, Baoshan Steel Company, Shanghai, China, 10.03.2000
3. Andrzej G. Chmielewski  
Energy and environment  
Institute of Instruments, Baoshan Steel Company, Shanghai, China, 10.03.2000
4. Andrzej G. Chmielewski  
Environmental impact  
Institute of Instruments, Baoshan Steel Company, Shanghai, China, 10.03.2000
5. Andrzej G. Chmielewski  
Air pollution control  
Institute of Instruments, Baoshan Steel Company, Shanghai, China, 11.03.2000
6. Andrzej G. Chmielewski  
Electron beam flue gas treatment  
Institute of Instruments, Baoshan Steel Company, Shanghai, China, 11.03.2000
7. Andrzej G. Chmielewski  
Radiation chemistry of gases  
Institute of Instruments, Baoshan Steel Company, Shanghai, China, 11.03.2000
8. Andrzej G. Chmielewski  
Akceleratorzy elektronów - fizyka bliska technologiom zaawansowanym (Electron accelerators - physics near advanced technologies)  
Training course for methodical advisors in physics, Elbląg, Poland, 16.03.2000
9. Andrzej G. Chmielewski  
Chemia atmosfery - pamiętajcie o ogrodach... (The chemistry of atmosphere - remember about gardens...)  
Training course for methodical advisors in chemistry, Elbląg, Poland, 29.03.2000
10. Andrzej G. Chmielewski  
Electron beam flue gas treatment  
University of Science and Technology of China, Hefei, China, 13.11.2000
11. Andrzej G. Chmielewski  
Environmental effects of fossil fuel combustion  
University of Science and Technology of China, Hefei, China, 13.11.2000
12. Leon Fuks  
Osobliwości ekstrakcji lantanowców i aktynowców (Peculiarities of solvent extraction of lanthanides and actinides).  
Faculty of Civil Engineering and Environmental Engineering, Białystok Technical University, Poland, 07.02.2000

13. Jacek Michalik  
ESR and optical studies of silver clusters in sodalites.  
National Institute for Research in Inorganic Materials, Tsukuba, Japan, 28.01.2000
14. Jacek Michalik  
Catalyst silver clusters in zeolites.  
Institute of Energy and Nuclear Research (IPEN), São Paulo, Brazil, 28.08.2000
15. Jacek Michalik  
Cationic silver clusters in zeolites.  
Department of Chemistry, University of Houston, Texas, USA, 25.10.2000
16. Jacek Michalik  
Radiation-induced silver agglomeration in molecular sieves.  
Department of Physics and Astronomy, Georgia State University, Atlanta, USA, 13.11.2000
17. Jerzy Narbutt  
High coordination numbers of metal ions in chelate complexes.  
Institute of Inorganic Chemistry, Zurich University, Switzerland, 14.11.2000.
18. Jerzy Narbutt  
High coordination numbers of metal ions in chelate complexes.  
Center for Radiopharmaceutical Science, Paul Scherrer Institute, Villigen, Switzerland, 17.11.2000
19. Jerzy Narbutt  
Liquid-liquid partition and hydration of amphiphilic chelates of metal ions.  
Institute for Bioinorganic and Radiopharmaceutical Chemistry, Research Center Rossendorf, Germany, 27.11.2000
20. Irena Szumiel  
Uszkodzenia DNA i mechanizmy naprawy (DNA damage and repair).  
Institute of Biostructure, Medical University of Warsaw, Poland, 13.12.2000
21. Marek Trojanowicz  
High performance capillary electrophoresis. Some environmental, physiological and chiral applications.  
Institute of Analytical Chemistry, University of Vienna, Austria, 15.09.2000
22. Marek Trojanowicz  
High performance capillary electrophoresis. Some environmental, physiological and chiral applications.  
Institute of Chemistry, University of São Paulo, Brazil, 27.10.2000
23. Andrzej Wójcik  
Micronuclei and centromeres.  
Biological Faculty, University of Essen, Germany, 07.10.2000
24. Andrzej Wójcik  
Biologische Wirkung ionisierender Strahlung (Biological effects of ionising radiation).  
Victoria School, Essen, Germany, 01.12 and 02.12.2000
25. Andrzej Wójcik  
Strahleninduzierte Schwesterchromatidaustausche (Post-irradiation sister chromatid exchanges).  
Institute of Medical Radiobiology, University Clinic Essen, Germany, 11.12.2000
26. Andrzej Wójcik  
Ionisierende Strahlung - muessen wir uns fuerchten? (Ionising radiation - must we be afraid?).  
Paul Ehrlich College, Dortmund, Germany, 18.12.2000
27. Zbigniew P. Zagórski  
Role of multi-ionization spurs in radiation-induced crosslinking of polyethylene.



University of Southern California, Los Angeles, USA, 26.01.2000

28. Zbigniew P. Zagórski

Two different chemistries in irradiated polymers: in and around single- and multi-ionization spurs.

University of Southern California, Los Angeles, USA, 02.11.2000

29. Zbigniew P. Zagórski

Radiation resistance of concrete and of sodium chloride.

Carlsbad Environmental Monitoring and Research Center, Carlsbad, USA, 08.11.2000

30. Zbigniew Zimek

Electron accelerator technology for radiation processing.

Malaysian Institute for Nuclear Technology Research, Kuala Lumpur, Malaysia, 15.08.2000

31. Zbigniew Zimek

Wykorzystanie akceleratora elektronów w procesie usuwania zanieczyszczeń gazowych (Electron accelerator application in gaseous pollutants removal process).

Faculty of Electrical and Electronic Engineering, Technical University of Łódź, Poland, 14.11.2000

## AWARDS IN 2000

1. Separation of water isotopomers by a porous hydrophobic membrane  
A.G. Chmielewski, G. Zakrzewska-Trznadel, N. Miljević, W.A. Van Hook  
Silver medal at the 28th International Exhibition of Inventions, New Techniques and Products, Geneva, Switzerland, 12-16.04.2000
2. Preparation and characterization of  $\text{LiCoO}_2$  and  $\text{LiMg}_{0.05}\text{Co}_{0.95}\text{O}_2$  thin films on porous Ni/NiO cathodes for MCFC by complex sol-gel process (CSGP)  
W. Łada  
Outstanding Poster Award on the 2000 Spring Meeting Chairs of the Materials Research Society, San Francisco, California, USA, 24-28.04.2000
3. Hanns Langendorff prize for the whole of work in the field of radiobiology and radiological protection  
A. Wójcik  
German-Austrian Congress of Radiation Protection, Baden-Baden, Germany, 12.05.2000
4. Application of ionizing radiation for removing 2,4-dichlorophenol from water and wastewater  
P. Drzewicz  
Honorable Mention at the Fifth International Symposium and Exhibition on Environmental Contamination in Central and Eastern Europe, Prague, Czech Republic, 12-14.09.2000, Prague 2000 Student Poster Competition
5. Electron beam flue gas treatment as an integrated method of  $\text{SO}_2$ ,  $\text{NO}_x$  and volatile organic compounds (VOCs) control  
A. Ostapczuk  
Honorable Mention at the Fifth International Symposium and Exhibition on Environmental Contamination in Central and Eastern Europe, Prague, Czech Republic, 12-14.09.2000, Prague 2000 Student Poster Competition
6. Membrane methods for the treatment of low and intermediate radioactive wastes  
G. Zakrzewska-Trznadel  
Best Scientific Paper at the 3rd International Yugoslav Nuclear Society Conference, Belgrade, Yugoslavia, 2-5.10.2000
7. Separation of water isotopomers by a porous hydrophobic membrane  
A.G. Chmielewski, G. Zakrzewska-Trznadel, N. Miljević, W.A. Van Hook  
The Cup of President of the Polish State Committee for Scientific Research on the 3rd International Exhibition of Invention "INNOWACJE'2000", Gdańsk, Poland, 10-13.10.2000
8. The method of making hollow spherical ceramic and metallic materials, reduced by hydrogen  
A. Deptuła, A.G. Chmielewski, W. Łada, T. Olczak  
Bronze medal at the 3rd International Exhibition of Invention "INNOWACJE'2000", Gdańsk, Poland, 10-13.10.2000
9. The method of making hollow spherical ceramic and metallic materials, reduced by hydrogen  
A. Deptuła, A.G. Chmielewski, W. Łada, T. Olczak  
Silver medal at the World Exhibition of Innovation, Research and New Technology "BRUSSELS EUREKA 2000", Brussels, Belgium, 14-20.11.2000
10. A.G. Chmielewski  
Gold Honourable Medal of the Polish Society of Inventors and Rationalizers

## INSTRUMENTAL LABORATORIES AND TECHNOLOGICAL PILOT PLANTS

### I. DEPARTMENT OF NUCLEAR METHODS OF MATERIAL ENGINEERING

#### 1. Laboratory of Materials Research

Activity profile: Studies of the structure and properties of materials and historical art objects.

- Scanning electron microscope

DSM 942, Zeiss (Germany)

Technical data: spatial resolution - 4 nm at 30 kV, and 25 nm at 1 kV; acceleration voltage - up to 30 kV; chamber capacity - 250x150 mm.

Application: SEM observation of various materials such as metals, polymers, ceramics and glasses. Determination of characteristic parameters such as molecule and grain size.

- Scanning electron microscope equipped with the attachment for fluorescent microanalysis

BS-340 and NL-2001, TESLA (Czech Republic)

Application: Observation of surface topology and elemental analysis of various materials.

- Vacuum evaporator

JEE-4X, JOEL (Japan)

Application: Preparation of thin film coatings of metals or carbon.

- Gamma radiation spectrometer

HP-Ge, model GS 6020; Canberra-Packard (USA)

Technical data: detection efficiency for gamma radiation - 60.2%, polarization voltage - 4000 V, energy resolution (for Co-60) - 1.9 keV, analytical program "GENIE 2000".

Application: Neutron activation analysis, measurements of natural radiation of materials.

### II. DEPARTMENT OF STRUCTURAL RESEARCH

#### 1. Track-Etched Membranes Studies and Application Laboratory

Activity profile: Studies on structural defects in polymers created under influence of heavy ion beam irradiation. Manufacturing and determination of physical and structural parameters of TEM (Track-Etched Membranes) - modern filtration materials, obtained by chemical etching of latent heavy ions tracks in polymer films. Modification of TEM surface properties by physical methods. Research and developments on application of TEM in the field of sterilization filtration and as microbiological barrier.

- Coulter Porometer II

Coulter Electronics Ltd (Great Britain)

Application: Pore size analysis in porous media.

- Vacuum chamber for plasma research

POLVAC Technika Próźniowa

Technical data: dimensions - 300x300 mm; high voltage and current connectors, diagnostic windows.

Application: Studies on plasma discharges influence on physicochemical surface properties of polymer films, particularly TEM.

#### 2. Laboratory of Diffractational Structural Research

Activity profile: Studies on magnetic properties of new materials using neutron diffraction method. X-ray diffraction structural studies on metal-organic compounds originating as degradation products of substances naturally occurring in the environment. Röntgenostructural phase analysis of materials. Studies on interactions in a penetrant-polymer membrane system using small angle scattering of X-rays, synchrotron and neutron radiation. Studies of structural changes occurring in

natural and synthetic polymers under influence of ionising radiation applying X-ray diffraction and differential scanning calorimetry.

- KM-4 X-ray diffractometer

KUMA DIFFRACTION (Poland)

Application: 4-cycle diffractometer for monocrystal studies.

- HZG4 X-ray diffractometer

Freiberger Präzisionsmechanik (Germany)

Application: powder diffractometers for studies of polycrystalline, semicrystalline and amorphous materials.

- URD 6 X-ray diffractometer

Freiberger Präzisionsmechanik (Germany)

Application: powder diffractometers for studies of polycrystalline, semicrystalline and amorphous materials.

### 3. Heavy Metal and Radioactive Isotopes Environment Pollution Studies Laboratory

Activity profile: Determination of elemental content of environmental and geological samples, industrial waste materials, historic glass objects and other materials by Energy Dispersive X-ray Fluorescence Spectrometry using a radioisotope excitation source as well as a low power X-ray tube and using 2 kW X-ray tube in total reflection geometry. Determination of radioactive isotopes content in environmental samples and historic glass objects by gamma spectrometry.

- Gamma spectrometer in low-background laboratory

EGG ORTEC

Technical data: HPGe detector with passive shield; FWHM - 1.9 keV at 1333 keV, relative efficiency - 92%.

- Total reflection X-ray spectrometer

Pico TAX, Institute for Environmental Technologies (Berlin, Germany)

Technical data: Mo X-ray tube, 2000 W; Si(Li) detector with FWHM 180 eV for 5.9 keV line; analysed elements: from sulphur to uranium; detection limits - 10 ppb for optimal range of analysed elements, 100 ppb for the others.

Application: XRF analysis in total reflection geometry. Analysis of minor elements in water (tap, river, waste and rain water); analysis of soil, metals, raw materials, fly ash, pigments, biological samples.

- X-ray spectrometer

SLP-10180-S, ORTEC (USA)

Technical data: FWHM - 175 eV for 5.9 keV line, diameter of active part - 10 mm, thickness of active part of detector - 5.67 mm.

Application: X-ray fluorescence analysis.

### 4. Sol-Gel Laboratory of Modern Materials Synthesis

Activity profile: Synthesis of modern ceramic materials (hydroxyapatite, high temperature superconductors of new generation e.g. doped SrTiO<sub>3</sub> or SrZrO<sub>2</sub> and on Hg basis, cathode materials for renewable lithium batteries) using developed in the INCT CSGP method (Complex Sol-Gel Method) in the form of spherical and irregularly shaped powders, monoliths (complete and porous), fibres as well as thin films on metallic and other substrates.

- DTA and TGA thermal analyser

OD-102 Paulik-Paulik-Erdey, MOM (Hungary)

Technical data: balance fundamental sensitivity - 20-0.2 mg/100 scale divisions, weight range - 0-9.990 g, galvanometer sensitivity -  $1 \times 10^{-10}$  A/mm/m, maximum temperature - 1050°C.

Application: Thermogravimetric studies of materials up to 1050°C.

- DTA and TGA thermal analyser 1500

MOM (Hungary)

Technical data: temperature range - 20-1500°C; power requirements - 220 V, 50 Hz.

Application: Thermal analysis of solids in the temperature range 20-1500°C.

- Research general-purpose microscope

Carl Zeiss Jena (Germany)

Technical data: General purpose microscope, enlargement from 25 to 2500 times, illumination of sample from top or bottom side.

- Metallographic microscope

EPITYP-2, Carl-Zeiss Jena (Germany)

Technical data: enlargement from 40 to 1250 times.

Application: Metallographic microscope for studies in polarized light illumination and hardness measurements.

- Laboratory furnace

CSF 12/13, CARBOLITE (Great Britain)

Application: Temperature treatment of samples in controlled atmosphere up to 1500°C with automatic adjustment of final temperature, heating and cooling rate.

### III. DEPARTMENT OF RADIOISOTOPE INSTRUMENTS AND METHODS

#### Laboratory of Industrial Radiometry

**Activity profile:** Research and development of non-destructive methods and measuring instruments utilizing physical phenomena connected with the interaction of radiation with matter: development of new methods and industrial instruments for measurement of physical quantities and analysis of chemical composition; development of measuring instruments for environmental protection purpose (dust monitors, radon meters); implementation of new methods of calibration and signal processing (multivariate models, artificial neural networks); designing, construction and manufacturing of measuring instruments and systems; testing of industrial and laboratory instruments.

- Multichannel analyser board with software for X and  $\gamma$ -ray spectrometry

Canberra

- Measuring stand for calibration and testing

Technical data: temperature sensors -  $-15 \div +70^\circ\text{C}$ , pressure sensors - 800-1050 hPa, humidity sensors - 0-100%.

### IV. DEPARTMENT OF RADIOCHEMISTRY

#### 1. Laboratory of Heavy Elements

**Activity profile:** Studies on chemical properties of the heaviest elements: nobelium, rutherfordium, dubnium, element 112. Studies on the influence of relativistic effects on the chemical properties (oxidation state, hydrolytic properties etc.) Elaboration of new analytical techniques for the determination of radium isotopes in natural waters.

#### 2. Laboratory of Radiopharmaceutical Chemistry

**Activity profile:** Preparation of novel complexes, potential radiopharmaceuticals, e.g. derivatives of tricarbonyltechnetium(I) ( $^{99\text{m}}\text{Tc}$ ) with chelating ligands: diketones and other similar extractants. Studying of their hydrophilic-lipophilic properties, structure and their interactions with peptides. The new complexes will be studied as prospective agents for labelling blood cells (leukocytes for inflammation imaging) and possibly in cerebral blood perfusion studies.

- Two radiometric sets

ZM 701, ZZUJ POLON (Poland)

Application: For measurements of radioactivity of radiotracers and radioelements.

- Spectrometric set

ORTEC

Multichannel analyser, type 7150, semiconductor detector GEM 08180

Application: Measurements and identification of  $\gamma$ - and  $\alpha$ -radioactive nuclides.

- Spectrometric set

TUKAN, IPJ (Świerk, Poland)

Multichannel analyser, type SILENA with a PC card type TUKAN; semiconductor detector GEM 08180

Application: Measurements and identification of  $\gamma$ -radioactive nuclides.

- Gamma radiation counter

ZR-11, ZZUJ POLON (Poland)

Application: For measurements of  $\gamma$ -radioactive samples, the volume of samples up to 5 ml.

- Counter of low activities

ZR-16, ZZUJ POLON (Poland)

Application: For measurements of low activities of  $\alpha$ - and  $\beta$ -radioactive nuclides, also of low energies.

- Gas chromatograph

610, UNICAM (England)

Description of usage: Analysis of the composition of mixtures of organic substances in the gas and liquid state.

- UV-VIS spectrophotometer

DU 68, Beckman (Austria)

Description of usage: Recording of electronic spectra of metal complexes and organic compounds in solution. Analytical determination of the concentration of these compounds.

- FT-IR spectrophotometer

EQUINOX 55, Bruker (Germany)

Description of usage: Measurements of the IR spectra of metal complexes and other species in the solid state and in solution.

## V. DEPARTMENT OF NUCLEAR METHODS OF PROCESS ENGINEERING

### 1. Pilot Plant for Flue Gases Treatment

Activity profile: Pilot plant was installed for basic and industrial research on radiation processing application for flue gases treatment at the PS Kawęczyn.

- Two accelerator ELW-3A

Technical data: 50 kW power, 800 kV

- Analyser of gases

Model 17, Thermo Instrument (USA)

Application: measurement of NO, NO<sub>2</sub>, NO<sub>x</sub>, NH<sub>3</sub> concentrations.

- Analyser 10AR (Shimadzu, Japan) with analysers NOA-305A for NO concentration determination and URA-107 for SO<sub>2</sub> determination
- Analysers CO/CO<sub>2</sub>, O<sub>2</sub>

### 2. Laboratory for Flue Gases Analysis

Activity profile: Experimental research connected with elaboration of technology for SO<sub>2</sub> and NO<sub>x</sub> and other hazardous pollutants removal from flue gases.

- Ultrasonic generator of aerosols

TYTAN XLG

- Gas chromatograph

Perkin-Elmer (USA)

- Gas analyser LAND

Application: determination of SO<sub>2</sub>, NO<sub>x</sub>, O<sub>2</sub>, hydrocarbons, and CO<sub>2</sub> concentrations.

- Impactor MARK III

Andersen (USA)

Application: measurement of aerosol particles diameter and particle diameter distribution.

### 3. Laboratory of Stable Isotope Ratio Mass Spectrometry

Activity profile: study of isotope ratio of stable isotopes in hydrogeological, environmental, medical and food (wines and juices) samples.

- Mass spectrometer DELTA<sup>plus</sup>

Finnigan MAT (Bremen, Germany) ...

Technical data: DELTA<sup>plus</sup> can perform gas isotope ratio measurements of H/D,  $^{13}\text{C}/^{12}\text{C}$ ,  $^{15}\text{N}/^{14}\text{N}$ ,  $^{18}\text{O}/^{16}\text{O}$ ,  $^{34}\text{S}/^{32}\text{S}$ .

Application: for measurements of hydrogen (H/D) and oxygen ( $^{18}\text{O}/^{16}\text{O}$ ) in water samples with two automatic systems: H/Device and GasBench II. The system is fully computerized and controlled by the software ISODAT operating in multiscan mode (realtime). The H/Device is a novel preparation system for hydrogen from water and volatile organic compounds determination. It is based on the reduction with hot chromium and is fully automated using an autosampler. Precision of hydrogen isotope ratio determination is about 0.5‰ for water. The GasBench II is a unit for on-line oxygen isotope ratio measurements in water samples by "continuous flow" techniques. The essence of the method consists in oxygen of isotope equilibration between water and  $\text{CO}_2$  in isothermal conditions. For water equilibration a precise thermostat sample tray is used for 96 vials. With GasBench II, water samples (0.5 ml) can be routinely analyzed with a precision and accuracy of 0.08‰. The total volume of water sample for oxygen and hydrogen determination is about 2 ml.

#### 4. Radiotracers Laboratory

Activity profile: Radiotracer research in the field of: environment protection, hydrology, underground water flow, sewage transport and dispersion in rivers and sea, dynamic characteristics of industrial installations and wastewater treatment stations studies.

- Heavy lead chamber (10 cm Pb wall thickness) for up to 1 Ci radiotracer activity preparations in liquid or solid forms
- Field radiometers for samples activity measurements
- Apparatus for liquid sampling
- Multichannel analyser DIDAC
- Liquid chromatograph Perkin-Elmer
- Turner fluorimeters for dye tracer concentration measurements
- Automatic devices for liquid tracers injection

#### 5. Membrane Laboratory

Activity profile: Research in the field of application of membranes for radioactive waste processing and separation of isotopes.

- Membrane distillation plant for concentration of solutions

Technical data: output  $\sim 0.05 \text{ m}^3/\text{h}$ , equipped with spiral-wound PTFE module G-4.0-6-7 (SEP GmbH) with heat recovery in two heat-exchangers.

- Multi-stage MD unit (PROATOM) with 4 chambers equipped with flat sheet membranes for isotope separations research
- US 150 laboratory stand (Alamo Water) for reverse osmosis tests

Technical data: working pressure - up to 15 bar, flow rate -  $200 \text{ dm}^3/\text{h}$ , equipped with two RO modules

- Laboratory stand with 5 different RP spiral wound modules and ceramic replaceable tubular modules
  - Laboratory set-up for small capillary and frame-and-plate microfiltration and ultrafiltration modules examination (capillary EuroSep, pore diameter  $0.2 \mu\text{m}$  and frame-and-plate the INCT modules)
  - The system for industrial waste water pretreatment
- Technical data: pressure - up to 0.3 MPa; equipped with ceramic filters, bed Alamo Water filters with replaceable cartridge (ceramic carbon, polypropylene, porous or fibrous) and frame-and-plate microfiltration module

- The set-up for chemically aggressive solutions (pH 0-14), high-saline solutions ( $\sim 50 \text{ g/l}$ ) in the whole pH range, and radioactive solutions treatment

Technical data: equipped with TONKAFLO high pressure pump, up to 7 MPa, chemically resistant Kiryat Weizmann module (cut-off 400 MW), and high-pressure RO module

## VI. DEPARTMENT OF RADIATION CHEMISTRY AND TECHNOLOGY

### 1. Pilot Installation for Radiation Processing of Polymers

Activity profile: The research is being performed in the field of polymer materials development particularly in relation with medical quality polypropylene suitable for radiation sterilization, thermomelttable glue and PE based composites for thermoshrinkable products applications.

- Accelerator ILU-6

INP (Novosibirsk, Russia)

Technical data: beam power - 20 kW, electron energy - 0.7-2 MeV.

Application: radiation processing.

- Extruder

PLV-151, BRABENDER-DISBURG (Germany)

Technical data: Plasti-Corder consists of: driving motor, temperature adjustment panel, thermostat, crusher, mixer, extruder with set of extrusion heads, (for foils, rods, sleeves, tubes) cooling tank, pelletizing machine, collecting device.

Application: preparation of polymer samples.

- Equipment for mechanical testing of polymer samples

INSTRON 5565, Instron Co. (England)

Technical data: High performance load frame with computer control device, equipped with Digital Signal Processing and MERLIN testing software; max. load of frame is 5000N with accuracy below 0.4% in full range; max. speed of testing 1000 mm/min in full range of load; total crosshead travel - 1135 mm; space between column - 420 mm; the environmental chamber 319-409 (internal dimensions 660x230x240 mm; temperature range from -70°C to 250°C).

Application: The unit is designed for testing of polymer materials (extension testing, tension, flexure, peel strength, cyclic test and other with capability to test samples at low and high temperatures).

### 2. Radiation Physics Laboratory

Activity profile: The influence of nuclear radiation (electrons, ions) on solid state, especially on semiconductor materials. Radiation lattice defects. The distribution of dose radiation in gaseous media.

- Electron accelerator

AS-2000 (Holland)

Technical data: Energy - 0.1-2 MeV, max. beam current - 100  $\mu$ A.

Application: Irradiation of materials.

- Spectrometer

DLS-82E, SEMITRAP (Hungary)

Application: Research in radiation physics of semiconductors.

- Argon laser

ILA-120, Carl Zeiss (Jena, Germany)

Application: Measurements of optical properties.

- Spectrometer

DLS-81 (Hungary)

Application: Measurements of semiconductor properties.

- Argon laser

LGN-503 (Russia)

Application: Measurements of optical properties.

### 3. Radiation Sterilization Pilot Plant of Medical Devices and Tissue Grafts

Activity profile: Research and development studies concerning new materials for manufacturing single use medical devices (resistant to radiation up to sterilization doses). Elaboration of monitoring



systems and dosimetric systems concerning radiation sterilization processing. Introducing specific procedures based on national and international recommendations of ISO 9000 and PN-EN 552 standards. Sterilization of medical utensils, approx. 50 million pieces per year.

- Electron beam accelerator

UELW-10-10, NPO TORIJ (Moscow, Russia)

Technical data: beam energy - 10 MeV, beam power - 10 kW, supply power - 130 kVA.

Application: Radiation sterilization of medical devices and tissue grafts.

#### 4. Laboratory of Radiation Microwave Cryotechnique

**Activity profile:** Radiation processes in solids of catalytic and biological importance: stabilization of cationic metal clusters in zeolites, radical reactions in polycrystalline polypeptides, magnetic properties of transition metals in unusual oxidation states; radical intermediates in heterogeneous catalysis.

- Electron spin resonance X-band spectrometer (ESR)

Bruker ESP-300, equipped with: microwave power meter HP 436A, continuous flow helium cryostat Oxford Instruments ESR 900, continuous flow nitrogen cryostat Bruker ER 4111VT, ENDOR-TRIPLE unit Bruker ESP-351.

Application: studies of free radicals, paramagnetic cations, atoms and metal nanoclusters as well as stable paramagnetic centers.

- Spectrophotometer UV-VIS

LAMBDA-9, Perkin-Elmer

Technical data: wavelength range - 185-3200 nm, equipped with 60 nm integrating sphere.

#### 5. Pulse Radiolysis Laboratory

**Activity profile:** Studies of charge and radical centres transfer processes in thioether model compounds of biological relevance in liquid phase by means of time-resolved techniques (pulse radiolysis and laser flash photolysis) and steady-state  $\gamma$ -radiolysis.

- Accelerator LAE 10 (nanosecond electron linear accelerator)

INCT (Warszawa, Poland)

Technical data: beam power - 0.2 kW, electron energy - 10 MeV, pulse duration - 7-10 ns and about 100 ns, repetition rate - 1, 12.5, 25 Hz and single pulse, pulse current - 0.5-1 A, year of installation 1999.

Application: research in the field of pulse radiolysis.

- Gas chromatograph

GC-14B, Shimadzu (Japan)

Specifications: two detectors: thermal conductivity detectors (TCD) and flame ionization detector (FID). Column oven enables installation of stainless steel columns, glass columns and capillary columns. Range of temperature settings for column oven: room temperature to 399°C (in 1°C steps), rate of temperature rise varies from 0 to 40°C/min (in 0.1°C steps). Dual injection port unit with two lines for simultaneous installation of two columns.

Application: Multifunctional instrument for analysis of final products formed during radiolysis of sulphur and porphyrin compounds and for analysis of gaseous products of catalytic reactions in zeolites.

- Dionex DX500 chromatograph system

Dionex Corporation

Specifications: The ED40 electrochemical detector provides three major forms of electrochemical detection: conductivity, DC amperometry and integrated and pulsed amperometry. The AD20 absorbance detector is a dual-beam, variable wavelength photometer, full spectral capability is provided by two light sources: a deuterium lamp for UV detection (from 190 nm) and a tungsten lamp for VIS wavelength operation (up to 800 nm). The GP40 gradient pump with a delivery system designed to blend and pump mixtures of up to four different mobile phases at precisely controlled flow rates. The system can be adapted to a wide range of analytical needs by choice of the chromatography columns: AS11 (anion exchange), CS14 (cation exchange) and AS1 (ion exclusion).

Application: The state-of-the-art analytical system for ion chromatography (IC) and high-performance liquid chromatography (HPLC) applications. Analysis of final ionic and light-absorbed products formed during radiolysis of sulphur compounds. The system and data acquisition are controlled by a Pentium 100 PC computer.

- Digital storage oscilloscope

9354AL, LeCroy

Specifications: Bandwidth DC to 500 MHz; sample rate 500 Ms/s up to 2 Gs/s (by combining 4 channels); acquisition memory up to 8 Mpt. with 2 Mpt per channel; time/div range: 1 ns/div to 1000 s/div; sensitivity: 2 mV/div to 5 V/div, fully variable, fully programmable via GPIB and RS-232C.

Applications: Digital storage oscilloscope (DSO) with high speed and long memory controls pulse radiolysis system dedicated to the nanosecond electron linear accelerator (LAE 10). The multiple time scales can be generated by a computer from a single kinetic trace originating from DSO since the oscilloscope produces a sufficient number of time points (up to 8 M points record length).

- Digital storage oscilloscope

9304C, LeCroy

Specifications: Bandwidth DC to 200 MHz; sample rate 100 Ms/s up to 2 Gs/s (by combining 4 channels); acquisition memory up to 200 kpt. per channel; time/div range: 1 ns/div to 1000 s/div; sensitivity: 2 mV/div to 5 V/div, fully variable.

Applications: Digital oscilloscope (DO) is used in pulse radiolysis system dedicated to the nanosecond electron linear accelerator (LAE 10).

## 6. Research Accelerator Laboratory

Activity profile: Laboratory is equipped with accelerators providing electron beams which make capable to perform the irradiation of investigated objects within wide range of electron energy from 100 keV to 13 MeV and average beam power from 0.1 W to 20 kW, as well as with gamma sources Co-60 with activity 0.5 kCi to 16 kCi and dose rate from 0.03 kGy/h to 1 kGy/h. The described above irradiators are completed in a unique in the world scale set of equipment which can be applied in wide range of electron beam and gamma-ray research and radiation processing.

- Linear electron accelerator

LAE 13/9, Institute of Electro-Physical Equipment (Russia)

Technical data: electron energy - 10-13 MeV; electron beam power - 9 kW.

Application: radiation processing.

- Cobalt source I

Co-60, OPIDI (Świerk, Poland)

Technical data: 32 sources - 500 Ci.

Application: radiation research.

- Cobalt source II

Issledovatel (Russia)

Technical data: 32 sources with a total activity of 16500 Ci.

Application: radiation research.

- Cobalt source III

Mineza, INR (Świerk, Poland)

Technical data: 6 sources with an initial activity of 720 Ci.

Application: radiation research.

- Transilluminator UV

STS-20M, JENCONS (United Kingdom)

Technical information: six 15 W bulbs, emitted 312 nm wavelength, which corresponds to the fluorescence excitation maximum of ethidium bromide. Product description: For visualisation of ethidium bromide - stained nucleic acids fluorescence detection systems. Fluorescence intensity is enhanced, while photobleaching and photoniccking of stained nucleic acids are reduced.

## VII. DEPARTMENT OF ANALYTICAL CHEMISTRY

### 1. Laboratory of Spectral Atomic Analysis

Activity profile: atomic absorption and emission spectroscopy, studies on interference mechanisms, interpretation of analytical signals, service analysis.

- Atomic absorption spectrometer

SH-4000, Thermo Jarrell Ash (USA); equipped with a 188 Controlled Furnace Atomizer (CTF 188), Smith-Heftie background correction system and atomic vapor (AVA-440) accessory.

Application: for analyses of samples by flame and furnace AAS.

- Atomic absorption spectrometer

SP9-800, Pye Unicam (England); equipped with SP-9 Furnace Power Supply, PU-9095 data graphics system, PU-9095 video furnace programmer and SP-9 furnace autosampler.

Application: for analyses of samples by flame and furnace AAS.

### 2. Laboratory of Neutron Activation Analysis

Activity profile: The sole laboratory in Poland engaged for 40 years in theory and practice of neutron activation analysis in which the following methods are being developed: reactor neutron activation analysis (the unique analytical method of special importance in inorganic trace analysis), radiochemical separation methods, ion chromatography.

- Laminar box

HV mini 3, Holten (Denmark)

Technical data: air flow rate 300 m<sup>3</sup>/h.

Application: protection of analytical samples against contamination.

- Ion chromatograph

2000i/SP, Dionex (USA)

Technical data: calculating program AI-450, conductivity detector, UV/VIS detector.

Application: analyses of water solutions, determination of SO<sub>2</sub>, SO<sub>3</sub> and NO<sub>x</sub> in flue gases and air.

- Well HPGe detector

GCW-3223, Canberra, coupled with analog line (ORTEC) and multichannel gamma-ray analyser TUKAN

Application: instrumental and radiochemical activation analysis.

- Coaxial HPGe detector

POP-TOP, ORTEC (USA), coupled with analog line (ORTEC) and multichannel gamma-ray analyser TUKAN

Application: instrumental and radiochemical activation analysis.

## VIII. DEPARTMENT OF RADIOBIOLOGY AND HEALTH PROTECTION

### Laboratory of Cellular Microbiology

Activity profile: The laboratory serves for production of plasmid DNA, subsequently used for studies on DNA recombination repair, determination of topoisomerase I activity and for EPR studies.

- Equipment for electrophoretic analysis of DNA

CHEF III, BIO-RAD (Austria)

Application: analysis of DNA fragmentation as a result of damage by various physical and chemical agents.

- Microplate reader

ELISA, ORGANON TEKNICA (Belgium)

Application: for measurement of optical density of solutions in microplates.

- Hybridisation oven

OS-91, BIOMETRA (Germany)

Technical data: work temperatures from 0°C to 80°C; exchangeable test tubes for hybridisation.

Application: for polymerase chain reaction (PCR).

- Spectrofluorimeter  
RF-5000, Shimadzu (Japan)  
Application: for fluorimetric determinations.
- Transilluminator for electrophoretic gels  
Biodoc, BIOMETRA (Great Britain)  
Application: for analysis of electrophoretic gels.
- Laminar flow cabinet  
1446, GV 1920  
Application: for work under sterile conditions.
- Liquid scintillation counter  
LS 6000LL, BECKMAN (USA)  
Application: for determinations of radioactivity in solutions.
- Research microscope universal  
NU, Carl Zeiss Jena (Germany)  
Application: for examination of cytological preparations.  
Comments: Universal microscope for transmission and reflected light/polarised light. Magnification from 25x to 2500x. Possibility to apply phase contrast.
- Incubator  
T-303 GF, ASSAB (Sweden)  
Technical data: 220 V, temperature range - 25-75°C.  
Application: for cell cultures under 5 % carbon dioxide.
- Laminar flow cabinet  
V-4, ASSAB (Sweden)  
Application: for work under sterile conditions.
- Image analysis system  
Komet 3.1, Kinetic Imaging (Great Britain)  
Application: for comet (single cell gel electrophoresis) analysis.

#### IX. LABORATORY FOR DETECTION OF IRRADIATED FOODS

Activity profile: Detection (identification) of irradiated foods. The analytical methods used are electron paramagnetic resonance spectroscopy (epr) and thermoluminescence measurements (TL). The research work is focused on the development of both methods mentioned as well as on the implementation of some other detection methods (gas chromatographic determination of volatile hydrocarbons in fats, comet assay method (DNA decomposition in single cells, statistical germination method). The quality assurance system has been adapted in the Laboratory in agreement with the PN-EN 45001 standard and ISO/IEC Guide 25:1990. The Laboratory has at disposal full documentation of the adapted quality assurance system. The Laboratory obtained a Certificate of Testing Laboratory Accreditation NR L 262/I/99 issued by the Polish Centre for Testing and Accreditation.

- Thermoluminescence reader  
TL-DA-15 Automated, Risø National Laboratory (Denmark)  
Technical data: 24 samples turntable, heating range 50-500°C, heating speed 0.5-10.0°C/s, stimulated luminescence (PSL) system.  
Application: detection of irradiated foods, research work on irradiated foods, thermoluminescence dosimetry.
- Fluorescence microscope  
OPTIPHOT Model X-2, NIKON (Japan)  
Technical data: halogen lamp 12 V-100 W LL; mercury lamp 100 W/102 DH; lenses (objectives) CF E Plan Achromat 4x, CF E Plan Achromat 40x; CF FLUOR 20x.  
Application: detection of irradiated foods by the comet assay method, research work on apoptosis in mammalian cells, biological dosimetry, analysis of DNA damage in mammalian cells.

- Compact EPR spectrometer

EPR 10-MINI, St. Petersburg Instruments Ltd. (Russia)

Technical data: sensitivity  $3 \times 10^{10}$ , operating frequency (X band) - 9.0-9.6 GHz, max. microwave power 80 mW, magnetic field range 30-500 mT, frequency modulation 100 kHz.

Application: detection of irradiated foods, bone and alanine dosimetry, research work on irradiated foods and bone tissues.

## X. EXPERIMENTAL PLANT FOR FOOD IRRADIATION

### 1. Microbiological laboratory

Activity profile: optimalization of food irradiation process by microbiological analysis.

- Sterilizer

ASUE, SMS (Warszawa, Poland)

Application: autoclaving of laboratory glass, equipment, and microbiological cultures.

- Fluorescence microscope

BX, Olympus (Germany)

Application: quantitative and qualitative microbiological analysis.

### 2. Experimental Plant for Food Irradiation

Activity profile: Development of new radiation technologies for the preservation and hygienization of food products and feeds. Development and standardization of the control system for electron beam processing of food and feeds. Development of analytical methods for the detection of irradiated food. Organization of consumer tests with radiation treated food products.

- Accelerator ELEKTRONIKA (10 MeV, 10 kW)

UELW-10-10, NPO TORIJ (Moscow, Russia)

Application: food irradiation.

## INDEX OF THE AUTHORS

**A**

Abedinzadeh Zohreh 25  
Al-Kaid Abeer 49  
Al-Mowed Abed A. 49  
Ambroz Hanna 19, 20

**B**

Barcz Adam 126  
Bartak Jakub 132  
Bartłomiejczyk Teresa 106  
Bartosik Jerzy 114  
Bergés Jacqueline 39  
Bernstorff Sigrud 78  
Bilewicz Aleksander 61, 64  
Bobrowski Krzysztof 23, 25, 26, 31, 39  
Bouzyk Elżbieta 101, 102, 103, 105  
Brede Ortwin 23  
Buczowski Marek 75, 76  
Bułka Sylwester 113  
Buraczewska Iwona 98, 99, 103, 104, 105

**C**

Callens Freddy 41  
Carewska Maria 79  
Carmichael Ian 26  
Chmielewski Andrzej G. 78, 79, 111, 112, 113, 114, 115, 117, 118, 119  
Cholerzyński Andrzej 115  
Chua David L. 81  
Chwastowska Jadwiga 72  
Cieśla Krystyna 46  
Croce Fausto 81

**D**

Dancewicz Antoni M. 47  
Danilczuk Marek 29  
Danko Bożena 62  
De Angelis Paula 97  
Degueldre Claude 65  
Dembiński Wojciech 67  
Deptuła Andrzej 79, 81  
Deptuła Danuta 81  
Derda Małgorzata 118  
Do-Hoang Cuong 135  
Drzewicz Przemysław 49  
Duarte Celina 49  
Dudek Jakub 71, 72  
Dybczyński Rajmund 62, 68, 70  
Dźwigalski Zygmunt 137

**E**

Eliasson Ann-Charlotte 46

**F**

Fessenden Richard W. 21  
Fiedler Rudolf 67  
Fuks Leon 65, 101, 102

**G**

Gasińska Anna 104  
Giorgi Leonardo 79  
Głuszeński Wojciech 46, 49  
Goovaerts Etienne 41  
Grądzka Iwona 95, 96, 98, 99  
Grigoriev Helena 78  
Grötzschel Rainer 33, 126, 127  
Gryz Michał 49  
Gustafsson Torbjörn 84

**H**

Harasimowicz Marian 115, 117  
Hofmann Michael 85  
Houée-Levin Chantal 39  
Hug Gordon L. 21, 26

**I**

Iller Edward 111, 114

**J**

Jagielski Jacek 127  
Janik Przemysław 95  
Jaworska Alicja 97

**K**

Kałuska Iwona 54  
Kapiszewska Maria 96  
Kasprzak Aleksandra J. 63  
Kierzek Joachim 63, 73  
Kobiątko Grażyna 105  
Kornacka Ewa 19, 20  
Korzeniowska-Sobczuk Anna 23, 26  
Kowalczyk Dariusz 95  
Kowalska Ewa 130, 131  
Kowalska Maria 105  
Kruszewski Marcin 44, 101, 102, 106  
Krynicki Janusz 33  
Kuduk-Jaworska Janina 103, 104

Kukielka Aleksandra 114  
Kulisa Krzysztof 68  
Kunicki-Goldfinger Jerzy 63

## L

Leciejewicz Janusz 85, 87, 88, 90  
Legocka Izabella 51  
Lehner Katarzyna 43  
Lewandowski Włodzimierz 101, 102  
Licki Janusz 111, 112, 113, 114  
Ligęza Maria 121  
Lipiński Paweł 106

## Ł

Łada Wiesława 79, 81  
Łukasiewicz Andrzej 124, 125

## M

Machaj Bronisław 133, 135  
Majerz Irena 84  
Malec-Czechowska Kazimiera 44, 47  
Malicki Wojciech 75  
Małożewska-Bućko Bożena 63, 73  
Matz Wolfgang 127  
Maurin Jan K. 90  
Michalik Jacek 29, 41, 114  
Migdał Wojciech 56  
Mikołajczuk Agnieszka 119  
Mikołajczyk Władysław 114  
Mioduski Tomasz 67  
Mirkowski Jacek 31  
Mirkowski Krzysztof 51  
Moreno Angelo 79

## N

Nałęcz-Jawecki Grzegorz 49  
Narbutt Jerzy 64  
Naumov Sergej 23

## O

Oikawa Hiroshi 49  
Olczak Tadeusz 79, 81  
Olovsson Ivar 84  
Ołdak Tomasz 101  
Orelowitch Oleg 123  
Ostapczuk Anna 112  
Owczarczyk Andrzej 117  
Owczarczyk Hanna B. 56

## P

Paluchowska Beata 90  
Panta Przemysław 49  
Pańczyk Ewa 121  
Parker Stewart F. 85

Parus Józef 73  
Pawlukojć Andrzej 85  
Penc Bogusław 85  
Piekoszewski Jerzy 126, 127, 128  
Pieńkos Jan P. 132  
Polkowska-Motrenko Halina 68  
Poniński Marek 67  
Priebe Waldemar 101, 102  
Prokert Fridrich 126, 128  
Przybytniak Grażyna 19, 20  
Pszonicki Leon 71, 72  
Ptasiewicz-Bąk Halina 83, 84, 87, 88

## R

Rafalski Andrzej 35  
Reitan Jon 97  
Remita Samy 25  
Richter Edgar 128  
Richter Lothar 23  
Rowińska Luzja 124, 125  
Rudawska Kinga 83  
Ryguła Czesław 114  
Rzewuski Henryk 33

## S

Sadło Jarosław 29  
Samczyński Zbigniew 62  
Samochocka Krystyna 101, 102  
Sampa Maria H.O. 49  
Sartowska Bożena 76, 79, 123  
Satyanarayana Jujjawarapu 64  
Sawicki Józef 49  
Scaccia Silvera 79  
Siekierski Sławomir 83  
Simonetti Elisabetta 79  
Skwara Witold 71, 72  
Sochanowicz Barbara 104  
Sołtyk Wojciech 117  
Stachowicz Wacław 41, 43, 44, 56  
Stanisławski Jacek 126, 127, 128  
Starosta Wojciech 76, 87, 88  
Sterlińska Elżbieta 72  
Struszczyk Henryk 114  
Strzelczak Grażyna 25, 39, 41, 56  
Stuglik Zofia 57  
Stupińska Halina 114  
Sun Yongxia 113  
Szewczyńska Małgorzata 49  
Szopa Zygmunt 70  
Szot Zbigniew 44  
Szumiel Irena 95, 96, 97, 103, 104  
Szymczyk Władysław 126  
Szytuła Andrzej 85

## Ś

Świstowski Edward 135

**T**

Tomczak Włodzimierz 115  
Tomkinson John 85  
Trojanowicz Marek 49  
Tymiński Bogdan 111, 114, 115, 117

**U**

Urbański Piotr 130, 131, 133

**V**

Vanhaelewyn Gauthier 41  
Varmenot Nicolas 25

**W**

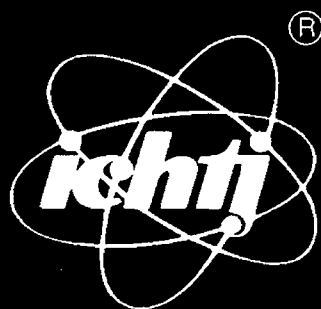
Walendziak Jolanta 117  
Waliś Lech 121, 124, 125, 128

Wachoł Stanisław 33  
Waszkiewicz Katarzyna 103, 104  
Wawszczak Danuta 75, 76  
Werner Zbigniew 126  
Wierzchnicki Ryszard 118, 119  
Wiśniowski Paweł 21, 23, 25, 31  
Włodzimirska Barbara 61  
Wojewódzka Maria 98, 99  
Wolińska-Grabczyk Aleksandra 78  
Wójcik Andrzej 105

**Z**

Zagórski Zbigniew P. 35, 37  
Zakrzewska-Trznadel Grażyna 114, 115, 117  
Zielonka Maria 51  
Zimek Zbigniew 51, 54, 111, 113, 114, 137  
Zygmunt Adam 85





**INSTITUTE OF NUCLEAR  
CHEMISTRY AND TECHNOLOGY**

**Dorodna 16, 03-195 Warszawa, Poland**  
**phone: (+48 22) 811 06 56, fax: (+48 22) 811 15 32,**  
**e-mail: [sekdyrn@orange.ichtj.waw.pl](mailto:sekdyrn@orange.ichtj.waw.pl)**